ACTA CHIMICA

ACADEMIAE SCIENTIARUM HUNGARICAE

TOMUS 61 FASCICULUS 1

AKADÉMIAI KIADÓ, BUDAPEST

1969

ACTA CHIM. ACAD. SCI. HUNG.

ACTA CHIMICA

A MAGYAR TUDOMÁNYOS AKADÉMIA KÉMIAI TUDOMÁNYOK OSZTÁLYÁNAK IDEGEN NYELVŰ KÖZLEMÉNYEI

Az Acta Chimica német, angol, francia és orosz nyelven közöl értekezéseket a kémiai tudományok köréből.

Az Acta Chimica változó terjedelmű füzetekben jelenik meg, egy-egy kötet négy füzetből áll. Évente átlag négy kötet jelenik meg.

A közlésre szánt kéziratok a szerkesztőség címére (Budapest 112/91 Műegyetem) küldendők.

Ugyanerre a címre küldendő minden szerkesztőségi levelezés. A szerkesztőség kéziratokat nem ad vissza.

Az Acta Chimica előfizetési ára kötetenként belföldre 120 Ft, külföldre 165 Ft. Megrendelhető a belföld számára az „Akadémiai Kiadó"-nál (Budapest V., Alkotmány utca 21. Bankszámla 05-915-111-46), a külföld számára pedig a „Kultúra" Könyv- és Hírlap Külkereskedelmi Vállalatnál (Budapest I., Fő utca 32. Bankszámla: 43-790-057-181) vagy annak külföldi képviseleteinél és bizományosainál.

Die Acta Chimica veröffentlichen Abhandlungen aus dem Bereiche der chemischen Wissenschaften in deutscher, englischer, französischer und russischer Sprache.

Die Acta Chimica erscheinen in Heften wechselnden Umfanges. Vier Hefte bilden einen Band. Jährlich erscheinen 4 Bände.

Die zur Veröffentlichung bestimmten Manuskripte sind an folgende Adresse zu senden:

Acta Chimica
Budapest 112/91 Műegyetem

An die gleiche Anschrift ist auch jede für die Redaktion bestimmte Korrespondenz zu richten.

Abonnementspreis pro Band: 165 Forint. Bestellbar bei dem Buch- und Zeitungs-Außenhandels-Unternehmen »*Kultúra*« (Budapest I., Fő utca 32. Bankkonto No. 43-790-057-181) oder bei seinen Auslandsvertretungen und Kommissionären.

ACTA CHIMICA

ACADEMIAE SCIENTIARUM HUNGARICAE

TOMUS 61

AKADÉMIAI KIADÓ, BUDAPEST

1969

ACTA CHIM. ACAD. SCI. HUNG.

ACTA CHIMICA

INDEX

TOMUS 61

Fasciculus 1: 1969
Fasciculus 2: 1969
Fasciculus 3: 1969
Fasciculus 4: 1969

APJOK, J. s. BARTÓK, M.

BABERNICS, L. s. TÉTÉNYI, P.

BARTÓK, M., APJOK, J., KARAKHANOV, R. A. and KOVÁCS, K.: Chemistry of 1,3- Bifunctional Systems, VI. Examination of the Transformations of 4-Methyl-1,3-Dioxane on Various Catalysts by Means of the Micro Reactor Technique 315

BERÉNYI, M.: Platinum and Palladium Catalyzed Oxidation of Ammonia under the Experimental Conditions of Differential Thermoanalysis (DTA) 257

BICZÓ, G. s. LADIK, J.

BITTER, I. s. CSŰRÖS, Z.

BOGNÁR, R., TŐKÉS, A. L. and FRENZEL, H.: Flavonoids, XVI. Mono- and Diglucosides of Phloracetophenone and Their Conversion into Glucosides of Chalcone, Flavanone and Phlorizin Type 79

BOKSAY, Z. and GURMAI, M.: Conductivity of Mixed Alkali Glasses Containing Aluminium Oxide 223

Book Reviews 429

BORBÉLY-KUSZMANN, A. s. NAGY, J.

BUZÁGH-GERE, É. s. PAULIK, F.

CYVIN, S. J. and HARGITTAI, I.: Mean Amplitudes of Vibration for Small Molecules Containing Sulphur, II. Sulphuryl Fluoride, Fluoro and Chloro Sulphonic Acids 159

CYVIN, S. J. s. HARGITTAI, I.

CSÁSZÁR, J. and HORVÁTH, E.: Physico-chemical Studies on Isomeric Compounds of Transition Metal Ions 13

CSŰRÖS, Z., SOÓS, R., BITTER, I., SZEGHY, L. and PETNEHÁZY, I.: Acylation Reactions with Phosgene 197

DÉVAY, J., MÉSZÁROS, L. and GARAI, T.: Calculation of the Influence of the Ohmic Resistance of the Cell on the Third Harmonic a.c. Polarographic Current in Case of a Reversible Electrode Reaction 279

DOBIS, E. s. MLINKÓ, S.

ERDEY, L. s. HANNA, Z. G.

ERDEY, L. s. INCZÉDY, J.

ERDEY, L. s. PAULIK, F.

FERENCZI-GRESZ, S. s. NAGY, J.

FREEMAN, D. E.: Stretching Force Constants in NO_2F and NO_2Cl 163

FRENZEL, H. s. BOGNÁR, R.

GANESCU, I. s. ZSAKÓ, J.

GARAI, T. s. DÉVAY, J.

GÖMÖRY, P. and SZEPES, L.: Preparation of ^{18}O-Labelled Methylsiloxanes 407

GÖMÖRY, P. s. SZÉKELY, T.

GÖRBICZ, M. s. UPOR, E.

GÖRÖG, S.: Analysis of Steroids, IX. Spectrophotometric Investigation of Oestra-5(10)-en-3,17-dione and its 3,3- Dimethyl Ketal 341

GURMAI, M. s. BOKSAY, Z.

HANKOVSZKY, O. H. and HIDEG, K.: Benzazoles, VII. Alkylation Reactions of 2-Thio-[1,3]-diazoles 69

HANNA, Z. G., KÁNTOR, T. and ERDEY, L.: Distribution of Arc Temperature Using Cathode Excitation 329

HARGITTAI, I. and CYVIN, S. J.: Mean Amplitudes of Vibration for Small Molecules Containing Sulphur, I. Thionyl and Sulphuryl Chlorides 51

HARGITTAI, I. s. CYVIN, S. J.

HIDEG, K. s. HANKOVSZKY, O.

HOLLY, S., SZABÓ, G., TÓTH, G. and VARSÁNYI, G.: Investigation of the Intermediates of the Nitration of Furfural by Infrared Spectroscopy 45

HOLZAPFEL, H. s. NENNING, P.

HORNYÁK, GY., LÁNG, L., LEMPERT, K. and MENCZEL, GY.: 1,2,4-Triazines and Condensed Derivatives, VIII. The Reaction of 6-Aza-2-Thiothymine with Acrolein and Related Compounds 93

HORNYÁK, GY., LEMPERT, K. and ZAUER, K.: 1,2,4-Triazines and Condensed Derivatives, IX. Synthesis of Some Imidazo-, Pyrimido- and [1,2,4]-Triazino-[1,2,4]-triazine Derivatives 181

HORVÁTH, E. s. CSÁSZÁR, J.

HUN-BOROSSAY, GY. s. TÖRÖK, F.

INCZÉDY, J., KLATSMÁNYI-GÁBOR, P. and ERDEY, L.: The Use of Complex-forming Agents in Ion Exchange Chromatography, I. Separation of Cobalt (II) and Nickel (II) Ions on Cation Exchange Column Using Oxalate Ions Containing Eluent ... 261

KÁNTOR, T. s. HANNA, Z. G.

KAPOSI, O. and RIEDEL, M.: Experimental Study of Positive Ion Emission from Tungsten, I 349

KARAKHANOV, R. A. s. BARTÓK, M.

KENDE, L. s. LADIK, J.

KISS, B. A.: Continuous Detection by Simultaneous TG and IR Measurements of NH_3 and H_2O Released in Thermal Decompositions 207

KLATSMÁNYI-GÁBOR, P. s. INCZÉDY, J.

KOVÁCS, K. s. BARTÓK, M.

KOZMUTZA, K. s. SCHMEER-ERDEY, A.

LADIK, J., BICZÓ, G., KENDE, L. and SÜMEGI, L.: Application of the Semiempirical Different Orbitals for Different Spins SCF LCAO MO Method for the Calculation of Spin Densities of Some Phenyl Nitric Oxide Radicals 381

LÁNG, L. s. HORNYÁK, GY.

LEMPERT, K. s. HORNYÁK, GY.

LÉGRÁDI, L.: Mechanism of Adsorption Indication, I. Nitronic Acids as Adsorption Indicators: *p*-nitro-α-naphtylred, a New Adsorption Indicator 115

LÉGRÁDI, L.: Mechanism of Adsorption Indication, II. Amphoteric Adsorption Indicators 125

MENCZEL, GY. s. HORNYÁK, GY.

MÉSZÁROS, L. s. DÉVAY, J.

MLINKÓ, S. and DOBIS, E.: Sulphur Determination in Organic Compounds by Radio-reagent Method 133

NAGY, J., FERENCZI-GRESZ, S., PÁLOSSY-BECKER, K. und BORBÉLY-KUSZMAN, A.: Dipolmomentuntersuchungen der Phenyl- und Benzylderivate von Elementen der vierten Hauptgruppe. (Investigation of the Dipole Moment of the Phenyl and Benzyl Derivatives of the Elements of Group IV/1 of the Periodic Table) 149

NENNING, P und HOLZAPFEL, H.: Quarternäre bororganische Verbindungen. (Quaternary Boron-organic Compounds) 421

PAÁL, É. and VARSÁNYI, GY.: Calculation of Infrared Band Contours of Planar Asymmetric Top Molecules, I. Construction of General Relationships 391

PÁLOSSY-BECKER, K. s. NAGY, J.

PAULIK, F., BUZÁGH-GERE, É. und ERDEY, L.: Derivatographische Untersuchung des Magnesiumammoniumphosphats. (Derivatographic Analysis of Magnesium Ammonium Sulfate) 29

PETNEHÁZY, I. s. CSŰRÖS, Z.

PULAY, P. s. TÖRÖK, F.

PUNGOR, E. und WESER, A.: Die Untersuchung von Boriden, Carbiden und Nitriden auf ihre Eignung als Indikatorelektrode für potentiometrische Messungen (The Investigation of Borides, Carbides and Nitrides for Their Suitability as Indicator Electrodes in Potentiometric Measurements) 241

RIEDEL, M. s. KAPOSI, O.

RÓNAI, S. s. UPOR, E.

RÓNAI, A. s. SZABOLCS, J.

ROST, L.: Physikalische Ursachen des Matrixeffektes bei der Spektralanalyse im Gleichstrombogen. (Physical Causes of the Matrix Effect in Spectral Analysis in a Direct-Current Arc) 271

RÖSNER, P. s. SZÉKELY, T.

SCHAY, G.: Árpád Kiss 1889—1968 107

SCHÄCHTER, K. s. TÉTÉNYI, P.

SCHNEER-ERDEY, A. and KOZMUTZA, K.: XeF_2 as an Analytical Reagent (Preliminary Communication) 325

SOÓS, R. s. CSŰRÖS, Z.

SÜMEGI, L. s. LADIK, J.

SZABÓ, G s. HOLLY, S.

SZABOLCS, J. and RÓNAI, Á.: Methanolysis of Lutein Ditri-chloroacetate. Preparation of 3-hydroxy-3'-methoxy-α-carotene and 3-hydroxy-5'-methoxy-4', 5'-dihydro-3', 4'-dehydro-α-carotene 301

SZABOLCS, J. and RÓNAI, Á.: The Structure of α-Cryptoxanthin and the Identity of Zeinoxanthin with α-Cryptoxanthin 309

SZAMMER, J.: A New Method for the Preparation of Amino Alcohols from Amino Acids 419

SZEGHY, L. s. CSŰRÖS, Z.

SZEJTLI, J.: A New Formula for the Description of the Conformation of Pyranoid Sugars 57

SZÉKELY, T., RÖSNER, P. and GÖMÖRY, P.: Contributions to the Heterofunctional Condensation of Silanes, I. Investigation of the Prepration of Sioxanes with Regular Structures 233

SZEPES, L. s. GÖMÖRY, P.

TÉTÉNYI, P., BABERNICS, L. and SCHÄCHTER, K.: Kinetic Study of Hydrocarbon Adsorption on Nickel Catalyst 367

TÓTH, G. s. HOLLY, S.

TÓTH, G. und ZSINKA, L.: Bestimmung der Oberfläche pulverförmiger Platinadsorbentien durch Messung der Jodadsorption mit der radioaktiven Indikator-Methode. (The Determination of the Surface of Powdered Platinum Adsorbents by the Measurement of Iodine Adsorption by Radioactive Tracer Method) 289

TŐKÉS, A. L. s. BOGNÁR, R.

TÖRÖK, F., PULAY, P. and HUN-BOROSSAY, GY.: On the Parameter Form of Force Constant Matrix, X. On the Coriolis Coupling Constants Compatible with the Normal Frequencies 39

TURÓS, J. s. ZSAKÓ, J.

UPOR, E., RÓNAI, Á. and GŐRBICZ, M.: Some Problems in the Separation, by Precipitation, of Traces of Elements, V. Sorption of Ammine Complex Forming Cations on Metal Hydroxides. Determination of Zinc in Rock Samples, after Separation with Ammoniumhydroxide 1

VARSÁNYI, G. s. HOLLY, S.
VARSÁNYI, GY. s. PAÁL, É.
VÁRHELYI, I. s. ZSAKÓ, J.
WESER, A. s. PUNGOR, E.
ZAUER, K s. HORNYÁK, GY.
ZSAKÓ, J., VÁRHELYI, Cs., GĂNESCU, I. and TURÓS, J.: Kinetics and Mechanism of Substitution Reactions of Complexes, XI. New Reinicke-salt-like Compounds Containing Paraphenetidine, and the Solvolysis of $[Cr(NCS)_4$-(*p*-phenetidine)$_2]^-$ in Ethanol–Water Mixtures 167
ZSINKA, L. s. TÓTH, G.

Acta Chimica Academiae Scientiarum Hungaricae, Tomus 61 (1), pp. 1—11 (1969)

SOME PROBLEMS IN THE SEPARATION, BY PRECIPITATION, OF TRACES OF ELEMENTS, V

SORPTION OF AMMINE COMPLEX FORMING CATIONS ON METAL HYDROXIDES. DETERMINATION OF ZINC IN ROCK SAMPLES, AFTER SEPARATION WITH AMMONIUM HYDROXIDE

E. UPOR, Á. RÓNAI and M. GÖRBICZ

(Mecsek Ore Mining Enterprise, Kővágószöllős)

Received January 23, 1968

Revised manuscript received: September 15, 1968

The adsorption of ammine-forming cations on iron(III) hydroxide has been studied as a function of the NH_4OH and ammonium salt concentrations. Though data in the literature are contradictory to one another, it has been found in agreement with KOLTHOFF's results that the adsorption of all ions decrease with increasing concentrations of NH_4OH and ammonium salts.

The pH-profile of adsorption is a bell-shaped curve with a maximum at about pH = 8. Cobalt(II) and zinc(II) are best adsorbed; by proper adjustment of the pH, these ions can be quantitatively directed into precipitate or kept in solution. Their elution from the precipitate is hindered by ageing.

The minimum concentrations of NH_4OH and ammonium salts at which the ions remain quantitatively in solution have been determined. The applicability of this separation method in the analysis of rocks has been demonstrated by tracer technique. The quantitative requirements of trace analysis can be met by a single separation, since only the loss in cobalt amounts to a few per cents.

The NH_4OH method is suitable for the separation of zinc from calcium. A method has been developed for the determination of small amounts of zinc in rocks using dithizone.

Introduction, review of the literature

Comparatively few communications deal with the losses occurring in metal hydroxides in the course of the separation of copper, zinc, nickel, and cobalt with ammonium hydroxide. Most of the papers [1—16] report on studies with standard solutions; several authors, however, discuss applications in the analysis of rocks, or metals [17—21].

Only the series publications of KOLTHOFF *et al.* [1—5] deal with this topic in details, and systematically.

All the authors agree that the separation of the above mentioned elements from iron(III) hydroxide and other metal hydroxides insoluble in ammonium hydroxide cannot be achieved without losses. There is, however, certain disagreement concerning the magnitude of the losses and the circumstances affecting the losses. Authors claim the principal factors influencing the sorption are those of ammonium hydroxide, and ammonium salts, in concentrations. Their considerations, however, are not unanimous.

KOLTHOFF *et al.* have shown that the increase of the NH_4OH and NH_4^+ concentration leads to the decrease of sorption. According to their data [3, 4] the sorption of copper, nickel, and zinc can be completely prevented, and the sorption of cobalt(II) can be reduced to 7 per cent if the concentration of the ammonium salt is sufficiently high (>2M). LUNDELL [15], however, claims that these conditions are favourable only for keeping copper and zinc in solution, and disadvantageous for cobalt and nickel. The same is the opinion of BAILEY [11] concerning the precipitation of cobalt(II) on $Cr(OH)_3$. According to IBBOTSON, cobalt and nickel losses decrease with the increasing concentration of ammonium hydroxide. MELLOR reports [17] that in ore analysis two or three precipitations are needed to achieve separation of zinc without any loss.

Under conditions not specified, IKRAMOV [22] found a 67 per cent loss of zinc in the presence of $Fe(OH)_3$. HOLYNSKA [21] estimates zinc losses to be about 10 to 20 per cent when rock samples are analysed.

Experimental considerations, methods of investigation

First the sorption as a function of the concentration of ammonium hydroxide and ammonium ions was studied. However, it seemed to be essential [29] that sorption should be represented as a function of pH instead of as a function of the concentration of ammonium hydroxide. Namely, preliminary experiments have shown that variation in the pH significantly affects the reproducibility of results.

The pH of the solutions was adjusted by an ammonium hydroxide solution. Thus instead of the dependence of sorption from pH, actually that from $(p_{OH} + p_{NH_3})$ is registered.

The pH-dependence of sorption at a constant ammonium hydroxide concentration will be described in a later communication.

Due to the volatility of ammonia the precipitation was carried out in ground glass stoppered vessels, and for rapid filtration (in general after a one hour standing) a wide pore filter paper was used. The pH of the filtrate was measured immediately. The results were reproducible, the pH values did not change within one hour.

From the macro-element used as the carrier 100 mg were taken; the precipitation was performed in a 100 ml volume. The concentration of the cations was between 10^{-5} and 10^{-2} M; most often the two limiting concentrations were employed.

Usually both the liquid and the solid phases were analysed. Precipitates were collected on paper filters and in order not to disturb sorption equilibria washing of the precipitates was omitted. Precipitates were weighed while

wet to allow correction for that quantity of the particular ion which remained in the incompletely removed solution (this was approximately 1—2 ml). Results were accepted as correct when the sum from the two phases was 100 ± ± 5 per cent that of the initially taken quantity.

Values noted on diagrams or curves are averages of at least two parallel measurements.

Analytical methods used were the following.

1. Radioactive tracer technique, and measurement of γ-activity

Determination of ^{65}Zn, ^{60}Co, and ^{110m}Ag activity was carried out in one of the following three apparatuses.

a) 20th Century Electronics 100-channel analyser (Type 1363d) with a Gamma ND-118 type measuring head and a NZ-111-BD type NaI/CsI well-crystal of 15 ml useful capacity.

b) Scaler, KFKI 1872 type, with the same sensor and measuring head as before.

c) Nuclear Enterprises single channel amplitude analyser, Type NE-8650.

The concentration of radioactive isotopes used for labelling was chosen so that background activity was not more than 0.1 per cent of the total activity.

2. Photometric methods

The determination of copper(II) was measured as copper(II) ammine complex, and cobalt(II) as cobalt-nitroso-R-salt complex [23]. When the precipitate was analysed, iron was extracted previously with tri-*n*-buthylphosphate, from a 1:1 hydrochloric acid medium. Sample weights were chosen so that 1 per cent of it should reliably be detectable.

3. Complexometric titration [24]

Zinc was titrated at pH 9—10 with EDTA using eriochrome-black T as indicator.

Cobalt(II) was measured by back-titrating an excess of EDTA pH 9—10 with a standard zinc solution using eriochrome-black T as indicator.

Nickel was titrated between pH 9—10 using murexide as indicator.

Copper was determined by back-titrating an excess of EDTA with manganese(II) standard solution using eriochrome-black T as indicator.

Sample weights were chosen so that in the parts an aliquot portion of the solution subjected to analysis, 1 per cent of the original quantity should correspond to 0.1 ml of EDTA.

The pH values were measured with a Radelkis OP 401/1 type potentiometric apparatus using an OP 801/1 type combined electrode.

The pH dependence of the sorption

Experiments were carried out mostly with $Fe(OH)_3$ as a carrier. The pH dependence of the sorption of zinc, and cobalt(II) is shown in Fig. 1. It can be concluded that by adjusting the pH suitably practically complete precipitation, or complete solution, can be achievable. A curve of similar character has been published by BERDNIKOV [25] for the sorption of cobalt(II) on peat, by REMPORT-HORVÁTH [26] for that of zinc(II) and cobalt on oxycellulose, and by KURBATOV [27] on filter paper.

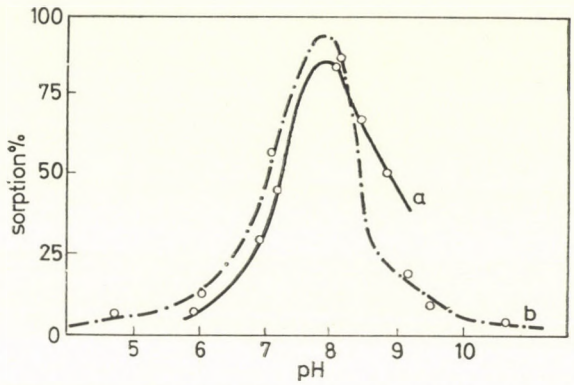

Fig. 1. Sorption of zinc(II), and cobalt(II) on iron(III) hydroxide from an ammonium hydroxide medium as a function of pH

(100 mg Fe^{3+} + zinc(II), or cobalt(II) + NH_4Cl, precipitated with various amounts of NH_4OH, at room temperature. Filtered after standing for one hour.)

a) 50 μg Zn^{++} (+ ^{65}Zn) + 0.9 *M* NH_4NO_3 *b)* 0.01 mM (58 mg) Co^{++} + 0.6 *M* NH_4NO

The dependence of the sorption on the ammonium concentration

Fig. 2 shows the pH-dependence of the sorption of cobalt(II), zinc, and silver, the pH being varied with ammonium hydroxide without addition of any ammonium salt. It can be seen that even at pH 10 the sorption of cobalt(II) is close to 90 per cent, and that of zinc to 70 per cent.

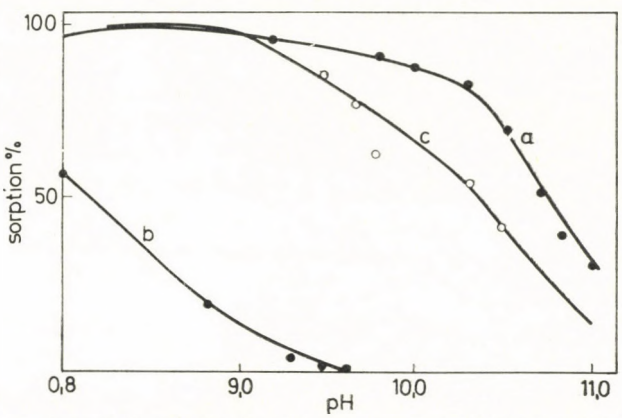

Fig. 2. Sorption of zinc(II), cobalt(II), and silver, on iron(III) hydroxide from an ammonium hydroxide medium, as a function of pH

(100 mg Fe^{3+} + zinc (cobalt, silver), precipitated with various amounts of NH_4OH, at room temperature; filtered after standing for one hour.)

a) 10 mg Co^{++}, *b)* 10 mg Ag^{+}, *c)* 10 mg Zn^{++}

Fig. 3 shows the sorption of zinc, at constant pH, as a function of the concentration of ammonium salt; Fig. 4 shows the sorption of cobalt(II)

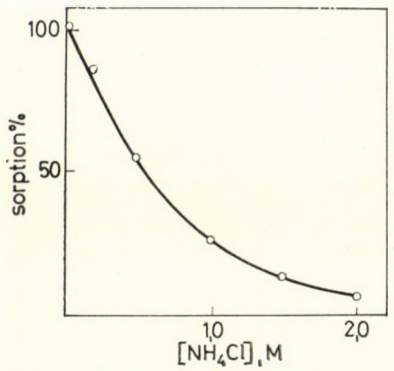

Fig. 3. Sorption of zinc(II) on $Fe(OH)_3$, as a function of the ammonium concentration (100 mg Fe^{3+} + 100 μg Zn^{++}, various amounts of NH_4Cl in 100 ml; pH 8.9—9.1, adjusted with NaOH.)

in function of pH at three different concentrations of ammonium salt. These results and those given in Figs 1 and 2 show an increase in ammonium concentration, and, as a result, a decrease of sorption.

Preliminary experiments with nickel, silver, and copper gave the same result. Curves of similar character as above were obtained for these. Thus claims [11, 15, 17] that an increase in the ammonium salt or ammonium hydroxide concentration decreases the sorption of some ions are disproved.

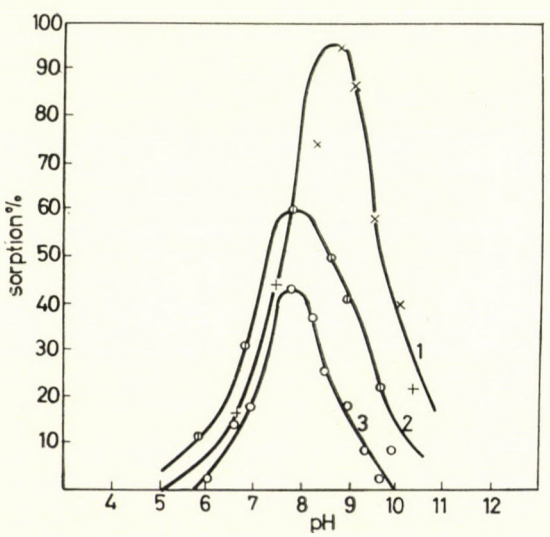

Fig. 4. Sorption of cobalt(II) as a function of pH, at various ammonium concentrations (100 mg Fe^{3+} + 50 mg Co^{++} + NH_4Cl, precipitated with various amounts of NH_4OH, at room temperature, filtered after standing for one hour.)
1. 0.18 *M* MH_4Cl. 2. 0.92 *M* MH_4Cl. 3. 1.85 *M* MH_4Cl

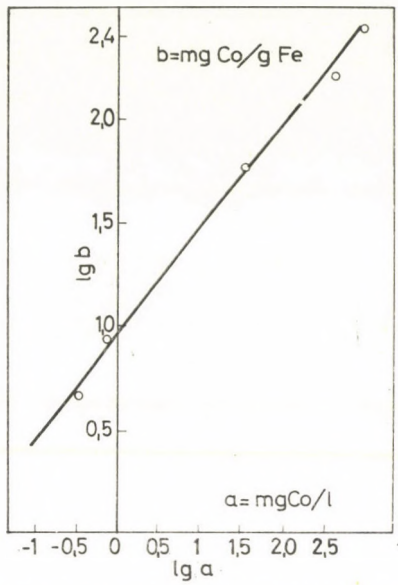

Fig. 5. Freundlich isotherm for the sorption of cobalt(II) on $Fe(OH_3)$ from an ammonium hydroxide medium
(100 mg Fe^{3+}, $5 \cdot 10^{-5}$ — $1.7 \cdot 10^{-2}$ *M* Co^{++}, 0.19 *M* NH_4Cl, 1 *M* NH_4OH; pH 9.1)

In Fig. 4 it is noteworthy that the concentration of the ammonium salt affects, in a certain measure, the position of the maximum; this may help in the elucidation of the mechanism of adsorption and desorption.

Optimum conditions for the separation of cations forming ammine complexes from metal hydroxides

Our results indicate that the separation according to the requirements of trace-analysis can be achieved by a single precipitation. Considering that the permissible limit of losses with regard to trace analysis is set at 2 per cent (with washing), the separation of several elements will be possible under the conditions given in Table I.

Values listed in the table are correlated concentrations of ammonium hydroxide and ammonium salt. The increase of the concentration of one of the components permits, within certain limits, the decrease of the other. Thus, for instance, with Ni^{++} a concentration of ammonium salt lower than 0.5 mole per litre suffices if concentration of ammonium hydroxide is higher than 1 molar, and, the other way round: when the ammonium salt concentration is above 2 *M* a few tenths of a mole per litre of ammonium hydroxide is sufficient. Of course, the possibility of variation is limited in the case of the most easily sorbed ions: Co^{++} and Zn^{++}, here high concentrations of ammo-

Table I

Conditions of separation without loss of some ions from $Fe(OH)_3$

100 mg Fe^{+++} + 0.1 to 10 mg of the ion studied in 100 ml.
Precipitates at room temperature with a mixture of NH_4Cl and NH_4OH.
Filtration five minutes after precipitation

Ion	NH_4OH *M*	NH_4Cl *M*	pH
Co^{++}	>4	>2	>10
Zn^{++}	>2	>2	>10
Cu^{++}	~2	>1	> 9.5
Ni^{++}	>2	>1.5	> 9.5
Ag^{+}	>1	>0.5	> 9.5

nium salt and hydroxide are required. According to the Freundlich isotherm ($b = k \cdot a^{1/n}$) the relative magnitude of sorption depends on the cation concentration. In order to present our experimental data for other concentrations we plotted the Freundlich isotherm for cobalt. The correlation is valid within the four orders of magnitude studied. The value of the exponent $1/n$ is 0.52. (According to KOLTHOFF, this is 0.41 for the sorption of zinc [4], and 0.46 for that of copper [3]. This means that at lower concentrations relative losses are greater, nevertheless, also with trace quantities separation can be made complete. In order to check the results from the point of view of the determination of traces of zinc and cobalt in rock, we studied the separation of ^{65}Zn and ^{60}Co added to various sandstone samples. These were digested in aqua regia, then the radioactive isotopes, ammonium chloride (3 *M*) and ammonium hydroxide (pH ~ 10) were added to the filtrates. After one hour standing the precipitate was collected on a filter paper, and was washed with a 2 *M* ammonium chloride solution (adjusted to pH = 9.6) several times. The zinc content of the samples was not higher than 100 μg/g, and the cobalt content not higher than 60 μg/g. The results are listed in Table II.

Table II

No. of the sample	Sorption loss, %	
	Zn	Co
XII 2360	0.8	1.8
XII 2322	0.9	1.5
XII 2280	0.6	0.9
XII 2260	—	1.1
XII 2229	1.0	1.3

As far as the requirements of trace analysis are considered, the separation is complete. However, it is important to filter within 10 minutes after precipitation. For, as we found it, due to ageing phenomena, the re-solubility of the cobalt and zinc incorporated by sorption into the precipitate will decrease with time. The loss, in the case of nickel, copper and silver, is less than 1 per cent. Accordingly, cations which form ammine complexes in solution can be separated without loss so as to comply with requirements of trace analysis, by a single precipitation. Thus the +10 per cent correction, proposed by KNYIPOVICH [28] for determinations of the copper content of rock samples, can be neglected. It should be mentioned, however, that rapid separation is a requirement in the case of cobalt, and also advantageous when zinc is measured.

A quantitative separation can be achieved both at room temperature, and at 80 °C water bath.

Preliminary experiments disclosed that only rapid precipitations from a homogeneous solution, or by means of ZnO [1, 15] gave satisfactory results. Since the pH of the separation is relatively close to the maximum of the sorption curve and the adjustment of the required value is not at all easy, separation cannot be kept well in hand. This is true also for the, otherwise best, precipitation with hexamethylenetetramine (cf. Table III). Even when the

Table III

Sorption of zinc(II), and of cobalt(II), on 100 mg of $Fe(OH)_3$, during various separation methods
100 μg Zn^{++} or Co^{++}, labelled with ^{65}Zn, and ^{60}Co

Ion	Method of separation	pH	NH_4Cl	% sorption
Zn^{++}	boiled with urea	7.15	0.19	93
Zn^{++}	warmed with hexamethylenetetramine	4.7	0.95	7.5
Zn^{++}	boiled with ZnO suspension	5.5	—	16.5
Co^{++}	boiled with urea	7.65	0.19	90
Co^{++}	warmed with hexamethylenetetramine	4.65	0.95	5.5
Co^{++}	with a ZnO suspension	6.2	—	7.5
Co^{++}	boiled with CH_3COONa	5.0	—	16

separation is carried out from a homogeneous medium, a certain ammonium salt concentration should be applied. Consequently, when routine analyses are contemplated, precipitation with ammonium hydroxide in the presence of ammonium salt is the most advantageous anyhow because the conditions of separation without loss are easy to ensure.

The application of separations performed using ammonium hydroxide

Determination of minute amount of zinc in rock samples with dithizone

As could be seen in Fig. 2, zinc can be quantitatively precipitated with iron(III) hydroxide in a relatively wide pH range. If the concentration of the ammonium salt is not high, *i.e.* < 0.1 *M*, the separation of zinc from calcium will be feasible. In the next step at a higher pH and ammonium salt concentration, the separation of zinc from iron can be carried out. It is advisable, however, to repeat the precipitation after redissolving the hydroxide precipitate, otherwise — when the analytical operations are carried out in the usual manner — losses due to ageing will occur. (When the precipitate is allowed to stand for an hour and then suspended in a mixture of a 2 *M* solution of NH_4Cl and a 3.5 *M* solution of NH_4OH, a 10—15 per cent zinc loss is to be observed.)

The dithizone method seems to be the most advantageous for the determination of minute amount of Zn; this is mostly used in water and in soil analysis [30, 31, 32] for orientative tests. Since our aim was to suggest a more accurate method, the possibility for the elimination of interfering ions and to obtain the best conditions for the procedure had to be studied.

All the elements which are extracted into the organic phase from a solution suitable for the extraction of zinc, interfere in the dithizone method [33]. From these elements several (Mn, Fe, Sn, Pb, Bi) can be removed by ammonium hydroxide precipitation, others (Ag, Cd, Hg) are present in ore or soil samples of average composition at concentrations lower by one order of magnitude than that of the zinc concentration thus no special concern is caused by these.

Only the interference of copper, cobalt, and nickel had to be eliminated. One way to perform this would be the masking of these ions *e.g.* with thiourea [34]. However, we wanted to determine the said elements after the separation with ammonium hydroxide had been carried out: thus we regarded it more advantageous to introduce suitable separation steps into the method.

Among the possibilities, the following proved to be the best.

Nickel. Extraction of its complex formed with dimethylglyoxime at pH 8—10.

Copper, cobalt. Extraction with dithizone, together with zinc, at pH 9, and re-extraction of zinc with a 0.1 *N* nitric acid solution.

In the course of these operations no loss of zinc (<1 per cent) occurs; nickel, cobalt, and copper are quantitatively removed. This was checked by tracer technique in the case of cobalt and nickel (^{60}Co, ^{63}Ni), and by photometry in the case of copper through its sodium diethyldithiocarbamate reaction.

An advantage of this method is that the pH of the solution obtained after separation with ammonium hydroxide is suitable for extraction.

In the extraction of zinc by dithizone we endeavoured to restrict excess dithizone to the lowest possible level, because the green dithizone has some absorption at 530 nm, proper for the measurement of the red zinc-dithizonate complex. To prevent this interference, two methods seemed to be advisable.

1. Extraction with small portions of a dithizone solution (0.5 to 1.0 ml) till a violet colour appears.

2. Extraction with excess dithizone followed by re-extraction of dithizone with a Na_2S solution.

A brief description of the method

The rock or soil sample (1 g) is evaporated to dryness with aqua regia (20 ml), the residue is dissolved in dilute hydrochloric acid and the insoluble part is filtered off. The solution is heated to boiling and ammonium chloride (10 g) and concentrated ammonium hydroxide (30 ml) are added. The hydroxide precipitates are filtered immediately, and the filtrate is diluted to 100 ml.

According to the expected zinc content, a 1 to 20 ml portion of the solution is treated with a 1 per cent solution (5 ml) of dimethylglyoxime, after ten minutes nickel is extracted with 2 portions (5 ml each) of chloroform, and the organic phase is discarded.

The portions of the aqueous solution are shaken with a 0.01 per cent solution of dithizone in chloroform till this keeps its original green colour. From the combined dithizone extracts zinc is recovered with a 0.1 *N* nitric acid solution (10 ml).

The aqueous solution is neutralized with ammonium hydroxide, then a buffer (5 ml) of pH 7.5 (a 1:4 mixture of a 1/15 *M* solution of disodiumhydrogen phosphate and a 0.1 *M* solution of sodium citrate) is added and zinc is extracted with 0.5 to 1.0 ml portions of a 0.001 per cent solution of dithizone (the last portion has a blue tint). The combined extracts are made up to 10 ml with chloroform, the light absorption measured of the solution in a 1-cm cuvette at 530 nm, using pure chloroform as a reference. A calibration curve, between 0.5 and 2.5 μg of Zn should be used. Extinction of 1 μg Zn is 0.16.

We may proceed also by extraction of zinc with a 0.01 per cent solution of dithizone and re-extraction of excess dithizone with a 0.15 per cent solution of Na_2S.

There is only one difficulty attached to this procedure, and this is the contamination of reagents, and of water, with zinc and other heavy metals. For this reason the reagents should be scrupulously purified *e.g.* distillation of water, after ion-exchange, in a quartz apparatus. Blank tests, for all the reagents, must be made in parallel runs. It is advisable to use the same vessels always for the same operations and to clean the vessels shortly before use.

The accuracy of the method is ± 10 per cent. We analysed standard rock samples prepared in the Geological Institute of Berlin, and obtained the following results (the zinc contents proposed are included for comparison).

Mark of sample	Found by our method	Proposed value
Granite (GM)	50 p. p. m. Zn	46 p. p. m. Zn [35]
Basalt (BM)	90 p. p. m. Zn	102 p. p. m. Zn [35]
Argillite (TS)	90 p. p. m. Zn	103 p. p. m. Zn [35]
Limestone (KH)	10 p. p. m. Zn	8 p. p. m. Zn [36]

REFERENCES

1. KOLTHOFF, I. M.: J. Phys. Chem. **36,** 862 (1932).
2. KOLTHOFF, I. M., STENGER, V. A.: J. Phys. Chem. **38,** 249 (1934).
3. KOLTHOFF, I. M., MOSKOVITZ, B.: J. Phys. Chem. **41,** 629 (1937).
4. KOLTHOFF, I. M., OVERHOLSER, G. I.: J. Phys. Chem. **43,** 762 (1939).
5. KOLTHOFF, I. M., OVERHOLSER, G. I.: J. Phys. Chem. **43,** 909 (1939).
6. LABY, T. H.: Chemical News, **1904,** 280.
7. ARDAGH, E. G. R., BONGARD, G. R.: Ind. Eng. Chem. **1924,** 297.
8. FUNK, W.: Z. Angew. Chem. **18,** 1687 (1905).
9. GELOSO, M. M., LEWY, L. S.: C. R. Acad. Sci. **1929,** 175.
10. THEODOROVICS, I. L.: Zs. Anal. Him. **9,** 293 (1954).
11. BAILEY, P. H.: Analyst **86,** 485 (1961).
12. SZTROMBERG, A. G.: Zav. Lav. **14,** 920 (1948).
13. GORDON, L.: Precipitation from Homogeneous Solution. New York, Wiley, 1959.
14. KOLTHOFF, I. M., SANDELL, E. B.: Textbook of Quantitative Inorganic Analysis. McMillan, New York, 1952.
15. LUNDELL, R., BRIGHT, H. A.: J. Am. Chem. Soc. **45,** 675 (1923).
16. ERDEY, L.: Súlyszerinti elemzés (Gravimetry) Vol. 2., Budapest, Akadémiai Kiadó, 1960.
17. MELLOR, J. W., THOMPSON, H. V.: Treatise on Quantitative Inorganic Analysis with Special Reference to the Analysis of Clays, Silicates, and Related Minerals. London, Ch. Griffin, 1938.
18. DOUGHERTY, G. T.: Chemical News, **1907** 261.
19. BRUJLE, E. S.: Zh. Prikl. Him. **36,** 2767 (1936).
20. KUNZ, K., DUCZYMINSKA, E , OSTACHOWSKA, J.: Rudy i Metalá Niezel, **9** (No. 1.) **35** (1964).
21. HOLYNSKA, B.: Rudy i Metala Niezel, **10** (No. 2.) **54** (1965).
22. IKRAMOV, L. T., IKRAMOV, M. V.: Sbornik Trudi V. Vsesojuznoj Konferencii Sudobni medikov. Riga, 1962. p. 570.
23. BABKO, A. K., PILIPENKO, A. T.: Kolorimetriás analízis (Colorimetry) Budapest, Akadémiai Kiadó, 1953.
24. SAJÓ, I.: Komplexometria (Complexometry) Budapest, Akadémiai Kiadó, 1959.
25. BERDNYIKOV, A. I., OVESKO, V. F.: Radiochimija **5,** 390 (1963).
26. REMPORT-HORVÁTH, Zs.: MTA kém. Oszt. Közl. **20,** 327 (1963).
27. KURBATOV, M. H., KRAMME, O. J.: J. Inorg. Nucl. Chem. **16,** 109 (1960).
28. KNYIPOVICH, Ju. N., MORACHEVSKIJ, Ju. V.: Analiz mineralnogvo sirja. Goshimizdat, Leningrad, 1959.
29. UPOR, E.: Adsorption of cations which form ammine complexes, on metal hydroxides and a study of the possibility of their desorption. (In Hungarian) II. Anal. Symp. of Baranyai Vegyészek, 1961, Pécs.
30. SOKOLOV, J. Ju.: Methodicheskoe rukovodstvo po opredelenju mikrokomponentov v prirodnih vodah pro poi'skah rudnih mestorozhdjenij. Gosgeolthizdat, Moskva, 1961.
31. LURJE, Ju. R., RIBNIKOVA, A. I.: Metodi himicheskovo analiza proizvodostvennih stochnih vod. Moscow, 1953.
32. HUBERT, G.: Méthodes d'analyse quantitative appliquées aux roches de la prospection géochimique. Mém. Bur. Rech. Géol. et Minières, No. 30., Paris 1964.
33. IVANCHEV, G.: Ditizon i evo primenenie. Izdatatinlit., Moskva, 1961.
34. DJACHENKO, I. P., CHUJKO, V. T.: Trudi komissii po anal. him., **14,** 307 (1963).
35. SCHINDLER, R.: Z. angew. Geologie, **12,** 188 (1966).
36. SCHINDLER, R.: Neuere Ergebnisse von Spurenelementbestimmungen verschiedener Laboratorien an den Standardgesteinen des ZGI. (Paper presented, in German, at a symposium on standard rock samples and their use in geological, geochemical practice) Berlin, 1967.

Endre UPOR; Pécs, 39-es Dandár út 3/a. Hungary

Ádám RÓNAI; Pécs, Móricz Zs. u. 15. Hungary

Margaret GÖRBICZ; Miskolc, Felszabadítók útja 4. Hungary

Acta Chimica Academiae Scientiarum Hungaricae, Tomus 61 (1), pp. 13—28 (1969)

PHYSICO-CHEMICAL STUDIES ON ISOMERIC COMPOUNDS OF TRANSITION METAL IONS

J. CSÁSZÁR and E. HORVÁTH

(Institute of General and Physical Chemistry, Attila József University, Szeged)

Received June 15, 1968

Physico-chemical investigation on coordination and polymerization complex isomers having Cr^{3+}-, Mn^{3+}-, Co^{3+}-, Ni^{2+}- and Cu^{2+}-ions as central ions are reported. Magnetic and spectral characteristics are explained on the basis of ligand field theory. All experimental data prove that complex ions retain their characteristic features also in isomeric adducts. RACAH parameters, infrared $\nu_s(NH_3)$ and $\nu_{as}(NO_2)$ values are used to draw conclusions regarding the character of the bonds.

1. Introduction

Compounds of Cr^{3+}-, Mn^{3+}-, Fe^{3+}-, Co^{3+}-, Ni^{2+}- and Cu^{2+}-ions, having various composition and geometry, are intensively studied from theoretical and practical (preparative) points of view. Many papers deal with their features and the theoretical interpretation of them on the basis of crystal field (CF), and ligand field (LF) theories and also the molecular orbital (MO) model [1—6]. Extremely stable complex anions and cations of these metal ions easily join with each other in the most varied combinations.

Only few papers deal with physico-chemical investigation of the isomeric adducts appearing in great variety. In this paper we report the results of our different spectroscopic and magnetic investigations on a series of compounds showing coordination and polymerization isomerism.

2. Experimental

The starting compounds were prepared according the methods described in the literature [7—10] from reagents of analytical grade, and purified by repeated recrystallization. When preparing the isomeric adducts equivalent quantities of the required components in solutions in water or water-ethanol mixture were mixed. After cooling to 0 °C the separated precipitate was filtered off, washed with some cold water and ethanol, then with ether and dried over P_2O_5 in a desiccator. Composition of the simple compounds and the isomers were checked by their spectra or by N-analysis, respectively. Characteristic data are summarized in Table I.

Table I

Characteristic features and analytical data of the prepared isomeric compounds

No.	Complex	Colour	Molecular weight	Polym. number	N %	
					Calcd.	Found
I.	$[Co(NH_3)_6]\ [Co(CN)_6]$	flesh coloured	376.18	—	44.68	44.51
II.	$[Co(NH_3)_5Cl]\ [Co(NH_3)_2(NO_2)_4]_2 \cdot 5H_2O$	tan	733.63	—	28.91	28.73
III.	$[Co(NH_3)_6]\ [Co(Ox)_3] \cdot 3H_2O$	pale green	484.13	—	15.62	15.48
IV.	$[Co(NH_3)_6]\ [Co(CO_3)_3] \cdot 4H_2O$	olive green	400.10	—	17.80	17.58
V.	$[Co(en)_3]\ [Co(CN)_6]$	tan	454.29	—	37.00	34.79
VI.	$[Co(en)_3]\ [Co(NO_2)_6]$	lemon coloured	574.23	—	29.27	29.16
VII.	$[Co(en)_3]\ [Co(O_X)_3] \cdot 4H_2O$	pale green	562.24	—	13.25	13.14
VIII.	$[Co(NH_3)_5H_2O]\ [Co(Ox)_3]$	brownish green	485.12	—	14.44	14.72
IX.	$[Co(NH_3)_4(NO_2)_2]\ [Co(NH_3)_2(NO_2)_4] \cdot 3H_2O$	ochre yellow	496.12	2	30.55	30.11
X.	$[Co(NH_3)_6]\ [Co(NO_2)_6]$	lemon coloured	496.12	2	33.88	33.86
XI.	$[Co(NH_3)_5NO_2]\ [Co(NH_3)_2(NO_2)_4]_2$	tan	744.18	3	33.88	33.95
XII.	$[Co(NH_3)_6]\ [Co(NH_3)_2(NO_2)_4]_3 \cdot 6H_2O$	ochre yellow	992.24	4	30.55	30.79
XIII.	$[Co(NO_2)_6]\ [Co(NH_3)_4(NO_2)_2]_3 \cdot 10H_2O$	ochre yellow	992.24	4	28.68	28.41
XIV.	$[Co(NO_2)_6]_2\ [Co(NH_3)_5(NO_2)]_3 \cdot 3H_2O$	reddish	1240.30	5	32.47	32.01
XV.	$[Cr(Ox)_3]\ [Co(NH_3)_6] \cdot 3H_2O$	tan	477.20	—	15.82	15.78
XVI.	$[Cr(Ox)_3]\ [Co(en)_3] \cdot 6H_2O$	light brown	555.31	—	12.67	12.60
XVII.	$[Cr(Ox)_3]\ [Cr(en)_3] \cdot H_2O$	greyish green	548.38	—	14.84	15.24
XVIII.	$[Mn(Ox)_3]\ [Co(NH_3)_6] \cdot 3H_2O$	magenta	480.12	—	15.73	15.62

XIX.	$[Mn(Ox)_3]\,[Co(en)_3] \cdot 3H_2O$	magenta	558.23	—	13.73	13.66
XX.	$[Mn(Ox)_3]\,[Cr(en)_3] \cdot 3H_2O$	violet-red	551.30	—	13.88	13.78
XXI.	$[Fe(Ox)_3]\,[Co(NH_3)_6]$	ochre yellow	481.04	—	17.47	16.58
XXII.	$[Fe(Ox)_3]\,[Co(en)_3] \cdot 5H_2O$	ochre yellow	559.15	—	12.95	12.88
XXIII.	$[Fe(Ox)_3]\,[Cr(en)_3] \cdot 3H_2O$	greenish yellow	552.22	—	13.86	13.76
XXIV.	$[Co(Ox)_3]\,[Cr(en)_3]$	dark green	555.31	—	15.14	15.02
XXV.	$[Co(NH_3)_6]\,[Fe(CN)_6]$	orange	373.09	—	45.06	44.97
XXVI.	$[Co(en)_3]\,[Fe(CN)_6]$	orange	451.20	—	37.26	37.22
XXVII.	$[Co(NH_3)_6]_4\,[Fe(CN)_6]_3$	pink	1280.40	—	45.95	45.92
XXVIII.	$[Co(en)_3]_4\,[Fe(CN)_6]_3$	pink	1592.83	—	36.94	36.98
XXIX.	$[Co(NH_3)_6]\,[CuCl_5]$	yellow	401.96	—	20.91	20.79
XXX.	$[Ni(NH_3)_6]\,[Co(NH_3)_2(NO_2)_4]_2$	ochre yellow	629.79	—	40.04	40.10
XXXI.	$[Cu(NH_3)_4]\,[Co(NH_3)_2(NO_2)_4]_2$	olive green	685.74	—	32.68	32.62

Table II

Possible Laporte-forbidden transitions in the O_h, C_{4v} (D_{4h}) symmetry classes, having

e^--config.	Sym. group	Transitions*		Energy
$(t_{2g})^3\,(e_g)^0$		$^{3,4}T_{2g}\,(F) \leftarrow {}^{3,4}A_{2g}\,(F)$:	ν_1^*	Δ
and	O_h	$^{3,4}T_{1g}\,(F) \leftarrow$	: ν_2^*	$\frac{15B+3\Delta-\sqrt{\Delta^2-18B\Delta+225B^2}}{2}$
$(t_{2g})^6\,(e_g)^2$		$^{3,4}T_{1g}\,(P) \leftarrow$	: ν_3^*	$\frac{15B+3\Delta+\sqrt{\Delta^2-18B\Delta+225B^2}}{2}$
		$^1T_1 \leftarrow {}^1A_1$	: ν_1^*	$\Delta - C$
	O_h	$^1T_2 \leftarrow$	: ν_2^*	$\Delta + 16B - C$
		$^3T_1 \leftarrow$	: $\nu_{t_1}^*$	$\Delta - 3C$
		$^3T_2 \leftarrow$	: $\nu_{t_2}^*$	$\Delta + 8B - 3C$
$(t_{2g})^6\,(e_g)^0$		$^1E_g^+ \leftarrow {}^1A_{1g}$	: $\nu_1^*(I)$	$\Delta - \frac{35}{4}Dt - C$
	C_{4v}	$^1A_{2g} \leftarrow$	: $\nu_1^*(II)$	$\Delta - C$
	D_{4h}	$^1B_{2g} \leftarrow$	: $\nu_2^*(I)$	$\Delta - 4Ds - 5Dt + 16B - C$
		$^1E_g^- \leftarrow$	: $\nu_2^*(II)$	$\Delta + 2Ds - \frac{25}{4}Dt + 16B - C$

Absorption and reflection spectra were recorded in the 320—1250 μm region on a Beckman DU spectrophotometer. Reflection curves were taken against magnesium oxide standard without dilution; calculation of the curves was carried out according to the KUBELKA—MUNK relation [11, 12].

Magnetic susceptibility was determined at room temperature with an electromagnet of Weiss-type, applying about 6500 Gauss field strength. The corrected [13] values were substituted into the $\mu_{B.M.} = 2{,}84(\chi_M T)^{1/2}$ formula to obtain the BM values. For standardisation $Hg[Co(SCN)_4]$ [14] and $[Ni(en)_3]S_2O_3$ [15] were used.

Infrared spectra were registered by a Unicam SP 100 recording spectrophotometer in KBr pellets at 30 °C.

3. Theoretical

Coordination isomerism is a well known type of isomerism [16], characteristic to compounds consisting of two complex ions at least. Such a pair of compounds are *e.g.* $[Co(NH_3)_6]\,[Cr(CN)_6]$ and $[Co(CN)_6]\,[Cr(NH_3)_6]$. This isomerism does not require different central ions in the complex ions, neither limits the number of complex ions among the constituents of the isomeric compound. Such are *e.g.* $[Co(NH_3)_6]\,[Co(NO_2)_6]$, $[Co(NH_3)_4(NO_2)_2]$ $[Co(NH_3)_2(NO_2)_4]$ or $[Co(NH_3)_6]\,[Co(NH_3)_2(NO_2)_4]_3$, $[Co(NO_2)_6]\,[Co(NH_3)_4$

d^3, d^8 and d^6 electrons, furthermore formulas used for calculation

$B_1(C)$**	B_2	Dt	Ds
$B_1 = \frac{\nu_2^* + \nu_3^* - 3\Delta}{16}$	$B_2 = \frac{3\nu_2^*\Delta - (\nu_2^*)^2 - 2\Delta^2}{27\Delta - 15\nu_2^*}$	—	—
$B = \frac{\nu_2^* - \nu_1^*}{16}$ $C = \frac{\nu_1^* - \nu_{t_2,1}^*}{2}$		—	—
$B = \frac{6\nu_2^* - 6\Delta + 6C + 35Dt}{96}$ $C = \Delta(O_h) - \nu_1^*$ (II)		$Dt = \frac{4}{35}[\nu_1^*$ (II) $- \nu_1^*$(I)$]$*** $Dt = \frac{8}{35}[\nu_1^*(O_h) - \nu_1^*]$****	$Ds = \frac{5}{24}Dt$

* According to the electron configuration, triplet and quartet levels exist in Ni^{2+} and Cr^{3+} atoms, resp.

** $B_{Cr^{3+}} = 947$; $B_{Co^{3+}} = 1065$; $B_{Ni^{2+}} = 1084$; $C_{Cr^{3+}} = 3850$; $C_{Co^{3+}} = 5120$; $C_{Ni^{2+}} = 4831$ cm^{-1}.

*** If ν_1^* is splitted enough to be evaluated or it can be disjoined by curve analysis.

**** If ν_1^* is not splitted.

$(NO_2)_2]_3$ compound pairs too. These compound pairs are polymerization isomers.

For our study we have chosen compounds of simple composition and structure, having ligands with no disturbing effects on assignation and identification of the characteristic bands.

In the case of parent compounds of O_h, D_{4h} and C_{4v} symmetry the structure and interpretation of their absorption spectra are well known. Functions are available for calculation of the LF parameters and through them quantities characteristic of the bonds can be determined.

Spectra of complexes of metal ions with $3d^3$, $3d^6$ and $3d^8$ electrons have been discussed in details in the literature [17—21]. Theory of Fe^{3+}-, Mn^{3+}- and Cu^{2+}-compounds, having $3d^5$, $3d^4$ and $3d^9$ electron structure, resp., was developed by BALLHAUSEN [6]. Table II shows the corresponding transitions and relations used in our work.

The LF parameters make possible calculation of $\beta = B/B_0$, $\gamma = C/C_0$ and $\delta\ \% = 100(1 - \beta)$ values [22], which sometimes allow interesting comparisons concerning the bond type.

Table III

Spectral-(kK) and magnetic data of the parent com-

No.	e^--configuration	Complex*	ν_1*	
			abs.	refl.
1.	$(t_{2g})^3$	$K_3[Cr(Ox)_3]$	17.70	17.75
2.		$Cr(En)_3Cl_3$	21.80	21.95
3.	$(t_{2g})^3 (e_g)^1$	$K_3[Mn(Ox)_3]$	9.58	9.60
4.	$(t_{2g})^3 (e_g)^2$	$K_3[Fe(Ox)_3]$**	—	—
5.	$(t_{2g})^6$	$[Co(CO_3)_3]^{3-}$	16.30	16.05
6.		$[Co(Ox)_3]K_3$	16.50	16.62
7.		$[Co(NH_3)_5Cl]Cl_2$	18.72	18.95
8.		$[Co(NH_3)_5H_2O]Cl_3$	20.50	20.76
9.		$[Co(NO_2)_6]K_3$	20.90	21.22
10.		$[Co(NH_3)_6]Cl_3$	21.05	21.30
11.		$[Co(En)_3]Cl_3$	21.45	21.52
12.		$[Co(NH_3)_5NO_2](NO_2)_2$	21.75	21.98
13.		tr-$[Co(NH_3)_4(NO_2)_2]NO_2$	22.73	22.80
14.		tr-$[Co(NH_3)_2(NO_2)_4]K$	23.05	23.25
15.		$[Co(CN)_6]K_3$	32.40	—
16.	$(t_{2g})^6 (e_g)^2$	$[Ni(NH_3)_6]Cl_2$	10.53	10.81
17.	$(t_{2g})^6 (e_g)^3$	$Cs_2[CuCl_4]$	12.50	$\sim$ 9.50
18.		$[Cu(NH_3)_4]Cl_2$	16.60	—

* $K_4[Fe(CN)_6]$ and $K_3[Fe(CN)_6]$ are not shown, as no $d-d$ transition is possible.
** No intensive $d-d$ band appears in the visible spectral region.

4. Discussion of the experimental data

4.1. Spectra of the parent compounds

Data of absorption and reflection spectra of the simple complexes, measured magnetic momentum values, together with the calculated ones are summarized in Table III. Explanation on the mechanism of their light absorption can be found in the literature [17—21]. Spectra of Cr^{3+} ($3d^3$), and Ni^{2+} ($3d^8$) and Co^{3+} ($3d^6$; O_h, C_{4v} and D_{4h} symmetry) are characterized by Laporte-forbidden transitions given in Table II. In these cases the corresponding LF parameters can easily be calculated. It is to be noted, that compounds of MeX_6 and MeL_3 type are considered as having O_h symmetry, *i.e.* we neglected the loss of symmetry caused by bidentate ligands.

In the spectrum of the Mn^{3+} complex two bands due to one spin-forbidden ($^3T_{1g} \leftarrow {}^5E_g$) and one spin-allowed ($^5T_{2g} \leftarrow {}^5E_g$) transitions are found [20]. High intensity of the latter results in complete overlap with the charac-

pounds and calculated B (RACAH) and β values

ν_2*		B		β		BM found
abs.	refl.	abs.	refl.	abs.	refl.	
24.10	24.35	621	646	0.66	0.68	3.93
28.50	28.60	628	622	0.66	0.66	3.82
20.02	20.10	—	—	—	—	4.88
—	—	—	—	—	—	5.76
22.80	22.96	406	432	0.38	0.41	0
23.80	23.96	456	459	0.43	0.43	0
27.50	27.58	500	—	0.47	—	0
30.40	30.72	630	—	0.59	—	0
~28.80	?	494	—	0.46	—	0
29.50	29.68	528	524	0.49	0.49	0
29.50	29.66	503	509	0.47	0.48	0
~30.80	?	551	—	0.52	—	0
~28.85	?	348	—	0.33	—	0
~29.60	?	404	—	0.38	—	0
39.00	—	413	—	0.39	—	0
17.24	17.35	912	868	0.84	0.80	3.13
—	23.50	—	—	—	—	1.99
—	—	—	—	—	—	1.96

teristic d—d band of the other complex-component present in its isomers. The spectrum of the Fe^{3+} compound — having $3d^5$ electrons — shows only combination bands of low intensity, as the ground term does not split and only spin-forbidden sextet-quartet transitions are possible. One broad, complex band is found in the spectrum of the tetrammine complex of the Cu^{2+} ion (with $3d^9$ electrons), its complexity is due to the JAHN—TELLER effect [23].

Considering that the isomeric compounds are very slightly or not at all soluble, the reflection spectra of the parent compounds were also determined — except of $[Co(CO_3)_3]^{3-}$ — and the corresponding parameters calculated. We ascertained, that absorption and reflection spectra of the Co^{3+} complexes are very similar [24], and the calculated B and β values can always be related as $B^0 \geq B^r$ and $\beta^0 \geq \beta^r$ (0 regarding the absorption-, and r the reflection spectra). This means a slight shift in the character of the bonds towards ionic one.

4.2. Co^{3+} isomers

All the Co^{3+} compounds are spin-paired, *i.e.* diamagnetic. Reflection spectra of the isomers contain the two characteristic Laporte-forbidden bands (Table II) (see *e.g.* Figs 1 and 2). The only exceptions are the nitro-ammine compounds, as the absorption of the nitro group prevents the observation of ν_2^*; in many cases also ν_1^* appears as a broad inflection only (Table IV). The bands of spin-forbidden transitions of low intensity, characteristic of

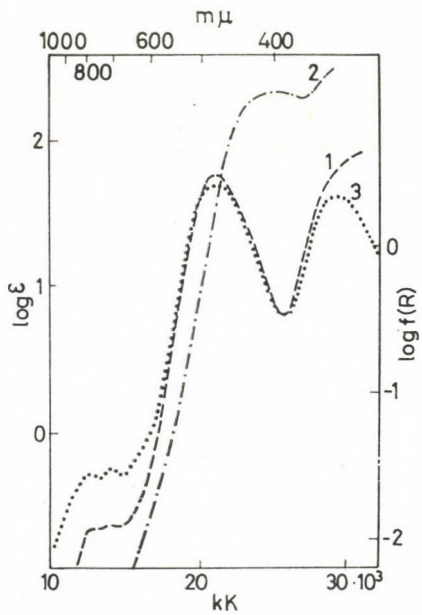

Fig. 1. Reflection spectra. 1: $[Co(NH_3)_6]$ $[Co(CN)_6]$; 2: $[Co(NH_3)_6]$ $[Co(NO_2)_6]$; 3: $[Co(NH_3)_6]Cl_3$ in water

Co^{3+} complexes can only be uncertainly identified, so the calculated values of C and γ should be regarded as approximative ones.

Values of B and C, calculated on the basis of spectral data [25] differ from those of the parent compounds. Here the ratio of C/B is lower. When comparing the spectra of the parent and isomeric compounds, those of the latters seem to be formed by additive combination of spectra of the former ones. The B values of the I—V and III—VII compound pairs are almost identical; it was to be expected by reason of the similarity of their structure.

Also the infrared spectra, recorded in the 375—8850 cm^{-1} region, prove this additivity [26]. Values of $\nu_s(NH_3)$ and $\nu_{as}(NO_2)$ are given in Table V. These are definitely observed in the case of the isomers too, always appearing between the corresponding values of purely covalent (NH_3, CH_3NO_2) and

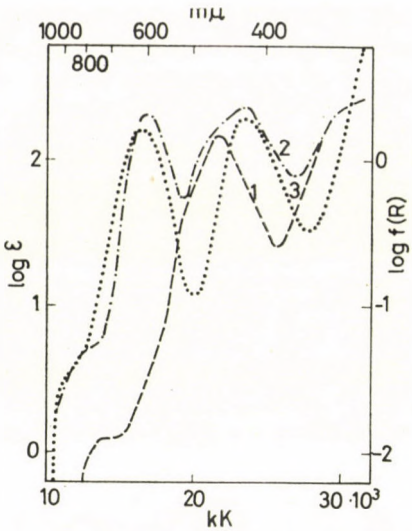

Fig. 2. Reflection spectra. 1: $[Co(en)_3]$ $[Co(CN)_6]$; 2: $[Co(en)_3]$ $[Co(Ox)_3]$; 3: $K_3[Co(Ox)_3]$ in water

Table IV*

Reflection spectral data of some Co^{3+} complex isomers, and calculated parameters

No.	$\nu^*_{1,1}$	ν^*_1	ν^*_2	B^r	β^r	C^r	C^r/B^r
I.	14.00	20.90	~31.20	~644	0.60	3450	5.4
II.	~18.80	~23.00	~28.20	—	—	—	—
III.	13.00	17.00	23.70	419	0.39	2000	4.8
IV.	~12.00	16.60	~25.00	~525	0.49	2300	4.4
V.	14.20	21.50	~31.80	~631	0.59	3750	4.9
VI.	~13.00	~24.00	—	—	—	—	—
VII.	12.60	16.80	23.50	419	0.39	2100	5.0
VIII.	—	16.60	~25.00	—	—	—	—
IX.	~15.00	~22.80	—	—	—	—	—
X.	—	~25.00	—	—	—	—	—
XI.	~14.50	~23.00	—	—	—	—	—
XII.	~14.00	22.50	~27.50	—	—	—	—
XIII.	~14.20	21.70	28.00	—	—	—	—
XIV.	~13.40	~22.00	~29.00	—	—	—	—

* Numbering corresponds to that of Table I.

purely ionic (NH_4Cl, ONO^-) forms [27]. This indicates partly ionic character of the $Co-NH_3$ and $Co-NO_2$ bonds. The covalent character of the bonds, expressed in per cents, ealculated according to the following equation [28]

$$\text{cov. } \% = \frac{\nu_k - \nu_i}{\nu_e - \nu_i} \cdot 100$$

are given in Table V. It is to be seen, that values of the two series are different, but show the same tendency.

Table V*

Two characteristic infrared frequencies of simple and isomeric compounds and covalent bond % values calculated from them

No.	covalent %			
	ν_s (NH_3)	calcd.	ν_{as} (NO_2)	calcd.
NH_3	3414	—	—	—
CH_3NO_2	—	—	1582	—
14.	3328	67.90	1440	51.05
IX.	3300	57.65	1440	51.05
13.	3300	57.65	1440	51.05
XI.	3300	57.65	1440	51.05
XII.	3290	54.10	1438	50.40
7.	3270	46.75	—	—
II.	3270	46.75	1435	49.45
12.	3260	43.13	1430	47.87
XIV.	3250	39.53	1420	44.71
9.	—	—	1420	44.71
XIII.	3220	28.79	1418	44.08
10.	3210	25.24	—	—
X.	3180	14.63	1417	43.76
NH_4Cl	3138	—	—	—
$(ONO)^-$	—	—	1335	—

* Numbering corresponds to that of Tables I and III.

4.3. Isomers of Cr^{3+}-, Mn^{3+}-, Fe^{3+}- and Co^{3+}-complexes

In this group the central ions are Cr^{3+}-$[(t_{2g})^3]$, $Mn^{3+}-[(t_{2g})^3(e_g)^1]$, $Fe^{3+}-[(t_{2g})^3(e_g)^2]$ and $Co^{3+}-[(t_{2g})^6]$ ions. In the studied region both Cr^{3+} and Co^{3+} complex ions show two Laporte-forbidden bands (Table II). The ν_3^* band of Cr^{3+} compounds can only rarely be observed because of overlap by bands due to charge-transfer and by those of the ligands too. Characteristic spectral data are given in Table VI.

Table VI

Characteristic data of Cr^{3+}, Mn^{3+}, Fe^{3+} and Co^{3+} isomers

No.	BM value		kK	Transition	B	β
	Calcd.*	Found**				
XV.	3.88	3.92	17.50	$^4T_{2g} \leftarrow {}^4A_{2g}$		
			~21.30	$^1T_{1g} \leftarrow {}^1A_{1g}$	552	0.58
			23.30	$^4T_{1g} \leftarrow {}^4A_{2g}$		
XVI.	3.88	3.90	17.70	$^4T_{2g} \leftarrow {}^4A_{2g}$		
			~20.50	$^1T_{1g} \leftarrow {}^1A_{1g}$	473	0.50
			22.80	$^4T_{1g} \leftarrow {}^4A_{2g}$		
XVII.	7.76	7.66	17.65	$^4T_{2g} \leftarrow {}^4A_{2g}$		
			22.90	$^4T_{1g} \leftarrow {}^4A_{2g}$	489	0.51
			~28.30	$^4T_{1g} \leftarrow {}^4A_{2g}$		
XVIII.	4.90	4.86	10.20	$^3T_{1g} \leftarrow {}^5E_g$		
			20.30	$^5T_{2g} \leftarrow {}^5E_g$		
XIX.	4.90	4.92	8.70	$^3T_{1g} \leftarrow {}^5E_g$		
			21.20	$^5T_{2g} \leftarrow {}^5E_g$		
XX.	8.78	8.67	9.70	$^3T_{1g} \leftarrow {}^5E_g$		
			20.40	$^5T_{2g} \leftarrow {}^5E_g$		
XXI.	5.92	5.82	21.00	$^1T_{1g} \leftarrow {}^1A_{1g}$		
			29.60	$^1T_{2g} \leftarrow {}^1A_{1g}$	537	0.50
XXII.	5.92	5.88	21.70	$^1T_{1g} \leftarrow {}^1A_{1g}$		
			29.00	$^1T_{2g} \leftarrow {}^1A_{1g}$	456	0.43
XXIII.	9.80	9.61	22.40	$^4T_{2g} \leftarrow {}^4A_{2g}$		
			29.20	$^4T_{1g} \leftarrow {}^4A_{2g}$	636	0.67
III.	0	0	17.00	$^1T_{1g} \leftarrow {}^1A_{1g}$		
			23.70	$^1T_{2g} \leftarrow {}^1A_{1g}$	419	0.39
VII.	0	0	16.80	$^1T_{1g} \leftarrow {}^1A_{1g}$		
			23.50	$^1T_{2g} \leftarrow {}^1A_{1g}$	419	0.39
XXIV.	3.88	3.85	17.10	$^1T_{1g} \leftarrow {}^1A_{1g}$		
			23.30	$^1T_{2g} \leftarrow {}^1A_{1g}$	388	0.36

* Calculated according to equation $\mu_{BM} = [4S(S+1)]^{1/2}$.

** Calculated from the corrected susceptibility value, according to the following formula: $\mu_{BM} = 2.84[\chi_M \cdot T]^{1/2}$.

Pairs of $Co^{3+}-Cr^{3+}$ (XV, XVI, XXIV) compounds show spectra (Figs 3, 6) with well-defined structure, the characteristic bands are easily observed and identified. Sometimes combination bands appear too, but their positions are uncertain.

In the case of $Fe^{3+}-Co^{3+}$ and $Fe^{3+}-Cr^{3+}$ compound pairs (XXI—XXIII) it is the structure of the spectrum of the complex cation (Fig. 5) which dominates [29]. In spectra of compounds containing Mn^{3+}-ions the extremely intensive $^5T_{2g} \leftarrow {}^5E_g$ band [6] overlaps the characteristic maxima of the Co^{3+} or Cr^{3+} compounds (Fig. 4).

We can state, that in spectra of isomeric pairs containing Fe^{3+} ions that of the complex cation, in other cases that of the complex anion is the domi-

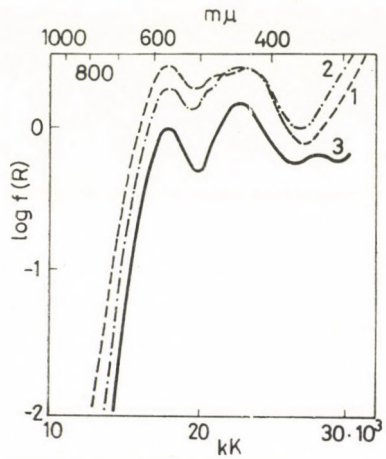

Fig. 3. Reflection spectra. 1: $[Cr(Ox)_3]$ $[Co(NO_3)_6]$; 2: $[Cr(Ox)_3]$ $[Co(en)_3]$; 3: $[Cr(Ox)_3]$ $[Cr(en)_3]$

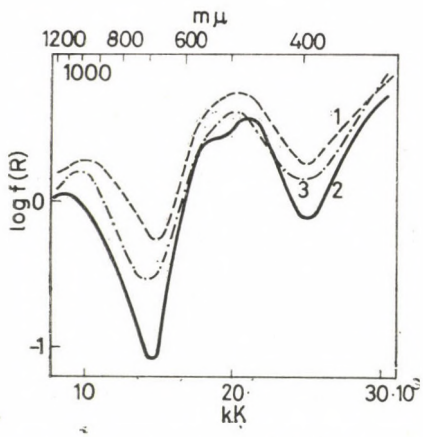

Fig. 4. Reflection curves. 1: $[Mn(Ox)_3]$ $[Co(NH_3)_6]$; 2: $[Mn(Ox)_3]$ $[Co(en)_3]$; 3: $[Mn(Ox)_3]$ $[Cr(en)_3]$

nating one, though the complexity of the individual bands can undoubtedly be proved at both type.

Calculated values of B and C (RACAH) parameters (Table II) are given in Table VI too. If the formulas, applied to the isomers, are selected with regard to the type of the curve, the obtained values change generally in $Cr^{3+}—Fe^{3+}—Co^{3+}$ order, corresponding to the nefelauxetic series of the central ions [30, 31].

Table VI shows very good agreement between measured and calculated spin-only values of paramagnetic moment. This indicates unchanged electron

structure of the complex constituents of the parent compounds in the adducts too, and also the magnitude of the contribution of orbital moment remains the same.

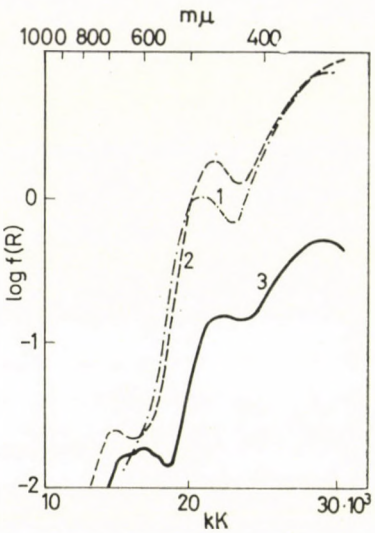

Fig. 5. Reflection spectra. 1: $[Fe(Ox)_3]\,[Co(NH_3)_6]$; 2: $[Fe(Ox)_3]\,[Co(en)_3]$; 3: $[Fe(Ox)_3]\,[Cr(en)_3]$

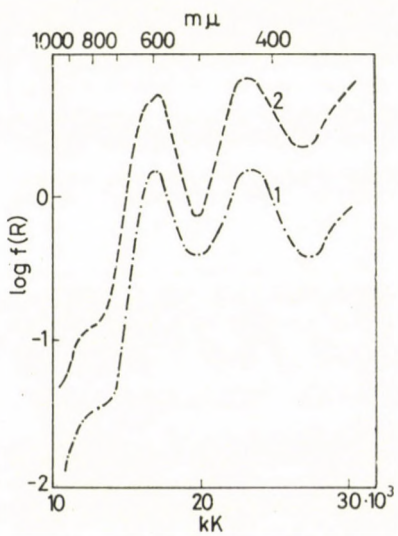

Fig. 6. Reflection curves. 1: $[Co(Ox)_3]\,[Co(NH_3)_6]$; 2: $[Co(Ox)_3]\,[Cr(en)_3]$

4.4. Other isomers

Characteristic data of some mixed isomers are summarized in Table VII.

In spectra of hexacyanoferrate(II) and hexacyanoferrate(III) of $[Co(NH_3)_6]^{3+}$ and $[Co(en)_3]^{3+}$ [32, 33] one single, sharp, well-defined band appears between 22.80 and 23.90 kK. In the hexacyanoferrate(III) adducts

Table VII

No.	Band maxima, kK (reflection spectra)				
XXV.	—	~15.90	23.90	—	—
XXVI.	—	19.80	23.50	—	—
XXVII.	—	—	~20.10	23.60	—
XXVIII.	—	—	22.80	—	—
XXIX.	~10.50	—	~24.00	—	—
XXX.	10.35	~16.60	~22.80	—	28.30
XXXI.	—	17.18	~23.20	—	28.50

(XXV, XXVI) the main band almost coincides with the band of the complex anion appearing at 23.80 kK, while the inflection, observed on the descending side indicates overlapped bands of the cations. The characteristic bands are shifted to 2058 and 2030 cm^{-1} in spectra of XXVII and XXVIII compounds, and to 2096 and 2094 cm^{-1} in those of XXV and XXVI, as compared to the $\nu(C{\equiv}N)$ [27] bands of hexacyanoferrate(II) and hexacyanoferrate(III) ions appearing at about 2031 and 2125 cm^{-1}. In accordance with the parent compounds hexacyanoferrates(II) are diamagnetic, while hexacyanoferrate(III) adducts are paramagnetic, having 2.48 and 2.43 BM values [32].

In $[Co(NH_3)_6]$ $[CuCl_5]$ the anion and the adduct are paramagnetic, with ~2.00 BM and 1.86 BM values, resp. In its reflection spectrum (Fig. 7) [34] a well-defined band appears at 10.50 kK and a broad, complex one between 21—28 kK. In aqueous solution the loose connection of the two complexes breaks off. Bands of $[Co(NH_3)_6]^{3+}$ appear almost in unchanged position. The complex anion loses its quasi-tetrahedral structure and an aquo-chloro, probably $[Cu(H_2O)_5Cl]^+$, complex is formed with a distorted octahedral structure. Bands at 12.5, 21.3 and 29.6 kK can be assigned to $d-d$ transitions of the complex anion and cation, resp. Calculated values of $B = 519$ and $\beta = 0.48$ show only a very weak interaction between the components. Value of λ calculated from the g-value [53] is -405 cm^{-1}.

The perfect additivity is well seen at compounds XXX and XXXI too. Characteristic bands of the cation complexes (Fig. 8) clearly appear in both cases, slight shift of them being disregarded. Ni^{2+} and Cu^{2+} compounds are paramagnetic, having 3.16 and 1.92 BM values, resp.

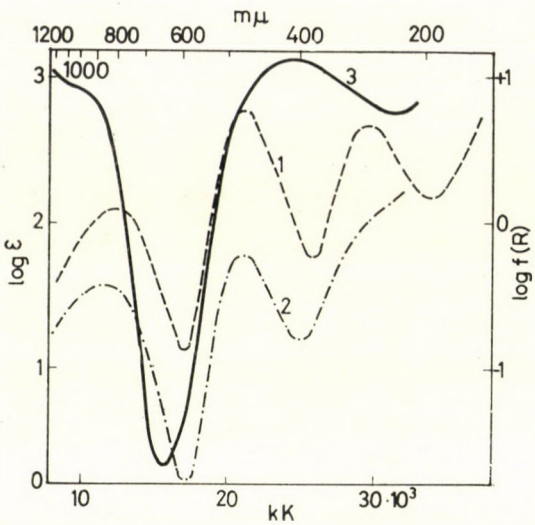

Fig. 7. 1: $[Co(NH_3)_6]$ $[CuCl_5]$ in water; 2: the same, in ~3 *M* HCl solution; 3: the same substance, its reflection curve

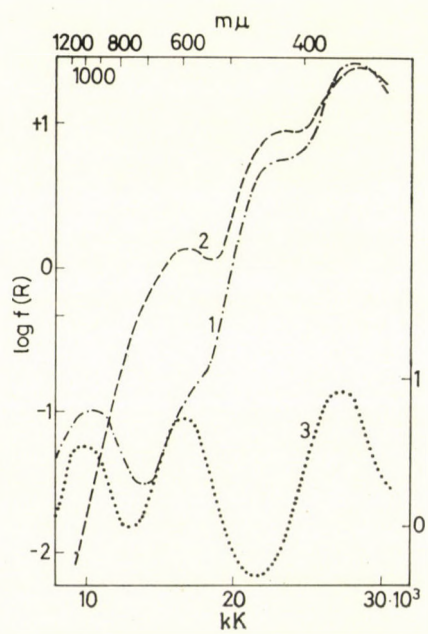

Fig. 8. 1: $[Ni(NH_3)_6]$ $[Co(NH_3)_2(NO_2)_4]_2$; 2: $[Cu(NH_3)_4]$ $[Co(NH_3)_2(NO_2)_4]_2$. Reflection spectra. 3: $[Ni(NH_3)_6]Cl_2$ in water

REFERENCES

1. YAMATERA, H.: Bull. Chem. Soc. Japan **31,** 95 (1958).
2. GRIFFITH, J. S. and ORGEL, L. E.: J. Chem. Soc. 4981 (1956).
3. MOFFIT, W., BALLHAUSEN, C. J.: J. Inorg. Nucl. Chem. **3,** 178 (1956).
4. SCHLÄFER, H. L., GLIEMANN, H.: Einführung in die Ligandenfeldtheorie. Akad. Vlg. Frankfurt am Main, 1967.
5. JÖRGENSEN, C. K.: Absorption Spectra and Chemical Bonding in Complexes. Pergamon Press, London, 1962.
6. BALLHAUSEN, C. J.: Introduction to Ligand Field Theory. McGraw Hill Incorp. New York, 1962.
7. BAILAR, J. C. Jr., FERNELIUS, W. C., ed.: Inorganic Syntheses. II—V., McGraw Hill Co., New York.
8. GMELIN, KRAUT: Handbuch anorg. Chem., 8. Aufl. Berlin, 1930. System Nr. 58.
9. MORI, M.: Bull. Chem. Soc. Japan **34,** 454, 1249 (1961).
10. BRAUER, G.: Handbuch prep. anorg. Chem. (Stuttgart) 1951.
11. KUBELKA, P.: J. Opt. Soc. Amer. **38,** 448 (1948).
12. KUBELKA, P., MUNK, F.: Z. techn. Physik, **12,** 593 (1931).
13. LEWIS, L., WILKINS, R. G.: Modern Coordination Chemistry, Intersci. Inc. New York, 1960.
14. MULAY, L. N.: Anal. Chem. **34,** 343 (1962).
15. KRÁL, M.: Coll. Czechoslov. Chem. Comm. **29,** 2841 (1964).
16. GRINBERG, A. A.: Bevezetés a komplex vegyületek kémiájába. Akad. Kiadó, Budapest, 1958.
17. BÁN, M., CSÁSZÁR, J.: Acta Chim. Acad. Sci. Hung. **53,** 7 (1967).
18. BÁN, M., CSÁSZÁR, J.: Acta Chim. Acad. Sci. Hung. **54,** 133 (1967).
19. GRIFFITH, J. S.: The Theory of Transition Metal Ions. Cambridge Univ. Press, London, 1961.
20. TANABE, Y., SUGANO, S.: J. Phys. Soc. Japan, **9,** 753, 766 (1954).
21. LIEHR, A. D., BALLHAUSEN, C. J.: Ann. of Physics (N. Y.), **6,** 134 (1959).
22. OWEN, J.: Proc. Roy. Soc. (London), **A. 227,** 183 (1955).
23. JAHN, H. A., TELLER, E.: Proc. Roy. Soc., **A. 161,** 220 (1937).
24. SZŐKE, J., CSÁSZÁR, J.: MTA Közp. Fiz. Kut. Közl., **11,** 46 (1963).
25. CSÁSZÁR, J., HORVÁTH, E.: Magy. Kém. Foly. **73,** 157 (1967).
26. CSÁSZÁR, J., HORVÁTH, E.: Magy. Kém. Foly. (In the press).
27. NAKAMOTO, K.: Infrared Spectra of Inorganic and Coordination Compounds. John Wiley and Sons Inc. New York, 1963.
28. SIEBERT, H.: Z. anorg. allg. Chem. **298,** 51 (1959).
29. CSÁSZÁR, J., HORVÁTH, E.: Magy. Kém. Foly. **73,** 441 (1967).
30. JÖRGENSEN, C. K., SCHÄFFER, C. E.: Internat. Symp. on the Chem. of Coord. Compounds. Suppl. Ricerca Sci., **8,** 143 (1958).
31. SCHÄFFER, C. E., JÖRGENSEN, C. K.: J. Inorg. Nucl. Chem. **8,** 143 (1958).
32. CSÁSZÁR, J., FELVÉGI, A.: Acta Chim. Acad. Sci. Hung. **47,** 37 (1966).
33. CSÁSZÁR, J., HORVÁTH, E.: Naturwiss. **53,** 476 (1966).
34. CSÁSZÁR, J.: Magy. Kém. Foly. **73,** 337 (1967).
35. HATFIELD, W. E., PIPER, T. S.: Inorg. Chem. **3,** 841 (1964).

József CSÁSZÁR
Erzsébet HORVÁTH
} Szeged, Rerrich B. tér, Hungary

Acta Chimica Academiae Scientiarum Hungaricae, Tomus 61 (1), pp. 29—37 (1969)

DERIVATOGRAPHISCHE UNTERSUCHUNG DES MAGNESIUMAMMONIUMPHOSPHATS

F. PAULIK, É. BUZÁGH-GERE und L. ERDEY

(Institut für Allgemeine und Analytische Chemie, Technische Universität, Budapest)

Eingegangen am 15. Juli 1968

Verschiedenartig hergestellte Magnesiumammoniumphosphat-Niederschläge wurden einer kombinierten derivatographischen thermogasanalytischen und dilatometrischen Untersuchung unterworfen. Es wurde u.a. festgestellt, daß aus Lösungen unter 75 °C das Hexahydrat, aus Lösungen über dieser Temperatur das Monohydrat ausfällt. Der Ammoniak- und Wassergehalt der Niederschläge entweicht bei monatelangem Aufbewahren verschiedenartig. Auch die thermische Zersetzung der Niederschläge ist je nach der Herstellungsweise unterschiedlich.

Die thermische Zersetzung des Magnesiumammoniumphosphat-hexahydrats besteht aus mehreren, einander überlappenden Teilvorgängen, über deren Verlauf die klassischen thermoanalytischen Methoden (DTA, TG) verhältnißmässig wenig auszusagen vermögen, woraus folgt, daß in der Literatur verschiedene Ansichten über die Art der thermischen Reaktionen zu finden sind [1—7].

Die mit dem Derivatographen von hohem Auflösungsvermögen erhaltenen mit *a* bezeichneten Kurven in Abb. 1 lassen zwei Phasen der thermischen Zersetzung erkennen, von denen die erste (70—180 °C) — auf Grund des resultierenden Gewichtsverlustes — dem Entweichen von 5 Molen Kristallwasser, die zweite (180—600 °C) dem gemeinsamen Entweichen des restlichen Kristallwassermoleküls von 1 Mol Ammoniak und 1/2 Mol Strukturwasser zu entsprechen scheinen [1].

Über weitere Einzelheiten der thermischen Zersetzung, über die Reihenfolge, Geschwindigkeiten und Verbundenheiten der Teilreaktionen erhält man jedoch auch im Besitze der derivatographischen Kurven keine weiteren Aufschlüsse.

Vor kurzem gelang es, mit Hilfe eines Mehrteller-Probehalters [10], eines thermogasanalytischen Adapters [11] und eines dilatometrischen Adapters [12], die Leistungsfähigkeit des Derivatographen [8, 9] weitgehend zu steigern. Unter diesen Voraussetzungen wurden die früher begonnenen [7] Untersuchungen bezüglich der thermischen Zersetzung des Magnesiumsammoniumphosphats wieder aufgenommen.

Tabelle I

Fällungsart		Nach WINKLER [13]						SAINT CHAMANT VIGIER [14]		Bisher nicht angegeben		Theoretischer H_2O- und NH_3-Gehalt
Grundlösung		$MgSO_4 + NH_4Cl + NH_4OH$						$MgSO_4 + NH_4Cl + (NH_4)_2HPO_4$				
Reagenslösung		$(NH_4)_2PO_4$-lösung						Äthanolamin (Hydrolyse in der Kälte)		$NaHCO_3$-Lsg. (Zersetzt sich siedend)		
Fällungstemperatur		100 °C	90 °C	80 °C	70 °C			25 °C		cca 75 °C		
Trocknung		am Glasfilter im Luftstrom, 40 Minuten					Im Vakuum bei 50 °C 10 Tage lang	am Glasfilter im Luftstrom, 40 Minuten				
Aufbewahrungszeit		—			—	2 Jahre	—	—	2 Jahre	—	2 Jahre	
Nr. der Niederschläge		1	2	3	4	5	6	7	8	9	10	
Molzahl NH_3	durch Destillation	1,05	1,02	1,02	1,01	0,93	0,55	1,03	0,99	1,97	0,96	1,00
	Thermogasanalytisch	0,95	1,00	0,94	0,99	0,92	0,52	—	0,93	—	0,95	
Molzahl** H_2O	durch Destillation	1,22	1,18	1,33	5,93	6,03	1,90	6,10	3,70	3,67	3,40	6,00
	Thermogasanalytisch	1,32	1,20	1,41	5,98	6,04	1,93	—	3,67	—	3,45	
Nummer der Abbildungen die die entsprechenden derivatographischen Kurven zeigen		2			1, 3, 6	3	5	3	4	4	4	

** indirekt, durch Berechnung

Experimenteller Teil

Zehn verschiedene, durch Änderungen der Fällungsmethode, der Fällungs- und Trocknungstemperatur sowie der Aufbewahrungszeit erhaltene Niederschläge wurden untersucht. Über die Herstellungsumstände und Zusammensetzung der einzelnen Niederschläge informiert Tab. I. Die derivatographischen Untersuchungen wurden teilweise im Tiegel, teilweise mit auf dem erwähnten Mehrteller-Probehalter [10] ausgebreiteten Proben unter-

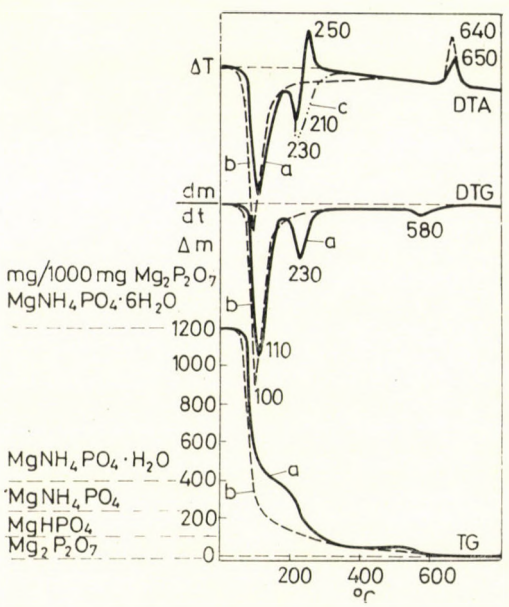

Abb. 1. Thermische Zersetzungskurven des Niederschlages Nr. 4; *a)* im Tiegel und in Luft, *b)* im Mehrteller-Probehalter und in Stickstoff, *c)* im Tiegel und in Stickstoff

nommen. Der thermogasanalytische Adapter [11] gestattete neben der üblichen Registrierung der Probetemperatur, der Gewichtsänderung (TG), der Geschwindigkeit der Gewichtsänderung (DTG) und der Geschwindigkeit der Entalpieänderung (DTA) auch die kontinuierliche, gleichzeitige Registrierung des entweichenden Ammoniaks und somit indirekt auch des Wassers. Der thermogasanalytische Adapter ermöglichte nämlich mit Hilfe von Trägergas die Überführung des freigesetzten Ammoniaks in einen Absorber, wo es in Wasser aufgefangen und mit $n/10$ HCl gegen Methylrot kontinuierlich titriert wurde. Die entweichenden Mengen des Ammoniaks als Funktion der Temperatur aufgezeichnet ergaben die mit NH_3 bezeichneten Kurven in den Abbildungen. Die mit H_2O bezeichneten Kurven, erhalten durch Differenzrechnung der TG und NH_3-Kurven zeigen den Austritt des Kristall- bzw. Struktur-

wassers (Abb. 2—5). Der NH_3-Gehalt eines jeden Niederschlags wurde auch durch Destillation bestimmt. Die in Molen ausgedrückten, derivatographisch und durch Destillation bestimmten NH_3- und rechnerisch ermittelten H_2O-Gehalte der einzelnen Niederschläge sind in Tab. I zusammengestellt. Um der Oxydation des Ammoniaks vorzubeugen, wurde bei den Versuchen Stickstoff als Trägergas verwendet, abgesehen von den Kurven *a* und *b* in Abb. 1, wo die Aufnahme in Luft erfolgte.

Niederschlag Nr. 4 wurde auch einer dilatometrischen Prüfung unterworfen, die mit Hilfe eines mit dem Derivatographen verbindbaren dilatometrischen Adapters [13] erfolgte. In zwei parallelen, unter Standard-Versuchsbedingungen ausgeführten Untersuchungen erhielt man hier die Temperatur-, Gewichts-(TG), und die der Volumenänderung entsprechende Längenänderung (TD), weiterhin die Geschwindigkeit der Entalpie- (DTA), Gewichts-(DTG) und Längenänderung der in zylindrische Form gepreßten Probe (Abb. 6). Die Aufheizungsgeschwindigkeit betrug stets 5 °C/Min.

Besprechung der Ergebnisse

Aus den Ergebnissen der Versuche geht hervor, daß Magnesiumammoniumphosphat-hexahydrat nur dann in stöchiometrischer Zusammensetzung ausfällt, wenn die Temperatur der Grundlösung unter 80 °C bleibt. Die Zusammensetzung der bei 100, 90 und 80 °C gefällten Niederschläge Nr. 1, 2 und 3 entsprach in jedem Fall nur dem Monohydrat (Abb. 2). Der Kristallwassergehalt des Niederschlages Nr. 9, gefällt bei Temperaturen zwischen 70 und 80°C (Wasserbad) betrug nur 3,7 Mol. Auf diesen Umstand muß Rücksicht genommen werden, sofern man Magnesium- oder Phosphationen gravimetrisch nach WINKLER [13] durch Wägen des getrockneten Niederschlags bestimmen will.

Der Niederschlag Nr. 4 wurde bei 50 °C, im Vakuum, bei 50 Torr getrocknet; während 200 Stunden sank der Kristallwassergehalt allmählich auf 1,9 Mol und der Ammoniakgehalt auf 0,5 Mol. Ein Jahr lang aufbewahrt änderte sich die Zusammensetzung von Niederschlag Nr. 4 überhaupt nicht, von Nr. 9 kaum, von Nr. 7 hingegen erheblich. Das Trocknen der Niederschläge ist demnach eine sehr heikliche Operation, es läßt sich hierfür nur die gut bewährte Winklersche Methode des Trocknens bei Zimmertemperatur im Luftstrom empfehlen.

Vergleicht man die Kurvenverläufe in Abb. 2—3, so zeigt sich, daß sich die Art der thermischen Zersetzung in Abhängigkeit von der Zusammensetzung der Niederschläge ändert. Verwendet man an Stelle des Tiegels den Mehrteller-Probehalter, bei dem der Partialdruck der gasförmigen Zersetzungsprodukte im Luftraum zwischen den Körnern geringer ist, so treten weitere Unterschiede im Verlauf der thermischen Zersetzung auf. Das weist darauf

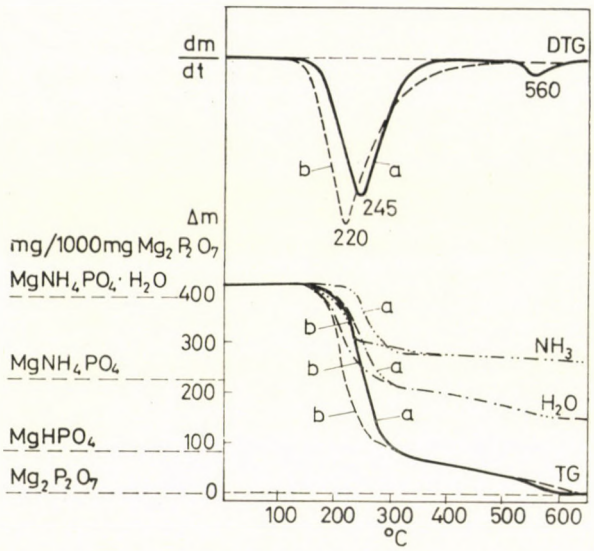

Abb. 2. Thermische Zersetzungskurven der Niederschläge Nr. 1, 2 und 3; *a)* im Tiegel, *b)* im Mehrteller-Probehalter

hin, daß in jenen Phasen der Zersetzung, wo die Zusammensetzungen der einzelnen Niederschläge auf Grund der TG (bzw. NH_3 und H_2O) einander gleich sind, in ihrer Kristallstruktur Differenzen bestehen. Die Zersetzungstemperatur ist nämlich ein empfindliches Kennzeichen der Stärke der zwischen den Atomen und Atomgruppen wirkenden Bindungskräfte.

Im Tiegel verwandeln sich die Niederschläge Nr. 4, 5, 7, 8, 9 und 10 (Kurven *a* in Abb. 3, 4) in der ersten Phase der thermischen Zersetzung, ungefähr bis 180 °C, in das Monohydrat (und zwar Nr. 8, 9 und 10 (Abb. 4) kontinuierlich, die übrigen in einer Stufe). Danach entweicht zwischen 180 und 600 °C, mit maximaler Geschwindigkeit zwischen 230 und 270 °C, gleichzeitig das restliche 1 Mol Kristallwasser, 1/2 Mol Strukturwasser und 1 Mol Ammoniak, ganz ähnlich wie bei den unmittelbar aus der Lösung als Monohydrate ausfallenden Niederschlägen Nr. 1, 2, 3 (Abb. 2). Niederschlag Nr. 6 geht zwischen 70 und 180 °C in das Anhydrid über (Abb. 5).

Im Mehrteller-Probehalter (Kurven *b*) entstehen aus den Niederschlägen Nr. 8, 9 und 10 in der ersten Phase der Zersetzung Monohydrate (Abb. 4), aus Nr. 5, 6 und 7 Anhydride (Abb. 3, 5) obzwar, wie Abb. 2 zeigt, das Monohydrat unter diesen Umständen bis 130 °C gewichtsbeständig war.

Es sei bemerkt, daß bei den Niederschlägen Nr. 6, 8, 9 und 10 mit defizitem Wassergehalt (Abb. 4, 5) im Mehrteller-Probehalter nicht nur das Kristallwasser, sondern auch das Ammoniak in zwei Stufen entweicht, während dies bei den stöchiometrischen Niederschlägen Nr. 1, 2, 3, 4 und 7 nicht der Fall war (Abb. 2, 3).

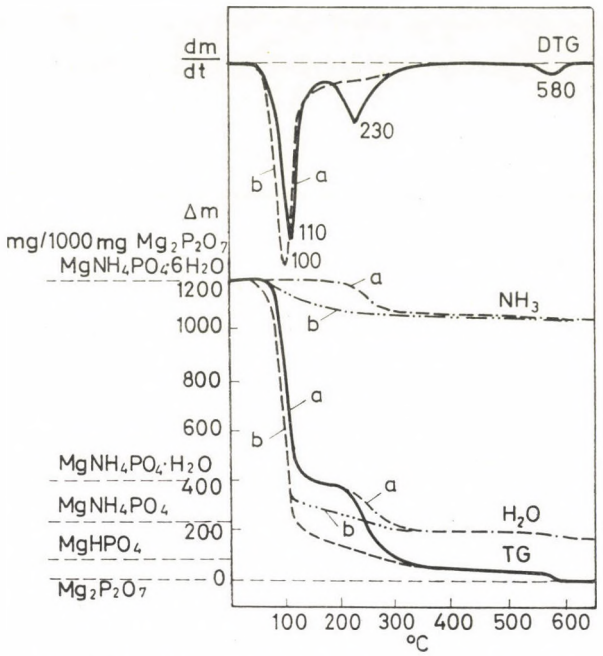

Abb. 3. Thermische Zersetzungskurven der Niederschläge Nr. 4 und 7; *a)* im Tiegel, *b)* im Mehrteller-Probehalter

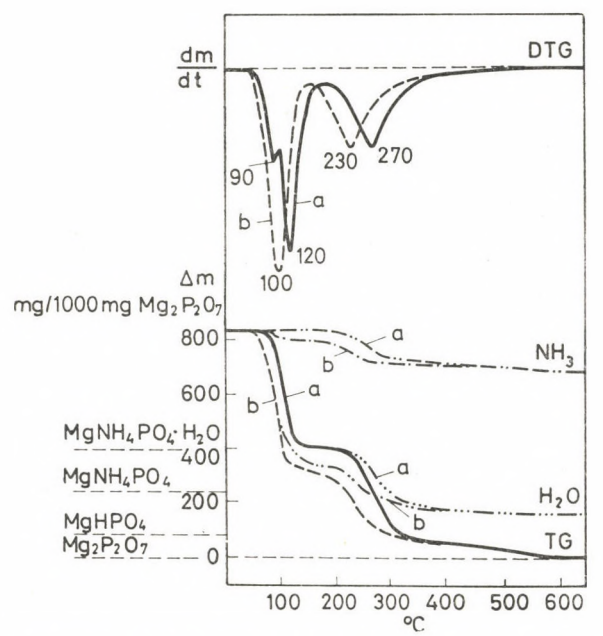

Abb. 4. Thermische Zersetzungskurven der Niederschläge Nr. 8, 9 und 10; *a)* im Tiegel, *b)* im Mehrteller-Probehalter

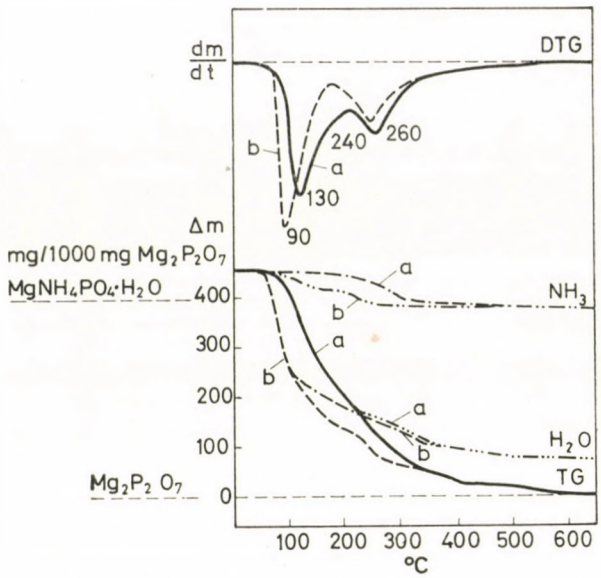

Abb. 5. Thermische Zersetzungskurven des Niederschlags Nr. 6; *a)* im Tiegel, *b)* im Mehrteller-Probehalter

Die Resultate der mit Präcipität Nr. 4 durchgeführten dilatometrischen Versuche sind ebenfalls bemerkenswert. Wahrscheinlich läuft hier in der ersten Phase der thermischen Zersetzung ein mit sich überlappender, zweimaliger Volumenveränderung verbundener Vorgang ab, wodurch die charakteristische Strecke bis 180 °C in der DTD-Kurve in Abb. 6 zustandekommt. Das Volumen der Probe zeigt zuerst eine zunehmende Tendenz, verursacht durch eine geringe Auflockerung der Kristallstruktur in Begleitung der Wasserabgabe. Bei 70 °C zeigt sich jedoch eine deutliche Volumverminderung, die mit der maximalen Geschwindigkeit des Austritts von 5 Molen Kristallwasser zusammenfällt, es scheint also, daß das Entweichen des Wassers aus der Gitterstruktur eine Verminderung der Gitterabstände verursacht. Diese Erscheinung war bei der dilatometrischen Prüfung der Hydrate anderer Verbindungen übrigens ebenfalls zu beobachten [15].

Der Verlauf der NH_3- und H_2O-Kurven beweist, daß die zweite Phase der thermischen Zersetzung aus einem ziemlich einheitlichen Reaktionsmechanismus besteht; die Teilreaktionen des Austritts von Ammoniak und Strukturwasser hängen miteinander organisch zusammen. Sie verlaufen streng parallel und ließen sich weder durch die Herstellungsmethoden (Abb. 2, 3, 4, 5) noch durch die thermischen Versuchsbedingungen (Kurven *a* und *b*) trennen. Die zweite Etappe der thermischen Zersetzung wird bei 220—270 °C in jedem Fall von einem raschen Gewichtsverlust eingeleitet, das Entweichen des restlichen Ammoniaks und Wassers ist jedoch lang hingezogen. Schon andere For-

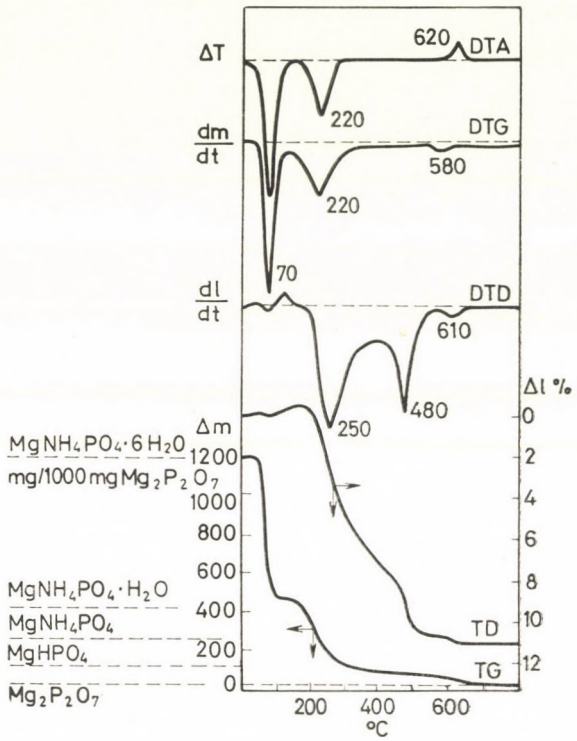

Abb. 6. Thermische Zersetzungskurven des Niederschlags Nr. 6, aufgenommen mit zylindrisch gepreßtem Probekörper

scher haben gezeigt [5], daß die über 230 °C beginnende Pyrophosphatbildung keine einfache Dimerisation ist, denn bei 500 °C kann schon eine beachtliche Menge von Trimeren und Polymeren nachgewiesen werden. Die Ursache des verzögerten Ammoniak- und Wasserverlustes ist also in dem verwickelten Mechanismus der Polymerisation zu suchen. Die erwähnten Forscher haben das Problem auch thermogasanalytisch untersucht.

Die Dilatationsversuche (Abb. 6) haben ergeben, daß diese zweite thermische Zersetzungsetappe ein Zweistufenvorgang ist. Die maximale Geschwindigkeit der eine Sinterung von etwa 7% verursachenden Strukturumwandlung fällt praktisch mit der Höchstgeschwindigkeit des Wasser- und Ammoniak-Austritts zusammen, während die zweite 4%ige Sinterung nur mit geringer Gewichts- und Entalpieänderung verbunden ist.

Das niedrige Maximum auf der DTA Kurve in Abb. 1 und 6 bei 620—650 °C wird durch die beginnende Ausbildung der Kristallstruktur des Magnesiumpyrophosphats aus dem amorphen Polymeren verursacht, durch welche das schnelle und restlose Entweichen der geringen noch anwesenden Menge

von Ammoniak und Wasser hervorgerufen wird. Diese Vorgänge sind auch in den TD- und DTD-Kurven erkennbar.

Das exotherme Maximum bei 250 °C auf der DTA Kurve in Abb. 1 läßt sich mit der partiellen Oxydation des entweichenden Ammoniaks erklären. Bei der Durchführung des Versuchs in Stickstoff erschien keine exotherme Spitze, nur eine endotherme bei 230 °C (gestrichelt). Merkwürdig ist der Umstand, daß die exotherme Spitze auch dann ausblieb, wenn die Probe im Mehrteller-Probehalter untersucht wurde (Kurve *b*, Abb. 1), obzwar hier eine noch intensivere Oxydation zu erwarten wäre. Im Tiegel erfolgt jedoch die Oxydation im Raum zwischen den Körnern, wodurch die Temperatur der Probe erhöht wird, bei der in sehr dünner Schicht ausgebreiteten Probe im Mehrteller-Probehalter hingegen spielt sich die Oxydation bereits außerhalb der Probe ab und so wirkt die freigesetzte Wärme auf die Probe nicht mehr. Umwandlungen, die sich nicht im Raum zwischen den Körnern, d. h. nicht innerhalb der Gasphase sondern in der festen Phase abspielen — wie z. B. Umwandlung der Kristallstruktur des Magnesiumpyrophosphats — konnten jedoch auch im Mehrteller-Probehalter eindeutig nachgewiesen werden.

*

Wir danken Frau M. Csonka und Frau E. Borsay für ihre Mithilfe bei den Versuchen.

LITERATUR

1. Struve, H.: Z. anal. Chemie, **37**, 495 (1898).
2. Sagortschev, B.: Z. physik Chem. (A) **182**, 31 (1938).
3. Duval, C.: Anal. Chim. Acta **4**, 159 (1950).
4. Ripan, R., Eger, J., Mirel, C.: Acad. rep. populare Romine, Filiala Cluj, Studii cercetari chim. **11**, 67—73 (1960).
5. Étienne, J. J., Sallier Dupin, A., Boullé, A.: Compt. rend. **256**, 172 (1963).
6. Berlin, A., Robinson, R. J.: Anal. Chim. Acta **24**, 224 (1961).
7. Erdey, L., Liptay, G., Gál, S., Paulik, F.: Period. Polytechn. Chem. Eng. **5**, 209 (1961).
8. Paulik, F., Paulik, J., Erdey, L.: Z. f. anal. Chem. **160**, 241 (1958).
9. Paulik, F., Paulik, J., Erdey, L.: Talanta (Review) **13**, 1405 (1966).
10. Paulik, J., Paulik, F., Erdey, L.: Anal. Chim. Acta **34**, 419 (1966).
11. Paulik, J., Paulik, F., Erdey, L.: Microchim. Acta 1966, 886.
12. Paulik, F., Paulik, J., Erdey, L.: Microchim. Acta (Wien) 1966, 894.
13. Winkler, L.: Z. angew. Chem. **31**, 211 (1918).
14. Saint Chamant, H., Vigier, R.: Bull. Soc. Chim. 1954, 180.
15. Paulik F., Paulik, J., Erdey, L.: Anal. Chim. Acta **41**, 170 (1968).

Ferenc Paulik
Éva Buzágh-Gere
László Erdey

Budapest XI., Gellért tér 4.

Acta Chimica Academiae Scientiarum Hungaricae, Tomus 61 (1), pp. 39—43 (1969)

ON THE PARAMETER FORM OF FORCE CONSTANT MATRIX, X

ON THE CORIOLIS COUPLING CONSTANTS COMPATIBLE WITH THE NORMAL FREQUENCIES

F. TÖRÖK, P. PULAY and Gy. HUN-BOROSSAY

(Institute of General and Inorganic Chemistry, L. Eötvös University, and Research Group for Inorganic Chemistry of the Hungarian Academy of Sciences, Budapest)

Received July 16, 1968

The Coriolis coupling constants compatible with the measured frequencies can be formed with the help of the parameter representation of force constants. By applying the method, formulas can be given to determine the partial derivatives of the Coriolis φ constants with respect to the parameters.

The energy of interaction between the rotational and vibrational motions of a molecula can be written as [1]:

$$\Omega_x \omega_x + \Omega_y \omega_y + \Omega_z \omega_z,$$

where ω_x, ω_y, ω_z are the components of the vector ω characterizing the angular velocity of the cartesian co-ordination system fixed on the molecule, and

$$\Omega_\alpha = \mathbf{Q}^T \zeta^\alpha \mathbf{Q}, \quad \alpha = x, y, z.$$

There $\mathbf{Q}$ designates the column matrix consisting of normal co-ordinates, and matrix ζ^α contains the so called Coriolis coupling constants whose values depend on the interaction between the rotation and vibration of the molecule.

The properties of matrices ζ^α have been investigated by MEAL and POLO [2]. They have shown that

$$\zeta^\alpha = l M^\alpha l^T,$$

where l is the transformation matrix between the normal and mass-weighted cartesian displacement co-ordinates. M^α designates simple matrices having along their main diagonal as many matrices

$$M^x = \begin{pmatrix} 0 & 0 & 0 \\ 0 & 0 & 1 \\ 0 & -1 & 0 \end{pmatrix}, \quad M^y = \begin{pmatrix} 0 & 0 & -1 \\ 0 & 0 & 0 \\ 1 & 0 & 0 \end{pmatrix}, \quad M^z = \begin{pmatrix} 0 & 1 & 0 \\ -1 & 0 & 0 \\ 0 & 0 & 0 \end{pmatrix}$$

as many atoms are in the molecule.

As the elements of matrix l depend on the force constants, the Coriolis coupling constants, which can be obtained from experimental data, also depend on them. Thus in the possession of the elements of ζ^α conclusions concerning the force field of the molecule can be drawn.

In the following it will be shown that with the help of the parametric method described in our earlier paper [4] the matrices ζ^α compatible with the measured frequencies of a molecule can be easily investigated.

According to MEAL and POLO [2] matrices can be expressed as

$$\zeta^\alpha = L^{-1} C^\alpha (L^{-1})^T,$$

where $C^\alpha = D M^\alpha D^T$. The transformation matrix D connects the S_i symmetry co-ordinates and the mass-weighted cartesian co-ordinates:

$$S = Dq$$

and matrix L^{-1} transforms the symmetry co-ordinates into the normal ones:

$$Q = L^{-1} S.$$

Matrix C^α can be formed in the knowledge of the geometry and atomic masses of the molecule, while matrix L can be obtained by solving the secular equation:

$$GFL = L\Lambda. \tag{1}$$

There G can also be calculated from the equilibrium geometry and atomic masses of the molecule, the elements of matrix F are the force constants, and the elements of the diagonal matrix Λ can be easily derived from the normal frequencies.

According to our previous paper [5] all the matrices L belonging to matrices F which reproduce the measured normal frequencies can be written as

$$L = G^{1/2} U,$$

where U is an arbitrary proper orthogonal matrix (*i.e.* with determinant equal to $+1$) which can be formed as function of $\binom{n}{2}$ parameters. Consequently all the Coriolis coupling constants being in harmony with the measured frequencies can be formed by the equation:

$$\zeta^\alpha = U^T G^{-1/2} C^\alpha G^{-1/2} U. \tag{2}$$

Taking into consideration that the multiplication of two proper orthogonal matrices yields also a proper orthogonal matrix, Eq. (2) means that as much as a

$$\zeta_a^\alpha = (L_a^{-1}) C^\alpha (L_a^{-1})^T$$

matrix was obtained then all the others can be formed by the equation:

$$\zeta^{\alpha} = U^{T} \zeta_a^{\alpha} U \,, \tag{3}$$

where U is again an arbitrary proper orthogonal matrix.

The relations above permit the partial derivatives of the elements of φ^{α} with respect to the parameters to be calculated.

Let us suppose that the partial derivatives of ζ_a^{α} are to be determined. It means that the partial $\delta\zeta_{st}^{\alpha}/\delta\alpha_{ij}$ are to be calculated from Eq. (3) when $U = E$ (E is the unit matrix), *i.e.* when the parameters are of zero value.

Using Eq. (3) the relation

$$\frac{\delta\,\zeta^{\alpha}}{\delta\,\alpha_{ij}} = \frac{\delta\,U^{T}}{\delta\,\alpha_{ij}}\bigg|_0 \zeta_a^{\alpha} + \zeta_a^{\alpha} \frac{\delta\,U}{\delta\,\alpha_{ij}}\bigg|_0$$

can be obtained, and from this equation applying the simple formula for the derivatives of matrices with respect to parameters at zero values [4], the partial derivatives can be expressed as

$$\frac{\delta\,\zeta_{st}^{\alpha}}{\delta\,\alpha_{ij}} = -\frac{\delta\,\zeta_{ts}^{\alpha}}{\delta\,\alpha_{ij}}$$

$$\frac{\delta\,\zeta_{sj}^{\alpha}}{\delta\,\alpha_{ij}} = (\zeta_a^{\alpha})_{is} \quad \text{if } s = 1,2,\ \ldots,\ n \text{ but } s \neq j$$

$$\frac{\delta\,\zeta_{it}^{\alpha}}{\delta\,\alpha_{ij}} = (\zeta_a^{\alpha})_{jt} \quad \text{if } t = 1,2,\ \ldots,\ n \text{ but } t \neq i$$

and

$$\frac{\delta\,\zeta_{st}^{\alpha}}{\delta\,\alpha_{ij}} = 0 \quad \text{if neither } s \text{ nor } t \text{ is equal to } i \text{ or } j.$$

The relations were applied to the molecule ONF. The harmonic frequencies 1876.8 cm^{-1}, 775.5 cm^{-1}, and 522.9 cm^{-1} correspond to the N—O stretching, N—F stretching and $\overset{O}{\diagdown}N\overset{F}{\diagup}$ angle deformation vibrations, respectively [7]. Some ζ sets compatible with the frequencies and the corresponding force constants are shown in Table I. The parameters of zero value give the force constant matrix:

$$F = \begin{pmatrix} 15.356 & 0.110 & 0.180 \\ & 2.818 & 0.345 \\ & & 1.313 \end{pmatrix}.$$

Table I

Some sets of Coriolis coupling constants and force constants compatible with the normal frequencies of ONF

In the blocks the sequences of the parameters and constants are as follows: α_{12}, α_{13}, α_{23} and ζ_{12}, ζ_{13}, ζ_{23} resp.

Parameters	Coriolis coupling constants	Force constants		
0	0.720	15.355	0.111	0.181
0	−0.555		2.818	0.345
0	0.417			1.313
0.1	0.720	15.281	2.275	−0.501
0	−0.461		3.029	0.205
0	0.518			1.381
0	0.624	17.656	2.580	3.050
0.1	−0.555		3.031	0.641
0	0.551			1.714
0	0.596	15.392	0.269	0.193
0	−0.686		3.217	0.571
0.1	0.417			1.213
−0.1	0.720	14.458	−1.943	0.861
0	−0.626		3.354	0.246
0	0.299			1.322
0	0.789	12.224	−1.860	−2.132
−0.1	−0.555		3.379	0.942
0	0.266			1.943
0.1	0.606	15.537	2.617	−0.278
0	−0.592		3.479	0.452
0.1	0.531			1.250

Matrix L_a corresponding to the force constants above gives the following matrix T:

$$T = (L_a^{-1})^T = \begin{pmatrix} 2.69291 & 0.22870 & 1.35403 \\ -0.10309 & 2.35477 & 2.27402 \\ -0.05899 & -0.75210 & 2.62080 \end{pmatrix}.$$

In Table II the partial derivatives of the ζ elements from the first row with respect to the force constants from the first column are shown.

Table II

The partial derivatives of ζ elements with respect to parameters in the case of ONF molecule

	ζ_{12}	ζ_{13}	ζ_{23}
α_{12}	0	0.417	0.555
α_{13}	−.417	0	0.720
α_{23}	−.555	−0.720	0

REFERENCES

1. WILSON, E. B., HOWARD, J. B.: J. Chem. Phys. **4**, 260 (1936).
2. MEAL, J. H., POLO, S. R.: J. Chem. Phys. **24**, 1119, 1126 (1956).
3. WILSON, E. B., DECIUS, J. C., CROSS, P. C.: Molecular Vibrations. McGraw-Hill Book Comp. Inc. 1955.
4. PULAY, P., TÖRÖK, F.: Acta Chim. Acad. Sci. Hung. **44**, 287 (1965).
5. PULAY, P., TÖRÖK, F.: Acta Chim. Acad. Sci. Hung. **47**, 273 (1966).
6. PULAY, P.: Acta Chim. Acad. Sci. Hung. **52**, 49 (1967).
7. JONES, L. H., ASPREY, L. B., RYAN, R. R.: J. Chem. Phys. **47**, 3371 (1967).

Ferenc TÖRÖK
Péter PULAY
Györgyi BOROSSAY-HUN

Budapest VIII., Múzeum krt. 6—8.

Acta Chimica Academiae Scientiarum Hungaricae, Tomus 61 (1), pp. 45—50 (1969)

INVESTIGATION OF THE INTERMEDIATES OF THE NITRATION OF FURFURAL, BY INFRARED SPECTROSCOPY

S. HOLLY,* G. SZABÓ,** G. TÓTH** and G. VARSÁNYI*

*(*Central Research Institute for Chemistry of the Hungarian Academy of Sciences, Budapest, and **Chinoin, Factory of Pharmaceutical and Chemical Products, Budapest)*

Received December 6, 1967; in revised form June 20, 1968

The infrared spectra of nitrotriacetoxy and nitrotripropionoxy derivatives formed during the nitration of furfural in acetic anhydride, and in propionic anhydride, respectively, and the infrared spectrum of 5-nitrofurfurylidene diacetate have been studied. The spectra of the intermediates formed during nitration correspond to those of 5-nitro-5-acetoxy-2,5-dihydrofurfurylidene diacetate and to 5-nitro-5-propionoxy-2,5-dihydrofurfurylidene dipropionate.

The starting material of α-nitrofurane derivatives, 5-nitrofurfurylidene diacetate, widely used and required in medical and veterinary practice, can be prepared by the nitration of furfural with concentrated nitric acid in the presence of acetic anhydride. KUPČÍK *et al.* [1] described a nitrotriacetoxy derivative formed as an intermediate of the nitration. On the basis of polarographic studies they suggested that treatment of furfural with a mixture of concentrated nitric acid and acetic anhydride gives rise to 1,1,5-triacetoxy-5-nitropentene-(3)-2-ol.

A comparison of the infrared spectra of nitrotriacetoxy and nitrotripropionoxy derivatives prepared from furfural, as described in Experimental, and of 5-nitrofurfurylidene diacetate (Fig. 1) showed that the intermediates

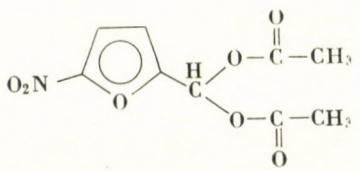

Fig. 1. Structure of 5-nitrofurfurylidene diacetate

formed during nitration were not linear compounds and did not contain hydroxyl group.

The infrared spectrum of 5-nitrofurfurylidene diacetate is shown in Spectrum 1. The characteristic frequencies are listed in Table I.

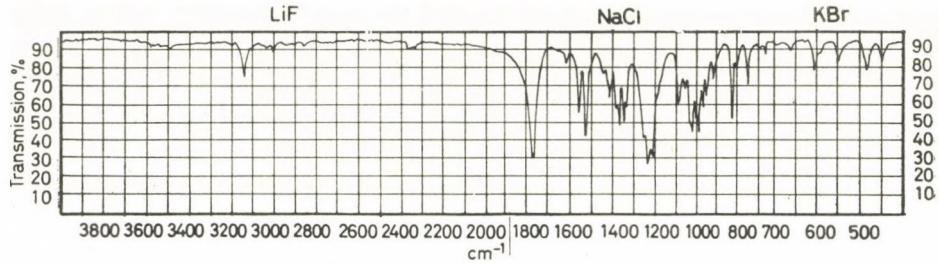

Spectrum 1. Infrared spectrum of 5-nitrofurfurylidene diacetate

Table I

Characteristic frequencies of 5-nitrofurfurylidene diacetate

Position of bands	Assignment	
3138 cm^{-1}	$\nu(=CH)$ (C—H stretching of hydrogen attached to the carbon atom in the five-membered heteroaromatic ring)	
1760 cm^{-1}	$\nu C=O$	
1605 cm^{-1}	Skeletal stretching (ν_{15})	[2]
1545 cm^{-1}	$\nu_{as}NO_2$	
1514 cm^{-1}	Skeletal stretching (ν_6)	[2]
1435 cm^{-1}	$\delta_{as}CH_3$ (Methyl groups of the acetoxy groups)	
1402 cm^{-1}	Skeletal stretching (ν_5)	[2]
1228 cm^{-1} 1210 cm^{-1}	$\nu_{as}O-\overset{\overset{O}{\|}}{C}-C$ (In-phase and out-of-phase vibrations of geminal diacetoxy groups)	

It is remarkable that the $\nu_{as}NO_2$ band of the nitro group is only of medium intensity. The same can be observed in the case of the ν_sNO_2 band. Because of this, the assignment of the latter is uncertain and therefore it is not shown in the Table. The bands at 1360 or 1340 cm^{-1} correspond to the mode ν_sNO_2. The band δ_sCH_3 (methyl group of the acetoxy group) also appears in this region; it may be assumed that the frequency 1373 cm^{-1} corresponds to the symmetric deformation C—H mode of the methyl groups. The band pairs at 1030 and 1017 cm^{-1} can be assigned to the $\nu_{as}C-\overset{\overset{O}{\|}}{C}-O-C$ vibrations.

The characteristic bands appearing in the spectrum of the nitrotriacetoxy derivative (Spectrum 2) are shown in Table II.

Spectrum 2 does not contain a band characteristic of the hydroxyl group; thus in our case the formation of 1,1,5-triacetoxy-5-nitropentene-(3)-2-ol is excluded.

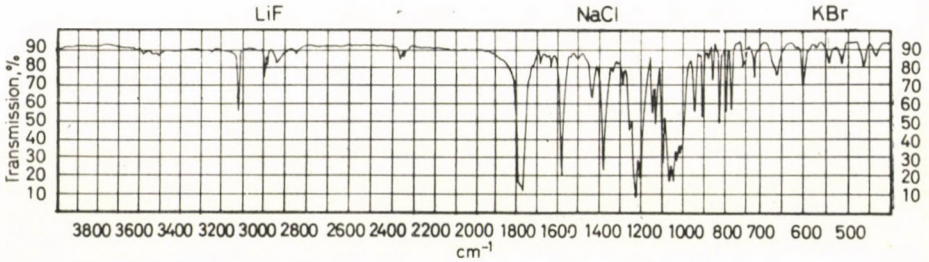

Spectrum 2. Infrared spectrum of 5-nitro-5-acetoxy-2,5-dihydrofurfurylidene diacetate

Table II

Characteristic frequencies of 5-nitro-5-acetoxy-2,5-dihydrofurfurylidene diacetate

Position of bands	Assignment	
3117 cm^{-1}	$\nu(=CH)$	(C—H stretching of olefinic hydrogen of a five-membered hetero ring)
1776 cm^{-1} 1765 cm^{-1}	$\nu C=O$	(C=O stretching of the 5-acetoxy and the geminal acetoxy groups)
1630 cm^{-1}	$\nu C=C$	
1577 cm^{-1}	$\nu_{as}NO_2$	
1435 cm^{-1}	$\delta_{as}CH_3$	(Methyl groups of the acetoxy groups)
1377 cm^{-1}	$\nu_s NO_2 + \delta_s CH_3$	
1222 cm^{-1} 1202 cm^{-1}	$\nu_{as}O-\overset{\overset{O}{\|}}{C}-C$	

The relatively high frequencies of the valence stretching vibrations of the nitro group show that the nitro group is attached to an aliphatic carbon atom bound to an atomic group or atom of strong $-I$ effect, such as the C-5 acetoxy group or the oxygen atom of the ring. At the same time, the $\nu C=O$ frequency of the band appearing at about 1776 cm^{-1} and originating, judging from its intensity, from the third acetoxy group (that is, not from one of the geminal diacetoxy groups) indicates that the ether oxygen atom of the "new" acetoxy group is linked to a carbon atom of strong $-I$ effect, in the present case, the one carrying the nitro group. Finally, it can be assumed that the 1065 and 1040 cm^{-1} bands originate from coupled vibrations between the oxygen atom of the ring and the oxygen atom in either linkage of the acetoxy group connected to C-5.

Taking into account that, according to the NMR spectrum, the nitro-triacetoxy derivative contains two olefinic hydrogen atoms in *cis* position,

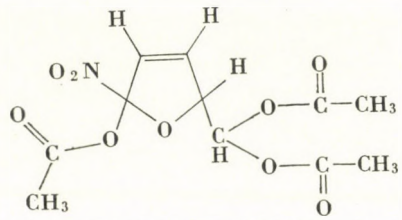

Fig. 2. Structure of 5-nitro-5-acetoxy-2,5-dihydrofurfurylidene diacetate

it can be stated with certainty that the compound formed as an intermediate is 5-nitro-5-acetoxy-2,5-dihydrofurfurylidene diacetate (Fig. 2).

When the spectrum of the nitrotripropionoxy derivative (Spectrum 3) is compared with the spectrum of 5-nitro-5-acetoxy-2,5-dihydrofurfurylidene

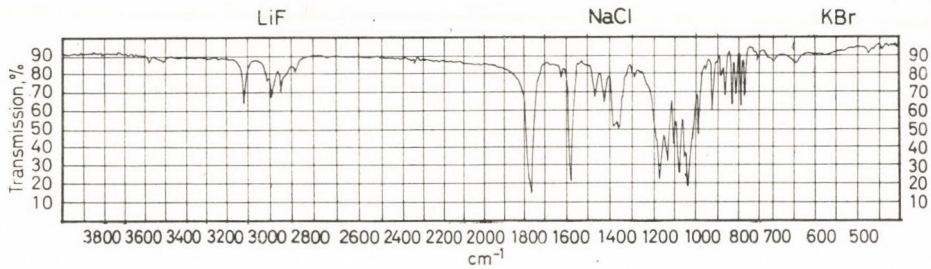

Spectrum 3. Infrared spectrum of 5-nitro-5-propionoxy-2,5-dihydrofurfurylidene dipropionate

diacetate (Spectrum 2), a significant change can be observed in three regions between 1480 and 1410, between 1400 and 1350 furthermore between 1230 and 1100 cm^{-1}.

The spectrum of the nitrotripropionoxy derivative has at 1466 cm^{-1} the $\delta_{as}CH_3$ band of the ethyl group, at 1423 cm^{-1} the $\beta_s CH_2$ band of the methylene group neighbouring the carbonyl group, at 1382 cm^{-1} the $\delta_s CH_3$ band of the ethyl group, at 1360 cm^{-1} the $\nu_s NO_2$ band of the nitro group, and at 1168 and 1135 cm^{-1} the ν_{as}O—C(=O)—C bands of the ester groups. The shift of the latter band pair toward smaller wave numbers, compared with the band pair seen in the spectrum of the triacetoxy derivative, is the consequence of mass increase.

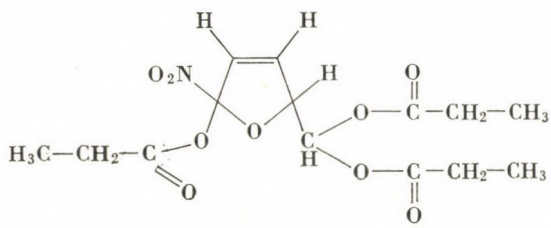

Fig. 3. Structure of 5-nitro-5-propionoxy-2,5-dihydrofurfurylidene dipropionate

Considering the similarities and deviations of Spectra 2 and 3, a structural formula similar to the one shown in Fig. 2 can be given for the nitrotripropionoxy derivative; consequently, in propionic anhydride medium the product is 5-nitro-5-propionoxy-2,5-dihydrofurfurylidene dipropionate (Fig. 3).

Experimental

5-Nitro-5-acetoxy-2,5-dihydrofurfurylidene diacetate

204 g (2 moles) of acetic anhydride was placed in a 1 litre flask equipped with a mechanical stirrer and a thermometer. This was cooled to 0 °C, and 0.5 g of cc. H_2SO_4 was added. The mixture was stirred for 10 min. and then the starting "mixed acid" was prepared by the addition of 5 g (0.08 mole) of 100% nitric acid and 0.5 g of water at 0 °C. This "mixed acid" was stirred and cooled, and 68 g (1.08 mole) of 100% nitric acid and 96 g (1.0 mole) of freshly distilled furfural were added to it simultaneously at 0 °C. The relative rates of adding the two components were adjusted so that the additions were finished about simultaneously. The nitrotriacetoxy derivative began to precipitate after the addition of about one-third of the furfural. After the addition of the total quantity of nitric acid and furfural, the reaction mixture was stirred between —2 °C and +2 °C until a thick crystal mass was obtained. The precipitate was washed with cold methanol and dissolved in hot methanol (2 ml per g), purified with decolourizing carbon and, after filtration, crystallized in an ice bath. After filtration and drying in vacuum at 40 °C the weight of the product was 162 g (53.2%), m. p. 109—111 °C.

The sample was repeatedly recrystallized from methanol.

$C_{11}H_{13}NO_9$ (303.22). Calcd. C 43.57; H 4.29; N 4.62. Found C 43.21; H 4.14; N 4.71%.

5-Nitro-5-propionoxy-2,5-dihydrofurfurylidene dipropionate

330 g (2.5 moles) of propionic anhydride was placed in a 1 litre flask equipped with a mechanical stirrer and a thermometer. This was cooled to 0 °C, 1 g of cc. H_2SO_4 was added, and after stirring for 10 min. at 0 °C, the "mixed acid" was prepared by the addition of 48 g (0.76 mole) of nitric acid. Stirring and cooling were continued, and 54 g (0.85 mole) of 100% nitric acid and 96 g (1 mole) of freshly distilled furfural were added simultaneously at 0 °C and at such a rate that the additions of the two components were finished at the same time. After completing the addition, the reaction mixture was stirred between —2 °C and +2 °C until a thick crystalline mass was obtained. The product was washed with cold methanol and dissolved in hot methanol (2 ml per g), purified with decolourizing carbon, and crystallized in an ice-bath. After filtration and drying in vacuum at 40 °C, the weight of the product was 62 g (18%), m. p. 87—89 °C.

This product was repeatedly recrystallized from methanol.

$C_{14}H_{19}NO_9$ (345.30). Calcd. C 48.70; H 5.55; N 3.62. Found C 48.31; H 5.41; N 3.74%.

Infrared spectra

The infrared spectra were obtained with a Carl Zeiss UR-10 infrared spectrometer, in KBr pellets.

*

The authors' thanks are due to Dr. L. RADICS, for obtaining and evaluation of the NMR spectra, to Miss I. SZABÓ for the infrared spectra, and to Miss E. PÁSZTOR for assistance in the preparative work.

REFERENCES

1. KUPČÍK, F., LIŠKA, M., KONUPČÍK, M.: Československá Farmacie **XI,** 63—66 (1962).
2. KATRITZKY, A. R., AMBLER, A. P.: Physical Methods in Heterocyclic Chemistry, Vol. II. Academic Press, Inc., New York, N. Y., 1963.

Sándor HOLLY; Budapest II., Pusztaszeri út 57—69.
Gábor SZABÓ, Géza TÓTH } Budapest IV., Tó u. 1—5.
György VARSÁNYI; Budapest II., Pusztaszeri út 57—69.

Acta Chimica Academiae Scientiarum Hungaricae, Tomus 61 (1), pp. 51—56 (1969)

MEAN AMPLITUDES OF VIBRATION FOR SMALL MOLECULES CONTAINING SULPHUR, I

THIONYL AND SULPHURYL CHLORID ES

I. HARGITTAI and S. J. CYVIN

(Laboratory for Research of Chemical Structures of the Hungarian Academy of Sciences, Budapest, and Institute of Theoretical Chemistry, Technical University of Norway, Trondheim)

Received August 14, 1968

Revised normal-co-ordinate analysis was performed for $SOCl_2$ and SO_2Cl_2 in order to attain consistence with mean amplitudes from electron diffraction. In particular the previous spectroscopic calculations tended to give somewhat too small values of l for the Cl . . . Cl distances. For $SOCl_2$ the force field of the present work gives perfect agreement with both observed frequencies and mean amplitudes. Also for SO_2Cl_2 a force field was produced which reproduces exactly the observed frequencies and gives mean amplitudes within the error limits of the electron-diffraction values. Another force field which gives a still better agreement for the mean amplitudes was found, whereas the lowest frequency (in SO_2Cl_2) changes from 218 to 175 cm^{-1}. No real conclusion could be drawn to this effect.

Small molecules containing sulphur have been subjected to many spectroscopic investigations, and have attained renewed interest in recent years. The present work concerns the vibrational analysis of $SOCl_2$ and SO_2Cl_2 made in connection with the electron diffraction investigations of HARGITTAI [1] reported in the preceding article.

Thionyl chloride

The mean amplitudes of vibration for $SOCl_2$ quoted in CYVIN's book [2] are taken from VENKATESWARLU *et al.* [3]. They used 114° as equilibrium value of the ClSCl angle. The later calculations of MÜLLER *et al.* [4] are based on structural parameters which include 97.5° for the ClSCl angle; this value has been confirmed by means of electron diffraction [1]. The mean amplitudes of vibration from MÜLLER *et al.* [4] differ largely from the others mentioned above [3]. In this connection it should be pointed out that the approximation method used by MÜLLER *et al.* [4] involving the neglect of all off-diagonal Σ matrix elements in general is very questionable.

The vibrational assignment for $SOCl_2$ employed in the cited spectroscopic works [3, 4] is the same, and the frequencies coincide in magnitude with those quoted by NAKAMOTO [5]. In a later compilation SIEBERT [6] adheres to the same assignment with practically the same (within few wave numbers) frequency values.

Recently the mean amplitudes of vibration were recalculated by CYVIN's group in collaboration with MÜLLER *et al.*, in order to get more reliable results from the rigorous method [2] of normal-co-ordinate analysis. Thesecal culations are based on the fundamental assumption of small harmonic vibrations. Force constants were obtained by the method of FADINI [7]. From these calculations, at 298 °K, the mean amplitudes of vibration for the S—Cl, S=O, Cl . . . Cl and Cl . . . O distances in $SOCl_2$ are: 0.0529, 0.0360, 0.0627 and 0.0968 Å, respectively. The force constants of these calculations all seemed reliable. In particular $f(S=O) = 9.384$ mdyne/Å is in good agreement with the values 9.30 [8], 9.49 [9] and 9.69 mdyne/Å [10], while also $f(S—Cl) = 2.155$ mdyne/Å is quite compatible with 1.80 mdyne/Å [10], although, somewhat higher than 1.4415 [9]. But in the latter work [9] the adopted assignment differs from that of the above cited more recent works [5, 6].

It was extremely interesting to compare the mean amplitudes given in the preceding paragraph with the observed values from electron diffraction [1]. The agreement was satisfactory for the two bonded distances, but significant discrepancies were found for the two nonbonded distances. Consequently we decided to modify the force field in such a way to attain agreement, if possible, for all the mean amplitudes of vibration and at the same time maintain the observed vibrational frequencies. After some trials with systematic changing of bending force constants in the totally symmetric species we really succeeded in producing such a force field. In these calculations the structural data from HARGITTAI [1] were adopted as equilibrium parameters; they are consistent with the parenthesized values in Table I. The final force constants are

Table I

Mean amplitudes of vibration (Å units) for thionyl chloride

$SOCl_2$	(Equil. dist.)	T = 0	298 °K	Electr. diff. [1]
S=O	(1.4425)	0.0359	0.0360	0.031 ± 0.010
S—Cl	(2.0755)	0.0466	0.0524	0.051 ± 0.0025
Cl . . . Cl	(3.0872)	0.0650	0.0959	0.101 ± 0.008
O . . . Cl	(2.8406)	0.0628	0.0774	0.076 ± 0.006

	303	313	323 °K
S=O	0.0360	0.0360	0.0361
S—Cl	0.0526	0.0530	0.0535
Cl . . . Cl	0.0966	0.0979	0.0992
O . . . Cl	0.0778	0.0787	0.0796

Table II

Symmetrized force constants (mdyne/Å) for thionyl chloride

A'	1	2.624	−0.006	0.055	0.149
	2		9.445	−0.002	0.120
	3			0.254	0.005
	4				0.455
A''	1	1.741	0.107		
	2		0.307		

shown in Table II and pertain to the tentatively standardized symmetry coordinates reported elsewhere [11]. This force field reproduces exactly the observed frequencies according to the quotation in SIEBERT's book [6]. The corresponding valence force-constants $f(S=O) = 9.445$ and $f(S-Cl) = 2.182$ mdyne/Å are still compatible with previous results (see above), and the calculated mean amplitudes are in perfect agreement with the electron-diffraction data for all distances. It is referred to Table I, where calculated values at several temperatures are reported.

Sulphuryl chloride

The only calculated mean amplitudes for SO_2Cl_2 available before our calculations were those from VENKATESWARLU *et al.* [12] also quoted by CYVIN [2]. We decided to perform some refined calculations in connection with the electron-diffraction work of HARGITTAI [1].

To start we set up an approximate force field with force constants mainly taken from HUNT *et al.* [13]. These force constants we adjusted to vibrational frequencies from NAKAMOTO [5] and from SIEBERT [6]; significant differences in the assignments for SO_2Cl_2 are found in these two books. The resulting mean amplitudes at 298 °K in Å units are shown below. The columns give: (a) Results of VENKATESWARLU *et al.* [3, 12] (at 300 °K), (b) present results consistent with frequencies from NAKAMOTO [5], and (c) from SIEBERT [6].

Distance	(a)	(b)	(c)
S=O	0.03976	0.0350	0.0349
S—Cl	0.05136	0.0538	0.0474
O . . . O	0.06121	0.0639	0.0637
Cl . . . Cl	0.08480	0.0831	0.0831
O . . . Cl	0.06428	0.0701	0.0689

The majority of these values are consistent with the electron-diffraction results [1] within their error limits. This is especially the case for all values in Set (c). On comparison with Set (b) the only significant difference is found

for the S—Cl distance. The observed value for l(S—Cl) [1] (see also below) clearly points in favour of Set (c). In the following we give the assignment from SIEBERT [6] with frequencies (included in parentheses) from NAKAMOTO [5] in the cases where they are different. The B_1 and B_2 species designation is ambiguous. The present notation is consistent with the conventions of symmetry co-ordinates given elsewhere [14] when the Cl and O atoms are considered as Y and Z, respectively, in the appropriate XY_2Z_2 model of C_{2v} symmetry. All values are wave numbers in cm^{-1}. *Species* A_1 : 1182, 560, 408 (405), 218. *Species* A_2 : 282 (388). *Species* B_1 : 1419 (1414), 388 (282). *Species* B_2 : 580 (380), 362. Throughout the present calculations we have adopted the structural data from HARGITTAI [1] as equilibrium parameters.

The observed value of l(Cl . . . Cl) [1] suggests that the calculated values in all the sets reported above are somewhat too low, although they fall within the relatively large error limits of the electron-diffraction experiment. A similar situation was encountered for thionyl chloride as described in the preceding section. Furthermore MORINO *et al.* [15] have observed a corresponding large value of l(Cl . . . Cl) = 0.102 ± 0.007 Å in SCl_2 [2, 15], while spectroscopic values about 0.093 Å for the same quantity have been reported [2]. In consequence we tried to modify the force field for SO_2Cl_2 in order to increase the calculated value for l(Cl . . . Cl) along the same procedure as was used for $SOCl_2$ (see above). Several attempts of varying the bending force constants within reasonable limits gave no substantial improvement for calculated mean amplitudes when compared to Set (c) reported above. All the mean amplitudes had a strong tendency to remain stable every time we insisted to maintain the observed frequencies. On the other hand, when we tolerated some deviations from the observed frequencies, we had no difficulties in producing a set of calculated mean amplitudes in still better agreement than Set (c) with electron-diffraction values. Below in the column (d) we give the best results of the present calculations. It was obtained with force constants practically the same as those of Set (c) except for $f\alpha$, which was put equal to 0.20 mdyne/Å.

Distance	(d)	Electron diffraction [1]
S=O	0.0349	0.035 ± 0.007
S—Cl	0.0475	0.046 ± 0.004
O . . . O	0.0665	0.061 (assumed)
Cl . . . Cl	0.0986	0.101 ± 0.018
O . . . Cl	0.0689	0.072 ± 0.006

The above column (d) again shows calculated mean amplitudes in Å units at 298 °K. The force constants used in this calculation give calculated frequencies different from those of SIEBERT [6] only in *Species* A_1, where they read: 1181, 557, 408 and 175 cm^{-1}. These considerations may be interpreted as a suggestion that the lowest frequency in SO_2Cl_2 should be somewhat lower

Table III

Mean amplitudes of vibration (Å units) for sulphuryl chloride
For the values at 298 °K, see column (c) in the text

SO_2Cl_2	(Equil. dist.)	T = 0	303	313	323 °K
S=O	(1.407)	0.0348	0.0349	0.0349	0.0350
S—Cl	(2.010)	0.0432	0.0476	0.0480	0.0483
O...O	(2.472)	0.0564	0.0640	0.0645	0.0650
Cl...Cl	(3.086)	0.0596	0.0836	0.0847	0.0858
O...Cl	(2.784)	0.0584	0.0692	0.0699	0.0706

Table IV

Symmetrized force constants (mdyne/Å) for sulphuryl chloride

A_1	1	3.925	0.124	0.122	0.333	A_2	0.313
	2		10.522	—0.048	—0.094		
	3			0.312	—0.014		
	4				1.287		
B_1	1	10.515	0.071	B_2 1	2.158	0.214	
	2		0.495	2		0.577	

than the magnitude (218 cm^{-1}) in the conventional assignments [5, 6]. However, this can hardly be considered as a real conclusion.

As the final spectroscopic values of mean amplitudes for SO_2Cl_2 we take those of Set (c) given above. Corresponding values at various temperatures are found in Table III, and the corresponding force field is given in Table IV. The reported force constants pertain to the symmetry coordinates reported elsewhere [14]. We repeat here that this force field reproduces exactly the vibrational frequencies according to SIEBERT [6], and the calculated mean amplitudes are all consistent with the electron-diffraction results within their error limits. The corresponding valence force-constants for stretchings are f(S=O) = 10.518 and f(S—Cl) = 3.041 mdyne/Å, which both seem to be reasonable.

REFERENCES

1. HARGITTAI, I.: Acta Chim. Acad. Sci. Hung. (in the Press)
2. CYVIN, S. J.: Molecular Vibrations and Mean Square Amplitudes. Universitetsforlaget, Oslo, and Elsevier, Amsterdam, 1968
3. VENKATESWARLU, K., RAJALAKSHMI, K. V.: Proc. Indian Acad. Sci. **A61,** 255 (1965)
4. MÜLLER, A., NAGARAJAN G.: Z. phys. Chem. **235,** 57 (1967)
5. NAKAMOTO, K.: Infrared Spectra of Inorganic and Coordination Compounds. Wiley, New York, 1963

6. SIEBERT, H.: Anwendungen der Schwingungsspektroskopie in der anorganischen Chemie Springer-Verlag, Berlin, 1966
7. FADINI, A.: Z. angew. Math. Mech. **44,** 506 (1964)
8. SIEBERT, H.: Z. anorg. allgem. Chem. **275,** 210 (1954)
9. VENKATESWARLU, K., SUNDARAM, S.: J. Chim. Phys., p. 202 (1957)
10. COTTON, F. A., HORROCKS, W. D. Jr.: Spectrochim. Acta **16,** 358 (1960)
11. CYVIN, S. J., BRUNVOLL, J., CYVIN, B. N., ELVEBREDD, I., HAGEN, G.: Mol. Phys. **14,** 43 (1968)
12. VENKATESWARLU, K., MALATHY DEVI, V.: Indian J. Pure Appl. Phys. **3,** 195 (1965)
13. HUNT, G. R., WILSON, M. K.: Spectrochim. Acta **18,** 959 (1962)
14. CYVIN, S. J., CYVIN, B. N., ELVEBREDD, I., HAGEN, G., BRUNVOLL, J.: To be published
15. MORINO, Y., MURATA, Y., ITO, T., NAKAMURA, J.: J. Phys. Soc. Japan **17,** Suppl. B-II, p. 37 (1962)

István HARGITTAI: Budapest, VIII., Puskin u. 11—13.
Sven J. CYVIN: Institute of Theoretical Chemistry, Technical University of Norway, Trondheim, Norway

Acta Chimica Academiae Scientiarum Hungaricae, Tomus 61 (1), pp. 57—68 (1969)

A NEW FORMULA FOR THE DESCRIPTION OF THE CONFORMATION OF PYRANOID SUGARS

J. SZEJTLI

(Universidad de La Habana, Facultad de Ciencias, Escuela Bioquimica Farmaceutica, Habana, Cuba)

Received January 25, 1968

REEVES' conformational formulas of aldopyranoses can be described by combinations of letters and numbers. This system may be especially useful when many conformational formulas would have to be printed. The C1 conformation of sugars in the D-series is to be visualized with the C_1 atom on the right, below, and the C_4 atom on the left, above in the chair form = $^4C_1$, and the ring members must be numbered clockwise. Applying these conventions, both in the D- and L-series the *axial* substituents attached to the C_1, C_3 and C_5 atoms in the C1 conformation are directed downwards, while those affixed to the C_2 and C_4 atoms point upwards relative to the plane of the ring. The C_5-substituent in pyranoses of C1 conformation is *axial* in the case of L-sugars, and *equatorial* in D-sugars. The axial position is designated in the formula by its location written in parentheses and the substituents other than —H and —OH are indicated behind the parentheses. $^4C_1$ means an aldopyranose ring of C_4 conformation. $^4C_1$(-)5-CH_2OH means β-D-glucopyranose, $^4C_1$(1,2)5-CH_2OH denotes α-D-mannopyranose. If the figure "5" also occurs in parentheses, the symbol represents an L-sugar, *e.g.*, $^4C_1$(1,2,5)5-CH_2OH means β-L-gulose, or $^4C_1$(1,2,5)5-COOH,3-deoxy is 3-deoxy-β-L-guloronic acid in C1 conformation. The 1C conformation is designated as $_1C^4$, B1 as $^4B^1$, B2 as $^5B^2$, etc. The ring members are numbered in the "alternative" conformations (1C, 1B, 2B, 3B) counter-clockwise.

Introduction

The knowledge of the conformation and its illustration is often inevitable in the delineation of various reactions of pyranoid sugars [1]. The demonstration of the real spatial arrangement of the sugar rings and their substituents has been performed so far mainly by REEVES' formulas [2]. These formulas, being drawings, can only circumstantially be written by typewriter and their typographical reproduction requires appropriate drawings and the preparation of costly plates: the printed formulas occupy a lot of place. Therefore, every author has to ponder to reduce the number of conformational formulas in his publication. Especially, in handbooks and textbooks, it would be very desirable to illustrate many of the conformations of the pyranoses discussed. However, this generally cannot be done because of the above-mentioned typographical reasons.

ISBELL and TIPSON [3] have proposed simple formulas for the delineation of the principal conformational forms of pyranoid sugars. Instead of the C1 and 1C symbols, ISBELL [4] proposed in 1956 to write C1 and C2, and in 1957, together with his co-workers [5] he suggested the use of C'1 and C'2 in order

to avoid a possible interchange with the REEVES formulas. In 1958 GUTHRIE [6], and in 1959 ISBELL and TIPSON [7] proposed a new nomenclature for the indication of the conformation. According to this nomenclature, the possible conformational forms of the pyranoside rings are indicated by the following symbols: C_1, B_1, B_2, B_3, $S_{1,3}$, $S_{2,0}$, $S_{2,4}$, $S_{3,5}$, $S_{4,0}$. The symbols C and B refer to the "chair" and "boat" forms, in accordance with REEVES' nomenclature, but they represent simultaneously both mirror-image isomers, *i.e.* in this case C means both C1 and 1C, as well as B means both the B1 and 1B forms. S indicates the skew conformation, which form was not treated in detail by REEVES' nomenclature. The numbers beside "S" refer to the exoplanar atoms.

The two mirror-isomers are distinguished on the basis of the configuration of the anomeric C-atom; if the position of the functional group on this atom is not *quasi*, the symbols C, B or S have to be completed by either "A" *(= axial)* or "E" *(= equatorial)*. In accordance with those said above the most stable conformation of an α-D-glucopyranoside is symbolized by CA, while the least probable conformation by CE (according to REEVES' C1 and 1C, respectively). As it follows, an ISBELL—TIPSON formula consists of three items: the systematic denomination of the sugar, characterization of shape of the sugar ring (C or B), and the position of the functional group on the anomeric carbon atom (A or E). In a more sophisticated form of the system, the above authors indicated the positions of all functional groups by adding "a" or "e" to the above-mentioned symbols; *e.g.*, the C1 conformation of α-D-galactose is delineated by the following formula: α-D-galactose-*(ascae)*. As it is seen, the ISBELL—TIPSON formula does not indicate the actual structure of a sugar; this is assumed to be known and is completed only by information concerning the shape of the sugar ring, as well as the configuration of the anomeric C-atom.

The present paper deals with a more simple method for the representation of the steric structures of pyranoid sugars. These new formulas may be regarded as descriptions of the widely used REEVES formulas by combinations of letters and numbers.

Basic conventions

The way of drawing REEVES' formulas is not uniform. The placing of the C_1 atom within the original REEVES formulas is not the most appropriate; many authors do not accept this form [2], where the C_1 atom is not placed on one or the other "peak" of the "chair". For this reason, the illustration of a glycosidic linkage or any reactions of the C_1 atom may lead to confusion (**Ia**). The formula is easy to survey only when the C_1 atom is placed on one or the other "peak" of the "chair" or "boat". Some authors draw the C1 conformation of REEVES with the C_1 atom on the left side, above (**Ib**), others

draw it on the right side, below (**Ic**). In the following, the location of the C_1 atom in chair formulas for D-sugars in C1 conformation will be fixed on the right side, below. This is basic convention No. 1. Above this to the left the ring oxygen atom, and under this latter the C_2 atom are to be written: *i.e.* the ring members are numbered clockwise. This is basic convention No. 2. The numbering of the so-called "alternative" conformations (1C, 1B, 2B, 3B) runs counter-clockwise, as it follows from their mirror-image character.

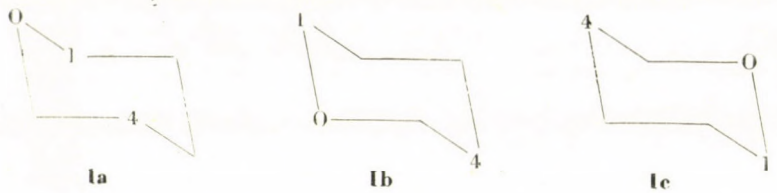

Ia **Ib** **Ic**

Formulas **IIa—IId** show the four possible chair conformations of an α-allose. An inspection of these formulas reveals the following facts. Conversion of the C1 conformation of a D-sugar into 1C conformation causes inversion in the ring skeleton, while all substituents change their position from axial to equatorial and vice versa (see **IIa → IIb**). Moving from the D—1C form (D-sugar in 1C conformation) to L—1C form (L-sugar in 1C conformation), the ring skeleton remains unchanged, while the substituents change their position (see **IIb ⟶ IId**). As a consequence, an L—1C sugar is always related to the D—C1 form of the same sugar, as an image reflected in a mirror. The same is true for an L—C1 and D—1C pair. Starting from D—C1 (see **IIa ⟶ IId**), one can get to L—1C also through L—C1; in this case, in the first step the substituents change their position, and in the second they return to their original position simultaneously with the inversion of the ring skeleton. The net result is only inversion of the ring skeleton.

Observing the mentioned first and second conventions, and applying the above-described train of thought to every pyranoid sugar, the following conclusion may be drawn for the spatial arrangement within the chair conformations:

(a) Considering that the C_4 atom is fixed in the C1 conformation on the left and in 1C conformation on the right side above, the *axial* substituent of the C_1 atom has to be directed downwards on the drawing, *i.e.* C_1. However, this defines the direction of every possible *axial* substituent $C_2 \uparrow C_3 \downarrow C_4 \uparrow C_5 \downarrow$, *i.e.* the 1-, 3- and 5-(unpaired) substituents may be staggered only downwards, the paired ones (2 and 4) only upwards, as related to the ring level. This conclusion is basic convention No. 3, while it is to be noted that in the case of the scarce B-conformations, both *axial* positions on the "peaks" are directed upwards, and all four axial ones on the "base" of the boat conformation are directed downwards.

(b) The C_5-substituent of a D-sugar in C1 conformation may never occupy *axial* position, only *equatorial* one ($C_{5\text{-}eq}$), while the main characteristic of an L-sugar in C1 conformation is the *axial* C_5-substituent ($C_{5\text{-}ax}$). In 1C conformation, these relations are reversed. This is basic convention No. 4. The suggested new delineation of the conformations is based on these four conventions.

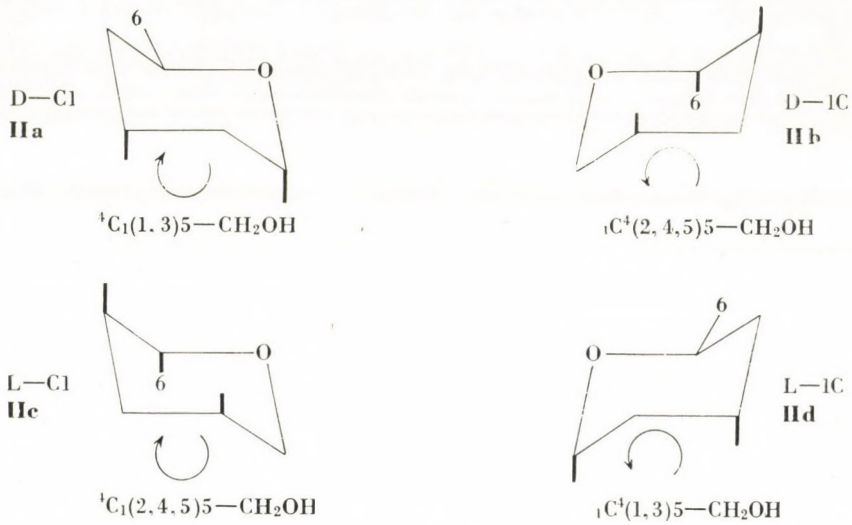

IIa—IId: The four possible chair conformations of α-allose. The arrows indicate the direction of numbering in the rings

Description of the C1 conformation

On the basis of the above conventions, the delineation of the conformations becomes simple. The delineation of the C1 ring is shown by **III**. Letter "C" denotes the "chair" conformation, while "4" on the left above, and "1" on the right below define the locations of the C_1 and C_4 atoms (Convention No. 1). According to Convention No. 2, numbering is done clockwise, therefore, the locations of the C_2, C_3 and C_5 atoms and of the ring oxygen are also fixed. Convention No. 3 defines the direction of the incidentally *axial* substituents. Both in the D- and L-series for both C-conformations (C1 and 1C), these are: $C_1 \downarrow C_2 \uparrow C_3 \downarrow C_4 \uparrow C_5 \downarrow$. Therefore, for an unambiguous definition of any sugar, it is sufficient to write the place number of the substituents in parentheses behind the ring symbol $^4C_1$; the direction of the substituents is fixed by their position in the ring. According to this the symbol $^4C_1(-)$ defines quite unambiguously the REEVES formula **IV**. The pyranoside having no *axial* substituent and no substituent on the C_5 atom (disregarding H and OH), is identical to β-D-xylose. Accordingly, α-D-xylose is designated as $^4C_1(1)$.

D-glucose differs from D-xylose by an $-CH_2OH$ group attached to the C_5 atom. This substituent has to be indicated outside the parentheses: $^4C_1(-)5-CH_2OH$ means β-D-glucopyranose, and $^4C_1(1)5-CH_2OH$ represents α-D-glucopyranose in C1 conformation (**Va** and **Vb**).

According to the fourth convention, the C_5-substituent is always *equatorial* within the D-series therefore, if there is no figure "5" within the parentheses behind the $^4C_1$ symbol, the formula represents a sugar belonging to the D-series, while figure "5" within the parentheses indicates an L-sugar. *E.g.*: $^4C_1(1,2,5)5-CH_2OH$ means β-L-gulose, and $^4C_1(1,2,5)5-COOH$ is β-L-guloronic acid (**VI**).

In case of pentopyranoses, the same statement is valid for the C_4 atom. If there is no figure "5" and attached substituent behind the parentheses the sugar in question is a pentopyranose. If there is a figure "4" in the parentheses, it indicates an L-pentopyranose, if there is not, a D-pentopyranose. *E.g.:* α-L-arabinose: $^4C_1(4)$; α-D-arabinose: $^4C_1(1,2,3)$. The homologous hexopyranoses are as follows: α-L-altrose: $^4C_1(4,5)5-CH_2OH$; α-D-altrose: $^4C_1(1,2,3)5-CH_2OH$.

An exceptional case is presented by C_5-methyl hexopyranoses, such as 6-deoxy-5-C-methyl-D-xylo-hexopyranose (=5,5-di-C-methyl-D-xylopyranose). Its curiosity is indicated by presence of a second bulky C_5-substituent. Such sugars may be classified both into the D-series and into the L-series. The abovementioned D-sugar in α-C1 form may be described by the following conformational formula: $^4C_1(1,5)5$-Me,5-Me; this is, however, identical to 6-deoxy-5-C-methyl-β-L-idose. Thus, C_5-dimethyl sugars represent transition forms between the D- and L-series. Another example for this kind of sugars is noviose: 6-deoxy-5-C-methyl-4-O-methyl-L-lyxo-hexopyranose. Its conformational formulas are as follows: L-1C form: $_1C^4(1,2,5)5$-Me,4-OMe; L-1C form: $^4C_1(3,4,5)5$-Me,4-OMe.

If the C_2 substituent is axial, and the C_1 substituent is not, *i.e.* we are dealing with a β-anomer of a D-sugar in C1 conformation, this results in every case in a $\Delta 2$-effect, therefore special indication of this fact is needless. This is the case. *e.g.*, with β-D-lyxose and β-D-mannose. In the α-anomers of D-sugars in C1 conformation, no $\Delta 2$-effect takes place.

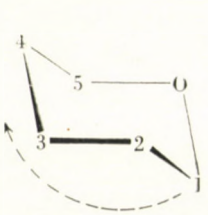

III

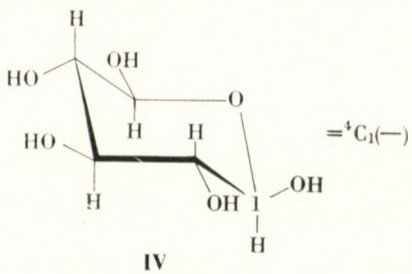

IV

Va

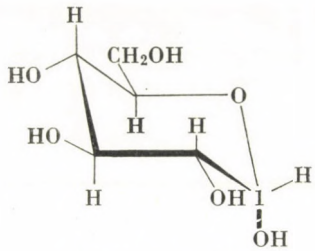

$^4C_1(1)5—CH_2OH$

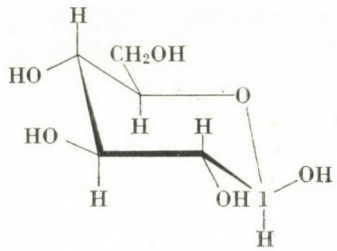

Vb

$^4C_1(-)5—CH_2OH$

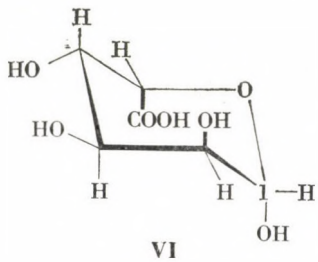

VI

$^4C_1(1,2,5)5—COOH$

In the C1 conformation within the D-series only α-anomers can have an *axial* C_1-substituent, whereas within the L-series the same applies to the β-anomers. Therefore, these new symbols render needless the use of D, L, α and β-letters in the description of the steric structures of pyranoid sugars.

Description of the conformations of disaccharides and glycosides

The new formula is also applicable for disaccharides. *E.g.*, β-D-maltose [$^4C_1(1)5$-CH_2OH,1-O-] [$^4C_1(-)5$-CH_2OH,4-] (**VIIa**). The location of the glycosidic bond in the non-reducing unit is indicated by 1-O-, while in the reducing one by 4-. Since the figure "1" occurs in parentheses in the non-reducing unit, it defines an *axial* position, *i.e.* in this case a linkage of an α-configuration ($C_{1\text{-}ax}$). The α-1,4-linked diglucose is identical to maltose. The β-configuration of the reducing unit is indicated by a sign "-" in parentheses, *i.e.* it means an $C_{1\text{-}eq}$ substituent. *E.g.*, the formula for α-isomaltose (**VIIb**), an α-1,6-linked diglucose, is the following: [$^4C_1(1)5$-CH_2OH,1-O-] [$^4C_1(1)5$-CH_2O-]. 1-O- means in every case an O-glycosidic linkage, similarly 1-N- denotes an N-glycoside and 1-S- means a 1-thioglycoside. Some examples to illustrate this point are as follows:

N-methyl-α-D-glycosaminide: $^4C_1(1)5$-CH_2OH,1-N-CH_3
β-cellobiose: [$^4C_1(-)5$-CH_2OH,1-O-] [$^4C_1(-)5$-CH_2OH,4-]
α,α-trehalose: [$^4C_1(1)$-5-CH_2OH,1-O-] [$^4C_1(1)5$-CH_2OH,1-]

α-D-methylglucopyranoside: $^4C_1(1)5\text{-}CH_2OH,1\text{-}O\text{-}CH_3$
1-deoxy-1-thio-β-D-ethylglucoside: $^4C_1(-)5\text{-}CH_2OH,1\text{-}S\text{-}C_2H_5$
2-deoxy-2-acetylamino-α-D-methylglucopyranoside: $^4C_1(1)5\text{-}CH_2OH,2\text{-}NH\text{-}CO\text{-}CH_3,1\text{-}O\text{-}CH_3$
2-deoxy-β-D-glucose: $^4C_1(-)5\text{-}CH_2OH,2\text{-deoxy}$

Scrutinizing these formulas — which are well suitable for data processing by punched card system — conclusion can be drawn concerning the stability of the sugars, since more *axial* substituents mean lower stability.

Table I contains the REEVES' formulas of aldopyranoses in C1 conformation as well as the suggested new formulas. An example for a 6-deoxy-sugar is 6-deoxy-β-D-idose: $^4C_1(2,3,4)5\text{-}CH_3$.

These formulas are also applicable for ketopyranoses, but in such cases the C_1 atom does not take part in the ring formation, therefore the C_4 and the ring-oxygen will form the "peaks" of the "chair", thus the appropriate symbol for ketopyranoses is $^4C_0(i)2\text{-}CH_2OH$.

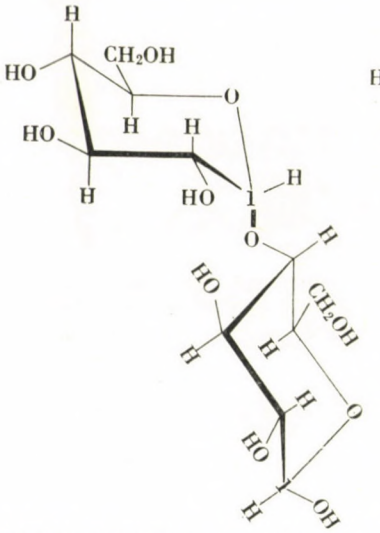

$[^4C_1(1)5—CH_2OH,1—0—][^4C_1(—)5—CH_2OH,4—]$
VII a: Maltose

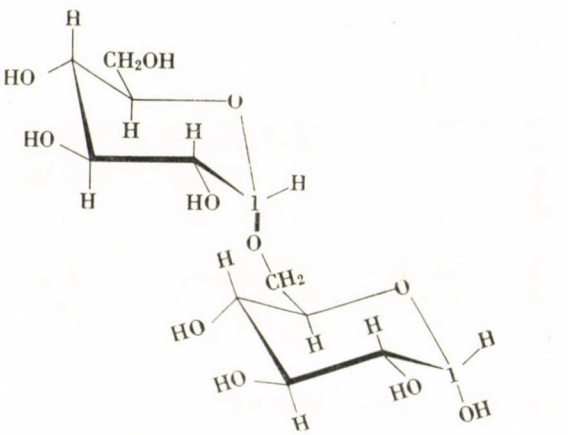

$[^4C_1(1)5—CH_2OH,1—0—][^4C_1(1)5—CH_2O—]$
VII b: Iso-maltose

Description of other conformational forms

The appropriate symbol for the 1C conformation follows simply from the mentioned conventions: $1C^4$. In this case, in the sense of the basic conventions, aldohexopyranoses belonging to the D-series are characterized by $C_{5\text{-}ax}$ and those in the L-series by $C_{5\text{-}eq}$ substituents. The 1C conformation — as it has

Table I

Formulas for delineation of α-D-aldo-pento- and

α-D-sugar	According to			
	Fischer	Haworth	Reeves	Present work
Ribose	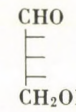	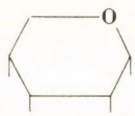	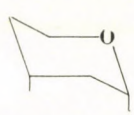	$^4C_1$ (1, 3)
Arabinose	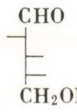		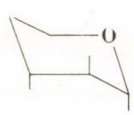	$^4C_1$ (1, 2, 3)
Xylose	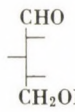	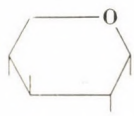		$^4C_1$ (1)
Lyxose	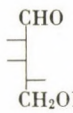			$^4C_1$ (1, 2
Allose		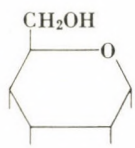	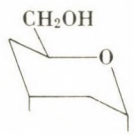	$^4C_1$ (1, 3) 5-CH_2OH
Altrose		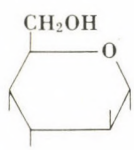	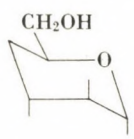	$^4C_1$ (1, 2, 3) 5-CH_2OH

been mentioned — is formed as a result of a "turning out" of the C1 conformation, with the consequence that the original and the new forms of the ring skeleton are related to each other as an object and its mirror-image. Simul-

hexopyranosides in C1 conformation

α-D-sugar	According to			
	Fischer	Haworth	Reeves	Present work
Glucose	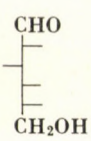	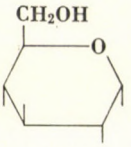	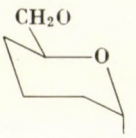	$^4C_1(1)5\text{-}CH_2OH$
Mannose	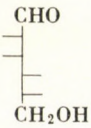	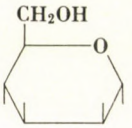	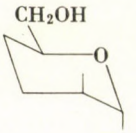	$^4C_1(1, 2)5\text{-}CH_2OH$
Gulose	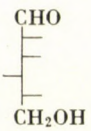	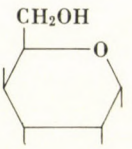	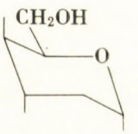	$^4C_1(1, 3, 4)5\text{-}CH_2OH$
Idose	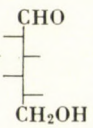	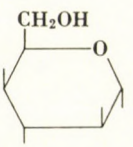	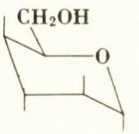	$^4C_1(1, 2, 3, 4)5\text{-}CH_2OH$
Galactose	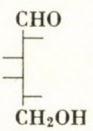	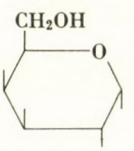	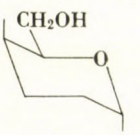	$^4C_1(1, 4)5\text{-}CH_2OH$
Talose	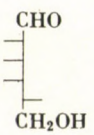	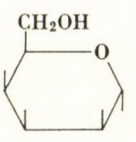	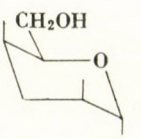	$C_1(1, 2, 4)5\text{-}CH_2OH$

taneously, the *equatorial* substituents are displaced into *axial* position, and *vice versa.*

The 1C conformation plays an important role — among others — in bicyclic derivatives of sugars. *E.g.*, the well known sugar anhydride, levo-

glucosan, can only be imagined in 1C conformation. Its designation is as follows (**VIII**): $_1C^4(1,2,3,4,5) < 1\text{-O-},5\text{-}CH_2\text{->}$. The 1,6-anhydride is designated as $<1\text{-O-},5\text{-}CH_2\text{->}$, while the 3,6-anhydride as $<3\text{-O-},5\text{-}CH_2\text{->}$. According to this, 3,6-anhydro-D-glucopyranose (**IX**) is designated as $_1C^4(1,2,3,4,5) <3,O\text{-},5\text{-}CH_2>$. D-Mannuronic acid 3,6-lactone may exist in 1C conformation (**X**), since it is only in this form that the C_3—OH and C_5—COOH groups are located on the same side of the ring. Its designation is: $_1C^4(1,3,4,5) < 3\text{-O},5\text{-CO-}>$. The 3,6-lactone is designated as $<3\text{-O-},5\text{-CO-}>$.

The B1 conformation is formed from the C1 conformation by turning the C_1 atom to the other side of the plane of the ring (**XI**). A similar displacement of C_1 in the 1C conformation (**XII**), or that of the C_4 atom in the C1 conformation (**XIII**), leads to 1B conformation. In this case, similarly to other "alternative" conformations (1C, 2B, 3B), the ring members are numbered counter-clockwise.

The designation of the B conformations are as follows:

B1: $^4B^1$	1B: $^1B^4$
B2: $^5B^2$	2B: $^2B^5$
B3: $^0B^3$	3B: $^3B^0$

The indication of substituents is similar to the case of C-conformations, taking into consideration that the *axial* positions on both "ends" of the boat are directed upwards, while on the base-forming four atoms, downwards. The B2 and 2B conformations of α-D-glucopyranose are shown by **XIVa** and **XIVb**. The directions of all possible axial positions in α-D-glucopyranoses [2,8], as well as the angles between the neighbouring hydroxyl groups are represented in Table II.

Table II

Steric positions of the substituents in α-D-glucopyranose in various conformations

Conformation	C_1—O—	C_2—OH	C_2—C_3*	C_3—OH	C_3—C_4*	C_4—OH	C_5—CH_2OH
C1	↓	—	— 60°	—	+ 60°	—	—
1C	—	↑	180°	↓	180°	↑	↓
B1	—	↓	—120°	—	+ 60°	—	—
1B	↑	—	—120°	↓	180°	↑	↓
B2	↓	—	— 60°	—	+120°	↓	↑
2B	—	↑	180°	↓	+120°	—	—
B3	↓	↓	180°	↑	180°	↓	—
3B	—	—	— 60°	—	+ 60°	—	↓

* = angle between the —OH groups.

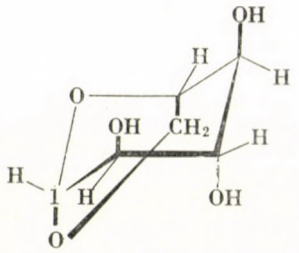

$_1C^4(1,2,3,4,5)\langle 1-0-,5-CH_2-\rangle$

VIII

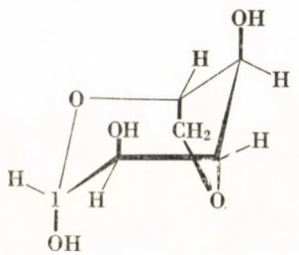

$_1C^4(1,2,3,4,5)\langle 3-0-,5-CH_2-\rangle$

IX

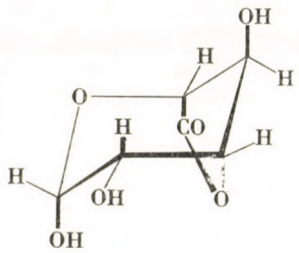

$_1C^4(1,3,4,5)\langle 3-0-,5-CO-\rangle$

X

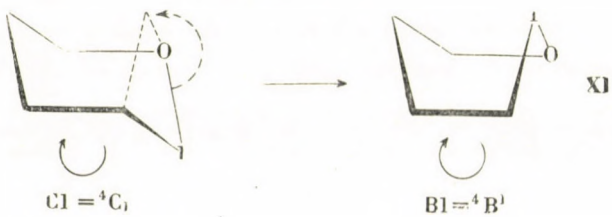

XI

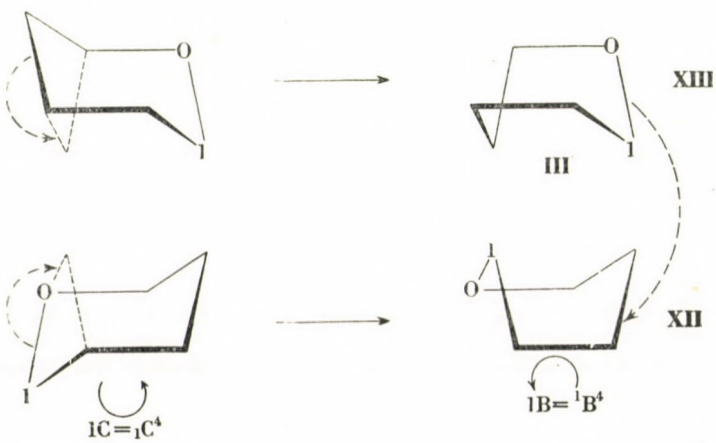

XIII

III

XII

XIVa

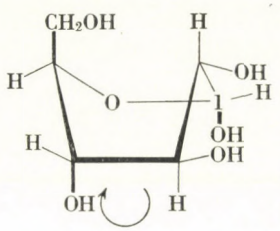

B2 = ${}^{5}B^{2}(1,4,5)5-CH_2OH$

XIVb

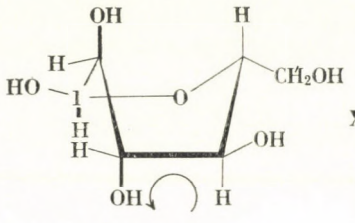

2B = ${}^{2}B^{5}(2,3)5-CH_2OH$

REFERENCES

1. FERRIER, R. J., OVEREND, W. G.: Quart. Revs. **13,** 265 (1959)
2. REEVES, R. E.: Advances in Carbohydrate Chem. 6, 107 (1951); J. Am. Chem. Soc. **73,** 957 (1951)
3. ISBELL, H. S., TIPSON, R. S.: J. Res. Nat. Bur. Standards **64A,** 171 (1960)
4. ISBELL, H. S.: J. Res. Nat. Bur. Standards **57,** 171 (1956)
5. ISBELL, H. S SMITH, F. A., CREITZ, E. C., FRUSH, H. L., MOYER, J. D., STEWARD, J. E.: J. Res. Nat. Bur. Standards **59,** 41 (1957)
6. GUTHRIE, R. D.: Chem. and Ind. **1958,** 1593
7. ISBELL, H. S., TIPSON, R. S.: Science **130,** 793 (1959)
8. GREENWOOD, C. T., ROSSOTTI, H.: J. Polymer Sci. **27,** 481 (1958)

József SZEJTLI; Universidad de La Habana, Facultad de Ciencias, Escuela Bioquimica Farmaceutica, Habana, Cuba

Acta Chimica Academiae Scientiarum Hungaricae, Tomus 61 (1), pp. 69—77 (1969)

BENZAZOLES, VII*

ALKYLATION REACTIONS OF 2-THIO-[1,3]-DIAZOLES

O. H. HANKOVSZKY and K. HIDEG

Institute of Pharmacology, Medical University, Pécs

Received July 18, 1968

2-Thio-[1,3]-diazoles have been reacted with halogenalkylpyridines in alkaline medium to synthesize 2-(thioalkylpyridyl)-[1,3]-diazole derivatives. The reactions of 2-(2'aminoethyl)pyridine with 2-thio-[1,3]-diazoles give 2-(thioethylpyridyl)-[1,3]-diazoles, with ammonia evolution. The mechanism of these reactions is nucleophilic addition involving β-elimination.

N_1-alkylpyridyl derivatives have been prepared from the corresponding nitroaniiines by reduction and ring closure with carbon disulphide in ethanol.

In one of the papers of this series the Mannich reactions of benzimidazole derivatives were reported; it was found that in the Mannich reaction of 2-mercaptobenzimidazole it was the thione tautomeric form which underwent aminomethylation according to an electrophilic substitution mechanism, to give 1,3-bis-(aminomethyl)benzimidazoline-2-thione (Part IV) [1].

In this paper we report that when 2-mercaptobenzimidazole is alkylated with an ω-halogenalkylpyridine in alkaline medium, it is always the 2-thiol form of the benzimidazole which undergoes the reaction, producing an S-alkyl derivative.

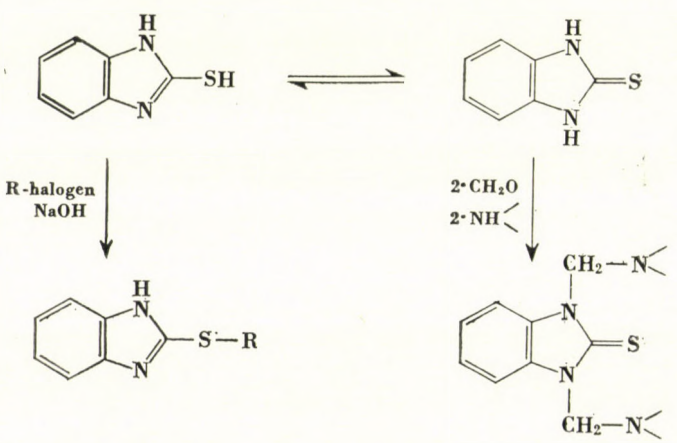

Method A

When a halogenalkylpyridine derivative was used as the reaction partner, 2-(S-alkylpyridyl)benzimidazoles were formed, as shown below.

* Part VI: Acta Chim. Acad. Sci. Hung. 57, 219 (1968)

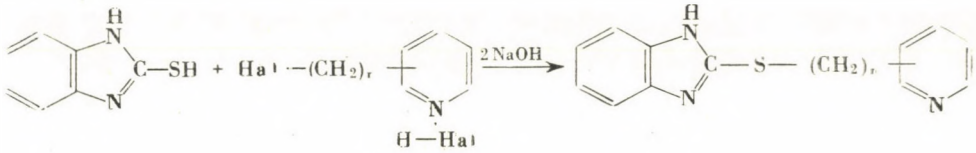

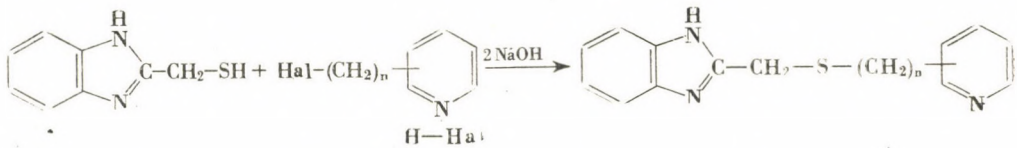

2-Mercaptomethylbenzimidazoles can also be alkylated by this method. This reaction was also applied to other 2-thiol-[1,3]-diazoles.

Method B

2-(2'-aminoethyl)pyridine was found to be able to react with benzimidazole-2-thiol derivatives, accompanied by ammonia evolution, according to the following reaction equation:

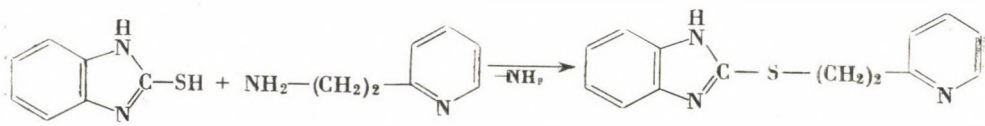

Using 2-(2'-bromoethyl)pyridine as the reaction partner in Method *A*, the products obtained by the two methods had identical physical and chemical constants.

The reactions can be generalized, since the conversions of 2-(2'-aminoethyl)pyridine with [1,3]-diazole-2-thiols give 2-(S-ethylpyridyl)-[1,3]-diazoles, as shown by the following reaction equations:

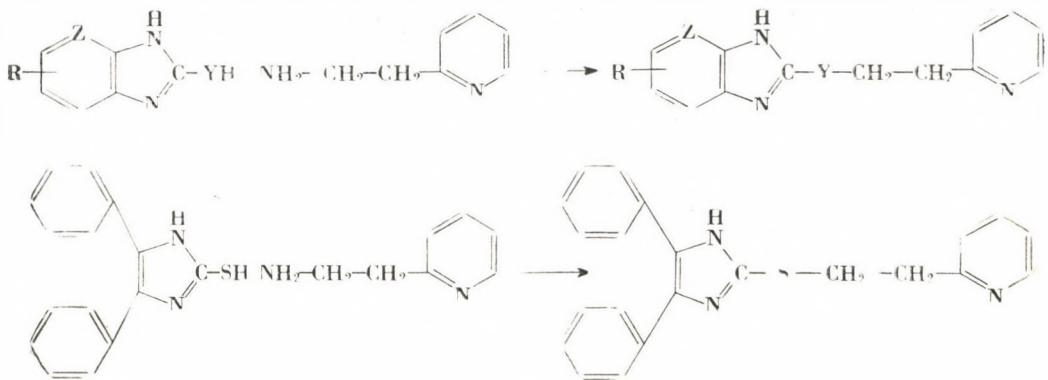

Applying suitable reaction partners, Method *A* and *B* resulted in identical products. The reactions given in the above equations can be generalized to different [1,3]-diazole-2-thiols, it is specific for 2-(2'-aminoethyl)pyridine, as no other amines show these reactions. Therefore, in our opinion, the mechanism of the reaction should be a nucleophilic addition involving β-elimination:

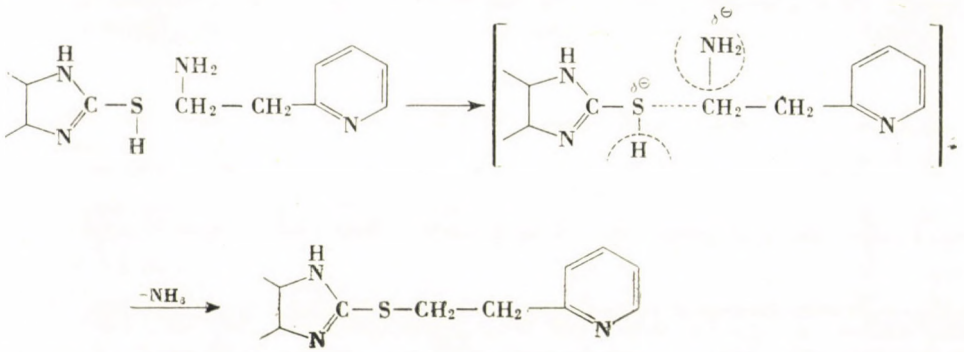

Method C

In order to show that the compounds obtained were other than 1-(alkylpyridyl)benzimidazole-2-thiols or their tautomers, 1-(alkylpyridyl)benzimidazoline-2-thiones, we synthesized 1-(picolyl)benzimidazoline-2-thiones by the following method:

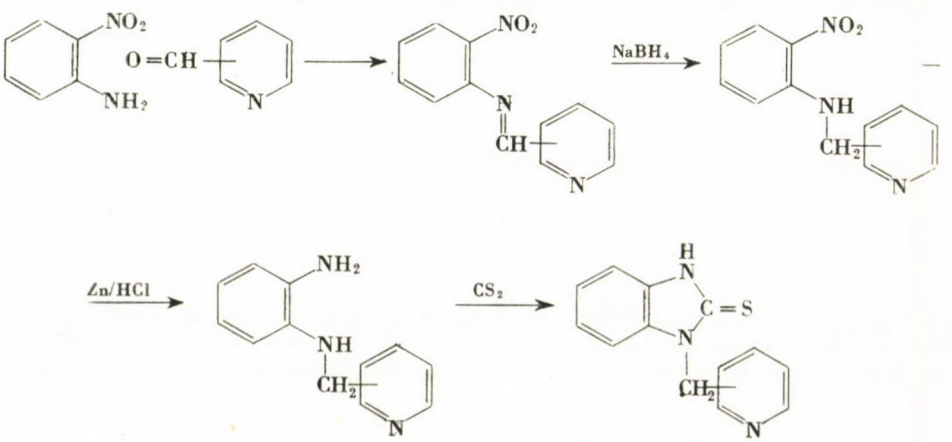

Table I

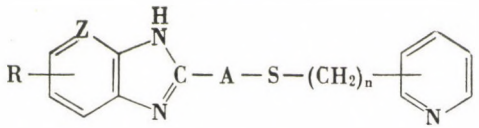

IR. No.	R	Z***	A	n	Position of attachment to pyridine	Method	M.p., °C	Formula (Molecular weight)	Analysis N Calcd	Analysis N Found	Analysis S Calcd	Analysis S Found	Analysis Cl Calcd	Analysis Cl Found	Sadtler No.*
1	H	CH	—	1	2	A	148—150	$C_{13}H_{11}N_3S \cdot 2HCl$ (314.25)	13.37	12.99	10.20	10.42	22.57	22.68	
2	H	CH	—	1	3	A	182—185	$C_{13}H_{11}N_3S \cdot 2HCl$ (314.25)	13.37	13.15	10.20	10.39	22.57	22.70	
3	H	CH	—	1	4	A	128—129	$C_{13}H_{11}N_3S$ (241.32)	17.42	17.36	13.28	13.27	—	—	
							180—183	$C_{13}H_{11}N_3S \cdot 2HCl$ (314.25)	13.37	13.17	10.20	9.98	22.57	22.78	
4	5(6)Cl	CH	—	1	2	A	172—174	$C_{13}H_{10}ClN_3S \cdot 2HCl$ (348.70)	12.05	12.23	9.20	9.42	30.50	30.29	
5	5(6)Cl	CH	—	1	3	A	160—165	$C_{13}H_{10}ClN_3S \cdot 2HCl$ (348.70)	12.05	11.90	9.20	9.00	30.50	30.45	
6	5(6)NO_2	CH	—	1	2	A	204—205	$C_{14}H_{12}N_4O_2S$ (300.34)	18.65	18.79	10.68	10.50	—	—	
							188—189	$C_{14}H_{12}N_4O_2S \cdot 2HCl$ (373.27)	15.01	14.85	8.59	8.44	19.79	19.69	
7	5,6-$(CH_3)_2$	CH	—	1	2	A	120—121	$C_{15}H_{15}N_3S$ (269.37)	15.60	15.42	11.91	11.67	—	—	
							198—200	$C_{15}H_{15}N_3S \cdot 2HCl$ (342.30)	12.28	12.26	9.36	9.73	20.72	20.80	

8	5,6-$(CH_3)_2$	CH	—	1	4	A	82—84 213—214	$C_{15}H_{15}N_3S$ (269.37) $C_{15}H_{15}N_3S \cdot 2HCl$ (342.30)	15.60 15.48 12.28 12.28	11.91 11.69 9.36 9.15	— — 20.72 20.60	
9	H	N	—	1	2	A	175—177 191—194	$C_{12}H_{10}N_4S$ (242.31) $C_{12}H_{10}N_4S \cdot 2HCl$ (315.24)	23.12 22.99 17.77 17.45	13.23 13.00 10.17 9.96	— — 22.50 22.49	34 286
10	H	N	—	1	3	A	200—201 128—129	$C_{12}H_{10}N_4S$ (242.31) $C_{12}H_{10}N_4S \cdot 2HCl$ (315.24)	23.12 22.90 17.77 17.69	13.23 12.98 10.17 9.97	— — 22.50 22.39	
11	H	N	—	1	4	A	162—165	$C_{12}H_{10}N_4S \cdot 3HCl$ (351.69)	15.93 15.98	9.12 9.06	30.25 29.85	
12	H	CH	—	2	2	A, B	75—77 198—201	$C_{14}H_{13}N_3S$ (255.34) $C_{14}H_{13}N_3S \cdot 2HCl$ (328.27)	16.46 16.18 12.80 12.63	12.55 12.75 9.76 9.57	— — 21.60 21.45	
13	5(6)CH_3	CH	—	2	2	A, B	45—47 188—193	$C_{15}H_{15}N_3S$ (269.37) $C_{15}H_{15}N_3S \cdot 2HCl$ (342.30)	15.60 15.54 12.28 12.31	11.91 11.89 9.36 9.58	— — 20.72 20.67	
14	5,6-$(CH_3)_2$	CH	—	2	2	B	67—68 196—198	$C_{16}H_{17}N_3S$ (283.40) $C_{16}H_{17}N_3S \cdot 2HCl$ (356.33)	14.83 14.64 11.80 12.05	11.31 11.49 9.00 9.08	— — 19.90 20.10	

Table I (cont.)

No.	R	Z***	A	n	Position of attachment to pyridine	Method	M.p., °C	Formula (Molecular weight)	Analysis			Sadtler IR No.*
									N	S	Cl	
									Calcd Found			
15	5(6)NO_2	CH	—	2	2	B	128—129 188—189	$C_{14}H_{12}N_4O_2S$ (300.34) $C_{14}H_{12}N_4O_2S \cdot 2HCl$ (373.27)	18.65 18.89 15.01 14.85	10.68 10.50 8.59 8.24	— — 19.00 19.27	
16	H	N	—	2	2	B	182—185	$C_{13}H_{12}N_4S \cdot 3HCl$ (365.73)	15.32 15.45	8.77 8.86	29.09 28.73	34 285
17	H	CH	—	3	3	A	104—106	$C_{15}H_{15}N_3S \cdot 2HCl$ (342.31)	12.28 11.97	9.36 9.33	20.72 20.47	
18	H	CH	CH_2	1	3	A	176—179	$C_{14}H_{13}N_3S \cdot 2HCl$ (328.27)	12.80 12.65	9.76 10.03	21.60 21.48	34 284 **5 674

* Sadtler IR Standard Spectra Catalog No.
** Sadtler NMR Spectra Catalog No.
*** Where Z=N, another isomer is also possible.

Table II

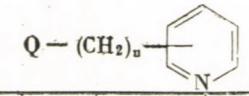

No.	Q	n	Position of attachment to pyridine	Method	Yield, %	B.p., °C/mm or M.p., °C	Formula (Molecular weight)	Analysis		
								N	S	Cl
								Calcd. Found		
19	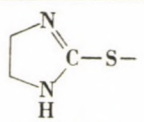	2	2	B	85	240/1.0 178—179	$C_{10}H_{13}N_3S$ (207.30) $C_{10}H_{13}N_3S \cdot HCl$ (243.76)	20.27 20.17 17.24 17.47	15.47 15.68 13.15 13.19	— — 14.54 15.07
20	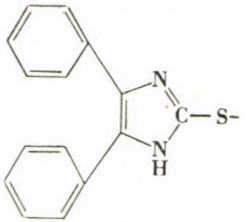	2	2	A(B)	82(87)	218—220 239—240	$C_{22}H_{19}N_3S$ (357.48) $C_{22}H_{19}N_3S \cdot HCl$ (393.94)	11.76 11.67 10.67 10.70	8.97 8.66 8.14 7.95	— — 9.00 9.47
21	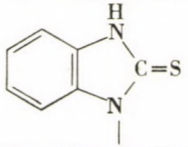	1	2	C	68	177—179	$C_{13}H_{11}N_3S$ (241.32)	17.41 17.71	13.28 13.41	—
22	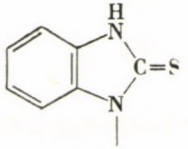	1	3	C	72	249—250	$C_{13}H_{11}N_3S$ (241.32)	17.41 16.93	13.28 12.93	— —

These compounds differed from the corresponding 2-isomers in their physical and chemical constants.

The prepared compounds are shown in Tables I and II; the methods are described in Experimental by way of actual examples that can be generalized.

Experimental

Method A

2-{[2-(4-pyridyl)methyl]-thio}benzimidazole (No. 3)

A solution of 8 g (0.2 mole) of sodium hydroxide in water and 16.4 g (0.1 mole) of 4-chloromethylpyridine hydrochloride were added to a solution of 15.0 g (0.1 mole) of 2-mercaptobenzimidazole in 200 ml of ethanol. The mixture was refluxed for 2 hrs. The NaCl formed (11 g) was filtered off, and the filtrate evaporated to dryness. After clarification of the acetone solution of the residue, it was diluted with water and the base 21.5 g (90%) was filtered off, m.p. 128—129 °C.

Dihydrochloride

The yellow crystals of the dihydrochloride separated when gaseous hydrogen chloride was introduced into an acetone solution of the base, m. p. 180—183 °C.

Method B

2-{[2-(2-pyridyl)ethyl]-thio}benzimidazole (No. 12)

15.0 g (0.1 mole) of 2-mercaptobenzimidazole and 12.2 g (0.1 mole) of 2-(2aminoethyl)pyridine were heated at 150 °C in a metal bath for 3 hrs., under a reflux condenser, until the evolution of ammonia ceased. After cooling, the melt was diluted with ethanol and the solution clarified. The base was obtained on diluting the filtrate with water. It was purified by recrystallization from a mixture of water–ethanol to obtain 20.50 g (80%), m. p. 75—77 °C.

Dihydrochloride

Acidification of an alcoholic solution of the base with a 1:1 mixture of cc. HCl and alcohol gave the dihydrochloride, m. p. 198—201 °C.
Sadtler IR No. 28137 (1966).

Dimethiodide

An acetone solution of the base was refluxed with methyl iodide. After cooling, the dimethiodide separated almost quantitatively as yellow crystals, m. p. 246—248 °C.
$C_{16}H_{19}I_2N_3S$ (539.22). Calcd. N 7.79; S 5.95. Found N 7.81; S 6.22%.
Sadtler IR No. 38128 (1966).

Method C

[1-(3-pyridyl)-methyl]benzimidazoline-2-thione (No. 22)

27.6 g (0.2 mole) of *o*-nitroaniline and 21.4 g (0.2 mole) of pyridine-3-aldehyde were heated in 150 ml of xylene until 3.6 ml of water was collected in the water trap (about 6 hrs). The xylene was distilled off in vacuum, and after dissolving the residue in 150 ml of absolute ethanol, 10 g of $NaBH_4$ was added to the cold solution, then it was refluxed for 1 hr. This time was enough to accomplish the reduction of the azomethine group. After decomposition of the complex with water the ethanol was evaporated; the aqueous residue was extracted with

ether, the solvent evaporated, and 2-nitro-N-(3-pyridyl)methylaniline was isolated as its monohydrochloride by means of a mixture of HCl-ethanol. Yield: 48 g (90%), m. p. 184—187 °C.

$C_{12}H_{11}N_3O_2 \cdot HCl$ (265.70). Calcd. N 15.81. Found 15.35%.

2-nitro-N-(3-pyridyl)methylaniline was reduced by zinc powder in water–hydrochloric acid (1:1), then the reaction mixture was made alkaline, and extracted with ether. The solvent was evaporated and the residual oil refluxed with 500 ml of anhydrous ethanol and 50 ml of carbon disulphide for 5 hrs. (the condenser was equipped with an outlet pipe for the gases). The product separated in yellow crystals. It could be recrystallized from alcohol to give m. p. 249—250 °C. Yield: 34.7 g (72%).

The infrared and NMR spectra were recorded and published by *Standard Spectra*, Philadelphia.

*

The present work was sponsored by the United Pharmaceutical and Dietetic Products, Budapest. Thanks are expressed to Mrs. M. Ott, Miss T. Huszár and Mrs. A. Halász for their technical assistance.

REFERENCE

1. Hideg, K., Hankovszky, O. H.: Acta Chim. Acad. Sci. Hung. **53,** 271 (1967).

Olga H.-Hankovszky
Kálmán Hideg
Pécs, Rákóczi út 2. Hungary

Acta Chimica Academiae Scientiarum Hungaricae, Tomus 61 (1), pp. 79—91 (1969)

FLAVONOIDS, XVI.*

MONO- AND DIGLUCOSIDES OF PHLORACETOPHENONE AND THEIR CONVERSION INTO GLUCOSIDES OF CHALCONE, FLAVANONE AND PHLORIZIN TYPE

R. BOGNÁR, A. L. TŐKÉS and H. FRENZEL

(Institute of Organic Chemistry, L. Kossuth University, Debrecen)

Received April 18, 1968

The glucosylation reaction of phloracetophenone has been re-investigated. It has been found that the coupling of phloracetophenone with α-acetobromoglucose in the presence of silver oxide in quinoline gives 2,4-di-(tetraacetyl-β-D-glucosyl)-phloracetophenone (**I**) as the only isolable product. On carrying out the glucosylation in acetone with a 10% solution of sodium hydroxide, 2,4-di(tetraacetyl-β-D-glucosyl)-phloracetophenone (**I**) is produced as the main product, but 4-(tetraacetyl-β-D-glucosyl)-phloracetophenone (**VII**) can also be isolated, though in a considerably lower yield.

The well-defined mono- and diglucosides of phloracetophenone were used to reproduce the experiments of ZEMPLÉN *et al.* [5, 13, 14]. The chalcone diglucosides prepared from 2,4-di-(tetraacetyl-β-D-glucosyl)-phloracetophenone with 4-hydroxy-, 4-methoxy-, 3,4-dihydroxy- and 3-hydroxy-4-methoxybenzaldehyde, and the dihydrochalcone diglucosides obtained by the hydrogenation of the chalcone diglucosides proved to be completely identical with the compounds described earlier.

4-(Tetraacetyl-β-D-glucosyl)-phloracetophenone has also been condensed with the above-mentioned benzaldehyde derivatives. Hydrogenation and ring closure, respectively, of the chalcone monoglucosides gives the corresponding phloretin derivatives and flavanone glucosides. The melting points and specific rotation values of the monoglucosides prepared are presented in Tables II, III and IV.

The glycosides of phloracetophenone are compounds of fundamental importance in the synthesis of flavonoid glycosides. With substituted aromatic aldehydes they can be condensed to the corresponding chalcone glycosides from which glycosides of phlorizin type of lower oxidation state can be prepared by hydrogenation, or flavanone glycosides of identical state of oxidation may be obtained by ring closure. These latter can be converted by known methods into the flavone and flavonol glycosides, etc. of higher oxidation state.

Syntheses of flavonoid glycosides carried out with phloracetophenone glycosides offer the advantage that the glycosyloxy group is introduced in this way directly into ring A of the flavonoid aglycone molecule and thus a great number of natural glycosides can be synthesized. Phlorizin, a compound of particular physiological effect, producing glucosuria, has been synthesized in 1942 by ZEMPLÉN and BOGNÁR [1].This glucoside, which is very wide-spread in plants [2], was first isolated by DE KONINCK [3] in 1835, but its structure was elucidated only almost a century later [4].

* Part XV: Acta Chim. Acad. Sci. Hung. **58**, 195 (1968); R. BOGNÁR, L. A. TŐKÉS, M. RÁKOSI: Magy. Kém. Folyóirat, 74, 457 (1968)

For the synthesis of phlorizin it was necessary to prepare the corresponding 2-glucosyl-phloracetophenone derivative, and to condense it with 4-hydroxybenzaldehyde. Hydrogenation of the obtained naringenin-chalcone glucoside gave phloretin-2'-glucoside, *i.e.* synthetic phlorizin.

In the course of our experiments to prepare phloracetophenone glucosides, direct glucosylation of phloracetophenone afforded a crystalline product which, on condensation with 4-hydroxybenzaldehyde and subsequent hydrogenation, gave a phloretin glucoside not identical with natural phlorizin but disclosing very similar properties [5]. It was presumed by ZEMPLÉN and BOGNÁR that this latter compound was the 4'-glucoside of phloretin. In order to distinguish it from natural phlorizin, the name *para*-phlorizin was suggested, in contrast to *ortho*-phlorizin proposed to denote natural phlorizin, on the basis of the site of linkage of glucose to the aglycone, phloretin.

The structure of the phloracetophenone glucoside obtained by direct synthesis was suggested by ZEMPLÉN and BOGNÁR on the basis of experimental evidence which showed that highest reactivity in phloracetophenone was exhibited by the hydroxyl group in 4-*(para)* position. Methylation of the phloracetophenone-glucoside tetraacetate by diazomethane failed to give a homogeneous derivative, or a crystalline hydrolytic cleavage product. This was explained by the probable simultaneous formation of 2,6-dimethyl and 2-methyl derivatives. The structure of the phloracetophenone glucoside derivative obtained by direct glucosylation was not checked unequivocally.

In 1959 JORIO [6] reported that partial hydrolysis of dihydronaringin gave phloretin-4'-glucoside, but this product was not identical with the compound synthesized by ZEMPLÉN and BOGNÁR and described as *para*-phlorizin. In 1961 WILLIAMS [7] succeeded in isolating, from the leaves of *Malus trilobata*, the natural *para*-phlorizin and proved its structure by chemical methods. Hydrolysis of the product afforded a 1 : 1 mixture of phloretin and glucose; alkaline degradation yielded florin (phloroglucinol glucoside), while methylation and subsequent hydrolysis gave phloretin-4,2',6'-trimethyl ether. These results unequivocally show that natural *para*-phlorizin is the 4'-glucoside of phloretin. In WILLIAMS' opinion, the compound prepared by JORIO was not identical with natural *para*-phlorizin.

In 1965 PACHECO and GROUILLER [8] reported that the presumed phloracetophenone-4-glucoside, which had been prepared and employed by ZEMPLÉN *et al.* for the preparation of various glucosides of the chalcone, flavanone and phlorizin type, was actually phloracetophenone-2,4-diglucoside. The French authors synthesized, through the corresponding chalcone diglucosides, flavanone diglucosides; partial hydrolysis of the latter with dilute acid gave isosakuranin, prunin and hesperetin-7-glucoside. Later in 1966, eriodictyol-7-glucoside, a compound isolated by WILLIAMS [10] from *Malus communis*,

and by PARIS and ETCHEPARE [11] from *Cratageus pyracantha*, was synthesized by HÖRHAMMER *et al.* [9] in the same way.

In this paper we report a reinvestigation of the glucosylation reaction of phloracetophenone. The structures of the products were proved, and the compounds were used for the synthesis of flavonoid glucosides. In the course of these experiments, earlier work of ZEMPLÉN *et al.* was, in part, also repeated and checked.

It has been found that the coupling of phloracetophenone and α-acetobromoglucose with silver oxide in quinoline affords, in relatively poor yield, only one isolable product: 2,4-di-(tetraacetyl-β-D-glucosyl)-phloracetophenone (**I**). However, if the glucosylation is carried out in the presence of 10% sodium hydroxide solution 2,4-di-(tetraacetyl-β-D-glucosyl)-phloracetophenone is obtained as the main product, in a yield essentially higher than in the former case. Besides, in a much lower yield, 4-(tetraacetyl-β-D-glucosyl)-phloracetophenone (**VII**) can also be isolated from the reaction mixture. The course of the coupling reaction was followed by chromatography (Kieselgel-G layer; solvent system benzene and methanol (93 : 7). It has been found that the mono- and the diglucoside acetates are formed simultaneously, in parallel reactions. In order to prove the structure and to identify the mono- and diglucoside acetates, analytical measurements (determination of the molecular weights, elemental analysis, determination of acetyl groups and glucose), and the following chemical conversions were carried out.

Saponification gave the free glucosides, 4-β-D-glucosylphloracetophenone(**VIII**) and 2,4-di-(β-D-glucosyl)-phloracetophenone (**II**), respectively.

Acetylation with acetic anhydride in pyridine of the diglucoside acetate (**I**) and the monoglucoside acetate (**VII**) and of the corresponding saponified acetyl-free glucosides (**II** and **VIII**) yielded 2,4-di-(tetraacetyl-β-D-glucosyl)-6-acetylphloracetophenone (**III**) and 4-(tetraacetyl-β-D-glucosyl)-2,6-diacetylphloracetophenone (**IX**), respectively.

The coupled products were methylated to obtain 2,4-di-(tetraacetyl-β-D-glucosyl)-6-methylphloracetophenone (**IV**) and, according to KUHN [12], 4-(tetraacetyl-β-D-glucosyl)-2,6-dimethylphloracetophenone (**X**), respectively. Acid hydrolysis of these compounds afforded 6-methylphloracetophenone (**V**) and 2,6-dimethylphloracetophenone (**XI**), respectively.

2,4-Di-(tetraacetyl-β-D-glucosyl)-phloracetophenone gave a crystalline oxime (**VI**) with hydroxylamine (Table I).

The condensation experiments conducted earlier by ZEMPLÉN *et al.* were then repeated with the well defined mono- and diglucoside derivatives of proved structure, using 4-hydroxy-, 4-methoxy-, 3,4-dihydroxy- and 3-hydroxy-4-methoxybenzaldehyde. The chalcone and dihydrochalcone diglucosides, respectively, obtained with the above-mentioned aldehydes and 2,4-di-(tetraacetyl-β-D-glucosyl)-phloracetophenone (**I**) were completely iden-

Table I

Phloracetophenone glucosides and compounds prepared by their conversion

I	R^1	= R^2	= $Gl(Ac)_4$;	R^3	=	H
II	R^1	= R^2	= Gl ;	R^3	=	H
III	R^1	= R^2	= $Gl(Ac)_4$;	R^3	=	Ac
IV	R^1	= R^2	= $Gl(Ac)_4$;	R^3	=	CH_3
V	R^1	= R^2	= H ;	R^3	=	CH_3
VI	R^1	= R^2	= $Gl(Ac)_4$;	R^3	=	H; C=O=C=N−OH
VII	R^1	= $Gl(Ac)_4$	;	R^2	=	R^3 = H
VIII	R^1	= Gl	;	R^2	=	R^3 = H
IX	R^1	= $Gl(Ac)_4$	;	R^2	=	R^3 = Ac
X	R^1	= $Gl(Ac)_4$	;	R^2	=	R^3 = CH_3
XI	R^1	= H	;	R^2	=	R^3 = CH_3

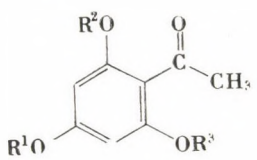

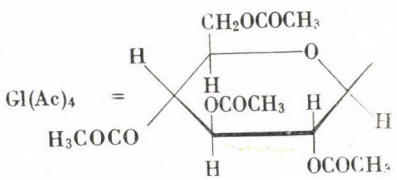

tical with the compounds synthesized by ZEMPLÉN *et al.* [5, 13, 14, 15]. Consequently, the statements of ZEMPLÉN *et al.* are to be corrected, because the product synthesized by them and presumed to be *para*-phlorizin is 2',4'-di-(β-D-glucosyl)-phloretin (**XIX**); the presumed 4-methyl-*para*-phlorizin is 2',4'-di-(β-D-glucosyl)-4-methylphloretin (**XX**); the presumed 3-hydroxy-*para*-phlorizin is 2',4'-di-(β-D-glucosyl)-3-hydroxyphloretin (**XXI**); and, finally the presumed 3-hydroxy-4-methyl-*para*-phlorizin is 2',4'-di-(β-D-glucosyl)-3-hydroxy-4-methylphloretin (**XXII**). Similarly, corrections are required in the case of the products prepared by PETRUCZ [16], since the compounds described as citronetin-chalcone-4'-β-D-glucoside and the corresponding flavanone, reported as citronetin-7-β-D-glucoside, are actually 2',4'-di-(β-D-glucosyl)-citronetin-chalcone and 5,7-di-(β-D-glucosyl)-citronetin. Further, the eriodictyol-7-β-D-glucosyde prepared by GARUSOVA *et al.* [17] is actually 5,7-di-(β-D-glucosyl)-eriodictyol (**XXVIII**), which fact has been already partly pointed out by PACHECO [8], and by HÖRHAMMER and FARKAS [9].

4-(Tetraacetyl-β-D-glucosyl) phloracetophenone (**VII**) was also condensed by us with 4-hydroxy-, 4-methoxy and 3-hydroxy-4-methoxy-benzaldehyde, preparing in this way 4'-β-D-glucosyl-naringeninchalcone (**XVI**), 4'-β-D-glucosyl-isosakuranetinchalcone (**XVII**) and 4'-β-D-glucosyl-hesperetin-

chalcone (**XVIII**). These chalcones were hydrogenated to *para*-phlorizin (**XXIII**), 4-methyl-*para*-phlorizin (**XXIV**) and 3-hydroxy-4-methyl-*para*-phlorizin (**XXV**), while ring closure in a buffer solution of disodium hydrogen phosphate and citric acid (pH 7) afforded 7-β-D-glucosyl-naringenin (**XXX**), 7-β-D-glucosyl-isosakuranetin (**XXXI**) and 7-β-D-glucosyl-hesperetin (**XXXII**), respectively.

Our attempts to condense 4-(tetraacetyl-β-D-glucosyl)-phloracetophenone (**VII**) with 3,4-dihydroxybenzaldehyde, in order to synthesize 3-hydroxy-*para*-phlorizin, failed. This compound has been synthesized by FARKAS *et al.* [18] by the partial hydrolysis of 2',4'-di-(β-D-glucosyl)3-hydroxyphloretin. The total synthesis of para-phlorizin has also been achieved starting with 2-benzoyl-4-(tetraacetyl-β-D-glucosyl)-phloracetophenone, through the known steps, while prunin has been prepared by the ring closure of the corresponding chalcone glucoside.

The course of the synthesis of the compounds prepared in the present experiments is as follows:

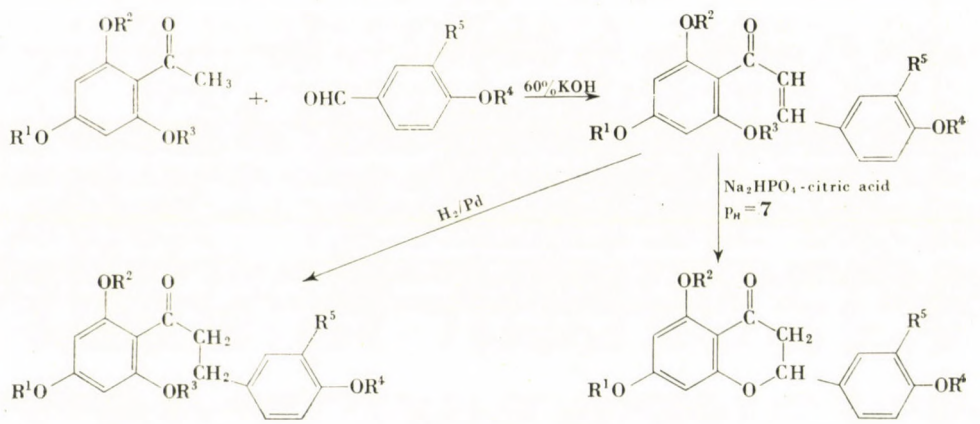

The melting points and values of specific rotation of the derivatives prepared in this work are listed in Tables II, III and IV.

*

The authors' thanks are due to Dr. É. RÁKOSI-DÁVID and to the staff of the micro-analytical laboratory for the analyses, and to Mr. P. KISS for his valuable help. The authors are grateful to the Hungarian Academy of Sciences for sponsoring the present investigations.

Experimental

All melting points are uncorrected.

2,4-Di-(tetraacetyl-β-D-glucosyl)-phloracetophenone (I)

(a) Coupling in acetone in the presence of 10% NaOH solution, according to ZEMPLÉN *and* BOGNÁR [5].

A crude product (5.52 g) of the reaction was repeatedly recrystallized to obtain 3.31 g (6%) of pure 2,4-di-(tetraacetyl-β-D-glucosyl)-phloracetophenone, m. p. 217—218 °C (lit. [5] m. p. 215—216 °C and [8] 220 °C $[\alpha]_D$ —48 (in anhydrous pyridine, $c = 1$). (Lit. [5] $[\alpha_D]$ —52.7, in pyridine, $c = 0.07$, and [8] —51.3 in pyridine, $c = 0.01$).

$C_{36}H_{44}O_{22}$ (828.71). Calcd. C 52.17; H 5.35; Ac 41.54. Found C 52.51; Ac 43.77%. Mol. wt. (Rast method):

Determination of glucose: 0.1 g of the pure product was saponified with 0.1 *M* sodium methoxide, and after hydrolysis with 10% HCl, sugar was determined according to BERTRAND. Calcd. 43 mg. Found 40.9 mg glucose (95.1% of the theoretical amount).

4-(Tetraacetyl-β-D-glucosyl)-phloracetophenone was separated from the methanolic mother liquor of 2,4-di(tetraacetyl-β-D-glucosyl)-phloracetophenone.

(b) Coupling in quinoline with silver oxide, according to ZEMPLÉN, BOGNÁR *and* SZEGŐ [14]

1.55 g of the crude product was recrystallized from a mixture of acetone and methanol; 0.75 g (4.2%) of a silky crystalline substance separated, m. p. 217—218 °C (lit. [14] m. p. 215 °C); $[\alpha]_D$ — 48° (anhydrous pyridine, $c = 1$) (lit. [14] $[\alpha]_D$ —37.1°, in pyridine).

$C_{36}H_{44}O_{22}$ (828.71). Calcd. C 52.17; H 5.35; Ac 41.5. Found C 52.65; H 5.55; Ac 42.89%. Mol. wt. (Rast method): 879. Determination of glucose as described under *(a)*. Calcd. 43 mg. Found 40.9 mg (95.1%).

4-(Tetraacetyl-β-D-glucosyl)-phloracetophenone (VII)

The methanolic mother liquor of 2,4-di-(tetraacetyl-β-D-glucosyl)-phloracetophenone obtained by method *(a)* was allowed to stand for a few days. The separated 4-(tetraacetyl-β-D-glucosyl)-phloracetophenone was recrystallized from methanol to yield 1g (2.6%, calculated for phloracetophenone) of **VII**, m. p. 176—177 °C.

After drying in vacuum, 1.5 mole water of crystallization was found. $[\alpha]_D$ — 42° (in anhydrous pyridine, $c = 1$).

$C_{22}H_{26}O_{13}$ (498.43). Calcd. C 53.01; H 5.25; Ac 34.54. Found C 53.58; H 5.32; Ac 33.05%. Mol. wt. (Rast method): 467. Glucose was determined as described under *(a)*. Calcd. 32 mg. Found 31.1. mg (97.3%).

2,4-Di-β-D-glucosyl-phloracetophenone (II)

1.7 g of 2,4-di-(tetraacetyl-β-D-glucosyl)-phloracetophenone was saponified in a mixture of 10 ml of anhydrous methanol and 6 ml of 0.1 *M* sodium methoxide. A white powder (0.51 g) was obtained which could not be crystallized, m. p. 93—95 °C; $[\alpha]_D$ —65° (in anhydrous pyridine $\varepsilon = 1$). (Lit. m. p. 95 °C; $[\alpha]_D$ —93°, in ethanol [8]).

2,4-Di-(tetraacetyl-β-D-glucosyl)-6-acetyl-phloracetophenone (III)

(a) From 2,4-di-(tetraacetyl-β-D-glucosyl)-phloracetophenone

5 ml of acetic anhydride was added in small portions to a suspension of 0.5 g of 2,4-di-(tetraacetyl-β-D-glucosyl)-phloracetophenone in 25 ml of anhydrous pyridine. The mixture was allowed to stand for 24 hrs. and poured onto ice. The amorphous white crude product was recrystallized from ethanol to give white needles, 0.41 g (78.8%); m.p. 182—183 °C (lit. [16] m. p. 180 °C); $[\alpha]_D$ —43.2° (in anhydrous pyridine, $c = 1$) (lit. [16] $[\alpha]_D$ —38.3°, in pyridine).

Mol. wt. 830 (in ethanol, by ebullioscopy) (calculated for $C_{38}H_{46}O_{23}$; 870.75).

Table II

Melting points and specific rotation values of chalcone glucosides prepared by the condensation reaction of **2,4** *di-(β-D-glucosyl)-phloracetophenone and* **4**-*β-D-glucosyl-phloracetophenone with aromatic aldehydes*

	R^1	R^2	R^3	R^4	R^5	M. p., °C	Lit. m.p., °C		$[\alpha]_D$	Lit. $[\alpha]_D$	
XII	Gl	Gl	H	H	H	190—191	191 191	[5] [8]	—30° (pyridine)	—40.4° (pyridine)	[5]
XIII	Gl	Gl	H	CH_3	H	175	173—175 190/174	[13] [8]	—68° (pyridine)	—32.8° (pyridine)	[13]
XIV	Gl	Gl	H	H	OH	193—194	193—194 194—196	[14] [17]	—34.7° (pyridine)	—34.3° (pyridine) —39° ($CHCl_3$)	[14] [17]
XV	Gl	Gl	H	CH_3	OH	200—205	200—204 205—210	[15] [8]	—42.1° (pyridine)	—32.6° (pyridine)	[15]
XVI	Gl	H	H	H	H	195—198	indefinite	[18]	—71° (ethanol)	—42° (ethanol)	[18]
XVII	Gl	H	H	CH_3	H	187			—44.5° (ethanol)		
XVIII	Gl	H	H	CH_3	OH	175—179			—19° (pyridine)		

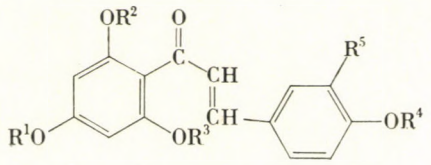

Table III

Melting points and specific rotation values of dihydrochalcone di- and monoglucosides prepared by the catalytic hydrogenation of chalcone di- and monoglucosides

	R^1	R^2	R^3	R	R^5	M. p., °C	Lit. m. p., °C		$[\alpha]_D$	Lit. $[\alpha]_D$	
XIX	Gl	Gl	H	H	H	166—167	170—173	[5]	—63.3° (pyridine)	—67.6° (pyridine)	[5]
XX	Gl	Gl	H	CH_3	H	170—175	143—144	[13]	—55° (pyridine)	—54.1° (pyridine)	[13]
XXI	Gl	Gl	H	H	OH	221	221	[14]	—47° (pyridine)	—47.5° (pyridine)	[14]
XXII	Gl	Gl	H	CH_3	OH	155—160	155—157	[15]	—53.8° (pyridine)	—59.7° (pyridine)	[15]
XXIII	Gl	H	H	H	H	164—166	164—166	[18]	—68° (ethanol)	—67° (ethanol)	[18]
							166	[7]		—70° (ethanol)	[7]
XXIV	Gl	H	H	CH_3	H	175—180			—36.5° (ethanol)		
XXV	Gl	H	H	CH_3	OH	178—180			—44° (pyridine)		

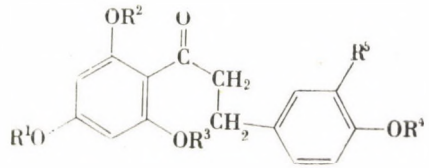

Table IV

Melting points and specific rotation values of flavanone di- and monoglucosides prepared by ring closure of chalcone di- and monoglucosides

	R^1	R^2	R^3	R^4	M. p., °C	Lit. m. p., °C		$[\alpha]_D$	Lit. $[\alpha]_D$	
XXVI	Gl	Gl	H	H	205—208	221	[8]	—61° (pyridine)	—74.9° (pyridine)	[8]
XXVII	Gl	Gl	CH_3	H	260	214	[13]	—72° (pyridine)	—73.4° (pyridine)	[13]
						265	[8]		—73.5° (pyridine)	[8]
XXVIII	Gl	Gl	H	OH	196—197	196—197	[17]	—66.6° (DMF)	—64.6° (DMF)	[17]
XXIX	Gl	Gl	CH_3	OH	249—250	250	[17]	—72.9° (pyridine)	—70.4° (pyridine)	[17]
						276	[8]		—71.2° (pyridine)	[8]
XXX	Gl	H	H	H	222—224	221—225	[18]	—40° (acetone)	—40° (acetone)	[18]
						222	[8]		—40.5° (acetone)	[8]
XXXI	Gl	H	CH_3	H	178—180	184—186	[8]	—50° (pyridine)	—55.3° (pyridine)	[8]
XXXII	Gl	H	CH_3	OH	180—185	189/180	[8]	—39.6° (pyridine)	—47.6° (pyridine)	[8]

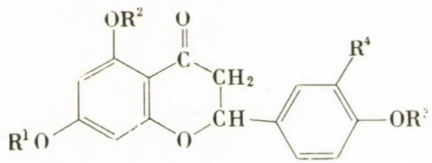

(b) From 2,4-di-β-D-glucosyl-phloracetophenone

0.2 g of 2,4-di-(β-D-glucosyl)-phloracetophenone in 10 ml of anhydrous pyridine was acetylated with 10 ml of acetic anhydride to yield 0.25 g (71.4%) of a white crystalline product, m. p. 182—183 °C (lit. [16] m. p. 180 °C); $[\alpha]_D$ —42° (in anhydrous pyridine, $c = 1$) (lit. [16] $[\alpha]_D$ —38°, in pyridine).

2,4-Di-(tetraacetyl-β-D-glucosyl)-6-methyl-phloracetophenone (IV)

1.24 g of silver oxide was added in portions, with continuous stirring to a solution of 1 g of 2,4-di-(tetraacetyl-β-D-glucosyl)-phloracetophenone and 1.24 g of methyl iodide in 15 ml of anhydrous acetone. The reaction mixture was maintained at 60 °C for 8 hrs., the precipitate removed by filtration, and the filtrate evaporated in vacuum. The residue was recrystallized from ethanol to obtain 0.80 g (76.2%) of **IV**, m. p. 195—196 °C; $[\alpha]_D$ —34.3° (in anhydrous pyridine, $c = 1$).

$C_{37}H_{46}O_{22}$ (842.74). Calcd. OCH_3 3.68. Found OCH_3 4.08%. Mol. wt.: 849 (in ethanol, by ebullioscopy).

2-Methylphloracetophenone (V)

1 g of 2,4-di-(tetraacetyl-β-D-glucosyl)-6-methylphloracetophenone was hydrolyzed for 6 hrs. with 30 ml of 10% H_2SO_4. The white amorphous crude product which precipitated on neutralization of the mixture, was recrystallized from aqueous ethanol to yield 0.13 g (60%) of **V**; m. p. 203—205 °C (lit. [19] m. p. 205—207 °C).

2,4-Di-(tetraacetyl-β-D-glucosyl)-phloracetophenone oxime (VI)

A solution of 1.6 g of 2,4-di-(tetraacetyl-β-D-glucosyl)-phloracetophenone, 0.14 g of hydroxylamine hydrochloride and 0.16 g of anhydrous sodium acetate in a mixture of 10 ml of ethanol and 3 ml of water was boiled for 3 hrs. Pouring the reaction mixture into ice-water gave a white amorphous product, which was recrystallized from ethanol to obtain 0.85 g (52.5%) of **VI**, m. p. 123—125 °C; $[\alpha]_D$ —33.8° (in anhydrous pyridine, $c = 1$).

$C_{36}H_{45}O_{22}N$ (834.72). Calcd. N 1.66. Found N 1.86%.

4-β-D-Glucosyl-phloracetophenone (VIII)

1 g of 4-(tetraacetyl-β-D-glucosyl)-phloracetophenone was refluxed for 1 hr. in 10 ml of 0.1 *M* sodium methoxide. The reaction mixture was acidified with acetic acid to pH 5, and evaporated in vacuum. Recrystallization of the residue from methanol yielded 0.22 g (33.4%) of pure **VII**, m. p. 235 °C; $[\alpha]_D$ —91° (in ethanol, $c = 1$).

4-β-D-glucosyl-phloracetophenone has been prepared by FARKAS *et al.* [18] from 4-(tetraacetyl-β-D-glucosyl)-2-benzylphloracetophenone. Their product had m. p. 228—229 °C, and $[\alpha]_D$ —90° (in ethanol, $c = 1$).

4-(Tetraacetyl-β-D-glucosyl)-2,6-diacetyl-phloracetophenone (IX)

(a) From 4-(tetraacetyl-β-D-glucosyl)-phloracetophenone

A suspension of 0.5 g of 4-(tetraacetyl-β-D-glucosyl)-phloracetophenone in 2 ml of anhydrous pyridine was mixed with 5 ml of acetic anhydride, and the mixture kept at room temperature for 24 hrs. It was then poured into ice-water, and the precipitated white amorphous product was recrystallized from ethanol to obtain 0.40 g (68.9%) of **IX**, m. p. 144—145 °C; $[\alpha]_D$ —39.6° (in anhydrous pyridine, $c = 1$).

Mol. wt. (Rast method); 523. Calculated for $C_{26}H_{30}O_{15}$: 582.50.

(b) From 4-β-D-glucosyl-phloracetophenone

0.2 g of 4-β-D-glucosyl-phloracetophenone was acetylated in 2 ml of anhydrous pyridine with 5 ml of acetic anhydride to yield 0.20 g (57.1%) of a white crystalline product, m. p. 144—145 °C; $[\alpha]_D$ —38° (in anhydrous pyridine, $c = 1$).

4-(Tetra acetyl-β-D-glucosyl)-2,6-dimethylphloracetophenone (**X**); 2,6-dimethylphloracetophenone

1 g of 4-(tetraacetyl-β-D-glucosyl)-phloracetophenone and 1 ml of methyl iodide were dissolved in 10 ml of dimethylformamide, and 1 g of silver oxide was added in portions, under continuous stirring. The reaction mixture was then stirred for further 3 hrs., the precipitate was filtered off and washed with some chloroform. The filtrate was shaken and washed with a 1% solution of potassium cyanide, then with water, dried over Na_2SO_4 and evaporated. The residual reddish-brown syrup was hydrolyzed directly with 25 ml of 1% HCl. After cooling, the hydrolyzate was neutralized with $NaHCO_3$. 2,6-Dimethylphloracetophenone (0.1 g; 25.6%) separated in the form of almost white needles, m. p. 183—185 °C (lit. [20] m. p. 185.5 °C).

4'-β-D-Glucosyl-naringenin-chalcone (XVI)

1 g of 4-(tetraacetyl-β-D-glucosyl)-phloracetophenone was saponified with 6.7 ml of a 60% solution of KOH, then 0.25 g of 4-hydroxybenzaldehyde was added. The reaction mixture was shaken for 72 hrs., acidified with 10% HCl to pH 5, the yellow crystalline product was filtered off by suction and washed with ice-water until free of acid. Recrystallization of the crude product (0.33 g; 37.9%) from hot water gave m. p. 195—198 °C (lit. [18] m. p.: non-characteristic); $[\alpha]_D$ —71° (in ethanol, $c = 1$); —27° (in anhydrous pyridine, $c = 0.5$). (lit. [18] $[\alpha]_D$ —42°, in ethanol, $c = 1.08$). $R_f = 0.65$, in *n*-butanol–benzene–acetic acid–water (40:10:5:45).

7-β-D-Glucosyl-naringenin (XXX)

0.2 g of 4'-β-D-glucosyl-naringenin-chalcone was boiled for 1 hr. with 10 ml of water. After cooling, the separated slightly yellowish product was filtered by suction and recrystallized from aqueous ethanol to obtain 0.11 g (55%) of **XXX**, m. p. 222—224 °C (lit. [8] m. p. 222 °C and [18] 221—225 °C); $[\alpha]_D$ —40° (in acetone, $c = 0.5$) (lit. [8] $[\alpha]_D$ —40.5°, in acetone, $c = 0.5$, and [18] —40°, in acetone, $c = 0.5$).

4'-β-D-Glucosyl-phloretin, para-phlorizin (XXIII)

4'-β-D-Glucosyl-naringenin-chalcone was hydrogenated in 10 ml of ethanol in the presence of palladium-on-carbon catalyst, at room temperature and atmospheric pressure. Recrystallization of the product from hot water yielded 0.12 g (60%) of **XXIII**, m. p. 164—166 °C (lit. [7] m. p. 166 °C and [18] 164—166 °C) $[\alpha]_D$ —68° (in ethanol, $c = 1$); —37° (in anhydrous pyridine, $c = 0.5$). (lit. [7] $[\alpha]_D$ —70°, in ethanol, $c = 2$, and [18] —67°, in ethanol, $c = 0.81$).

4'-β-D-Glucosyl-isosakuranetin-chalcone (XVII)

1 g of 4-(tetraacetyl-β-D-glucosyl)-phloracetophenone was saponified with 6.7 ml of a 60% solution of KOH. After the addition of 0.32 g of 4-methoxybenzaldehyde, the reaction mixture was shaken for 72 hrs., and acidified with 10% HCl to pH 5. The yellow, oily crude product was separated and recrystallized from hot water to yield 0.32 g (35.9%) of a yellow crystalline substance, m. p. 187 °C (shrinking from 150 °C). $[\alpha]_D$ —44.5° (in ethanol, $c = 0.5$). $R_f = 0.58$, in *n*-butanol–benzene–acetic acid–water (40:10:5:45).

$C_{22}H_{24}O_{10}$ (448.41). Calcd. C 58.91; H 5.39. Found C 58.23; H 5.31%.

7-β-D-Glucosyl-isosakuranetin, isosakuranin (XXXI)

A solution of 0.2 g of 4'-β-D-glucosyl-isosakuranetin-chalcone in 4 ml of methanol was mixed with 5 ml of a buffer mixture of disodium hydrogen phosphate and citric acid (pH 7), and the mixture was refluxed for 30 min. The orange-red precipitate was filtered off, washed with cold methanol and recrystallized from 50% methanol to obtain 0.1 g (50%) of **XXXI**; m. p. 178—180 °C (lit. [8] m. p. 184—186 °C); $[\alpha]_D$ —50° (in anhydrous pyridine, $c = 0.5$) (lit. [8] $[\alpha]_D$ —55.3°, in pyridine).

4'-β-D-Glucosyl-4-methylphloretin; 4-methyl-para-phlorizin (XXIV)

0.2 g of 4'-β-D-glucosyl-isosakuranetin-chalcone was hydrogenated in 10 ml of ethanol in the presence of palladium-on-carbon catalyst. After processing the reaction mixture in the conventional way, 0.1 g (50%) of the pure product was obtained, m. p. 175—180 °C; $[\alpha]_D$ —36.5° (in ethanol, $c = 0.5$).

$C_{22}H_{26}O_{10}$ (450.42). Calcd. C 58.65; H 5.81. Found C 58.02; H 5.78%.

4-Methylphloretin

Hydrolysis of 0.1 g of 4'-β-D-glucosyl-4-methylphloretin with 1% HCl gave 0.05 g (83.3%) of 4-methylphloretin, m. p. 194—195 °C (lit. [13] m. p. 196 °C).

4'-β-D-Glucosyl-hesperetin-chalcone (XVIII)

1 g of 4-(tetraacetyl-β-D-glucosyl)-phloracetophenone was saponified with 6.7 ml of a 60% solution of KOH and 0.30 g of 3-hydroxy-4-methoxybenzaldehyde was added to the reaction mixture which was then shaken for 72 hrs., and acidified with 10% HCl to pH 5. The oily substance which separated was repeatedly recrystallized from hot water to yield 0.28 g (30%) of a yellow product, m. p. 175—179 °C; $[\alpha]_D$ = —19° (in anhydrous pyridine, c = 0.5); R_f = 0.61, in *n*-butanol–benzene–acetic acid–water (40:10:5:45).

$C_{22}H_{24}O_{11}$ (464.41). Calcd. C 56.89; H 5.20. Found C 56.75; H 5.17%.

7-β-D-Glucosyl-hesperetin (XXXII)

0.2 g of 4'-β-D-glucosyl-hesperetin-chalcone was dissolved in 1 ml of methanol, 2 ml of a buffer solution of disodium hydrogen phosphate and citric acid (pH 7) was added, and the reaction mixture refluxed for 30 min. The orange-red solution was allowed to stand for a few hours, when a slightly yellowish crude product separated. This was recrystallized from 50% ethanol to yield 0.03 g (15%) of **XXXII**, m.p. 180—185 °C (lit. [8] m. p. 189/180 °C); $[\alpha]_D$ —39.6° (in anhydrous pyridine, c = 0.5). (lit. [8] $[\alpha]_D$ —47.6°, in pyridine).

4'-β-D-Glucosyl-3-hydroxy-4-methylphloretin; 3-hydroxy-4-methyl-para-phlorizin (XXV)

A solution of 0.2 g of 4'-β-D-glucosyl-hesperetin-chalcone in 40 ml of ethanol was hydrogenated in the presence of palladium-on-carbon catalyst at room temperature and atmospheric pressure. Processing of the reaction mixture in the usual way gave 0.098 g (49.3%) of dihydrochalcone glucoside; m. p. 178—180 °C; $[\alpha]_D$ —44° (in anhydrous pyridine, c = 0.5).

$C_{22}H_{26}O_{11}$ (466.42). Calcd. C 56.64; H 5.61. Found C 56.31; H 5.37%.

3-Hydroxy-4-methylphloretin

0.1 g of 4'-β-D-glucosyl-3-hydroxy-4-methylphloretin was hydrolyzed with 1% HCl. A slightly yellowish product (0.05 g; 83.3%) was obtained, m. p. 194—195 °C (lit. [15] m. p. 194—195 °C).

REFERENCES

1. ZEMPLÉN, G., BOGNÁR, R.: Ber. **75,** 1040 (1942).
2. KLEIN, G.: Handbuch der Pflanzenanalyse. Band III. Verlag J. Springer, Wien, 1932.
3. DE KONICK: Ann. **15,** 15 (1835).
4. WESSELY, F., STORM, K.: Monatsh. Chem. **53/54,** 554 (1929); JOHNSON, F. R., ROBERTSON, A.: J. Chem. Soc. **1930,** 21.
5. ZEMPLÉN, G., BOGNÁR, R.: Ber. **75.** 645 (1942).
6. JORIO, M. A.: Annali di Chimica **49,** 1929 (1959).
7. WILLIAMS, A. H.: J. Chem. Soc. **1961,** 4133.
8. PACHECO, H., GROUILLER, A., HOURFAR, M. A.: Bull. soc. chim. France **1965,** 2937.
9. HÖRHAMMER, L., WAGNER, H., KRÄMER, H., FARKAS, L.: Tetrahedron Letters **42,** 5133 (1966).
10. WILLIAMS, A. H.: Ann. Rep. Long Ashton Res. Station 31.
11. PARIS, R. P., ETCHEPARE, S.: Ann. pharm. France **23,** 627 (1965).
12. KUHN, R., TRISCHMANN, A., LÖW, J.: Angew. Chem. **67,** 32 (1955).
13. ZEMPLÉN, G., BOGNÁR, R., MESTER, L.: Ber. **75,** 1433 (1942).
14. ZEMPLÉN, G., BOGNÁR, R., SZEGŐ, L.: Ber. **76,** 1112 (1943).
15. ZEMPLÉN, G., BOGNÁR, R.: Ber. **75,** 1043 (1942).
16. PETRUCZ, K.: A citronetin glikozidjainak szintézise. (Synthesis of the glucosides of citronetin.) Dissertation. Budapest, 1944 (In Hungarian).

17. GARUSOVA, N. B., VETROV, A. N., PREOBRAZHENSKII, N. A.: Zhurn. Obschch. Khem. **10,** 3300 (1964).
18. FARKAS, L., MAJOR, Á., NÓGRÁDI, M.: Ber. **98,** 2926 (1965).
19. SONN, A., BÜLOW, W.: Ber. **58,** 1691 (1925).
20. CANTER, F. W., CURD, F. H., ROBERTSON, A.: J. Chem. Soc. **1931,** 1245.

Rezső BOGNÁR
Adrienne L. TŐKÉS
University, Debrecen 10, Hungary
Heiner FRENZEL; Karl Marx Univ., Pharmaceutical Inst. Leipzig, GDR.

Acta Chimica Academiae Scientiarum Hungaricae, Tomus 61 (1), pp. 93—105 (1969)

1,2,4-TRIAZINES AND CONDENSED DERIVATIVES, VIII*

THE REACTION OF 6-AZA-2-THIOTHYMINE WITH ACROLEIN AND RELATED COMPOUNDS

Gy. HORNYÁK (1), L. LÁNG (2), K. LEMPERT (1) and Gy. MENCZEL (3)

(1) *(Department of Organic Chemistry, Technical University, Budapest;*
(2) *Department of Spectroscopy, Hungarian Optical Works,** Budapest;*
(3) *Department of Experimental Physics, L. Eötvös University, Budapest)*

Received June 6, 1968.

6-Aza-2-thiothymine (**1**) adds readily to activated olefinic double bonds. Depending on the quality of the reaction partner, the reaction starts with the nucleophilic attack of either the sulfur or the nitrogen atom at position 2 of **1** (sometimes, in addition, with that of the nitrogen atom at position 4) on the β-carbon of the activated olefinic bond. The addition is often accompanied or followed by cyclization. Acrylonitrile, acrolein, crotonaldehyde and methyl γ-bromocrotonate were used as activated olefins. The structures of the products have been elucidated by chemical and spectroscopical methods.

Urea, thiourea as well as their analogues and derivatives may, as it is well known, readily add to the activated olefinic double bond of acrylic acid and related compounds [1—3]. Urea and thiourea units incorporated into cyclic structures are also capable of this reaction [4—8]. Since the thiourea moiety, particularly in anionic form, generally exhibits ambident reactivity, either *N*-(β-substituted ethyl)thioureas [1,2,5,6,8] or *S*-(β-substituted ethyl)-isothioureas [1—3] may be formed by this reaction.

6-Methyl-3-thio-1,2,4-triazine-3,5(2*H*,4*H*)-dione ("6-aza-2-thiothymine", **1**) [9], which has been used several times as a starting material for studies described in previous parts of the present series, is a cyclic thiourea or, more precisely, a cyclic thiosemicarbazide derivative; therefore, it was thought reasonable to investigate its reactions with acrylic acid derivatives and related compounds, all the more so, because the products obtainable in this way were promising as potential starting materials for the synthesis of condensed 1,2,4-triazine derivatives.

First the reaction of **1** with acrylonitrile was investigated. Under the conditions applied, two molecules of acrylonitrile reacted with **1** to yield **2**; thus *S*-cyanoethylation did not occur. The structure of the product could unequivocally be deduced from its spectral properties, its UV spectrum being

* Part VII: ZAUER, K., PUSKÁS, J., NYITRAI, J., HORNYÁK, Gy., WOLFNER, A., DOLESCHALL, G. and LEMPERT, K.: Periodica Polytechn. Budapest, Ser. Chem. Engng. **12**, 259 (1968)

** Magyar Optikai Művek.

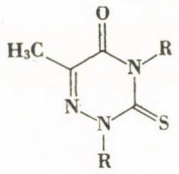
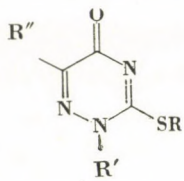
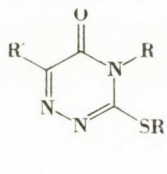
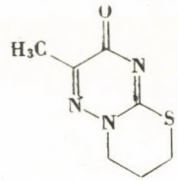

1: R = H **4**: R″ = H; R = R′ = CH_3 **7**: R′ = H; R = CH_3
2: = — CH_2CH_2CN **5**: R″ = H; R = R′ = — CH_2CH_2CN **8**: R′ = CH_3; R = CH_2CH_2CN **9**
3: R = — CH_3 **6**: R = CH_3; R = — CH_2COOH;
R′ = H

almost identical with that of the model compound **3** [10] and, at the same time, significantly differing from those of model compounds **4** and **6** [10].* Moreover, the position of the $\nu C{=}O$ band in the IR spectrum of the product was in complete agreement with structure **2** (cf. Table I), therefore, the isomeric structures **5** and **8** could be definitely excluded.

Since both NH hydrogens of **1** were substituted during the formation of **2**, the latter cannot be used as a starting material for the synthesis of condensed 1,2,4-triazine derivatives. For this purpose the *mono*cyanoethylation product of **1** would be suitable. However, before starting our experiments with the aim to develop methods for the synthesis of compounds of the latter type, Czechoslovak researchers reported a detailed investigation of cyanoethylation reactions of 6-azauracils and 6-aza-2-thiouracils [6, 8]; therefore, our work towards the above aim was abandoned. Instead, a study of the reactions of **1** and α,β-unsaturated aldehydes (acrolein and crotonaldehyde) was initiated.

At about 50 °C, in the presence of triethylamine, a 1:1 adduct (**13**) is formed from **1** and acrolein (the proof of structure is given below), whose IR spectrum contains neither an aldehydic carbonyl band nor an NH band. On the other hand, a sharp νOH band may be readily detected in addition to a $\nu C{=}O$ band characteristic for derivatives of 6-aza-2-thiouracils containing a cross-conjugated double bond system. The UV spectrum, too, exhibited the characteristics of the spectra of such cross-conjugated derivatives, *e.g.* **4** and **9** [10], cf. Table I. Since **1** fails to react with simple carbonyl compounds, such as butyraldehyde, benzaldehyde, or acetone, but, at the same time, as shown by its reaction with acrylonitrile, is capable to add to an activated olefinic double bond, the reaction leading to the formation of the adduct could be assumed to start with the addition of **1** to the olefinic bond of acrolein and to end with a cyclization under participation of the now intramolecular alde-

* Compounds **3**, **4** and **6** have been kindly furnished by Dr. J. GUT, Institute of Organic Chemistry and Biochemistry of the Czechoslovak Academy of Sciences, Prague.

Table I

UV and IR spectra

Compound	UV Spectra		IR Spectra (KBr pellets)	
	λ_{max} (log ε)	Solvent	νC=O, ring, cm^{-1}	Other bands, cm^{-1}
2	222 (4.13); 270 (4.21); 300 (3.69) sh.	ethanol	1700	νC≡N: 2260/2250, doublet
3*	223 (4.04); 266 (4.22); 302 (3.60) sh.	methanol	1695	
4* [11]	235 (4.38)	methanol	1670	
7* [11]	208 (4.11); 226 (3.76) sh.; 298 (3.92)	methanol	1695	
9 [10]	238 (4.36)	ethanol	1645	
13	238 (4.38)	ethanol	1640	νOH: 3335
15	235 (4.47); 359 (4.32)	ethanol	1630	νNH: 3300 and 3110
6 + EtCH=N—NH 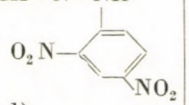 (1 : 1)	235 (4.47; 359 (4.32)	ethanol		
16	221 (4.38); 270 (4.40); 354 (4.32)	ethanol	1720	νNH: 3300 and 3110
1 + EtCH=N—NH 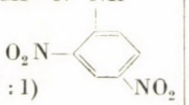 (1 : 1)	270 (4.40); 354 (4.32)	ethanol		
17	238 (4.44)	ethanol	1665	νC=O, ester: 1750
18	240 (4.36)	ethanol	1650	
19	220 (4.12); 270 (4.32); 305 (3.64) sh.	ethanol	1710	νOH: 3440, νNH: 3200—2600 with a maximum at 3080
21	239 (4.38)	ethanol	1670 (weak) + 1630 (strong)**	νOH: 3150 (broad)
	238 (4.38)	dioxane		
22	238 (4.34)	dioxane	1665	νC=O, ester: 1750
24	231 (4.12)	ethanol	1665	νC=O, ester: 1745

* Compounds **3**, **4** and **7** have been kindly furnished by Dr. J. GUT, Institute of Organic Chemistry and Biochemistry of the Czechoslovak Academy of Sciences, Prague

** Cf. footnote** on p. 100

hyde group.* In principle, either the sulfur atom of **1** or its nitrogen atom at position 2 could attack on the β-carbon atom of acrolein; therefore, the possible formation of either of two products, **11** and **13** through the corresponding intermediates **10** and **12**, respectively,** had to be taken into consideration. Actually, only a single adduct could be isolated, between whose two alternative structures (**11** and **13**) a decision could have easily been made if a monocyclic intermediate could have been isolated which, however, was not the case.

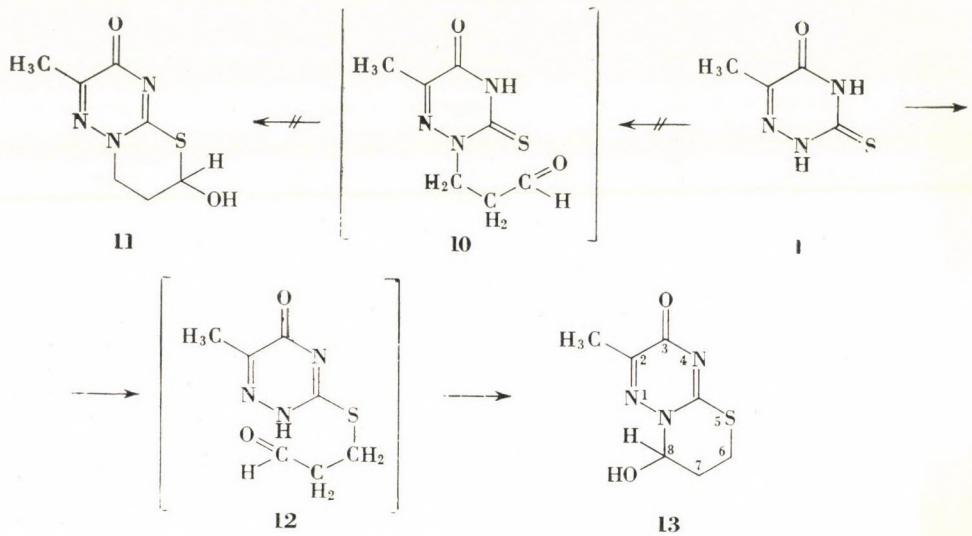

In order to elucidate the structure of the adduct, X-ray diffraction and chemical studies were performed. The present paper deals mainly with the results of the latter and, in addition, preliminary results of the former are presented in Experimental.

As an obvious route for the structure determination, selective fission of the newly formed *m*-thiazine ring of the adduct in the vicinity of either of the hetero atoms was attempted with the aim to derive the structure of the original adduct from that of its cleavage product, which latter was hoped to be determinable by spectroscopical means. Thus, desulfuration of the adduct by Raney nickel, as well as its hydrolysis by prolonged refluxing of its aqueous solution was attempted; however, treatment with Raney nickel resulted in complete destruction of the adduct while, on refluxing in aqueous solution, the acrolein moiety was cleaved completely from at least part of

* For cyclizations with the participation of NH groups incorporated into a heterocycle and aldehyde groups in side chains attached to the same ring, see, *e.g.*, [16, 17].

** It should be pointed out that the possibility of the reaction to proceed in a single step by simultaneous reaction of both reactive centres of acrolein with **1** is not excluded by our results.

the adduct and was found in the destillate; from the gummy residue only small amounts of **1** could be recovered. Similarly, only tarry products were formed as a result of attempted hydrolysis by concentrated hydrochloric acid (3 hrs. at 110 °C in a sealed tube). Under less vigorous conditions the hydrochloride of the adduct was simply formed (either in anhydrous form or as the monohydrate), from which, by treatment with aqueous sodium hydrogen carbonate solution, the adduct could be recovered.

Finally, the desired selective ring cleavage was achieved by reacting the adduct with 2,4-dinitrophenylhydrazine, whereby one of the 2,4-dinitrophenylhydrazones, **14** or **15**, was formed, possibly through the corresponding intermediate **10** or **12**. Since the UV spectrum in alcoholic solution of the

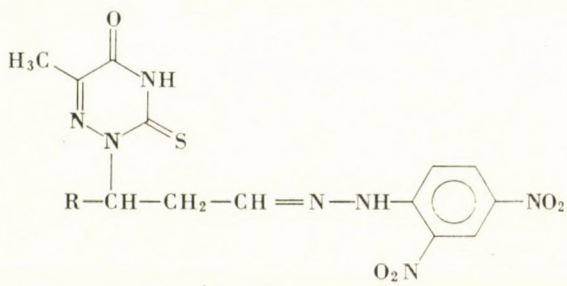

14 : R = H
16 : R = CH_3

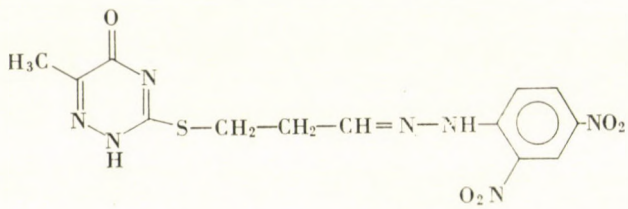

15

dinitrophenylhydrazone thus obtained was found to be practically identical with that of an equimolecular mixture of **6** [12] and propionaldehyde 2,4-dinitrophenylhydrazone and, at the same time, differed considerably from that of an equimolecular mixture of **1** and propionaldehyde 2,4-dinitrophenylhydrazone (see Figs. 1 and 2), the correct structure of the dinitrophenylhydrazone obtained from the adduct must be **15** and, consequently, that of the adduct itself **13**.

Acetylation and chlorination of **13** gave the *O*-acetyl and the chloro derivatives **17** and **18**, respectively, whose UV and IR spectra were consistent

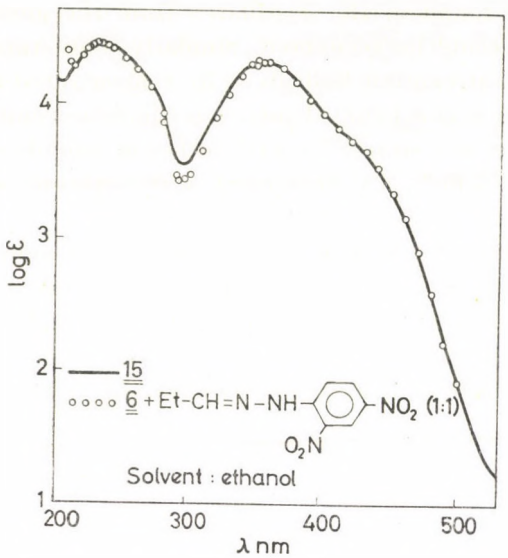

Fig. 1

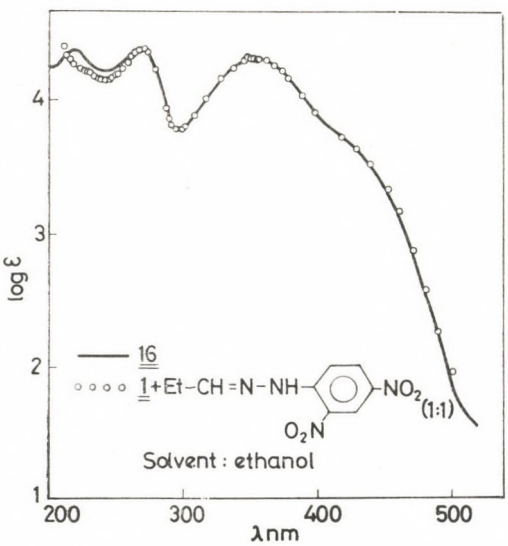

Fig. 2

with their assumed structures. Hydrolysis of **17** with hydrochloric acid gave back **13.** The chlorine atom of **18** could not be substituted by such nucleophiles as potassium cyanide, ammonia, or primary amines.

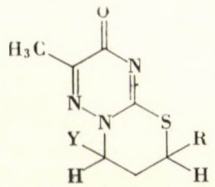
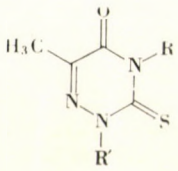
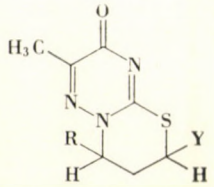

17:Y=CH_3COO–;R=H **19**:R=H; R′=—$CH(CH_3)CH_2CH(OH)OC_2H_5$ **21**:Y=OH; R=CH_3
18:Y=Cl; R=H **20**:R=—$CH(CH_3)CH_2CH(OH)OC_2H_5$; R′=H **22**:Y=$CH_3COO$–;R=$CH_3$

The reaction of **1** with crotonaldehyde was slightly different. After short refluxing of an ethanolic solution of the components in the presence of triethylamine, a ternary adduct could be isolated consisting of 1 molecule each of **1**, crotonaldehyde and ethanol. Since the UV and IR spectra of this product were characteristic for 3-thio-1,2,4-triazine-3,5(2*H*, 4*H*)-diones *(e.g.*, **1—3**; see Table I), the alternative structures **19** and **20** were considered. These structures were in accord with the NMR spectrum as well. A decision between the alternative structures was rendered possible by our finding that, on repeated recrystallization from acetone, one molecule of ethanol was gradually eliminated from the ternary adduct (accompanied by a gradual rise of the melting — decomposition — point and as expected for a presumably unstable hemiacetal-like structure), yielding a binary 1 : 1 adduct consisting of **1** and crotonaldehyde, which melted without decomposition.* The UV and IR spectra of this product differed considerably from those of the original ternary adduct, exhibiting the characteristics of the spectra of cross-conjugated 3-alkylthio-1,2,4-triazin-5(2*H*)-ones *(e.g.*, **4** and **6**). This change of the spectral properties could only be interpreted by assuming structures **19** and **21**** for the ternary and binary adducts, respectively. Structure **19** for the former is corroborated also by the course of its reaction with 2,4-dinitrophenylhydrazine yielding, under elimination of one molecule each of ethanol and water, a dinitrophenylhydrazone (**16**) whose UV spectrum is practically identical with that of an equimolecular mixture of **1** and propionaldehyde 2,4-dinitrophenylhydrazone, differing at the same time considerably from that of an equimolecular mixture of the latter and **6** [12] (see Figs. 1 and 2).

Thus, in the reaction of **1** with acrolein and crotonaldehyde, respectively, different orientations are experienced: while the β-carbon of acrolein is attacked by the sulfur atom, that of crotonaldehyde by the N(2) atom of **1**. The reason for the different behaviour of the two closely related unsaturated aldehydes is apparently the presence of an extra methyl group

* The fact that the ternary adduct melts under decomposition suggests that elimination of ethanol occurs even on simple heating. This change — as traced by the changes in the carbonyl region of the IR spectra — occurs indeed even on drying the adduct over P_2O_5 in vacuum at about 70—80°, or for several days at room temperature.

** Since **21** contains two centers of chirality, two diastereomeric pairs of racemates are theoretically possible. As concluded from the sharp melting point of the product, only one of the racemates has been isolated in our experiments.

in crotonaldehyde and not the slight differences of the conditions applied. If, namely, the reaction of **1** with acrolein was performed — similarly to that with crotonaldehyde — by short refluxing, formation of the adduct **13** likewise occurred, though in much lower yield because the greatest part of the aldehyde was simply polymerized. On the other hand, if the reaction of **1** and crotonaldehyde was performed — similarly to that with acrolein — at lower temperatures, the already known ternary adduct **19** could be isolated as the only product though, again, in lower yield.

A further characteristic difference of the reactions of **1** with acrolein and crotonaldehyde, respectively, is that a monocyclic intermediate of the cycloaddition — or more precisely its hemiacetal-like derivative (**19**) — could be isolated only in the latter case.* It would, however, be wrong to draw from this the conclusion that the monothiohemiacetal-like functional group partly incorporated into the *m*-thiazine ring of the *binary* adduct (**21**) formed with crotonaldehyde is less stable than the aldehyde-ammonia like functional group partly incorporated into the *m*-thiazine ring of the adduct (**13**) formed with acrolein. In fact, the situation is just reversed since, in contrast to the *m*-thiazine cycle of **13**, the ring of **21** fails to undergo cleavage under similar conditions with 2,4-dinitrophenylhydrazine, *i.e.* the reaction **21** → **16** cannot be achieved.

Similarly to **13**, **21** may be acetylated, and the acetyl derivative **22** is reconverted by hydrochloric acid into **21**.**

Preparation of the hydrazone **16** was also attempted starting with the acetyl derivative **22** but, in view of the negative results obtained with **21**, the cleavage of the thiazine cycle was forced by the use of hydrochloric acid. Though the cleavage of the thiazine ring was achieved by this treatment, it did not occur in the desired direction: the crotonaldehyde moiety became completely detached from the triazine ring and could be isolated in 60% yield as its 2,4-dinitrophenylhydrazone, instead of the desired **16**.

Direct preparation of the dinitrophenylhydrazones **15** and **16** starting with **1** and the dinitrophenylhydrazone of acrolein and crotonaldehyde, respectively, was also attempted, however, without success.

In addition, the reaction of **1** with methyl γ-bromocrotonate [13] was investigated. As a result of this reaction, the components are linked together under elimination of hydrogen bromide, as shown by the elemental composition of the product. Since 6-aza-2-thiouracils are known to yield always

* The hemiacetal-like functional group of **19** plays, apparently, an important part in the subsequent formation of the *m*-thiazine ring of **21**. When the triethylamine-catalyzed reaction of **1** and crotonaldehyde was performed in dioxane instead of an alcohol — *i.e.* under conditions where the possibility of intermediate formation of the hemiacetal function was excluded — no **21** could be isolated.

** The latter reaction also had importance in checking the purity of **21**. In the IR spectrum of **21** (Table I) splitting of the carbonyl band had been observed, which might have been attributed — in spite of a correct analysis — to the presence of impurities. Since, however, the IR spectrum of **21**, recovered from **22** (whose purity was beyond doubt on the basis of its IR spectrum), was found to be identical with that of a specimen directly obtained, the splitting of the carbonyl band is not due to the presence of impurities.

S-alkyl derivatives on treatment with one molecule of an alkyl halide [14], it was likely that the product had structure **23**. However, its IR spectrum did not show the presence of any NH band, thus obviously the reaction proceeded further to yield **24**, by intramolecular addition of the NH group to the activated olefinic double bond of **23**. The spectroscopic properties of the product are consistent with structure **24**. The isomeric alternative structure,

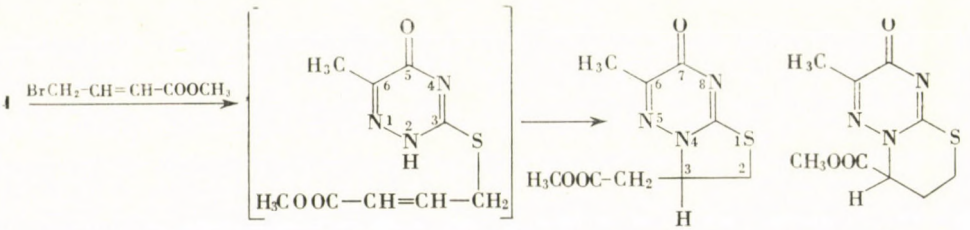

23 **24** **25**

25, is excluded by general experience concerning the orientation in Ad_N reactions of α,β-unsaturated esters. The structure of the product, **26**, obtained from the reaction of thioacetamide and methyl γ-bromocrotonate, elucidated by British authors by NMR spectroscopy [15], may be considered as further evidence, based on analogy.

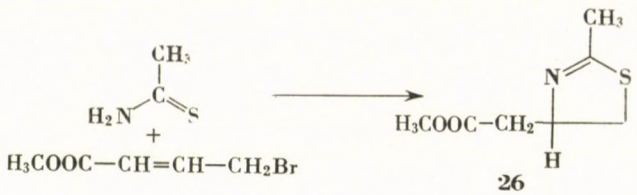

26

Experimental*

6-Methyl-5-oxo-3-thioxo-1,2,4-triazine-2,4(3*H*,5*H*)-dipropionitrile (2)

A mixture of 6-aza-2-thiothymine (**1**; 2.86 g; 20 mmoles), acrylonitrile (2 ml; 30 mmoles), dioxane (12 ml) and triethylamine (9 ml) was refluxed 4 hrs. The yellow oily residue obtained on evaporation in vacuum was dissolved in 20 ml of ethanol and treated with Norite. Petroleum ether was added to the solution until faintly opalescent, and the mixture was allowed to stand for 3 days in a refrigerator to yield 1.2 g (32%, based on acrylonitrile) of a colourless crystalline powder, m.p. 97—8 °C (from ethanol).

$C_{10}H_{11}N_5OS$ (249.3). Calcd. N 28.10; S 12.78 Found N 27.97; S 12.90%.

7,8-Dihydro-8-hydroxy-2-methyl-3*H*,6*H*-[1,3]thiazino[3,2-b] [1,2,4]triazin-3-one (13)

6-Aza-2-thiothymine (**1**; 2.86 g; 20 mmoles) was dissolved in hot methanol (30 ml). After cooling to 50°C, triethylamine (0.5 ml) and acrolein (1.5 ml; 22 mmoles) were added, and the mixture was allowed to stand 2 hrs. at room temperature. After chilling in ice, the crystals (2.2 g; 55%) of **13** were filtered off and washed with ether to obtain colourless needles, m.p. 176—8 °C(d.) (from water).

* All m.p.'s are uncorrected.

$C_7H_9N_3O_2S$ (199.3). Calcd. N 21.08; S 16.10. Found N 21.02; S 16.23%.

Preliminary X-ray diffraction investigations have been performed on single crystals of this compound. The specimens were colourless monoclinic needles elongated in the direction of the *b* axis.

Laue and oscillation photographs showed the Laue group to be 2/m. Systematical absence of reflexions indicated the presence of a twofold screw axis and of a glide plane in the unit cell. Taking the direction of the *y* axis fixed parallel to the twofold axis and changing the directions of the *x* and *z* axes, the space group and unit cell dimensions can be choosen in the following three ways:

(1) Space group $P2_1/c$
$a_1 = 9.76$ Å, $b = 9.56$ Å, $c_1 = 11.25$ Å, $\beta = 125.2°$

(2) Space group $P2_1/n$
$a_2 = 9.76$ Å, $b = 9.56$ Å, $c_2 = 9.76$ Å, $\beta = 109.6°$

(3) Space group $B2_1/c$
$a_3 = 15.95$ Å, $b = 9.56$ Å, $c_3 = 11.25$ Å, $\beta = 90°$

The data given above were measured with an accuracy of 0.02 Å and 0.1° respectively.

The density, measured by flotation in mixtures of carbon tetrachloride and acetone, is 1.523 g/cm³. With four molecules in the primitive unit cell (Z = 4), the calculated density is 1.542 g/cm³.

Weissenberg photographs of 6 layers around the *b* axis and of 5 layers around the c_3 axis were made in order to determine the crystal structure by X-ray methods.

Hydrochloride

13 (2.0 g; 10 mmoles) was refluxed 2 hrs. with 20% aqueous hydrochloric acid (30 ml). The oily residue obtained on evaporation in vacuum was dissolved in ethanol (10 ml) and allowed to stand 2 days in a refrigerator to yield 0.7 g (28%) of a crystalline powder which was filtered off and washed with ether, m.p. 125—7 °C (d.) (from ethanol, saturated with hydrogen chloride, and ether).

$C_7H_9N_3O_2S \cdot HCl \cdot H_2O$ (253.7). Calcd. Cl 13.97; N 16.56. Found Cl 13.86; N 16.53%.

Treatment with 5% aqueous $NaHCO_3$ solution reconverted the salt into **13.**

The salt was obtained in anhydrous form by passing dry hydrogen chloride into a solution of **13** in a mixture of ethanol and ether. M. p. 145—7 °C (d.) (from ethanol, saturated with hydrogen chloride, and ether). The IR spectrum was — apart from the H_2O band — identical with that of the monohydrate.

Acetylation

13 (4.0 g; 20 mmoles) was refluxed for 30 min. with acetic anhydride (40 ml); the solution turned faintly yellow. The crystals, obtained on allowing the mixture to stand 2 days in a refrigerator, were filtered off and washed with ether to yield 3.7 g (77%) of **17**, faintly yellow crystalline powder, m. p. 189—91 °C (from acetic anhydride and ether).

$C_9H_{11}N_3O_3S$ (241.3). Calcd. N 17.42; S 13.28. Found N 17.50; S 13.05%.

Deacetylation

17 (2.0 g; 8.3 mmoles) was refluxed for 30 min. with 20% aqueous hydrochloric acid. The oily residue obtained on evaporation of the brown solution to dryness in vacuum, was triturated with 5% aqueous $NaHCO_3$ solution to give 0.9 g (54%) of crystalline **13**, m. p. 176—8 °C (d.) (from water); the product gave no m. p. depression with an authentic sample.

Reaction with thionyl chloride

13 (5.0 g; 25 mmoles) was mixed under vigorous stirring with thionyl chloride (20 ml); complete dissolution occurred under the evolution of heat. After evaporation of the excess $SOCl_2$ in vacuum, the oily residue was dissolved in water (20 ml) and neutralized with 20% aqueous Na_2CO_3 solution, when 4.1 g (75%) of **18** precipitated as faintly yellow, long needles, m. p. 182—4 °C (d.) (from water).

$C_7H_8ClN_3OS$ (217.7). Calcd. Cl 16.29; N 19.30; S 15.07. Found Cl 16.18; N 19.18; S 14.68%.

Reaction with 2,4-dinitrophenylhydrazine

A mixture of **13** (1.0 g; 5 mmoles), 2.4-dinitrophenylhydrazine (1.0 g; 5 mmoles) and ethyl acetate (50 ml) was refluxed for 16 hrs. The colour of the solution turned from orange gradually to faintly yellow. The mixture was allowed to stand overnight in a refrigerator, and the crystals of **15** (1.4 g; 74%) were filtered off and washed with ether to obtain a bright yellow crystalline powder, m. p. 196 °C (d.) (from DMF and water).

$C_{13}H_{13}N_7O_5S$ (379.4) Calcd. C 41.15; H 3.45; S 8.45. Found C 41.56; H 3.71; S 8.03%.

β-Methyl-(4,5-dihydro-6-methyl-5-oxo-3-thioxo-2(3*H*)-1,2,4-triazine)-propionaldehyde hemiacetal (19)

A mixture of 6-aza-2-thiothymine (**1**; 2.9 g; 20 mmoles), crotonaldehyde (2 ml; 24 mmoles), triethylamine (0.5 ml) and anhydrous ethanol (25 ml) was refluxed for 30 min., filtered hot and allowed to stand overnight in a refrigerator to yield 2.7 g (52%) of **19** in form of an almost colourless microcrystalline powder which, after being filtered off, was washed with petroleum ether. M. p. 128—130 °C (d.) (after a *single* recrystallization* from ethanol-petroleum ether).

$C_{10}H_{17}N_3O_3S$ (259.3). Calcd. C 46.32; H 6.61; S 12.37. Found C 46.28; H 6.23; S 12.31%.

NMR spectrum (δ values)

1.2	ppm:	CH_3—(CH_2),	triplet	(J = 6 cps)
1.4	ppm:	CH_3—(CH),	doublet	(J = 8 cps)
2.25	ppm:	CH_3—C,	singlet	
2.9	ppm:	(CH)—CH_2—(CH),	triplet	(J = 6 cps)
3.7	ppm:	CH_2—(CH_3),	quadruplet	(J = 6 cps)
~4.8	ppm:	CH—(CH_2),	triplet	(J = 6 cps)
6.0	ppm:	(CH_3)—CH—(CH_2),	multiplet	(J = 6 cps)
~9.75	ppm:	NH,	singlet	

Reaction with 2,4-dinitrophenylhydrazine

A mixture of **19** (1.85 g; 7.1 mmoles), 2.4-dinitrophenylhydrazine (1.8 g; 9 mmoles) and ethyl acetate (50 ml) was refluxed for 10 hrs. and subsequently evaporated to dryness in vacuum. The yellow crystalline residue was recrystallized from nitromethane (25 ml) and washed with ether to yield 2.4 g (85%) of **16**, bright yellow crystalline powder, m. p.190—1°C (from DMF-water).

$C_{14}H_{15}N_7O_5S$ (393.4). Calcd. C 42.74; H 3.84; S 8.15. Found C 42.57; H 4.03; S 8.13%.

7,8-Dihydro-6-hydroxy-2,8-dimethyl-3*H*,6*H*-[1,3]thiazino-[3,2-b] [1,2,4]triazin-3-one (21)

This compound was prepared by threefold recrystallization of **19** from acetone-petroleum ether, followed by two recrystallizations from pure acetone. After the last recrystallization no rise of the m. p. was observed. Yield: 45% of **21**, m. p. 152—4 °C.

$C_8H_{11}N_3O_2S$ (213.3). Calcd. N 19.70; S 15.04. Found N 19.65; S 14.48%.

No reaction occurred with dinitrophenylhydrazine under the condition described above, and 85% of the starting material could be recovered unchanged.

Acetylation

21 (1.1 g; 5 mmoles) was refluxed for 10 min. in acetic anhydride (10 ml) and the resulting solution allowed to stand overnight in a refrigerator to yield colourless crystalline needles (0.6 g; 47%) of **22** which were washed with ether. M. p. 200—2 °C (from acetic anhydride–ether).

$C_{10}H_{13}N_3O_3S$ (255.3). Calcd. C 47.07; H 5.13; S 12.56. Found C 47.14; H 5.12; S 12.47%.

* Repeated recrystallization causes gradual rising of the m. p. and, finally, transformation of the product under elimination of ethanol into **21**.

Deacetylation

A mixture of **22** (0.5 g; 2 mmoles) and 20% aqueous HCl (4 ml) was refluxed for 30 min. The solution, which became slightly coloured, was evaporated to dryness in vacuum. In order to remove traces of water, the residue was mixed with dry benzene and again evaporated to dryness. Finally, the partly crystalline residue was triturated with ethereal diazomethane solution to remove any hydrochloric acid bound. The product solidified completely to yield 0.2 g (47%) of **21**, m. p. 152—4 °C (from acetone).

Reaction of the acetyl derivative 22 with 2,4-dinitrophenylhydrazine

A mixture of **22** (0.5 g; 2 mmoles), 2,4-dinitrophenylhydrazine (0.4 g; 2 mmoles), dioxane (40 ml) and 20% aqueous HCl (1 ml) was refluxed for 10 hrs. During this period, small amounts of tars were deposited from the red solution. After treatment with Norite, the solution was evaporated to dryness in vacuum and the red, partly solid residue was triturated with ethereal diazomethane solution. The excess of the reagent was evaporated in vacuum, and the crystalline residue was filtered off after addition of a small amount of ether to yield 0.3 g (60%) of a red crystalline powder, m. p. 180—5° (crude product), whose IR spectrum proved to be identical with that of an authentic sample of crotonaldehyde 2,4-dinitrophenylhydrazone, m. p. 190 °C (from nitromethane).

2,3-Dihydro-6-methyl-3-(methoxycarbonylmethyl)-7*H*-thiazolo-[3,2-b] [1,2,4]triazin-7-one (24)

6-Aza-2-thiothymine (**1**; 1.4 g; 10 mmoles) and methyl γ-bromocrotonate [13] (1.2 ml; 10 mmoles) were dissolved in a solution of sodium (0.23 g; 10 mg—at) in anhydrous methanol (15 ml.). The solution was refluxed for 1 hr. and subsequently evaporated to dryness in vacuum. The residue was triturated with 50 ml of anhydrous acetone and filtered to remove the insoluble sodium bromide. The filtrate was evaporated to dryness in vacuum at room temperature and the crystalline residue was triturated with petroleum ether and filtered off to yield 1.9 g (79%) of faintly yellow crystalline needles of **24**, m. p. 94—5 °C (from benzene–petroleum ether).

$C_9H_{11}N_3O_3S$ (241.3). Calcd. C 44.80; H 4.59; S 13.28. Found C 44.72; H 4.52; S 13.86%.

*

The authors wish to express their gratitude to Miss K. Ófalvi, Mrs. S. Viszt-Simon and Mrs. I. Zauer-Csüllög for the microanalyses; to Mrs. F. Kubik for valuable technical assistance; to Dr. P. Sohár for the NMR, to Mr. M. Vörös for the UV and to Mrs. Gy. Karsai-Sas and Mrs. M. Szirányi-Kiss for the IR spectra; and to the United Works of Pharmaceutical and Dietetic Products (Egyesült Gyógyszer- és Tápszergyár), Budapest, for financial support.

REFERENCES

1. Терентев, А. П., Кост, А. Н.: Реакции и Методы Исследования органических Соединений (под Редакцией С. С. Наметкина, В. М. Родионова и Н. Н. Мельникова), Госхимиздат, Москва—Ленинград, Том 2, стр. 72, 1952. (With references to the earlier literature)
2. Behringer, H., Zillikens, P.: Liebigs Ann. Chem. **574,** 140 (1951)
3. Kataev E. G., Barinova, L. K.: Dokl. Akad. Nauk SSSR **141,** 1373 (1961)
4. Shvachkin, Yu. P., Azarova, M. T., Rapanovich, I. I.: Vestn. Mosk. Univ., Ser. II, Khim. **18** (5), 68 (1963)
5. Shvachkin, Yu. P., Rapanovich, I. I., Azarova, M. T.: Vestn. Mosk. Univ., Ser. II, Khim. **20** (1), 73 (1965)
6. Nováček, A.: Coll. Czechoslov. Chem. Commun. **30,** 2480 (1965)
7. Nováček, A.: Coll. Czechoslov. Chem. Commun. **32,** 3565 (1967)
8. Nováček, A., Lissnerová, M.: Coll. Czechoslov. Chem. Commun. **33,** 604 (1968)
9. Gut, J.: Chem. Listy **51,** 1947 (1957); Coll. Czechoslov. Chem. Commun. **23,** 1588 (1958)

10. NYITRAI, J., BÉKÁSSY, S., LEMPERT, K.: Acta Chim. Acad. Sci. Hung. **53,** 311 (1967)
11. GUT, J., PRYSTAŠ, M., JONÁŠ, J.: Coll. Czechoslov. Chem. Commun. **26,** 986 (1961)
12. GUT, J., PRYSTAŠ, M.: Coll. Czechoslov. Chem. Commun. **24,** 2986 (1959)
13. ZIEGLER, K., SPÄTH, A., SCHAAF, E., SCHUMANN, W., WINKELMANN, E.: Liebigs Ann. Chem. **551,** 80 (1942)
14. GUT, J. in *Advances in Heterocyclic Chemistry* (Edited by A. R. Katritzky), Vol. 1., p. 223. Academic Press, New York and London, 1963
15. DINGWALL, J. G., REID, D. H., SALMOND, W. G.: J. Chem. Soc. [London] **1965,** 4271
16. ZONDLER, H. and PFLEIDERER, W.: Chem. Ber. **99,** 2984 (1966)
17. HORNYÁK, Gy.: Dr. Techn. Thesis, Technical University, Budapest, 1967

Gyula HORNYÁK; Budapest XI., Gellért tér 4.
László LÁNG; Budapest XII., Csörsz u. 35—43.
Károly LEMPERT; Budapest XI., Gellért tér 4.
György MENCZEL; Budapest VIII., Múzeum krt. 6—8.

INDEX

INORGANIC AND ANALYTICAL CHEMISTRY – ANORGANISCHE UND ANALYTISCHE CHEMIE – НЕОРГАНИЧЕСКАЯ И АНАЛИТИЧЕСКАЯ ХИМИЯ

UPOR, E., RÓNAI, Á. and GÖRBICZ, M.: Some Problems in the Separation, by Precipitation, of Traces of Elements, V. Sorption of Ammine Complex Forming Cations on Metal Hydroxides. Determination of Zinc in Rock Samples, After Separation with Ammonium Hydroxide 1

CSÁSZÁR, J. and HORVÁTH, E.: Physico-Chemical Studies on Isomeric Compounds of Transition Metal Ions 13

PAULIK, F., BUZÁGH-GERE, É. und ERDEY, L.: Derivatographische Untersuchung des Magnesiumammoniumphosphats. (Derivatographic Analysis of Magnesium Ammonium Sulfate) 29

TÖRÖK, F., PULAY, P. and HUN-BOROSSAY, Gy.: On the Parameter Form of Force Constant Matrix, X. On the Coriolis Coupling Constants Compatible with the Normal Frequencies 39

PHYSICAL CHEMISTRY – PHYSIKALISCHE CHEMIE – ФИЗИЧЕСКАЯ ХИМИЯ

HOLLY, S., SZABÓ, G., TÓTH, G. and VARSÁNYI, G.: Investigation of the Intermediates of the Nitration of Furfural, by Infrared Spectroscopy 45

HARGITTAI, I. and CYVIN, S. J.: Mean Amplitudes of Vibration for Small Molecules Containing Sulphur. I. Thionyl and Sulphuryl Chlorides 51

ORGANIC CHEMISTRY – ORGANISCHE CHEMIE – ОРГАНИЧЕСКАЯ ХИМИЯ

SZEJTLI, J.: A New Formula for the Description of the Conformation of Pyranoid Sugars 57

HANKOVSZKY, O. H. and HIDEG, K.: Benzazoles, VII. Alkylation Reactions of 2-Thio-[1,3]-diazoles 69

BOGNÁR, R., TŐKÉS, A. L. and FRENZEL, H.: Flavonoids, XVI. Mono- and Diglucosides of Phloracetophenone and their Conversion into Glucosides of Chalcone, Flavanone and Phlorizin Type 79

HORNYÁK, Gy., LÁNG, L., LEMPERT, K. and MENCZEL, Gy.: 1,2,4-Triazines and Condensed Derivatives, VIII. The Reaction of 6-Aza-2-thiothymine with Acrolein and Related Compounds 93

Printed in Hungary

A kiadásért felel az Akadémiai Kiadó igazgatója — Műszaki szerkesztő: Farkas Sándor

A kézirat nyomdába érkezett: 1969. III. 17. — Terjedelem: 9,25 (A/5) ív, 58 ábra

69.67446 Akadémiai Nyomda, Budapest — Felelős vezető: Bernát György

ACTA CHIMICA

ТОМ. 61 ВЫП. 1

РЕЗЮМЕ

О НЕКОТОРЫХ ВОПРОСАХ РАЗДЕЛЕНИЯ СЛЕДОВ ЭЛЕМЕНТОВ С ПОМОЩЬЮ ВЫСАЖДЕНИЯ, V

Сорбция катионов, образующих аммин-комплексы, на гидроокисях металлов в среде NH_4OH. Зависимость сорбции от pH и от концентрации аммонийной соли. Определение цинка из горных пород

Э. УПОР, А. РОНАИ и М. ГЁРБИЦ

Проводились исследования для определения зависимости сорбции катионов, образующих аммино-комплексы, на гидроокиси железа (III) от концентрации NH_4OH аммонийной соли. В согласии с результатами Колтгоффа (среди остальных противоречивых литературных данных) было найдено, что увеличение концентрации NH_4OH и аммонийной соли приводит к уменьшению сорбции каждого исследованного иона.

Зависимость сорбции от pH представляет кривую колокольной формы, максимум которой лежит в области pH = 8. Наиболее хорошо сорбируемые кобальт(II) и цинк(II), с помощью изменения pH, могут переводится количественно либо в осадок, либо в раствор. Растворение из осадка портится явлением старения.

Определили минимальные концентрации NH_4OH и аммонийной соли, необходимые для количественного сохранения отдельных ионов в растворе. На основе изотопной индикации было показано, что разделение может быть использовано и в анализе горных пород. С помощью одного высаждения — с точки зрения требований анализа следов элементов — может быть достигнуто количественное разделение.

Разделение гидроокисью аммиака позволяет отделить и цинк от кальция.

Был разработан метод дитизонного определения небольших количеств цинка из горных пород.

Физико-химическое исследование изомерных соединений ионов переходных металлов

Й. ЧАСАР и Е. ХОРВАТ

Авторы приводят физико-химические исследования координационных и полимеризационных изомеров комплексов, содержащих следующие центральные ионы: Cr^{+3}, Mn^{+3}, Fe^{+3}, Co^{+3}, Ni^{+2} и Cu^{+2}. Магнитные и спектральные свойства этих комплексов объясняются на основе теории поля лигандов. Экспериментальные данные показывают, что ионы комплекса даже в изомерном аддукте сохраняют свои характерные свойства. На основе RACAH-параметров, а также величин $_s(NH)_3$ и $_{as}(NO_2)$ из ИК-спектров были сделаны заключения относительно характера связей.

Дериватографическое изучение магнийаммонийфосфата

Ф. ПАУЛИК, Э. БУЗАГ-ГЕРЕ и Л. ЭРДЕИ

При различных экспериментальных условиях были получены осадки магнийаммонийфосфата, которые изучались комбинированными исследованиями дериватографии термическо-газового анализа дилатационных измерений. Было установлено, что при

температуре ниже приблизительно 75° С выделяется гексагидрат, а выше — моногидрат. Содержание воды и аммония в некоторых осадках уменьшается при месячных стояниях или при вакуумной сушке. Ход термораспада осадков различного состава отличается друг от друга.

О параметрическом определении F-матриксы силовых постоянных, X

Изучение постоянных связи Кориолиса, согласуемых с нормальными частотами

Ф. ТЁРЁК, П. ПУЛАИ и ДЬ. БОРОШШАИ

Используя метод параметрического определения силовых постоянных, могут быть просто получены постоянные связи Кориолиса, соответствующие нормальным частотам молекул. На основе данного метода может быть получена легко используемая формула для частных производных постоянных связи Кориолиса по силовым постоянным.

Изучение промежуточных продуктов нитрования фурфурола на основе ИК-спектров

Ш. ХОЛЛИ, Г. САБО, Г. ТОТ и ДЬ. ВАРШАНИ

Изучались ИК-спектры нитро-триацетокси и нитро-пропионокси-производных, а также 5-нитро-фурфурилиден-диацетата, образующихся при нитровании фурфурола в средах ангидридов уксусной и пропионовой кислот, соответственно. Было установлено, что ИК-спектры промежуточных продуктов реакции нитрования соответствуют диацетату 5-нитро-5-ацетокси-2,5-дигидро-фурфурилидена и дипропионату 5-нитро-5-пропионокси-2,5-дигидро-фурфурилидена.

Спектроскопический анализ и средние амплитуды колебания для $SOCl_2$ и SO_2Cl_2

И. ХАРГИТТАИ и С. Й. СИВИН

Проведен уточнённый анализ нормальных координат для $SOCl_2$ и SO_2Cl_2 с целью достижения соответствия с средними амплитудами колебания, полученными в результате электронографического исследования. В частности, в прежних спектроскопических расчётах было получено завышенное значение для l(Cl...Cl) по сравнению с электронографическими данными. В настоящей работе было достигнуто совершенное согласие для силового поля $SOCl_2$ как с наблюдаемыми частотами так и с средними амплитудами. Для SO_2Cl_2 тоже можно было получить силовое поле, которое точно соответствует наблюдаемым частотам и даёт средние амплитуды в пределах ошибки электронографических величин. Можно было получить и другое силовое поле, находящееся в лучшем соответствии с средними амплитудами, но в этом случае величина низшей частоты (для SO_2Cl_2) изменяется. Авторы работы не думают, что из этого следует делать какой-нибудь вывод.

Новая формула для описания конформаций пираноидных сахаров

Й. СЕЙТЛИ

Конформационные формулы Ривса для альдопираноз могут быть изображены в виде комбинаций букв и цифр. Это особенно удобно, когда необходимо печатать большое количество конформационных формул. Конформация Cl для сахаров в D-серии визуально

представляется атомом C_1 справа и внизу и атомом C_4 слева и вверху в форме стула $= {}^4C_1$, и нумерация членов кольца должна проводиться по часовой стрелке. Применяя эти конвенции как в D-, так и в L-сериях, аксиальные заместители на атомах C_1, C_3 и C_5 в конформации Cl направлены вниз, а заместители на C_2 и C_4 — вверх, по отношению к уровню кольца. Заместитель на C_5 пираноз в конформации Cl является аксиальным в L-сахарах и экваториальным в D-сахарах. Аксиальное положение обозначается в формуле его позицией, заключенной в скобки, и заместители иные, чем —H и —OH указываются после скобок. ${}^4C_1$ означает альдопиранозное кольцо с конформацией Cl. ${}^4C_1(-)5\text{-}CH_2OH$ означает O-D-глюкопиранозу, ${}^4C_1(1,2)5\text{-}CH_2OH$ означает α-D-маннопиранозу. Если цифра «5» также находится в скобках, то это означает L-сахара. Так например: ${}^4C_1(1,2,5)5\text{-}CH_2OH$ означает β-L-гулозу, ${}^4C_1(1,2,5)5\text{-}COOH$, 3-дезокси означает 3-дезокси-β-L-гулуроновую кислоту с конформациями Cl. Конформация 1C обозначается через ${}_1C^4$, B1 — через ${}^4B^1$, B2 — через ${}^5B^2$, и т. д. Нумерация в кольцах «альтернативных» конформаций (1C, 1B, 2B, 3B) происходит в направлении против часовой стрелки.

Бензазоли, VII.

X. O. ХАНКОВСКИЙ и К. ХИДЕГ

Реакции алкилирования 2-тио-(1,3)диазолей

Проводились исследования для получения пиридиловых производных 2-тио-13, диазолей. 2-тио-1,3-диазоли, реагируя с галогеналкилпиридинами (в щелочной среде) дают 2-тио-алкил-пиридиловые производные 1,3-диазоля. 2-тио-1,3-диазоли при взаимодействии с 2(2'-аминоэтил)-пиридином с выделением аммиака по механизму нуклеофильного-β-элиминации присоединения дают 2(тио-этилпиридил)-1,3-диазоли.

N_1-Алкилпиридиловые производные можно было синтезировать из соответствующих производных нитроанилина с помощью их восстановления с последующей сероуглеродной циклизацией в спиртовой среде.

Флаваноиды, XVI.

Моно- и диглюкозиды флорацетофенона и их превращение в глюкозиды типа халкон, флавонон и флоризин

Р. БОГНАР, А. Л. ТЁКЕШ и Х. ФРЕНЦЕЛЬ

Авторами пересматривалась реакция глюкозилирования флорацетофенона, т. к. согласно новым исследованиям [6, 7, 8], полученное Земплэном и Богнаром [1] соединение, которое ранее считалось 4-(тетраацетил-O-D-глюкозил)-флорацетофеноном (VII), в действительности оказалось производным бис-глюкозида флорацетофенона. (1).

Было установлено, что при хинолинном связывании флорацетофенона с O-ацетобром-глюкозой под влиянием окиси серебра в действительности может быть выделен лишь 2,4-ди(тетраацетил-O—D-глюкозил)-флорацетофенон (1); при щелочном-ацетоновом связывании, однако, наряду с этим основным продуктом, с небольшим выходом может быть выделен VII. Структура этих соединений подтверждалась соответствующими химическими превращениями (см. табл. 1. и относящиеся к ней формулы).

Производные моно- и диглюкозидов определенного строения повторно подвергались исследованиям, проведенным Земплэном и сотрудниками [5, 13, 14, 15]. Производные халкона, дигидрохалкона и флавона, полученные из 1, полностью совпадают с соединениями, полученными вышеупомянутыми авторами, и, таким образом, это диглюкозидные производные.

Аналогичные исследования, проведенные с VII, привели к 4'- и 4-моно-глюкозил-окси-производным халконов, дигидрохалконов и флавононов.

Данные к моно- и диглюкозидам приводятся в таблицах 2., 3. и 4.

1,2,4-Триазины и их конденсированные производные, VIII.

Реакция 6-аза-2-тиотимина с акролеином и родственными соединениями

ДЬ. ХОРНЯК, Л. ЛАНГ, К. ЛЕМПЕРТ и ДЬ. МЕНЦЕЛЬ

6-аза-2-тиотимин (*1*) может быть легко принужден к реакции присоединения по активированной олефиновой связи. В зависимости от природы реакционного партнера, присоединение начинается с нападанием β-углерода активированной олефиновой связи или атомом серы, или атомом азота во 2-ом и гораздо реже в 4-ом положении соединения *1*; циклизация часто сопровождает или следует за присоединением.

В качестве компонента с активированной олефиновой связью использовались акрилонитрил, акролеин, кротоновый альдегид и метиловый эфир γ-бромкротоновой кислоты. Строение продуктов реакции определялось на основе их химических и спектральных свойств.

The Acta Chimica publish papers on chemistry in English, German, French and Russian.

The Acta Chimica appear in volumes consisting of four parts of varying size, 4 volumes being published a year.

Manuscripts should be addressed to

Acta Chimica
Budapest 112/91 Műegyetem

Correspondence with the editors should be sent to the same address.

The rate of subscription is 165 forints a volume. Orders may be placed with "*Kultúra*" Foreign Trade Company for Books and Newspapers (Budapest I., Fő utca 32. Account No. 43-790-057-181) or with representatives abroad.

Les Acta Chimica paraissent en français, allemand, anglais et russe et publient des mémoires du domaine des sciences chimiques.

Les Acta Chimica sont publiés sous forme de fascicules. Quatre fascicules seront réunis en un volume (4 volumes par an).

On est prié d'envoyer les manuscrits destinés à la rédaction à l'adresse suivante:

Acta Chimica
Budapest 112/91 Műegyetem

Toute correspondance doit être envoyée à cette même adresse.

Le prix de l'abonnement est de 165 forints par volume.

On peut s'abonner à l'Entreprise pour le Commerce Extérieur de Livres et Journaux «*Kultúra*» (Budapest I., Fő utca 32. Compte-courant No. 43-790-057-181) ou à l'étranger chez tous les représentants ou dépositaires.

«*Acta Chimica*» издают трактаты из области химической науки на русском, французском, английском и немецком языках.

«*Acta Chimica*» выходят отдельными выпусками разного объема. 4 выпуска составляют один том. 4 тома публикуются в год.

Предназначенные для публикации рукописи следует направлять по адресу:

Acta Chimica
Budapest 112/91 Műegyetem

По этому же адресу направлять всякую корреспонденцию для редакции.

Подписная цена «*Acta Chimica*» — 165 форинтов за том. Заказы принимает предприятие по внешней торговле книг и газет «*Kultúra*» (Budapest I., Fő utca 32. Текущий счет № 43-790-057-181) или его заграничные представительства и уполномоченные.

42,— Ft

Reviews of the Hungarian Academy of Sciences are obtainable at the following addresses:

ALBANIA
Ndermarja Shtetnore e Botimeve
Tirana

AUSTRALIA
A. Keesing
Box 4886, GPO
Sydney

AUSTRIA
Globus Buchvertrieb
Salzgries 16
Wien I

BELGIUM
Office International de Librairie
30, Avenue Marnix
Bruxelles 5
Du Monde Entier
5, Place St. Jean
Bruxelles

BULGARIA
Raznoiznos
1, Tzar Assen
Sofia

CANADA
Pannonia Books
2, Spadina Road
Toronto 4, Ont.

CHINA
Waiwen Shudian
Peking
P. O. B. 88

CZECHOSLOVAKIA
Artia
Ve Směčkách 30
Praha 2
Poštovná Novinová Služba
Dovoz tisku
Vinohradská 46
Praha 2
Mad'arská Kultura
Václavské nám. 2
Praha I
Poštová Novinová Služba
Dovoz tlače
Leningradská 14
Bratislava

DENMARK
Ejnar Munksgaard
Nörregade 6
Copenhagen

FINLAND
Akateeminen Kirjakauppa
Keskuskatu 2
Helsinki

FRANCE
Office International de Documentation et Librairie
48, rue Gay Lussac
Paris 5

GERMAN DEMOCRATIC REPUBLIC
Deutscher Buch-Export und Import
Leninstraße 16
Leipzig 701
Zeitungsvertriebsamt
Fruchtstrasse 3—4
1004 Berlin

GERMAN FEDERAL REPUBLIC
Kunst und Wissen
Erich Bieber
Postfach 46
7 Stuttgart S.

GREAT BRITAIN
Collet's Holdings Ltd.
Dennington Estate
London Rd.
Wellingborough, Northants.
Robert Maxwell and Co. Ltd.
Waynflete Bldg. The Plain
Oxford

HOLLAND
Swetz and Zeitlinger
Keizersgracht 471—487
Amsterdam C.
Martinus Nijhof
Lange Voorhout 9
The Hague

INDIA
Current Technical Literature
Co. Private Ltd.
India House OPP
GPO Post Box 1374
Bombay I

ITALY
Santo Vanasia
Via M. Macchi 71
Milano
Libreria Commissionaria Sansoni
Via La Marmora 45
Firenze

JAPAN
Nauka Ltd.
92, Ikebukur O-Higashi 1-chome
Toshima-ku
Tokyo
Maruzen and Co. Ltd.
P. O. Box 605
Tokyo-Central
Far Eastern Booksellers
Kanda P. O. Box 72
Tokyo

KOREA
Chulpanmul
Phenjan

NORWAY
Johan Grundt Tanum
Karl Johansgatan 43
Oslo

POLAND
RUCH
ul. Wronia 23
Warszawa

ROUMANIA
Cartimex
Str. Aristide Briand 14—18
Bucureşti

SOVIET UNION
Mezhdunarodnaya Kniga
Moscow G—200

SWEDEN
Almquist and Wiksell
Gamla Brogatan 26
Stockholm

USA
Stechert Hafner Inc.
31. East 10th Street
New York, N. Y. 10003
Walter J. Johnson
111, Fifth Avenue
New York, N. Y. 10003

VIETNAM
Xunhasaba
19, Tran Quoc Toan
Hanoi

YUGOSLAVIA
Forum
Vojvode Mišića broj 1
Novi Sad
Jugoslovenska Knjiga
Terazije 27
Beograd

29. VIII. 1969

Index: 26.007

ACTA CHIMICA

ACADEMIAE SCIENTIARUM HUNGARICAE

TOMUS 61 FASCICULUS 2

AKADÉMIAI KIADÓ, BUDAPEST

1969

ACTA CHIM. ACAD. SCI. HUNG.

ACTA CHIMICA

A MAGYAR TUDOMÁNYOS AKADÉMIA KÉMIAI TUDOMÁNYOK OSZTÁLYÁNAK IDEGEN NYELVŰ KÖZLEMÉNYEI

Az Acta Chimica német, angol, francia és orosz nyelven közöl értekezéseket a kémiai tudományok köréből.

Az Acta Chimica változó terjedelmű füzetekben jelenik meg, egy-egy kötet négy füzetből áll. Évente átlag négy kötet jelenik meg.

A közlésre szánt kéziratok a szerkesztőség címére (Budapest 112/91 Műegyetem) küldendők.

Ugyanerre a címre küldendő minden szerkesztőségi levelezés. A szerkesztőség kéziratokat nem ad vissza.

Az Acta Chimica előfizetési ára kötetenként belföldre 120 Ft, külföldre 165 Ft. Megrendelhető a belföld számára az „Akadémiai Kiadó"-nál (Budapest V., Alkotmány utca 21. Bankszámla 05-915-111-46), a külföld számára pedig a „Kultúra" Könyv- és Hírlap Külkereskedelmi Vállalatnál (Budapest I., Fő utca 32. Bankszámla: 43-790-057-181) vagy annak külföldi képviseleteinél és bizományosainál.

Die Acta Chimica veröffentlichen Abhandlungen aus dem Bereiche der chemischen Wissenschaften in deutscher, englischer, französischer und russischer Sprache.

Die Acta Chimica erscheinen in Heften wechselnden Umfanges. Vier Hefte bilden einen Band. Jährlich erscheinen 4 Bände.

Die zur Veröffentlichung bestimmten Manuskripte sind an folgende Adresse zu senden:

Acta Chimica
Budapest 112/91 Műegyetem

An die gleiche Anschrift ist auch jede für die Redaktion bestimmte Korrespondenz zu richten.

Abonnementspreis pro Band: 165 Forint. Bestellbar bei dem Buch- und Zeitungs-Außenhandels-Unternehmen »*Kultúra*« (Budapest I., Fő utca 32. Bankkonto No. 43-790-057-181) oder bei seinen Auslandsvertretungen und Kommissionären.

Árpád Kiss
1889 — 1968

On 10th November, 1968, died, at the age of seventy-nine, Árpád Kiss, corresponding member of the Hungarian Academy of Sciences, retired professor of the József Attila University in Szeged, Hungary. A week later, a good many of his colleagues, disciples and admirers gathered to accompany this outstanding representant of Hungarian physico-chemists on his last journey, at Budapest.

Árpád Kiss, born at Sárospatak, Hungary, on 16th September, 1889, absolved his academic studies at the University of Budapest and obtained there his degree of Ph. D., in the institute of the late Professor Gustave Buchböck and under his personal guidance, as his assistant. The topic of his doctor's dissertation, entitled "On the rate of interaction between nitric oxide and chlorine", was quite up-to-date at its time, having been one of the first examples of the rare homogeneous gas reactions of the third order. The work of Árpád Kiss contributed materially to prove that the formation of nitrogen oxychloride is in fact a pure example of this highly interesting type of reactions, the theoretical interpretation of which, mainly of their very small and sometimes even negative temperature coefficients, raised considerable interest among the scientists concerned. The reliable experiments of Árpád Kiss could serve as a firm basis for these theoretical efforts, and so his name became indelible in any modern book on reaction kinetics.

A serious break in his scientific career was caused by the first world war. Soon after his recruitment, in August 1914, he fell, after having been wounded, in captivity and stayed on after the end of the war for several years in the Soviet Union, appointed by the Soviet Geographical Society as phytopathologist resp. botanist. It was in 1920 that he returned to Hungary. In those difficult times, following war and revolution, his scientific activity could hardly develop in the then so-called Third Chemistry Institute of the University, and before it could rise to fruitfulness, Árpád Kiss left the Insitute, recommended by G. Buchböck and the authorities of the University, to spend the years from 1921 to 1924 at Leyden University as an assistant of Schreinemakers. During his stay there, he resumed his research work in the field of reaction kinetics with remarkable success. He studied the catalytic effect of

bromine and nitrogen dioxide, respectively, on the formation of nitrogen oxychloride as well as the photochemical decomposition of the latter. These studies, too, furnished valuable data for the vigorously developing branch of reaction kinetics, *i. e.* that of clearing up reaction mechanisms. Á. Kiss himself was also interested in problems of reaction mechanisms, as shown by his papers on the mechanism of the formation of acetic acid and on homogeneous gas catalysis. In connexion with the latter, he was among the first to prove the occurrence of distinct intermediate compounds.

He returned to Hungary in 1924, to become professor at the University of Szeged, head of the Institute of General and Physical Chemistry, where he worked throughout his career, not only until his retirement but also afterwards, as far as his physical condition allowed it. At Szeged, he got intensively involved in another branch of reaction kinetics opening new perspectives at that time, namely in the so-called neutral salt effect on ionic reactions in aqueous solutions. He studied a considerable number of such reactions, not only with respect to the effect of varying salt concentration but also to that of temperature, so that enthalpy and entropy changes could be computed besides isothermal activity coefficients, making possible to link up the BRÖNSTED theory with that of DEBYE and HÜCKEL. Owing to their exemplary careful planning and to their exactitude, these studies contributed much to support the theory and to clear some controversial questions. Much later, Á. Kiss reverted to the same problems again, but now he studied the neutral salt effect on the activation parameters of the reactions, in view of the theory of absolute reaction rates, proving again his never relenting susceptibility to new ideas and views.

In natural connexion with the above kinetic studies, problems concerning the mechanisms of some of the reactions did arise, and Á. Kiss treated such questions repeatedly, too [reaction between iron(III), persulfate, iron(III)-cyanide ions, respectively, and iodide ions, investigation of triiodide equilibrium, mechanism of the reaction between monobromo-acetate and hydroxide ions].

Another study belonging to the sphere of salt effects was that of the salt error of the quinhydrone electrode, and the electrochemical methods used herein may have induced him to start, after having recognized their economical importance, electrochemical corrosion studies in Hungary, assisted by a group of his disciples. Though he did not achieve any significant scientific discoveries, his activities in this field were important because many of those who are concerned now with corrosion studies in Hungary came from his school.

It was a logical extension of his interests that he engaged himself in questions of the catalysis of ionic reactions, too. In this connexion, his attention was drawn to the catalytic effect of certain complexes, but soon it became the study of the complexes themselves, by the method of light absorption, which

took possession of his activities. His first publication dealing with light absorption dates back to 1934, and this remained, until the end, the domain of his further scientific interests.

He studied intensely the changes of the spectra characteristic of different metal ions in aqueous solution, caused by different salt additions, and could show that these changes are brought about by complex formation: entry of different anions into the coordination sphere of the central ion, instead of water molecules, results in characteristic band shifts and in the appearance of new bands, respectively. The evaluation of the experimental results was highly promoted by the method of band analysis, evolved for the resolution of overlapping bands. Later on, he extended his studies to metallic ion complexes formed with organic ligands. His measurements tell of great experimental reliability and circumspect planning, with elimination of disturbing effects, careful elucidation and consideration of any solvent effects. The vast experimental material gathered could serve afterwards as a firm basis for the elaboration of the ligand field theory; H. HARTMANN *e.g.* relied to a great extent on the experimental results of Á. Kiss. After the appearance of the theory, the new aspects opened by it were successfully applied by Á. Kiss himself to the interpretation of his experimental results. It may be noted that he was the first to ascertain complex formation with some metal ions whose tendency towards complexing was doubtful at that time. The last years of his activity were devoted to the task of putting the vast amount of experimental data into a systematic order, guided by the theoretical aspects, by assigning the found optical bands to certain spectroscopic transitions.

Besides the study of light absorption by complexes, he started extensive research work on the spectra of several groups of organic compounds (*e.g.* hydrocarbons with angularly condensed rings) in solution. Here too, experimental data of value have been compiled, and their explanation attempted on the basis of the so-called theory of oriented light absorption.

Á. Kiss was a never relenting searcher, exemplary as to experimental reliability and always accessible to new ideas. It was with this good example that he launched on their career generations of his disciples who are working now as valued experts in quite diverse fields of activities. His activity as professor was rewarded by the title of "Distinguished worker of high-school education" in 1953, and a year later by the Order of Labour. In appreciation of his research work, he was elected corresponding member of the Hungarian Academy of Sciences in 1954 and was awarded by the government with the "Kossuth Prize", in 1955.

Á. Kiss was, until his death, an active member of the Commission of Physical Chemistry of the Hungarian Academy and chairman of the Subcommission for Corrosion as long as this latter was in existence. Thus, he contributed successfully not only as professor but also as an active member of

the Chemistry Section of the Academy to the realisation of the goals set in our science policy.

The name of Á. Kiss will remain indelible not only in the history of physico-chemical research in Hungary, but also in the international literature of this special branch of science, so that his memory shall stay immune against fading.

G. SCHAY

List of papers published by Á. KISS

1. KISS, Á.: A radioaktivitás jelenségeinek tárgyalása kémiai szempontból (Discussion of radioactive phenomena from the chemical viewpoint). Sárospatak (1911) 1—136
2. KISS, Á.: A nitrogénoxid és chlor egymásrahatásának sebességéről (On the rate of the interaction between nitrous oxide and chlorine). Magyar Chemikusok Lapja **1** (1913) 1—26
3. KISS, Á.: Katalyse der Nitrosylchloridbildung durch Brom. Rec. Trav. Chim. Pays-Bas, **42** (1923), 112—145
4. Á. KISS: Über den Lichtzerfall des Nitrosylchlorids. Rec. Trav. Chim. Pays-Bas **42** (1923) 665—675
5. KISS, Á.: De stralingshypothese van de chemische reactiesnelheid. Chemisch Weekblad **20** (1923) 585—587
6. KISS, Á.: Theorie en experiment bei gasreacties. Chemisch Weekblad **21** (1924) 26—28
7. KISS, Á.: Katalyse der Nitrosylchloridbildung durch Nitrogendioxyd. Rec. Trav. Chim. Pays-Bas **43** (1924) 68—83
8. KISS, Á. und DEMÉNY, L.: Über den Mechanismus der Essigsäurebildung aus Aldehyd und Sauerstoff. Rec. Trav. Chim. Pays-Bas **43** (1924) 221—299
9. KISS, Á.: Über die Katalyse bei homogenen Gasreaktionen. Chemisch Weekblad **24** (1927) 46—49
10. KISS, Á. und BRUCKNER, Gy.: Über die Neutralsalzwirkung bei Ionreaktionen. I. Über die spezifische Ionenwirkung. Z. physik. Chem. **128** (1927) 71—86
11. KISS, Á. und LEDERER, E.: Über die Neutralsalzwirkung bei der durch Eisenionen katalysierten Zersetzung der Hydrogenhyperoxydlösungen. Z. physik. Chem. **129** (1927) 186—198
12. KISS, Á. und LEDERER, E.: Über den Mechanismus der durch Metallionen katalysierten Zersetzung der Hydrogenhyperoxyd-Lösungen. Rec. Trav. Chim. Pays-Bas **46** (1927) 453—456
13. KISS, Á. und ZOMBORY, L.: Über die Katalyse der Reaktion zwischen Persulfat- und Jodionen. Rec. Trav. Chim. Pays-Bas **46** (1927) 225—239.
14. KISS, Á.: Neutrális sóhatás iónreakciók esetén (Neutral salt effect in ionic reactions). Magy. Tud. Akad. Mat. Termtud. Értesítője **45** (1928) 193—198
15. KISS, Á. und BOSSÁNYI, I.: Über den Temperaturkoeffizienten der Neutralsalzwirkung. Rec. Trav. Chim. Pays-Bas **47** (1928) 619—626
16. KISS, Á. und BOSSÁNYI, I.: Über die Neutralsalzwirkung in konzentrierten Salzlösungen. Z. physik. Chem. **134** (1928) 26—32
17. KISS, Á. and BOSSÁNYI, I.: Über die spezifische Ionenwirkung. Acta Chem. Mineral. Physica Univ. Szeged **1** (1928) 60
18. KISS, Á.: Über die Katalyse der Reaktion zwischen Persulfat- und Jodionen. Rec. Trav. Chim. Pays-Bas **48** (1929) 508—526
19. KISS, Á.: A Brönsted féle reakciósebességi elmélet alapvonalai (Fundamentals of Brönsted's theory on the reaction rate). Magy. Chem. Folyóirat **35** (1929) 139—144
20. KISS, Á. und HATZ, E.: Über den Einfluss von Nichtelektrolyten auf die Geschwindigkeit der Ionreaktionen. Rec. Trav. Chim. Pays-Bas. **48** (1929) 7—17
21. KISS, Á.: A ferri- és jódion reakciójának mechanizmusáról (On the reaction mechanism of ferric and iodine ions). Magy. Chem. Folyóirat **36** (1930) 49
22. KISS, Á. und BOSSÁNYI, I.: Über die Neutralsalzwirkung der Ferri-Jodionen-Reaktion in verdünnten Lösungen. Z. anorg. allg. Chem. **19** (1930) 289—308
23. KISS, Á.: A neutrális sóhatás és katalízis ionreakciók esetén (Neutral salt effect and catalysis in ionic reactions). Magy. Chem. Folyóirat **37** (1931) 17—23
24. KISS, Á. und BOSSÁNYI, I.: Neutrális sóhatás a ferri- jódion-reakciónál tömény sóoldatokban (Neutral salt effect in the ferric-iodine ion reaction in concentrated salt solutions). Magy. Chem. Folyóirat **37** (1931) 121—133

25. KISS, Á. und BOSSÁNYI, I.: Über die Neutralsalzwirkung der Ferri-Jodionen-Reaktion in konzentrierten Lösungen. Z. anorg. allg. Chem. **198** (1931) 102—115
26. KISS, Á. und URMÁNCZY, A.: Über die Löslichkeit des Jodes in wässerigen Salzlösungen. Z. anorg. allg. Chem. 202 (1931) 172—190
27. KISS, Á. und BOSSÁNYI, I.: Über den Mechanismus der Persulfat-Jodionen-Reaktion. Rec. Trav. Chim. Pays-Bas **51** (1932) 434—444
28. KISS, Á., BOSSÁNYI, I. und URMÁNCZY, A.: Über die Katalyse der Persulfat—Jodionen-Reaktion durch Kobaltikomplexe. Acta Chem. Mineral. Physica Univ. Szeged **2** (1932) 210—220.
29. KISS, Á. und BOSSÁNYI, I.: Über die Neutralsalzwirkung in konzentrierten Salzlösungen. Z. physik. Chem. **A. 160** (1932) 290—294
30. KISS, Á. und VASS, P.: Über den Einfluss von Nichtelektrolyten auf die Geschwindigkeit der Ferri-Jodionen-Reaktion. Z. Anorg. allg. Chem. **206** (1932) 196—208
31. KISS, Á. und VASS, P.: Über die Neutralsalzwirkung der Thiosulfat- und Monobromazetationen-Reaktion. Z. anorg. allg. Chem. **209** (1932) 236—240.
32. KISS, Á.: A neutrális sóhatás törvényszerűségei tömény sóoldatokban (The laws of the neutral salt effect in concentrated salt solutions). Magy. Chem. Folyóirat **39** (1933) 162—168
33. KISS, Á. und KUKAI, R.: Über die Neutralsalzwirkung bei Ionenreaktionen in konzentrierten Lösungen. Z. Physik Chem. **A. 167** (1933) 354—364
34. KISS, Á. und KOCSIS, I.: Über die Neutralsalzwirkung bei der Hydrolyse des Essigsäureanhydrids. Acta Chem. Mineral. Physica Univ. Szeged **3** (1933) 50—66
35. KISS, Á. und URMÁNCZY, E.: Über die Neutralsalzwirkung bei der Reaktion zwischen Ameisensäure und Jod. Z. anorg. allg. Chem. **213** (1933) 353—364
36. KISS, Á. und BOSSÁNYI, I.: Über den Mechanismus der Ferricyan- und Jodionen-Reaktion. Rec. Trav. Chim. Pays-Bas **52** (1933) 289—297
37. KISS, Á., BOSSÁNYI, I. und VASS, P.: Über den Einfluss von Nichtelektrolyten auf die Geschwindigkeit von Ionenreaktionen. Acta Chem. Mineral. Physica Univ. Szeged **3** (1933) 20—35
38. KISS, Á. und BOSSÁNYI, I.: Über den Mechanismus der Monobromacetat- und Xanthogenationen-Reaktion. Acta Chem. Mineral. Physica Univ. Szeged **3** (1934) 99—111
39. KISS, Á. und BOSSÁNYI, I.: Über die Neutralsalzwirkung in konzentrierten Salzlösungen bei der Monochloracetat- und Xanthogenationen-Reaktion. Rec. Trav. Chim. Pays-Bas **53** (1934) 903—916
40. KISS, Á. und GESZNER, M.: Über die Ursache der Farbenänderungen der Kobaltosalze in Neutralsalzlösungen. Acta Chem. Mineral. Physica Univ. Szeged **4** (1934) 124—232
41. KISS, Á. und URMÁNCZY, A.: Messungen mit Wasserstoff- und Chinhydronelektroden in konzentrierten Salzlösungen. Z. Physik. Chem. *A.* **169** (1934) 31—40
42. KISS, Á. und URMÁNCZY, A.: Über die Dissoziationskonstanten von Ameisen- und Essigsäure in konzentrierten Salzlösungen. Z. physik. Chem. **A. 171** (1934) 257—267
43. KISS, Á. und VASS, P.: Über den Einfluss der Temperatur auf die Geschwindigkeit von Ionenreaktionen. Z. anorg. allg. Chem. **217** (1934) 305—320
44. KISS, Á. und URMÁNCZY, A.: Die Dunkelreaktion zwischen Natriumformiat und Jod. Z. anorg. allg. Chem. **219** (1934) 348—356
45. KISS, Á. und KUKAI, R.: Über den Einfluss der Temperatur auf die Geschwindigkeit von Ionenreaktionen II. Z. anorg. allg. Chem. **223** (1935) 149—160
46. KISS, Á. und BOSSÁNYI, I. Über den Einfluss der Temperatur auf die Geschwindigkeit von Ionreaktionen in wässerigen Nichtelektrolytlösungen. Z. anorg. allg. Chem. **224** (1935) 38—39
47. KISS, Á. und GERENDÁS, M.: Über die Feststellung der Extinktionskurven von gelösten Stoffen nach der photographischen Methode. Acta Chem. Mineral. Physica Univ. Szeged **4** (1935) 272—286
48. KISS, Á. und KUKAI, R.: Über die Neutralsalzwirkung der Acetylglycolat- und Hydroxylionen-Reaktion in verdünnten Lösungen. Rec. Trav. Chim. Pays-Bas **54** (1935) 337—344
49. KISS, Á., BOÉR, P. und GERENDÁS, M.: Über die Ursachen der Farbenänderungen von Nickelsalzen in Neutralsalzlösungen. Acta Chem. Mineral. Physica Univ. Szeged **4** (1935) 259—271
50. KISS, Á. und URMÁNCZY, A.: Über den Mechanismus von Reaktionen bei welchen die Reaktionskomponenten durch eine Membran diffundieren. Z. anorg. allg. Chem. **224** (1935) 40—48
51. KISS, Á. und KUKAI, R.: Über den Mechanismus der Acetylpropionat- und Hydroxylionen-Reaktion. Acta Chem. Physica Univ. Szeged **5** (1936) 17—29

52. KISS, Á. und BOSSÁNYI, I.: Über den Mechanismus der Monobromacetat- und Hydroxylionen-Reaktion. Acta Chem. Mineral. Physica Univ. Szeged **5** (1936) 10—23
53. KISS, Á.: Zur Konstitution der Sulfatoverbindungen. Z. anorg. allg. Chem. **226** (1936) 141—144
54. KISS, Á. und GERENDÁS, M.: Zur photographischen Aufnahme der Absorptionsspektren im Ultraviolett. Acta Chem. Mineral. Physica Univ. Szeged **5** (1937) 153—165
55. KISS, Á. und GERENDÁS, M.: Zur Lichtabsorption von Kobaltchloridlösungen. Z. physik. Chem. **A. 180** (1937) 117—130
56. KISS, Á., LAJTAI, I. und THURY, G.: Über die Löslichkeit von Gasen in Wasser-Nichtelektrolyt Gemischen. Z. anorg. allg. Chem. **233** (1937) 346—352
57. KISS, Á.: Zur Analyse der Extinktionskurven von Lösungen. Acta Chem. Mineral. Physica Univ. Szeged **6** (1937) 101—124
58. KISS, Á.: Erős elektrolitek elnyelési színképéről (On the absorption spectra of strong electrolytes). Magy. Chem. Folyóirat **42** (1937) 185—192
59. KISS, Á.: Hőmérséklet hatása ionreakciók sebességére (The effect of temperature on the rate of ionic reactions). Magy. Chem. Folyóirat **46** (1938) 14—21
60. KISS, Á. und URMÁNCZY, A.: Über die Löslichkeit des Chlors in wässerigen Salzlösungen. Acta Chem. Mineral. Physica. Univ. Szeged **6** (1938) 305—316
61. KISS, Á. und CZEGLÉDY, D.: Zur Lichtabsorption der Kobaltikomplexe, I. Z. anorg. allg. Chem. **235** (1938) 407—427
62. KISS, Á. und CZEGLÉDY, D.: Zur Konstitution der zweischaligen Komplexverbindungen. Z. anorg. allg. Chem. **239** (1938) 27—38
63. KISS, Á.: Zur Katalyse der Komplexverbindungen. Acta Chem. Mineral. Physica Univ. Szeged **7** (1939) 26—32
64. KISS, Á., CSOKÁN, P. und RICHTER, M.: Über den Wechsel der Koordinationszahl als Ursache der Farbenänderungen von Kobaltosalzlösungen. Acta Chem. Mineral. Univ. Szeged **7** (1939) 119—132
65. KISS, Á. und GEGŐ, M.: Zur Bestimmung von Ionengewichten nach der Dialysenmethode. Z. anorg. allg. Chem. **244** (1940) 57—66
66. KISS, Á. und CSOKÁN, P.: Zur Lichtabsorption der Kobaltrhodanid-Lösungen. Z. Physik. Chem. **A. 186** (1940) 239—247
67. KISS, Á. und RICHTER, M.: Zur Lichtabsorption von Kobaltchloridlösungen, 2. Nichtwässerige Lösungsmittel. Z. physik. Chem. **A. 187** (1940) 211—226
68. KISS, Á. und URMÁNCZY, A.: Über die Neutralsalzwirkung in der Reaktion zwischen Acetaldehyd und Chlor. Acta Chem. Mineral. Physica Univ. Szeged **7** (1940) 204—218
69. KISS, Á., ÁBRAHÁM, I. und HEGEDÜS, I.: Zur Lichtabsorption der Ferrikomplexe. Z. anorg. allg. Chem. **244** (1940) 98—110
70. KISS, Á. und CSOKÁN, P.: Zur Lichtabsorption von Kobaltrhodanidlösungen, 2. Wasser-Nichtelektrolyte als Lösungsmittel. Z. physik Chem. **A. 188** (1940) 27—40
71. KISS, Á. und CSOKÁN, P.: Zur Lichtabsorption von Nickelrhodanidlösungen. Z. anorg. allg. Chem. **245** (1941) 355—364
72. KISS, Á. und ÁCS, V.: Zur Bestimmung von Ionengewichten nach der Dialysenmethode, II. Z. anorg. allg. Chem. **247** (1941) 190—204
73. KISS, Á. und AUER, Gy.: Zur Lichtabsorption von organischen Verbindungen, I. Z. physik. Chem. **A. 189** (1941) 344—363
74. KISS, Á. und MAJOR, E.: Zur Lichtabsorption von Kobaltthiosulfatlösungen. Z. physik. Chem. **A. 189** (1941) 364—372
75. KISS, Á., AUER, Gy. und MAJOR, E.: Zur Lichtabsorption der Kobaltikomplexe, II. Z. anorg. allg. Chem. **246** (1941) 28—34
76. KISS, Á. und CSOKÁN, P.: Zur Lichtabsorption von Nickelrhodanidlösungen, 2. Nichtwässerige Lösungen. Z. anorg. allg. Chem. **247** (1941) 205—210
77. KISS, Á., BÁCSKAI, GY. und VARGA, E.: Zur Lichtabsorption der aromatischen Schiff-Basen. Acta Chem. Physica Univ. Szeged **1** (1942) 156—168
78. KISS, Á., CSOKÁN, P. und NYIRI, G.: Zur Lichtabsorption der polycyklischen innerkomplexen Verbindungen. Z. physik. Chem. **A. 190** (1942) 65—80
79. KISS, Á., BÁCSKAI, GY. und CSOKÁN, P.: Zur Lichtabsorption der polycyklischen Komplexverbindungen, II. I. prakt. Chem. N. F. **160** (1942) 1—20
80. KISS, Á. und NYIRI, G.: Zur Lichtabsorption der polycyklischen innerkomplexen Verbindungen, III. Z. anorg. allg. Chem. **249** (1942) 340—352
81. KISS, Á. und SZABÓ, R.: Zur Lichtabsorption der polycyklischen innerkomplexen Verbindungen, IV. Z. anorg. allg. Chem. **252** (1943) 172—184
82. KISS, Á., FODOR, G. and LÓZSA, A.: Investigations of the interaction of several chromophores in the same molecule. Acta Chem. Physica Univ. Szeged **21** (1948) 25—30

83. KISS, Á. und CSETNEKY, E.: Über die Mesomerie der Sulfogruppe. Acta Chem. Physica Univ. Szeged **2** (1948) 30—32
84. KISS, Á. und BÁCSKAI, Gy.: Zur Lichtabsorption der Antipyrinkomplexe. Acta Chem. Physica Univ. Szeged **2** (1948) 48—49
85. KISS, Á.: A Szegedi egyetem általános és szervetlen kémiai intézetének munkássága (The activity of the Institute for General and Inorganic Chemistry of the University of Szeged). Magyar Kém. Lapja **3** (1948) 141—144
86. KISS, Á.: Szerves vegyületek fényelnyeléséről (On the light absorption of organic compounds). Magyar Kém. Lapja **3** (1948) 349—395
87. KISS, Á. et SÁNDORFY, K.: Sur les méthodes d'analyse des courbes d'absorption. Acta Chem. Physica Univ. Szeged **2** (1948) 71—76
88. KISS, Á. and PAUNCZ, R.: On the absorption of light by isomeric derivatives of benzylaniline. Acta Chem. Physica Univ. Szeged **2** (1948) 83—89
89. KISS, Á., MOLNÁR, I. et SÁNDORFY, K.: Les spectres d'absorption phénoliques et leur interprétation théorique. Compt. Rend. Acad. Sci. Paris **227** (1948) 724—727
90. KISS, Á. und HYROSS, J.: Zur Lichtabsorption der Nitroderivate des Benzols. Acta Chem. Physica Univ. Szeged **2** (1948) 76—82
91. KISS, Á. und CSETNEKY, E.: Über den Einfluss der Ionisation auf die Extinktionskurven von Benzolderivaten. Acta Chem. Physica Univ. Szeged **2** (1948) 37—47
92. KISS, Á. und CSETNEKY, E.: Über die mesomere und induktive Wirkung der Aminogruppe. Acta Chem. Physica Univ. Szeged **2** (1948) 132—138
93. KISS, Á. and BIRÓ, K.: On the light absorption of polychromates. Acta Chem. Physica Univ. Szeged **2** (1948) 90—95
94. KISS, Á.: Zur Lichtabsorption der *o*-, *m*- und *p*-disubstituierten Benzolderivate. Acta Chem. Physica Univ. Szeged **2** (1948) 129—132
95. KISS, Á. und SZŐKE, S.: Zur Lösungsmittelabhängigkeit der Extinktionskurven von polycyklischen Komplexen. Acta Chem. Physica Univ. Szeged **2** (1949) 155—162
96. KISS, Á., FODOR, G. and MOLNÁR, I.: The mesomerism of propenylbenzene and allylbenzene derivatives. Acta Chem. Physica Univ. Szeged **2** (1949) 189—191
97. KISS, Á. et SÁNDORFY, K.: Les spectres d'absorption des ions hydratés. Revue Scientifique Paris **87** (1949) 37—41
98. KISS, Á., MOLNÁR, I. et SÁNDORFY, K.: Les spectres d'absorption des dérivés phénoliques. Bull. Soc. Chim. France **16** (1949) 275—282
99. KISS, Á.: Sur les spectres d'absorption de dérivés naphtaléniques. Compt. Rend. Acad. Sci. Paris **229** (1949) 762—763
100. KISS, Á. und FAREDIN, I.: Zur Lichtabsorption der Komplexe von Aminobenzolsulfosäuren. Acta Chem. Physica Univ. Szeged **2** (1949) 212—217
101. KISS, Á., VINKLER, E. und CSETNEKY, E.: Zur Lichtabsorption der N-(aryl-thioalkyl)-phthalimid-Derivate. Acta Chem. Physica Univ. Szeged **2** (1949) 192—196
102. KISS, Á. et CSETNEKY, E.: L'influence de l'ionisation sur les courbes d'absorption des dérivés benzéniques. Compt. Rend. Acad. Sci. Paris **228** (1949) 1423—1426
103. KISS, Á.: Spektroszkópiai irányú kutatásaink eredményei és célkitűzései (Results and objects of our research work in spectroscopy). Magy. Kém. Folyóirat **56** (1950) 41—43
104. KISS, Á.: Über den Einfluss von Lösungsmitteln auf die Extinktionskurven von organischen Verbindungen. Acta Chem. Physica Univ. Szeged **2** (1950) 235—238
105. KISS, Á.: Az orientált fényelnyelés elméletének kísérleti ellenőrzése (Experimental verification of the theory of oriented light absorption). Magy. Tud. Akad. Kém. Osztályk. **2** (1952) 329—338
106. KISS, Á.: Eine Theorie der Lichtabsorption von Komplexverbindungen. Z. anorg. allg. Chem. **282** (1955) 141—148
107. KISS, Á.: Zur Lichtabsorption von Komplexverbindungen. Tagungsber. Chem. Ges. DDR Hauptjahrestagung 1954. Akad. Verlag Berlin 1955, 45—54
108. KISS, Á.: A hidratált ionok fényelnyeléseinek törvényszerűségei (Principles of the light absorption of hydrated ions). Magy. Tud. Akad. Kém.Osztályk. **6** (1955) 37—46
109. KISS, Á.: Az elekrosztatikus kötésű komplexek fényelnyelése (The light absorption of complexes with electrostatic bonding). Magy. Tud. Akad. Kém. Osztályk. **6** (1955) 77—87
110. KISS, Á.: A naftalinszármazékok fényelnyelése (The light absorption of naphthaline derivatives). Magy. Tud. Akad. Kém. Osztályk. **6** (1955) 47—61
111. KISS, Á.: Az angulárisan kondenzált aromás szénhidrogének fényelnyelése (The light absorption of aromatic hydrocarbons with angularly condensed ring systems). Magy. Tud. Akad. Kém. Oszt. Közl. **6** (1955) 63—76
112. KISS, Á.: A sztérikus gátlás hatása a fényelnyelésre (The effect of steric hindrance on light absorption). Magy. Tud. Akad. Kém. Osztályk. **6** 27—35 (1955)

113. KISS, Á.: A kobalti komplexek fényelnyelésének mechanizmusa (On the mechanism of the light absorption of cobaltic complexes). Magy. Tud. Akad. Kém. Osztályk. **8** 59—66 (1956)
114. KISS, Á., CSÁSZÁR, J. and LEHOTAI, L.: Az acetilaceton komplexek fényelnyelése (The light absorption of acetylacetone complexes). Magy. Tud. Akad. Kém. Osztályk. **8** 149—155 (1956)
115. KISS, Á.: Zur Lichtabsorption der kondensierten aromatischen Verbindungen. I. Weiterbau der Theorie der orientierten Lichtabsorption. Acta Chim. Acad. Sci. Hung. **8** 345—354 (1956)
116. KISS, Á.: Az atomkötésű komplexek fényelnyelése (The light absorption of complexes with atomic bonds). Magy. Tud. Akad. Kém. Osztályk. **7** 367—377 (1956)
117. KISS, Á.: Über den Mechanismus der Lichtabsorption von hydratisierten Atomionen. Acta Chim. Acad. Sci. Hung. **10** 39—49 (1956)
118. KISS, Á.: Über die Beeinflussung der Lichtabsorption durch sterische Hinderung. I. Systematik der Wirkungsarten. Acta Chim. Acad. Sci. Hung. **10** 208—216 (1956)
119. KISS, Á.: Über die Bedeutung der Absorptionskurven in der Strukturforschung gelöster Komplexe. Acta Phys. et Chem. Szeged **11** 102—109 (1956)
120. KISS, Á.: Zur Lichtabsorption der kondensierten aromatischen Verbindungen. II. Die Lichtabsorption der linear kondensierten aromatischen Verbindungen. Acta Chim. Acad. Sci. Hung. **11** 85—98 (1957)
121. KISS, Á.: Zur Lichtabsorption der kondensierten aromatischen Verbindungen. III. Die Lichtabsorption der annular kondensierten aromatischen Verbindungen. Acta Chim. Acad. Sci. Hung. **11** 99—111 (1957)
122. KISS, Á.: Mechanismus der Lichtabsorption der Komplexe mit kovalenten Bindungen. Acta Chim. Acad. Sci. Hung. **11** 113—123 (1957)
123. KISS, Á.: Mechanismus der Lichtabsorption der Komplexe mit elektrostatischen Bindungen. Acta Chim. Acad. Sci. Hung. **10** 373—386 (1957)
124. KISS, Á. and MUTH, B. A.: Ultraviolet light absorption of monosubstituted benzene derivatives containing elements of the oxygen group. Acta Chim. Acad. Sci. Hung. **22** 397—480 (1960)
125. KISS, Á. und CSÁSZÁR, I.: Lichtabsorption der *o*-Phenanthrolinkomplexe. Acta Chim. Acad. Sci. Hung. **38** 405—419 (1963)
126. KISS, Á. und CSÁSZÁR, I.: Lichtabsorption der 2,2'-Dipyridylkomplexe. Acta Chim. Acad. Sci. Hung. **38** 421—434 (1963)
127. KISS, Á.: Theorie der Lichtabsorption der Cyclopentadienyl-Komplexe der Übergangselemente. Acta Chim. Acad. Sci. Hung. **56** (1968) 215—219

Acta Chimica Academiae Scientiarum Hungaricae, Tomus 61 (2), pp. 115—124 (1969)

MECHANISM OF ADSORPTION INDICATION, I

NITRONIC ACIDS AS ADSORPTION INDICATORS: *p*-NITRO-α-NAPHTHYL RED, A NEW ADSORPTION INDICATOR

L. LÉGRÁDI

(Nitrochemical Works Fűzfőgyártelep)

Received February 2, 1968

A new adsorption indicator, *p*-nitro-α-naphthyl red is recommended for the titration of cyanide, bromide and iodide ions. Titration of cyanide should be performed in neutral or alkaline medium (pH 9—10.5), and of iodide and bromide ions in alkaline medium. The indicator has acid–base properties, but the mechanism is different from that of any other basic dye known so far. The dye adsorbate is an acid–base indicator on uncharged or positively charged precipitates, and forms nitronic acid on alkalizing, which process is accompanied by a colour change. In the titration of cyanide ions nitronic acid is formed when silver ions are present in excess, the original structure is restored however on adding cyanide ions. In titrations made in alkaline medium the reason for the colour change is that the dissociation constant of the dye adsorbate, which is very small when anions are in excess, increases on adding silver ions in excess, and the dye adsorbate forms nitronic acid. The indicator effect can be demonstrated by the variation of the dissociation constant of the dye adsorbate with increasing excess of self-ions and by the formation of nitronic acid on positively charged precipitate on alkalizing the solution.

Phenyl-azo-α-naphthyl-amine, or α-naphthyl red is a suitable adsorption indicator in the titration of bromide, iodide and thiocyanate ions [1]. The *o*-ethyl- [2] and *p*-ethoxy [3] derivatives of the compound have been prepared, and their application as adsorption indicators reported earlier. Furthermore, also nitro group was introduced into the phenyl-azo-α-naphthyl-amine molecule. Nitroaniline isomers were diazotized and coupled with α-naphthyl-amine-hydrochloride. The synthesis can be described by the following reaction equation, for *p*-nitroaniline:

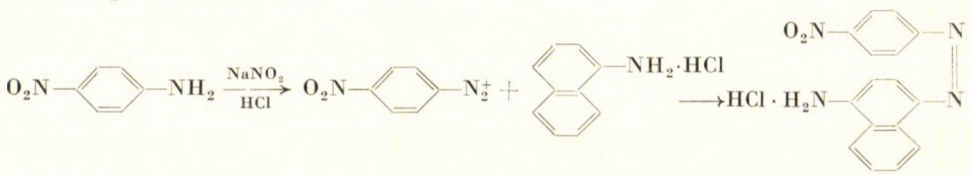

Experimental

Our investigations disclosed that out of the nitro-phenyl-azo-α-naphthyl amines, the *meta* compound is an indicator base with a pH interval of 3—4.5, the *ortho* compound is an amphoteric indicator, in which the acidic character is weak, the pH intervals are between 3.8 and 5.5, and between 8.4 and 9.6.

With the *para* compound the indicator-acid and indicator-base characteristics are equally strong, the latter being observable only in alcoholic medium, its pH interval is between 3.5 and 5.5. The colour of the indicator bases is red in acid and yellow in alkaline medium.

Of the mentioned compounds *p*-nitro-α-naphthyl red proved to be the best as an argentometric indicator. Further experiments were performed with this indication. In Table I the results of argentometric titrations are given. Volumes of consumed standard solution are the mean values of three measurements. The results of titrations carried out in the presence of indicator were compared to the results of potentiometric titrations. The latter were made with a Titri-pH-meter (Radelkisz, Budapest), with silver and saturated calomel electrodes. To characterize the accuracy of measurements the standard deviations in the titration of 10 ml portions of solution were determined. In the titration of cyanide with 0.1 *M* silver nitrate the standard deviation was found to be ± 0.044 ml, of cyanide with 0.01 *M* silver nitrate, ± 0.052 ml, in the titration of bromide and iodide with 0.1 *M* standard solution, ± 0.040 ml. The measurements were made in alkaline medium, to 50 ml solution 1—2 drops of 1 *M* sodium hydroxide were added (pH = 9.0—10.5). In acid medium, in contrast to the former derivatives [1, 2, 3], no colour change was observed. 0.1% solution of the indicator in alcohol was used in each case. With 0.01 *M* silver nirate solution only cyanide and iodide ions could be titrated. With titration of anions, after reaching colour change, the original colour can be resumed by adding small excess of anions.

Investigation of the mechanism of indication

Using *p*-nitro-α-naphthyl red as model substance, the mechanism of azo dyes, containing both nitro and amino groups as absorption indicators was investigated. For this purpose the following measurements were made: a) the variation of the dissociation constant of the dye adsorbate was measured with increasing concentration of excess self ion; b) the acid–base character of the indicator was investigated on different precipitates. Proton releasing or uptake, as indicated by pH changes, could not be observed during titration.

1. *Measurement of the variation of the dissociation constant*

Measurements were carried out similarly to those described in our earlier papers [2, 3]. The results are given in Table II. As shown by the data, dye adsorbates are amphoteric indicators, except silver bromide. The change of the dissociation constant of the indicator base caused by excess self ions is very small, therefore the indicator cannot be used in the titration of anions in weakly acid medium. The change of the dissociation constant of the indicator

Table I

Titration of anions with silver nitrate in the presence of p-nitro-α-naphthyl red as indicator

Ion	$AgNO_3$ standard solution	Indicator ml	Medium	Colour change	Consumed $AgNO_3$, ml (potentiometric indicator)		Deviation	
							ml	%
Cyanide	0.1 *M*	1	—	from violet-red to blue	4.90	4.92	+0.02	0.4
Cyanide	0.01 *M*	0.3	1 drop of 1 *M* NaOH; pH = 9	from violet to blue	9.78	9.85	+0.07	0.7
Bromide	0.1 *M*	0.4	2 drops of 1 *M* NaOH; pH = 10.5	from yellow to blue	10.01	10.03	+0.02	0.2
Iodide	0.01 *M*	0.3	2 drops of 1 *M* NaOH; pH = 10.5	from yellow to green	10.12	10.9	—0.03	0.3

Acta Chim. Acad. Sci. Hung. 61, 1969

Table II

The dye-adsorbate as acid–base indicator

Adsorbed substance: 4-(4'-nitrophenyl-azo)-1-naphthyl-amine hydrochloride

Adsorbent	Excess self ion, equiv.	pH interval	Dissociation constant		Colour change
			K_1	K_2	
Silver cyanide	50% Ag^+	3.3—4.0 and 6.0— 6.5	$2.24 \cdot 10^{-4}$	$5.62 \cdot 10^{-7}$	From red to violet-red and from violet to blue
	10% Ag^+	4.0—4.5 and 7.0— 8.5	$5.62 \cdot 10^{-5}$	$1.78 \cdot 10^{-8}$	
	Equiv. point	4.5—5.5 and 8.0— 9.5	$1.00 \cdot 10^{-5}$	$1.78 \cdot 10^{-9}$	
	10% CN^-	4.5—5.5 and 10.5—11.5	$1.00 \cdot 10^{-5}$	$1.00 \cdot 10^{-11}$	difficult
	50% CN^-	4.5—5.5 and 11.5—13	$1.00 \cdot 10^{-5}$	$5.62 \cdot 10^{-13}$	to see
Silver iodide	50% Ag^+	2.8—3.2 and 6.5— 7.5	$1.00 \cdot 10^{-3}$	$1.00 \cdot 10^{-7}$	From pale pink to orange and from orange to green
	10% Ag^+	3.0—3.5 and 7.0— 8.0	$5.62 \cdot 10^{-4}$	$3.16 \cdot 10^{-8}$	
	Equiv. point	3.2—3.6 and 8.0— 9.0	$3.98 \cdot 10^{-4}$	$3.16 \cdot 10^{-9}$	
	10% I^-	3.2—3.6 and 11 —13.0	$3.98 \cdot 10^{-4}$	$1.00 \cdot 10^{-12}$	difficult to observe in acid medium
	50% I^-	— above 14		below 10^{-14}	
Silver bromide	50% Ag^+	3.0—4.0 and 6.0— 7.5	$3.16 \cdot 10^{-4}$	$1.78 \cdot 10^{-7}$	From orange grey to grey and from grey to dark grey
	10% Ag^+	6 —7.5		$1.78 \cdot 10^{-7}$	
	Equiv. point	6 —7.5		$1.78 \cdot 10^{-7}$	From brownish violet to grey
	10% Br^-	6.5—8.0		$1.78 \cdot 10^{-8}$	
	50% Br^-	6.5—8.0		$1.78 \cdot 10^{-8}$	From violet to brown
Silver chloride	50% Ag^+	3.5—4.0 and 7.6— 8.0	$1.78 \cdot 10^{-4}$	$1.59 \cdot 10^{-8}$	From pale pink to orange
	10% Ag^+	3.0—3.6 and 7.5— 8.5	$5.01 \cdot 10^{-4}$	$1.00 \cdot 10^{-8}$	which turns to pale violet;
	Equiv. point	3.0—4.0 and 8.5— 9.9	$3.16 \cdot 10^{-4}$	$6.31 \cdot 10^{-10}$	weak colour change
	10% Cl^-	3.0—4.0 and 10.8—11.5	$3.16 \cdot 10^{-4}$	$7.08 \cdot 10^{-12}$	
	50% Cl^-	3.0—4.0 and 12.5—13.5	$3.16 \cdot 10^{-4}$	$1.00 \cdot 10^{-13}$	
Silver thiocyanate	50% Ag^+	3.8—4.3 and 7.1— 8.0	$8.91 \cdot 10^{-5}$	$2.82 \cdot 10^{-8}$	From red to yellow and from
	10% Ag^+	3.8—4.3 and 7.0— 8.2	$8.91 \cdot 10^{-5}$	$2.51 \cdot 10^{-8}$	yellow to grey
	Equiv. point	3.8—4.3 and 8.5— 9.5	$8.91 \cdot 10^{-5}$	$1.00 \cdot 10^{-9}$	From red to violet then to blue
	10% CSN^-	3.8—4.3 —	$8.91 \cdot 10^{-5}$	—	no colour change
	50% CSN^-	3.8—4.3 —	$8.91 \cdot 10^{-5}$	—	From red to violet then to blue no colour change

as indicator acid is remarkable, especially on adding anion in excess, therefore the indicator can be used in the titration of anions in alkaline medium. Greatest changes were observed, and best results obtained with cyanide and iodide ions. The change of the dissociation constant is sufficiently great in the case of silver chloride, but the colour change is weak, and so it is in the end-point of the titration of chloride ions. With silver bromide, the dye adsorbate is a weak indicator acid, showing only a small change on the addition of excess self ions, accordingly the colour change in the end-point of titrations is only small. In the case of silver thiocyanate there occurs no acid–base indication in the presence of excess self ion, consequently the indicator shows no colour change at the end-point of the titration of thiocyanate ions, even with 0.1 *M* silver nitrate standard solution.

2. *Colour change of the indicator on various precipitates*

In Table III the colour changes of *p*-nitro-α-naphthyl red on various silver precipitates are presented, depending on the charge of precipitate and pH of the medium. The negatively charged precipitates showed no acid–base indicator properties. With uncharged precipitates, the dye adsorbed on silver thiocyanate and silver cyanide is a good acid–base indicator, *i.e.* there is a great difference between the neutral and alkaline colours, while on silver halides the colour difference is only small. Accordingly, nitronic acid indication does not occur on silver halide precipitates on adding self ion excess, only on alkalizing. In the case of positively charged precipitates remarkable difference between neutral and alkaline colour can only be observed for silver cyanide. The greatest difference can be observed between the neutral and alkaline colours of the indicator absorbed on positively charged precipitates, which is most favourable from the point of view of the sharpness of transition at the end-point of titrations.

Discussion

All adsorption indicators with acid–base properties are azo dyes which are positively charged in acid, and uncharged in alkaline medium. They work as adsorption indicators as follows: in the presence of cation excess the adsorbed dye releases proton and shows its neutral or alkaline colour, in the presence of anion excess it takes up proton and shows its acid colour [4].

In the case of *p*-nitro-α-naphthyl red also acid–base indication is in question. The difference from the former is that this is an indicator acid, titrations have to be made in alkaline medium, and colour change takes place

Table III

Colourchange of p-nitro-α-naphthyl red on silver precipitates

Adsorbent	Positively charged precipitate			Uncharged precipitate			Negatively charged precipitate		
	acid	neutral	alkaline	acid	neutral	alkaline	acid	neutral	alkaline
	medium			medium			medium		
AgCl	grey	violet-grey	Ag_2O precipitated	violet-red	violet-grey	grey	pale violet	light grey	grey
AgBr	greyish white	greyish white	Ag_2O precipitated	pink	yellow	greenish grey	grey	grey	grey
AgI	greyish white	yellow	greenish yellow	flesh-pink	yellow	greenish yellow	dark yellow	yellow	light yellow
AgSCN	brownish red	orange-brown	grey	red	violet-red	violet-blue	violet-red	violet-red	violet
AgCN	violet-red	orange	blue	red	orange	violet-blue	pink	orange-grey	grey

without uptake or release of proton. Although nitronic acids have not yet been used as adsorption indicators, argentometric titrations have already been made in weakly alkaline medium. Titrations were carried out in the presence of resorcinol-quinoline as indicator, in aqueous ammonia [5]. Earlier also ammonium carbonate was used in the determination of chloride and iodide ions in the presence of eosine as indicator [6]. Dilute sodium hydroxide was used in the case of Rodamin 6G and phenosafranine [7], and also phthalein-complexone and xylenol orange can be used in dilute, aqueous ammonia or sodium hydroxide [8]. In these cases the application of alkaline medium is a possible way of performing the titration, but not the only way. The mentioned indicators are of quite different structure and the mechanism of their operation is also different, they work on the basis of surface precipitate formation or redox reaction. These compounds cannot help us to understand the operation of *p*-nitro-α-naphthyl red as adsorption indicator.

The mechanism of indication can be given as follows: *p*-nitro-α-naphthyl red is an indicator base in aqueous medium:

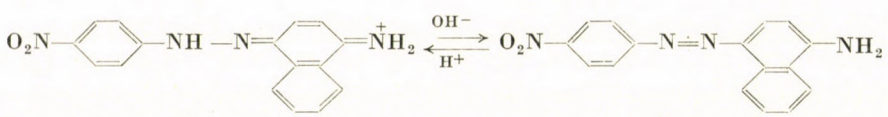

red yellow

In aqueous medium no indicator acid is formed. In alcohol the dye is red, turning to violet-red on acidifying. Nitronic acid is formed also in neutral solution, which causes red colour, but the process is promoted by adding alkali solutions:

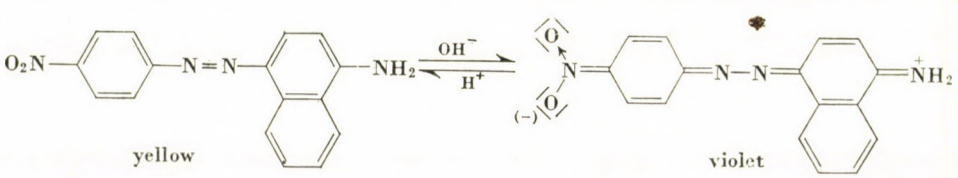

yellow violet

The dye adsorbed on uncharged or positively charged silver cyanide precipitate shows acid–base properties. This acid–base indicator is amphoteric, and turns to red from violet on acidifying and to blue from violet on alkalizing:

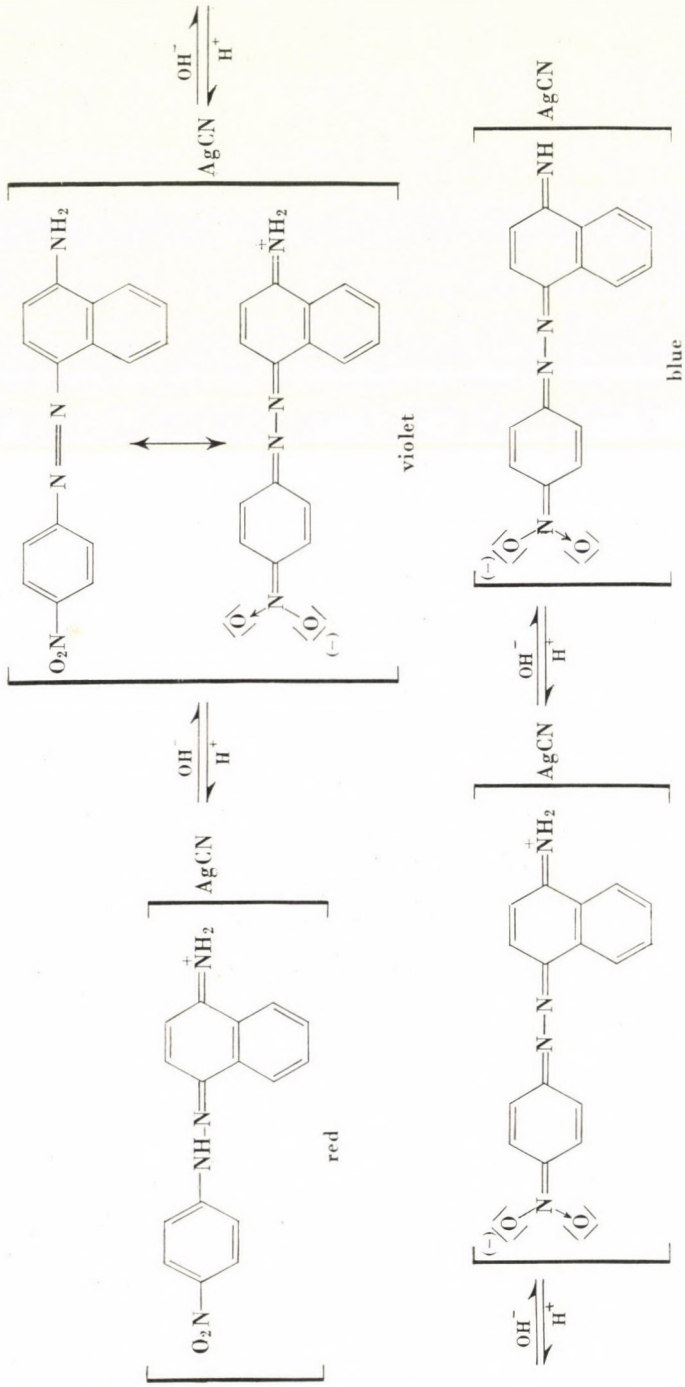
OH⁻
H⁺
AgCN
violet
red
blue

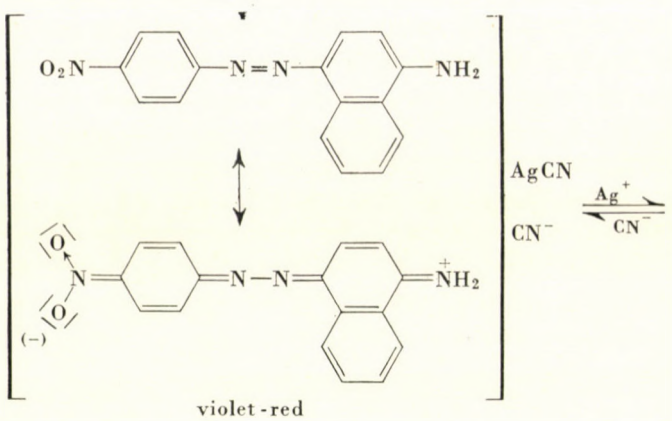

violet-red

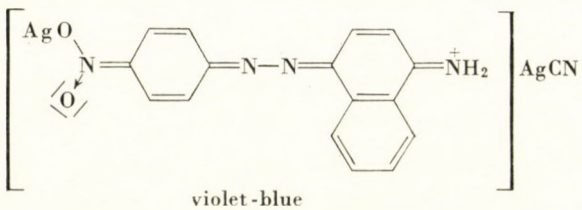

violet-blue

In argentometric titrations violet-blue colour occurs at silver ion excess and violet-red at cyanide ion excess. The effect of silver ions is the same as that of alkali, and that of cyanide ions as that of acid, the shades being, however, different, not pure red and blue colours but the violet shades are obtained. On adding silver and cyanide ions, the same structural change takes place as on alkalizing or acidifying. Silver ion can produce a salt with nitronic acid. On adding 10—20% excess of silver ions, the silver salt of the dye decomposes, the violet-blue colour turns to greyish violet, which turns to brown on longer standing, probably due to oxidation. The above mechanism is supported by the experimental evidence that when silver ions are titrated with potassium cyanide in the presence of *p*-nitro-α-naphthyl red as indicator, no violet-blue colour can be obtained. The colour turns to light violet from dark violet, the change being perceptible about 5% after the equivalence point. The violet-blue colour is caused by the formation of a positively charged silver salt of nitronic acid which cannot be formed here on positively charged precipitate in the presence of excess silver ions, therefore no blue colour appears.

If the solution is alkalized with sodium hydroxide, not only cyanide, but also halide ions can be titrated with silver nitrate standard solution in the presence of *p*-nitro-α-naphthyl red as indicator. In the titration of iodide ions the indicator shows no colour change until the equivalence point is reached. Here, on adding silver ions in excess, the indicator turns to green from yellow. This process does not take place in the absence of alkali. The degree of alkalizing

depends on the dissociation constant of the dye adsorbate. Too high alkali concentration is disadvantageous, since a not distinct colour change takes place before the equivalence point. The green colour formed in the presence of excess silver ions turns to yellow again on adding iodide in excess. The mechanism of indication here can be explained as follows: in the presence of anions in excess, the dissociation constant of the dye adsorbate is small, so nitronic acid cannot be formed even in alkaline medium, the dye shows its acid colour. In the presence of silver ions in excess the dissociation constant increases and in alkaline medium nitronic acid is formed.

This mechanism in the alkaline medium is evidenced by the following facts: a) Remarkable decrease of the dissociation constant on adding the anion in excess; this decrease is greater than found for any other basic dye known so far. b) The dye adsorbate is an acid–base indicator on uncharged or positively charged precipitates, the alkaline colour being the same as that produced by excess silver ions during argentometric titrations.

The position of the nitro group in the indicator molecule. Indicators were prepared from three isomeric nitro-anilines by diazotizing and coupling with α-naphthyl amine. The position of the nitro group proved to be important from the point of view of indicator properties. Only the *p*-nitro compound can be used for determining cyanide ions, iodide and cyanide ions can be titrated by means of the *m*-nitro compound only in the presence of alkali and the colour change is not sharp, while the *o*-nitro derivative cannot be used at all as an indicator.

REFERENCES

1. TANDON, K. N., MEHROTRA, R. C.: Anal. Chim. Acta **27,** 97 (1962)
2. LÉGRÁDI, L.: Magyar Kém. Folyóirat, **70,** 27 (1964); Acta Chim. Acad. Sci. Hung. **42,** 107 (1964)
3. LÉGRÁDI, L.: Magyar Kém. Folyóirat **70,** 404 (1964); Acta Chim. Acad. Sci. Hung. **47,** 103 (1966)
4. PUNGOR, E., SCHULEK, E.: Z. anal. Chem. **150,** 116 (1956)
5. MEHROTRA, R. C.: Proc. Nat. Acad. Sci. (Alld.) **15,** 148 (1946); **16,** 31 (1947)
6. KOLTHOFF, I. M.: Z. anal. Chem. **70,** 395 (1927); **71,** 235 (1927)
7. MARTINEZ, S. P.: Anales Univ. Murcia **15,** 41 (1956—57)
8. MEHROTRA, R. C., TANDON, K. N.: Talanta **11,** 1093 (1964)

László LÉGRÁDI; Fűzfőgyártelep, Hungary

Acta Chimica Academiae Scientiarum Hungaricae, Tomus 61 (2), pp. 125—131 (1969)

MECHANISM OF ADSORPTION INDICATION, II

AMPHOTERIC ADSORPTION INDICATORS

L. LÉGRÁDI

(Nitrochemical Works Fűzfőgyártelep)

Received February 2, 1968

The acid–base and adsorption indicator properties of the phenylazo-α-naphthylamine molecule substituted with groups having $+M$ and $-M$ effect were investigated. It was found that the properties of the substance are determined by the nature of the group situated in the para position to the azo-nitrogen. An amphoteric adsorption indicator was prepared by diazotizing 4-nitro-2-anisidine and coupling the diazotized product with α-naphthylamine. In the presence of amphoteric adsorption indicators an ion can be titrated both in acid and in alkaline medium, when different colour changes can be observed. The indicators operate according to the acid–base principle, which can be demonstrated by measuring the pH change during the titration in acid medium and by determining the change of the dissociation constant in acid and alkaline medium on adding self ion in excess.

By introducing ethoxy group which has $+M$ effect into phenylazo-α-naphthylamine a strong indicator base [1], and by introducing nitro group which has $-M$ effect, an indicator acid was obtained [2], which proved to be good adsorption indicators.It was also examined, how the acid–base character and adsorption indicator properties of the compound change when two substituents with $+M$ and $-M$ effect, respectively are introduced. Nitroanisidines were diazotized and coupled with α-naphthylamine. The following azo compounds were obtained:

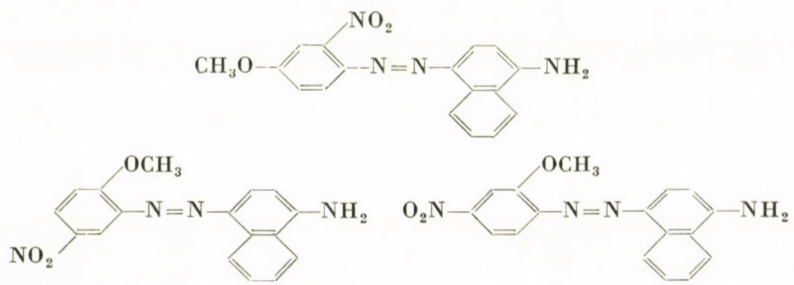

Experimental

The first and second compounds are indicator bases with pH intervals of 2.2—3.6 and 2.5—3.8, respectively, while the third compound is an amphoteric indicator, although showing no colour change in solution. The acid colour of the first and second compounds is red, the alkaline colour orange or yellow. The indicators were used in argentometric titrations. All three

indicators were applied as 0.1—0.2% solution in alcohol, in two ways: in weakly acid medium as indicator base, and in weakly alkaline medium, as indicator acid. The *p*-methoxy-*o*-nitro derivative could only be used in acid medium as indicator base, while the *m*-nitro-*o*-methoxy derivative both in acid and alkaline medium, the colour change in alkaline medium being, however, weak. The *p*-nitro-*o*-methoxy compound shows sharp colour change both in acid and alkaline medium in the titration of bromide and iodide ions. The results of titrations are given in Table I. The volumes of consumed titrant are the mean values of three measurements. The volume of titrated solution was 50 ml. The results were compared with those obtained by the potentiometric method. Potentiometric titrations were made with a Titri-pH-meter (Radelkisz, Budapest), with silver and saturated calomel electrodes. With 0.01 *M* silver nitrate solution only iodide ions could be titrated. Thiocyanate ions could not be titrated with either of the three indicators studied. In the titration of anions, after the colour change has taken place, the original colour can be resumed by adding anions in a small excess. Silver nitrate could only be titrated with 0.1 *M* potassium iodide solution in acid medium; with the *o*-methoxy-*m*-nitro compound the colour changes from yellow to red, with the *o*-nitro-*p*-methoxy derivative from brown to blue, while with the *p*-nitro-*o*-methoxy compound the colour change is weak. With the compounds as indicator acids titrations have to be carried out at pH = 10—11. The standard deviation was ± 0.06 ml in the titration of iodide ions in neutral solution, and ± 0.05 ml in the titration of cyanide ions and also of bromide and chloride ions in alkaline solution.

Mechanism of indication

The examinations were made with *p*-nitro-*o*-methoxyphenylazo-α-naphthylamine, the indicator being applicable both in acid and alkaline medium. In order to demonstrate the operation on the basis of acid–base principle the variation of the pH during argentometric titrations was measured, and the change of the dissociation constant of the dye adsorbate with increasing self-ion excess determined [3, 4].

1. pH changes during titration

50 ml of water and 0.3 ml of 0.2% solution of *p*-nitro-*o*-methoxyphenylazo-α-naphthylamine were added to 10 ml of 0.01 *M* solution of the anion and the solution titrated with 0.01 *M* silver nitrate standard solution. The pH change was measured during titration, and also in the titration of silver ions with anions. During the titration of iodide and bromide ions 0.1—0.15 pH decrease was observed in the equivalence point, with thiocyanate and chloride ions only a slight change, while in the titration of silver ions with ions a 0.2—0.3 pH increase. This is in accordance with the results of titrations, namely that only iodide and bromide ions can be titrated in neutral medium. So *p*-nitro-*o*-methoxyphenylazo-α-naphthylamine functions on acid–base principle in neutral and weakly acid medium. If the titrations were performed in alkaline medium at pH = 10, no pH change could be observed in the equivalence point.

2. Determination of the change of the dissociation constant of the dye adsorbate

The measurements were made similarly to those described in an earlier paper [1]. The results are given in Table II. According to the data, the *p*-nitro-*o*-methoxyphenylazo-α-naphthylamine indicator adsorbate has an amphoteric character. The dye adsorbed on silver cyanide exhibits a change of the dissociation constant only in alkaline solution, consequently, cyanide ions can be titrated in neutral or alkaline medium. The dissociation constant of the dye adsorbed on silver iodide changes both in acid and alkaline medium. In the presence of excess anion the change is not perceptible owing to the fast decomposition. In the titration of iodide ions the indicator can be used both in acid and alkaline solution. On uncharged silver iodide precipitate the indicator shows colour change only between pH 12 and 13, the compound containing no methoxy group between pH 9 and 10. Although it decreases to pH = 8—9 on adding silver ions in 10% excess, this means that the titration should be performed at higher pH in the presence of the *p*-nitro-*o*-methoxy derivative than in the presence of the nitro compound containing no methoxy group. With silver bromide the colour change cannot be perceived since the precipitate turns brown. With silver chloride the dissociation constant changes both in acid and alkaline solution with increasing self ion excess, in alkaline medium remarkably, in acid only slightly. Consequently, the colour change is sharp in the titration of chloride ions in alkaline, and only weak in acid medium.

Table I

Titration of anions in the presence of 4-(4'-nitro-2-methoxyphenylazo)-1-naphthylamine as indicator

Ion	$AgNO_3$ standard solution	Indicator, ml	Medium	Colour change	Consumed $AgNO_3$ ml		Deviation	
					(pontentiometric)	(indicator)	ml	%
Iodide	0.1 *M*	0.7 ml, 0.2%	—	from violet to orange	5.04	5.01	—0.03	0.6
Iodide	0.01 *M*	0.4 ml, 0.2%	—	from violet to orange	10.14	10.13	—0.01	0.1
Iodide	0.1 *M*	0.7 ml, 0.2%	2 drops of 2 *M* NaOH; pH = 10.8	from yellow to green	4.30	4.33	+0.03	0.7
Iodide	0.01 *M*	0.5 ml, 0.2%	2 drops of 2 *M* NaOH	from yellow to green	8.84	8.88	+0.04	0.5
Cyanide	0.1 *M*	0.7 ml, 0.2%	—	from violet to blue	4.56	4.57	+0.01	0.2
Bromide	0.1 *M*	0.7 ml, 0.2%	—	from violet to orange	5.00	5.01	+0.01	0.2
Bromide	0.1 *M*	0.7 ml, 0.2%	2 drops of 2 *M* NaOH	from yellow to greyish blue	5.00	5.03	+0.03	0.6
Chloride	0.1 *M*	0.7 ml, 0.2%	2 drops of 2 *M* NaOH	from violet-orange to bluish grey	5.02	5.04	+0.02	0.4

Table II

The dye adsorbate as acid–base indicator

Adsorbed substance 4-(4'-nitro-2'methoxyphenylazo)-1-naphthylamine

Adsorbent	Excess self-ion equiv.	pH interval	Dissociation constant		Colour change
			K_1	K_2	
Silver cyanide	50% Ag^+	3.5—4.5 and Ag_2O precipitation	$1.00 \cdot 10^{-4}$	—	Difficult to see owing to the fast browning of the precipitate
	10% Ag^+	3.0—4.1 and 7.3— 8.6	$2.82 \cdot 10^{-4}$	$1.12 \cdot 10^{-8}$	
	Equiv. point	3.0—4.0 and 7.8— 9.1	$3.16 \cdot 10^{-4}$	$3.55 \cdot 10^{-9}$	
	10% CN^-	3.0—4.0 and 10.5—11.5	$3.16 \cdot 10^{-4}$	$1.00 \cdot 10^{-11}$	From red to violet, then from violet to blue
	50% CN^-	13.0—14.0		$3.16 \cdot 10^{-14}$	
Silver iodide	50% Ag^+	imperceptible 7.6— 8.4	—	$1.00 \cdot 10^{-8}$	In the presence of excess silver ions the precipitate browns quickly
	10% Ag^+	2.0—2.5 and 8.0— 9.0	$5.62 \cdot 10^{-3}$	$3.16 \cdot 10^{-9}$	
	Equiv. point	3.0—4.0 and 12.0—13.0	$3.16 \cdot 10^{-4}$	$3.16 \cdot 10^{-13}$	From yellowish brown to yellow and then from yellow to green
	10% I^-	not perceptible	—	—	
Silver bromide	The colour change caused by acid and alkali is hardly perceptible				
Silver chloride	50% Ag^+	2.5—3.5 and 7.5— 8.5	$1.00 \cdot 10^{-3}$	$1.00 \cdot 10^{-8}$	From violet to orange-brown and then from orange-brown to violet-grey
	10% Ag^+	3.2—4.0 and 8.1— 9.0	$2.51 \cdot 10^{-4}$	$2.82 \cdot 10^{-9}$	
	Equiv. point	3.5—4.5 and 9 —10.2	$1.00 \cdot 10^{-4}$	$2.51 \cdot 10^{-10}$	
	10% Cl^-	4.0—5.0 and 10 —11.2	$3.16 \cdot 10^{-5}$	$2.51 \cdot 10^{-11}$	
	50% Cl^-	4.0—5.5 and 13.1—14	$1.78 \cdot 10^{-5}$	$3.55 \cdot 10^{-14}$	
Silver thiocyanate	50% Ag^+	7.5— 8.5		$1.00 \cdot 10^{-8}$	From red to orange grey (There is only one colour change)
	10% Ag^+	7.5— 8.5		$1.00 \cdot 10^{-8}$	
	Equiv. point	7.5— 8.5		$1.00 \cdot 10^{-8}$	
	10% CSN^-	no change			
	50% CSN^-	no change			

According to our earlier investigations [2] the acid–base indication on positively charged precipitates is important if the adsorbed indicator can form nitronic acid. On silver cyanide and silver iodide there is a great difference between the neutral and alkaline colours. Accordingly, sharp colour change is observed in the titration of cyanide and iodide ions in alkaline medium. With bromide and chloride ions there is only a slight difference between the neutral and alkaline colours, so there is only a weak colour change during the titration.

Discussion

When anions are titrated in the presence of *p*-nitro-*o*-methoxyphenylazo-α-naphthylamine as adsorption indicator in neutral or weakly acid medium, the colour turns from violet to orange. The indicator works on acid–base principle, under the condition reported by PUNGOR and SCHULEK [3].

In the presence of an anion excess, before the equivalence point of the titration, the indicator takes up proton and shows its acid colour, while in the equivalence point, when excess silver ion is added, it releases proton and shows its neutral colour:

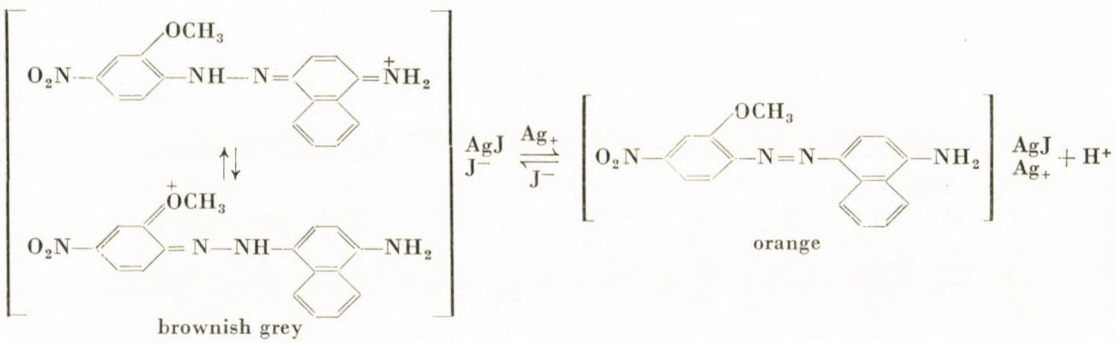

This mechanism was proved by demonstrating the pH change during titration and by determining the change of dissociation constant in acid medium.

In the argentometric titration of sodium cyanide the mechanism of the operation of indicator is the same as it is in the case of *p*-nitro-α-naphthyl red [2].

According to this interpretation nitronic acid is formed as its silver salt on adding one drop of silver nitrate solution in excess.

This mechanism was proved, similarly to our earlier investigations by the following facts: a) The dissociation constant of the dye adsorbate changes remarkably with increasing self ion excess in alkaline medium. b) On positively charged precipitates the dye adsorbate works as an acid–base indicator in neutral and alkaline solution. c) The blue silver salt of nitronic acid formed on silver cyanide precipitate decomposes in the presence of a great (10—20%) excess of silver ions.

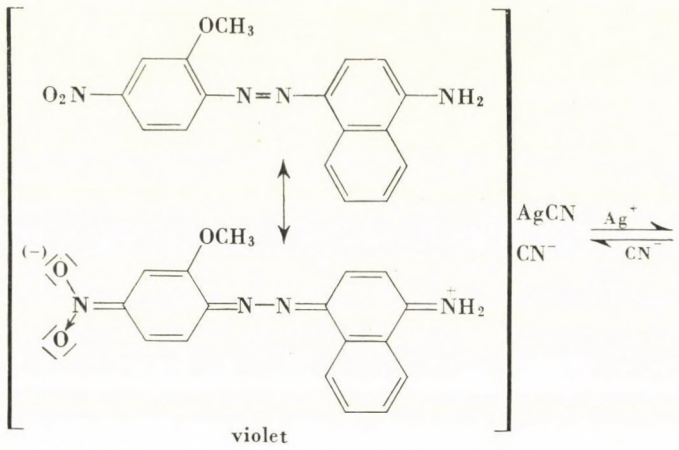

violet

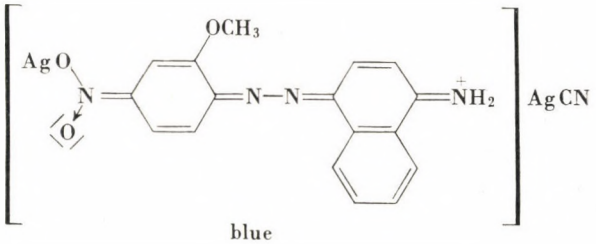

blue

During the argentometric titration of halide ions the dye adsorbate forms nitronic acid owing to the presence of alkali, that gives rise to colouration. While at anion excess nitronic acid is formed only in strongly alkaline solution, at cation excess, however, in weakly alkaline solution too. Therefore during titration nitronic acid is formed only in the equivalence point, when the first drop of silver nitrate solution is added in excess. This way of indication was demonstrated by determining the change of the dissociation constant of the dye adsorbate in the presence of self ion excess.

p-Nitro-*o*-methoxyphenylazo-α-naphthylamine as an adsorption indicator, has amphoteric properties. Amphoteric adsorption indicators are compounds in the presence of which an ion can be titrated both in acid and alkaline solution, and the colour change of which is different in the two media. In acid solution the indicator behaves as a base, and turns from a darker to a lighter colour on adding silver ions in excess, while in alkaline solution from a lighter colour to a darker one. The lighter and darker colours are not the same in the two different media, since they are attributed to different structures. Amphoteric adsorption indicator functions on acid–base principle, the mechanism of their operation can be proved by determining the pH change during the

titration in weakly acid or neutral solution, and the change of the dissociation constant of the dye adsorbate in acid and alkaline medium in the presence of self ions in excess. The advantage of amphoteric adsorption indicators over other types of adsorption indicator is that they can be used in a wide pH range (pH 3—11).

REFERENCES

1. LÉGRÁDI, L.: Magy. Kém. Folyóirat, **70,** 404 (1964); Acta Chim. Acad. Sci. Hung., **47,** 103 (1966)
2. LÉGRÁDI, L.: Magy. Kém. Folyóirat **73,** 525 (1967)
3. PUNGOR, E., SCHULEK, E.: Z. anal. Chem. **150,** 116 (1956)
4. SCHULEK, E., PUNGOR, E.: Anal. Chim. Acta **4,** 213 (1950)

László LÉGRÁDI; Fűzfőgyártelep, Hungary

Acta Chimica Academiae Scientiarum Hungaricae, Tomus 61 (2), pp. 133—148 (1969)

SULPHUR DETERMINATION IN ORGANIC COMPOUNDS BY RADIOREAGENT METHOD

S. MLINKÓ and E. DOBIS

(Central Research Institute for Chemistry, Hungarian Academy of Sciences, Budapest)

Received June 16, 1968

A procedure and an apparatus are described for the radiometric determination of the sulphur content of organic compounds. The sulphur content of organic compounds is converted by destructive hydrogenation to hydrogen sulphide and the hydrogen sulphide conducted with hydrogen carrier gas through a $Cd^{14}CO_3$ filling. From the cadmium carbonate and hydrogen sulphide cadmium sulphide, water and carbon dioxide are formed at room temperature in the presence of water. The activity of carbon dioxide formed in the course of the reaction was measured according to the carbon-14 analyses with methane counting gas in the proportional region. For the elaboration of the procedure oxide-hydrate-free cadmium carbonate was synthesized. The thermal properties of the radioactive reagent were studied in air- and hydrogen-atmosphere. According to the assumed adsorptive ion exchange an explanation of the reaction was given. The conditions of the basic reaction taking place quantitatively were examined during the formation of the sulphide content. The restricted efficiency of the cadmium carbonate — derived from the experimental data — was accounted for by the formation of the solid solutions of cadmium carbonate and cadmium sulphide and with the restricted mixed crystal formation.

The present method is based on the gas–solid reaction between $Cd^{14}CO_3$ and hydrogen sulphide. A procedure has been described for the determination of some gases by radioactive reagent [1—3]. However, no radiometric sulphur determination through $S \rightarrow H_2S \rightarrow$ gas–phase–solid reactions is known so far.

For the radiometric determination of the sulphur content of organic compounds the TER-MEULEN hydrogenation principle was employed [4—5]. According to the procedure, the organic compounds are thermally decomposed in streaming hydrogen and the sulphur containing pyrolysis products are converted into hydrogen sulphide using a platinized quartz wool catalyst. Hydrogen sulphide is swept with hydrogen carrier gas into a reactor filled with $Cd^{14}CO_3$, where the following reaction proceeds:

$$Cd^{14}CO_3 + H_2S = CdS + H_2O + {}^{14}CO_2 \qquad (1)$$

Water is fixed with calcium chloride and the carbon dioxide gas is frozen out in a cooling trap connected to an atmospheric counting tube. Gas activity is measured with methane counting gas in the proportional region as described earlier [6].

(a) Apparatus

Hydrogen is fed from a paraffin oil filled pressure regulator and the gas flow rate is adjusted to 25—30 ml/minute. The oxygen content of hydrogen is converted into water in the purification tube *A* in the presence of copper and the water is absorbed in absorber *B*. A platinized quartz wool catalyst is

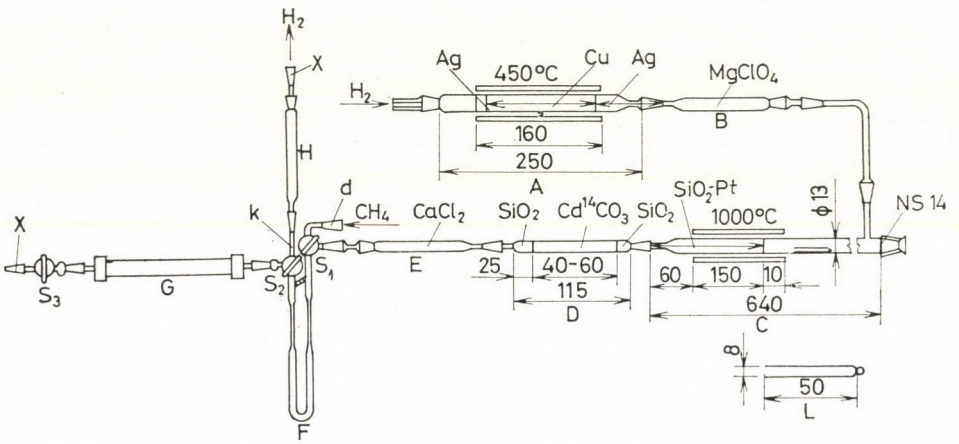

Fig. 1. Apparatus for the radiometric determination of the sulphur content of organic compounds. *A:* purification tube, *B* and *E:* absorption tubes for the absorption of water, *C:* hydrogenation tube, *D:* reaction tube, *F:* carbon dioxide trap, *G:* atmospherical counting tube, *H:* carbon dioxide absorption tube with ascarite and anhydrone filling, *L:* quartz weighing vessel

placed into the hydrogenating tube *C* [7] and the filling is heated to 1000°C. A portion of the catalyst protrudes from the furnace. In this section of the tube a continuous temperature gradient — advantageous for the formation of hydrogen sulphide — is established. Hydrogen sulphide partly decomposes at 1000°C, therefore, the conversion should take place quantitatively in the reaction zone after the furnace, this zone being of lower temperature. The cadmium carbonate is placed between the quartz wool plugs in the reactor *D* connected to the hydrogenating tube. The water leaving the reaction vessel is removed by calcium chloride or phosphorus pentoxide, the carbon dioxide gas is frozen out in trap *F*. The hydrogen carrier gas is leaving the trap through the absorption tube *H* filled with sodium asbestos. Activity measurements are performed by means of the atmospheric counting tube *G* [7—8]. A methane filling and purification system [6] is connected to the counting tube through ground joint *d*.

(b) Analyses

The apparatus is heated in a hydrogen flow. In the course of the heating period the hydrogen is allowed to pass through trap F and counter G. Samples to be analyzed are weighed into a platinum boat or into quartz vessel L (shown in Fig. 1), and placed at 5—6 cm from the furnace into the hydrogenating tube. Before the introduction of the sample, stopcock S_2 is temporarily turned off and trap F is immersed into liquid air or nitrogen. The pressure drop occurring upon cooling in trap F having been equalized from the direction of the hydrogenating tube, stopcock S_2 is turned on again, after the introduction of the sample.

When using quartz vessels the samples are approached with a gas burner — according to the principle of the counter current pyrolysis — from the direction of the furnace. The pyrolysis of the sample is accomplished in 5—10 minutes. With a gas flow rate of 25—30 ml/minute, 15 minutes are needed to sweep out the combustion products. Then the stopcocks of the counter are turned off (S_1, S_2, S_3), a vacuum rubber tube is connected to ground joint x of the counter and the effective volume is pumped out (5—10 seconds). With a momentary turn of stopcock S_2, the hydrogen is also partly removed. With stopcock S_2 open, the frozen carbon dioxide is allowed to evaporate and the gas left over in the trap is quantitatively swept out with purified methane into the counting tube from the direction of ground joint d. The method for activity measurements has been described in our earlier papers [6—8]. During the decontamination of the counting tube absorber H is connected to the counting tube along ground joint x and the radioactive carbon dioxide gas is trapped in the absorber. The decontamination of the counting tube is automatically performed by the hydrogen flow during the pyrolysis of the next sample.

(c) Synthesis of $Cd^{14}CO_3$ and its properties

The formation of carbon dioxide takes place according to reaction (1) if the preparate is hydroxide-free. Otherwise, a part of the hydrogen sulphide reacts with the hydroxide content of the basic cadmium carbonate:

$$Cd(OH)_2 + H_2S \rightarrow CdS + H_2O \qquad (2)$$

This reaction reduces the carbon dioxide yield. Nevertheless, it does not exclude in itself the analytical utilization of the fundamental reaction, as the carbon dioxide loss caused by the simultaneous reaction can be compensated by increasing the specific activity of cadmium carbonate. In the case of radiometric procedures the activity equivalent — that is, the radiostoichiometric factor — can be adjusted to a corresponding value. The activity equivalent

can be determined by isotope analysis and chemical analysis of the substance or by conversion measurements also in the case of basic cadmium carbonate. Sulphide formation from cadmium carbonate and cadmium hydroxide, in the presence of water, takes place quantitatively already at room temperature. In the reaction rates no significant difference can be observed, even in the case of considerable excess of water.

The unfavourable property of the oxide hydrate content is encountered, then the carbon dioxide gas, formed during the reaction, is swept out from the reaction tube. Actually the carbon dioxide leaving with the hydrogen is bound by the hydroxide content of the reagent as long as the latter is not saturated with carbon dioxide:

$$Cd(OH)_2 + {}^{14}CO_2 \rightarrow Cd^{14}CO_3 + H_2O \qquad (3)$$

The subsequent dry saturation of the basic precipitate with carbon dioxide gas of the same molar activity is rather complicated, as in the case of pre-dried and partially dehydrated precipitates the rate of carbon dioxide uptake decreases.

Considering the above points, it can be established that, for the utilization of the reaction, hydroxide-free cadmium carbonate is necessary, the formation of which is determined by the conditions of precipitation. According to literature data, the aqueous preparation of chemically pure cadmium carbonate is rather difficult [9—13]. All modifications of cadmium carbonate contain water which is difficult to eliminate. The chemical structure of the precipitate greatly depends on the cadmium- and carbonate-ion excess, respectively, employed for the precipitation. From the contradictory experimental data the conclusion can be drawn that the composition of the carbonate precipitate sensitively depends on the pH-value of the medium.

Reproducing the experimental data of former authors we found that a practically neutral and oxide hydrate free product can be obtained if dilute solutions are used and a cadmium acetate solution is added dropwise in nearly twofold excess into boiling sodium carbonate or sodium hydrogen carbonate solution. After hot water decantation and washing, the precipitate is neutral, and according to analytical results, in the freshly precipitated substance carbonate ion excess is present. Taking into consideration the conditions of precipitation the following micella formula can be given for the structure of the adsorption layer:

$$n(CdCO_3)CO_3^{2-} \mid Cd^{2+}$$

During the separation of the precipitates the formation of the adsorption layer is governed by the Paneth—Fajans rule. Because of the solubility properties of the cadmium carbonate, a significant amount of carbonate ion excess is present in the solution, therefore in the presence of bivalent carbonate ions the acetate ions are displaced from the double adsorption layer.

During the separation of the precipitates the occlusion of a considerable amount of water can be observed, caused by the hydrophilic character of the surface. If the precipitates are dried for the adjustment of constant water content during two hours at 120°C, then with the standardization of the conditions of precipitation we obtain nearly reproducible precipitate compositions (Table I). From the point of view of the procedure it is of importance that the

Table I

Chemical composition of the $CdCO_3$ *precipitates*

Precipitating solution	*$CdCO_3$%	H_2O%	CdO%	CO_2%	CdO : CO_2
Na_2CO_3	97.92	1.68	72.99	24.38	1.0052
Na_2CO_3	98.02	1.85	73.07	24.94	1.0040
Na_2CO_3	99.15	1.03	73.82	25.24	1.0024
Na_2CO_3	96.80	2.90	72.10	24.56	1.0057
$NaHCO_3$	97.42	2.31	72.58	24.55	1.0130
$NaHCO_3$	98.74	1.42	73.35	24.89	0.9473
$Na^{14}CO_3$	98.60	1.38	72.53	24.87	0.9992

* Measured volumetric alley

mole ratio of cadmium oxide–carbon dioxide is 1 : 1 in all precipitates in spite of the different water content. Extending the drying period by two hours each, the pre-dried precipitate yields 0.4 per cent additional water during the second drying period, and only 0.2 per cent additional water during the third period. In the precipitate dried for 6 hours a further water content of 1 per cent can be detected which can be totally eliminated only during the thermal decomposition of the substance. Variable amounts of water may occupy lattice points fixed within the crystals, in the form of solid solution, depending on the crystal regularity, that is, in increasing rate with increasing regularity. The structural water is firmly bound and can be displaced with more difficulty than the water adsorbed at the surface taking part in the formation of relatively labile hydrates. According to BALAREW [14], this water hydrates the self ions adsorbed within the crystals.

According to our observations the presence of water is the preliminary condition for the reaction, therefore we do not aim at its further elimination. The entirely dehydrated cadmium carbonate does not react with hydrogen sulphide at room temperature. For example, if the cadmium carbonate is applied to the surface of hygroscopic substances (magnesium perchlorate, calcium chloride, phosphorus pentoxide), the hydrogen sulphide flows through the reaction vessel and can be quantitatively titrated iodometrically.

Similarly, no reaction was observed between ammonium sulphide, ammonium hydrogen sulphide and cadmium carbonate. This observation is of importance, as in the pyrolysis and in the destructive hydrogenation of organic compounds with nitrogen content, ammonia can be formed which has to be eliminated. This can be attained by increasing the temperature of the platinum catalyst. At 1000°C the catalytic decomposition of ammonia is complete, even in case of hydrogen excess. At the same time, at 1000°C, in case of hydrogen

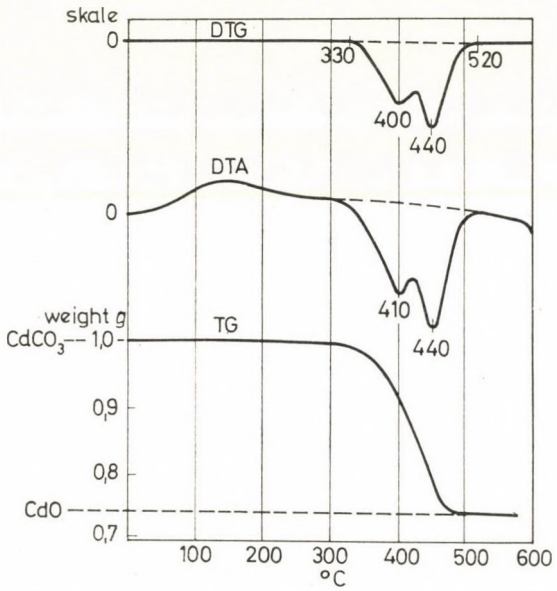

Fig. 2. Thermoanalytical curves of cadmium carbonate in nitrogen flow

excess, the equilibrium of the water–gas reaction is practically displaced in the direction of the carbon monoxide formation:

$$CO_2 + H_2 \rightarrow CO + H_2O \qquad (4)$$

therefore, the carbon dioxide appearing among the pyrolysis products cannot enter into an exchange reaction. The establishment of the equilibrium is accelerated by the platinum catalyst.

The thermal properties of neutral cadmium carbonate can be derived from the thermoanalytical curves (Fig. 2). On the DTA and DTG curves of the pre-dried cadmium carbonate a double endothermic peak can be observed. The place of the endothermal maxima falls approximately into the region of the dissociation temperature of cadmium carbonate (357°C; $p_{CO_2} = 760$ torr). The retardation of dissociation can be related to an induction period studied in details in the literature [15]. The double maximum found on the DTA and DTG

curves indicates the intermediary structural change of the precipitate, to the forming of solid solution of cadmium oxide and cadmium carbonate. For the thermal pretreatment of the precipitates and elimination of the adsorptively bound carbon dioxide the initial decomposition temperature of the cadmium carbonate has to be known which cannot be read from thermoanalytical curves. The chemical and structural changes of the basic cadmium carbonate were studied by SCHRÖDER [13] and more precisely with the emanation method of HAHN [16]. According to the curve showing the weight loss, SCHRÖDER found a small carbon dioxide loss at 300°C. At 350°C the carbon dioxide loss increased to 2 per cent, and at 400°C the carbonate was practically completely decomposed. CENTNERSZWER and ANDRUSOW [17] heated the cadmium carbonate at 265°C in a carbon dioxide-free air flow for several days and noticed only a very slight dissociation. In the experiments of ROSE [10], the cadmium carbonate, after having been heated for several hours at 300°C, lost only a small fraction of its water and carbon dioxide content; at the same time, one part of the carbon dioxide remained fixed even when heated continuously in a platinum crucible. According to our experiments the basic cadmium carbonate proved to be thermostable up to 120°C in hydrogen flow, the neutral carbonate, however, slightly decomposed above 50°C. The amount of carbon dioxide formed in the decomposition was followed by activity measurement and plotted against the gas volume passing through the reactor (see Table II). Taking into consideration the thermal decomposition of the substance, results not necessitating blank tests can be obtained only in case if the temperature in the reactor is kept at 50°C or lower during the analyses.

Table II

Decomposition of $Cd^{14}CO_3$ at 130°C in hydrogen stream

Sweeping time, min	Volume of passed gas, ml	Activity found, cpm
15	450	558
30	900	1249
30	900	1309
45	1350	1920
60	1800	2426
60	1800	2636

Background: 220 cpm
Gas velocity: 30 ml/min

The reaction of hydrogen sulphide with cadmium carbonate may be considered as an adsorptive ion exchange. As a first step the hydrogen sulphide is adsorbed on the surface of the cadmium carbonate, thereafter the adsorption

is followed by the electrolytic dissociation of the hydrogen sulphide. On the surface cadmium sulphide is formed by ion exchange, that is, the following equilibrium takes place:

$$CdCO_3 + S^{2-} \rightleftharpoons CdS + CO_3^{2-} \qquad (5)$$

The carbonate ions of the surface are displaced by sulphide ions, as in the adsorption layer the dissociation equilibrium shifts in favour of the undissociated molecules. Accordingly, the reaction cannot take place without the presence of water, that is, the electrolytic dissociation of the hydrogen sulphide and $CdCO_3$ as well. The less soluble is the product formed in comparison with the original precipitate, the more complete is the adsorptive ion exchange. The formation of cadmium sulphide is practically quantitative, as the ratio of the solubility products of the cadmium carbonate and cadmium sulphide is: $L_{CdCO_3}/L_{CdS} = 0.7 \cdot 10^{15}$.

From the point of view of the reaction not all the surface sites can be considered as equally active. Cadmium carbonate contains water in a certain surface concentration. According to the analytical results it can be assumed that the active fraction is very small, compared to the entire surface. Therefore, the impact of a hydrogen sulphide molecule from the gas phase exactly into an active site is rare. It is much more probable that the adsorbed hydrogen sulphide, as a two-dimension gas, migrates freely on the surface until, by its diffusion in the adsorption layer, it reaches the reaction centres.

The reaction between hydrogen sulphide and cadmium carbonate can be utilized for analytical purposes only up to the formation of a certain sulphide content. The amount of carbon dioxide to be produced optimally from cadmium carbonate with hydrogen sulphide was determined in a series of experiments, taking into consideration the conditions of quantitative conversion. Our experimental results are summarized in Tables III and IV. The rate of sulphur uptake, related to the sulphide content, is given in mg values. In the experiments sulphanilic acid, or alternately sulphur and sulphanilic acid were pyrolyzed. In order to check the completion of the reaction the carbon dioxide formed was measured gravimetrically. The formation of carbon dioxide can be considered as quantitative depending on the conditions of the synthesis of the reagent and especially on its water content up to 20—25 mg sulphur uptake. The sulphur capacity of the reagent (42—44 mg) can be doubled if it is deposited from an alcoholic suspension in a thin layer on a glass frit carrier (Table IV, series of experiments V). After the uptake of 43 mg of sulphur the capacity of the precipitate can be improved temporarily by increasing the sweeping time or the flow rate of the carrier gas. However, this additional sulphur uptake is not significant.

Data obtained under different experimental conditions of the pyrolysis of organic compounds, are compiled in Table III. It can be seen that the optimal

Table III

Series of experiments	Weight of sulphanilic acid, mg	Total sulphur, mg	CO_2, mg		Yield CO_2, %	Reaction temperature, °C		Gas velocity, ml/min
			found	calculated		SiO_2—Pt	$Cd^{14}CO_3$	
I	7.230	1.338	1.725	1.837	93.90	1000	30	10
	4.215	2.118	0.910	1.071	84.97	1000	30	10
	7.038	3.421	1.700	1.788	95.08	1000	30	10
	4.037	4.168	0.980	1.026	95.52	1000	30	10
	6.800	5.427	1.413	1.728	81.77	1000	30	10
	6.442	6.619	1.400	1.637	85.52	1000	30	10
	4.247	7.405	1.028	1.079	95.27	1000	30	10
	5.985	8.513	1.300	1.521	85.47	1000	30	10
	5.102	9.457	1.292	1.296	99.69	1000	30	20
	5.353	10.448	1.394	1.360	102.50	1000	50	20
	4.900	11.355	1.234	1.245	99.11	1000	50	20
	4.462	12.181	1.114	1.134	98.24	1000	50	20
	4.844	13.078	1.224	1.231	99.43	950	50	20
	3.369	13.702	0.840	0.856	98.13	950	50	20
	4.540	14.542	1.155	1.154	100.09	950	50	20
	4.200	15.319	1.081	1.067	101.31	900	50	20
	4.123	16.082	1.040	1.048	99.24	900	50	20
	4.577	16.929	1.128	1.163	96.99	850	50	20
	4.232	17.712	1.125	1.075	104.65	1000	50	25
	4.923	18.623	1.274	1.251	101.84	1000	50	25
	5.305	19.605	1.379	1.348	102.30	1000	30	30
	5.522	20.627	1.405	1.403	100.14	1000	30	30
	4.005	21.368	1.162	1.018	114.14	1050	50	30
	5.760	22.434	1.500	1.464	102.46	1050	50	30

reaction conditions are 1000°C and 30 ml/minute hydrogen flow rate. To decrease the adsorption of carbon dioxide and hydrogen sulphide on the reagent surface containing sulphide, the temperature of the cadmium carbonate is suitably adjusted to 50°C. The decrease of the sulphide and carbon dioxide formation during the progress of the reaction has two reasons:

1) With the increase of the sulphide content the cadmium sulphide can take up the hydrogen sulphide in the form of a surface compound and of hydrogen sulphide as well and releases it only at a very low rate. The hydrogen sulphide uptake of the cadmium sulphide was examined in a separate series of experiments. One part of the hydrogen sulphide originating from the first sample of sulphanilic acid was bound irreversibly by the fresh cadmium sul-

Table IV

Series of experiments	Weight of		Total sulphur, mg	CO_2, mg		Yield CO_2, %
	sulphanilic acid, mg	sulphur, mg		found	calculated	
I		5.053	5.053			
	4.165		5.824	1.084	1.058	102.45
	5.795		6.897	1.515	1.473	102.85
		5.819	12.716			
	4.950		13.633	1.292	1.258	102.70
	5.265		14.608	1.372	1.338	102.54
		5.118	19.726			
	4.014		20.469	1.050	1.020	102.94
	8.550		22.051	2.233	2.173	102.76
		6.223	28.274			
	3.226		28.871	0.748	0.820	91.22
	6.004		29.982	1.200	1.525	78.68
II		5.992	5.992			
	5.811		7.068	1.520	1.477	102.91
	3.974		7.803	1.037	1.009	102.77
		5.786	13.589			
	4.255		14.376	1.113	1.081	102.96
	4.076		15.130	1.066	1.036	102.90
		5.166	20.296			
	4.778		21.180	1.163	1.214	95.79
	4.334		21.982	1.131	1.101	102.72
	4.948		22.898	0.830	1.257	66.03
	6.293		24.063	1.442	1.599	90.18
III	5.628		1.068	1.628	1.430	113.84
	4.753		1.947	1.243	1.208	102.90
	4.278		2.379	1.121	1.087	103.13
	3.865		3.454	1.011	0.982	102.95
		4.578	8.032			
	5.096		8.975	1.333	1.295	102.93
	3.344		9.594	0.870	0.849	102.47
	5.418		10.596	1.055	1.377	76.62
		10.632	21.228			
	4.450		22.051	1.167	1.131	103.18
	3.365		22.673	0.881	0.855	103.04

(Continuation of Table IV)

Series of experiments	Weight of		Total sulphur, mg	CO_2, mg		Yield CO_2, %
	sulphanilic acid, mg	sulphur, mg		found	calculated	
III		6.276	28.949			
	3.709		29.635	0.971	0.942	103.08
	5.471		30.647	0.477	1.390	34.31
	5.456		31.637	1.018	1.386	73.45
IV		12.511	12.511			
		21.825	34.336			
		18.890	53.225			
	2.790		53.741	0.585	0.709	82.51
	4.398		54.555	0.805	1.117	72.06
V	4.273	0.791	0.791	1.110	1.086	102.20
	3.648	0.675	1.466	0.830	0.927	89.54
	2.251	0.417	1.883	0.537	0.572	93.88
	16.526	3.060	4.943	4.162	4.199	99.12
	10.865	2.012	6.955	2.565	2.761	92.90
	12.273	2.272	9.227	2.954	3.118	94.74
	30.035	5.561	14.788	7.570	7.633	99.17
	28.098	5.203	19.991	7.100	7.140	99.44
	32.446	6.008	25.999	8.042	8.245	97.54
	22.223	4.115	30.114	5.630	5.647	99.70
	17.083	3.163	33.277	4.308	4.341	99.24
	19.062	3.530	36.807	4.845	4.844	100.02
	24.049	4.453	41.260	5.987	6.106	98.05
	14.070	2.605	43.865	3.665	3.580	102.37
	28.766	5.326	49.191	6.205	7.310	84.88
	24.358	4.510	53.701	5.710	6.190	92.25
	30.125	5.578	59.279	6.540	7.656	85.42
	29.170	5.401	64.680	7.615	7.412	102.74
	22.380	4.144	68.824	5.707	5.687	100.35
	26.686	4.941	73.765	6.845	6.782	100.93
	27.105	5.019	78.784	7.007	6.888	101.73
		6.105	84.889	8.000	8.380	95.47
		5.328	90.217	6.570	7.313	89.84
		5.712	95.929	7.145	7.839	91.14
		5.870	101.799	7.330	8.056	90.99

Reaction parameters; $t_{Pt} = 1000°C$; $t_{CdCO_3} = 25-50°C$. Hydrogen flow rate: 25—30 ml/min. Sweeping time: 30 minutes

phide. After saturation of the filling the hydrogen sulphide obtained from the second sample was regained quantitatively at 80—100°C, by an increased reaction time and gas flow rate. In the sorption process a strongly activated sorption of hydrogen sulphide can also take place, in addition to its rapid physical and reversible adsorption on cadmium sulphide. The desorption of hydrogen sulphide can be carried out only if the surface regions suitable for the binding of hydrogen sulphide in a stable form are saturated, that is, if the rate of formation of the surface compounds is low at the experimental temperature during the time of a given experiment. The rapid adsorption can be considered as the intermediary step of the hydrogen sulphide formation. The hydrogen sulphide formed during the decomposition of the cadmium hydrogen sulphide can be partly chemisorbed to the sulphide phase. To achieve the complete decomposition of these formations and to release the hydrogen sulphide, much higher temperatures should be employed than the dissociation temperature of the cadmium hydrogen sulphide. The surface compounds of metal sulphides formed with hydrogen sulphide are more stable than the corresponding hydrogen sulphide, therefore they cannot be considered as the intermediary step of the hydrogen sulphide formation. The activated sorption can be interpreted as the side reaction of the hydrogen sulphide decomposition.

The crystalline structure of cadmium carbonate is different from that of cadmium sulphide, therefore, the formation of the solid solutions of the two substances in a broader concentration interval — in the absence of isomorphy — is unlikely. It is conceivable that initially a solid solution of cadmium carbonate and cadmium sulphide is formed; then, at a given concentration ratio, a two phase region begins to form, as the cadmium carbonate becomes saturated with respect to the sulphide. As long as the concentration of cadmium sulphide in cadmium carbonate is low and the carbonate contains the sulphide in a homogeneous disperse distribution, the reaction will take place, as the disturbing factor of the chemisorption cannot be operative. The loosely bound hydrogen sulphide can move freely on the surface until it reaches the reaction points. Later, with the increase of the sulphide content, the cadmium sulphide separates from the mixed crystal and a recrystallization process occurs as a consequence of the Brownian movement of the crystal centres. The crystalline structure of cadmium sulphide progressively assumes a macroscopic structure which entails the increased uptake of hydrogen sulphide. The free mobility of the adsorbed gas — because of the unequality of the forces acting at different points of the adsorbing surface — permits one or more molecules to occupy sites of higher activity and to be bound there permanently. The occurrence range of the surface compound is not restricted by a given equilibrium pressure-temperature curve. The establishment of the crystalline structure of cadmium sulphide impedes the diffusion of hydrogen sulphide from the surface layer to the inner ones and probably eliminates the intermolecular water, essential for the reaction.

The recrystallization process and the exhaustion of the filling can be followed also by the colour change of the reagent. The colour of the filling containing sulphide is light yellow at the beginning and the reaction zone is sharply limited. When the quantitative formation of carbon dioxide decreases, the colour of the reagent changes into orange. Because of the restricted mixed crystal formation cadmium sulphide separates from the solid solution, its degree of dispersity decreases, it becomes heterodisperse and its colour covers the mixed colour formed from those of cadmium carbonate and cadmium sulphide. The recrystallization may be followed also by an intermediate change in crystal modification, which goes parallel with the appearance of the brick-red colour.

2) The other responsible factor lies in the fact that the diffusion of carbon dioxide from the reaction zone bordered by cadmium sulphide is hindered or it is so slow that it renders the reaction useless from the analytical point of view. The water formed in the reaction remains on the surface of the reagent. The water dissolves the carbon dioxide, therefore appreciable water condensation increases the length of rinsing time necessary for the recovery of carbon dioxide. Because of the diffusion and adsorption phenomena of the formation of intermediate compounds, of the activated adsorption, of the restricted solubility and of the change of the crystalline structure, a continuous increase in the analysis time can be expected.

According to the above series of experiments the cadmium carbonate fillings can be utilized up till the uptake of 20—22 mg sulphur; afterwards, the reactor is turned over and a fresh filling is applied. During the experiment a sulphide containing reaction zone of maximum 25 mm length is formed, therefore we do not use fillings of more than 60 mm length. Actually, the length of filling depends on the surface area on which the cadmium carbonate is dispersed. For conversion measurements and for hydrogen sulphide capacity determinations, an originally 10 cm long (5.28 g) filling of carrier-free granulate (size of granule 0.5—1 mm) was placed into reaction tube *D*. After uptake of 22.434 mg sulphur (Table III, series of experiments I) the filling containing cadmium sulphide of the reactor was separated from the unreacted cadmium carbonate and the weight of the reaction product determined. The weight of the reacted part of filling was 0.636 g. 22.434 mg sulphur is equivalent to 120.6 mg cadmium carbonate, that is, in the separated filling the cadmium carbonate is still present in nearly fivefold excess. The inner part of the granulate is ineffective from the point of view of the reaction, therefore 2 · 650 mg labelled cadmium carbonate is deposited on the glass frit carrier, in nearly 6 cm length.

When synthesizing labelled cadmium carbonate we started from $Ba^{14}CO_3$. The specific activity of cadmium carbonate is chosen so that 1 mg sulphur should be equivalent to approximately $2 \cdot 10^4$ impulses. Under such conditions

— taking into account micro-weights (1—5 mg) — 5 to 10 minutes of detection time are necessary for obtaining 10^5 impulses, thus the mean square deviation of the activity measurement is smaller than ± 0.3 relative per cent.

Synthesis of $Cd^{14}CO_3$

Let us suppose that 50 g (nearly enough for 4 fillings) of labelled reagent have to be synthesized with 83.804 μc overall activity. The activity of the original $Ba^{14}CO_3$ is 71 μc/g; theoretically, 1.18 mg is necessary for the synthesis. The radioactive substance is diluted with inactive barium carbonate in 60—80-fold excess in order to render the activity loss smaller at the carbon dioxide evolution. The measured sample weights are:

$$Ba^{14}CO_3 = 1.556 \text{ mg}; \qquad BaCO_3 = 106.466 \text{ mg}.$$

The weighed samples are placed in a gas-generating vessel, the carbon dioxide is liberated with conc. sulphuric acid and the gas absorbed in an absorber containing sodium hydroxide solution. For the quantitative rinsing of carbon dioxide nitrogen gas is employed and the reaction flask is simultaneously heated. 20 ml 0.1 *n* NaOH solution is measured into the absorption vessel (about twofold excess) in order to obtain a quantitative absorption. The content of the absorber is rinsed into a 100 ml measuring flask and afterwards the solution is diluted with distilled water to the mark. 100 ml of the $Na^{14}CO_3$ stock solution contains 110.426 μc carbon-14 activity, thus 83.804 μc is present in 75.9 ml solution, with a $Na^{14}CO_3$ content of 44.03 mg. The separation of 50 g $Cd^{14}CO_3$ necessitates 44.03 mg radioactive, 30.7 g inactive sodium carbonate and 133.62 g cadmium acetate, the latter taken in a twofold excess. For precipitation sodium carbonate and cadmium acetate are dissolved each in 500 ml of water. The calculated amount of radioactive solution is added to the sodium carbonate solution, then it is heated to boiling and cadmium acetate solution is added dropwise. The precipitate is decanted with hot water, transferred to a G_3 filter, then dried for two hours at 120°C. Weight of the precipitate: 24.16 g, yield: 48.38 per cent. The greater part of cadmium carbonate remains in solution. To prevent activity loss, the radioactive precipitate is stored in a carbon dioxide-free atmosphere. Immediately before use the precipitate is deposited from alcoholic suspension on the surface of G_2 sintered glass rubble (granule size: 2—3 mm), the alcohol is sucked off and the excess alcohol evaporated.

To calculate the radiostoichiometric factor the specific and molar activity of the reagent has to be known. The empirical formula can be written in a simple way if the amount of water bound to cadmium carbonate is given in the fractional values of the mole number, related to 1 mole cadmium carbonate. As a consequence of the variable water content the hydrate formula cannot be written in such a way that only an integral number of water or cadmium carbonate molecules be contained in it. The isotopic and chemical analysis of the substance was performed in the following way:

10—15 mg of pre-dried precipitate were weighed into a platinum boat and the substance, together with the platinum vessel, placed into the combustion tube of a carbon-14 determining apparatus. The substance was thermally decomposed in a purified air stream, the separated water retained in an absorption tube filled with anhydron. First, the activity of the carbon dioxide gas was measured in a proportional counting tube, then, with the decontamination of the counting tube, the carbon dioxide was swept into a previously conditioned absorption tube. From the weight increase of the absorption tube the water- and carbon dioxide content of cadmium carbonate can be directly calculated. For the determination of the cadmium oxide content the measuring vessel was heated to 800°C and its weight measured again. The weight difference corresponds to the cadmium oxide content of the sample. According to the analytical results the CdO : CO_2 mole ratio in the cadmium carbonate is 1 : 1; this proves that the product is hydroxide-free (Table I).

Mean value of the specific activities according to six parallel measurements:

$$4387 \text{ cpm/mg}; \qquad \sigma_{rel} = 0.17\%$$

According to the analytical results (Table I) the following empirical formula can be given for the composition of our cadmium carbonate:

$$Cd^{14}CO_3 \cdot 1.134\ H_2O; \quad \text{specific activity: } 767270 \text{ cpm/mM}.$$

Table V

Substance	Weight, mg	Activity, cpm		S cpm/mg	Sulphur, %		Deviation, %
		found	calculated		found	calculated	
Sulphanilic acid	11.191	49 156	49 580	23 766	18.75	18.51	—0.16
	10.631	46 870	47 100	23 813	18.42	18.51	—0.09
	10.968	47 590	48 590	23 980	18.13	18.51	—0.38
Sulphur	2.755	66 517	65 922	24 144	100.90	100.00	+0.90
	2.670	64 162	63 890	24 030	100.44	100.00	+0.44
L-Methionine	7.010	34 675	36 047	22 986	20.67	21.49	—0.82
	7.062	34 784	36 314	22 920	20.58	21.49	—0.91
	7.644	39 184	39 307	23 853	21.42	21.49	—0.07
Thiourea	4.002	38 376	40 340	22 764	40.07	42.12	—2.05
	4.111	41 224	41 440	23 805	41.91	42.12	—0.21
Dibenzyl-disulphide	1.216	7 099	7 573	22 430	24.40	26.03	—1.63
	1.724	10 500	10 738	23 395	25.45	26.03	—0.58
Aminonaphthol-sulphonic acid	2.234	7 020	7 165	23 440	13.13	13.40	—0.29
	2.581	8 075	8 275	23 358	13.07	13.40	—0.33
S-Methylthiourea sulphate	3.660	28 668	29 168	22 641	32.74	34.58	—1.84
	4.560	38 706	36 340	24 644	35.48	34.58	—0.10
	2.803	22 066	22 333	22 763	32.90	34.58	—1.68
N-Methyl-N-toluene-sulphonic-naphtholamine	2.715	6 182	6 689	22 118	9.51	10.30	—0.79
	2.090	4 836	5 149	22 472	9.67	10.30	—0.63
2-Methyl-mercapto-4-amino-triazine	3.787	22 057	20 450	25 809	24.34	22.56	+1.78
	2.747	15 476	14 828	24 973	23.54	22.56	+0.98
Tetraacetyl-D-glucose-dimethyl-dithiocarbonate	1.904	6 289	6 471	23 256	23.80	14.20	—0.40
	2.077	6 988	7 059	23 688	14.06	14.20	—0.14
1,2,3,4-Tetraacetyl-6-tosylglucose	2.618	3 815	4 297	21 244	6.09	6.86	—0.77
	4.640	6 701	7 615	21 054	6.03	6.86	—0.73
Sulphanilic acid + *p*-bromobenzoic acid	6.119	25 541	24 555	24 888	17.44	16.78	+0.66
	6.570	27 382	26 364	24 850	17.41	16.78	+0.63
Sulphanilic acid + *p*-bromoacetanilide	5.608	22 930	22 504	24 380	17.08	16.78	+0.30
	4.216	17 675	16 557	25 544	17.90	16.78	+1.12
	6.180	25 481	24 805	24 644	17.23	16.78	+0.45
Sulphanilic acid + 1-chloro-2,4-dinitrobenzoic acid	6.110	25 192	24 520	24 585	17.23	16.78	+0.45
	5.350	22 276	21 469	24 828	17.40	16.78	+0.62
Sulphanilic acid + *p*-chlorobenzoic acid	5.365	22 179	21 529	24 650	17.27	16.78	+0.51
	3.083	12 628	12 371	24 424	17.12	16.78	+0.34

The radiostoichiometric factor calculated from the molar activity is 23928 cpm/mg sulphur equivalent. The given data are relative activity values. The determination of the absolute activity of the reagent can be omitted if the same counting tube is used for the radiometric analysis and for the determination of the specific activity.

The results of radiometric analyses are summarized in Table V. For calculating the analytical results the following formula is used:

$$S\% = \frac{(I - I_0) \cdot 100}{B \cdot A}$$

I = activity measured in cpm (relative value)
I_0 = background in cpm
B = sample weight in mg
A = activity equivalent, in our experiments 23928 cpm/mg sulphur equivalent.

The activity equivalent is the product of the stoichiometric factor F and the specific activity C.

$$F = \frac{Cd^{14}CO_3 \cdot 1.134\, H_2O}{S}\,; \quad F \cdot C = \frac{174883}{32.066} \cdot 4378 = 23928 \text{ cpm/mg}$$

sulphur equivalent. By the radiometric procedure the sulphur content of organic compounds can be determined within ± 2 per cent experimental error.

REFERENCES

1. Chleck, D. J., Ziegler, C. A.: Nucleonics **17,** No. 9, 130 (1959)
2. Hommel, C. O., Chleck, D. J., Brousaides, F. J.: Nucleonics **19,** No. 4, 94 (1961)
3. Hommel, C. O., Brousaides, F. J., Bersin, R. L.: Anal. Chem. **34,** 1608 (1962)
4. Ter Meulen, H.: Rec. trav. Chim. Pay-Bas **33,** 118 (1934)
5. Mázor, L.: Szerveskémiai analízis II. Műszaki Könyvkiadó, Budapest 1962
6. Mlinkó, S., Szarvas, T., Hegede, B.: Mikrochim. Acta **1963,** 139
7. Mlinkó, S., Szarvas, T., Gács, I.: Int. J. appl. Rad. Isotopes **18,** 457 (1967)
8. Mlinkó, S., Gács, I., Szarvas, T.: Acta Chim. Acad. Sci. Hung. **52,** 359 (1967)
9. Lefort, I.: Compt. rend. **27,** 268 (1848)
10. Rose, H.: Pogg. Ann. **85,** 304; Journ. prakt. Chem. **55,** 458 (1852)
11. Follenius, O.: Zschr. analyt. Chem. **13,** 292 (1874)
12. Kraut, K.: Zschr. anorg. Chem. **13,** 14 (1897)
13. Schröder, W.: Zschr. Elektrochem. **47,** 196 (1941)
14. Balarew, D.: Kolloid-Beih. **34,** 444 (1932)
15. Centnerszwer, M., Bruzs, B.: Zschr. phys. Chem. **119,** 405 (1926)
16. Hahn, B. O.: Applied Radiochemistry. Cornell University Press 1936
17. Centnerszwer, M., Andrusow, L.: Zschr. phys. Chem. **111,** 79 (1924)

Sándor Mlinkó
Emilia Dobis
Budapest II., Pusztaszeri út 57/69

Acta Chimica Academiae Scientiarum Hungaricae, Tomus 61 (2), pp. 149—158 (1969)

DIPOLMOMENTUNTERSUCHUNGEN DER PHENYL- UND BENZYLDERIVATE VON ELEMENTEN DER VIERTEN HAUPTGRUPPE

J. NAGY, S. FERENCZI-GRESZ, K. PÁLOSSY-BECKER und A. BORBÉLY-KUSZMANN

(Institut für Anorganische Chemie der Technischen Universität, Budapest)

Eingegangen am 24. Juni 1968

Das Dipolmoment der Verbindungen vom Typ

$(CH_3)_3E$—⬡ und $(CH_3)_3E—CH_2$—⬡

(wo E = C, Si, Ge und Sn) wurde mittels der ONSAGER-Methode im flüssigen Zustand bestimmt.

Es wurde festgestellt, daß der Dipolmomentwert im Falle der Phenylderivate bei der Silicium-Verbindung ein Minimum aufweist und im Falle der Benzylderivate monoton zunimmt.

Im Laufe unserer Forschungen haben wir uns mit den Bindungsstrukturproblemen der Trimethylvinylderivate der Elemente der vierten Hauptgruppe auf Grund der Dipolmomentmessungen schon befaßt [5]. Wir haben festgestellt, daß der Dipolmomentwert in der untersuchten Verbindungsreihe vom Typ $(CH_3)_3ECH = (CH_2)$ (E = C, Si, Ge, Sn) beim Siliciumderivat ein Minimum zeigt. Diese Tatsache ist damit zu erklären, daß mit Ausnahme des Kohlenstoffderivates im Falle der anderen Elemente auch ein $-M$ Effekt neben einem $+I$ Effekt auftritt. Der $-M$ Effekt ist beim Siliciumderivat am größten und vermindert das resultierende Dipolmoment in hohem Maße.

Eine ähnliche Erscheinung tritt auch bei den Trimethylphenyl- und Trimethylbenzyl-Derivaten der Elemente der vierten Hauptgruppe auf, wie dies auch von HUANG und HUI [1] im Zuge von Dipolmomentbestimmungen der Phenyl- und Benzylzinnderivate bewiesen wurde. Da HUANG und HUI nur die Dipolmomente der Trimethylphenyl- und Trimethylbenzylzinn-Verbindungen gemessen haben, ergänzten wir ihre experimentellen Ergebnisse nun mit der Bestimmung der Dipolmoment-Daten der Kohlenstoff-Silicium und Germanium-Derivate. Die Dipolmomentwerte wurden abweichend von den in der Literatur beschriebenen Methoden unter Berücksichtigung der richtigen Atompolaritätswerte und unter Ausschluß des Lösungsmittelfehlers nach der ONSAGER-Methode [2] bestimmt.

Die von uns untersuchten Verbindungsgruppen können mit den folgenden Formeln charakterisiert werden:

$(CH_3)_3E$—⬡ und $(CH_3)_3E—CH_2$—⬡

wo E = C, Si, Ge, Sn.

Die Dipolmomentmessungen wurden in allen Fällen im Flüssigkeitszustand nach ONSAGER durchgeführt, da die Kohäsionskräfte bei den untersuchten Verbindungen vernachlässigbar sind.

Zur Berechnung der richtigen Dipolmomentwerte war die Bestimmung der genauen Atompolaritätswerte der Phenyl-Silicium-Gruppe notwendig. Zu diesem Zweck wurden die Elektronen- und Atompolaritätswerte des Tetraphenylsilans in benzolischer Lösung bestimmt ($P_\infty = P_A + P_e$). Das Tetraphenylsilan Molekül besitzt kein Dipolmoment. Da der Richtpolaritätswert gleich Null ist, kann der Atompolaritätswert in Kenntnis der Elektronenpolarität berechnet werden. Die Bestimmung der Atompolarität wurde auf folgende Weise durchgeführt: Es wurden Dichte, Brechungsindex, Dispersionswert und Dielektrizitätskonstante der verdünnten benzolischen Lösungen des Tetraphenylsilans gemessen. Tabelle I enthält die gemessenen Werte.

Tabelle I

Physikalische Konstanten verdünnter benzolischer Tetraphenylsilan-Lösungen

	Lösung		
	1	2	3
N_2	0,00288	0,00398	0,00478
d	0,8738	0,8751	0,8760
n_D	1,4988	1,4992	1,4996
z	35,51	35,35	35,38
ε	2,2812	2,2827	2,2850
P_e	25,3300	25,4114	25,4751

Durch Extrapolation der Dichte und der Dielektrizitätskonstante auf unendlich verdünnte Lösung konnte der Wert der Gesamtpolarität auf Grund der Gleichung von Hedestrand berechnet werden:

$$P_\infty = \frac{\varepsilon_1 - 1}{\varepsilon_1 + 2}\left(\frac{M_2}{d_1} - \frac{M_1\beta}{d_1}\right) + \frac{3M_1\alpha}{(\varepsilon_1 + 2)^2 d}.$$

Die durch graphische Extrapolation erhaltenen Werte sind die folgenden:

$$\left.\begin{aligned} d_1 &= 0{,}8707 \\ \varepsilon_1 &= 2{,}2746 \\ \alpha &= 2{,}269 \\ \beta &= 1{,}111 \end{aligned}\right\} \quad P_\infty = 114{,}49 \text{ ml.}$$

Die Elektronenpolarisation der einzelnen Lösungen wurde mit Hilfe der auf den unendlichen Wellenlängenwert (n_∞) bezogenen aus z berechneten Dispersion ($n_F - n_C$) nach folgender Gleichung erhalten:

$$P_{e_{12}} = \frac{n_\infty^2 - 1}{n_\infty^2 + 2} V.$$

Tabelle I enthält auch diese Werte (P_e). Die Elektronenpolarisation der gelösten Substanz (P_e^*) haben wir durch Extrapolation dieser P_e-Werte auf unendlich hoch verdünnte Lösung erhalten.

$$P_e^* = 104{,}41 \text{ ml}$$

$$P_A = P_\infty - P_e^*.$$

Der Atompolarisationswert (P_A) beträgt 10,08 ml. Dementsprechend ist das Inkrement der Atompolarisation der Phenyl-Silicium Gruppe ein Viertel des obigen Wertes

$$P_A(\text{Si} - \text{C}_6\text{H}_5) = 2{,}52 \text{ ml}.$$

Auf diese Weise wurden die Dipolmomentwerte der folgenden Verbindungen bestimmt (über deren Herstellung im experimentellen Teil berichtet wird):

$C_6H_5C(CH_3)_3$, $C_6H_5CH_3$, $C_6H_5Si(CH_3)_3$, $C_6H_5Ge(CH_3)_3$, $C_6H_5CHC(CH_3)_3$,
$C_6H_5CH_2Si(CH_3)_3$ und $C_6H_5CH_2Ge(CH_3)_3$.

Zur Bestimmung der Dipolmomente war die Kenntnis der folgenden charakteristischen physikalischen Daten nötig: Brechungsindex ($n_D^{25°}$), Dichte (d_4^{25}), Dispersion ($n_F - n_C$) und Dielektrizitätskonstante ($\varepsilon^{25°C}$), welche letztere mit einem selbsthergestellten Kapazitätmeßgerät bei 10^4 Hz bestimmt wurde [4].

Auf Grund dieser Werte wurden die Molrefraktionen der einzelnen Verbindungen berechnet, welche mit den aus den Bindungsinkrementen berechneten Werten gut übereinstimmten. Die Elektronenpolarisationswerte (P_e) wurden mit Hilfe des aus den Dispersionswerten erhaltenen n_∞-Wertes [5] unter Berücksichtigung des Molvolumens bestimmt.

Die Atompolarisationswerte wurden im Falle der Kohlenstoff- und Siliciumverbindungen auf Grund der Arbeiten von AUDSLEY [6] und ALTSHULLER [7] mit der Additivitätsregel der Bindungsinkremente berechnet. Das Bindungsinkrement der C_6H_5Si-Gruppe wurde auf Grund der obigen Ausführungen mit 2,52 angesetzt. Die exakten Dipolmomentwerte wurden in Kenntnis der zusammengehörigen Atom- und Elektronenpolarisationswerte nach der ONSAGER-

Tabelle II

Charakteristische physikalische Konstanten der Trimethylphenyl- und Trimethylbenzyl-Verbindungen der Elemente der IV/1 Gruppe

	C_6H_5—$(CH_3)_3$	C_6H_5—CH_3	$(CH_3)_3SiC_6H_5$	$(CH_3)_3GeC_6H_5$	C_6H_5—CH_2—$C(CH_3)_3$	C_6H_5—$CH_2Si(CH_3)_3$	$C_6H_5CH_2Ge(CH_3)_3$
n_D^{25}	1,4900	1,4935	1,4887	1,5126	1,4858	1,4912	1,5091
d^{25}	0,86064	0,8583	0,8686	1,09906	0,86145	0,8604	1,0914
ε_{25}	2,356	2,376	2,3616	2,4887	2,4545	2,5866	2,6538
V	155,96	108,17	173,0	177,24	172,09	191,01	191,13
$MR_{D\ \text{theor.}}$	45,04	31,15	50,10	53,68	49,67	54,67	58,31
$MR_{D\ \text{gemessen}}$	45,09	31,46	49,91	53,24	49,39	55,34	57,08
$n_F - n_C$	0,01359	0,0158	0,01477	0,01448	0,01344	0,01464	0,01600
n_∞	1,4695	1,4697	1,4664	1,59065	1,4600	1,4691	1,4850
P_2	43,47	30,16	47,96	51,30	47,14	52,44	54,78
P_A	1,44	1,00	4,808	—	1,556	5,90	—
$P_A + P_e = R_\text{I}$	44,91	31,16	52,77	—	48,69	58,34	—
$MR_D \cdot 1{,}05 = R_\text{II}$	$R = MR_D$	$R = MR_D$			$R = MR_D$		
	45,09	31,46	52,41	55,90	49,39	58,1	59,94
$\varepsilon_{\text{eff I}}$	2,21	2,2144	2,3164	—	2,184	2,3193	—
$\varepsilon_{\text{eff II}}$	2,22	2,2305	2,3034	2,312	2,207	2,3115	2,3704
P^*_I	3,695	2,887	1,2512	—	7,6875	7,927	—
P^*_II	3,515	2,579	1,6187	2,9125	6,9586	8,022	8,2049
μ_I	0,425	0,376	0,248	—	0,614	0,623	—
μ_II	0,415	0,355	0,281	0,378	0,584	0,627	0,634

Formel berechnet. Außerdem wurden die Dipolmomentwerte auch auf Grund des bekannten empirischen Zusammenhanges

$$MR_D \cdot 1{,}05 = P_e + P_A$$

bestimmt.

Da die Gruppeninkrement-Werte der Germaniumverbindungen bisher nicht bekannt sind, wurden deren Dipolmomentwerte nur mit Hilfe dieser letzteren Gleichung gewonnen. Die Ergebnisse sind in Tabelle II angegeben, wo μ_I den mit der exakten Methode und μ_{II} den mit der empirischen Formel berechneten Dipolmomentwert bedeuten.

Tabelle III enthält die von uns bestimmten und in der Literatur angegebenen Dipolmomentwerte der Verbindungen $C_6H_5CH_3$; $C_6H_5C(CH_3)_3$; $C_6H_5Si(CH_3)_3$ und $C_6H_5CH_2Si(CH_3)_3$.

Tabelle III

Dipolmomentwerte der Trimethylphenyl- u. Trimethylbenzyl-Verbindungen der Elemente der IV/1 Gruppe

Formel	Gemessener Wert μ[D]	Literaturwert μ[D]
$C_6H_5CH_3$	0,376	0,63[8] (flüss); 0,40[9] (flüss); 0,06[10]; 0,5[11]; 0,39[12]; 0,3[13]; **0,37**[14]; 0,34[15]; 0,53[16]; 0,3[17]; **0,37**[18]; 0,39[19]; 0,37[20]
$C_6H_5{-}C(CH_3)_3$	0,425	0,53[15]; **0,70**[18]; 0,52[21]; 0,41[19]; 0,45[22]
$C_6H_5{-}Si(CH_3)_3$	0,248	0,44[23]; 0,42[24]; 0,00[25]
$C_6H_5{-}CH_2{-}Si(CH_3)_3$	0,623	0,71[23]; 0,55[24]; 0,68[26]

Aus den Daten der Tabelle III ist ersichtlich, daß das Dipolmoment des Toluols infolge der Wirkung der tertiären Butylgruppe kleiner ist als das des *tert.* Butylbenzols. Aus den Angaben der Tabelle III geht auch hervor, daß das von uns gemessene Dipolmoment des Toluols mit dem in der Literatur [14] angegebenen Wert (Dampfzustand) übereinstimmt, was die Genauigkeit unserer Meßmethode und der Berechnungen bestätigt.

Ein den Literaturangaben entsprechendes Dipolmoment haben wir auch im Falle des *tert.* Butylbenzols gemessen.

Mehrere Forscher haben sich auch mit der Bestimmung des Dipolmomentes des Trimethylphenylsilans befaßt. Amerikanische Verfasser [23] haben

0,44 D, sowjetische 0,42 D [24] bzw. 0,00 D [25] gemessen. In den ersten zwei Fällen wurde der Atompolarisationswert kleiner und beim Wert 0,00 D größer gewählt als der von uns aus den Atompolarisationsinkrementen berechnete Wert.

Auch der Dipolmomentwert des Trimethylbenzylsilans wurde von mehreren Verfassern bestimmt. ROBERTS und Mitarbeiter [23] fanden $\mu = 0{,}71$ D. Dieser Wert war wegen des falsch gewählten Atompolarisationswertes größer, das von KARZEW und Mitarb. [24] bestimmte Dipolmoment, 0,55 D, war kleiner als der von uns berechnete Wert ($\mu_I = 0{,}623$ D). ČER und Mitarbeiter [26] fanden für den Dipolmomentwert des Trimethylbenzylsilans $\mu = 0{,}68$ D. Die Differenz zwischen dem von uns bestimmten und dem obigen Wert kann auf die unterschiedlichen Meßmethoden und auf den Unterschied der Berechnung des Atompolarisationswertes zurückgeführt werden. Im Laufe unserer Berechnungen gebrauchten wir den von KARZEW [24] für die Benzyl-Siliciumgruppe gewählten Atompolarisationswert: 5,9 ml. Auch die Berechnung des Bindungdipolmomentes der C_6H_5—E Gruppe war ein interessantes Problem. Sein Wert kann unter Annahme tetraedrischer Symmetrie auf Grund des folgenden Dipolenvektor-Bildes wie folgt berechnet werden:

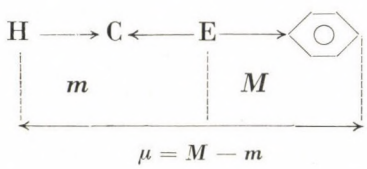

m = Dipolvektor der $(CH_3)_3E$ Gruppe, welcher auf Grund der Literaturangaben folgende Werte annehmen kann:

CH_3 — C	0,00 D	[5]
CH_3 — Si	0,20 D	[27]
CH_3 — Ge	0,30 D	[28]
CH_3 — Sn	0,60 D	[29]

M = Dipolvektor der  — E Gruppe, mit den möglichen Werten:

 — C	0,425 D	bzw. 0,425 D
 — Si	0,445 D	bzw. → 0,048 D
 — Ge	0,678 D	bzw. 0,078 D
 — Sn	1,232 D	bzw. 0,032 D

Werden die Dipolmomentwerte der Benzyl- und Phenyl-Derivate als Funktion der Hauptquantenzahl — ähnlich dargestellt, wie die Vinyl-Derivate der vierten Hauptgruppe, so kann bei den Phenyl-Silicium-Derivaten — ähnlich wie bei ihren Vinyl-Derivaten — ein Minimum beobachtet werden, während die Dipolmomentwerte der Benzyl-Derivate eine monotone Zunahme aufweisen (Abb. 1).

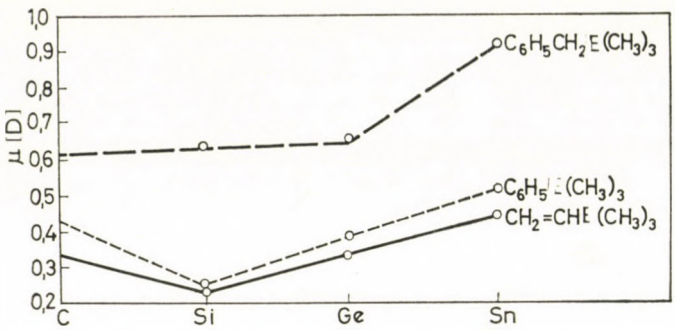

Abb. 1. Änderung des Dipolmomentwertes der Trimethylphenyl, Trimethylbenzyl- und Trimethylvinyl-Verbindungen der IV/1 Gruppe als Funktion der Ordnungszahl

Die Erklärung solcher Änderungen der Dipolmomente auf Grund der Bindungsstruktur wurde schon in einer unserer früheren Arbeiten [30] beschrieben, wo wir darauf hingewiesen haben, daß das Zentralatom in den Trimethylphenylderivaten der Elemente der vierten Hauptgruppe — ähnlich den Trimethylvinylverbindungen (die Kohlenstoffverbindungen ausgenommen) — nicht nur einen $+I$, sondern auch einen $-M$ Effekt besitzt, welcher den Vektorwert des Dipolmomentes vermindert. Die Existenz der $+I$ und $-M$ Effekte beweist auch jene Tatsache, daß die Darstellung der Dipolmomentwerte der Trimethylphenyl- und Trimethylvinyl-Verbindungen der Elemente der vierten Hauptgruppe eine Gerade ergibt (Abb. 2). Bei den Trimethylbenzylderivaten gelangt in jedem Falle nur der $+I$ Effekt zur Geltung, dessen Richtung mit der des Hyperkonjugationseffektes der CH_2-Gruppe identisch ist und zunehmende Dipolmomente ergibt.

Die partielle Ladungsverteilung des σ- und π-Bindungssystems wurde im Falle des Trimethylphenylsilans mit quantenchemischen Berechnungen bestimmt.

Die Einzelheiten der quantenchemischen Berechnungen haben wir an anderer Stelle bereits beschrieben [31]. Das in Kenntnis der partiellen Ladungsanteile berechnete resultierende σ,π-Dipolmoment beträgt 0,08 D und stimmt mit dem gemessenen Wert ($\mu = 0{,}25$ D) gut überein. Dies beweist die zwei entgegengesetzten σ und π-Effekte, d.h. daß das π-Sextett der Phenylgruppe eine $p\pi - d\pi$ Wechselwirkung mit dem *d* Orbital des Si Atoms zustandebringt.

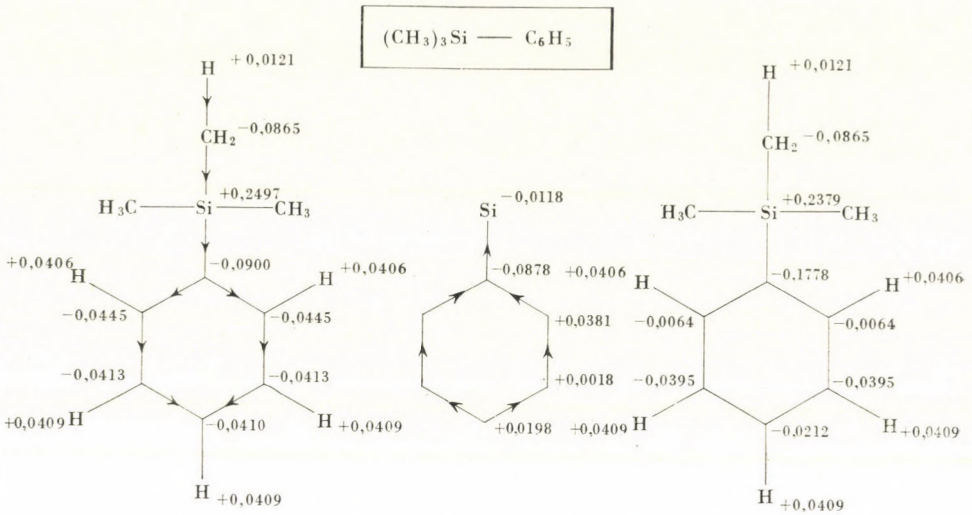

Abb. 2. Partielle Ladungsverteilung im σ- und π-Bindungssystem des Trimethylphenylsilans

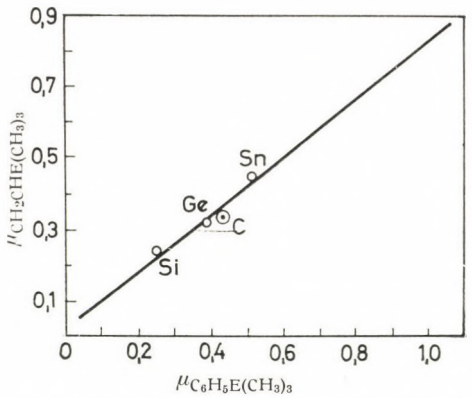

Abb. 3. Korrelation zwischen den Dipolmomentwerten der Trimethylphenyl- und Trimethylvinyl-Verbindungen der Elemente der IV/1 Gruppe

Experimenteller Teil

1. *tert.*-Butylbenzol

tert.-Butylbenzol [$C_6H_5C(CH_3)_3$] wurde aus Benzol und *tert.*-Butylchlorid mit der Friedl-Crafts Synthese hergestellt.

50 g wasserfreies $AlCl_3$ und 200 ml abs. Benzol wurden in einem Dreihalskolben (mit Rührer, Rückflußkühler und Tropftrichter versehen) unter 0°C gekühlt. 49 g *tert.*-Butylchlorid wurden langsam eingetragen, wobei die Temperatur unter +5°C gehalten wurde. Das Reaktionsgemisch wurde noch eine Stunde gerührt und danach auf Eis gegossen. Die organische Phase wurde mit $NaHCO_3$-Lösung, dann mit Wasser neutral gewaschen und über $CaCl_2$ getrocknet. Das Produkt wurde durch Destillation gereinigt. Kp.: 168,5°C/760 Torr. Ausbeute: 45 g (67%). Die Reinheit der Substanz wurde gaschromatographisch kontrolliert [32].

2. Neopenthylbenzol

Die Verbindung wurde aus Benzylchlorid und *tert.*-Butylchlorid nach der Grignard-Methode hergestellt. In einen Dreihalskolben (Rückflußkühler, Rührer und Tropftrichter) wurden 5 g Mg-Späne mit 150 ml abs. Äther übergossen, die Reaktion mit 1—2 ml Äthylbromid in Gang gesetzt und 26 g (0,2 Mol) Benzylchlorid wurden zugetropft. Die Suspension wurde 3 Stunden und nach Zugabe von 18,5 g (0,2 Mol) *tert.*-Butylchlorid weitere 3 Stunden unter Rückfluß gekocht. Das Reaktionsgemisch wurde auf Eis gegossen und die abgetrennte organische Phase mit Wasser gewaschen und über $CaCl_2$ getrocknet. Das nach Abtreiben des Lösungsmittels erhaltene Produkt wurde durch Destillation bei 10 Torr (Kp_{10}: 64° C) gereinigt. Ausbeute 16 g (54%). Die Reinheit des Produktes wurde gaschromatographisch geprüft. Kp_{10}: 64° C, Kp_{12}: 72° C [32].

3. Trimethylphenylsilan

Die Verbindung wurde aus 48 g (0,3 Mol) Brombenzol, 32,5 g (0,3 Mol) Trimethylchlorsilan und 7,5 g Magnesium-Spänen in 150 ml abs. Äther analog wie die vorstehende Verbindung hergestellt. Das Endprodukt wurde durch Destillation bei 15 Torr gereinigt. Kp_{15}: 55° C, Kp_{760}: 172° C. Ausbeute 21 g (46,7%). Die Reinheit der Verbindung wurde gaschromatographisch geprüft. Kp_{760}: 172° C; $n_D^{25°}$: 1,4883 [33].

4. Trimethylbenzylsilan

Die Verbindung wurde aus 26 g (0,2 Mol) Benzylchlorid, 23 g (0,2 Mol) Trimethylchlorsilan und 5 g Magnesium-Spänen in 200 ml abs. Äther analog wie die vorstehende Verbindung hergestellt. Das durch Destillation bei 35 Torr gereinigte Endprodukt (Kp_{35}: 93° C; Kp_{748}: 191—192° C) wog 17 g (51,7%). Kp_{760}: 191° C [23].

*

Dr. V. F. Mironov möchten wir für das zu unseren Messungen zur Verfügung gestellte Trimethylphenylgermanium und Trimethylbenzylgermanium an dieser Stelle danken.

LITERATUR

1. Huang, H., Huiy, K.: Journ. Organometal. Chem. **2**, 288 (1964)
2. Onsager, L.: Journ. Am. Chem. Soc. **58**, 1486 (1936)
3. Hedestrand, G.: Z. physik. Chem. **2B**, 428 (1929)
4. J. Nagy, I. Gresz, Ferenczi-Gresz S.: Periodica Polytechnica **10**, 335 (1966)
5. Nagy, J., Ferenczi-Gresz, S., Durgarjan: Acta Chim., im Druck
6. Audsley, A., Goss, F. R.: Journ. Am. Chem. Soc. **72**, 2989 (1950)
7. Altshuller, A. P., Rosenblum, R.: Journ. Am. Chem. Soc. **77**, 272 (1955)
8. Lertes, P.: Z. Phys. **6**, 56 (1921)
9. Krchma, I. J., Williams, J. W.: Journ. Am. Chem. Soc. **49**, 2408 (1927)
10. Williams, J. W., Krchma, I. J.: Journ. Am. Chem. Soc. **49**, 2416 (1927)
11. Daily, C. R.: Phys. Rev. **34**, 548 (1929)
12. Tiganik, L.: Z. phys. Chem. **B13**, 425 (1931)
13. Higashi, K.: Bull. Inst. Phys. Chem. Res. (Tokyo) **12**, 22 (1933)
14. Alpine, K. B., Smith, C. P.: Journ. Am. Chem. Soc. **55**, 453 (1933)
15. Le Fèvre, C. G., Le Fèvre, R. J. W., Robertson, K. W.: Journ. Chem. Soc. 480 (1935)
16. Mohler, H., Sorga, J.: Helv. Chim. Acta **20**, 1447 (1937)
17. Müller, F. H.: Z. Phys. **38**, 283 (1937)
18. Baker, J. W., Grover, L. G.: Journ. Chem. Soc. 1144 (1939)
19. Altshuller, A. P.: Journ. Phys. Chem. **58**, 392 (1954)
20. Cumper, C., Vogel, A. Y., Walker, S.: Journ. Chem. Soc. 3640 (1957)
21. Lumbroso, H.: Ann. Fac. sci. univ. Toulouse. Sci. Math. et sci. Phys. **14**, 9 (1950)
22. Shiereci, L., Lumbroso, H., Passerini, R.: C. v. Acad. Sci. **237**, 611 (1953)
23. Roberts, J. D. M., Elhill, E. A., Armstrong, R.: Journ. Am. Chem. Soc. **71**, 2923 (1949)
24. Karzew, G. N. und Mitarb.: Dokl. Akad. Nauk USSR **122**, 99 (1958)
25. Karzew, G. N. und Mitarb.: Shurnal schtrukturnoj chimii **6**, 309 (1965)
26. Čer, Vaiserová, V., Chvalovsky, V.: Collection **32**, 3784 (1967)

27. NAGY, J., FERENCZI-GRESZ, S. MIRONOV, F. V.: Zeitschrift f. Anorg. u. Allg. Chemie, **347,** 191 (1966)
28. NAGY, J., FERENCZI-GRESZ, S. NEFJODOV, S. L.: Periodica Polytechn. **10,** 319 (1966)
29. LORBERTH, J., NOTH, H.: Berichte **98,** 969 (1965)
30. NAGY, J., RÉFFY, J., BORBÉLY-KUSZMANN, A., BECKER-PÁLOSSY, K.: J. Organometallic Chem. **7,** 393 (1967)
31. NAGY, J., RÉFFY, J., BORBÉLY-KUSZMANN, A., BECKER-PÁLOSSY, K., FERENCZI-GRESZ, S., GERGŐ, É.: Periodica Polytechnica, im Druck
32. VOGEL, A. J.: Textbook of Practical Organic Chemistry. Longmans, Green and Co., London (1956)
33. Gmelins Handbuch der Anorg. Chemie. Silicium. Weinheim, 1958.

József NAGY
Sarolta FERENCZI-GRESZ
Katalin PÁLOSSY-BECKER
Anna BORBÉLY-KUSZMANN

Budapest XI., Gellért tér 4.

Acta Chimica Academiae Scientiarum Hungaricae, Tomus 61 (2), pp. 159—161 (1969)

MEAN AMPLITUDES OF VIBRATION FOR SMALL MOLECULES CONTAINING SULPHUR, II

SULPHURYL FLUORIDE, FLUORO AND CHLORO SULPHONIC ACIDS

S. J. CYVIN and I. HARGITTAI

(Institute of Theoretical Chemistry, Technical University of Norway, Trondheim and Laboratory for Research of Chemical Structures of the Hungarian Academy of Sciences, Budapest)

Received August 14, 1968

Mean amplitudes of vibration were calculated for SO_2F_2, $(OH)SO_2F$ and $(OH)SO_2Cl$ from spectroscopic data. For the two latter compounds the results should be considered as somewhat uncertain. In any way the calculations for all these compounds may no doubt be helpful in future electron-diffraction investigations.

In this paper we communicate the calculated mean amplitudes of vibration for some further molecules containing sulphur, in addition to our work on thionyl and sulphuryl chlorides [1]. In contrast to the situation for the latter molecules no electron-diffraction data of mean amplitudes are available for the compounds considered in the present work. But the results of the present calculations are believed to be very helpful for future electron-diffraction investigations, which actually are scheduled at least for some of the molecules in question.

Sulphuryl fluoride

Following the same procedure as we used for sulphuryl chloride [1] we started with force constants mainly taken from HUNT *et al.* [2], and adjusted them to vibrational frequencies from (b) NAKAMOTO [3] and (c) SIEBERT [4]. Below we give the resulting mean amplitudes in Å units at 298°K, along with calculated values from VENKATESWARLU *et al.* [5, 6] (at 300°K) listed under column (a).

Distance	(a)	(b)	(c)
S = O	0.03969	0.0340	0.0339
S — F	0.04282	0.0405	0.0406
O . . . O	0.05830	0.0520	0.0604
F . . . F	0.06612	0.0571	0.0599
O . . . F	0.05476	0.0643	0.0601

Table I

Mean amplitudes of vibration (Å units) for fluoro and chloro sulphonic acids

$(OH)SO_2F$	(Equil. dist.)	T = 0	298°K
O—H	(0.957)	0.070_2	0.070_2
S—O (hydroxyl)	(1.560)	0.047_7	0.050_3
S—F	(1.530)	0.046_3	0.049_0
S=O	(1.405)	0.037_0	0.037_4
O (hydroxyl) . . F	(2.297)	0.064_6	0.073_0
O . . . O	(2.481)	0.049_9	0.050_9
O (hydroxyl) . . O	(2.405)	0.057_9	0.061_5
F . . . O	(2.380)	0.059_5	0.065_5
H . . . S	(2.147)	0.111_5	0.114_1
H . . . F	(3.198)	0.096_7	0.101_8
H . . . O	(2.733)	0.132_9	0.137_4
$(OH)SO_2Cl$	(Equil. dist.)	T = 0	298°K
O—H	(0.957)	0.070_7	0.070_7
S—O (hydroxyl)	(1.560)	0.044_6	0.046_7
S—Cl	(2.010)	0.043_1	0.048_0
S=O	(1.407)	0.036_1	0.036_4
O (hydroxyl) . . Cl	(2.759)	0.074_8	0.106_6
O . . . O	(2.472)	0.055_0	0.058_1
O (hydroxyl) . . O	(2.399)	0.060_2	0.065_7
Cl . . . O	(2.784)	0.059_0	0.069_8
H . . . S	(2.147)	0.103_3	0.105_1
H . . . Cl	(3.676)	0.099_4	0.120_3
H . . . O	(2.717)	0.129_0	0.135_2

The vibrational assignment for SO_2F_2 from SIEBERT [4] is given in the following, with frequency values (included in parentheses) from NAKAMOTO [3] in the cases where they are different. All values are wave numbers in cm^{-1}. *Species* A_1: 1269, 848, 544 (545), 384 (544). *Species* A_2: 388 (360). *Species* B_1: 1502, 553 (386). *Species* B_2: 885, 539 (545). As equilibrium parameters we have used [7] R(SF) = 1.53 Å, D(SO) = 1.405 Å, 2A(FSF) = 96.1° and 2B(OSO) = = 124°. Observed mean amplitudes from electron diffraction might be decisive in favour of one of the above listed alternatives. At present we consider Set (c) to represent the most reliable values. The corresponding set in the calcula-

tions for the chlorine compound [1] showed its superiority. Moreover all the vibrational frequencies for SO_2F_2 of the SIEBERT assignment [4] are exactly equal to those of a recent Raman reinvestigation [8]. The valence force-constants for stretchings from our calculations corresponding to Set (c) are: f(S = O) = 11.724 and f(S — F) = 5.570 mdyne/Å.

Fluoro and chloro sulphonic acids

Here we give only a brief report on our calculations of mean amplitudes for $(OH)SO_2F$ and $(OH)SO_2Cl$, since the results are rather uncertain for several reasons. As to the structure of these molecules the HOSX (X = F, Cl) atoms are assumed to lie in one plane, while SO_2 forms another plane perpendicular to the former. The calculations are based on vibrational assignments of frequencies collected from two works [9, 10], but this assignment is certainly not unquestionable. On the other hand, using these frequencies the procedure of our normal-coordinate analysis worked very well. We started with an initial valence force field, which should reproduce the observed frequencies not too badly. Next this force field was adjusted to the exact frequency values. After some few runs of this type using an iteration procedure we obtained reasonable force constants, and we made no further refinements. Further refinements and modifications seem not to be justified at least before some observed mean amplitudes are available. The equilibrium parameters used for $(OH)SO_2F$ and $(OH)SO_2Cl$ in our calculations are transferred from related compounds according to various sources from literature. Their magnitudes are consistent with the bonded and nonbonded distances included in parentheses in Table I. In this table the final mean amplitudes from our calculations are collected.

REFERENCES

1. HARGITTAI, I., CYVIN, S. J.: Acta Chim. Acad. Sci. Hung. **61** (1969). This paper is considered as Part I of the article series.
2. HUNT, G. R., WILSON, M. K.: Spectrochim. Acta **18**, 959 (1962)
3. NAKAMOTO, K.: Infrared Spectra of Inorganic and Coordination Compounds. Wiley, New York, 1963
4. SIEBERT, H.: Anwendungen der Schwingungsspektroskopie in der anorganischen Chemie. Springer-Verlag, Berlin 1966
5. VENKATESWARLU, K., MALATHY DEVI, V.: Indian J. Pure Appl. Phys. **3**, 195 (1965)
6. CYVIN, S. J.: Molecular Vibrations and Mean Square Amplitudes. Universitetsforlaget, Oslo, and Elsevier, Amsterdam 1968
7. LIDE, D. R., MANN, D. E., FRISTROM, R. M.: J. Chem. Phys. **26**, 734 (1957)
8. BIRCHALL, T., GILLESPIE, R. J.: Spectrochim. Acta **22**, 681 (1966)
9. GILLESPIE, R. J., ROBINSON, E. A.: Can. J. Chem. **40**, 644 (1962)
10. CHACKALACKAL, S. M., STAFFORD, F. E.: J. Am. Chem. Soc. **88**, 4815 (1966)

Sven J. CYVIN, Institute of Theoretical Chemistry, Technical University of Norway, Trondheim, Norway
István HARGITTAI, Budapest VIII., Puskin u. 11—13

Acta Chimica Academiae Scientiarum Hungaricae, Tomus 61 (2), pp. 163—166 (1969)

STRETCHING FORCE CONSTANTS IN NO_2F AND NO_2Cl

D. E. FREEMAN

(Air Force Cambridge Research Laboratories)

Received November 28, 1968

The stretching force constants of NO_2F and NO_2Cl recently obtained in two different systems of symmetry coordinates by NEMES are physically incompatible unless (a) they refer to quite different solutions among the multiplicity of possible solutions to the vibrational problem and/or (b) NEMES' dispersions of the force constants are grossly underestimated.

In the latest paper of NEMES [1] dealing with the force fields of NO_2Cl and NO_2F, the revised normal frequency assignments of BERNITT *et al.* [2] are used. In this paper [1], which supersedes his earlier efforts [3], NEMES reports and compares symmetry force constants based on two different sets of symmetry coordinates, only one set of which contains a redundant angular coordinate. The purpose of the present note is to indicate that the two sets of stretching force constants obtained are physically incompatible unless (a) they refer to quite different solutions among the multiplicity of possible solutions of the vibrational problem and/or (b) the stated dispersions of the force constants are grossly underestimated and possess not even relative validity. In either case, doubt is cast upon the usefulness of the calculation.

When different sets of symmetry coordinates satisfying the molecular symmetry requirements exist, the relationship between the corresponding sets of force constants is defined by the invariance of the vibrational potential energy to the choice of coordinate system. Generally, for a given molecule, no physically meaningful direct comparison can be made between analogous force constants belonging to different coordinate systems. In Table IV (for NO_2F) and Table V (for NO_2Cl) of NEMES' paper [1], the symmetry force constants based on his Set I symmetry coordinates (containing a redundancy) are directly compared to those based on his Set II symmetry coordinates (containing, it is claimed, no redundancy). To render such a comparison meaningful the symmetry force constants calculated in different coordinate systems should be transformed to a common basis which may here conveniently be chosen as Set I, Set II, or the internal coordinate system. Due to the angular redundancy in the Set I coordinates, the corresponding force constants cannot all be transformed uniquely to a redundancy-free basis, but, because the redundancy for planar XY_2Z molecules involves only angles, the nonangular

portion, *i.e.*, the bond-stretching portion, of the potential function is unaffected by the purely angular redundancy. Consequently, the Set I stretching coordinates S^{I}, the Set II stretching coordinates S^{II}, and the internal stretching coordinates r are linearly and uniquely related, in accordance with the formulae

$$S^{I} = \begin{bmatrix} S_1^{I} \\ S_2^{I} \\ S_4^{I} \end{bmatrix} = \begin{bmatrix} 3^{-1/2} & 3^{-1/2} & 3^{-1/2} \\ -6^{-1/2} & -6^{-1/2} & 2(6)^{-1/2} \\ 2^{-1/2} & -2^{-1/2} & 0 \end{bmatrix} \begin{bmatrix} d_1 \\ d_2 \\ D \end{bmatrix} \equiv A^{I} r \tag{1}$$

and

$$S^{II} = \begin{bmatrix} S_1^{II} \\ S_2^{II} \\ S_4^{II} \end{bmatrix} = \begin{bmatrix} 2^{-1/2} & 2^{-1/2} & 0 \\ 0 & 0 & 1 \\ 2^{-1/2} & -2^{-1/2} & 0 \end{bmatrix} \begin{bmatrix} d_1 \\ d_2 \\ D \end{bmatrix} \equiv A^{II} r\,. \tag{2}$$

If F,^{I} F^{II}, and f denote, respectively, force constant matrices (of stretching force constants only) based on coordinates S^{I}, S^{II}, and r, then, since A^{I} and A^{II} are orthogonal, the formulae

$$f = \tilde{A}^{I}\ F^{I}\ A^{I} \tag{3a}$$

$$= \tilde{A}^{II}\ F^{II}\ A^{II} \tag{3b}$$

and

$$F^{I} = (A^{I}\,\tilde{A}^{II})\,F^{II}(A^{I}\,\tilde{A}^{II})^{\sim} \tag{4}$$

describe the transformation properties of the purely stretching portion of the potential function.

The results of applying Eq. (4) to the Set II symmetry stretching force constants listed in Tables IV and V of Ref. [1] are given in Table I. In a similar

Table I

NO_2X stretching force constants obtained from calculations in two different systems of symmetry coordinates

	NO_2F		NO_2Cl	
mdyn A^{-1}	Calc. I[a]	Calc. II[b]	Calc. I[a]	Calc. II[b]
F_{11}^{I}	12.587±0.036	9.380	10.057±0.012	8.731
F_{12}^{I}	−3.630±0.034	−3.036	−2.260±0.011	−1.312
F_{22}^{I}	4.370±0.035	5.175	7.127±0.012	7.055

[a] These force cons ants are those given for Set I coordinates by NEMES [1] in his Tables IV and V.
[b] These force constants are expressed relative to the Set I coordinates S^{I} of Eq. (1) and are obtained through Eq. (4) from the Set II force constants in Tables IV and V of NEMES [1].

fashion, Eq. (3a) and Eq. (3b) can be used separately to obtain values of stretching force constants relative to the common set of internal stretching coordinates r, defined in Eq. (1) and Eq. (2). These results are given in Table II.

Since the weighted sum of squared frequency errors cited by NEMES for his Set I and Set II calculations in his Tables IV and V are of comparable magnitude for a particular molecule, both calculations are judged comparable in their ability to fit the frequencies of that molecule. Moreover, since the vectors

$$[F^{I}_{11}, F^{I}_{12}, F^{I}_{22}, F^{I}_{44}], [F^{II}_{11}, F^{II}_{12}, F^{II}_{22}, F^{II}_{44}], \quad \text{and} \quad [f_D, f_d, f_{Dd}, f_{dd}]$$

are linearly related by transformations which may be shown from Eqs (3) and (4) to be well-conditioned and not nearly singular, it follows that small changes or errors in force constants are not unduly magnified by transformations among these coordinate systems. The results in Table I lead therefore to the conclusion that (a) the stretching force fields converged upon in the Set I and Set II calculations of NEMES do not belong to the same solution of the vibrational problem (which admits of multiple solutions unless constraints are imposed, for example, by the requirement that vibration-rotation interaction constants be fitted in addition to the vibrational frequencies) and/or (b) the dispersions quoted by NEMES and shown in Table I are grossly underestimated and possess not even the relative validity claimed for them [1]. This conclusion is corroborated by the results given in Table II for the force constants derived from NEMES' values for his Set I and Set II calculations and re-expressed in terms of a common basis, *viz.*, the internal stretching coordinates. For both NO_2F

Table II

NO_2X stretching force constants based on internal coordinates

	NO_2F			NO_2Cl		
mdyn A^{-1}	Calc. I[a]	Calc. II[b]	BERNITT[c]	Calc. I[a]	Calc. II[b]	BERNITT[c]
f_D	3.686	3.724	2.657	5.973	6.377	2.456
f_d	10.330	9.111	11.214	9.993	9.093	10.431
f_{Dd}	1.883	0.688	0	0.444	0.250	0
f_{dd}	2.940	1.721	1.534	1.217	0.317	1.569

[a] These force constants are obtained through Eq. (3a) from the Set I values in Tables IV and V of NEMES [1].
[b] These force constants are obtained through Eq. (3b) from the Set II values in Tables IV and V of NEMES [1].
[c] From Table 3 of Ref. [2].

and NO_2Cl, it also seems that the internal stretching force constants of NEMES* and those of BERNITT *et al.* [2] belong to different solutions of the vibrational problem. These considerations, together with the inability of NEMES' force fields to reproduce the isotopic frequencies well, cast doubt on the usefulness of these force fields for NO_2Cl and NO_2F and stress the necessity for the inclusion of experimental data on vibration-rotation interaction constants in any future calculations of the force fields for these molecules.

Note added in proof. For NO_2F, A. M. MIRRI, G. CAZZOLI, and L. FERRETTI [J. Chem. Phys. **49,** 2775 (1968)] have recently shown that even the use of centrifugal distortion coefficients derived from the millimeter wavelength spectrum, in addition to the infrared frequencies, does not permit determination of a unique force field. Two alternative force fields are obtained, and these results seem closer to those of BERNITT *et al.* [2] than to those of NEMES [1].

REFERENCES

1. NEMES, L.: Acta Chim. Acad. Sci. Hung. **56,** 153 (1968)
2. BERNITT, D. L., MILLER, R. H., HISATSUNE, I. C.: Spectrochim. Acta **23A,** 237 (1967)
3. NEMES, L.: Acta Chim. Acad. Sci. Hung. **52,** 169, 179, 189 (1967)

D. E. FREEMAN; Air Force Cambridge Research Laboratories. L. G. Hanscom Field, Bedford, Massachusetts 01730.

* It would be possible, by an appropriate transformation, to compare the bending force constants of BERNITT *et al.* (who employ non-redundant coordinates) to those based on NEMES' Set II coordinates if this latter set were generated from a complete non-redundant set of internal coordinates. However, the five symmetry coordinates (S_1^{II}, ... S_5^{II}) specifying the five degrees of planar freedom are defined by NEMES in terms of six internal coordinates (d_1, d_2, D, A, a_1, a_2).

Acta Chimica Academiae Scientiarum Hungaricae, Tomus 61 (2), pp. 167—179 (1969)

KINETICS AND MECHANISM OF SUBSTITUTION REACTIONS OF COMPLEXES, XI

NEW REINECKE-SALT-LIKE COMPOUNDS CONTAINING PARA-PHENETIDINE, AND THE SOLVOLYSIS OF $[Cr(NCS)_4(p\text{-PHENETIDINE})_2]^-$ IN ETHANOL–WATER MIXTURES

J. ZSAKÓ, Cs. VÁRHELYI, J. GĂNESCU and J. TURÓS

(Faculty of Chemistry, Babeş-Bolyai University, Cluj, Roumania)

Received June 16, 1968

Twenty new complexes were synthesized, containing the complex anion-$[Cr(NCS)_4(p\text{-phenetidine})_2]^-$. Synthesis, analysis and characterization of these compounds are given.

The solvolysis of the $[Cr(NCS)_4(p\text{-phenetidine})_2]^-$ complex ion was studied in various ethanol–water mixtures. The experimental results were explained by assuming two parallel processes. The substitution of the first NCS is a first order reaction in respect to the initial complex ion. Its activation energy is about 30 kcal/mole and its activation entropy of about 10—15 Cl. The rate of this reaction is practically not influenced by the composition of the solvent. The substitution of the *p*-phenetidine molecules seems to be a second order reaction (first order in respect to the complex ion and first order in respect to ethanol). This reaction has an activation energy of about 22—23 kcal/mole and nearly a zero activation entropy. The substitution of NCS ions is practically not influenced by the hydrogen ion concentration, the substitution of *p*-phenetidine, however, is faster in the presence of a mineral acid.

We have reported in earlier papers [1—3] that in $K_3[Cr(NCS)_6]$ the NCS-groups can be easily partially substituted with aromatic or with heterocyclic amines as aniline derivatives (pK = 9—12) and pyridine, picoline respectively, by heating these reagents in the absence of solvent. We observed that *p*-phenetidine, with a base strength close to that of aniline, enters easily into the internal co-ordination sphere of $K_3[Cr(NCS)_6]$: $[Cr(NCS)_6]^{3-} + 2p\text{-phenetidine} = [Cr(NCS)_4(p\text{-phenetidine})_2]^- + 2NCS^-$ [4].

The physico-chemical properties of $[Cr(NCS)_4(p\text{-phenetidine})_2]^-$ are very similar to those of the rhodanilate ion $[Cr(NCS)_4(aniline)_2]^-$ obtained by BERGMAN [5]. It is a suitable precipitating agent for a great number of heterocyclic N-bases and can be used *e.g.* for the separation of alkaloids. In the present paper 8 new compounds formed between the above complex ion and chlorohydrates of alkaloids and of heterocyclic N-bases are described. These are listed in Table I.

The solubility of the alkaloid salts is very slight and therefore these organic bases can be determined quantitatively either by a gravimetric or a photometric method in the same manner as the reineckeate.

Meanwhile the anion $[Cr(NCS)_4(p\text{-phenetidine})_2]^-$ (abbreviated as Phen.R. is a very effective precipitating agent for the separation of metal-amine complex cations, as $[Me^{II}(NH_3)_n]^{2+}$, $[Me^{II}(en)_n]^{2+}$, with Me^{II} = Zn, Cd, Cu

Table I

New compounds of the type amine. H[Cr(NCS)$_4$(p-phenetidine)$_2$] (Amines are organic N-bases)

No.	Formula	Mol. weight calcd.	Analysis				Solubility, in water mole/l (20—22°C)
			Calcd.	Found	Appearance	Yield %	
1.	*p*-phenetidine H [Phen. R]	696.8	Cr 7.46 S 18.40	7.50 18.47	red-violet thin prisms	80	—
2.	8-oxychinoline H [Phen. R]	703.8	Cr 7.39 S 18.19	7.32 18.22	red-violet thin plates	85	$1.16 \cdot 10^{-3}$
3.	atropine H [Phen. R]	849	Cr 6.12 N 11.54	6.08 11.19	red-violet thin prisms	63	$1.84 \cdot 10^{-3}$
4.	cinchonidine H [Phen. R]	854	Cr 6.09 N 11.45	6.24 11.60	red-violet thin plates	78	$1.49 \cdot 10^{-3}$
5.	chinine H [Phen. R]	884	Cr 5.88 S 14.48	6.08 14.53	red-violet thin prisms	87	$1.50 \cdot 10^{-3}$
6.	ephedrine H [Phen. R]	724.9	Cr 7.17 S 17.66	6.93 17.68	red-violet thin prisms	71	$1.50 \cdot 10^{-3}$
7.	morphine H [Phen. R]	845	Cr 6.15 N 11.60	6.21 11.85	red-violet irregular plates	78	$8.4 \cdot 10^{-4}$
8.	pylocarpine H [Phen. R]	767.9	Cr 6.77 N 13.11	6.88 13.11	red-violet thin plates	80	$4.4 \cdot 10^{-3}$

[Phen. R] = $[Cr(NCS)_4(p\text{-phenetidine})_2]^-$

and Ni, $[Cr(en)_3]^{3+}$, $[Cr(NH_3)_5H_2O]^{3+}$, $[Cr(en)_2(NCS)_2]^+$ and a large number of cations of the hexamine, mono-acido-pentamine and diacido-tetramine-cobalt(III)-type. The precipitation reactions with cobalt(III)- and chrom(III)-amines have no analytical significance because of the specific formation conditions, but they can be used for the isolation and chemical characterization of readily soluble complex cations. In Table II 12 cobalt(III)-amine compounds are compiled.

From the above compounds those of the hexamine type are slightly soluble in water. All the cobalt(III)-amine derivatives given in Table II are

Table II

New cobalt(III)-amine derivatives of the acid $H[Cr(NCS)_4(p\text{-phenetidine})_2]$

No.	Formula	Mol. weight calcd.	Analysis			Yield %
			Calcd.	Found	Appearance	
	a) Hexamine type					
1.	$[Co(en)_3]$ (Phen. R)$_3$	1914.9	Co+3Cr 11.23 S 20.09	11.41 19.98	light red microcryst.	68
2.	$[Co(NH_3)_6]$ (Phen. R)$_3$	1835.8	Co+3Cr 11.70 S 20.94	11.88 20.77	red-violet microcryst.	70
3.	$[Co(NH_3)_5H_2O]$ (Phen. R)$_3$	1837.8	Co+3Cr 11.68 S 20.93	11.64 20.73	violet rectangular plates	55
	b) Monoacido-pentamine type					
4.	$[Co(en)_2Cl\ NH_3]$ (Phen. R)$_2$	1348.8	Co+2Cr 12.08 N 11.44	12.20 11.30	red microcryst.	60
5.	$[Co(en)_2Cl$ benzylamine] (Phen. R)$_2$	1438.8	Co+2Cr 11.32 S 17.82	11.03 17.64	light red microcryst.	50
6.	$[Co(en)_2Cl$ aniline] (Phen. R)$_2$	1424.9	Co+2Cr 11.44 N 10.81	11.50 10.90	red-violet microcryst.	52
	c) Diacido-tetramine type					
7.	trans-$[Co(en)_2Cl_2]$ (Phen. R)	808.6	Co+Cr 13.77 S 15.86	13.44 15.88	light pink microcryst.	65
8.	cis-$[Co(en)_2Cl_2]$ (Phen. R)	808.6	Co+Cr 13.77	13.60	violet microcryst.	60
9.	cis-$[Co(NH_3)_4(NO_2)_2]$ (Phen. R)	777.8	Co+Cr 14.26 N 21.60	14.40 21.40	orange microcryst.	60
10.	$[Co(DH)_2(\beta$-toluidine$)_2]$ (Phen. R)	1063.8	Co+Sr 10.43 C 12.05	10.20 11.99	golden yellow microcryst.	88
11.	$[Co(DH)_2(\beta$-picoline$)_2]$ (Phen. R)	1035.8	Co+Cr 10.47 S 12.38	10.57 12.35	light pink microcryst.	80
12.	$[Co(DH)_2$(o-anisidine$)_2]$ (Phen. R)	1095.8	Co+Cr 10.13 S 11.68	10.06 11.67	thin, golden yellow plates	75

en = $C_2H_8N_2$, DH = $C_4H_7N_2O_2$

readily soluble in some polar solvents as acetone, methyl-ethyl-ketone, acetyl-acetone, ethyl acetate, dimethyl-formamide and pyridine; they are, however, insoluble in nonpolar solvents as benzene, toluene, carbon tetrachloride, chloroform. Their solubility in methanol is quite different. The most soluble are some derivatives of the diacido-tetramine-type as $[Co(DH)_2(amine)_2]$ Phen.R.

The anion $[Cr(NCS)_4(p\text{-phenetidine})_2]^-$ is unstable in solutions: in aqueous alcohol solutions ligand exchange reactions take place.

We have studied the solvolysis of the anion of two similar Reinecke-salt-like compounds (anilinium resp. *p*-toluidinium $[Cr(NCS)_4(amine)_2]$) in ethanol–water mixtures [6], [7]. Our experiments showed that two parallel ligand exchange reactions occur, the replacement of thiocyanate ion and the replacement of the aromatic amine molecule by solvent molecules. In this respect the solvolysis of the studied compounds differs fundamentally from the solvolysis of the Reinecke salt, studied by ADAMSON [8].

He has proved that in the solvolysis of $[Cr(NCS)_4(NH_3)_2]^-$ only NCS is replaced, ammonia, however, is not liberated. In ethanol–water mixtures the solvolysis kinetics are practically not influenced by the composition of the solvent. In the case of the analogous compounds containing aromatic amines the NCS exchange is also not affected by the alcohol content of the solvent, but the amine is liberated too and the rate of its exchange is considerably increased by higher ethanol concentration. The amine exchange process is a second order reaction, being first order in ethanol [7]. Mineral acids have a similar accelerating effect upon the amine exchange.

In this paper the ligand exchange reactions with the $[Cr(NCS)_4(p\text{-phenetidine})_2]^-$ ion are reported. The change in time of the concentration of this ion at different temperatures was followed in 4 ethanol–water mixtures, containing 24.2; 48.5; 72.7 and 97.0 v/v per cent ethanol, respectively. These measurements enabled us to study the kinetics of the total process. A plot of $\lg c/c_0$ versus time gave a good linearity (Fig. 1).

Thus the overall process is apparently a first order reaction. As seen from Fig. 1, rate constants are highly dependent on the composition of the solvent, similarly as in the case of the analogous aniline and *p*-toluidine derivatives. From the experimental data the rate constants were calculated for various temperatures and ethanol–water mixtures. The corresponding rate constants are given in Table III.

Using the Arrhenius equation the apparent activation energy $E_a^{\ddagger}$ and the frequency factor PZ were calculated for the different solvent compositions. These values are given in Table IV.

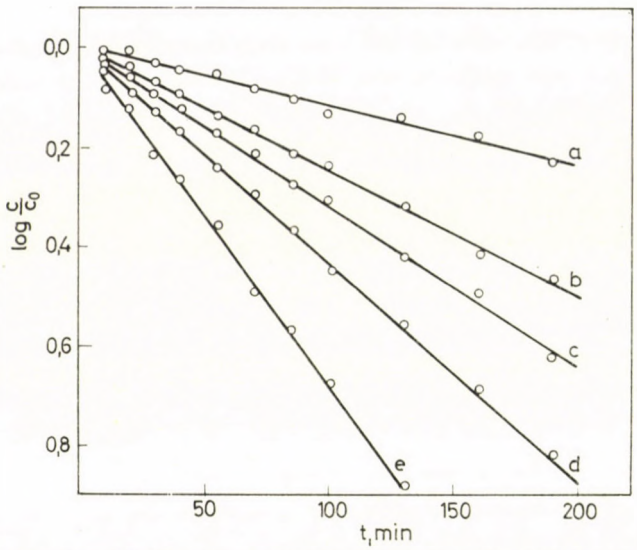

Fig. 1. Determination of the rate constants of the overall reaction. a — 24.2% ethanol, 40.1°C; b — 24.2% ethanol, 45.1°C; c — 48.5% ethanol, 45.0°C; d — 97.0% ethanol, 40.2°C; e — 97.0% ethanol 45.0°C

Table III

Rate constants of the overall process ($k \cdot 10^4$, s^{-1})

t°C	Ethanol concentration v/v per cent			
	24.2	48.5	72.7	97.0
40.1	0.46	0.68	—	—
40.2	—	—	1.04	1.69
45.0	—	1.23	1.79	2.65
45.1	0.97	—	—	—
50.1	1.64	2.78	3.82	4.83
53.5	2.94	—	—	—
54.8	—	4.27	—	—
55.0	—	—	5.88	8.93

Table IV

Apparent activation energy and activation entropy of the overall process

t°C	Ethanol concentration v/v per cent			
	24.2	48.5	72.7	97.0
$E_a^{\ddagger}$, kcal/mole	27.3	26.3	24.6	23.1
lg PZ	14.7	14.1	13.2	12.3
$\Delta S_{298}^{\ddagger}$Cl	8.7	6.2	1.7	—2.1

In the same table are given also the apparent activation entropy values, obtained by means of the well known formula:

$$\Delta S^{\ddagger} = 2{,}3\, R \ \lg \frac{PZ\,h}{kT}.$$

The apparent activation energy and also the activation entropy decrease with increasing ethanol content of the solvent.

In order to separate the two parallel solvolysis processes, both the concentration of the unchanged complex and that of the free NCS^- was measured. Thus we obtained the ratio $r = [NCS^-]/(c_0 - c)$, where c_0 and c stand for the

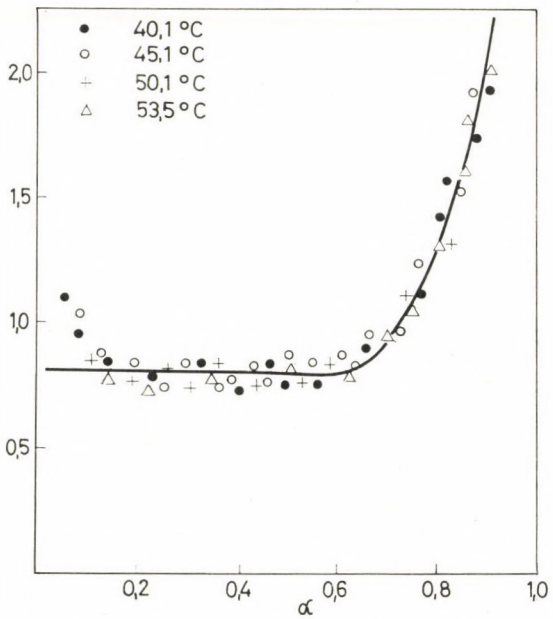

Fig. 2. Ratio $r = [NCS^-]/(c_0 - c)$ versus transformation degree of the initial complex ion Ethanol content of the solvent: 24.2%

initial and for the actual concentration of the studied complex ion. This ratio is constant in the case of the solvolysis of the Reinecke salt. According to ADAMSON [8], it is about $r = 2$. ADAMSON assumed that the solvolysis of the first NCS^- was followed by the instantaneous replacement of the second thiocyanate ion. In the case of the corresponding aniline and *p*-toluidine derivatives we found also a constant ratio r [6, 7], when not more than 80—85% of the initial complex was transformed. These values are less than 2 and are depending on the ethanol content of the solvent. We suppose that also the aniline or the *p*-toluidine

molecules are replaced during the solvolysis process. Our measurements concerning the ratio r in the case of the solvolysis of the *p*-phenetidine derivative give the same general picture as at the earlier studied compounds. The plot of the ratio r *versus* the transformation degree α of the initial complex gives a single curve for each solvent composition, irrespective of the temperature. The ratio r is practically constant until the transformation of the initial complex ion is nearly complete; no systematic variation of this ratio with temperature was observed, but an irregular scattering of experimental values round the common curve. These results are illustrated in Fig. 2.

It can be seen that r has about the same value during the solvolysis at all studied temperatures and begins to increase only after the transformation of the majority of the initial complex ions. The mean value of r, corresponding to the horizontal portion of the curve in Fig. 2, depends on the composition of the solvent. For this practically constant r value we obtained the following figures in the different solvent mixtures:

Ethanol content v/v per cent	24.2	48.5	72.7	97.0
Ratio r	0.79	0.51	0.33	0.22

These values are also less than those found by ADAMSON for the Reinecke salt and r decreases with increasing ethanol content. These results can be explained by means of the following hypotheses:

1. The solvolysis of the complex ion involves two parallel processes:

$$[Cr(NCS)_4(p\text{-Phen})_2] + ROH = [Cr(NCS)_3(ROH)(p\text{-Phen})_2] + NCS^- \quad (1)$$

$$[Cr(NCS)_4(p\text{-Phen})_2]^- + ROH = [Cr(NCS)_4(p\text{-Phen})(ROH)]^- + p\text{-Phen} \quad (2)$$

where *p*-Phen stands for *p*-phenetidine and ROH for a molecule of solvent, either water or ethanol.

2. Reaction (1) is succeeded by a practically instantaneous process:

$$[Cr(NCS)_3(ROH)(p\text{-Phen})_2] + ROH = [Cr(NCS)_2(ROH)_2(p\text{-Phen})_2]^+ + NCS^- \quad (3)$$

This assumption seems to be probable for the following reasons:

a) In the case of the Reinecke salt, where NH_3 is not substituted, ADAMSON found the ratio $r = 2$.

b) In the case of the aniline derivatives the ratio r is near to $r = 2$ at low ethanol content and otherwise it varies with the ethanol content like the *p*-phenetidine derivative, studied in the present paper.

Supposing that the above hypotheses are correct we can calculate the rate constants of the processes (1) and (2) from the overall rate constant.

For this purpose we can use the formulas given in our earlier paper [6]:

$$k_1 = k\frac{r}{2} \quad \text{and} \quad k_2 = k\left(1 - \frac{r}{2}\right). \tag{4}$$

In these formulas k, k_1 and k_2 stand for the rate constant of the overall reaction and of reactions (1) and (2) respectively. In order to eliminate the scattering of experimental data, k_1 and k_2 were not calculated using the experimental overall rate constants k (given in Table III), but from "theoretical" ones obtained from the Arrhenius equation, using the activation energies and lg PZ values from Table IV. From these "theoretical" overall rate constants k_1 and k_2 were calculated according to formulas (4). The obtained values are presented in Tables V and VI.

Table V

Rate constants of reaction (1) ($k_1 \cdot 10^4$, s^{-1})

t°C	Ethanol concentration v/v per cent			
	24.2	48.5	72.7	97.0
40.1	0.18	0.17	—	—
40.2	—	—	0.17	0.18
45.0	—	0.33	0.31	0.34
45.1	0.36	—	—	—
50.1	0.71	0.64	0.58	0.60
53.5	1.10	—	—	—
54.8	—	1.14	—	—
55.0	—	—	1.02	1.03

Table VI

Apparent rate constants of reaction (2) ($k_2 \cdot 10^4$, s^{-1})

t°C	Ethanol concentration v/v per cent			
	24.2	48.5	72.7	97.0
40.1	0.28	0.51	—	—
40.2	—	—	0.87	1.42
45.0	—	0.97	1.57	2.47
45.1	0.56	—	—	—
50.1	1.09	1.87	2.89	4.40
53.5	1.70	—	—	—
54.8	—	3.36	—	—
55.0	—	—	5.15	7.52

These data indicate that the rate constant k_1 of reaction (1) is almost independent from the concentration of ethanol, *i.e.* reaction (1) is, in first approximation, not influenced by the composition of the solvent. This conclusion is in a good agreement with ADAMSON's observation concerning the independence of the solvolysis rate from the alcohol content of the solvent in the case of the Reinecke salt, where only the thiocyanate is exchanged.

In contrary to reaction (1), the rate constant of reaction (2) increases strongly with increasing ethanol concentration. This enables us to look for a partial reaction order with respect to ethanol. The quotient of the rate constant k_2 and the molar concentration of ethanol is nearly constant at a given temperature. Thus reaction (2) seems to be a second order reaction: first order both with respect to the complex ion and to ethanol.

On the basis of the above results we assume that *p*-phenetidine is replaced by ethanol in reaction (2). The corresponding second order rate constants are given in Table VII.

Table VII

Second order rate constants of reaction (2)
($k_2 \cdot 10^5$, l^{-1} $mole^{-1}$)

t°C	Ethanol concentration v/v per cent			
	24.2	48.5	72.7	97.0
40.1	0.67	0.61	—	—
40.2	—	—	0.69	0.85
45.0	—	1.17	1.26	1.49
45.1	1.34	—	—	—
50.1	2.62	2.25	2.31	2.62
53.5	4.07	—	—	—
54.8	—	4.04	—	—
55.0	—	—	4.12	4.47

Considering the activation energy and activation entropy of both processes we can say the following: Since the apparent activation energy of the solvolysis decreases with increasing ethanol concentration and meanwhile the relative rate of reaction (2) increases, we can presume that reaction (1) requires a larger activation energy than reaction (2). On the basis of apparent activation energy data given in Table IV, the activation energy of reaction (1) is about 30 kcal/mole, while the activation energy of reaction (2) about 22—23 kcal/mole. Similarly we presume that reaction (1) has a larger activation entropy, about 10—15 Cl, while reaction (2) a far smaller and even a negative one.

Further the influence of an acid on these solvolysis reactions was studied. The same kinetic measurements were carried out in 24.2 v/v per cent ethanol

in the presence of different perchloric acid concentrations. The overall rate of solvolysis is strongly influenced by the acidity of the solution: the solvolysis rate increases with increasing perchloric acid concentration. In Table VIII are given the rate constants obtained at different temperatures and different acid concentrations together with the activation energy, lg *PZ* and activation entropy values.

Table VIII

Influence of the perchloric acid concentration on the kinetics of the overall process in an ethanol–water mixture containing 24.2 v/v per cent ethanol

Concentration of $HClO_4$ mole/l	$k \cdot 10^4$, s^{-1}				$E_a^{\ddagger}$ kcal/mole	lg *PZ*	$\Delta S_{298}^{\ddagger}$ Cl	*r*
	40°C	45°C	50°C	55°C				
$3 \cdot 10^{-4}$	0.50	0.98	1.84	3.56	26.2	14.0	5.5	0.74
$1 \cdot 10^{-3}$	0.54	1.06	1.97	3.66	25.5	13.6	3.6	0.69
$3 \cdot 10^{-3}$	0.59	1.13	2.08	3.81	25.0	13.2	1.9	0.54
$1 \cdot 10^{-2}$	0.64	1.21	2.19	3.94	24.4	12.85	0.3	0.45
$3 \cdot 10^{-2}$	0.68	1.28	2.31	4.18	24.4	12.85	0.3	0.41
$1 \cdot 10^{-1}$	0.73	1.35	2.42	4.49	24.2	12.75	−0.2	0.39

It can be seen that both the apparent activation energy and activation entropy decrease with increasing acidity.

The ratio (r) of the concentration of free NCS^- to transformed complex ion was determined, and the obtained values are also included in Table VIII. Since ratio r decreases, the rate of solvolysis, however, increases with increasing hydrogen ion concentration, we can conclude that reaction (2) is strongly accelerated by the hydrogen ions.

Using the kinetic parameters given in Table VIII, "theoretic" overall rate constants were calculated, and by means of formulae (4) the rate constants, k_1 and k_2, were obtained.

Table IX

Influence of perchloric acid upon the rate constants of reactions (1) and (2)

Conc. of $HClO_4$ mole/l	$k_1 \cdot 10^4$, s^{-1}				$k_2 \cdot 10^4$, s^{-1}			
	40°C	45°C	50°C	55°C	40°C	45°C	50°C	55°C
$3 \cdot 10^{-4}$	0.18	0.36	0.68	1.31	0.31	0.61	1.16	2.25
$1 \cdot 10^{-3}$	0.19	0.37	0.68	1.26	0.35	0.69	1.29	2.40
$3 \cdot 10^{-3}$	0.16	0.30	0.56	1.02	0.43	0.83	1.52	2.79
$1 \cdot 10^{-2}$	0.14	0.27	0.49	0.88	0.49	0.94	1.70	3.06
$3 \cdot 10^{-2}$	0.14	0.26	0.48	0.86	0.54	1.02	1.84	3.32
$1 \cdot 10^{-1}$	0.15	0.27	0.49	0.89	0.59	1.08	1.96	3.69

It can be seen from Table IX that both rate constants k_1 and k_2 are differently influenced by the hydrogen ion concentration. The rate constant of reaction (1) decreases with increasing acidity, up to perchloric acid concentrations of $3 \cdot 10^{-3}$ to 10^{-2} mole/l. Thus reaction (1) shows a similar behaviour as many other aquation reactions, where a minimum acidity is needed to hinder the basic hydrolysis. Since basic hydrolysis is much faster than the acid one, increasing acidity lowers the hydrolysis rate. In the case of some bis-ethylenediamine-chloro-amino-cobaltous(III) complexes the basic hydrolysis can be suppressed completely at $pH \leq 3$ in aqueous solutions [11, 12]. According to the kinetic data of Table IX, in our ethanol–water mixtures some more hydrogen ions are needed to hinder basic hydrolysis of the studied $[Cr(CNS)_4(p\text{-Phen})_2]^-$, since rate constant values k_1 are practically independent of acidity only if the perchloric acid concentration is not less than 10^{-2} mole/l.

Reaction (2) is greatly accelerated by perchloric acid. Rate constants k_2 are increasing with the perchloric acid concentration all over the studied acidity range. This increase is not directly proportional to an integer power of the hydrogen ion concentration, it is, however, closely linear with the pH.

In some respect the influence of perchloric acid is similar to the influence of the ethanol content of the solvent, as the increase of the concentration of the added component (perchloric acid or ethanol) leads to the acceleration of reaction (2). Since reaction (2) has a smaller activation energy and activation entropy than reaction (1), the apparent activation energy and entropy of the overall process decrease in both cases (see Tables IV and VIII).

Meanwhile, there is a great difference too, between the influence of ethanol content and acidity. Reaction (1) is practically not influenced by the ethanol content of the solvent, while the presence of perchloric acid hinders basic hydrolysis and thus the increase of its concentration diminishes the rate constant k_1, at $pH > 2$. Reaction (2) is accelerated by the increase of both ethanol concentration and acidity. While it is possible to establish a first order with respect to ethanol, one cannot find a partial reaction order with respect to the hydrogen ions.

Experimental

Preparation of p-phenetidine.H[Cr(NCS)$_4$(p-phenetidine)$_2$]

60 g (0.1 mole) of anhydrous $K_3[Cr(NCS)_6]$ and 70 g (0.6 mole) of *p*-ethoxy-aniline (*p*-phenetidine) are thoroughly mixed and the mixture is kept on water bath in a corked flask. The mixture should be stirred frequently. The initially violet mass gradually turns to dark red. In order to separate the product from the KCNS, which is formed in the reaction between $K_3[Cr(NCS)_6]$ and the organic base, the mixture is treated with 250 ml of 50% acetic acid after cooling. It is stirred vigorously and filtered. The precipitate is washed with an aqueous solution of acetic acid, and the residue is dissolved in 200 ml of ethanol. The alcoholic solution is given dropwise to 1500 ml of water, and *p*-phenetidine.H$[Cr(NCS)_4(p\text{-phenetidine})_2]$ precipitates. It is filtered, washed with distilled water and dried on air.

Preparation of derivatives of the type: amine.H[Cr(NCS)$_4$(p-Phen)$_2$]

To 10 mmole of the corresponding amine 10 ml of conc. HCl is added. The obtained amine-chlorhydrate is dissolved in 80—100 ml of water. 2.5 mmole of *p*-phenetidine. H[Cr(NCS)$_4$(*p*-Phen)$_2$] (1.8 g) is dissolved in 30—35 ml alcohol separately. In 10—30 minutes after mixing the two solutions the complex salt precipitates. The product is filtered, washed with some distilled water 3—4 times and dried on air at room temperature. The compounds are given in Table I.

Analysis. The chromium content of the products was determined iodometrically, sulphur gravimetrically, as $BaSO_4$ and nitrogen by Dumas' method.

Solubility measurements. Saturated solutions of the complex salts were submitted to alkaline decomposition in the presence of H_2O_2 and the chromium content was determined iodometrically.

Synthesis of cobalt(III)-amine derivatives

Hexamine-cobalt(III) derivatives: 2 mmoles of the chloride of the hexamine type complex are dissolved in 150 ml of water. To this liquid the solution of 2 mmole *p*-phenetidine. H[Cr(NCS)$_4$(*p*-phenetidine)$_2$] in 30 ml of alcohol is added. The reaction mixture is allowed to stand for 20—30 minutes and the product of the double exchange reaction is filtered then washed with water and dried on air.

Monoacido-pentamine-cobalt(III) derivatives: 3 mmoles of trans-[Co(en)$_2$Cl$_2$]Cl (0.82 g) are treated with 3—3.5 mmoles of amine (ammonia, benzylamine or aniline) at room temperature in 10 ml aqueous solution. After allowing to stand for one day the reaction mixture is diluted to 100 ml and filtered [9]. To the filtrate the solution of 2 mmole *p*-phenetidine. H[Cr(NCS)$_4$(*p*-Phen)$_2$] in 30 ml alcohol is added and a precipitate is formed. The above described procedure is followed further.

Diacido-tetramine-cobalt(III) derivatives

2 mmoles of the diacido-tetramine complex (in chloride form) are dissolved in 200 ml of water. To this liquid the solution of 2 mmole *p*-phenetidine. H[Cr(NCS)$_4$(*p*-Phen)$_2$] in 30 ml alcohol is added. The obtained complex salts are worked up as directed above. The dimethylglyoxime (DH_2) containing cobalt(III) chelate compounds were synthesized by ABLOV's method [10]. The aqueous–alcoholic solution of cobalt(III) chloride, dimethylglyoxime and the corresponding amine (molar ratio 1 : 2 : 3) was oxidized by bubbling air through the mixture.

The data on this type of compounds are compiled in Table II.

Analysis. Sulphur and nitrogen were determined as above. The sum of the metals was determined gravimetrically in the form of $Co_3O_4 + Cr_2O_3$ after ignition at 900—920°C.

Kinetic measurements. The samples on the complex salt were dissolved in the calculated amount of preheated ethanol and diluted with preheated water to a certain volume, to obtain solutions with initial concentration of the complex ion from 3 to $7 \cdot 10^{-3}$ mole/l. The solutions were kept in an ultrathermostat. The samples taken at various times were cooled quickly in ice and the concentration of the free thiocyanate ion and that of the unchanged complex ion were determined.

Determination of CNS^-. Free thiocyanate ion was determined photocolorimetrically. To a sample an aqueous solution of iron(III)-perchlorate (0.1 *M*) was added in excess and the extinction of the solution was measured, using a blue filter. The corresponding concentration values were obtained by the aid of a calibration curve.

Determination of the unchanged complex ion. For this purpose we used a precipitation reaction with 8-quinolinol(oxine)chlorhydrate. This salt gives an insoluble product with the studied complex ion. The solvolysis products, however, do not precipitate since at the substitution of NCS are formed a nonelectrolyte or cations, which cannot combine with the 8-quinolinolium ion and the 8-quinolinolium salt of the product obtained by the substitution of the *p*-phenetidine is soluble in water. The 8-quinolinolinium salt of the studied complex ion is soluble in alcohol, and for this reason an excess of aqueous oxine solution (containing 1 mole/l 8-quinolinol and 3 mole/l HCl) should be used. The final solution should not contain more than 13 per cent of ethanol. The precipitate is filtered through a Gooch filter, G_4, and washed with distilled water. Then the precipitate is dissolved in methanol and the extinction

of the obtained reddish violet solution is measured photocolorimetrically, using a green filter. A calibration curve should be used.

The calculation of rate constants, activation energies and lg *PZ* values was carried out by means of the least square method.

REFERENCES

1. VÁRHELYI, Cs. and GĂNESCU, I.: Monatshefte **98,** (2) 472 (1967)
2. GĂNESCU, I. and VÁRHELYI, Cs.: Revue roum. chim. **12** (4) 395 (1967)
3. RIPAN, R., GĂNESCU, I. and VÁRHELYI, Cs.: Z. anorg. Chem. **357** (3) 140 (1968)
4. VÁRHELYI, Cs., GĂNESCU, I. and OPRESCU, D.: Studia Univ. Babeş-Bolyai, Chem. **13** (2) 41 (1968)
5. BERGMANN, M.: J. Biol. Chem. **110,** 476 (1935)
6. ZSAKÓ, J. VÁRHELYI, Cs. and GĂNESCU, I.: Revue roum. chim. **13** (5) 577 (1968)
7. ZSAKÓ, J., VÁRHELYI, Cs. and GĂNESCU, I.: Monatshefte **99,** 2235 (1968)
8. ADAMSON, A. W.: J. Amer. Chem. Soc. **80,** 3183 (1958)
9. MEISENHEIMER, J. and KIDERLEN, E.: Liebigs Ann. **438,** 238 (1924)
10. ABLOV, A. V.: Bull. Soc. Chim. France **7,** 140 (1940)
11. ZSAKÓ, J., VÁRHELYI, Cs. and BANICI, L.: Studia Univ. Babeş-Bolyai, Chem. **13,** (2) 21 (1968)
12. ZSAKÓ, J., VÁRHELYI, Cs. and DOBOCAN, D.: J. Inorg. Nuclear Chem. **31,** 1459 (1969)

János ZSAKÓ
Csaba VÁRHELYI
Jon GĂNESCU
János TURÓS

Cluj, str. Arany János 11, Roumania

Acta Chimica Academiae Scientiarum Hungaricae, Tomus 61 (2), pp. 181—196 (1969)

1,2,4-TRIAZINES AND CONDENSED DERIVATIVES, IX*

SYNTHESIS OF SOME IMIDAZO-, PYRIMIDO- AND [1,2,4]-TRIAZINO-[1,2,4]TRIAZINE DERIVATIVES

GY. HORNYÁK, K. LEMPERT and K. ZAUER

(Department of Organic Chemistry, Technical University, Budapest, and Research Group for Alkaloid Chemistry of the Hungarian Academy of Sciences, Budapest)

Received June 21, 1968

The reaction of 6-methyl-3-methylthio-1,2,4-triazin-5(2*H*)-one (**3**) with 2-aminoethanol and 3-aminopropanol gives, depending on the reaction conditions, derivatives either of 3,5-diamino-1,2,4-triazine (**4**) or of 3-amino-1,2,4-triazin-5(2*H*)-one (**2c, 2d**). As intermediates of the reactions leading to the latter products, salt-like 1 : 1 adducts (**5, 10**) of **3** and the aminoalcohol can be isolated.

The products (**6,** $n = 2,3$) obtained from **2c** and **2d** with thionyl chloride undergo cyclization, depending on the reaction conditions, to yield 7,8-dihydro-3-methylimidazo[2,1-c][1,2,4]triazin-4(6*H*)-one (**7,** $n = 2$), or 6,7-dihydro-2-methylimidazo-[1,2-b][1,2,4]triazin-3(5*H*)-one (**8,** $n = 2$) and 6,7,8,9-tetrahydro-3-methyl-4*H*-pyrimido[2,1-c][1,2,4]triazin-4-one (**7,** $n = 3$), or the isomeric 5,6,7,8-tetrahydro-2-methyl-3*H*-pyrimido[1,2-b][1,2,4]triazin-3-one (**8,** $n = 3$), respectively.

Methods have been developed for the synthesis of the dioxo compound, **21,** containing the same fundamental ring system as **8** ($n = 2$), and of the triazinotriazine derivative **28.**

The directions of the ring closure reactions and other orientation problems, as well as the fine structures of the potentially tautomeric products have been clarified by spectroscopic methods.

The observed orientation phenomena are related to the order of nucleophilic reactivity of the nitrogen atoms in the 1,2,4-triazine ring.

In previous papers [1—2] of the present series some methods have been described by the aid of which a sulfur-containing second ring could be fused to sides *b* and *c* of 3-thio-1,2,4-triazine-3,5(2*H*,4*H*)-diones (**1**), by making use of the sulfur and the nitrogen atoms in positions 2 and 4, respectively, of the latter for the construction of the new ring (see Scheme 1). Starting with 3-amino-1,2,4-triazin-5(2*H*)-ones (**2**) we now succeeded in extending these

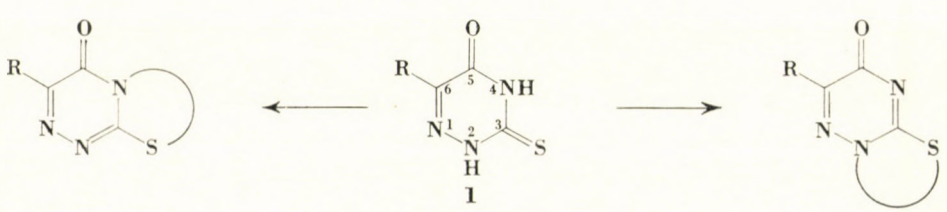

1

* Part VIII: HORNYÁK, Gy., LÁNG, L., LEMPERT, K. and MENCZEL, Gy.: Acta Chim. Acad. Sci. Hung. **61,** 93 (1969).

methods to the synthesis of bicyclic 1,2,4-triazine derivatives in which the second ring, too, contains only nitrogens as the hetero atoms (see Scheme 2).

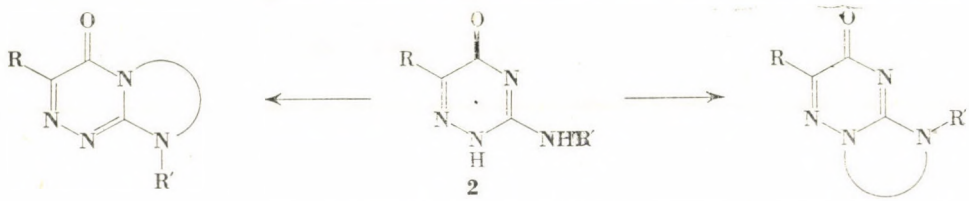

2

a: R = HOC_2H_4—; R′ = H
b: R = HOC_3H_6—; R′ = H
c: R = CH_3; R′ = HOC_2H_4—
d: R = CH_3; R′ = HOC_3H_6—

According to the literature [3], the starting compounds of type **2** may be prepared either by cyclization of the guanylhydrazones of α-oxo acids in neutral or weakly alkaline solutions, or by *S*-alkylation of thioxo compounds of type **1** and subsequent aminolysis. Compounds **2** — in which hydrogen is attached to at least one of the nitrogen atoms — are potentially tautomeric. According to spectroscopic evidence [4], their cross-conjugated forms (depicted in the above schemes) are by far the most stable, consequently, compounds **2** always exist in these forms except, of course, if the C=N double bond at C—3 is shifted to another position by the introduction of substituents.

By the second synthesis method mentioned above, four new 3-amino-1,2,4--triazin-5(2*H*)-ones (**2a—d**) have been prepared, the latter two being, at the same time, suitable starting compounds for some representative bicyclic triazine derivatives of the desired types (see Scheme 3). In order to prepare **2c** and **2d**, 6-methyl-3-methylthio-1,2,4-triazin-5(2*H*)-one (**3**) was first refluxed with excess 2-aminoethanol and 3-aminopropanol, respectively; the reagent served at the same time also as the solvent. However, in addition to the expected reaction, which was the selective aminolysis of the methylthio group, aminolysis of the carbonyl group of **3** also occurred, giving rise to the formation of 3,5-diamino-1,2,4-triazine derivatives, **4**. The latter reaction points to enhanced liability of the carbonyl carbon in **3** to nucleophilic attack as compared with the case of "ordinary" amides, and is in complete agreement with the liability of the carbonyl group of **3** and its analogues to alcoholysis, experienced previously [5, 6]. However, while alcoholysis can only be performed by means of acid catalysis, aminolysis smoothly proceeded in the above and related cases [7] in the absence of acid catalysts.

The desired transformation **3** → **2c** could, finally, be achieved by refluxing **3** with 1—1.1 mole of 2-aminoethanol for a few hours in methanol or ethanol. The product was found to consist of two components: the desired **2c**

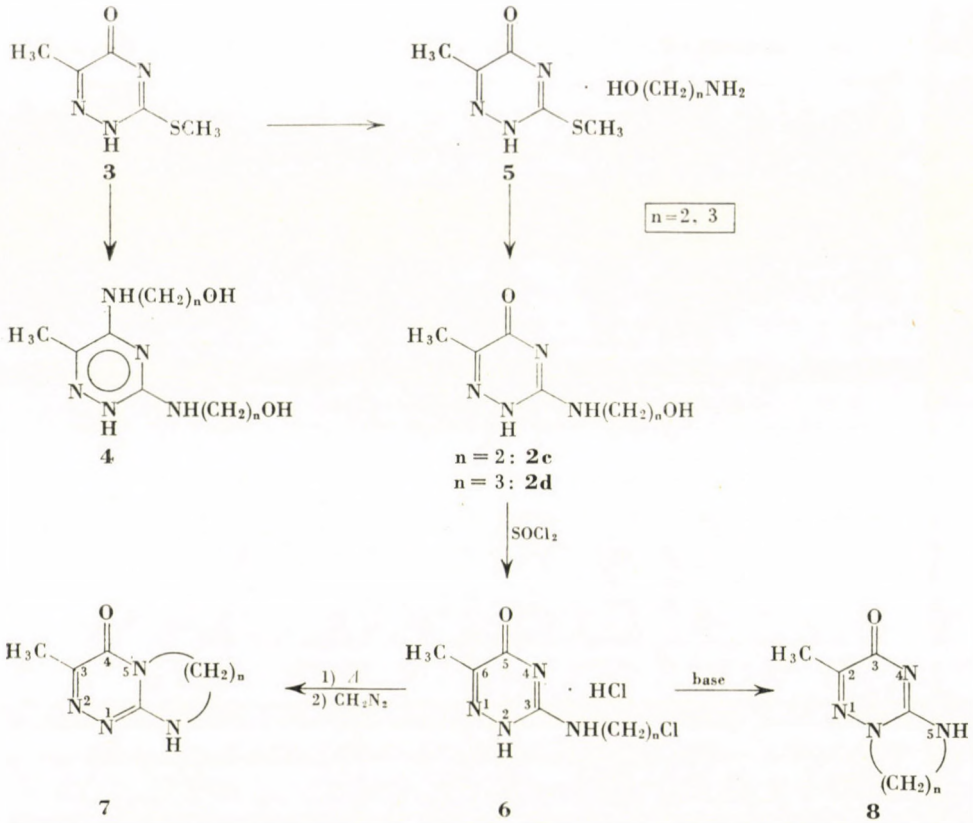

was formed in comparatively low yields, and the main product proved to be a 1 : 1 adduct (**5**, $n = 2$) of **3** and 2-aminoethanol. This adduct, however, on being heated to 150°C or refluxed with tetralin, was converted into **2c** under the evolution of methanethiol. Neither was a single product formed in the reaction of **3** and 3-aminopropanol. In the latter case the two products (**5**, $n = 3$, and **2d**) expected by analogy* were not separated but, instead, the whole amount of the residue obtained on evaporation of the solvent was thermally transformed into **2d.**

The adduct **5** ($n = 2$) was also formed when **3** was covered with ethanol (in which it is rather insoluble) and, subsequently, the calculated amount of 2-aminoethanol was added. On shaking, **3** dissolved under the evolution of considerable heat, and the residue obtained on evaporation of the solvent proved after recrystallization to be identical with **5** ($n = 2$). A similar but less vigorous reaction was observed between **3** and 3-aminopropanol, but this

* This expectation was completely supported by the IR spectrum of the crude product when compared with that of pure **2d.** By the same technique it was also shown that after 1—2 hrs. practically no **2d** was yet formed.

adduct proved to be less stable: its recrystallization presented difficulties, and no satisfactory analysis figures could be obtained. Thus, the length of the carbon chain of the aminoalcohol component seems to be of great importance in determining the stability of the adduct [8].

Adduct **5** ($n = 2$) — and obviously adduct **5** ($n = 3$) as well — have, as evidenced by the UV spectrum of the former, salt-like character (**10**). While, namely, the UV spectra of **3** obtained in ethanolic solutions at concentrations not less than 10^{-3} moles/l (or in more diluted solutions which, however, have been acidified by a few drops of cc. hydrochloric acid) contain a single maximum at 236 nm ($\log \varepsilon = 4.26$ [9, 10]) diagnostic for cross-conjugated 3-methylthio--1,2,4-triazine-5(2*H*)-ones, the spectrum of **5** ($n = 2$), recorded in ethanol, shows the same characteristic differences with respect to the former — *viz.* broadening of the absorption band at 236 nm in the direction of shorter wave lengths and appearance of a second, less intensive maximum at 286 nm — which were observed also if the spectrum of **3** was run in ethanolic solutions at concentrations of 10^{-5} moles/l or less (or in a more concentrated solution which, however, had been treated previously with a few drops of alkali) and which were attributed to the presence of the anion (**9**) corresponding to **3** [9, 10]. Structure **10** for the adduct is also supported by its IR spectrum in which no carbonyl band can be found.

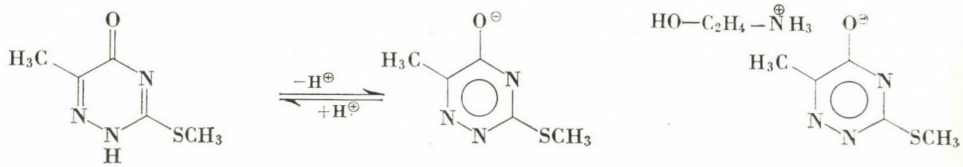

3 **9*** **10**

* Limiting structure of greatest relative weight.

Treatment of **2c** by thionyl chloride yielded the hydrochloride (**6**, $n = 2$) of the corresponding 3-(2-chloroethylamino) derivative, which cyclized on heating to the hydrochloride (**7**, $n = 2$) of 7,8-dihydro-3-methylimidazo[2,1-c]-[1,2,4]triazin-4(6*H*)-one with the elimination of 1 mole of hydrochloric acid. The corresponding base could be liberated by treatment with diazomethane. If, on the other hand, the salt **6** ($n = 2$) was treated with ethanolic sodium ethoxide, ring closure in the other direction took place, and the isomeric 6,7-dihydro-2-methylimidazo[1,2-b][1,2,4]triazin-3(5*H*)-one (**8**, $n = 2$) was obtained.

The direction of the cyclizations can be most easily deduced from the UV spectra of the products. While the UV spectrum (run in ethanol) of the product obtained on thermal cyclization contains two bands (at about 220 and 300 nm), similarly to 3-amino-1,2,4-triazin-5(4*H*)-ones (**11**) containing a

continuously conjugated chromophoric system [4], that of the isomeric product, obtained on ring closure with sodium ethoxide, contains only a single distinct maximum (at about 210 nm) and a shoulder (at about 245 nm), similarly to cross-conjugated 3-amino-1,2,4-triazin-5(2*H*)-ones (**2**) [4].

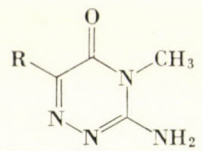

11 [4]

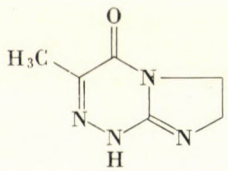

12

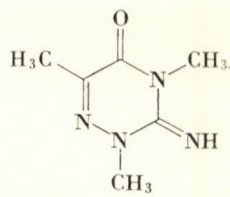

13 [4]

These structure assignments were corroborated also by the IR spectra of the products. The carbonyl band of the thermal cyclization product was found at higher wave numbers than that of its isomer obtained on ring closure by sodium ethoxide, in complete accordance with earlier observations (*e.g.*, [1, 2]) according to which in isomeric 1,2,4-triazin-5-ones the carbonyl band of the continuously conjugated compound is always found at higher wave numbers than that of the cross-conjugated isomer.

2d and thionyl chloride reacted similarly. In this case, however, isolation of the reaction product in pure form was not attempted; instead the crude product was directly cyclized thermally or by sodium ethoxide to **7** ($n = 3$) and **8** ($n = 3$), respectively. The direction of ring closure could again be deduced from the UV and IR spectra.

The fine structures of compounds **6** and **7** ($n = 2, 3$) could also be deduced from the spectra. Being potentially tautomeric, these compounds could exist theoretically — at least partly — in another modification than hitherto assumed, *viz.* in one which contains the C=N double bond in exocyclic position with respect to the triazine ring (*e.g.*, **12**). However, by comparison with the known spectra [4] of triazinones (*e.g.* **13**) containing the latter type of chromophore, this possibility may definitely be excluded.

The cyclization of compounds **6** in the presence of a base to yield compounds of type **8** is, as an intramolecular alkylation reaction at the nitrogen atom in position 2 of the triazine cycle, consistent with the reactivity of 1,2,4--triazines experienced in other cases. The nucleophilic reactivity of the nitrogen atom at position 2 in derivatives of 1,2,4-triazine is, namely, generally found to be enhanced as compared with that of the nitrogen atom at position 4 [1, 2, 11—13]. The thermal cyclization of compounds **6** yielding, under participation of the nitrogen atom at position 4, compounds of type **7**, is an exception to the above rule. Salt formation, apparently, inverts the order of nucleophilic reactivity of the two nitrogen atoms. This change may be explained

by assuming that during salt formation the nitrogen atom at position 2 of the triazine ring (being not only the most nucleophilic but also the most basic centre) has been protonated, *i.e.* that the structure of the salts **6** is correctly represented by formula **14.** As a result of protonation, the nitrogen atom at position 2 is no longer nucleophilic, and ring closure must, of necessity, proceed under participation of the other nitrogen atom. Our assumption regarding

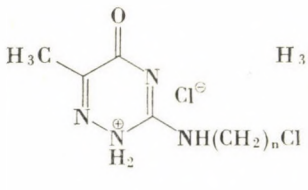

14

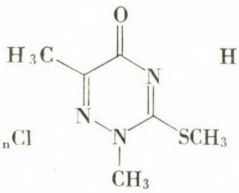

15

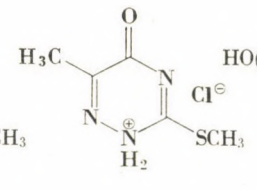

16

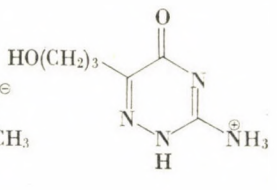

17

the site of protonation is also supported by the IR spectra. The carbonyl band of **2c** is found at 1660 cm^{-1}, but this band is shifted in the spectrum of **6** ($n = 2$) up to 1735 cm^{-1}. A similar hypsochromic shift is observed when the IR spectra of **15** ($\nu C{=}O$: 1670 cm^{-1}) and the hydrochloride of **3** ($\nu C{=}O$: 1720 cm^{-1}), whose structure **16** has been already proved [5], are compared;* in both cases the shift may be attributed to the introduction of a positive pole.

*

Synthesis of dioxo derivatives containing the same fundamental ring skeleton as **8** ($n = 2$) was also attempted (see Scheme 7). With this aim **3** was allowed to react with ethyl bromoacetate and bromoacetamide to yield **19a** and **22,** respectively; the former was then subjected to butylaminolysis and the product **20a** cyclized under acidic conditions to yield the desired **21.**

Attempts to prepare the related compound **23,** unsubstituted at N(5), starting with **19a** or **22** proved unsuccessful because no homogeneous product was obtained. If, on the other hand, **18** instead of **3** was reacted with ethyl bromoacetate, **20b** was obtained in a low yield, but the product could not be cyclized to the 2-(2-hydroxyethyl) analogue of **21.**

The sites of "alkylation" in the course of the reactions of **3** and **18** with ethyl bromoacetate and bromoacetamide could be ascertained by spectroscopical means: compounds **19a** and **22,** as well as **20b,** obtained through the

* Interestingly, the protonation of **2b,** which compound is related to the hypothetical base corresponding to **14,** occurs, as already demonstrated, at the exocyclic nitrogen to give the cation **17** [6]. The different behaviour towards protons is also manifested in the IR spectra: the carbonyl band of **2b** is found at 1655 cm^{-1}, and it is shifted as a result of the formation of **17** only to 1675 cm^{-1}.

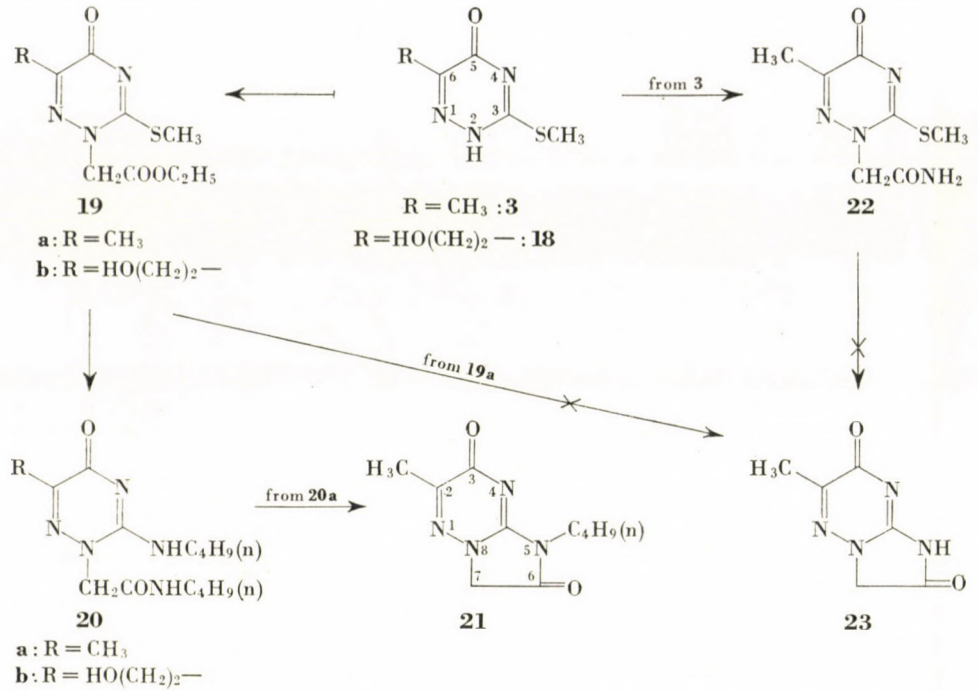

uncrystallizable **19b** — and, of course, **21** as well — produced IR and UV spectra characteristic of cross-conjugated 3-alkylthio- and 3-amino-1,2,4--triazin-5(2*H*)-ones. This orientation is in complete harmony with previous observations [1, 2, 11].

*

Finally, experiments were made with the aim of synthesizing compound **28** which contains the [1,2,4]triazino[4,3-b][1,2,4]triazine ring system (see Scheme 8). In order to achieve this goal, thiosemicarbazide was methylated to yield the hydroiodide of *S*-methyl-isothiosemicarbazide. The latter was then reacted with 2-hydrazinoethanol to yield **24** and, finally, this product was condensed with pyruvic acid in aqueous solution.

According to the analytical results, two alternative structures, **25** and **26,** had to be taken into consideration for the product which melted at 190—191°. The UV spectrum (λ_{max} = 220 and 300 nm; log ε = 3.88 and 3.78, respectively) showed the product to be a continuously conjugated 3-amino-1,2,4--triazin-5(4*H*)-one, rendering thereby structure **25** highly probable. If, namely, the structure of the product were represented by **26,** the assumption that the tautomeric equilibrium **26a** ⇌ **26b** is highly shifted in the direction of **26a** would be necessary in order to interpret the characteristics of the UV spectrum,

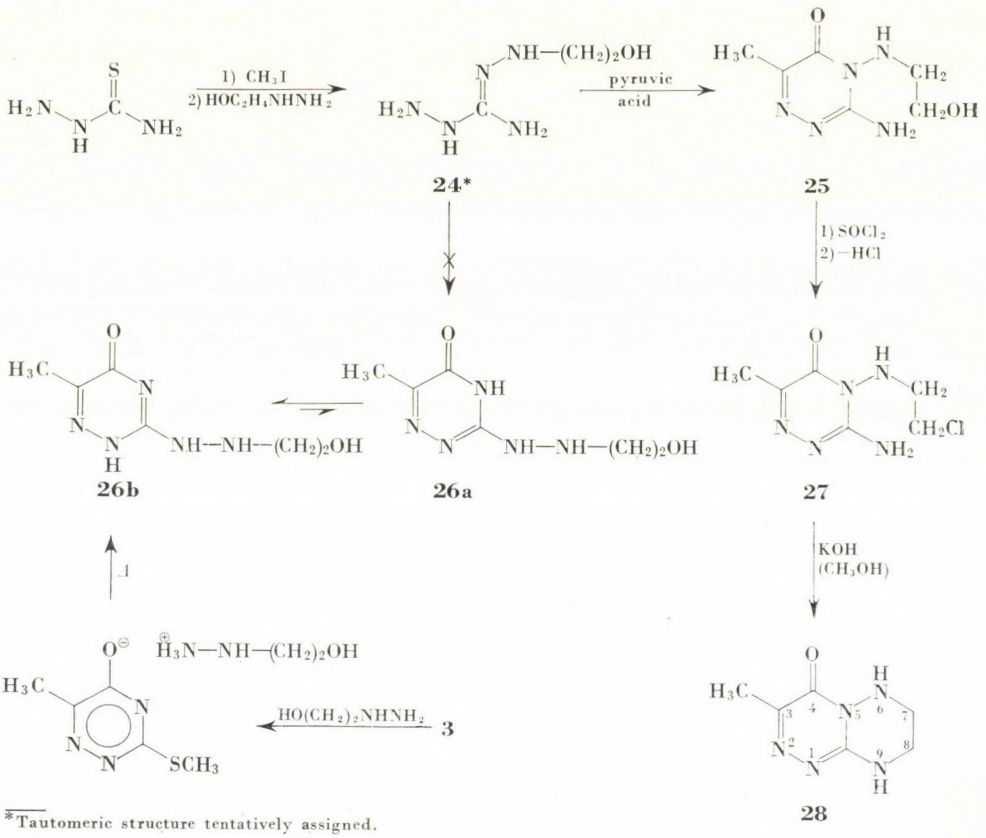

*Tautomeric structure tentatively assigned.

whereas, according to all experiences hitherto gained [4], it is form **26b** which should be the more stable.

For the sake of complete certainty, compound **26** was prepared by a structure proving synthesis starting with **3.** This product was found both according to its m.p. (162°C) and its spectroscopical properties to be different from the product of the synthesis starting with **24.**

The synthesis of **26** was achieved by reacting **3** with hydrazinoethanol, when a salt-like 1 : 1 adduct, analogous to **10,** was first formed which, on heating, transformed under evolution of methanethiol into **26.** According to its UV spectrum (ethanolic solution), this compound exists indeed, as expected, in the cross-conjugated modification, **26b.** The difference in the type of conjugation of **25** and **26b** is reflected by their IR spectra as well: the carbonyl band of the continuously conjugated **25** is found at 1690 cm^{-1}, while that of the cross-conjugated **26b** is shifted to 1665 cm^{-1}.

25, whose structure was established by the above facts beyond doubt, was reacted with thionyl chloride to yield **27** (in form of its hydrochloride) and the latter was cyclized by ethanolic potassium hydroxide to the desired **28.**

Experimental*

3-Amino-6-(2-hydroxyethyl)-1,2,4-triazin-5(2*H*)-one (2a)**

6-(2-Hydroxyethyl)-3-methylthio-1,2,4-triazin-5(2*H*)-one [6] (2.0 g; 11 mmoles) was heated in a sealed tube with saturated ethanolic ammonia solution (10 ml), prepared at 0°C, for 8 hrs. to 120°C. On cooling 1.4 g (82%) of **2a** separated; colourless crystalline powder, m.p. 268—9°C (from water).

$C_5H_8N_4O_2$ (156.2). Calcd. C 38.46; H 5.15; N 35.88. Found C 38.46; H 5.17; N 35.46%.

3-Amino-6-(3-hydroxypropyl)-1,2,4-triazin-5(2*H*)-one (2b)** was prepared similarly, starting with 6-(3-hydroxypropyl)-3-methylthio-1,2,4-triazin-5(2H)-one [6] (2.0 g; 10 mmoles). The yield was 1.1 g (64%), colourless plates, m.p. 267—8°C (from water).

$C_6H_{10}N_4O_2$ (170.2). Calcd. C 42.35; H 5.92; N 32.92. Found C 42.27; H 5.68; N 32.67%.

2-Hydroxyethylammonium 6-methyl-3-methylthio-1,2,4-triazin-5-olate (5, $n = 2$; 10)

A mixture of **3** (3.1 g; 20 mmoles), 2-aminoethanol (1.5 ml; 25 mmoles) and anhydrous methanol (40 ml) was refluxed for 3 hrs. and subsequently evaporated in vacuum. The slowly crystallizing oily residue was recrystallized from ethanol–petroleum ether to yield 4.1 g (94%) of **5** ($n = 2$), colourless crystalline powder, m.p.: 107—8°C.

$C_7H_{14}N_4O_2S$ (218.3). Calcd. C 38.51; H 6.46; S 14.69. Found C 38.57; H 6.55; S 14.10%.

3-(2-Hydroxyethylamino)-6-methyl-1,2,4-triazin-5(2*H*)-one (2c)

(a) A mixture of **3** (3.1 g; 20 mmoles), 2-aminoethanol (1.5 ml; 25 mmoles) and anhydrous ethanol (80 ml) was refluxed for 32 hrs. After standing overnight in a refrigerator, the crystals of **2c** (0.4 g = 12%) were filtered off and washed with a small amount of water. Colourless needles, m.p. 256°C (d.) (from water).

$C_6H_{10}N_4O_2$ (170.2). Calcd. C 42.35; H 5.92; N 32.93. Found C 42.29; H 5.93; N 33.19%.

The ethanolic mother liquor of the crude **2c** was evaporated to dryness in vacuum and the partly solidifying residue recrystallized from ethanol–petroleum ether to yield 3.7 g (85%) of **5** ($n = 2$), m.p. and mixed m.p. with the product prepared as described above: 107—8°C. The identity of the two substances was also established by their IR spectra.

(b) The crude, partly solid compound **5** ($n = 2$), obtained by refluxing a mixture of **3** (3.1 g; 20 mmoles), 2-aminoethanol (1.5 ml; 25 mmoles) and anhydrous methanol (40 ml) for 5 hrs. and subsequently evaporating it to dryness in vacuum, was heated for 3 hrs. to 130—140°C in an oil bath. The mixture, which was a liquid at the beginning of the heating period, gradually turned under evolution of methanethiol into a solid mass, which was recrystallized from DMF (40 ml), and the crystals of **2c** thus obtained (2.5 g; 73%) were washed with ether to give a colourless crystalline powder, m.p. 256°C (d.).

The two specimens of **2c**, prepared according to *(a)* and *(b)*, proved to be identical by m.p., mixed m.p. and IR spectra.

3-(3-Hydroxypropylamino)-6-methyl-1,2,4-triazin-5(2*H*)-one (2d)

A mixture of **3** (3.1 g; 20 mmoles), 3-aminopropanol (1.6 ml; 21 mmoles) and anhydrous methanol (50 ml) was refluxed for 5 hrs. and subsequently evaporated to dryness in vacuum. The oily residue (**5**, $n = 3$) was heated for 3 hrs. in an oil bath to 130—140°C and the crystalline product thus obtained recrystallized from DMF (about 20 ml) and washed with ether to yield 2.6 g (68%) of **2d**, colourless crystalline powder, m.p. 247—8°C (d.).

$C_7H_{12}N_4O_2$ (184.2). Calcd. C 45.64; H 6.57; N 30.42. Found C 45.55; H 6.43; N 30.04%.

* All m.p.'s are uncorrected.

** Experiments performed by Mrs. M. HORNYÁK-HÁMORI.

Table I

UV and

Compound	Type of chromophore[b]	UV Spectra in ethanol λ_{max} [nm] (log ε)
2a	B_N	205 (4.43); 249 (3.78)
2b	B_N	
2c	B_N	210 (4.42); 240 (3.86), sh
2d	B_N	211 (4.41); 240 (3.86), sh
4 ($n=2$)	D_N	212 (4.36); 234 (4.12); 309 (3.75)
4 ($n=3$)	D_N	212 (4.38); 230 (4.09), sh; 314 (3.64)
5 ($n=2$)=**10** ($n=2$)	D_S	220 (4.18); 230 (4.17); 286 (3.59)
6 ($n=2$)=**14** ($n=2$)	$B_N^{d)}$	210 (4.38); ~ 250 (~3.8), sh
	B_N	210 (4.42); 244 (3.86), sh[e]
7 ($n=2$) HCl salt	A_N	220 (4.05); 300 (3.70)
7 ($n=3$) HCl salt	A_N	231 (4.05); 316 (3.85)
8 ($n=2$)	B_N	210 (4.42); 244 (3.86), sh
8 ($n=3$)	B_N	212 (4.42); 255 (3.82)
19a	B_S	238 (4.34)
20a	B_N	212 (4.43); 248 (3.94), sh
21	B_N	215 (4.34); 235 (4.13)
		214 (4.28); 268 (3.84), sh[i]
22	B_S	238 (4.11)
25	A_N	220 (3.88); 300 (3.78)
26b	B_N	211 (4.36); 244 (3.85), sh
27	A_N	218 (3.93); 302 (3.83)
28	A_N	226 (4.11); 311 (3.84)
Model compounds:		
3	$B_S^{k)}$	236 (4.30)[l]
	$D_S^{m)}$	218 (4.24); 290 (3.90)
11 (R=CH_3) [4]	A_N	222 (3.90); 299 (3.89)
13 [4]	C	216 (3.88); 266 (3.58); 308 (~2.4), sh
15	B_S	235 (4.38)[o]
16	$B_S^{d)}$	

(a) The UV Spectra were obtained with a Spectromom instrument (Type 201) of the Hungarian Optical Works (Magyar Optikai Művek), Budapest.
IR Spectra were recorded with a double beam spectrograph, type UR 10 of Zeiss, Jena

(b) A_N: Continuously conjugated in triazine ring, with nitrogen attached in position 3[c)]
B_N: Cross-conjugated in triazine ring, with nitrogen attached in position 3[c)]
B_S: Cross-conjugated in triazine ring, with sulfur attached in position 3[c)]

IR Spectra

IR Spectra (KBr pellets) Characteristic bands of the double bond region [cm^{-1}]	Compound
1665, 1640 (m), 1545, 1490 (vs)	**2a**
1665, 1645 (m), 1540 (vs), 1490 (vs)	**2b**
1660, 1600 (vs), 1555/45 (doublet), 1525 (m), 1480	**2c**
1665, 1615 (w), 1560, 1475	**2d**
1620, 1570/60 (doublet, vs), 1525	**4** (n=2)
1640 (sh), 1575 (vs), 1530 (sh), 1490 (sh), 1475 (m)	**5** (n=2)
1735, 1690, 1640 (m), 1590 (m)	**6** (n=2)
1680, 1635 (vs), 1545, 1490	**7** (n=2)
1720, 1675 (vs), 1610, 1565	HCl salt
1680, 1625 (vs), 1555, 1455	**7** (n=3)
1720, 1660 (vs), 1625 (m), 1585	HCl salt
1660, 1600 (vs), 1560—20 (broad, vs), 1480	**8** (n=2)
1635 (vs), 1590, 1525, 1470 (m)	**8** (n=3)
1755[f], 1660 (vs), 1595 (m), 1490 (vs)	**19a**
1675[g], 1645[g], 1610—1560 (broad, vs), 1520	**20a**
1770[h], 1665, 1605 (vs), 1540 (vs), 1520	**21**
1695 (vs)[j], 1655, 1600 (sh), 1485 (vs)	**22**
1690, 1650 (vs), 1560/40 (doublet, m), 1510	**25**
1670, 1610 (vs), 1560 (vs), 1520 (m), 1470	**26b**
1690, 1630 (vs), 1560 (m), 1540 (m), 1510	**27**
1665, 1620 (vs), 1565, 1460	**28**
1610 (m), 1590 (m), 1535 (m)	**3**
1670 (vs), 1470 (vs)	**15**
1720 (vs), 1610, 1550, 1500	**16**

C: Semicyclic C=N double bond at position 3[c] of triazine ring
D_N: Aromatic triazine ring with nitrogen attached in position 3[c]
D_S: Aromatic triazine ring with sulfur attached in position 3[c]
(c) According to the numbering of the *individual* triazine ring
(d) Protonated at N-2
(e) In ethanol containing a few drops of 0.001 *N* aqueous NaOH

3,5-Di(2-hydroxyethylamino)-6-methyl-1,2,4-triazine (4, $n = 2$)

3 (2.0 g; 12.5 mmoles) was refluxed for 3 hrs. with 2-aminoethanol (15 ml) and the resulting solution evaporated to dryness in vacuum to yield a crystalline residue which was recrystallized from ethanol (about 30 ml). 1.9 g (71%) of **4** ($n = 2$) was obtained as a colourless crystalline powder, m.p. 170—1°C.

$C_8H_{15}N_5O_2$ (213.2). Calcd. C 45.06; H 7.09; N 32.84. Found C 45.20; H 7.12; N 33.06%.

3,5-Di(3-hydroxypropylamino)-6-methyl-1,2,4-triazine (4, $n = 3$) was prepared similarly. The product (2.4 g; 78%) was initially a faintly yellow oil which slowly solidified within a week to give a colourless crystalline powder, m.p. 126—7°C (from ethanol–petroleum ether).

$C_{10}H_{19}N_5O_2.1/4\ H_2O$ (245.8). Calcd. C 48.86; H 7.99; N 28.50. Found C 48.90; H 7.93; N 28.44%.

3-(2-Chloroethylamino)-6-methyl-1,2,4-triazin-5(2*H*)-one hydrochloride (6, $n = 2$)

2c (1.7 g; 10 mmoles) was added in portions at room temperature to thionyl chloride (8 ml). After the addition of a drop of triethylamine, the mixture was kept for 30 min at 40—50°C in a water bath. Subsequently, the excess thionyl chloride was removed in vacuum, the temperature of the mixture being maintained at 40°C. The crystalline residue was rubbed with anhydrous ether and filtered off to yield 1.9 g (84%) of **6** $n = 2$, faintly yellow crystalline powder, m.p. 172—4°C (d.)* (from anhydrous methanol–ether).

$C_6H_{10}Cl_2N_4O$ (225.1). Calcd. C 32.01; H 4.48; Cl 31.51. Found C 32.15; H 4.78; Cl 31.58%.

7,8-Dihydro-3-methylimidazo[2,1-c][1,2,4]triazin-4(6*H*)-one, (7, $n = 2$)

6 ($n = 2$) (1.0 g; 4.5 mmoles) was refluxed for 3 min in anhydrous DMF (10 ml). After cooling, an about equal volume of ether was added to precipitate 0.7 g (82%) of the *hydrochloride* of **7** ($n = 2$); faintly yellow needles, m.p. 273—3°C (from anhydrous methanol–ether).

$C_6H_9ClN_4O$ (188.6). Calcd. C 38.21; H 4.81; Cl 18.80. Found C 38.37; H 4.55; Cl 18.87%.

The salt (1.9 g) was suspended in a small amount of ether. Freshly prepared ethereal diazomethane solution was added under continuous shaking until its yellow colour persisted for about 3 min., and the crystalline product was filtered off; the free base was obtained (1.4 g; 92%) as faintly yellow needles, m.p. 291—2°C (from water).

$C_6H_8N_4O$ (152.2). Calcd. C 47.36; H 5.30; N 36.82. Found C 47.37; H 5.19; N 36.76%.

6,7-Dihydro-2-methylimidazo[1,2-b][1,2,4]triazin-3(5*H*)-one (8, $n = 2$)

Sodium (0.46 g; 20 mg-atom) was dissolved in anhydrous methanol (50 ml), **6** ($n = 2$) (2.2 g; 10 mmoles) was added, and the mixture was refluxed for 8 hrs. The precipitated sodium chloride was removed by filtration, and the pH of the filtrate adjusted to about 6.5 by the

(f) Ester grouping of side chain
(g) One of the two Amide I bands has its origin in the amide group of the side chain
(h) ν C=O of γ-lactam grouping
(i) In dioxane
(j) Amide I band of side chain
(k) Hydrogen bridged
(l) $c = 10^{-3}$ moles/l
(m) Anionized
(n) $c = 5 \cdot 10^{-6}$ moles/l
(o) In methanol

* After slight decomposition, the melt resolidified at 174°C and decomposed finally above 265°C. *Cf.* the preparation of the hydrochloride of **7** ($n = 2$), see below.

addition of a few drops of acetic acid. On standing overnight in a refrigerator 1.1 g (65%) of **8** ($n = 2$) crystallized. The product was filtered off, washed with ether and recrystallized from water to obtain small, colourless needles, m.p. 262°C.

$C_6H_8N_4O \cdot H_2O$ (170.2). Calcd. C 42.34; H 5.92; O 18.80. Found C 42.40; H 5.96; O 18.85%.

6,7,8,9-Tetrahydro-3-methyl-4*H*-pyrimido[2,1-c][1,2,4]triazin-4-one (7, $n = 3$)

2d (1.8 g; 10 mmoles) was added in portions to thionyl chloride (10 ml). After the addition of a drop of triethylamine, the mixture was kept 30 min. at 50°C in a water bath. The excess thionyl chloride was then removed in vacuum, and the crystalline residue thus obtained rubbed with anhydrous ether and filtered off to yield 2.1 g of the *hydrochloride* of **6** ($n = 3$). The obtained powder was recrystallized from DMF and washed with ether to yield 1.5 g (74%) of the *hydrochloride* of **7** ($n = 3$), faintly yellow crystalline powder, m.p. 245—7°C (d.).

$C_7H_{11}ClN_4O$ (202.8). Calcd. C 41.45; H 5.46; Cl 17.48. Found C 41.28; H 5.77; Cl 17.23%.

The free base **7** ($n = 3$) was obtained in 90% yield similarly as in the case of the lower ring homologue **7** ($n = 2$), see above. Faintly yellow needles, m.p. 277°C (d.) (from water).

$C_7H_{10}N_4O$ (166.2). Calcd. C 50.59; H 6.07; N 33.72. Found C 50.56; H 6.01; N 34.18%.

5,6,7,8-Tetrahydro-2-methyl-3*H*-pyrimido[1,2-c][1,2,4]triazin-3-one (8, $n = 3$)

Sodium (0.4 g; 17 mg-atom) was dissolved in anhydrous methanol (50 ml). Crude **6** ($n = 3$; hydrochloride) (2.1 g), prepared from **2d** (1.8 g; 10 mmoles) as described above, was added, and the mixture refluxed for 6 hrs. The sodium chloride was removed and the pH of the filtrate adjusted to about 6.5 by the addition of a few drops of acetic acid. The solution was evaporated to dryness in vacuum and the crystalline residue rubbed with ether and filtered off to yield 1.3 g (78%) of **8** ($n = 3$), colourless needles, m.p. 295—6°C (from water).

$C_7H_{10}N_4O$ (166.2). Calcd. C 50.59; H 6.07; N 33.72. Found C 50.40; H 5.90; N 33.56%.

Ethyl 6-methyl-3-methylthio-5-oxo-1,2,4-triazine-2(5*H*)-acetate (19a)

Sodium (0.46 g; 20 mg-atom) was dissolved in anhydrous ethanol (30 ml). **3** (3.2 g; 20 mmoles) and ethyl bromoacetate (3.3 g; 20 mmoles) were added, and the solution refluxed for 30 min., and then evaporated in vacuum to about half of its original volume. Water (70 ml) was added to the solution while still hot. On cooling 1.7 g (38%) of **19a** separated, faintly yellow crystalline powder, m.p. 112—3°C (from water).

$C_9H_{13}N_3O_3S$ (243.3). Calcd. N 17.27; S 13.18. Found N 17.99; S 13.47%.

6-Methyl-3-methylthio-5-oxo-1,2,4-triazine-2(5*H*)-acetamide (22) was prepared similarly, starting with **3** (20 mmoles) and using bromoacetamide (2.8 g; 20 mmoles) instead of ethyl bromoacetate. The reaction mixture was evaporated to dryness in vacuum, the crystalline residue rubbed with cold water (10 ml), and filtered off to yield 1.1 g (26%) of **22**; colourless crystalline powder, m.p. 228—30°C (from ethanol).

$C_7H_{10}N_4O_2S$ (214.3). Calcd. N 26.10; S 14.95. Found N 26.08; S 14.51%.

N-(n-Butyl)-3-(n-butylamino)-6-methyl-5-oxo-1,2,4-triazine-2(5*H*)-acetamide (20a)

A mixture of **19a** (1.20 g; 5 mmoles), *n*-butylamine (2.4 ml; 10 mmoles) and anhydrous ethanol (15 ml) was refluxed for 7 hrs., and then evaporated to dryness in vacuum. The partly crystalline residue was recrystallized from a mixture of methanol and water (1 : 1 v/v) to yield 0.9 g (61%) of **20a**; long colourless needles, m.p. 188—9°C.

$C_{14}H_{25}N_5O_2$ (295.4). Calcd. C 56.92; H 8.35; N 23.71. Found C 56.61; H 8.33; N 24.05%.

N-(n-Butyl)-3-(n-butylamino)-6-(2-hydroxyethyl)-5-oxo-1,2,4-triazine-5(2*H*)-acetamide (20b)

Sodium (0.23 g; 10 mg-atom) was dissolved in anhydrous ethanol (20 ml). **18** (1.87 g; 10 mmoles) and ethyl bromoacetate (1.1 ml; 10 mmoles) were added and the mixture refluxed for 2 hrs. After cooling, the sodium bromide was removed and the filtrate evaporated to dryness in vacuum. The resulting yellow oil (**19b**) was mixed with *n*-butylamine (4.8 ml; 20 mmoles) and ethanol (30 ml). After refluxing for 2 hrs., the mixture was evaporated to dryness in vacuum to yield a dark brown oil which was dissolved in hot water (40 ml) and treated with Norite. On cooling 0.5 g (15%) of **20b** crystallized, m.p. 190—1°C (from acetic acid–ether).

$C_{15}H_{27}N_5O_3$ (325.4). Calcd. C 55.36; H 8.36; N 21.54. Found C 55.02; H 8.17; N 20.76%.

5-(n-Butyl)-2-methylimidazo[1,2-b][1,2,4]triazine-3,6(5*H*,7*H*)-dione (21)

20a (1.5 g; 5 mmoles) was refluxed for 1 hr. with 20% aqueous HCl (10 ml) and the mixture evaporated to dryness in vacuum to yield an oily residue which slowly solidified on standing for several days. The product was recrystallized from water to yield 0.7 g (63%) of **21**; colourless crystalline powder, m.p. 126°C.

$C_{10}H_{14}N_4O_2$ (222.2). Calcd. C 54.04; H 6.35; N 25.21. Found C 54.05; H 6.12; N 24.86%.

3-Amino-4-(2-hydroxyethylamino)-6-methyl-1,2,4-triazin-5(4*H*)-one (25)

A mixture of equimolecular amounts of thiosemicarbazide and methyl iodide in 5 parts of methanol was allowed to stand 1 hr. The reaction mixture was then refluxed for an additional hr. and evaporated to dryness in vacuum to yield crude crystalline hydriodide of *S*-methyl-isothiosemicarbazide, m.p. 141—3°C. Lit. m.p. [14]: 140°C.

A mixture of the crude hydriodide (24.5 g; 0.1 mole), 2-hydrazinoethanol (8.0 g; 0.1 mole) and methanol (100 ml) was allowed to stand for 4 days and finally refluxed for 2 hrs. The gummy *N*-amino-*N*'-(2-hydroxyethylamino)guanidinium iodide (**24** · HI), obtained on evaporation of the solvent, could not be crystallized.* Therefore, it was dissolved in water (60 ml) and treated with pyruvic acid (9.3 g; 0.11 moles). Heat was evolved spontaneously and, after being allowed to stand 1 hr., the mixture was refluxed for 30 min. After cooling, the pH was adjusted to 7.0 by the addition of aqueous $NaHCO_3$ solution. The slowly precipitating loose crystals were filtered off next day; two additional crops of the product were obtained by evaporating the filtrate in two steps to about 1/4 of its original volume, the total yield of **25** being 5.9 g (24%); m.p. 190—1°C (from water).

$C_6H_{11}N_5O$ (185.2). Calcd. C 38.91; H 5.99; N 37.82. Found C 39.27; H 6.35; N 37.76%.

The yield could not be raised above 32% by variation of the reaction conditions; the reason may be partly that the intermediate was not pure **24** · HI, *cf.* footnote.

3-[β-(2-Hydroxyethyl)-hydrazino]-6-methyl-1,2,4-triazin-5(2*H*)-one (26b)

A mixture of **3** (1.6 g; 10 mmoles),2-hydrazinoethanol (0.76 g; 10 mmoles) and anhydrous ethanol (40 ml) was refluxed for 3 hrs., and then evaporated to dryness in vacuum. During these operations only slight evolution of methanethiol was observed. The faintly yellow, oily residue, consisting mainly of the hydroxyethylhydrazinium salt of **3**, was heated 5 hrs. in an oil bath to 120—30°C, when vigorous evolution of methanethiol took place. The glassy product obtained on cooling was dissolved in hot ethanol (about 15 ml). After the addition of petroleum ether (10 ml) the mixture was allowed to stand overnight in a refrigerator to precipitate 1.3 g (70%) of **26b**, faintly yellow crystalline powder, m.p. 162°C (from ethanol-petroleum ether).

$C_6H_{11}N_5O_2$ (185.2). Calcd. C 38.91; H 5.99; O 17.28. Found C 39.17; H 5.72; O 16.59%.

* The product was possibly a mixture of **24** · HI and the isomeric *N*,*N*'-diamino-*N*-(2-hydroxyethyl)guanidinium iodide.

3-Amino-4-(2-chloroethylamino)-6-methyl-1,2,4-triazin-5(2*H*)-one (27)

Thionyl chloride (10 ml) was added in small portions within a few minutes to **25** (3.1 g; 16.8 mmoles). A vigorous reaction started giving rise to the formation of a viscous liquid product. In order to achieve complete dissolution of **25**, the mixture was kept for 10—15 min. at 35—40°C after the main reaction had subsided. On cooling the mixture gradually turned into a crystalline mass. Most of the excess thionyl chloride was removed in vacuum at room temperature, and the residue was rubbed with dry ether (20 ml). Filtration gave 3.7 g (92%) of crude **27**.HCl, m.p. 188—90°C, which, as shown by the analysis, was sufficiently pure.

$C_6H_{11}Cl_2N_5O$ (240.1). Calcd. C 30.02; H 4.58; Cl 29.55; N 29.15. Found C 30.56; H 5.32; Cl 29.36; N 28.55%.

The free base was precipitated from an aqueous solution of the salt by aqueous $NaHCO_3$ in 72% yield, m.p. 136—7°C (from methanol).*

$C_6H_{10}ClN_5O$ (203.6). Calcd. C 35.39; H 4.95; Cl 17.41. Found. C 35.84; H 5.69; Cl 17.10%.

The base **27** could also be obtained by treating an ethereal suspension of its hydrochloride with ethereal diazomethane solution. As shown by the identity of the IR spectrum of the product with that of the base obtained with $NaHCO_3$, no methylation took place under these conditions.

6,7,8,9-Tetrahydro-3-methyl-4*H*-[1,2,4]triazino[4,3-b][1,2,4]-triazin-4-one (28)

27 (6.8 g; 33 mmoles) was refluxed in a methanolic solution (60 ml) of KOH (2.2 g; 39 mmoles) for 20 min. During this period precipitation of a crystalline product started which was filtered off after cooling, and washed with methanol and ether to yield 4.4 g (79%) of **28**, m.p. 299—300°C (from aqueous methanol, 1 : 1). The product could be advantageously purified also by sublimation in vacuum.

$C_6H_9N_5O$ (167.2). Calcd. C 43.11; H 5.43. Found C 42.79; H 5.50%.

*

Acknowledgement: The authors wish to express their gratitude to Mr. I. KÁDAS for his valuable assistance in performing part of the experimental work, to Dr. P. SOHÁR, Mrs. Gy. KARSAI-SAS and Mrs. M. SZIRÁNYI-KISS for the IR, to Dr. L. LÁNG and Mr. M. VÖRÖS for the UV spectra, to Miss K. ÓFALVI, Mrs. S. VISZT-SIMON and Mrs. I. ZAUER-CSÜLLÖG for the microanalyses, and to the United Works of Pharmaceutical and Dietetic Products (Egyesült Gyógyszer és Tápszergyár), Budapest, for financial support.

REFERENCES

1. NYITRAI, J., BÉKÁSSY, S., LEMPERT, K.: Acta Chim. Acad. Sci. Hung. **53,** 311 (1967)
2. DOLESCHALL, G., HORNYÁK, Gy., HORNYÁK-HÁMORI, M., LEMPERT, K., WOLFNER, A.: Acta Chim. Acad. Sci. Hung. **53,** 385 (1967)
3. GUT, J., HESOUN, D., NOVÁČEK, A.: Coll. Czechoslov. Chem. Commun. **31,** 2014 (1966); with references to earlier literature
4. PIŤHA, J., FIEDLER, P., GUT, J.: Coll. Czechoslov. Chem. Commun. **31,** 1864 (1966)
5. DOLESCHALL, G.: Acta Chim. Acad. Sci. Hung. **53,** 395 (1967)
6. DOLESCHALL, G., HORNYÁK-HÁMORI, M., LEMPERT, K.: Acta Chim. Acad. Sci. Hung. **55,** 319 (1968)
7. DOLESCHALL, G., LEMPERT, K.: Unpublished results
8. HORNYÁK, Gy., KÁDAS, I.: Unpublished results
9. DOLESCHALL, G., HORNYÁK, Gy., LÁNG, L., LEMPERT, K., ZAUER, K.: Acta Chim. Acad. Sci. Hung. **57,** 191 (1968)
10. SZIVÓS, K.: Thesis, L. Eötvös University, Budapest, 1967

* On melting a profound change takes place: after resolidification on cooling, the product melts again only at 215—20 °C under decomposition.

11. GUT, J., in *Advances in Heterocyclic Chemistry* (Edited by Katritzky, A. R.), Vol. 1, pp. 223—228. Academic Press, New York and London, 1963
12. DORNOW, A., ABELE, W., MENZEL, H.: Chem. Ber. **97,** 2179 (1964)
13. DORNOW, A., MENZEL, H., MARX, P.: Chem. Ber. **97,** 2185 (1964)
14. FREUND, M., PARADIES, T.: Ber. **34,** 3114 (1901)

Gyula HORNYÁK
Károly LEMPERT
Károly ZAUER
Budapest XI., Gellért tér 4.

Acta Chimica Academiae Scientiarum Hungaricae, Tomus 61 (2), pp. 197—205 (1969)

ACYLATION REACTIONS WITH PHOSGENE

Z. Csűrös, R. Soós, I. Bitter, L. Szeghy and I. Petneházy

(Department of Organic Chemical Technology, Technical University, Budapest)

Received July 31, 1968

The kinetics and mechanism of the formation of carbamic acid chlorides have been studied in the reactions of aromatic primary amines with phosgene. The rate constants and the activation enthalpies were determined for aniline, substituted anilines, and for tolylene-2,4- and -2,6-diamines. The equilibria between carbamic acid chlorides and the isocyanates have been investigated and the kinetical data measured for phenylcarbamyl chloride, substituted phenylcarbamyl chlorides, and tolylene-2,4- and 2,6-dicarbamic acid chlorides. The effect of various solvents on the extent and rate of decomposition has been determined, and a mechanism of the decomposition is suggested.

In earlier communications [1, 2] we dealt mainly with the qualitative aspects of the reactions between aromatic amines and phosgene, and results pertaining to the manufacture of isocyanates were reported. Parts of the preceding research were only included to illustrate the great variety of problems which arose in the course of the work with technological aim.

In this paper we discuss the kinetics of the two main steps in the previously described [1] reaction sequence, the acylation resulting in a derivative of carbamyl chloride, and the dehydrohalogenation leading to isocyanate.

1. Acylation of aromatic amines with phosgene

The acylation proceeds according to the following overall equation:

$$2\ ArNH_2 + COCl_2 \rightarrow ArNHCOCl + ArNH_2HCl$$

No literature was available on the kinetics and mechanism of this reaction, but our preliminary experiments had revealed an extremely high reaction rate making traditional methods useless. We therefore studied the literature on the kinetics of fast reactions [3], and selected the so-called "quenching-flow" method [4], which seemed to be the most appropriate for our purpose. This method combines flow technique with the quenching of the reaction, and subsequent analysis.

The reaction was stopped with sodium or potassium methoxide or ethoxide, and the free amine content in the reaction mixture was determined in non-aqueous medium glacial acetic acid with perchloric acid. The analytical method was reported in one of our earlier publications [1].

For the purpose of the kinetical measurements, we constructed, on the basis of literature data [4], the tube reactor shown in Fig. 1. The reactants were transferred by indifferent gas (nitrogen) pressure into a mixing chamber where the reaction started. From here the reaction mixture passed through a narrow (1—2 mm diam.) tube reactor into the quenching solution. The reaction time was determined from the measured volume velocity of the reaction mixture and from the dimensions of the reactor, and it could be varied by varying these dimensions. Each point on the concentration *vs.* time curve represents the result of one experiment. The method has a reproducibility of $\pm 7\%$.

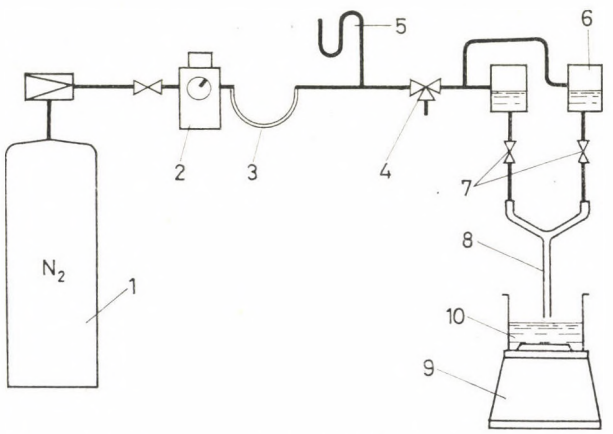

Fig. 1. Tube reactor experimental apparatus. 1. Nitrogen cylinder; 2. Pneumatic feeder; 3. Calcium chloride tube; 4. Three-way valve; 5. Mercury manometer; 6. Solvent storage vessels in a thermostated jacket; 7. Flow-through; 8. Tube reactor; 9. Magnetic stirrer; 10. Quenching fluid

We found that for reproducible results the following conditions must be carefully observed:

1. Adequate thermostating of the reactants
2. Turbulent flow in the reactor
3. Constant flow rate
4. Accurate measurement of flow through time
5. Adequate mixing of the quenching agent and the reaction mixture.

The measurements were carried out at $-5°C$, $+5°C$ and $+25°C$ in toluene, with aniline, *o*- and *p*-toluidine, *p*-chloroaniline, tolylene-2,4- and -2,6-diamine as the model substances, always using an excess of phosgene.

With each model substance 15—20 measurements were carried out by varying the initial amine concentration between 0.005 and 0.03 mol/litre. Since the sojourn time in the reactor could be varied only between 0.07 and 0.3 sec (in the case of aniline only between 0.07 and 0.15 sec due to the very high rate of the reaction), a graphic representation of the experimental results would

provide little information, since a heap of points scattered along a straight line would be obtained. For this reason, individual rate constants were calculated from the related C-t parameter pairs by means of the rate equation for reactions of second order (accounting for the fact that the hydrochloric acid liberated in the course of the reaction binds an equivalent quantity of amine). The averages of the rate constants are given in Table I. Since the values of the individual constants deviate by less than 7—8% from the average, it is resonable to assume that this reaction follows second order kinetics.

Table I

Amine	Rate constant, k ($l \cdot mol^{-1} \cdot sec^{-1}$)			Activation enthalpy, $\Delta H^{\ddagger}$	Activation entropy $\Delta S^{\ddagger}$
	—5°C	+5°C	25°C	kcal / mole	cal / mole · °K
Aniline	116	183	359	5.46	—28.5
p-Chloroaniline	56.7	87.5	157	6.58	—26.5
	0°C	10°C			
p-Toluidine	315	438	708	3.92	—27.6
o-Toluidine	85.2	123	288	6.44	—25.5
Tolylene-2,4-diamine	39.0	58.3	113	5.40	—27.5
Tolylene-2,6-diamine	18.8	27.6	57.2	5.86	—27.7

The mechanism of this reaction, like that of other N-acylation reaction, is of type S_{N_2} (bimolecular nucleophilic substitution).

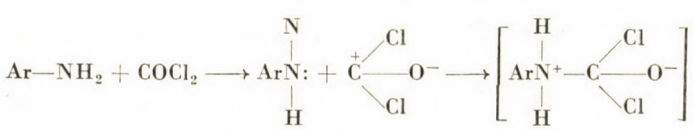

$$\xrightarrow{Ar—NH_2} Ar—NHCOCl + Ar—NH_2 \cdot HCl$$

The reaction begins with a nucleophilic attack by the amine, followed by the stabilization of the intermediate in the form of aryl carbamyl chloride, with the loss of hydrogen chloride.

The amine participates in the reaction as an electron donor. Consequently, if there are electron withdrawing groups in the aromatic ring which reduce the basicity of the amine, the reaction rate will decrease, while in the presence of electron donor groups which enhance the basicity of the amine, the reaction rate will increase. The steric vicinity of *ortho* substituents greatly reduces the reaction rate.

Graphic representation of Hammet's equation results in a straight line with a slope of $\varrho = -0.66$ (Fig. 2). The activation entropies were found to be nearly equal indicating that the structures of the activated complexes are similar for the substances investigated.

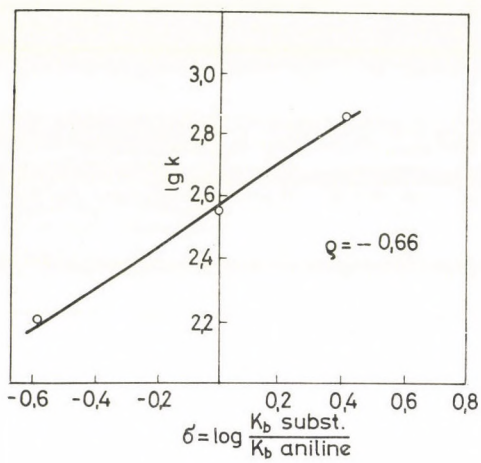

Fig. 2

HINSHELWOOD [5] observed a similar substituent effect and constancy of the activation entropies when studying the reaction between aniline and benzoyl chloride.

2. Decomposition of aromatic carbamyl chlorides

The conversion of a carbamyl chloride into isocyanate is an equilibrium elimination reaction in which the carbamyl chloride loses one molecule of hydrogen chloride. We have reported [1] that, contrary to literature data, the infrared spectrum of phenylcarbamyl chloride in various solvents has a characteristic isocyanate band at 2260 cm^{-1}, indicating the beginning of decomposition at room temperature, probably owing to an interaction with the solvent.

For a more thorough study of this problem, the carbamyl chloride-isocyanate equilibrium was studied at room temperature in the cases of *p*-chloro- and *p*-bromophenylcarbamic acid chloride by means of infrared spectrophotometry. An increase in the intensity of the isocyanate bands was observed in the order: toluene, benzene, chlorobenzene, indicating that the equilibrium is shifted (in the above order) towards decomposition. Tolylene-2,4- and 2,6-dicarbamic acid chlorides were studied in benzene, *o*-dichlorobenzene and carbon tetrachloride, and it was found that the extent of equilibrium transfor-

mation increased in the order: benzene, *o*-dichlorobenzene, carbon tetrachloride (Fig. 3).

These results reveal the important roles of both the substituents in the aromatic ring and the solvent in the decompositions of carbamyl chlorides.

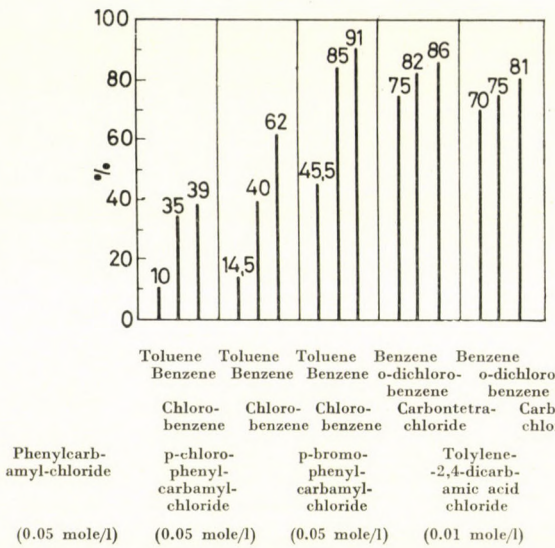

Fig. 3. Free isocyanate content of carbamyl chloride

In the same solvent, a carbamyl chloride containing halogen in para position decomposes more readily than the non-substituted carbamic acid chloride.

The rate of dehydrohalogenation of carbamyl chlorides was also studied with the same model substances and solvents. Direct measurement of the hydrochloric acid liberated in the decomposition reaction was rather difficult because of the low concentrations involved in the kinetical measurements and owing to the presence of the carbamyl chloride which continues to decompose under the conditions of the determination of hydrochloric acid.

It was not possible to apply a spectroscopic method, since we did not possess a sodium chloride cell which could be kept at constant temperature. Therefore, an indirect method was developed for the study of the reaction. The decomposition was effected in the presence of excess triethylamine which bound the hydrochloric acid liberated in the form of a salt; the amine hydrochloride precipitated quantitatively from the solvent. Sufficiently rapid filtration, washing with petroleum ether, drying and weighing gave the hydrochloric acid content at any given time with $\pm 1\%$ accuracy.

Since the salt is rapidly formed, the rate determining step is the decomposition of the carbamyl chloride. Because of the presence of triethylamine, the

reaction does not stop in an equilibrium state, but proceeds to completion until all carbamyl chloride in the solution has been used up.

A further problem is introduced by the fact that during the dissolution of the carbamyl chloride, its concentration drops to the equilibrium value. Consequently, there is a certain amount of hydrochloric acid in the solution right at the beginning of the measurement, since part of the acid chloride has already suffered decomposition. This fact has to be taken into account in the calculations.

If the change of the carbamyl chloride concentration was plotted logarithmically *vs.* the reaction time, a straight line was obtained in all cases indicating that the reaction followed first order kinetics. The calculated reaction rate constants are listed in Table II.

Table II

Carbamyl chloride	Solvent	$k_{average}$ (min^{-1})				Activation enthalpy, cal/mole
		0°C	10°C	25°C	40°C	
Phenylcarbamyl chloride	Benzene	—	0.0155	0.0694	0.2630	16.500
	Toluene	—	0.0440	0.0645	0.0925	4.370
	Chlorobenzene	0.0072	0.0250	0.1320	—	20.400
p-Chlorophenyl-carbamyl chloride	Benzene	—	0.0170	0.0745	0.2880	16.850
	Toluene	—	0.0295	0.0760	0.1780	10.260
	Chlorobenzene	0.0102	0.0340	0.1780	—	16.300
p-Bromophenyl carbamyl chloride	Benzene	—	0.0150	0.0720	0.2900	13.870
	Toluene	—	0.0236	0.0695	0.1750	10.960
	Chlorobenzene	0.0093	0.0295	0.1500	—	17.800

It appears from the rate constants that the various solvents have a significant influence on the rate of the reaction. At the same temperature, the rate constant generally increases in the order: toluene, benzene, chlorobenzene. If the aromatic ring contains an electron-withdrawing halogen atom in para position, the decomposition rate will again increase. The value of activation enthalpy is the lowest for the decomposition in toluene, and it is unexpectedly low in the case of phenylcarbamyl chloride. For the time being, we have no explanation for this phenomenon.

In the knowledge of the kinetical data, we attempted to draw conclusions on the mechanism of the reaction (Fig. 4).

Since the reaction rate is increased by the presence of an electron-withdrawing substituent in para position, we assume that the reaction starts with the cleavage of a proton ion, which is the rate determining step. Under the influence of a substituent X, the NH bond is loosened, and finally the proton

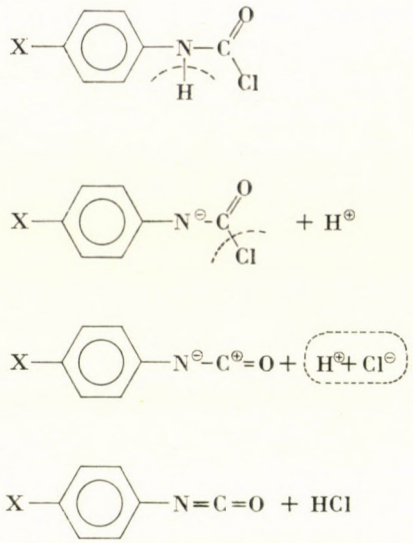

Fig. 4. X = electron-withdrawing substituent (halogen)

is split off. The transition complex formed in this way is stabilized by the elimination of a chloride ion in such a way that the unshared electron pair on the nitrogen is linked to the carbon atom whereby a carbon-nitrogen double bond is formed.

The method described above was only suitable for studying the decomposition rates of monocarbamic acid chlorides. Dicarbamic acid chlorides are scarcely soluble in inert solvents, furthermore, the equilibrium in the solution is markedly shifted in the direction of decomposition. Thus the above gravi-

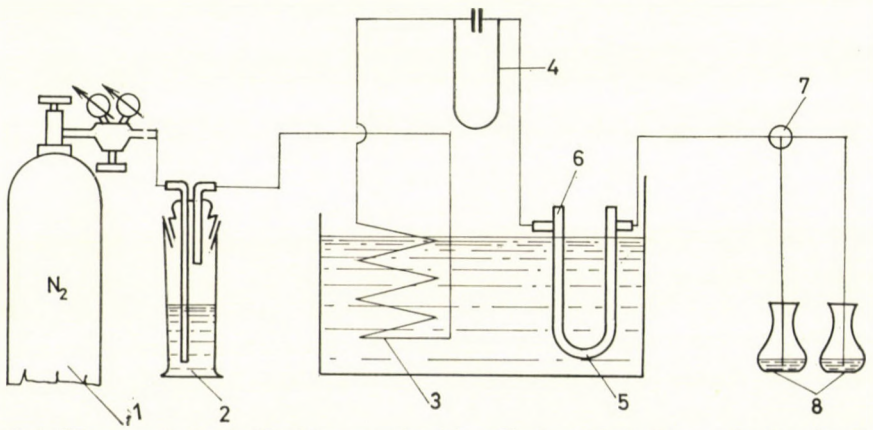

Fig. 5. 1. Nitrogen flask; 2. Washing vessel with sulfuric acid; 3. Brass tube for the thermostating of nitrogen; 4. Differential manometer; 5. Sample; 6. Reaction vessel; 7. Three-way valve; 8. Absorber with alkali

metric method cannot be used to measure the rate of decomposition of dicarbamyl chlorides.

The thermal decomposition of solid dicarbamic acid chlorides can be studied in the apparatus shown in Fig. 5.

Dry, thermostated nitrogen gas is passed in turbulent flow through a known quantity of thermostated acid chloride in a U-tube. The hydrochloric acid formed by decomposition leaves the system together with the inert gas, and is absorbed in alkali. Back-titration of the excess alkali gives the hydrochloric acid formed per unit time. (The fact that the carrier gas entrained some isocyanate interfered with the measurement. This isocyanate was converted in the wash-bottle into carbonate which also consumed alkali. This error was eliminated by applying WARDER's method [6] for the determination of carbonate and total alkali.)

The measurements were carried out at 70°C, 90°C and 110°C. The logarithm of the decrease of amount of the dicarbamic acid chloride as a function of time gave again a straight line indicating that the decomposition reaction has first order kinetics.

There was no change in the slope of the straight lines when the initial quantity of acid chloride and the flow rate of the carrier gas were varied. This confirms the first kinetical order of the decomposition reaction and shows that diffusion is not the rate determining step.

Table III contains the rate constants calculated from the slope of the straight lines and the activation enthalpies obtained from the temperature dependence of the rate constants.

Table III

Rate constants and activation enthalpies of the thermal decompositions of 2,4- and 2,6-tolylene dicarbamic acid chlorides

	Rate constant (min^{-1})			Activation enthalpy, kcal/mole
	70°C	90°C	110°C	
2,4-isomer	0.032	0.055	0.080	6.1
2,6-isomer	0.018	0.095	0.219	10.8

Investigation of the decomposition of tolylene dicarbamic acid chlorides by means of this method did not reveal a difference between the decompositions of the two types of acid chlorides. A derivatographic study of the decomposition processes indicated a certain difference in the behaviour of the 2,4- and 2,6-isomers. Since with our apparatus it was impossible to achieve quite accurate adjustment of constant temperatures, and to remove hydrogen chloride as soon as it was formed, quantitative data have not been calculated. It appears, however, probable that consecutive reactions with slightly different rates

take place and that in the case of the 2,4-isomer the cleavage of the first, in the case of the 2,6-isomer of the second hyrogen chloride molecule proceeds at higher rate. An investigation of this effect and its confirmation by means of accurate numerical data will be the subject of forthcoming experiments.

REFERENCES

1. CSŰRÖS, Z., SOÓS, R., SZEGHY, L., BITTER, I.: Periodica Polytechnica **10/4,** 495 (1966)
2. CSŰRÖS, Z., SOÓS, R., DANCSÓ, J., SZEGHY, L.: Periodica Polytechnica **10/4,** 503 (1966)
3. CALDIN, E. F.: Fast Reactions in Solution. Blackwell, Oxford, 1964
4. PINSET, J.: Disc. Faraday Soc. **17,** 140 (1954)
5. BOSE, A. N., HINSHELWOOD, C.: J. Chem. Soc. **1958,** 4085
6. ERDEY, L.: Introduction into Chemical Analysis (in Hungarian), Vol. II. Tankönyvkiadó, Budapest, 1958

Zoltán CSŰRÖS
Rudolf SOÓS
István BITTER
Lajos SZEGHY
Imre PETNEHÁZY

Budapest XI., Műegyetem rkp. 3.

INDEX

NORGANIC AND ANALYTICAL CHEMISTRY – ANORGANISCHE UND ANALYTISCHE CHEMIE – НЕОРГАНИЧЕСКАЯ И АНАЛИТИЧЕСКАЯ ХИМИЯ

SCHAY, G.: Árpád Kiss 1889—1968 107
LÉGRÁDI, L.: Mechanism of Adsorption Indication, I. Nitronic Acids as Adsorption Indicators: *p*-nitro-α-naphthyl red, a New Adsorption Indicator 115
LÉGRÁDI, L.: Mechanism of Adsorption Indication, II. Amphoteric Adsorption Indicators 125
MLINKÓ, S. and DOBIS, E.: Sulphur Determination in Organic Compounds by Radioreagent Method 133

PHYSICAL CHEMISTRY – PHYSIKALISCHE CHEMIE — ФИЗИЧЕСКАЯ ХИМИЯ

NAGY, J., FERENCZI-GRESZ, S., PÁLOSSY-BECKER, K. und BORBÉLY-KUSZMANN, A.: Dipolmomentuntersuchungen der Phenyl- und Benzylderivate von Elementen der vierten Hauptgruppe (Investigation of the Dipole Moment of the Phenyl and Benzyl Derivatives of the Elements of Group IV/1 of the Periodic Table) 149
CYVIN, S. J. and HARGITTAI, I.: Mean Amplitudes of Vibration for Small Molecules Containing Sulphur, II. Sulphuryl Fluoride, Fluoro and Chloro Sulphonic Acids 159
FREEMAN, D. E.: Stretching Force Constants in NO_2F and NO_2Cl 163

ORGANIC CHEMISTRY – ORGANISCHE CHEMIE — ОРГАНИЧЕСКАЯ ХИМИЯ

ZSAKÓ, J., VÁRHELYI, CS., GĂNESCU, J. and TURÓS, J.: Kinetics and Mechanism of Substitution Reactions of Complexes, XI. New Reinicke-salt-like Compounds Containing Para-phenetidine, and the Solvolysis of $[Cr(NCS)_4$-(*p*-phenetidine)$_2]^-$ in Ethanol–Water Mixtures 167
HORNYÁK, GY., LEMPERT, K. and ZAUER, K.: 1,2,4-Triazines and Condensed Derivatives, IX. Synthesis of Some Imidazo-, Pyrimido- and [1,2,4]-Triazino-[1,2,4]triazine Derivatives 181
CSŰRÖS, Z., SOÓS, R., BITTER, I., SZEGHY, L. and PETNEHÁZY, I.: Acylation Reactions with Phosgene 197

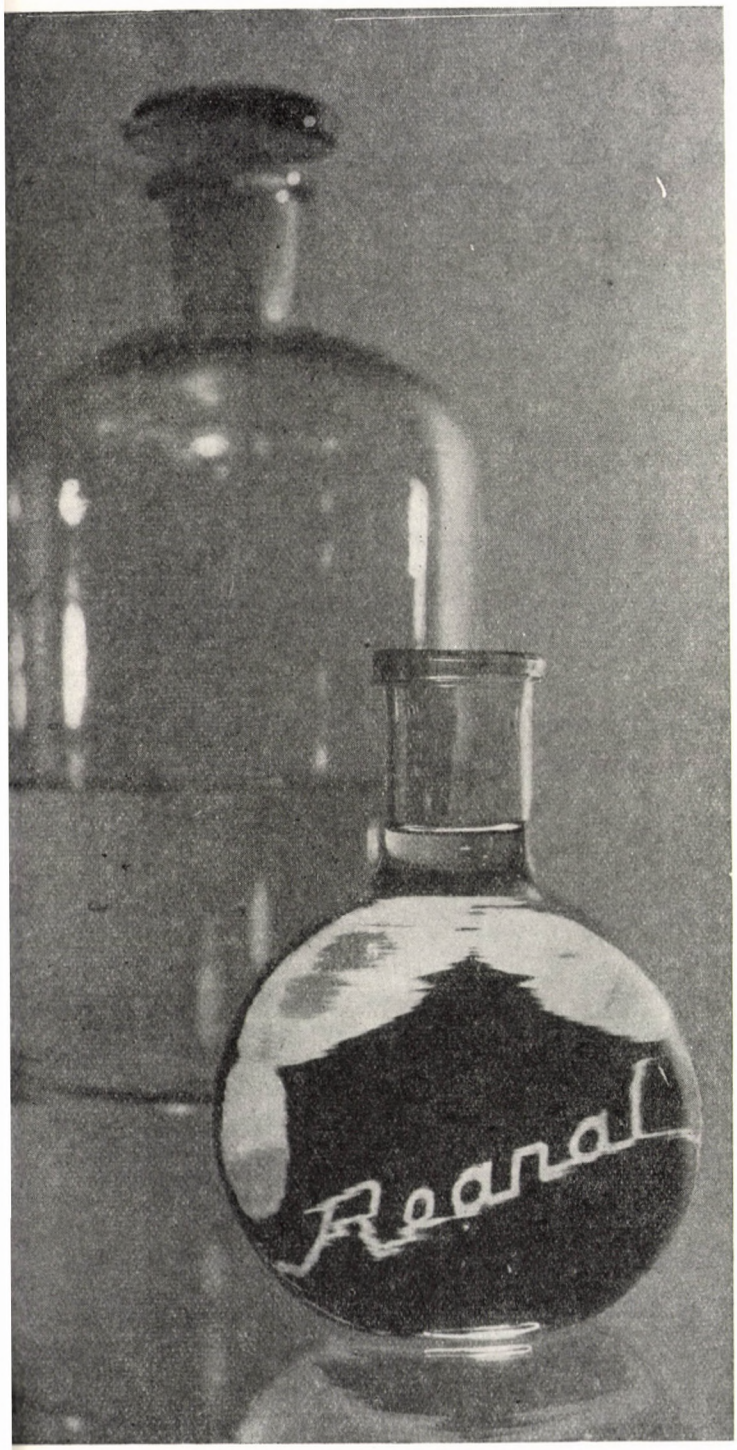

ANORGANISCHE UND ORGANISCHE FEINCHEMIKALIEN

Garantiert reine Reagenzien für analytische Zwecke

Laboratoriumspräparate für die Forschung und Technik

Biochemikalien:

Aminosäuren und Derivate · Peptide und Derivate · Enzyme und Koenzyme · Nukleoproteide · Purine

Indikatoren

Tetrazoliumsalze

Präparate für Mikroskopie und Biologie

Kohlenhydrate

»Selecton«-Reagenzien für Komplexometrie

R E A N A L FABRIK FÜR FEINCHEMIKALIEN

Budapest · Ungarn

INFORMATION
UND LITERATUR
MEDIMPEX
BUDAPEST 5 . POSTFACH 126

Printed in Hungary

A kiadásért felel az Akadémiai Kiadó igazgatója — Műszaki szerkesztő: Farkas Sándor

A kézirat nyomdába érkezett: 1969. IV. 3. — Terjedelem: 9 (A/5) ív, 26 ábra

69.67656 Akadémiai Nyomda, Budapest — Felelős vezető: Bernát György

ACTA CHIMICA

ТОМ 61 — ВЫП. 2

РЕЗЮМЕ

Механизм адсорбционной индикации, I.

Нитрокислоты как адсорбционные индикаторы: п-нитро-α-нафтилкрасный — новый адсорбционный индикатор

Л. ЛЕГРАДИ

Автором предлагается новый адсорбционный индикатор — п-нитро-α-нафтилкрасный, который может быть использован для определения ионов цианида, бромида и иодида. Титрование необходимо проводить в нейтральной или щелочной средах (pH = = 9—10,5) для цианистого иона и в щелочной среде для иодистого и бромистого ионов. Индикатор работает по кислотно-основному принципу, но механизм его действия отличается от известного до сих пор для основных красителей. Адсорбат красителя является кислотно-основным индикатором на нейтральном или положительно заряженном осадке и под влиянием щелочи образуется нитроновая кислота, которая вызывает изменение окраски. При титровании ионов цианида под влиянием избытка иона серебра также образуется нитроновая кислота, которая затем превращается обратно под влиянием цианистых ионов. При титровании в щелочной среде изменение окраски вызвано тем, что избыток иона серебра повышает константу диссоциации адсорбата-красителя, которая является слишком низкой при избытке аниона, и за счет этого адсорбат красителя дает нитроновую кислоту. Влияние индикатора может быть обнаружено при изменении константы диссоциации адсорбата-красителя, происходящем при избытке собственного иона, а также при подщелачивании положительно заряженного осадка, сопровождающегося образованием нитроновой кислоты.

Механизм адсорбционной индикации, II.

Амфотерные адсорбционные индикаторы

Л. ЛЕГРАДИ

Автором изучались кислотно-основные и адсорбционные индикаторные свойства, появляющиеся при совместном введении заместителей с эффектом +M и —M в молекулу фенил-азо-α-нафтил-амина. Заместитель фенильного кольца, находящийся в пара-положении по отношению к азоту азо-группы, оказывает решающее влияние на кислотно-основные и адсорбционные индикаторные свойства молекулы. При диазотировании 4-нитро-2-анизидина и сочетании с α-нафтил-амином образуется амфотерный адсорбционный индикатор. С помощью амфотерного адсорбционного индикатора можно титровать как в кислых, так и в щелочных средах; при этом случаются различные изменения окраски, соответствующие различным структурным изменениям. Действие индикатора происходит на основе кислотно-основного принципа, что может быть доказано измерением изменения pH в течение титрования в кислой среде и определением изменения константы диссоциации адсорбата красителя, имеющего место при избытке собственного иона в кислой и основной средах.

Радиометрическое определение серы в серорганических соединениях

Ш. МЛИНКО и О. ДОБИШ

Приводится метод и описывается установка для радиометрического измерения содержания серы в органических соединениях. Сера в органических соединениях превращается с помощью деструктивного гидрирования в сероводород, который с помощью водорода — газа-носителя пропускается через наполнитель — $Cd^{14}CO_3$. Из карбоната кадмия и сероводорода образуются в присутствии воды при комнатной температуре

сульфид кадмия, вода и двуокись углерода. Активность двуокиси углерода, образующейся в реакции, измерялась по образцу анализа углерода-14, наряду с метаном — счетным газом, в пропорциональной области. В процессе разработки данного метода был синтезирован карбонат кадмия, свободный от оксида-гидрата. Термические свойства радиоактивного реагента изучались в воздушной и водородной атмосферах. Протекание реакции объяснялось на основе полагаемого адсорбционного ионного обмена. Исследовались условия количественного протекания основной реакции по мере образования сульфида. Ограниченная емкость карбоната кадмия — согласно экспериментальным данным — объяснялась образованием твердого раствора карбоната и сульфида кадмия и органиченной способностью образования смешанных кристаллов.

Исследование дипольных моментов для фенильных и бензиловых производных элементов IV/I группы

Й. НАДЬ, Ш. ФЕРЕНЦИ-ГРЕС, К. БЕКЕР-ПАЛОШИ и А. БОРБЕЙ-КУСМАН

1. С помощью метода Онзагера в жидком состоянии определялись дипольные моменты соединений типа:

(где E = C, Si, Ge, Sn).

2. Было установлено, что в случае фенильных производных величина дипольного момента достигает минимума в случае фенил-кремниевых соединений, а для бензиловых производных возрастает монотонно.

Средние амплитуды колебания для малых молекул, содержащих атом серы. Часть II: SO_2F_2 $(OH)SO_2F$ и $(OH)SO_2Cl$

С. Й. СИВИН и И. ХАРГИТТАИ

Средние амплитуды колебания были рассчитаны для SO_2F_2, $(OH)SO_2F$ и $(OH)SO_2Cl$ из спектроскопических данных. Для двух последних молекул полученные результаты являются несколько неопределёнными. Однако данные проведенных расчётов несомненно будут служить полезной ориентацией для будущих электронографических исследований.

Растягивающие силовые постоянные в NO_2F и NO_2Cl

Д. Е. ФРИМАН

Растягивающие силовые постоянные в молекулах NO_2F и NO_2Cl, рассчитанные недавно Немешем, исходя из двух различных систем координат симметрии, являются физически несовместимыми разве, что а) они относятся к совершенно различным решениям среди мультиплетностей возможных решений проблемы колебаний и б) дисперсия силовых постоянных, полученных Немешем, значительно недооценен.

Кинетика и механизм реакций замещения в комплексах, XI.

Новые соединения типа солей Рейнеке, содержащие п-фенетидин, и сольволиз $[Cr(NCS)_4(п\text{-фенетидин})_2]^-$ в смесях этанол-вода

Я. ЖАКО, Ч. ВАРХЕЛЬИ, И. ГЭНЕСКУ и Я. ТУРОШ

Приводится синтез, результаты анализа и краткие характеристики 20 новых соединений, содержащих комплексный анион $[Cr(NCS)_4(п\text{-фенетидин})_2]^-$. Исследовали сольволиз комплексного иона $[Cr(NCS)_3(п\text{-фенетидин})_2]^-$ в смесях этанол-вода, различного со-

става, измеряя концентрации неразложившегося комплексного иона и выделяющегося иона NCS^- в зависимости от времени. Для объяснения экспериментальных результатов предполагалось протекание двух параллельных процессов обмена лигандов. Первый — это замещение группы NCS, реакция первого порядка по комплексному иону с энергией активации около 30 ккал/моль и энтропией активации 10—15 ккал/моль · °С. Состав раствора практически не оказывает влияния на скорость этой реакции. Кажущийся порядок второй параллельной реакции равен двум (первый по комплексному иону и первый по этанолу). Энергия активации этой реакции равна 22—23 ккал/моль, а энтропия активации — почти нулю. Концентрация иона водорода в растворе практически не оказывает влияния на замещение групп NCS, в то время как замещение п-фенетидина сильно ускоряется присутствием минеральных кислот.

1,2,4-Триазины и их конденсированные производные, IX.

Получение некоторых имидазо-, пиримидо- и [1,2,4]триазино-производных [1,2,4)]триазина

ДЬ. ХОРНЯК, К. ЛЕМПЕРТ и К. ЗАУЭР

6-Метил-3-метилтио-1,2,4-триазин-5(2*H*)-он **(3)**, взаимодействуя с 2-аминоэтанолом и 3-аминопропанолом, образует в зависимости от условий реакции производные 3,5-диамино-1,2,4-триазина **(4)** или 3-амино-1,2,4-триазин-5(2*H*)-она **(2c, 2d)**. Могут быть изолированы промежуточные продукты последней реакции, представляющие собой солеобразные аддукты **3** с аминоспиртами, с составом 1:1 **(5, 10.)**

Продукты взаимодействия **2c** и **2d** с тионилхлоридом **(6,** $n = 2,3$), в зависимости от применяемых условий, циклизируются в 7,8-дигидро-3-метилимидазо[2,1-c][1,2,4] триазин-4(6*H*)-он **(7,** $n = 2$) или 6,7-дигидро-2-метилимидазо[1,2-b] [1,2,4]триазин-3 (5*H*)-он **(8,** $n = 2$), и в 6,7,8,9-тетрагидро-3-метил-4*H*-пиримидо [2,1-c] [1,2,4]триазин-4-он **(7,** $n = 3$) или изомерный 5,6,7,8-тетрагидро-2-метил-3*H*-пиримидо[1,2-b] [1,2,4] триазин-3-он **(8,** $n = 3$).

Был разработан метод получения диоксо-**(21),** а также триазино-**(28)** производных триазина, со скелетом соединения **8** ($n = 2$).

Спектроскопически были определены направление замыкания кольца и некоторые другие ориентационные проблемы, а также тонкая структура потенциально таутомерных соединений. Наблюдаемые ориентационные эффекты были связаны с порядком нуклеофильности атомов азота в 1,2,4-триазиновом скелете.

Изучение реакций ацилирования, протекающих с помощью фосгена

З. ЧЮРЁШ, Р. ШОШ, И. БИТТЕР, Л. СЕГИ и И. ПЕТНЕХАЗИ

В настоящей работе исследовались кинетика и механизм образования хлоридов карбаминовых кислот, получаемых в реакции первичных ароматических аминов с фосгеном. Определялись константы скоростей, энтальпии активации и величины энтропии для анилина и его замещенных производных, а также для толуилен-2,4- и -2,6-диаминов. Также исследовалось равновесие хлорид карбаминовой кислоты — изоцианат, и измерялись кинетические данные в случае хлоридов фенилкарбаминовой и замещенных фенилкарбаминовых кислот, а также хлоридов толуилен-2,4- и -2,6-дикарбаминовых кислот. Было установлено, что различные растворители влияют на степень разложения и ее скорость. Предлагается механизм реакции разложения.

The Acta Chimica publish papers on chemistry in English, German, French and Russian.

The Acta Chimica appear in volumes consisting of four parts of varying size, 4 volumes being published a year.

Manuscripts should be addressed to

Acta Chimica
Budapest 112/91 Műegyetem

Correspondence with the editors should be sent to the same address.

The rate of subscription is 165 forints a volume. Orders may be placed with "*Kultúra*" Foreign Trade Company for Books and Newspapers (Budapest I., Fő utca 32. Account No. 43-790-057-181) or with representatives abroad.

Les Acta Chimica paraissent en français, allemand, anglais et russe et publient des mémoires du domaine des sciences chimiques.

Les Acta Chimica sont publiés sous forme de fascicules. Quatre fascicules seront réunis en un volume (4 volumes par an).

On est prié d'envoyer les manuscrits destinés à la rédaction à l'adresse suivante:

Acta Chimica
Budapest 112/91 Műegyetem

Toute correspondance doit être envoyée à cette même adresse.

Le prix de l'abonnement est de 165 forints par volume.

On peut s'abonner à l'Entreprise pour le Commerce Extérieur de Livres et Journaux «*Kultúra*» (Budapest I., Fő utca 32. Compte-courant No. 43-790-057-181) ou à l'étranger chez tous les représentants ou dépositaires.

«*Acta Chimica*» издают трактаты из области химической науки на русском, французском, английском и немецком языках.

«*Acta Chimica*» выходят отдельными выпусками разного объема. 4 выпуска составляют один том. 4 тома публикуются в год.

Предназначенные для публикации рукописи следует направлять по адресу:

Acta Chimica
Budapest 112/91 Műegyetem

По этому же адресу направлять всякую корреспонденцию для редакции.

Подписная цена «*Acta Chimica*» — 165 форинтов за том. Заказы принимает предприятие по внешней торговле книг и газет «*Kultúra*» (Budapest I., Fő utca 32. Текущий счет № 43-790-057-181) или его заграничные представительства и уполномоченные.

Reviews of the Hungarian Academy of Sciences are obtainable at the following addresses:

ALBANIA

Ndermarja Shtetnore e Botimeve
Tirana

AUSTRALIA

A. Keessing
Box 4886, GPO
Sydney

AUSTRIA

Globus Buchvertrieb
Salzgries 16
Wien I

BELGIUM

Office International de Librairie
30, Avenue Marnix
Bruxelles 5
Du Monde Entier
5, Place St. Jean
Bruxelles

BULGARIA

Raznoiznos
1. Tzar Assen
Sofia

CANADA

Pannonia Books
2. Spadina Road
Toronto 4, Ont.

CHINA

Waiwen Shudian
Peking
P. O. B. 88

CZECHOSLOVAKIA

Artia
Ve Směčkách 30
Praha 2
Poštová Novinová Služba
Vinohradská 46
Dovoz tisku
Praha 2
Mad'arská Kultura
Václavské nám. 2
Praha I
Poštová Novinová Služba
Dovoz tlace
Leningradská 14
Bratislava

DENMARK

Ejnar Munksgaard
Nörregade 6
Copenhagen

FINLAND

Akateeminen Kirjkauppa
Keskuskatu 2
Helsinki

FRANCE

Office International de Documentation et Librairie
48, rue Gay Lussac
Paris 5

GERMAN DEMOCRATIC REPUBLIC

Deutscher Buch-Export und Import
Leninstraße 16
Leipzig 701
Zeitungsvertriebsamt
Fruchtstrasse 3—4
1004 Berlin

GERMAN FEDERAL REPUBLIC

Kunst und Wissen
Erich Bieber
Postfach 46
7 Stuttgart S.

GREAT BRITAIN

Collet's Holdings Ltd.
Dennington Estate
London Rd.
Wellingborough. Northants.
Robert Maxwell and Co. Ltd.
Waynflete Bldg. The Plain
Oxford

HOLLAND

Swetz and Zeitlinger
Keizersgracht 471—487
Amsterdam C
Martinus Nijhof
Lange Voorhout 9
The Hague

INDIA

Current Technical Literature
Co. Private Ltd.
India House OPP
GPO Post Box 1374
Bombay 1.

ITALY

Santo Vanasia
Via M. Macchi 71
Milano
Libreria Commissionaria Sansoni
Via La Marmora 45
Fireze

JAPAN

Nauka Ltd.
92, Ikebukur O-Higashi 1-chome
Toshima-ku
Tokyo
Maruzen and Co. Ltd.
P. O. Box 605
Tokyo-Central
Far Eastern Booksellers
Kanda P. O. Box 72
Tokyo

KOREA

Chulpanmul
Phenjan

NORWAY

Johan Grundt Tanum
Karl Johansgatan 43
Oslo

POLAND

RUCH
ul. Wronia 23
Warszawa

ROUMANIA

Cartimex
Str. Aristide Briand 14—18.
Bucureşti

SOVIET UNION

Mezhdunarodnaya Kniga
Moscow G—200

SWEDEN

Almquist and Wiksell
Gamla Brogatan 26
Stockholm

USA

Stechert Hafner Inc.
31, East 10th Street
New York, N. Y. 10003
Walter J. Johnson
111 Fifth Avenue
New York, N. Y. 10003

VIETNAM

Xunhasaba
19, Tran Quoc Toan
Hanoi

YUGOSLAVIA

Forum
Vojvode Mišića broj 1
Novi Sad
Jugoslovenska Knjiga
Terazije 27
Beograd

ACTA CHIMICA

ACADEMIAE SCIENTIARUM HUNGARICAE

TOMUS 61 FASCICULUS 3

AKADÉMIAI KIADÓ, BUDAPEST

1969

ACTA CHIM. ACAD. SCI. HUNG.

ACTA CHIMICA

A MAGYAR TUDOMÁNYOS AKADÉMIA KÉMIAI TUDOMÁNYOK OSZTÁLYÁNAK IDEGEN NYELVŰ KÖZLEMÉNYEI

Az Acta Chimica német, angol, francia és orosz nyelven közöl értekezéseket a kémiai tudományok köréből.

Az Acta Chimica változó terjedelmű füzetekben jelenik meg, egy-egy kötet négy füzetből áll. Évente átlag négy kötet jelenik meg.

A közlésre szánt kéziratok a szerkesztőség címére (Budapest 112/91 Műegyetem) küldendők.

Ugyanerre a címre küldendő minden szerkesztőségi levelezés. A szerkesztőség kéziratokat nem ad vissza.

Az Acta Chimica előfizetési ára kötetenként belföldre 120 Ft, külföldre 165 Ft. Megrendelhető a belföld számára az „Akadémiai Kiadó"-nál (Budapest V., Alkotmány utca 21. Bankszámla 05-915-111-46), a külföld számára pedig a „Kultúra" Könyv- és Hírlap Külkereskedelmi Vállalatnál (Budapest I., Fő utca 32. Bankszámla: 43-790-057-181) vagy annak külföldi képviseleteinél és bizományosainál.

Die Acta Chimica veröffentlichen Abhandlungen aus dem Bereiche der chemischen Wissenschaften in deutscher, englischer, französischer und russischer Sprache.

Die Acta Chimica erscheinen in Heften wechselnden Umfanges. Vier Hefte bilden einen Band. Jährlich erscheinen 4 Bände.

Die zur Veröffentlichung bestimmten Manuskripte sind an folgende Adresse zu senden:

Acta Chimica
Budapest 112/91 Műegyetem

An die gleiche Anschrift ist auch jede für die Redaktion bestimmte Korrespondenz zu richten.

Abonnementspreis pro Band: 165 Forint. Bestellbar bei dem Buch- und Zeitungs-Außenhandels-Unternehmen »*Kultúra*« (Budapest I., Fő utca 32. Bankkonto No. 43-790-057-181) oder bei seinen Auslandsvertretungen und Kommissionären.

Acta Chimica Academiae Scientiarum Hungaricae, Tomus 61 (3), pp. 207—222 (1969)

CONTINUOUS DETECTION BY SIMULTANEOUS TG AND IR MEASUREMENTS OF NH_3 AND H_2O RELEASED IN THERMAL DECOMPOSITIONS

A. B. Kiss

(Industrial Research Institute for Electronics "HIKI", Imre Bródy Laboratory (TUNGSRAM), Budapest-Újpest)

Received July 16, 1968

An IR-spectroscopic method was developed to follow the release of NH_3 and H_2O during thermal decompositions. The effect of the sample-weight, the flow-rate of the carrier-gas, and the heating-rate of the furnace on the area under the maxima of the resulting curves was studied. The conditions ensuring proportionality of the area under the maxima to the amount of released gases were determined.

The measurement of H_2O was performed using its secondary reaction with CaC_2. The maxima were standardized with $CuSO_4 \cdot 5H_2O$. Simultaneous TG- and IR-measurements gave results throwing light on some details of the decomposition of ammonium paramolybdate and paratungstate which have not been studied so far.

In an earlier paper we described a study of thermal decomposition where, in addition to recording the changes in the solid phase, those in the gaseous phase were followed and recorded by infrared spectroscopy. This technique has been used first for the continuous detection of released CO_2 during the thermal decomposition of manganese(II) carbonate. A description of the procedure has been given together with the experimental results [1].

Titrimetric methods for the continuous measurement of NH_3 released in thermal decompositions have been described in the literature, among others, by Eikoh [2] and Ahn [3]. By plotting the titrimetric data against the temperature, an integral curve, similar to the TG-curve, is obtained which is a source of useful information about the reaction. Due to certain difficulties we prefer IR-spectroscopic measurements.

The method described earlier has been extended to the continuous detection of gases other than CO_2. In the present paper we report the experimental results obtained when NH_3 and H_2O vapours evolve.

Experimental

The measurements were carried out with a Chevenard-type thermobalance and a type UR 10 spectrophotometer. A 10 cm long gas-cell with a volume of 125 ml was used. The flow-rate of the carrier gas was kept at the desired level with a calibrated capillary manometer. The following settings of the spectrophotometer were used in all cases: Feste Wellenzahl, Spaltprogramm 4, Regi-

striergeschwindigkeit 50 cm^{-1}/min, Schreibzeit f. Vollausschlag 32 sec, Registriermaßstab 4 mm/100 cm^{-1}.

Ammonium paramolybdate [$3(NH_4)_2O.7MoO_3 \cdot 4H_2O$, Analar, G.R.] and ammonium paratungstate [$5(NH_4)_2O.12WO_3 \cdot 5H_2O$, Fluka, G.R.] were used in the preliminary experiments. Standardization for H_2O measurements was performed with $CuSO_4 \cdot 5H_2O$. According to X-ray diffraction data, the molybdate and the tungstate had the well-known heptamolybdate and paratungstate structures, respectively, and their composition corresponded to the above formulas.

a) Measurement of gaseous NH_3

The sample-holder of the thermobalance [1] was connected to the gas-cell of the spectrophotometer. Thus, it was possible to measure the concentration of the released gas in the cell as a function of time and temperature. The concentration was determined using the sensitive maximum at 965.0 cm^{-1}.

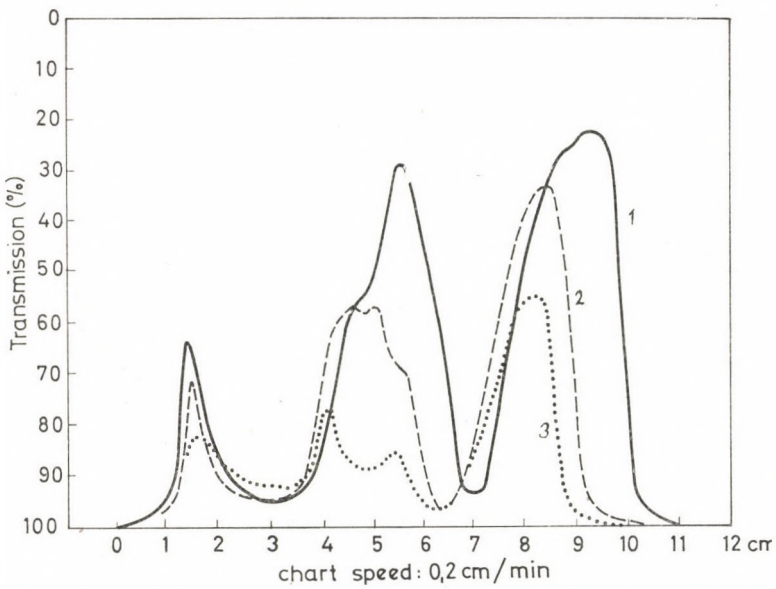

Fig. 1. IR-curve for NH_3 (ammonium paramolybdate). 1. 400 mg, 2. 200 mg, 3. 100 mg

The effect of sample-weight, flow-rate, and rate of heating was studied. The transmission *vs.* time curves for 400, 200, and 100 mg paramolybdate samples are shown in Fig. 1 (heating rate: 300°C/hr, flow-rate: 16.65 lit/hr).

Three large ammonia peaks are observed under the conditions given on Fig. 1, in agreement with the TG-curves that will be discussed later. The heights and relative areas of the peaks are strongly dependent on the sample weight.

According to the results of control measurements, this is due to the lack of proportionality between the optical density and ammonia concentration, rendering direct quantitative evaluation impossible. To circumvent this difficulty, a calibration curve was constructed by plotting transmission against the amount of NH_3 (mg) in the spectrophotometric cell. A treatment of the data in Fig. 1 using the calibration curve leads to the maxima shown in Fig. 2.

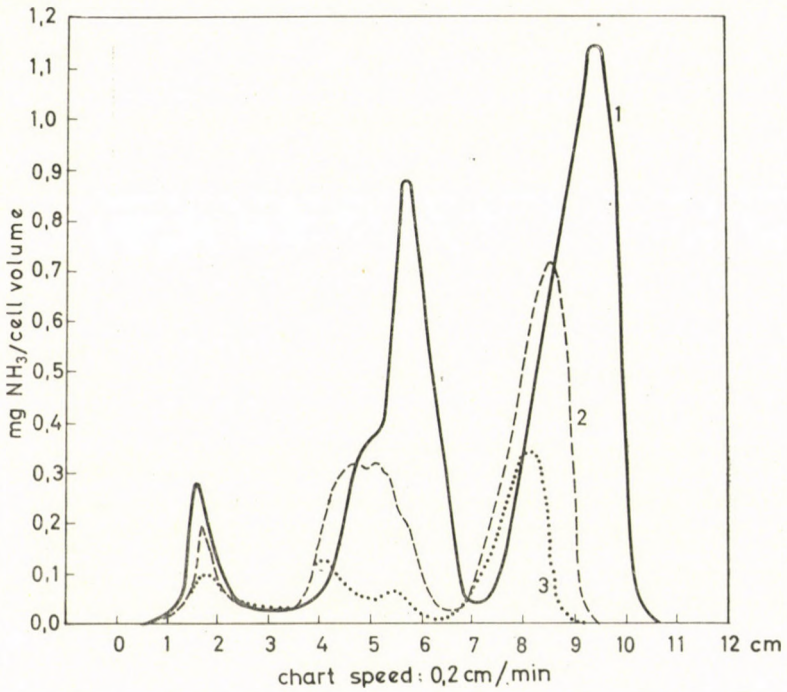

Fig. 2. IR-curve for NH_3 (ammonium paramolybdate). 1. 400 mg, 2. 200 mg, 3. 100 mg

By weighing the total areas under the curves in Fig. 2, the following results were obtained:

Sample weight (mg):	100	200	400
Index proportional to the area:	46.6 (T_1)	96.5 (T_2)	190.0 (T_3)

The surface areas are in the ratio $T_1 : T_2 : T_3 = 1 : 2.07 : 4.07$, therefore, under the present conditions, the total area under the IR-maxima is proportional to the sample weight, *i.e.* to the amount of released NH_3.

In order to study the effect of the flow-rate of the carrier-gas, measurements were performed with a 400 mg paramolybdate sample at flow-rates of

16.65, 29.26, and 40.0 (lit/hr) rate of heating: 300°C/hr. The determination of the areas gave the following results:

Flow-rate (lit/hr):	16.65 (V_1)	29.26 (V_2)	40.0 (V_3)
Index proportional to the area:	190.0 (T_1)	106.0 (T_2)	78.5 (T_3)

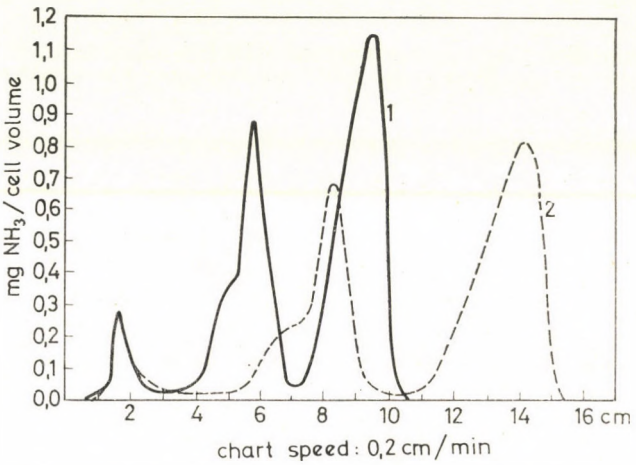

Fig. 3. IR-curve for NH_3 (ammonium paramolybdate). Sample weight: 400 mg, 1. 300°C/hr 2. 150°C/hr

The increase of the flow-rate proportionally decreases the area under the curve, as demonstrated by the following ratios:

$$\frac{V_3}{V_1} = 2.40 \quad \frac{V_2}{V_1} = 1.76 \quad \frac{V_3}{V_2} = 1.37$$

$$\frac{T_1}{T_3} = 2.42 \quad \frac{T_1}{T_2} = 1.79 \quad \frac{T_2}{T_3} = 1.35$$

In general, the heating-rate of the furnace is not linear in the whole range, therefore, for quantitative purposes one can only use recordings where the horizontal axis (time) corresponds to the linear displacement of the chart-paper (mm), similarly to Figs 1 and 2. Obviously, if the heating rate in a given interval is decreased by a factor of 1/2, only half of the original amount of NH_3 will flow through the cell in unit time, *i.e.* the area under the curve will decrease by 1/2, too. However, the total areas obtained with different heating-rates but identical chart-speeds must be equal to each other. This was proved by performing the measurements on a 400 mg sample at a flow-rate of 16.65 lit/hr, using heat-

ing-rates of 300°C/hr and 150°C/hr. The curves obtained with the above procedure are shown in Fig. 3.

The total areas under the curves in Fig. 3 are actually equal within the experimental error. The area-index is 190.0 at 300°C/hr and 188.7 at 150°C/hr.

The release of NH_3 from an 800 mg ammonium paratungstate sample was followed under experimental conditions identical with those given in Figs 1 and 2 (Fig. 4).

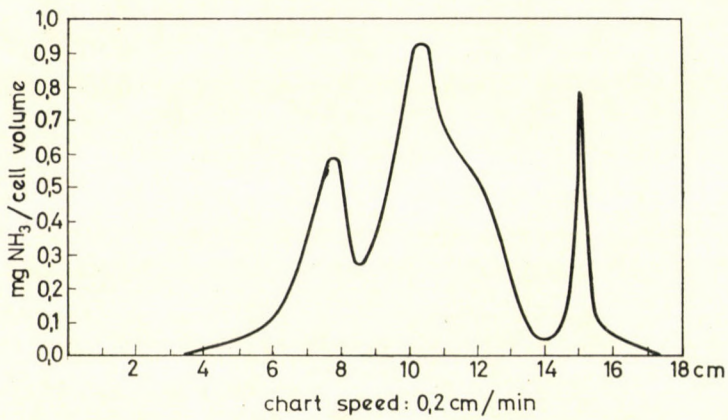

Fig. 4. IR-curve for NH_3 (ammonium paratungstate). Sample weight: 800 mg

The relative amount of NH_3 in the two compounds calculated from their formulas is in agreement with the ratio of the areas under curve 1 in Fig. 2, and the curve in Fig. 4.

$$\frac{NH_3\,mg\,(Mo)}{NH_3\,mg\,(W)} = \frac{33.07}{43.28} = 0.765 \qquad \frac{T\,(Mo)}{T\,(W)} = \frac{190.0}{245.0} = 0.775$$

b) Measurement of H_2O-vapour

Under conditions similar to those used with ammonia the direct IR-spectrometric detection of H_2O is not possible because the absence of hydrogen-bridges strongly diminishes the sensitivity of the measurement. The detection of H_2O was based on the GC studies by FORBES[4], KNIGHT and WEISS [5], SUNDBERG and MARESH [6], and DUSWALT and BRANDT [7], using the reaction

$$CaC_2 + H_2O = Ca(OH)_2 + C_2H_2$$

The amount of acetylene was measured by means of the sensitive peak at 728.0 cm^{-1}. The gases released in the thermobalance were led through a tube

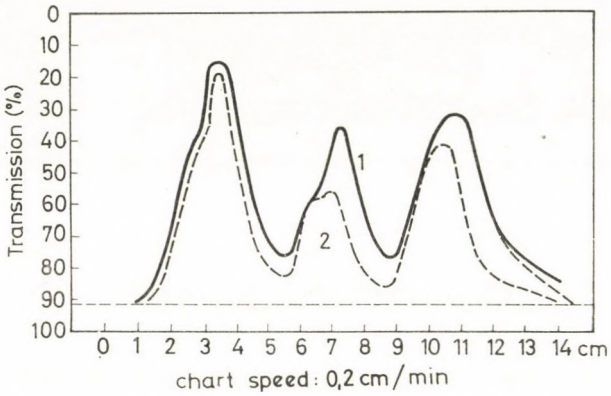

Fig. 5. IR-curve for H_2O (ammonium paramolybdate). 1. 400 mg, 2. 200 mg

(length: 25 cm, inner diameter: 1.2 cm) filled with granular CaC_2 (average grain size: 0.1—0.2 cm). The tube was connected to the gas-cell where the amount of acetylene formed in the above reaction was determined. The simultaneous determination of NH_3 and H_2O (C_2H_2) requires two experiments under identical conditions, using the wave-numbers which correspond to NH_3 and acetylene, respectively. At the above mentioned peaks the two gases do not interfere in the analyses.

Since compressed air used as carrier-gas contains some water, an acetone/dry ice trap was installed to remove water vapour. The complete dehydration of the gas, however, is unnecessary. It is sufficient if the meter indicates *e.g.* a steady 90% transmission after the carrier-gas has been flowing through the system for a time long enough to ensure equilibration.

In principle, the flow can be parted after the trap, and acetylene can be evolved at identical flow-rate from a second CaC_2-tube connected to a compensation gas-cell which is used to adjust 100% transmission. However, the presence of two CaC_2-columns introduced new sources of error which can only be eliminated by a more complex technique. The single-column procedure was found to be similar and easier to control.

Direct recordings obtained with 400 and 200 mg paramolybdate samples at 300°C/hr (flow-rate: 16.65 lit/hr) are shown in Fig. 5. Using the calibration curve for acetylene, the curves shown in Fig. 6 are obtained. The considerations mentioned in connection with NH_3 also hold for the optical density *vs.* C_2H_2-concentration relationship.

The horizontal line in Fig. 5 drawn at 90% transmission corresponds to the equilibrium amount of acetylene formed due to the humidity of the carrier-gas leaving the trap. The amount of acetylene formed during the measurement is added to this level. Thus, the horizontal band in Fig. 6 should be cut off when

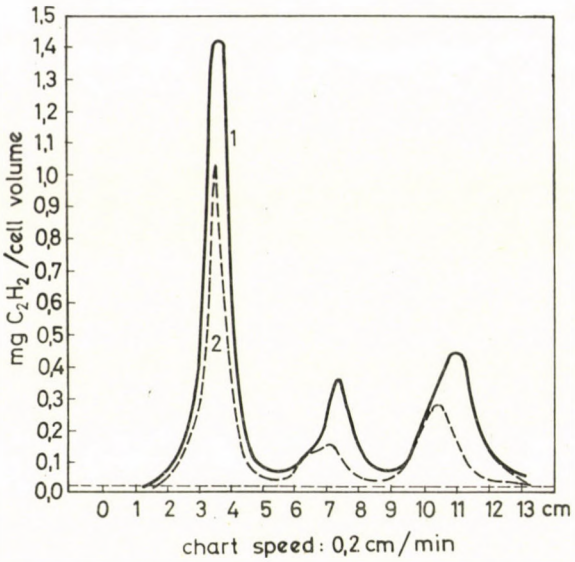

Fig. 6. IR-curve for H_2O (ammonium paramolybdate). 1. 400 mg, 2. 200 mg

determining the area. With the present two-stage freezing technique the equilibrium is reached in 30—40 min. The area-index for a 400 mg sample was 158.5, while for 200 mg it equaled 80.5, demonstrating that the ratio of the sample weights is equal to the ratio of the areas (1.96).

b) Standardization of the H_2O-Determination with $CuSO_4 \cdot 5H_2O$

Since the measurement of H_2O needed an additional reaction, the curves obtained for acetylene were standardized by IR-recordings on $CuSO_4 \cdot 5H_2O$. According to DUVAL [8] and MARIN [9], $CuSO_4 \cdot 5H_2O$ loses 4 moles of water in the interval of 67—153°C, the fifth water being released but slowly. The anhydrous salt is formed at 300°C.

The recordings obtained with 20, 40, and 60 mg of $CuSO_4 \cdot 5H_2O$ at a heating-rate of 300°C/hr (flow-rate: 16.65 lit/hr) in the above CaC_2-reactor are shown in Fig. 7.

On comparing the areas under the maxima of the IR-curves for $CuSO_4 \cdot 5H_2O$ and paramolybdate with the theoretical water-content of the samples, the data shown in Table I are obtained. According to the formula $3(NH_4)_2O.7MoO_3 \cdot 4H_2O$, the total amount of released water should be corrected for the amount of water present in the $(NH_4)_2O$ group: $(NH_4)_2O \rightarrow 2NH_3 + H_2O$.

It can be seen from Table I that the experimentally determined areas are proportional to the corresponding amount of H_2O. The proportionality indi-

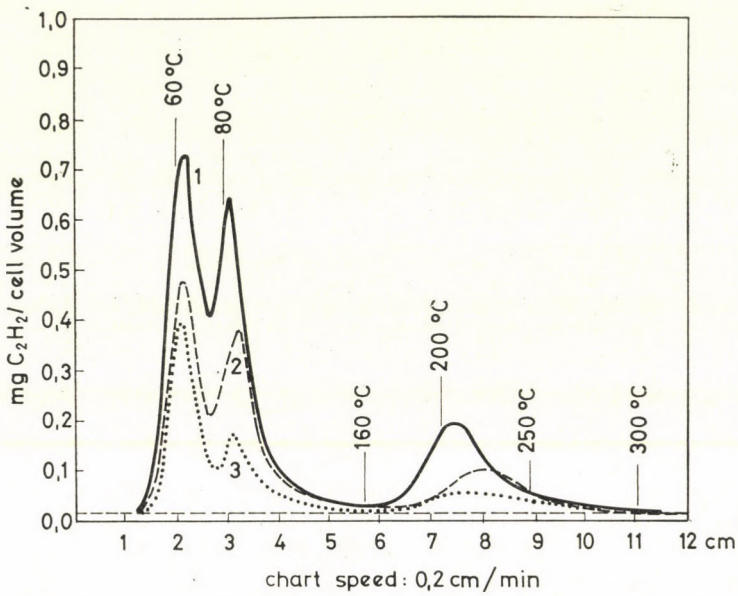

Fig. 7. IR-curve for H_2O ($CuSO_4 \cdot 5H_2O$). 1. 60 mg, 2. 40 mg, 3. 20 mg

Table I

Weight (mg)		Area $T_{(H_2O)}$	$\frac{H_2O\ (mg)}{T_{H_2O}} \times 10^{-2}$	Compound
Sample	H_2O			
20.0	7.21	28.0	25.6	$CuSO_4 \cdot 5H_2O$
40.0	14.43	56.6	25.5	
60.0	21.64	86.0	25.1	
400.0	40.70	158.5	25.7	Paramolybdate
200.0	20.35	80.5	25.2	

cates that in the CaC_2 reactor various types of water are converted to acetylene to the same degree.

The reaction between CaC_2 and water is known to take place in two steps:

$$CaC_2 + 2H_2O = Ca(OH)_2 + C_2H_2 \quad (1)$$

$$CaC_2 + Ca(OH)_2 = 2CaO + C_2H_2 \quad (2)$$

The first fast reaction is the only one to be taken into account in water analyses by gas-liquid chromatography [5, 7]. In order to obtain information

about the reaction with CaC_2 under the present conditions, we determined the total amount of acetylene formed in the CaC_2-reactor due to the thermal decomposition of $CuSO_4 \cdot 5H_2O$. The results obtained with the titration method of BARNES and MOLININI [10] are shown in Table II.

Table II

	Weight (mg)		Result (mg)		Derivation (mg)	Error %	Factor (f)
	$CuSO_4 \cdot 5H_2O$	H_2O	C_2H_2	H_2O			
o	40.0	14.43	8.81	12.20	2.23	—15.45	1.182
x	40.0	14.43	8.96	12.40	2.03	—14.05	1.163
o	60.0	21.64	13.38	18.50	3.14	—14.48	1.171
x	60.0	21.64	13.30	18.41	3.23	—14.90	1.177
o	60.0	21.64	13.42	18.60	3.04	—14.00	1.165

x: The reactor was filled with new CaC_2
o: The reactor was used three or four times

The data in Table II show that no interference from reaction *2* is observed in the thermal decomposition up to 1 hr, *i.e.* up to 300°C (at 300°C/hr). However, reaction *1* does not go to completion either, the efficiency being about 85%. Similar results, though for water-contents smaller by several orders of magnitude, were reported by KNIGHT and WEISS [5]. These authors calibrated the detector with acetylene solutions in acetone of known composition. For benzene containing known amount of water, the gas-chromatographic results were smaller than those obtained with the Fischer method.

The length of the reactor-column did not affect the results. Part of the released water may be adsorbed on the colder surfaces of the furnace tubes leading to incomplete recovery of water, *i.e.* to low water contents. An essentially identical efficiency was observed when the colder surfaces were heated with warm air (50—60°C) to decrease or eliminate adsorption of H_2O.

Since the deviation is approximately constant, as demonstrated by the data in Table II, the incomplete reaction seems not to affect the relative surface areas.

Reaction *2* was found to be very slow. However, after prolonged standing, the C_2H_2 formed in reaction *2* accumulates in the closed reactor. Before starting the measurement, this acetylene should be removed by flushing with the carrier-gas.

It should be mentioned that after the reactor had been repeatedly used, the CaO formed in reaction *2* may also bind water thus leading to low results. This source of error can be eliminated by passing air through the column for several minutes immediately before the measurement when CaO is rapidly converted to $Ca(OH)_2$ by H_2O in the air [5].

Comparison of the TG and IR measurements

Useful information about the course of thermal decomposition is obtained by plotting TG curves and IR-maxima together for the individual components against temperature. This was done for ammonium paramolybdate and ammonium paratungstate, the results being shown in Figs 8 and 9, respectively.

The time-course of the reactions is illustrated by Figs 10 and 11 constructed by the aid of the calibration curves. On the basis of Figs 10 and 11,

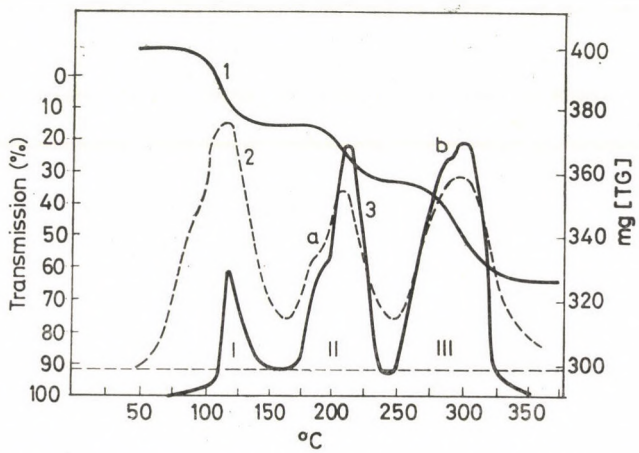

Fig. 8. Ammonium paramolybdate. Sample weight: 400 mg, 1. TG-curve, 2. IR-curve for H_2O, 3. IR-curve for NH_3

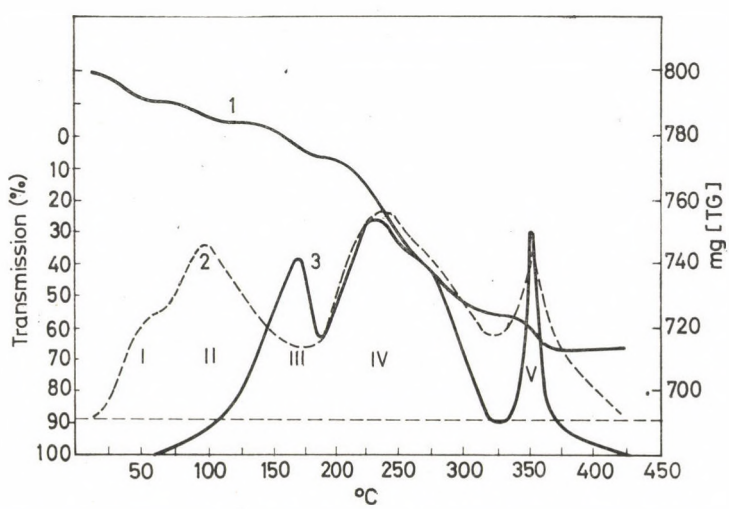

Fig. 9. Ammonium paratungstate. Sample weight: 800 mg, 1. TG-curve, 2 IR-curve for H_2O 3. IR-curve for NH_3

it is possible to make a quantitative evaluation by determining the areas under the curves.

The thermal decomposition of ammonium paramolybdate has been the subject of several papers [2, 11, 12, 13, 14]. According to thermoanalytical and X-ray diffraction studies, the reaction is composed of the following steps:

$$3(NH_4)_2O \cdot 7MoO_3 \cdot 4H_2O \xrightarrow{155-130\ ^\circ C} 2(NH_4)_2O \cdot 5MoO_3 \longrightarrow$$

$$\xrightarrow{225-245\ ^\circ C} 2(NH_4)_2O \cdot 8MoO_3 \xrightarrow{320-350\ ^\circ C} MoO_3$$

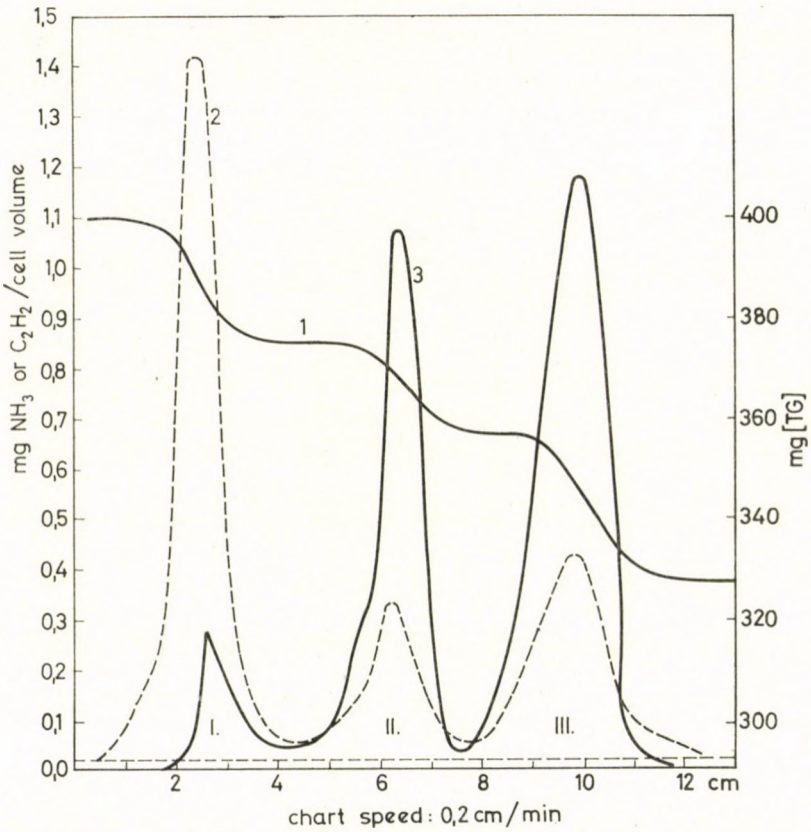

Fig. 10. Ammonium paramolybdate. Sample weight: 400 mg, 1. TG-curve, 2. IR-curve for H_2O, 3. IR-curve for NH_3

The IR-measurements yield three maxima according to the TG curves in Figs 8 and 10 for the above decomposition reaction. All three steps involve the simultaneous release of given amounts of NH_3 and H_2O. The decomposition, however, does not explain the presence of inflexion points in Fig. 8 at the locations marked by *a* and *b* on the left-hand side of maxima II and III. We have

shown by IR- and X-ray diffraction studies that the inflexion at point *a* is due to octamolybdate having a slightly different structure, while that at point *b*, to the formation of unknown intermediate phases is stable in only a narrow temperature range. Therefore, the decomposition is more complex than it was thought earlier [15].

Regardless of these observations, we consider first only the known main steps of the decomposition, and make an attempt at relating the area under

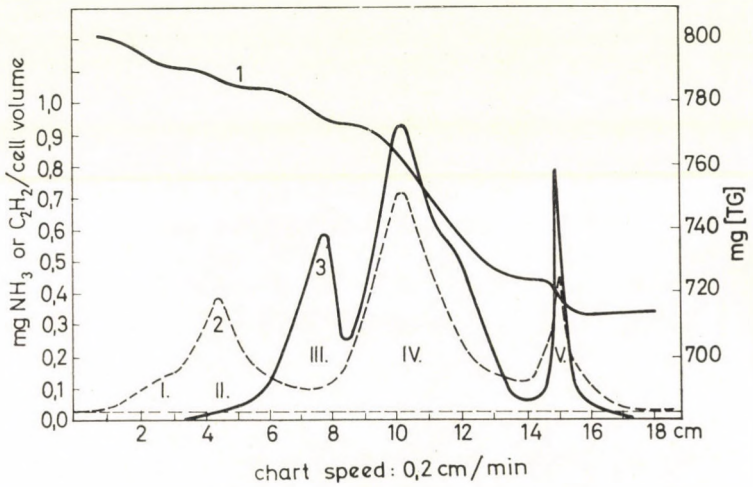

Fig. 11. Ammonium paratungstate. Sample weight: 800 mg, 1. TG-curve, 2. IR-curve for H_2O, 3. IR-curve for NH_3

the IR-maxima to the decomposition reactions. The ratios of the calculated amounts of NH_3 and H_2O (moles) released at the individual stages are

$$0.4 : 2.1 : 3.5 = 1.0 : 5.25 : 8.75 \ (NH_3)$$
$$4.2 : 1.05 : 1.75 = 4.0 : 1.0 : 1.66 \ (H_2O)$$

The ratio of the areas under the maxima in Fig. 10 is

$$\begin{array}{lllll} T_1 & T_2 & T_3 & & \\ 12.4 : 67.0 : 107.0 & = & 1.0 : 5.40 : 8.62 & (NH_3) \\ 94.0 : 23.8 : 41.0 & = & 3.94 : 1.0 : 1.72 & (H_2O) \end{array}$$

in satisfactory agreement with the theoretical proportion.

These data can be used to form an approximate picture about the reaction even if no other information is available.

Ammonium paramolybdate is an ideal model substance for the measurement of areas under the IR-maxima because the individual stages of the decom-

position are well separated. Therefore, the maxima are also well-separated, and the areas can easily be determined.

The data in the literature for the decomposition of paratungstate are much less informative than in the case of paramolybdate [3, 16]. None the less, the IR-measurements permit to draw a few qualitative conclusions which help to understand the nature of the reaction. It can be directly seen from Figs 9 and 11 that after the removal of the water of crystallization at stages I and II,

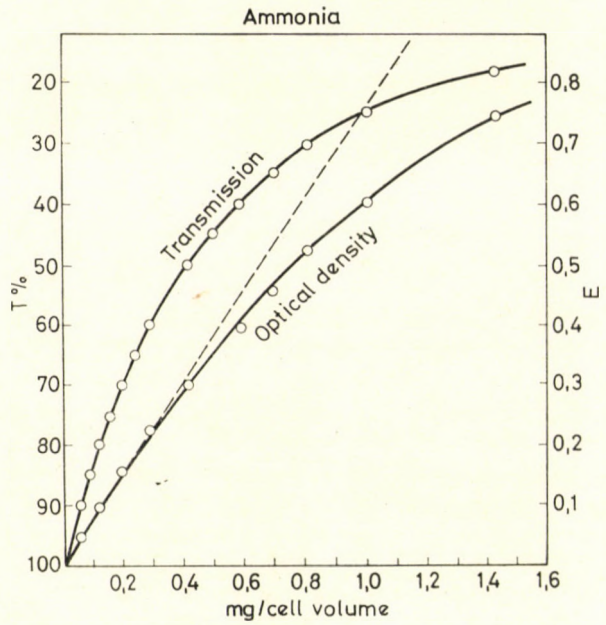

Fig. 12. Calibration curves for NH_3

dry ammonia is also formed in stage III, as opposed to ammonium paramolybdate. At stages IV and V NH_3 and H_2O are simultaneously released, probably in the proportion determined by the composition of the $(NH_4)_2O$ group. These experimental results modify the views held up till now [3, 16]. The differences between the observations for molybdate and tungstate are closely related to the mechanism of their decomposition.

The results indicate that the decomposition of paratungstate consists of overlapping steps. Therefore, the area under the maxima can only be determined by more complex graphical methods.

On comparing the TG-curves with the IR-maxima, it can be established that the maxima are located at the inflexion points of the corresponding TG-curves. The concentration of the gases in the cell gradually increases with increasing loss of weight. From the inflexion point to the beginning of the TG-

plateau, the gas-concentration, *i.e.* the absorption, gradually decreases. Qualitatively, the IR-curves characterize the thermal decomposition more sensitively than the TG-curves. This is illustrated by Figs 8 and 9 where the IR-curve clearly shows the release of water when the loss of weight is still insignificant according to the early parts of the TG-curve. Also, the inflexion points at *a* and *b* in Fig. 8 represent changes that cannot be observed on the corresponding TG-curves, at least with this particular sample-weight. Finally, the calibration curves are given in Figs 12 and 13.

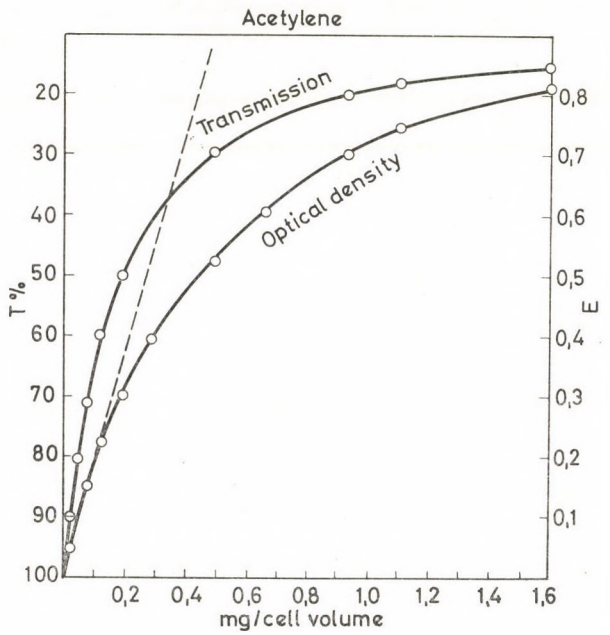

Fig. 13. Calibration curves for C_2H_2

Discussion

It can be concluded from the experimental results that simultaneous IR-measurements help to identify the reaction which takes place at the individual stages of the TG-curve, especially when more than one gas is independently released during thermal decomposition.

The method has the advantage that several gaseous products can be followed independently, thus the TG-curve referring to the total change of weight is resolved into its components.

The thermogram represents the sum of all processes accompanied by loss of weight, the DTG-curve being its derivative. The IR-curves with the maxima, too, can be regarded as derivatives of a TG-curve. More specifically, they correspond to the derivatives of an integral function involving all the components

of the TG-curve, at least in the case when the change of weight is the result of releasing only the two gases which are measured. The method is suitable for studying thermal decompositions where gases such as NH_3, CO, CO_2, NO, NO_2, SO_2, and H_2O are released. However, if the cells and the connections are thermostated, the method, in principle, can be extended to the study of thermal decompositions leading to any volatile product, provided the latter is measurable by IR-spectroscopy. Reductions leading to the formation of H_2O may be followed, too. Similar studies have been carried out for paramolybdate and paratungstate [17].

If a calibration curve is available, the measurement of the above gases becomes a matter of routine, it being necessary to include a secondary reaction only in the case of H_2O. A few points of interest should be made on the latter.

As it has been mentioned in the Experimental Part, reaction *1* leading to acetylene is fast. From Figs 8, 9, 10, and 11 one concludes that, under those experimental conditions, the reaction rate is high enough to ensure that the acetylene concentration followed that of the released water without a time-lag. The coincidence of the H_2O-maxima with the inflexion points on the TG-curves is as good as for NH_3. If the reaction with CaC_2 had involved a time-lag, the NH_3 and the H_2O peaks could not have coincided (*cf.* steps II and III in Figs 8 and 10), although it is certain that NH_3 and H_2O are, at these stages, released simultaneously in the ratio determined by the composition of the $(NH_4)_2O$ group. The decomposition of molybdate thus proves that the reaction with CaC_2 does not introduce any time-lag.

One can only speculate about the decreasing efficiency of reaction *1*. Since we used CaC_2 containing 10—15% of CaO, the decrease in efficiency may be due to the binding of H_2O by CaO. The CaO present as an impurity differs significantly from that formed in reaction *2*. The latter is located on the outer surfaces of the grains and can easily be converted to $Ca(OH)_2$ with humid air. The original CaO-impurity, on the other hand, becomes accessible for H_2O only as CaC_2 is being gradually used up. Therefore, during the measurement it gradually reaches the surface and consumes water. These considerations indicate that reaction *1* only appears to be incomplete.

The objective of the present work was to further develop this method of investigation. The new information about the thermal decomposition of molybdate and tungstate obtained by X-ray, IR and derivatographic techniques will be presented in subsequent papers.

*

The author is indebted to Dr. A. J. HEGEDÜS for directing his attention to the problem and performing the TG-measurements, as well as for helpful comments in the course of the work. The assistance by Mr. P. GADÓ in connection with the X-ray studies is gratefully acknowledged.

REFERENCES

1. HEGEDÜS, J. A., KISS, A. B.: Acta Chim. Acad. Sci. Hung. **51,** 251 (1967). Magy. Kém. Foly. **73,** 41 (1967).
2. EIKOH, Ma.: Bull. Chem. Soc. Japan **37,** 171 (1964); **37,** 648 (1964).
3. AHN, Y.: Japan Soc. Powder Metallurgy **8,** 253 (1961).
4. FORBES, I. W.: Anal. Chem. **34,** 1125 (1962).
5. KNIGHT, H. S., WEISS, F. T.: Anal. Chem. **34,** 749 (1962).
6. SUNDBERG, O. E., MARESH, C.: Anal. Chem. **32,** 274 (1960).
7. DUSWALT, A. A., BRANDT, W. W.: Anal. Chem. **32,** 272 (1960).
8. DUVAL, C.: Anal. Chim. Acta **16,** 223 (1957).
9. MARIN, Y., DUVAL, C.: Anal. Chim. Acta **6,** 47 (1952).
10. BARNES, L. JR., MOLININI, L. J.: Anal. Chem. **27,** 1025 (1955).
11. DUVAL, C.: Inorganic Thermogravimetric Analysis. Elsevier, Amsterdam (1953), p. 332.
12. HEGEDÜS, J. A., SASVÁRI, K., NEUGEBAUER, J.: Z. anorg. allg. Chem. **293,** 56 (1957).
13. FUNAKI, K., SEGAWA, T.: J. Electrochem. Soc. Japan **18,** 152 (1950).
14. RODE, E. YA., TVERDOKHLEDOV, V. N.: Zhur. Neorg. Khim. **3,** 2343 (1958).
15. GADÓ, P., HEGEDÜS, J. A., KISS, A. B.: to be published.
16. WANEK, W.: Silikaty **6,** 70 (1962).
17. KISS, A. B.: Progress Report, Telecommunication Research Institute (1967).

András B. KISS; Budapest IV., Váci út 77

Acta Chimica Academiae Scientiarum Hungaricae, Tomus 61 (3), pp. 223—231 (1969)

CONDUCTIVITY OF MIXED ALKALI GLASSES CONTAINING ALUMINIUM OXIDE

Z. BOKSAY and M. GURMAI

(Department of General and Inorganic Chemistry, Eötvös Loránd University, Research Group for Inorganic Chemistry of the Hungarian Academy of Sciences, Budapest)

Received August 2, 1968

The electric resistivity and transference numbers of cations in glasses which belong into the Na_2O—K_2O—Al_2O_3—SiO_2 system were determined. While the resistivity at 400°C of sodium aluminium silicate glasses changes in function of aluminium/alkali ratio within one order of magnitude, the resistivity of potassium glasses increases by about three orders of magnitude, in a narrow range of composition. The unusually high electric resistivity of K_2O—Al_2O_3—SiO_2 glasses with a high aluminium content can be explained on the basis that an excess of activation energy is needed to form breaches among oxygen ions in the rigid network for the jumping potassium ions.

A rather consistent and detailed picture on the electric conductivity of alkali-aluminium silicate glasses, containing sodium as the univalent ion, can be formed on the basis of the literature [1—9]. First, it has been supposed [2, 4] and later proved [10] that all the aluminium ions in the glass are fourfold coordinated if the mole per cent of the aluminium oxide is lower than that of the sodium oxide. From the point of view of conductivity it is important that AlO_4 tetrahedra, composed of several atoms and carrying one negative charge, bind sodium ions less strongly than do the non-bridging oxygen ions. ISARD supposed also [4] that in the neighbourhood of the AlO_4 tetrahedron the sodium ion was located in a hole bigger than its diameter, like in the structure of some crystalline aluminium silicates.

Thus, on the basis of this supposition it seems to be possible to replace a sodium ion with a somewhat larger ion without causing a significant distortion of the lattice. In more simple silicate (and borate) glasses which do not contain aluminium, the site of a smaller ion cannot be occupied by a larger one without difficulty. To support this idea we may point to the so-called mixed alkali glasses containing *e.g* potassium and sodium in which during the electrical conduction it quite often occurs that a potassium ion has to occupy the site of a sodium ion. According to our interpretation [11—13], the hindrance in the way of such steps causes the resistivity of a mixed alkali glass to be higher by several orders of magnitude than that of a glass containing only one type of alkali ions. Mixed alkali glasses with aluminium oxide were studied by GRETCHANIK [3] who found that when silicium oxide was replaced by a 1 : 1 mixture of sodium and potassium oxides at given aluminium oxide contents, $T_{\varkappa 100}$ (*i.e.* the temperature at which the specific conductivity is $100 \cdot 10^{10}\ \Omega^{-1}\ cm^{-1}$) generally

diminished. However, there exists a certain range of composition in which the increase of the concentration of the conducting ions (Na^+ and K^+) makes unexpectedly the $T_{\varkappa 100}$ higher.

Since no solution for the question concerning the possibility of occupying the sites of sodium ions by potassium ions is forthcoming from experiments described by GRETCHANIK because of lack of data (*e.g.* the $T_{\varkappa 100}$ value of pure potassium glass), the phenomenon gave further impulse to study aluminium glasses more thoroughly.

The ratio of alkali ions to oxygen ions in our glasses was constant and that of aluminium oxide to alkali oxide, x, was severally $\frac{1}{2}$, $\frac{1}{4}$, $\frac{1}{8}$, and in the marginal case, zero (*cf.* Table I). Within the mixed alkali glass system the mole

Table I

Mole per cent composition of the glasses

x	Me_2O	Al_2O_3	SiO_2
0	21.4	—	76.6
1/8	21.7	2.72	75.58
1/4	22.0	5.50	72.50
1/2	22.64	11.32	66.04

fraction of potassium, $n_K = \frac{K}{Na + K}$ was zero, 0.25, 0.50, 0.75, or 1.0. Glasses with lower alumina content ($x = 0$, or 1/8) were fused in platinum crucibles and in an electrical furnace at 1350°C, the other glasses were prepared in mullite crucibles at 1500°C. The potassium glasses having high transformation temperature were remelted in a hydrogen—oxygen flame. For measuring electric resistances, the apparatus described earlier [12] was used.

Table II lists the logarithms ($\lg \varrho$) of the resistivity at 400°C of sodium- and potassium-aluminium silicate glasses, and of mixed alkali glasses containing equal quantities of these alkali metals. In this Table also the values of the Rasch—Hinrichsen constants α and β in the equation $\lg \varrho = \frac{\alpha}{T} - \beta$ are included. Measured data as functions of the ratio of aluminium to alkalies are plotted in Figs 1, 2 and 3. The curves of the sodium glasses and of the mixed alkali glasses are of similar shape at least in Figs 1 and 2 and indicate that, according to expectation, the resistivity and the α values — which include the activation energies — of mixed alkali glasses are higher throughout. Quite surprisingly, the curves for the potassium glasses show in all three instances a steep rise in the

Table II

Specific resistance, constants α and β of the glasses as a function of the aluminium to alkali ratio

n_K	x	lg ϱ 400°C	α 400°C	β 400°C
0.00	0	3.02	3560	2.27
	$\frac{1}{8}$	3.08	3880	1.96
	$\frac{1}{4}$	3.84	3630	1.54
	$\frac{1}{2}$	3.60	3530	1.64
0.5	0	4.98	5540	3.49
	$\frac{1}{8}$	5.16	5730	3.37
	$\frac{1}{4}$	5.24	5500	2.92
	$\frac{1}{2}$	5.24	4600	1.59
1.0	0	3.78	3640	2.41
	$\frac{1}{8}$	3.52	3590	1.82
	$\frac{1}{4}$	6.51	8700	6.41
	$\frac{1}{2}$	6.61	8700	6.31

range between $x = \frac{1}{8}$ and $\frac{1}{4}$; unusually high resistivity, α and β values are in evidence which hardly change with the further increase of x.

Since pure potassium glasses form the extreme cases of mixed alkali glasses with constant value of x, it is to be expected that a rise of x from $\frac{1}{8}$ to $\frac{1}{4}$ will cause a significant change in the behaviour of mixed alkali glasses. In the experimental study of this phenomenon, of two series of glasses ($x = \frac{1}{8}$, respectively $\frac{1}{4}$) specific resistance, α and β values, further, transference numbers of cations were measured. Since the determination of transference number was carried out at 270°C in order to compare it with log ϱ values, in Table III the data for 270°C beside those for 400°C are listed. (However, from this Table

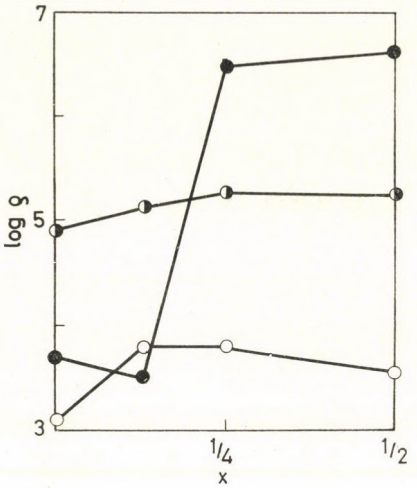

Fig. 1. Resistivity as a function of the ratio of aluminium to alkali. ○ $n_{Na} = 1$; ● $n_K = 1$; ◑ $n_{Na} = n_K = 0.5$

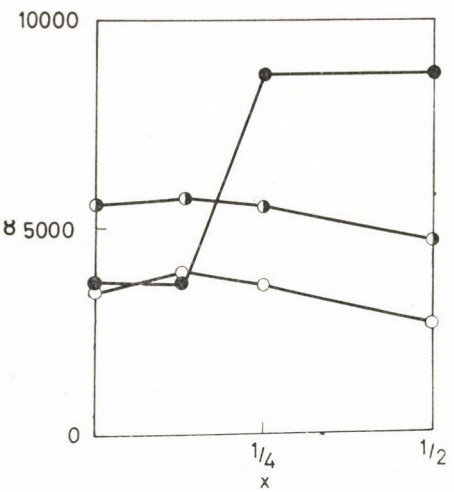

Fig. 2. The value of α as a function of the ratio of aluminium to alkali (x). ○ $n_{Na} = 1$; ● $n_K = 1$; ◑ $n_{Na} = n_K = 0.5$

resistivity value for 270°C of pure potassium glasses is lacking because this falls outside the measuring range of the apparatus available.)

Specific resistance as a function of the mole fraction of the potassium ions is by and large independent of x in the range $n_K \leq 0.5$ (*cf.* Fig. 4), and there is a constant difference between the respective α and β values of the two series of glasses (Figs 5 and 6).

However, in the range around $n_K = 0.75$ there is a significant deviation in lg ϱ values and in the potassium ion transference number, v_K, as shown in Fig. 7. The fact that, at ratio $x = \frac{1}{4}$, α is somewhat higher, v_K somewhat lower

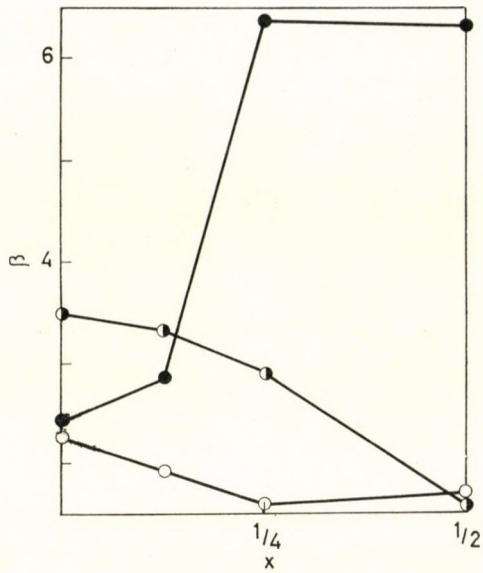

Fig. 3. The value of β as a function of the ratio of aluminium to alkali. ○ $n_{Na} = 1$; ● $n_K = 1$; ◑ $n_{Na} = n_K = 0.5$

Table III

Specific resistance, constants α and β, potassium ion transference number of mixed alkali glasses as functions of composition

x	n_K	lg ϱ (270°C)	lg ϱ (400°C)	α (400°C)	β (400°C)	v_K (270°C)
$\frac{1}{8}$	0.00	5.24	3.80	3800	1.96	0.00
	0.25	6.48	4.67	4830	2.94	0.01
	0.50	7.20	5.16	5730	3.37	0.19
	0.75	6.93	5.05	5300	2.84	0.87
	1.00	4.80	3.52	3590	1.82	1.00
$\frac{1}{4}$	0.00	5.10	3.84	3630	1.54	0.00
	0.25	6.15	4.48	4500	2.20	0.01
	0.50	7.20	5.24	5500	2.92	0.22
	0.75	7.59	5.64	5450	2.46	0.44
	1.00	—	6.61	8700	6.31	1.00

in comparison to the other series, indicates in glasses the presence in significant concentrations of potassium ions which require high activation energies and participate only to a lesser degree in conduction. A significant proportion of immobile potassium ions diminish the conductivity also in the sense that they

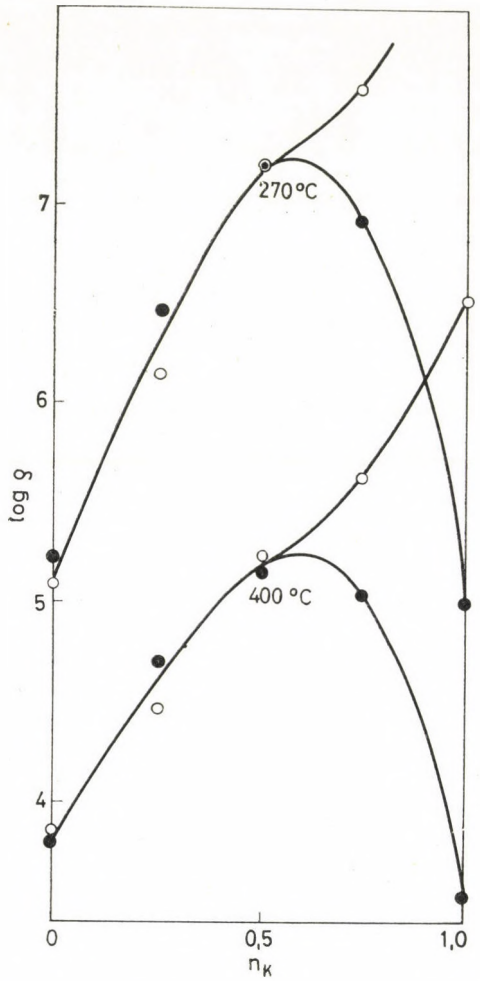

Fig. 4. Resistivity as a function of potassium mole fraction: ● $x = \frac{1}{8}$; ○ $x = \frac{1}{4}$

prevent the migrating of sodium ions as do calcium, barium or other bivalent ions of similar size.

Also the behaviour observed by GRETCHANIK may be the consequence of impeded migration of sodium ions (and thus of an overall decrease of conductivity or increased $T_{\varkappa 100}$) caused by the immobile potassium ions introduced with the sodium-potassium mixture, though the concentration of the univalent ions increased in that particular range of composition. The original question whether a potassium ion can fit easily into the space vacated by a sodium ion will be left unanswered for the time being because one potassium ion cannot easily migrate to the site of any other potassium ion if the concentration of AlO_4 tetrahedrons is sufficiently high.

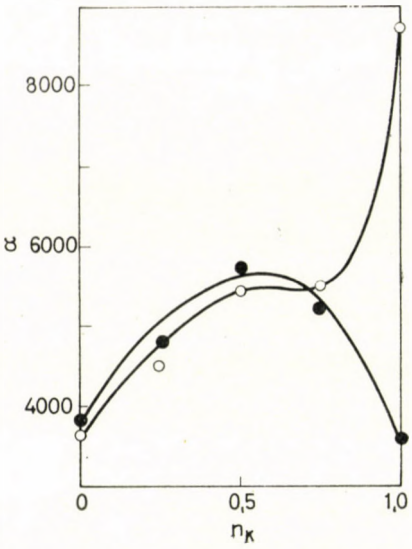

Fig. 5. α as a function of potassium mole fraction; ● $x = \frac{1}{8}$, ○ $x = \frac{1}{4}$

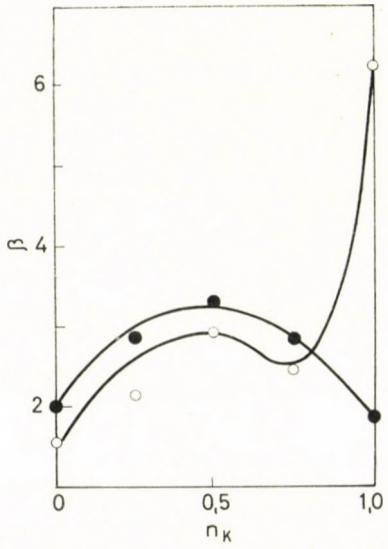

Fig. 6. β as a function of potassium mole fraction; ● $x = \frac{1}{8}$, ○ $x = \frac{1}{4}$

Thus the problem might be formulated: why is the activation enthalpy of potassium ion migration so high in glasses containing Al_2O_3 (39.7 kcal·mole^{-1} calculated from the α value of a pure potassium glass)?

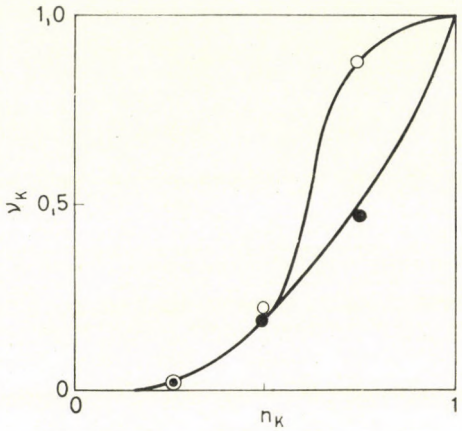

Fig. 7. Correlation between the transference number and mole fraction of potassium ions; $\bullet\ x = \frac{1}{8}, \circ\ x = \frac{1}{4}$

This might be interpreted as follows. A comparatively large potassium ion can pass from one hole into the other if the groups of the network separate sufficiently from each other. The movements of a network structure composed of silicium and oxygen are not greatly restricted if enough non-bridging oxygen ions interrupt the network and loosen the rigidity of the structure [16]. In structures like this, potassium ions move as easily as sodium ions [7]. If concentration of aluminium ions increases then the number of non-bridging oxygen ions will become less and the structure more rigid. At the beginning this change does not significantly affect the conductivity since the potassium ions being out of the environment of the AlO_4 tetrahedrons can migrate without difficulty. When the concentration of aluminium has reached a value (aluminium ions have bound one fourth of the non-bridging oxygen ions) that causes restriction of mobility to spread over the entire network structure, potassium ions can change their position only at the expense of a considerable high energy.

REFERENCES

1. Gehlhoff, G., Thomas, M.: Z. Techn. Phys. **6,** 544 (1925).
2. Moore, H., DeSilva, R. C.: J. Soc. Glass Technol. **36,** 5 (1952).
3. Gretchanik, L. A.: Zh. Prikl. Him. **31,** 1164 (1958).
4. Isard, J. O.: J. Soc. Glass Technol. **43,** 113T (1959).
5. Tsehotski, V. A., Mazurin, O. V., Evstropev, K. K.: Fiz. Tverd. Tela **5,** 586 (1963).
6. Mjuller, R. L., Pronkin, A. A.: Zh. Prikl. Him. **36,** 1192 (1963).
7. Pronkin, A. A.: Zh. Prikl. Him. **37,** 887 (1964).
8. Ivanov, O. A., Galant, E. I.: Electricheskie svoistva i stroenie stekla. Izdat. "Himia", Moskva—Leningrad.
9. Lengyel, B., Boksay, Z., Varga, M.: Z. phys. Chem. In the press.

10. DAY, D. E., RINDONE, G. R.: J. Am. Ceram. Soc. **45,** 579 (1962).
11. LENGYEL, B., BOKSAY, Z.: Z. phys. Chem. **203,** 93 (1954).
12. LENGYEL, B., BOKSAY, Z.: Z. phys. Chem. **204,** 154 (1955).
13. LENGYEL, B., BOKSAY, Z.: Z. phys. Chem. **223,** 49 (1963).
14. LENGYEL, B., BOKSAY, Z., DOBOS, S.: Z. phys. Chem. **223,** 186 (1963).
15. LENGYEL, B., BOKSAY, Z.: Z. phys. Chem. In the press.
16. DAY, D. E., RINDONE, G. E.: J. Am. Ceram. Soc. **45,** 496 (1962).
17. LENGYEL, B.: Glastechn. Ber. **18,** 177 (1940).

Zoltán BOKSAY; Budapest VIII., Múzeum krt. 6/8
Mihály GURMAI; Budapest XI., Budafoki út 91

Acta Chimica Academiae Scientiarum Hungaricae, Tomus 61 (3), pp. 233—239 (1969)

CONTRIBUTIONS TO THE HETEROFUNCTIONAL CONDENSATION OF SILANES, I

INVESTIGATION OF THE PREPARATION OF SILOXANES WITH REGULAR STRUCTURES

T. SZÉKELY, P. RÖSNER and P. GÖMÖRY

(Research Group of Inorganic Chemistry, Hungarian Academy of Sciences and Department of General and Inorganic Chemistry of the Loránd Eötvös University, Budapest)

Received August 4, 1968

Heterofunctional condensation between alkoxy silanes and chlorosilanes was studied with the aim to establish how far this reaction is suitable for the preparation of "tailor made" siloxane polymers or oligomers with regular structures. It was found that when the reaction proceeds in a solvent the equilibration which is one of the interfering side-reactions can be eliminated, but substituent exchange limits the possibility of producing molecules with regular structure to the range of low molecular weights.

By varying the alkyl radical in the alkoxy group certain conclusions may be drawn on the mechanism of the reaction and the role of the catalyst.

The siloxane chain, that is the molecular skeleton, may be easily prepared by the condensation of silanols:

$$\equiv Si{-}OH + HO{-}Si \equiv \longrightarrow \equiv Si{-}O{-}Si \equiv + H_2O \qquad (1)$$

Silanols on the other hand are readily formed by the hydrolysis of compounds, most generally chlorosilanes, containing a silicon functional (hydrolysable) group:

$$\equiv Si{-}Cl + H_2O \longrightarrow \equiv Si{-}OH + HCl \qquad (2)$$

Starting from a silane containing a functional group, or from the mixture of silanes possessing various functional groups, processes (2) and (1) will take place subsequently. Thus the polymer product may be obtained from the starting monomer, or mixture of monomers by a single operation.

Simultaneously with the introduction of this reaction which is used in the large scale production of silicones, a so-called "non-aqueous" method was suggested for the preparation of siloxanes. This method is based on the fact that silanes containing two different functional groups condense in the presence of a catalyst ($FeCl_3$, $FeCl_3 \cdot 6\ H_2O$ or $ZnCl_2$) in a single step, according to the following reaction:

$$\equiv Si{-}OY + X{-}Si \equiv \xrightarrow{\text{catalyst}} \equiv Si{-}O{-}Si \equiv + XY \qquad (3)$$

The reaction is known as heterofunctional condensation and this leads to the preparation of both linear [1] and branched siloxanes [2].

Although this reaction is slower than the hydrolytic one and requires in general a catalyst, it displays, however, several advantageous features [3, 5], and its more thorough study seemed to be challenging. The reaction has the advantage that if no other process except the heterofunctional condensation proceeds, a molecular structure with regular sequences can be obtained and, in addition, valuable by-products are formed (not only a hydrochloric acid solution, as in the hydrolytic reaction).

Heterofunctional condensation is important from both preparative and practical aspects also because it enables the co-condensation of monomers with different functional groups and consequently with widely different hydrolysis and condensation rates. Thus, for instance, di- and tetrafunctional units may in fact be coupled only by heterofunctional condensation, since simple hydrolysis results only in very slight co-condensation.

Experiments were carried out to select the most suitable catalyst, since beyond a few concrete examples like $FeCl_3$, $AlCl_3$ etc. literature mentions only that the catalysts are in general Lewis acids. On the basis of these experiments — on which we shall report in detail in a forthcoming publication — we found that for our present purposes from the point of view of reproducibility and simplicity the most suitable catalyst seems to be $Fe_2(SO_4)_3 \cdot H_2O$.

We wished to employ heterofunctional condensation for the synthesis of branched molecules of known structure. The simplest model is a molecule which contains but a single branching (trifunctional unit) [3, 4]. This "star molecule" is illustrated by the following formula:

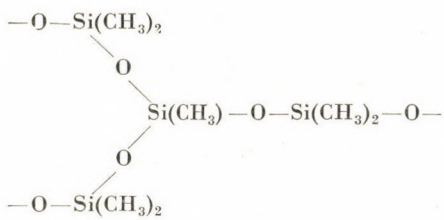

In the synthesis methyltriethoxysilane (I) was the branching centre which reacted with a chain increasing heterofunctional monomer, namely dimethyl-*n*-butoxychlorosilane (II):

$$(CH_3)-Si\equiv(OC_2H_5)_3 + 3n\,(CH_3)_2{=}SiCl(OC_4H_9) \xrightarrow{\text{catalyst}}$$
$$\longrightarrow (CH_3)-Si\equiv\left\{[OSi{=}(CH_3)_2]_{n-1}\,[OSi{=}(CH_3)_2\,(OC_4H_9)]\right\}_3 +$$
$$+ (3n-3)\,C_4H_9Cl + 3\,C_2H_5Cl \qquad (4)$$

It was found that in accordance with Eq. (4) the reaction indeed starts in all four directions. This will be discussed later in greater detail.

It is possible to achieve very low local concentration of compound II by the slow addition of the same, and condensation of compound II according to

reaction (5)

$$n(CH_3)_2SiCl(OC_4H_9) \xrightarrow{\text{catalyst}} Cl\,(CH_3)_2SiO[(CH_3)_2SiO]_{n-2}-\underset{\displaystyle (CH_3)_2}{\overset{\displaystyle OC_4H_9}{\overset{|}{\underset{\|}{Si}}}} + \\ + (n-1)\,C_4H_9Cl \qquad (5)$$

does not occur. With increasing molecular weight this is of course more difficult to ensure and therefore shorter or longer chain molecules, respectively sequences are formed. In fact, this accompanying reaction does not essentially interfere with the synthesis of regular structured "star molecules", since the molecular weight of the former is considerably lower than that of the latter and a very effective separation can be achieved by subsequent fractionation.

In addition we were interested in the interfering effect of the side reactions on the heterofunctional condensation, namely such side reactions might limit the formation of molecules with regular structures. Under the given reaction conditions the interfering effects of two side reactions should be considered: a) the catalytic equilibration (scrambling reaction) [5, 6], b) the statistic rearrangement of the functional groups [7]. The experiments were concerned mainly with ascertaining the extent of these reactions.

Experimental

1. Effect of equilibration

So-called equilibration (scrambling) is a catalytic process leading to equilibrium molecular weight distribution by way of polymerization and depolymerization reactions, resulting in thermodynamical equilibrium. The catalysts are acids and bases, primarily Lewis acids and bases. Thus we must reckon with the equilibrating effect of the catalyst of heterofunctional condensation, which in the given case leads to the formation of high molecular weight compounds.

A) A mixture of 20 g octamethyl-cyclo-tetrasiloxane (D_4) and 0,2 g of $Fe_2(SO_4)_3 \cdot H_2O$ was refluxed for 6 hours at about 100°C. During this period an increase in the viscosity of the mixture could be observed. After 6 hours the product was dissolved in 50 ml of benzene, filtered and washed to iron-free. The distillation residue was 17.1 g (85.6%) of polymer with an average number-molecular weight of 1480 determined by means of the Hewlett-Packard VPO 301 A Vapour Pressure Osmometer.

B) 60 g D_4 and 0.6 g of $Fe_2(SO_4)_3 \cdot H_2O$ were dissolved in 50 ml of dehydrated benzene and refluxed as above. The product was filtered, washed to iron-free, dried and distilled. After these operations the quantity of polymer was only 1.3 g with a number-average molecular weight of 1023.

2. Statistical rearrangement (substituent exchange)

Since both substituent exchange and heterofunctional condensation proceed with the participation of silicon functional groups, substituent exchange — whenever it occurs — is always accompanied by condensation, thus unfortunately the former cannot be studied alone.

Substituent exchange for this case is illustrated by Eq. (6):

$$\equiv Si^{(1)}-X + \equiv Si^{(2)}-Y \xrightarrow{\text{catalyst}} \equiv Si^{(1)}-Y + \equiv Si^{(2)}-X \qquad (6)$$

The following experiments served to demonstrate this reaction.

A) 112 g of $(CH_3)_2SiCl(OC_2H_5)$ was boiled in an 80 cm long distillation column, packed with glass helices, without take off. Head temperature was 94°C, corresponding to the boiling point of the substance. After 6 hours boiling the head temperature dropped to 90°C, but after taking off some distillate the temperature rose again to 94°C. The quantity of the distillate was 1.6 g.

B) In 56 g of $(CH_3)_2SiCl(OC_2H_5)$ 0.56 g of the catalyst was dissolved, the mixture boiled in the distillation column of par. A) and 11.0 g of distillate was collected. The rest of the substance being a low volatility polymer its vapours did not reach the head of the column.

C) 0.56 g of the catalyst was dissolved in 56 g of $(CH_3)_2SiCl(OC_2H_5)$, the solution mixed with 50 ml of dehydrated benzene and the mixture treated in the distillation column as above. The yield was 10.42 g of distillate.

The compositions of the distillates were analysed by gas chromatography. Due to catalytic substituent exchange $(CH_3)_2SiCl_2$ was present in the distillate. The quantities of this compound for identical quantities (0.40 mol) of the starting material are shown in Table I. It should be noted that the starting substance contained no detectable amount of $(CH_3)_2SiCl_2$.

Table I

Sample	Distillate, ml	Solvent, ml (benzene)	Catalyst, g	Volatile fraction $(CH_3)_2SiCl_2$, %	Total quantity of *D* in sample, ml
A	0.8	—	—	13.4	0.2
B	11.0	—	0.56	24.8	2.7
C	16.2	25	0.56	10.4	1.7

D) 47.95 g of $(CH_3)_2SiCl_2$ and 55.20 g of $(CH_3)_2Si(OC_2H_5)_2$ were mixed with 46 ml of benzene and 1.03 g of catalyst was dissolved in the mixture. During the six hours refluxing ethylchloride evolved and heterofunctional condensation took place. Provided this is not accompanied by substituent exchange due to the nature of the reaction, beside chains terminated by functional groups only cyclic compounds with even numbers of silicon atoms in the ring should be present in the product. In fact gas chromatographic analysis of the volatile portion (9.38 g, contrary to 40.44 g of non-volatile residue) of the reaction product resulted the following figures (Table II).

Table II

D_4	D_5	D_6	D_7	Benzene
88.0%	11.0%	0.7%	trace	0.3%

E) An example of radical exchange as a side-reaction beside heterofunctional condensation is illustrated by the following experiment. Condensation-reaction can be performed according to Eq. (7):

$$(CH_3)_2SiCl_2 + 2(CH_3)_3SiOC_4H_9 \xrightarrow{\text{catalyst}} [(CH_3)_3SiO]_2 \cdot Si(CH_3)_2 + 2C_4H_9Cl \qquad (7)$$

Provided reaction (7) is not accompanied by radical exchange, condensation will lead to the single trimer-compound.

47.85 g of trimethyl-*t*-butoxysilane and 21.15 g of dimethyl-dichlorosilane were dissolved together with 0.7 g of catalyst in 21.0 ml of dehydrated benzene. The mixture was boiled in a flask provided with a Vigreaux fixture to which a Marcusson fixture was joined for the collection of the *t*-butylchloride, formed during the reaction. After the Marcusson fixture a reflux condenser with a $CaCl_2$-trap was applied. In its first phase the reaction was so strongly

exothermic that no heating was necessary. After 6 hours boiling the product was again isolated by distillation and the volatile portion subjected to gas chromatographic analysis. The yields are shown in Table III.

Table III

Volatile fractions		Polymer
$[(CH_3)_3Si]_2O$	$[(CH_3)_3SiO]_2Si(CH_3)_2$	
22.7%	6.9%	0.2%

3. Heterofunctional condensation

A) 1.1 g of catalyst was dissolved in 112 g of $(CH_3)_2SiCl(OC_2H_5)$, diluted with 50 ml of dehydrated benzene, refluxed and the evolved ethylchloride collected in a deep cooled receiver. By frequent weighing of the condensed reaction product the progress of heterofunctional condensation could be followed. The reaction rate was rather low already after two hours and after six hours no further reaction could be observed. To free the reaction mixture from the small quantity of chain-ending chlorine the product was mixed with ethanol, filtered and washed to iron-free. Distillation at 100 mm Hg and 150°C yielded volatile and polymeric fractions. The volatile fraction amounted to 26.4% of the total, its gas chromatographically established composition is shown in Table IV.

Table IV

D_4	D_5	D_6	Benzene
81.5%	13.4%	2.0%	0.5%

The number-average molecular weight of the polymeric fraction was 2600.

B) The procedure was similar to that described in par. A) with the difference that the reaction was carried out without solvent. No volatile fraction was obtained, the number-average molecular weight of the polymer was 3550.

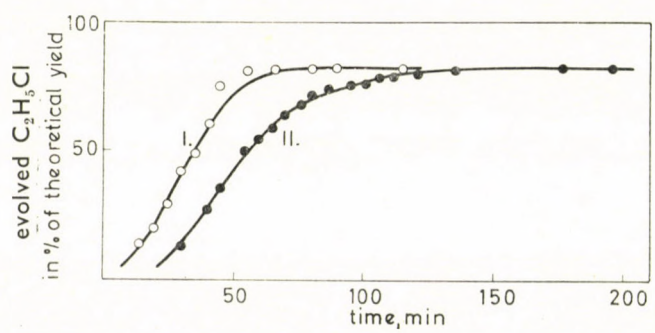

Fig. 1. Ordinate: evolved C_2H_5Cl in % of theoretical yield. Abscissa: time, min; Curve I: condensation without solvent; Curve II: condensation in the presence of solvent

It should be mentioned here that by prolonging polymerization at an appropriate temperature condensation in the absence of solvent yielded products of very high molecular weight.

Figure 1 shows the evolved ethylchloride [in experiments A) and B)] plotted against time.

C) Next we wished to investigate a very important problem from the aspect of the development of the regular structure, namely whether in the case of starting from a mixture of trifunctional and chain growth promoting difunctional monomers the three branches of the star molecule will grow simultaneously.

For this reason 110.15 g of dimethyl-2-chloroethoxy-chlorosilane and 37.74 g of methyltriethoxysilane were dissolved in 40 ml of dehydrated benzene. 1.5 g of catalyst was mixed to the mixture. In refluxing 85% of the theoretical quantity of ethylchloride was recovered which means that practically all three functional groups participated in the condensation reaction. It should however be mentioned that according to these experiments in the case of $Fe_2(SO_4)_3 \cdot H_2O$ catalyst the chloroethoxy group was found entirely inactive from the aspect of heterofunctional condensation.

D) Results similar to the above were obtained also with other functional groups.

80.2 g of dimethyl-*n*-butoxychlorosilane, 18.86 g of methyltriethoxysilane and 1.0 g of catalyst were dissolved in 18.6 ml of toluene and boiled in an 80 cm high distilling column packed with glass helices. The butylchloride formed in course of the reaction condensed in the cooler, while the ethylchloride passed into the deep cooled receiver where it liquified. The quantity of this ethylchloride amounted to 88% of the theoretical, which allows the conclusion that with good approximation in this case too the growth of the molecule proceeded in all three directions, though at the same time the chain also grew linearly, as indicated by the quantity of butylchoride. Thus this method led indeed to star molecules.

Discussion

Experiments concerning the side-reactions indicate that performing the condensation without a solvent both considerable equilibration and substituent exchange occur. Under these conditions heterofunctional condensation is not appropriate to furnish polymeric or oligomeric molecules with regular "tailored" structure. The experiments proved further that by the application of solvents, equilibration can be practically eliminated. Heterofunctional condensation will proceed in solvents too, though at a considerably lower rate and the maximum attainable molecular weight *i.e.* polymerization degree will also be considerably lower. In the case of star-molecule polymethylsiloxanes this limit molecular weight was found around 2500—3000 which could not be raised by the application of other solvents either.

A certain substituent exchange was observed with condensation processes in solvents too. The data in Table II permit the conclusion that as expected the progress of the reaction is concentration dependent. Beyond this qualitative finding the present experiments permit no further quantitative conclusions, since the exchange reaction is always accompanied by an intensive condensation process, but apparently in benzene solution too the exchange reaction limits the possibility of the synthesis of molecules with regular structures.

Change in the alkyl radical of the alkoxy group bound to silicon has a significant influence on condensation rate. Thus, while butoxy silane reacts already without catalyst with chlorosilanes and when heated methoxysilanes too may be condensed in the absence of catalysts, the ethoxysilanes will react only in the presence of catalysts. The reaction of chloroethoxysilanes indicated the loss of reactivity by the alkoxy group due to the presence of the highly

electronegative alkyl radical. The mechanism of condensation can be represented by the following scheme:

or with catalyst

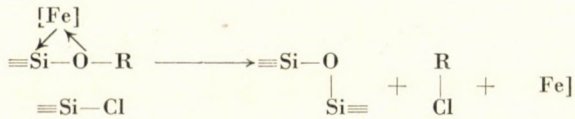

In the above equation [Fe] stands for an iron complex which will be studied more thoroughly in the future.

It is obvious that the prerequisite for the elimination of the alkyl halogenide is a bond rearrangement facilitated by the above-mentioned electron displacement. Increased electronegativity of the alkyl group causes, on the other hand, a reversed electron displacement inhibiting thereby the condensation process.

The high catalytic activity of the transition metal compounds refers not only to a simple Lewis acid—base interaction of the oxygen — bound to the silicon — and the metal ion, but also to the enhancement of the σ-bond in Fe—O probably through the π-acceptor property of the empty *d*-orbital of the silicon atom. To support this assumption it is worth mentioning that contrary to literature data strong Lewis acids as *e.g.* $AlCl_3$ or boron halogenides have practically no catalytic effect on heterofunctional condensation.

REFERENCES

1. Servais, P. C.: US Patent 2,485,928.
2. Philip, C. S.: French Patent 1,037,111.
3. Andrianov, K. A., Zavin, B. G., Persova, N. V.: Vysokomol. Soed. **10,** 46 (1968).
4. Andrianov, K. A., Ganina, T. N., Sokolov, N. N.: Zh. Obsch. Khim. **26,** 1691 (1956).
5. Chevalier, P. J.: Swiss Patent 282,740.
6. Wright, J. C. E.: US Patent 2,389,477.
7. Kumada, M., Tamara, K. J.: Chem. Soc. Japan **55,** 31 (1952).

Tamás Székely
Péter Rösner
Pál Gömöry

Budapest VIII., Múzeum krt. 6/8

Acta Chimica Academiae Scientiarum Hungaricae, Tomus 61 (3), pp. 241—255 (1969)

DIE UNTERSUCHUNG VON BORIDEN, CARBIDEN UND NITRIDEN AUF IHRE EIGNUNG ALS INDIKATORELEKTRODE FÜR POTENTIOMETRISCHE MESSUNGEN

E. PUNGOR und A. WESER*

(Universität für die Chemische Industrie, Lehrstuhl für Analytische Chemie, Veszprém)

Eingegangen am 17. August 1968

Bei der Untersuchung von Carbiden, Boriden und Nitriden der Übergangsmetalle auf ihre Eignung als Indikatorelektroden in sauren Hexacyanoferratlösungen fanden wir einen Zusammenhang zwischen der Kristallstruktur des Indikatorelektrodenmaterials und seiner Eignung als Indikatorelektrode.

Potentiometrische Messungen in Redoxsystemen ergeben Potentiale, die von dem untersuchten System und unter Umständen von dem Elektrodenmaterial abhängig sind. Bei solchen Messungen wurden vor allem Gold-, Platin- und Platinrhodiumelektroden verwendet.

Besonders gern werden Platinelektroden sowohl für Redoxmessungen als auch für pH-Titrationen eingesetzt, die auf Redoxvorgänge zurückzuführen sind, wie aus den Zusammenstellungen hervorgeht [4, 8, 27, 43, 44, 50, 51, 53]. Platinindikatorelektroden eignen sich für die gleichen Verfahren in wasserfreien Lösungsmitteln [18, 45].

Der Anwendungsbereich der Platinindikatorelektrode wird durch die Bildung von Oberflächenoxydschichten festgelegt, deren Bildung von LINGANE [2, 32], KOLTHOFF [28] und ROSS [54] gezeigt wurde. Ähnliche Oxydschichten fanden LEE, ADAMS und BRICKER [30] an Gold, Platin und Palladium, deren Potentiale bei den den Oxyden entsprechenden Werten sich einstellen.

Goldelektroden fanden eine ähnliche breite Anwendung wie Platinelektroden [4, 8, 27]. REICHERT, MCNEIGHT und RUDEL fanden, daß Goldelektroden bei der potentiometrischen Titration von Wasserstoffperoxyd Platinelektroden überlegen sind, da Gold die Zersetzung von Wasserstoffperoxyd weniger stark katalysiert [49] als Platin.

Platinrhodiumlegierungen besitzen ähnliche Eigenschaften wie reine Platinelektroden, was von MALMSTADT und FETT gezeigt wurde [33].

Es wurde berichtet, daß mit Zinndioxyd [58] und mit Titanoxydschichten [12] überzogene Indikatorelektroden auf Redoxsysteme ansprechen. Das gleiche Verhalten wurde für Indikatorelektroden aus PbO_2 [20] und W_2O_5 [57]

* Aspirant von der Bergakademie Freiberg, DDR, Institut für anorganische und analytische Chemie.

gefunden. Nach MAUSER und NICKEL soll sich das Redoxpotential von Phenol-Phenoxyl-Systemen an Platinelektroden nicht, wohl aber an Sinterborcarbidelektroden reversibel einstellen [34].

Bei den oben angeführten Edelmetallen wird das Verhalten als Indikatorelektrode weitgehend von den gebildeten Oberflächenoxyden bestimmt. MÜLLER und ADAMS fanden im Borcarbid ein Elektrodenmaterial, an dem keine Oberflächenoxyde gebildet werden sollen und obige Erscheinungen entfallen müßten [40, 41, 42]. Zu den gleichen Ergebnissen gelangten auch andere Autoren [39, 55]. Neueste Untersuchungen von Borcarbidelektroden weisen aber auf die Existenz von Oberflächenoxyden hin [17].

Titandiborid, Zirkondiborid und Molybdändisilicid wurden von MÜLLER und OLSON wegen ihrer hohen chemischen Beständigkeit als Elektroden für voltametrische Bestimmungen untersucht [42]. Sie erwiesen sich aber als der Borcarbidelektrode unterlegen. Dieselben Stoffe prüften MAZZA und TRASSATTI mit dem gleichen Ergebnis [35]. Weiterhin untersuchten sie das Verhalten von Wolframcarbid, Titancarbid und Titannitrid mit Hilfe von Messungen der Austauschstromdichte in verschiedenen Redoxsystemen unterschiedlicher Wasserstoffionenkonzentration. Wolframcarbid, Borcarbid und Titannitrid erwiesen sich nach MAZZA und TRASSATTI als Elektroden für Redoxsysteme gleichwertig, wobei Wolframcarbid am besten für saure und Titannitrid für alkalische Lösungen geeignet ist.

Titancarbid und Tantalcarbid zeigten weniger befriedigende Ergebnisse.

Siliciumcarbid wurde auch als Indikatorelektrode bei potentiometrischen Titrationen vorgeschlagen [22, 23, 24]. Da Siliciumcarbid in verschiedenen Modifikationen auftritt und schon durch sehr geringe Verunreinigungen stark in seinen elektrischen Eigenschaften verändert wird, finden sich teilweise widersprechende Veröffentlichungen, in denen Siliciumcarbid einmal als Indikatorelektrode oder auch als Bezugselektrode vorgeschlagen wird [1, 5, 6, 7, 19, 21, 31].

GINNER und SWETTE fanden Titannitridelektroden in alkalischen Lösungen besonders zur Sauerstoffreduktion geeignet [15].

Es hat nicht an Versuchen gefehlt, die teuren Edelmetallelektroden durch andere Materialien zu ersetzen. Als günstigstes Elektrodenmaterial bewährte sich Graphit, der von vielen Autoren als Indikatorelektrode bei potentiometrischen Redox- und pH-Titrationen vorgeschlagen wurde [9, 10, 11, 13, 14, 38]. Die günstigen Eigenschaften von pyrolytischem Graphit als Indikatorelektroden wurden festgestellt [56]. Die aus pyrolytischem Graphit gefertigten Elektroden sind dicht und gasundurchlässig und auch für nichtwäßrige Lösungsmittel und Salzschmelzen geeignet, wie von LAITINEN gezeigt wurde [29]. Die verschiedenen Arten der Graphitelektrode (mit Wachs imprägnierte Graphitelektroden und pyrolytische Graphitelektroden), beschrieben ELVING, FRIED und TURNER [11]. Ein besonderer Vorteil von Graphitindikatorelektroden ist, daß

leicht eine neue Oberfläche erzeugt werden kann, die reproduzierbare Eigenschaften besitzt.

Wie aus der Literatur hervorgeht, eigen sich nicht alle Stoffe als Elektrodenmaterial, auch wenn sie sich chemisch inert verhalten. Um nähere Aussagen über die Eignung von Verbindungen als Redoxindikatorelektroden machen zu können und eventuelle Beziehungen zwischen dieser Eigenschaft mit der Kristallstruktur zu zeigen, untersuchten wir eine Reihe von Boriden, Carbiden, Nitriden und anderen Verbindungen der Übergangsmetalle. Es trat die Frage auf, in welcher Form wir die zu untersuchenden Stoffe einsetzen sollten, um reproduzierbare Werte zu erhalten. Wir stellten in der Hauptsache heterogene Membranelektroden aus den zu untersuchenden Stoffen mit Silikonkautschuk her, da auf diesem Gebiet mit ionenselektiven Membranelektroden beste Erfahrungen vorliegen [46, 47, 48]. Von einigen Verbindungen wurden auch homogene Elektroden durch Schmelzen oder Sintern hergestellt.

Experimentelles

1. Angewandte Elektroden

a) *Carbidelektroden*

Tabelle I gibt Auskunft über die von uns gefertigten Carbidelektroden. Der Widerstand der Elektroden wurde mit einer Brückenmethode gemessen. Die manchmal bei ein und demselben Stoff variierenden Werte hängen von dem Verhältnis Silikonkautschuk zu Carbidanteli ab. Das Verhältnis von Carbid zu Silikonkautschuk verhielt sich etwa wie 4 : 1.

Tabelle I

Physikalische Eigenschaften und Herstellung von Carbid-Elektroden

Nr.	Zeichen	Widerstand 10^x Ohm	Phasen	Gittertyp des Hauptbestandteils	Herstellungsart der Verbindung	Art der Elektrode
1.	Pt	0,5	Pt	AI	—	H
2.	C	0,5	C		I.	S,H
3.	B_4C	5—5,2	B_4C, C	B_4C	II.	S
4.	SiC	3			III.	S,H
5.	TiC 1	0,5	TiC, wenig C	NaCl	1	S
6.	TiC 2	0,5	TiC, wenig C	NaCl	1	S
7.	TiC 3	0,5	TiC	NaCl	1	S
8.	TiC 7	0,5	TiC, viel C	NaCl	1	S
9.	ZrC 1	1,5	ZrC	NaCl	2	S
10.	VC	5—6	VC	NaCl	1	S
11.	NbC 6	1—3	NbC + Oxyde	NaCl	1	S

Tabelle I. Fortsetzung

Nr.	Zeichen	Widerstand 10^x Ohm	Phasen	Gittertyp des Hauptbestandteils	Herstellungsart der Verbindung	Art der Elektrode
12.	TaC 1	4—5	TaC, wenig WC	NaCl	IV.	S
13.	Cr_7C_3 1	7—8	Cr_7C_3	Cr_7C_3	2	S
14.	Cr_3C_2 1	7—8	Cr_3C_2	Cr_3C_2	2	S
15.	Mo_2C 3	7—8	Mo_2C, MoC	Mo_2C	2	S
16.	MoC 1	0,5	Mo_2C, MoC	MoC	2	S,H
17.	W_2C 1	2	W_2C, wenig C	Mo_2C	2	S
18.	W_2C 2	1—1.5	W_2C	Mo_2C	2	S
19.	WC 1	7—8	WC	MoC	IV.	S
20.	Fe_3C	3		Fe_3C	3	S
21.	$WTiC_2$ 1	4	$WTiC_2$	NaCl	IV.	S
22.	$WTiC_2$ 2	3	$WTiC_2$	NaCl	IV.	S
23.	$WTiC_2$ 3	4—5	$WTiC_2$	NaCl	IV.	S

I. Wir verwendeten spektralreinen Graphit.
II. Das verwendete Borcarbid stammte vom Schleifmittelwerk Salgótarján.
III. Gleiche Herkunft wie Borcarbid.
IV. Die Proben wurden vom Hartmetallwerk Immebort DDR zur Verfügung gestellt.

In der 1. Spalte ist die laufende Nummer der Elektrode enthalten.
In der 2. Spalte folgt die Bezeichnung der Elektrode.
In der 3. Spalte wird der Widerstand der fertigen Elektroden angegeben.
In der 4. Spalte führen wir die von uns mit Hilfe der Röntgenanalyse gefundenen und bestimmten Phasen des in die Membran eingebauten Materials an.
In der 5. Spalte wird der Gittertyp des Hauptbestandteils des eingebauten Materials vermerkt.
In der 6. Spalte verweisen wir auf die Herstellung der betreffenden Verbindung, die im Anhang beschrieben wird.
In der 7. Spalte geben wir die Art der Elektrode an, da von einigen nicht nur mit Silikonkautschuk gebundene Elektroden (S), sondern auch homogene Elektroden (H) aus dem betreffenden Material gefertigt wurden.

Tabelle II

Physikalische Eigenschaften und Herstellung von Nitridelektroden

Nr.	Zeichen	Widerstand 10^x Ohm	Phasen	Gittertyp des Hauptbestandteils	Herstellungsart der Verbindung	Art der Elektrode
1.	TiN 3	4	TiO_2 (50%) TiN (50%)		5a(700°C)	S
2.	TiN 4	5	TiO_2 (85%) TiN (15%)		5a(700°C)	S
3.	TiN 17	3	TiN	NaCl	5a(3×1000°C)	S

Tabelle II. Fortsetzung.

Nr.	Zeichen	Widerstand 10x Ohm	Phasen	Gittertyp des Hauptbestandteils	Herstellungsart der Verbindung	Art der Elektrode
4.	TiN 19	3	TiN	NaCl	4	S,H
5.	ZrN 3	2	ZrO_2, ZrH, ZrH_2		5a(600°C)	S
6.	ZrN 8	3,2	ZrN, ZrO_2 10%		4	S
7.	ZrN 10	4—5	ZrN, ZrO_2 5%	NaCl	4	S,H
8.	VN 7	5—6	VN	NaCl	6(900°C)	S
9.	VN 12	1—3	VN, V_2O_3		6,8	H
10.	VN 13	1—3	VN	NaCl	6.8	H
11.	CrN 11	3—5	CrN	NaCl	5a	S
12.	CrN 16	3—5	Cr_2N, CrN		6,8	H
13.	CrN 17	3—5	Cr_2N, Cr_2O_3		6,8	H
14.	CrN 18	3—5	Cr_2N, $Cr_2O_3 \sim 5\%$		5a	H

b) *Nitridelektroden*
Über Eigenschaften und Herstellung der Nitridelektroden gibt Tabelle II Auskunft.

c) *Boridelektroden*
Über Eigenschaften und Herstellung der Boridelektroden gibt Tabelle III Auskunft.

Tabelle III

Physikalische Eigenschaften und Herstellung von Boridelektroden

Nr.	Zeichen	Widerstand 10^x Ohm	Phasen	Gittertyp des Hauptbestandteils	Herstellungsart der Verbindung	Art der Elektrode
1.	TiB_2 6	3—4	TiB_2	AlB_2	2	S,H
2.	TiB_2 18	3—4	TiB_2	AlB_2	2	H
3.	Cr_2B	0,5	Cr_2B + unbekannte Phase		2	S,H
4.	CrB	0,5	Cr_2B + unbekannte Phase		2	S,H
5.	CrB_2	0,5	CrB	TaB	2	S,H
6.	MoB	0,5	Gemische von		2	S,H
7.	Mo_2B	0,5			2	S,H
8.	Mo_2B_5	0,5	Mo_2B, Mo		2	S,H
9.	MoB_2	0,5	MoB		2	S,H
10.	MgB_4	8	MgO versch. Boride		2	H

d) *Weitere von uns untersuchte Elektrodenmaterialien* sind in Tabelle IV aufgeführt.

Tabelle IV

Physikalische Eigenschaften und Herstellung einiger Redoxelektroden

Nr.	Zeichen	Widerstand 10^x Ohm	Phasen	Gittertyp des Hauptbestandteils	Herstellungsart der Verbindung	Art der Elektrode
1.	Ti_2BN 7	3—4	Ti_2BN, wenig TiB_2	NaCl	9	S,H
2.	Ti_2BN 16	3—4	Ti_2BN, wenig TiB_2	NaCl	9	S,H
3.	Ti_2B_2N	3	TiN, TiB_2	TiSi	9	S,H
4.	TiSi	3	TiSi	TiSi	2	H
5.	Zr_2BN	3—4	Zr, N, ZrB_2		9	S,H
6.	Cr_3Si	2—3	Cr_3Si	β-W	2	H
7.	Mn_3Si	4	Mn_3Si	α-Fe	2	H
8.	$MoSi_2$	2	$MoSi_2$	$MoSi_2$	2	H
9.	MoS_2	2	MoS_2	MoS_2	2	S

2. Vorbereitung der Elektroden

a) *Mit Silikonkautschuk gebundene Elektroden*

Das Reaktionsgut wurde mit einer Kugelmühle (Fritsch Pulverisette) zu einem feinen Pulver entsprechend den Anforderungen der Röntgenanalyse vermahlen. Dieses Pulver vermischten wir mit einem in der Kälte auspolymerisierenden Silikonkautschukmonomeren und dem entsprechenden Katalysator. Aus der noch plastischen Masse wurden Folien gefertigt, aus denen nach der Erhärtung Scheibchen von 3 mm ∅ geschnitten wurden. Diese Scheibchen kitteten wir mit einem Silikongummikleber auf ein Glasrohr, welches einige Tropfen Quecksilber und einen eingekitteten Kupferdraht zum Kontaktübertrag besaß. Vor und nach den Messungen wurden die so gefertigten Elektroden mit dest. Wasser abgespült.

b) *Homogene Elektroden*

Bei der Herstellung dieser Elektroden kitteten wir ein Bruchstück von dem Sinter- oder Schmelzkörper analog auf ein mit einer Ableitung versehenes Glasrohr. Die freistehende Oberfläche der Elektrode wurde mit Borcarbidpulver angeschliffen und poliert.

3. Benutzte Meßkette

Bei allen Messungen verwendeten wir eine gesättigte Kalomelelektrode als Referenzelektrode, die über einen mit Kaliumchlorid gefüllten Stromschlüssel in das Meßgut eintauchte. Die Messungen wurden unter Argon als Schutzgas ausgeführt.

4. Meßgeräte

Die Potentiale maßen wir anfangs mit zwei verschiedenen Geräten, um apparativen Einfluß auszuschalten. Wir verwendeten das ungarische Modell RADELKIS OP-203 und ein Seibold pH-Meter. Letzteres bewährte sich bei Elektrodenwiderständen von mehr als 10 MΩ am besten. Die Röntgenanalysen führten wir an dem Philips-Goniometer aus.

5. Messungen im Hexacyanoferrat(II)—(III)-System

Um unsere Elektroden zu prüfen, wählten wir das Hexacyanoferrat(II)—(III)-System. Dieses Redoxpaar steht im reversiblen Gleichgewicht und gibt an Platin- oder Graphitelektroden reproduzierbare Potentiale. Verschiedene Störungen des Gleichgewichts (Fremdsalzzusätze, pH-Änderungen) beeinflussen das Redoxpotential in reproduzierbarer Weise [25, 26]. Der Grundelektrolyt war 0,05 *N* an Schwefelsäure und immer 5×10^{-3} *N* an $K_3Fe(CN)_6$. Die Konzentration des $K_4Fe(CN)_6$ wurde von 5×10^{-2} bis 5×10^{-4} *N* variiert. Für das Hexacyanoferrat-System wird ein Formalpotential von +0.69 V in 1 *f* H_2SO_4 angegeben [16]. Das Formalpotential in neutraler Lösung liegt bei +0.36 V.

Die mit Platin- oder Graphitelektroden gemessenen und übereinstimmenden Potentiale betrachteten wir als die reversiblen Potentiale und bewerteten nach ihnen das Verhalten der übrigen Elektrodenmaterialien. Die Meßergebnisse sowie die zu Potentialeinstellung erforderlichen Zeiten sind in der Tabelle V angegeben.

Tabelle V

Gemessene Redoxpotentiale in $K_3Fe(CN)_6$—$K_4Fe(CN)_6$-Lösungen in 0,05 N H_2SO_4

Nr.	Zeichen	Einstellzeit des Potentials	5×10^{-3} 5×10^{-2} 5×10^{-2}	Elektrolytzusammensetzung		
				5×10^{-3} 5×10^{-3} 5×10^{-2}	5×10^{-3} 5×10^{-4} 5×10^{-2}	*N* $K_3Fe(CN)_6$ *N* $K_4Fe(CN)_6$ *N* H_2SO_4
1.	Pt	1—2 sec	189±1	300±1	378±1	mV
2.	C	1—2 sec	189±1	300±1	378±1	mV
3.	B_4C	20—60 sec	191±1	302±1	378±2	mV
4.	SiC	10—15 min	189±2	300±2	378±3	mV
5.	TiC 1	1—2 sec	189±1	300±2	378±1	mV
6.	TiC 2	1—2 sec	189±1	300±1	378±1	mV
7.	TiC 3	1—2 sec	189±1	300±1	378±1	mV
8.	TiC 7	1—2 sec	189±1	300±1	378±1	mV
9.	ZrC	2—5 sec	189±1	300±1	300±1	mV
10.	VC			keine Abhängigkeit		
11.	NbC 6	2—5 sec	188±2	300±2	377±2	mV
12.	TaC 1	2—5 sec	189±2	300±2	375±2	mV
13.	Cr_7C_3 1	2—5 sec	63±5	75±5	148±7	mV
14.	Cr_3C_2 1	2—5 sec	128±5	165±5	210±8	mV
15.	Mo_2C 3			keine Abhängigkeit		
16.	MoC 1	2—5 sec	185±4	296±5	350±5	mV
17.	W_2C 1	1—2 sec	189±1	296±2	378±2	mV
18.	W_2C 2	1—2 sec	189±1	308±2	378±1	mV
19.	WC			keine Abhängigkeit		
20.	Fe_3C	2—5 sec		Siehe Text		
21.	$WTiC_2$ 1	1—2 sec	189±1	300±1	376±1	mV
22.	$WTiC_2$ 2	1—2 sec	189±1	300±1	378±1	mV
23.	$WTiC_2$ 3	1—2 sec	185±1	300±1	378±1	mV
24.	TiN 3			keine Abhängigkeit		
25.	TiN 4			keine Abhängigkeit		

Table V. Fortsetzung.

Nr.	Zeichen	Einstellzeit des Potentials	5×10^{-3} 5×10^{-2} 5×10^{-2}	Elektrolytzusammensetzung		
				5×10^{-3} 5×10^{-3} 5×10^{-2}	5×10^{-3} 5×10^{-4} 5×10^{-2}	N $K_3Fe(CN)_6$ N $K_4Fe(CN)_6$ N H_2SO_4
26.	TiN 17	5—10 sec	176±5	280±5	315±10	mV
27.	TiN 19	5—10 sec	177±5	283±5	322±10	mV
28.	ZrN 3			keine Abhängigkeit		
29.	ZrN 8			keine Abhängigkeit		
30.	ZrN 10	2—5 sec	188±4	298±5	370±8	mV
31.	VN 7	1—2 sec	203±4	299±4	379±5	mV
32.	VN 12	1—2 sec	189±1	300±1	378±2	mV
33.	VN 13	1—2 sec	189±1	300±1	378±2	mV
34.	CrN 11	1—2 sec	189±1	300±1	378±1	mV
35.	CrN 16	1—2 sec	185±2	299±2	377±2	mV
36.	CrN 17	1—2 sec	189±1	300±1	379±2	mV
37.	CrN 18	1—2 sec	183±3	297±2	370±2	mV
38.	TiB_2 6			keine Abhängigkeit		
39.	TiB_2 18	2—5 sec	188±3	299±2	378±3	mV
40.	Cr-Boride			keine Abhängigkeit		
41.	Mo-Boride			keine Abhängigkeit		
42.	MgB_4	2—5 sec	159±5	235±5	280±5	mV
43.	Ti_2BN 7	1—2 sec	189±1	300±1	378±1	mV
44.	Ti_2BN 16	1—2 sec	189±1	300±1	378±1	mV
45.	Ti_2B_2N	10—20 sec	150±15	282±15	310±20	mV
46.	Zr_2BN	10—20 sec	181±2	285±10	stark streuend	
47.	TiSi	10—20 sec	181±2	285±4	379±5	mV
48.	Cr_3Si	2—5 sec	189±2	302±3	381±4	mV
49.	Mn_3Si			keine Abhängigkeit		
50.	MoS_2			keine Abhängigkeit		
51.	$MoSi_2$	1—2 sec	185±2	300±2	370±2	mV

Alle Potentiale wurden gegen die ges. Kalomelelektrode bei 25°C gemessen.

6. Ergebnisse und Schlußfolgerungen

a) Carbide

Wir bewerteten die Elektroden nach zwei Kriterien, nach dem Potential im Vergleich zur Platinelektrode und der zur Potentialeinstellung erforderlichen Zeit. Wir stellten fest, daß ein Teil der Elektroden wie Edelmetallelektroden reversibel auf das Redoxsystem anspricht.

Geeignete Indikatorelektroden

C, TiC, TiC+C, ZrC, $WTiC_2$, W_2C, Fe_3C, NbC und TaC. Interessant ist das Verhalten von Fe_3C. Diese Elektroden zeigen unmittelbar nach dem Eintauchen in das Meßgut das gleiche Potential wie die Platinelektrode, welches sich aber dann bald verändert. Wir führen dies auf eine chemische Reaktion mit der Lösung zurück, da sich Fe_3C in Schwefelsäure leicht auflöst. Wir fanden noch eine Anzahl von Stoffen, an denen das theoretische Potential nur langsam erreicht wird. Dieses Verhalten weist darauf hin, daß sich das Gleichgewicht an der Elektrodenoberfläche nur langsam einstellt, da wir diese Erscheinung auch an Elektroden mit einem Widerstand von weniger als 100 K Ohm beobachten konnten.

Zu dieser Gruppe zählen auch Stoffe, die das theoretische Potential nicht erreichen, wohl aber auf das Redoxsystem ansprechen. Derartige Carbide sind: SiC, B_4C, MoC und Chromcarbide.

Ungeeignete Carbide

WC, VC, Mo_2C, Cr_7C_3, Cr_3C_2 und $Cr_{23}C_6$.

b) Nitride

Mit den Nitriden der Übergangsmetalle stellten wir analoge Untersuchungen an. Wir können auch diese in zwei entsprechende Gruppen einteilen.

Geeignete Indikatorelektroden

VN, CrN

Ungeeignete Indikatorelektroden

ZiN, ZrN

c) Boride

Die große Ähnlichkeit zwischen Carbiden, Nitriden und Boriden der Übergangsmetalle veranlaßte uns, auch diese Stoffklasse zu untersuchen, weil einige Veröffentlichungen über das Verhalten dieser Boride bereits vorliegen. Entgegen den Erwartungen zeigten die meisten der untersuchten Boride keine Eignung als Indikatorelektrode für unser Redoxsystem. Im allgemeinen traten schlecht reproduzierbare negative Potentiale auf. Folgende Boride verwendeten wir bei unseren Messungen: TiB_2, Cr_2B, CrB, Mo_2B, MoB und MgB_4. Elektroden aus TiB_2 folgten zwar dem Potentialgang des Redoxsystems, die Potentiale stellten sich jedoch nur langsam und mit nicht allzu großer Genauigkeit ein.

Von den anderen Boriden sprach nur das MgB_4 auf das Redoxsystem an, erreichte aber nicht die Potentiale der Platinelektrode.

d) Silicide und gemischte Verbindungen

Neben den aufgeführten Carbiden, Nitriden und Boriden gibt es eine Reihe chemisch verwandter Stoffe mit ähnlichen Strukturen und großer Beständigkeit gegen viele Reagenzien.

Geeignete Indikatorelektroden

Ti_2BN, $MoSi_2$, Cr_3Si, TiSi

Ungeeignete Indikatorelektroden

Ti_2B_2N, Te, MoS_2, Mn_3Si.

Bei Folgerungen der Übersicht dieser Verbindungen scheint sich ein Zusammenhang zwischen der Kristallstruktur und der Eignung als Indikatorelektrode zu ergeben. Der größte Teil der guten Indikatorelektroden kristallisiert in der kubisch-flächenzentrierten Steinsalzstruktur.

Eine ganz ähnliche kubische Struktur hoher Symmetrie finden wir bei den als klassische Elektrodenmaterialien bekannten Metallen Gold, Silber, Palladium und Platin.

Es ist auffallend, daß demgegenüber die chemisch sehr ähnlichen Verbindungen, wie die Boride und Silicide, im allgemeinen inaktiv sind. Sie kristallisieren alle mit Strukturen niederer Symmetrie.

Die Bedeutung der Kristallstruktur konnten wir an einem Mischkristall aus Titannitrid und Titanmonoborid zeigen. Da TiB, welches ebenfalls zum Steinsalztyp gehört, bei Raumtemperatur instabil ist und von uns nicht hergestellt werden konnte, versuchten wir einen Mischkristall der Formel Ti_2NB aus Titan, Bor und Titannitrid herzustellen. Im Anhang sind die Röntgenaufnahmen von einigen reinen Titanboridproben, der Verbindung Ti_2BN und Ti_2B_2-Pulver hergestellt. Die Röntgenaufnahmen zeigen deutlich die Steinsalzstruktur von Ti_2BN. Das Gemisch aus TiN und TiB_2 zeigte auch nach mehrmaligem Glühen in Argon die Linien von TiN und TiB_2 in unveränderter Intensität. Es wurde noch eine Aufnahme von $WTiC_2$ angeführt, welches ebenfalls Steinsalzstruktur besitzt und in seiner Aktivität dem Titancarbid überlegen ist. Reines WC kristallisiert im hexagonalen MoC-Typ und eignet sich nicht als Indikatorelektrode im Hexacyanoferrat-System.

*

An dieser Stelle sei den Herrn Prof. Dr. E. Nemecz und K. Nagy unser Dank für die Unterstützung bei der Anfertigung der Röntgenaufnahmen und der präparativen Arbeit ausgesprochen.

Anhang

Verfahren 1. Das entsprechende Metalloxyd wird mit Zuckerkohle verpreßt und bei 1200°C im Argonstrom 12 Stunden geglüht. Die Preßlinge werden gemahlen und erneut dem gleichen Glühprozeß unterworfen. Zur vollständigen Homogenisierung wird das gleiche verfahren noch ein drittes Mal durchgeführt. Der Ansatz kann so variiert werden, damit man Produkte mit verschiedenem Kohlenstoffgehalt gewinnt.

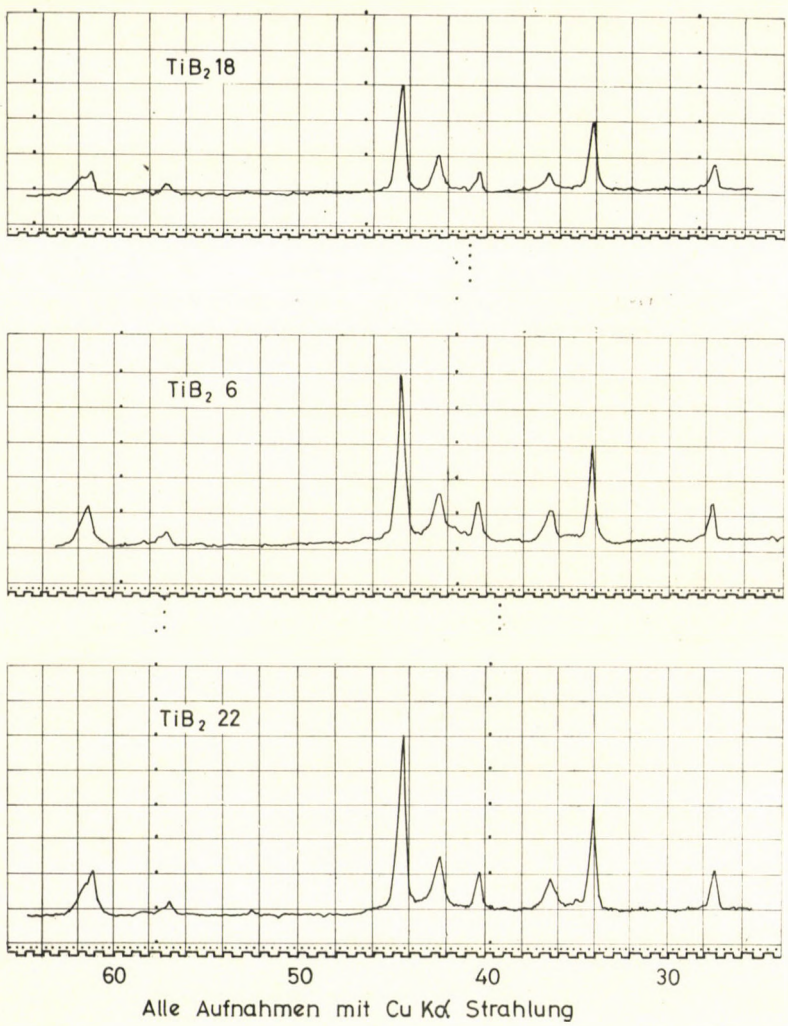

Verfahren 2. Die Elemente werden miteinander vermahlen und zu Formlingen verpreßt, die bei 1200°C 12 Stunden in Argon oder Wasserstoff geglüht werden. Um völlig homogene Proben zu erhalten, muß noch zweimal pulverisiert und geglüht werden.

Verfahren 3. Ein Überschuß der Metallkomponente wird mit dem Nichtmetall zu Formlingen verpreßt und bei 1000°C 12 Stunden im Argonstrom gesintert. Das Reaktionsprodukt wird mit verdünnter Essigsäure gelöst, um den Überschuß der Metallkomponente zu entfernen.

Verfahren 4. Das Metall wird 12 Stunden im Stickstoffstrom bei 1200°C geglüht, wobei es spröde wird und sich dann mahlen läßt. Das Mahlgut wird in Pyrolanschiffchen erneut bei 1200°C im Stickstoffstrom geglüht, gemahlen und noch einmal 12 Stunden bei 1200°C im Stickstoffstrom gehalten.

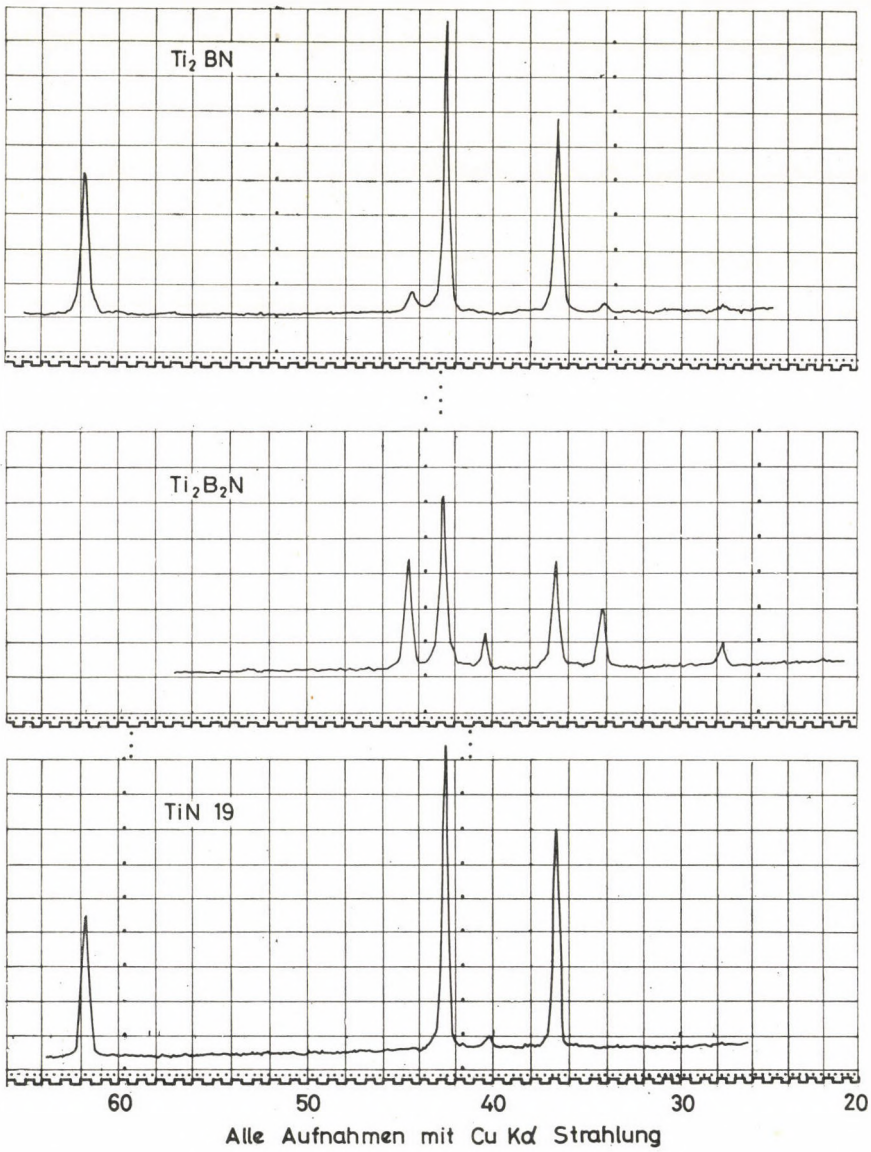

Verfahren 5. Das Metall (5a) oder das Oxyd (5b) werden bei der angegebenen Temperatur im Ammoniakstrom geglüht.

Verfahren 6. Die Ammoniumfluoride werden im Ammoniakstrom bei der angegebenen Temperatur pyrolysiert.

Verfahren 7. Das Metalloxyd wird mit Magnesiumpulver im Stickstoffstrom reduziert. Das Reaktionsprodukt wird mit NH_4Cl-Lösung ausgelaugt. Dieses Verfahren wird noch zweimal ausgeführt.

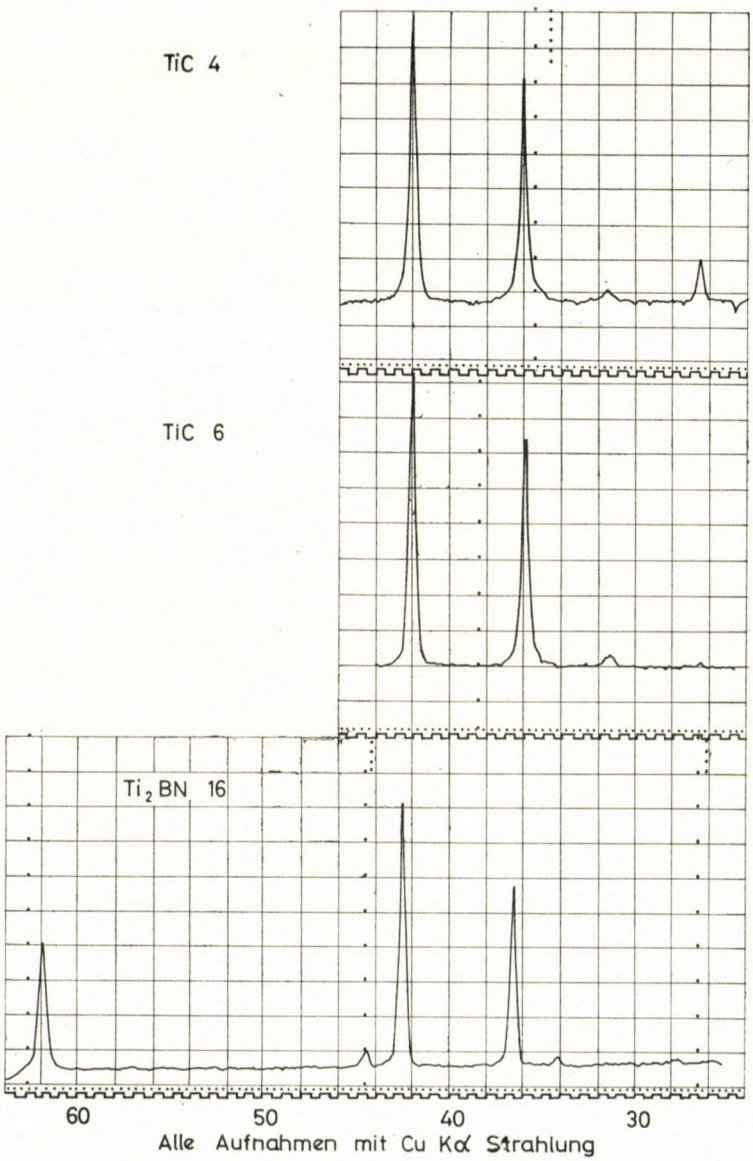

Verfahren 8. Die feinvermahlene Probe wird verpreßt und bei 1200°C 12 Stunden in Argon homogenisiert.

Verfahren 9. Ti_2BN und Zr_2BN wurden aus den entsprechenden Nitriden, Metallen und Bor hergestellt nach Verfahren 2.

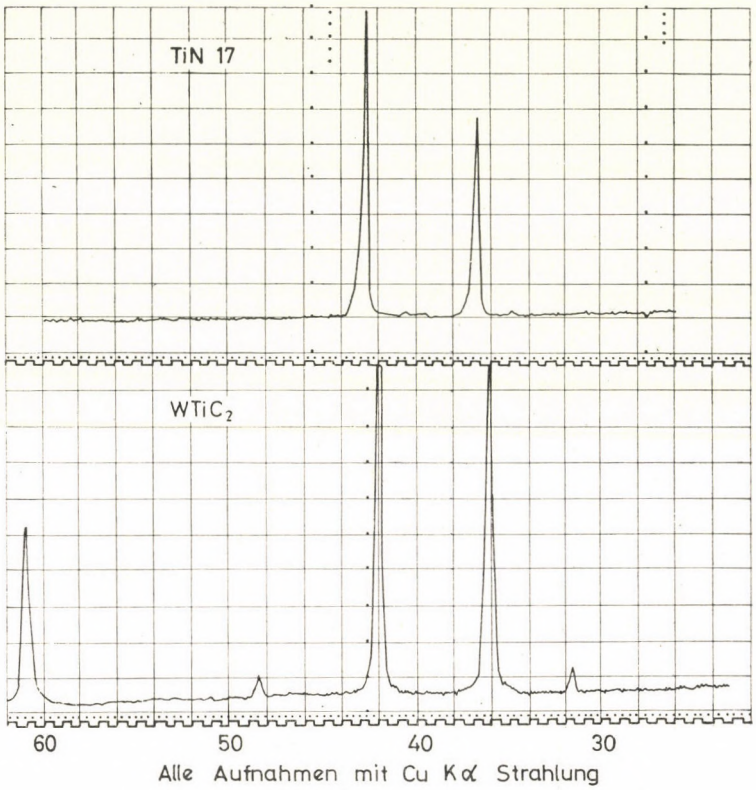

Alle Aufnahmen mit Cu Kα Strahlung

LITERATUR

1. Anastasiu, J. A., Velculescu, A. J.: Z. anal. Chem. **85,** 120 (1931).
2. Anson, F., Lingane, J. J.: J. Am. Chem. Soc. **79,** 4961 (1957).
3. Beilby, A. L., Brooks, W., Lawrence, G. L.: Anal. Chem. **36,** 22 (1964).
4. Berka, A., Vulterin, I., Zyka, J.: Maßanalytische Oxydations- und Redoxmethoden. Akad. Verlagsgesellschaft Geest und Portig K. G., Leipzig, 1964.
5. Boltunov, Iu. A., Isakova, K. K.: Zurnal obsch. Chim. **7,** 2838 (1937).
6. Boltunov, Iu. A., Kozmina, Z. P.: Zurnal obscij Chim. **7,** 2899 (1937).
7. Chlopin, N. Ja.: Zavodskaja Labor **6,** 548 (1937).
8. Cihalik, J.: Potentiometrie. Verlag Tschech. Akad. der Wissenschaften, Prag 1961.
9. Elving, P. J. Smith, D. L.: Anal. Chem. **32,** 1849 (1960).
10. Elving, P. J., Smith, D. L.: Analyt. Chem. int. Sympos., Birmingham, **1962, 1963,** 204.
11. Elving, P. J., Fried, I., Turner, W. R.: C 00—1148—84 Michigan Univ., Ann. Arbor, Apr. 28, 1964.
12. Flis, I. J., Woroblew, I. M.: Betriebs-Labor. UdSSR **29,** 538 (1963).
13. Gaylor, V. F., Conrad, A. L., Elving, P. L.: Anal. Chem. **25,** 1078 (1953).
14. Gaylor, V. E., Conrad, A. L., Landerl, H. J.: Anal. Chem. **29,** 224 (1957).
15. Giner, J., Swette, L.: Nature **211,** 1291 (1966).
16. Handbook of Chemistry and Physics. 47th Edition 1966—67. The Chemical Rubber Co., Cleveland, Ohio.
17. Hartley, A. M., Axelrod, H. D.: J. Electroanal. Chem. **18,** 115 (1968).
18. Hladky, Z.: Z. Chem. **5,** 424 (1965).
19. Hume, D. N., Kolthoff, I. M.: J. Am. Chem. Soc. **63,** 2805 (1941).
20. Issa, I. M., Abdul, Azim, A. A.: Egypt. J. Chem. **2,** 67 (1959).
21. Kahlenberg, L., Krueger, A. G.: Trans. Am. Electrochem. Soc. **56,** 201 (1929).

22. KAMIENSKI, B.: Przemyst. Chem. **11,** 769 (1927).
23. KAMIENSKI, B.: Z. phys. Chem. A. **145,** 48 (1928).
24. KAMIENSKI, B.: Z. phys. Chem. A. **138,** 345 (1928).
25. KOLTHOFF, I. M.: Chem. Weekblad **16,** 1406 (1919).
26. KOLTHOFF, I. M.: Z. anorg. Chem. **110,** 143 (1920).
27. KOLTHOFF, I. M., FURMAN, H.: Potentiometric Titrations. John Wiley and Sons Inc., New York 1949.
28. KOLTHOFF, I. M., TANAKA, N.: Anal. Chem. **26,** 632 (1954).
29. LAITINEN, H. A., RHODES, D. R.: J. Electrochem. Soc. **109,** 413 (1962).
30. LEE, J. K., ADAMS, R. N., BRICKER, C. E.: Anal. Chim. Acta **17,** 321 (1957).
31. LIFSCHNITZ, I., REGGIANI, M.: Gazz. **61,** 915 (1931).
32. LINGANE, J. J., LANGFORD, G. H., ANSON, F. C.: Anal. Chim. **16,** 165 (1957).
33. MALMSTADT, H. V., FETT, E. R.: Anal. Chem. **27,** 1757 (1955).
34. MAUSER, H., NICKEL, B.: Angew. Chem. **77,** No. 8, 378 (1965).
35. MAZZA, F., TRASSATTI, S.: J. Electrochem. Soc. **110,** 847 (1963).
36. MILLER, F. J.: Anal. Chem. **35,** 929 (1963).
37. MILLER, F. M., ZITTEL, H. E.: Anal. Chem. **35,** 1866 (1963).
38. MORRIS, J. B., SCHEMPF, J. M.: Anal. Chem. **31,** 286 (1959).
39. MOUNTCASTLE, W. R.: Anal. Chim. Acta **32,** 332 (1965).
40. MUELLER, T. R., ADAMS, R. N.: Anal. Chim. Acta **23,** 467 (1960).
41. MUELLER, T. R., OLSEN, C. L., ADAMS, R. N.: Advances in Polarography, Vol. 1, p. 198, London, 1960.
42. MUELLER, T. R., OLSON, C. L.: Advances in Polarography Int. Congr., Cambridge, Vol. **1,** pp. 198, 1959.
43. MURRAY, R. M., REILLEY, CH. N.: Anal. Chem. **34,** 313R—322R (1962).
44. MURRAY, R. M., REILLEY, CH. N.: Anal. Chem. **36,** 370R—380R (1964).
45. PELLERIN, F., DEMAY, D.: Ann. pharmac. franc. **22,** 307, (1964).
46. PUNGOR, E., HAVAS, J., TÓTH, K.: Acta Chim. Acad. Sci. Hung. **41,** 239 (1964).
47. PUNGOR, E., HAVAS, J., TÓTH, K.: Z. Chem. **5,** 9 (1965).
48. PUNGOR, E., HAVAS, J., TÓTH, K.: Acta Chim. Acad. Sci. Hung. **48,** 17 (1966).
49. REICHERT, J. S., MACNEIGHT, S. A., RUDEL, H. W.: Ind. Eng. Chem. Anal. Ed. **11,** 194 (1939).
50. REILLEY, CH. N.: Anal. Chem. **28,** 671 (1965).
51. REILLEY, CH. N.: Anal. Chem. **30,** 765 (1958).
52. REILLEY, CH. N.: Anal. Chem. **32,** 185R—193R (1960).
53. ROE, D. K.: Anal. Chem. **38,** 461R (1966).
54. ROSS, J. W., SHAIN, I.: Anal. Chem. **28,** 548 (1956).
55. SAWYER, D. T., SIEV, E. T.: J. Electroanal. Chem. **3,** 410 (1962).
56. SWOFFORD, H. S., CARMAN, ROY, L.: Anal. Chem. **38,** 966 (1966).
57. Treatise on Analytical Chemistry, Part I, Vol. 4, pp. 2402. Interscience Publishers, New York, 1963.
58. ZACHAREVSKIJ, M. S., L'VOVA, T. I., KUZNECOVA, I. N., KRYZANOVSKIJ, B. B.: Zav. Labor **30,** 1196 (1964).
59. ZITTEL, H. E., MILLER, F. J.: Anal. Chem. **36,** 45 (1964).

Ernő PUNGOR; Veszprém, Schönherz Z. u. 10, Hungary
A. WESER; Bergakademie Freiberg, DDR

Acta Chimica Academiae Scientiarum Hungaricae, Tomus 61 (3), pp. 257—260 (1969)

PLATINUM AND PALLADIUM CATALYZED OXIDATION OF AMMONIA UNDER THE EXPERIMENTAL CONDITIONS OF DIFFERENTIAL THERMOANALYSIS (DTA)

M. BERÉNYI

(Department of Urology, University of Medical Sciences, Budapest)

Received August 26, 1968

Under the conditions of differential thermoanalytical tests at temperatures higher than 230°C ammonia is oxidized by atmospheric oxygen with a considerable rate by the catalytic effect of the sample holder made of platinum. A detector for following processes accompanied by the cleavage of ammonia above 100°C was prepared by using platinum and palladium catalysts of high specific surfaces. Less than 1 mg of ammonia could be detected.

In earlier communications [1, 2] we have drawn attention to the fact that when using platinum sample holders for the DTA of decomposition processes which involve the cleavage of ammonia we have to reckon with the catalytic oxidation of ammonia.

Thermoanalysts have in all probability left this problem out of consideration, because in the industrial nitric acid production the contact temperature of platinum is generally 700—900°C; partial oxidation of ammonia, in the presence of platinum, however, proceeds already between 400 and 700°C [3]. Under the experimental conditions of differential thermoanalysis (DTA) this oxidation is detectable already at 230°C applying a platinum sample holder.

The experiments were carried out by means of the derivatograph [4]. A platinum crucible or plate [5], washed with concentrated hydrochloric acid and ignited was placed on the rod of the sample holder and a ceramic or glass crucible was fitted above the thermocouple used for temperature measurement of the inert substance. Air was bubbled through a 25% ammonium hydroxide solution from where it was led into the furnace space without exhaustion. The rate of heating was 10°C per minute. At 230°C the pointer of the DTA galvanometer began to deflect from the base line obtained without the introduction of ammonia and proceeded with increasing rate in exothermic direction (Fig. 1, curve *a*). After the oxidation of the major part of ammonia, which had accumulated in the furnace during the time till 230°C was reached, the DTA signal dropped to a value corresponding to the quantity of oxygen present and to the rate of ammonia input. A mixture of oxygen and ammonia behaved in a similar manner. The DTA curves were the steeper the higher the temperature at which the introduction of ammonia was begun (Fig. 1, curves *b* and *c*). Ammonia of course

oxidizes also at the solders of the Pt/Rh–Pt thermocouples which may be proved simply by protecting the solder of one of two counter-connected thermocouples in the furnace by means of a small glass cap from the attack of the ammonia.

During the decomposition of compounds the liberation of ammonia is an endothermic process, but with simultaneous oxidation the endothermic character will be less pronounced, moreover, provided the sample holder has a sufficiently large and active platinum surface, the process may appear definitely exothermic [1].

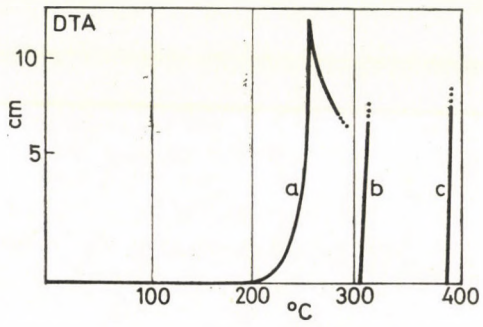

Fig. 1. Oxidation of ammonia on a Pt plate. Changes in the DTA signal at constant ammonia input (curve *a*) and when ammonia input is started at 305°C and 385°C, respectively (curves *b* and *c*). Sample: 13 mm diameter empty Pt crucible. DTA galvanometer sensitivity: 1/10

Neglection of the possibility of oxidation may cause an error mainly when the DTA curve is used for quantity evaluations, *e.g.* in the determination of decomposition enthalpies or of activation energies.

The catalytic effect of platinum was used to follow processes accompanied by the cleavage of ammonia. A sample spread over a large surface on a platinum plate in the manner shown in Fig. 2 was covered by a dense (1024 knots per sq.cm) platinum net made of 0.062 mm platinum wire. This arrangement helped to maintain the advantages of the plate sample holder, while at the same time the thermal changes accompanying the decomposition process were only slightly sensed by the thermocouple, but the heat liberated on the platinum net in the temperature interval of ammonia cleavage was detected with unchanged sensitivity.

When a catalyst precipitated on some thermally neutral carrier was placed in a few tenth of mm thickness on the platinum net, a detector operating at temperatures considerably below 230°C was obtained. Thus, for instance, a catalyst containing 10% of palladium which was precipitated on active charcoal by hydrogenation will oxidize the ammonia above 100°C. Platinum or palladium containing catalysts obtained by hydrogenation have to be heated before use to 80—100°C to eliminate any interference by the oxidation of the adsorbed

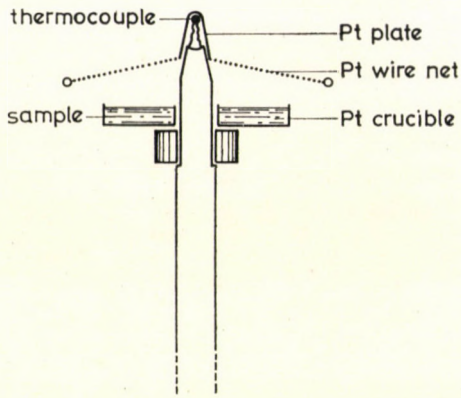

Fig. 2. Detector to follow the evolution of gases which are oxidized on platinum

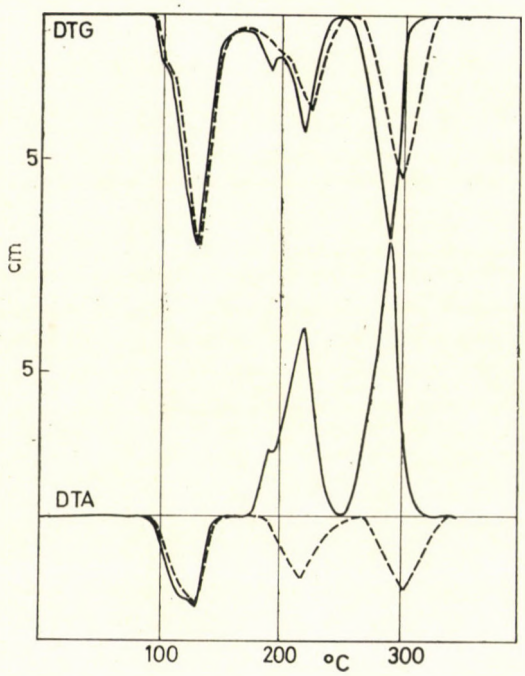

Fig. 3. Derivatogram of $(NH_4)_6Mo_7O_{24} \cdot 4H_2O$ by using a platinum plate (dashed line) and an ammonia detector (continuous line). Weight of sample: 101 mg. The net of the detector was covered with 75 mg of platinum obtained by hydrogenation. Sensitivity of the galvanometers: 1/3

hydrogen with the measurements. Because of the combustion of coal Pd/C can be used only up to temperatures of 300—330°C.

The applicability of the detector is shown through the decomposition of ammonium heptamolybdate (Fig. 3, continuous curve). It appears from the

DTA curve that 6 mols of ammonia are removed not in one step, as might be assumed from the customary DTA and TG curves [6], but in three. Due to oxidation each process associated with ammonia cleavage is accelerated, as shown by the DTG curve which is proportional to the weight loss rate and was plotted for the sake of comparison without the use of the ammonia detector (Fig. 3, dashed line). Although the distance between the plate and the Pt net is 4—6 mm, the DTA curve follows the process satisfactorily and lags behind the DTG curve by not more than 5 °C. The sensitivity of the detector is reflected by the 10 mm high peak on the DTA curve for the 0.7 mg of ammonia which evolves from ammonium urate at 280—320 °C in 4 minutes.

Platinum and palladium exert catalytic effect not only on the oxidation ammonium and hydrogen, but also *e.g.* carbon monoxide and the decomposition products of organic compounds. We shall report elsewhere on experiments concerning this problem.

REFERENCES

1. BERÉNYI, M., LIPTAY, GY.: Acta Chim. Acad. Sci. Hung. **58,** 23 (1968).
2. LIPTAY, GY., BERÉNYI, M., SÁRKÁNY, E.: Hung. Sci. Instr. 1968/15, 31—35.
3. Gmelins Handbuch der anorganischen Chemie, 8. Aufl. 1942, Syst. No. 68, Platin, Teil B, 329.
4. PAULIK, F., PAULIK, J., ERDEY, L.: Z. anal. Chem. **160,** 241 (1958).
5. PAULIK, J., PAULIK, F., ERDEY, L.: Anal. Chim. Acta **34,** 419 (1966).
6. ERDEY, L., GÁL, S., LIPTAY, G.: Talanta **11,** 913 (1964).

Mihály BERÉNYI; Budapest VIII., Üllői út 78/b

Acta Chimica Academiae Scientiarum Hungaricae, Tomus 61 (3), pp. 261—269 (1969)

THE USE OF COMPLEX-FORMING AGENTS IN ION EXCHANGE CHROMATOGRAPHY, I

SEPARATION OF COBALT(II) AND NICKEL(II) IONS ON CATION EXCHANGE COLUMN USING OXALATE IONS CONTAINING ELUENT

J. INCZÉDY, P. KLATSMÁNYI-GÁBOR and L. ERDEY

(Institute for General and Analytical Chemistry, Technical University, Budapest)

Received September 17, 1968

The volume distribution coefficients of nickel(II) and cobalt(II) ions on cation exchange resin in the presence of oxalate ions were calculated, and the optimum pH value of the eluent for the best separation and the peak eluent volumes were predicted using ion exchange equilibrium, complex stability constants and other data taken from the literature. The calculated peak eluent volumes were compared with those obtained in experiments, and good agreement was found.

Ion exchange chromatography as an operation can be compared to conventional partition chromatography in principle: the distribution of a species between the fixed and mobile phase is not controlled by solubility but rather by electrolytic equilibria, since the ions to be separated are bound electrostatically.

The rate of travelling of the adsorption band of an ion on the ion exchange resin column is depending on its distribution coefficient.

If the travelling ion is denoted by B, the following basic equation is valid for the rate of travelling:

$$\left(\frac{dx}{dv}\right)_B = \frac{[B]}{(B)} = \frac{1}{D_B} \tag{1}$$

where dx denotes the infinitesimally thin layer of the column — expressed as volume or rather volume increment — in which the ion B is driven forward by dv ml incoming eluent. The term in round brackets is the concentration of the ion in the resin, that in square ones, in the solution phase. D_B is the distribution coefficient of the ion B, defined as the ratio of the concentration of the ion in the resin phase to that in the mobile *i.e.* liquid phase.

Separating the variables in Eq. (1) and taking the entire volume X of the ion exchange column into consideration, integrating the equation from $v = 0$ to $v = V$ and $x = 0$ to $x = X$, the net eluent volume V can be obtained

$$V = X \cdot D_B \tag{2}$$

The distribution coefficient is considered as constant during elution. Taking also the dead volume of the ion exchange column into consideration, or rather adding it to the net eluent volume, the following equation — very useful in practice — is obtained:

$$V_{\max} = X(D + a) \tag{3}$$

This equation, deduced first by GLUECKAUF [1], gives the relationship between the distribution coefficient and the peak volume of eluent passing through the column until the ion appears in the effluent in maximum concentration. a is the void fraction of the column.

Different ions of similar behaviour can be separated by ion exchange chromatography if the values of $V_{\max}$ and distribution coefficients, respectively, are different. The greater the ratio of the peak eluent volumes of the ions, the more efficient is the separation.

The efficiency of the separation depends also on kinetic factors, which are responsible for the form of the chromatographic curves. On the basis of equilibrium calculations only the approximate position of the peaks, and the possibility of the separation can be predicted.

An attempt was made to calculate the most convenient parameters necessary for the separation of bivalent cobalt and nickel ions by ion exchange chromatography. The calculations were based mainly on the concept of RINGBOM, who used successfully the complex equilibrium calculations in various fields of analytical chemistry [2].

The distribution coefficient of a bivalent metal ion on cation exchange resin column in the absence of any complex forming substance can be calculated approximately from the ion exchange equilibrium equation in the following way:

$$K^x = \frac{(M)\,[A]^2}{[M]\,(A)^2} \tag{4}$$

K^x is the apparent equilibrium constant expressed with concentrations of the ions taking part in the ion exchange process. M denotes the bivalent metal ion to be eluted and A the monovalent cation (sodium, hydrogen, etc.) present in the eluent solution.

The distribution coefficient can be expressed as

$$D_M = \frac{(M)}{[M]} = K^x \left(\frac{(A)}{[A]}\right)^2 \tag{5}$$

Since the amount of the ion A is always much higher in ion exchange chromatographic operations than that of the ion M to be eluted, as a first approximation the capacity of the column (Q) can be written instead of the concentration of A

in the resin phase, and the K^x value can be assumed as constant. The distribution coefficient can be approximately calculated by the following logarithmic formula [2]:

$$\log D_M \approx \log(K^x Q^2) - 2 \log [A] \tag{6}$$

Since K^x and Q are constants for a given ion pair and ion exchange column, the logarithms of the distribution coefficients of bivalent ions change in the same way with the logarithm of the eluent concentration as can be seen in

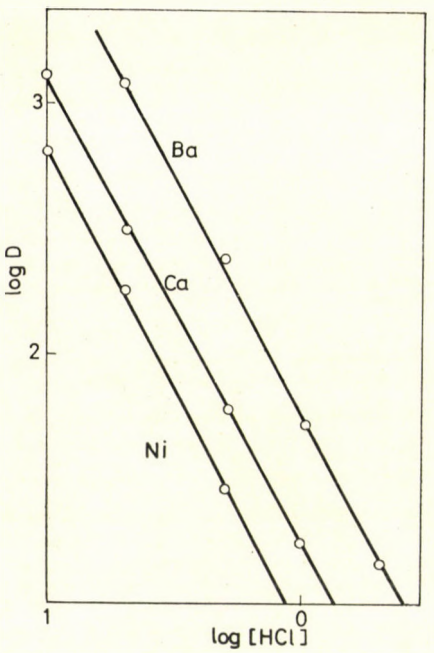

Fig. 1. Logarithmic diagram of distribution coefficients of some bivalent metal ions in function of the eluent concentration. (Data taken from experimental results of STRELOW et al. [4])

Fig. 1. The position of the lines depends on the value of K^x but the lines run similarly, all having a slope of -2 (corresponding to the charge ratio of the ions: 2/1). The ratio of the distribution coefficients — the difference of the logarithms — is constant at any eluent concentration; so its value cannot be influenced this way.

The efficiency of the separation can be increased by means of complexing agents, which form neutral or negatively charged complexes of different stabilities with the ions to be separated. According to RINGBOM [2] the logarithm of the distribution coefficient can be calculated from the following equation if the

eluent contains *e.g.* a dibasic acid H_2Y as complexant:

$$\log D_M \approx \log K^x - \log \alpha_{M(Y)} + 2 \log Q - 2 \log[A] \tag{7}$$

where $\alpha_{M(Y)}$ is the complex formation function which can be calculated if the total concentration and dissociation constants of the complexant and also the complex products of the complexes formed are known

$$\alpha_{M(Y)} = 1 + \left[\frac{C_Y}{\alpha_{Y(H)}}\right]\beta_{MY} + \left[\frac{C_Y}{\alpha_{Y(H)}}\right]^2 \beta_{MY_2} + \cdots$$
$$\cdots + \left[\frac{C_Y}{\alpha_{Y(H)}}\right][H]\beta_{MHY} + \cdots \tag{8}$$

C_Y denotes the total analytical concentration of the complexing agent, the β-s denote the complex products and $\alpha_{Y(H)}$ the protonation function of the complex forming ligand.

$$\alpha_{Y(H)} = 1 + [H]\frac{1}{k_2} + [H]^2\frac{1}{k_1 k_2} \tag{9}$$

k_1 and k_2 are the dissociation constants of the acid H_2Y.

In order to find the optimum composition of the eluent for the chromatographic separation of two metal ions of same valence, the total analytical concentration of the complexing agent can be varied, or it can be kept constant and the pH varied. Both from theoretical and practical points of view it is more expedient to change the pH of the solution and keep the ion concentration constant.

By varying the pH, the free ligand concentration can be changed very sensitively and in most cases one can find the value of pH at which the distribution coefficients of the ions to be separated make possible the best separation. Whether stepwise or gradient elution is used for the separation of metal ion mixtures the detection can be facilitated if the ionic strength of the effluent is nearly constant and only the pH is varied.

Nickel(II) and cobalt(II) ions cannot be separated by means of a cation exchange column if dilute hydrochloric acid or sodium chloride solution is used as eluent. The ion exchange constants, the K^x values of the two ions referring to hydrogen or sodium ions are close together. According to investigations, however, these ions can be separated successfully using a 0.1 *M* oxalic acid—sodium oxalate eluent. Oxalate ions have a suitable mobility and form complexes of different stabilities with nickel(II) and cobalt(II) ions.

Using Eqs (7), (8) and (9) and literature data, the distribution coefficients of nickel(II) and cobalt(II) ions were calculated at different pH in solutions containing 0.1 *M* oxalic acid.

The weight ion exchange constant data taken from literature were the following: $K^{w}_{Co-H} = 1.99$; $K^{w}_{Na-H} = 1.29$ [3]. The K^{w}_{Ni-H} was estimated as 1.94, considering the distribution coefficient data of nickel(II) and cobalt(II) ions obtained by STRELOW [4]. The complex products of the nickel(II)- and cobalt(II)-oxalate complexes: $\log \beta_{NiY} = 4.5$; $\log \beta_{NiY_2} = 7.2$; $\log \beta_{NiY_3} = 8.5$ [5]; $\log \beta_{CoH_2Y_2} = 10.9$; $\log \beta_{CoHY} = 5.6$; $\log \beta_{CoY} = 3.72$; $\log \beta_{CoY_2} = 6.03$ (ionic strength 0.2) [6].

The dissociation constants of oxalic acid: $\log k_1 = -1.4$; $\log k_2 = -3.8$ (ionic strength: 0.1) [7].

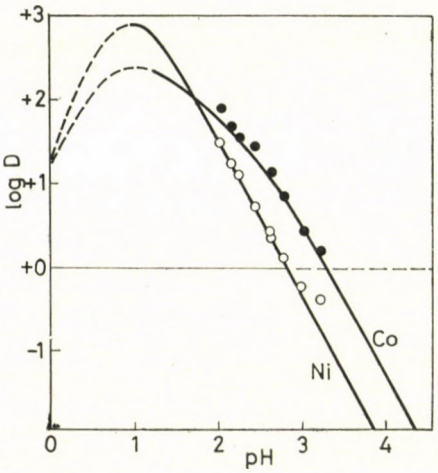

Fig. 2. Volume distribution coefficients of nickel(II) and cobalt(II) ions at different pH, using 0.1 *M* oxalic acid—sodium oxalate as eluent. The points of the curve were calculated by means of equations (7), (8), and (9). The empty and full circles were evaluated from the peak eluent volumes found in experiments using equation (3)

The capacity of the ion exchange resin Amberlite CG—120 Type I used in the experiments was found to be $Q = 1.9$ mval/ml; column density $\sigma = 0.42$ g/ml.

Since in the calculation the values of volume distribution coefficients were required, the weight ion exchange constants were converted to volume constants in the following way:

$$K^{x}_{CoH} = \frac{K^{w}_{CoH};}{\sigma}; \qquad K^{x}_{CoNa} = \frac{K^{w}_{CoH}}{K^{w\,2}_{NaH}} \cdot \frac{1}{\sigma}$$

where σ is the column density. The constants of nickel(II) ions were calculated similarly.

The complex products taken from the literature were used in the calculations without correction, since the ionic strength of the eluent in the experiments did not differ much from those for which the data were given.

From the calculated distribution coefficients a logarithmic diagram was constructed (Fig. 2).

To obtain the optimum pH value for the elution, the ratios

$$\frac{D_{Co} + a}{D_{Ni} + a} \tag{10}$$

(which correspond to the ratios of the peak eluent volumes) were also calculated and their logarithms plotted against the pH of the solution. The obtained diagram can be seen in Fig. 3 (full line). The curve has two

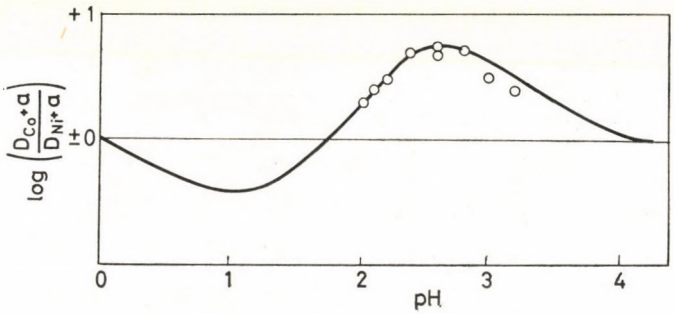

Fig. 3. Comparison of the peak eluent volume ratios found in experiments (circles) to the $(D_{Co} + a)/(D_{Ni} + a)$ fractions. Full line calculated using equations (7), (8) and (9) at different pH

extreme values, one of which is in the acidic region, which does not ensure good separation; the maximum at pH 2.6, however, is really the optimum pH for the best separation. At higher pH values, the ratio of the distribution coefficients does not decrease, but the ratio of the peak eluent volumes tends to 1.

The calculation of the distribution coefficients at pH 2.6, and also of the peak eluent volumes using equations (7), (8), (9) and (3) are given as follows. The data of the ion exchange column used later in experiments were considered.

$\log \alpha_{oxH)} = 1.3$

$\alpha_{Ni(ox)} = 1 + 10^{-2.3} \cdot 10^{-4.1} + 10^{-4.6} \cdot 10^{7.2} + 10^{-6.9} \cdot 10^{8.5} \approx 10^{2.65}$

$\log D_{Ni} = 0.44 + 0.56 - 2.65 + 2 = 0.35$

$D_{Ni} = 2.24$; $V_{max\ Ni} = 3.08\ (2.24 + 0.4) \approx 8.1$ ml

$\alpha_{Co(ox)} = 1 + 10^{-2.6} \cdot 10^{-2.3} \cdot 10^{5.6} + 10^{-5.2} \cdot 10^{-4.6} \cdot 10^{10.9} + 10^{-2.3} \cdot$
$\cdot 10^{3.7} + 10^{-4.0} \cdot 10^{6.03} \approx 10^{1.84}$

$\log D_{Co} = 0.45 + 0.56 - 1.84 + 2 \approx 1.17$

$D_{Co} = 14.8$

$V_{max,\ Co} = 3.08\ (14.8 + 0.4) = 46.8$ ml

To estimate the error caused by the simplification of Eqs (6) and (7), *i.e.* the substitution of (Na) with Q, elution experiments were carried out with different amounts of nickel(II) ions but with the same eluent and under the same conditions. In this series of experiment 1 M ammonium chloride solution was used as eluent. V_{max} values evaluated from the obtained chromatograms are presented in Fig. 4. As can be seen from the figure, the shift of the V_{max} value — and of the corresponding distribution coefficient — is not greater than about 6% in the range investigated if the amount of the eluted ion is not higher than 1% of the column capacity; the probable error is of the same order of magnitude as the reproducibility of elution experiments.

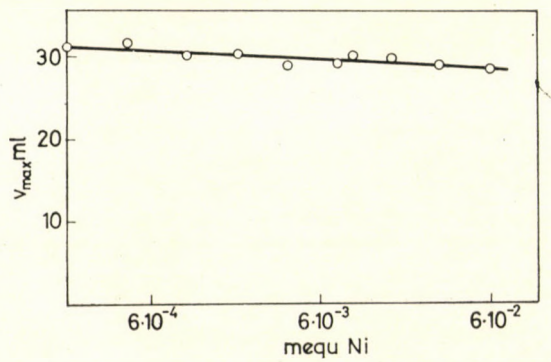

Fig. 4. The variation of the peak eluent volume with the amount of the eluted ion. Eluent: 1 M ammonium chloride. Ion exchange column: Amberlite CG—120 Type I; 7×82 mm. Total capacity cca 6 mval. Flow rate: 0.4 ml/min

Elution experiments with nickel(II) and cobalt(II) ions were carried out using 0.1 M oxalic acid—sodium oxalate as eluent of different pH; from the obtained chromatograms the V_{max} values were evaluated, and also the volume distribution coefficients calculated using equation (3). The ratios of the peak eluent volumes found experimentally are summarized in Fig. 3. The distribution coefficients calculated from the experimental data are presented in Fig. 2.

The chromatogram obtained at the separation of nickel(II) and cobalt(II) ions using an eluent of pH 2.6 can be seen on Fig. 5. The peak eluent volumes were found to be as follows:

$$V_{max,Ni} = 10 \text{ ml}$$

$$V_{max,Co} = 45 \text{ ml}$$

On the basis of the results of experiments and by comparing the calculated and experimental data one can say that equation (7) was suitable for the calculation of the volume distribution coefficients of nickel(II) and cobalt(II)

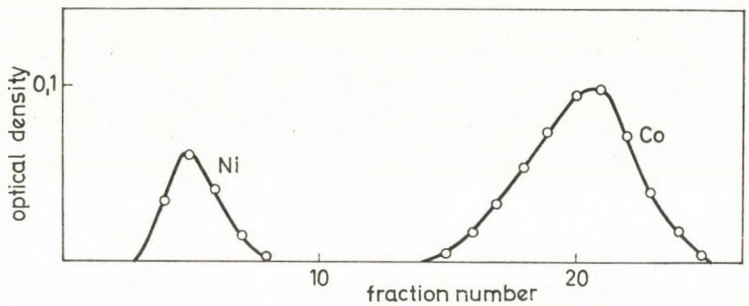

Fig. 5. Chromatographic separation of nickel(II) and cobalt(II) ions using 0.1 *M* oxalic acid—sodium oxalate solution of pH 2.6 as eluent. Ion exchange column: Amberlite CG—120 Type I; 7×80 mm; fraction volume: 2 ml. Flow rate: 0.4 ml/min

ions. On the basis of the calculated distribution coefficients at different pH but constant eluent concentration also the optimum pH could be predicted.

The difference between the calculated and experimentally found peak eluent volumes (at pH 2.6) is smaller than 20 per cent.

Experimental

Reagents. In all experiments A. G. reagents were used.

Oxalic acid—sodium oxalate eluent solutions of different pH were prepared from 0.2 *M* oxalic acid solution. After diluting 500 ml 0.2 *M* oxalic acid solution to about 900 ml under stirring and checking the pH, 1 *M* sodium hydroxide solution was added from a burette unti the required pH was reached. After dilution to one litre, the pH of the solution was checked by a pH-meter.

0.05 *M* nickel(II) sulphate and cobalt(II) sulphate stock solutions were prepared by weighing and dissolving the crystalline chemicals. The concentration of the solutions was also checked by complexometric titration.

Ion exchange column. Ion exchange column with a resin bed of 7 mm diameter and 80 mm length was prepared from Amberlite CG—120 Type I cation exchange resin after the usual preliminary treatment [8]. The column was equilibrated with the eluent and washed before the elution experiments.

Elution experiments for the investigation of the effect of the amount of the eluted ion on the peak eluent volume. Ion exchange column of 7 mm diameter and 80 mm height was prepared, converted to the ammonium form and washed. 30 microliter of the nickel(II) sulphate stock solution of given concentration was given on the column with a micropipette and after washing with some drops of water, the elution with 1 *M* ammonium chloride solution as teluen was started with a flow rate of 0.4 ml/min. The effluent was collected by means of an automatic fraction collector (Fractomat Y—2, HAKO, GFR) in 1 ml fractions, and analysed (see later). From the obtained optical density data elution diagrams were constructed and the peak eluent volumes in ml evaluated.

Elution experiments for separation of trace amounts of nickel(II) and cobalt(II) ions using oxalate ions containing eluent of different pH. The elution experiments were carried out with single ions and also with ion pairs in the following way: The ion exchange column (7×80 mm) was first equilibrated with the eluent and washed with water. 30 microliters of a 0.05 *M* nickel(II) sulphate and 0.05 *M* cobalt(II) sulphate solution was then given on the column and washed with some drops of water. The elution was carried out with a flow-rate of 0.4 ml/min. The effluent was collected in 1—4 ml fractions automatically and analysed. On the basis of the obtained data elution diagrams were constructed and peak eluent volumes evaluated.

Estimation of nickel(II) and cobalt(II) ions in the effluent. For the estimation of nickel(II) ions 1.5 ml of DMG reagent solution and 1 ml of 0.625% potassium iodate solution was given to the effluent portion filled up to 10 ml and after 30 min the optical density measured at 520 nm by means of a Spekol (Zeiss, Jena, GDR) spectrophotometer. DMG reagent solution: equal parts of 20% tartaric acid, 25% sodium hydroxide and 0.5% ammoniacal dimethyl glyoxime were mixed [9].

For the estimation of cobalt(II) ions 0.5 ml of buffer solution, 1 ml of 1 : 4 ammonia and 0.5 ml of 0.05% 2-nitroso-1-naphthol solution was given to the fraction diluted to 10 ml and the optical density measured at 520 nm after 30 min. Buffer solution: 500 g citric acid was dissolved in 250 ml of water and filled up to 1 litre with cc. ammonia solution [10].

REFERENCES

1. GLUECKAUF, E. I.: Ion exchange and its applications. Soc. Chem. Ind. London, 1954, 34.
2. RINGBOM, A.: Complexation in Analytical Chemistry. Interscience Publ., New York, 1963.
3. KRAUS, K. A., RARIDON, R. J.: J. Phys. Chem. **63,** 1901 (1959).
4. STRELOW, F. W. E.: Anal. Chem. **32,** 1185 (1960).
5. WATTERS, I. I., DEWITT, R.: J. Am. Chem. Soc. **82,** 1333 (1960).
6. SCHUBERT, J., LIND, E. L., WESTFALL, W. M., PFLEGER, R. Li, N. C.: J. Am. Chem. Soc. **80,** 4799 (1958).
7. MCAULEY, A., NONCOLLAS, G. H.: Trans. Faraday Soc. **56,** 1165 (1960).
8. INCZÉDY, J.: Analytical Applications of Ion Exchangers. Pergamon Press, Oxford, 1966.
9. COOPER, W. D.: Anal. Chem. **23,** 875 (1951).
10. YOE, J. H., BARTON, CH. J.: Ind. Eng. Chem. Anal. Ed. **12,** 405 (1940).

János INCZÉDY
Piroska KLATSMÁNYI-GÁBOR
László ERDEY
Budapest XI., Gellért tér 4

Acta Chimica Academiae Scientiarum Hungaricae, Tomus 61 (3), pp. 271—277 (1969)

PHYSIKALISCHE URSACHEN DES MATRIXEFFEKTES BEI DER SPEKTRALANALYSE IM GLEICHSTROMBOGEN*

L. Rost

(Sektion Geowissenschaften der Bergakademie Freiberg, DDR)

Eingegangen am 27. Mai 1968

Für die Matrixeffekte der quantitativen Spektralanalyse kommen zwei Ursachenkomplexe in Betracht, nämlich chemische Vorgänge bei der Probeverdampfung (chemisch bedingte Matrixeffekte) und physikalische Vorgänge im Plasma der Strahlungsquelle (physikalisch bedingte Matrixeffekte). Gegenstand der vorliegenden Arbeit sind nur die physikalisch bedingten Matrixeffekte, die am Beispiel eines frei brennenden Gleichstrombogens näher untersucht werden. Dabei lassen sich im wesentlichen vier mögliche Einzelursachen feststellen, die in komplizierter Weise zusammenwirken können. Diese Ursachen sind: die Kopplung aller Teilchenkonzentrationen im Plasma, die Kopplung zwischen Teilchenkonzentrationen und Bogentemperatur, die Transportvorgänge in der Bogensäule und die Wechselwirkung des in die Entladungszone einströmenden Probedampfes mit dem Plasma.

Die quantitative Spektralanalyse beruht auf dem Zusammenhang zwischen Linienintensität und Teilchendichte im Plasma der Strahlungsquelle. Dabei macht man normalerweise die Voraussetzung, daß die Konzentrationsverhältnisse der Elemente, wie sie in der Probe vorliegen, sich entweder im Plasma wiederfinden oder wenigstens in stets gleicher Weise abgeändert werden. Ist das nicht der Fall, dann liegen »chemisch bedingte« Matrixeffekte vor, die auf die Vorgänge bei der Probeverdampfung zurückzuführen sind. Diese Vorgänge können unter anderem als Verdampfungsbehinderung durch Bildung thermisch stabiler Systeme [1, 2, 3] oder als unterschiedliche Verdampfbarkeit infolge von unterschiedlicher chemischer Bindung [4] in Erscheinung treten. Auch wenn derartige Effekte keine Rolle spielen, besteht die Schwierigkeit immer noch darin, daß der Zusammenhang zwischen Linienintensität und Teilchendichte im Plasma der Strahlungsquelle nicht eindeutig ist. Die Ursache dafür ist im physikalischen Verhalten des Entladungsplasmas zu suchen. Es ist deshalb sinnvoll, den Gesamtkomplex der Erscheinungen, die auf Störungen der Intensitäts-Konzentrations-Beziehung im Plasma zurückzuführen sind, als »physikalisch bedingten« Matrixeffekt zu bezeichnen.

Am Beispiel des Normaldruck-Niederstrombogens sollen die Probleme des physikalisch bedingten Matrixeffektes im folgenden etwas genauer betrachtet werden. Dabei ist zu bedenken, daß in der Praxis zwischen chemisch und physikalisch bedingten Matrixeffekten oft eine enge Wechselbeziehung zu beobachten ist, die zu sehr unübersichtlichen Verhältnissen führt.

* Nach einem im Januar 1968 in Berlin gehaltenen Vortrag.

I

Im Lichtbogen herrscht mit hinreichender Genauigkeit thermisches Gleichgewicht. Bei Emission aus optisch dünner Schicht ist die Intensität dann bestimmt durch den Emissionskoeffizienten ε. Für die Linie eines neutralen Atoms gilt:

$$\varepsilon = \frac{1}{4\pi} A\, h\nu \frac{g_{0,a}}{u_0} n_0 e^{-\chi_{0,a}/kT} \tag{1}$$

Dabei bedeuten A die Übergangswahrscheinlichkeit, h die PLANCKsche Konstante, ν die Frequenz des ausgestrahlten Lichtes, $g_{0,a}$ das statistische Gewicht des angeregten Zustandes, u_0 die Zustandssumme des neutralen Atoms, n_0 die Zahl pro cm^{-3} der neutralen Atome im Grundzustand oder in irgendeinem angeregten Zustand, $\chi_{0,a}$ die Anregungsenergie, k die BOLTZMANN Konstante und T die absolute Temperatur.

Im Temperaturbereich des Niederstrombogens kommen praktisch nur neutrale und einfach ionisierte Atome der Analysenelemente vor. Die Gesamtzahl pro cm^{-3} einer bestimmten Sorte ist dann $n_0 + n_1$, wobei der Index auf die Ionisierungsstufe hinweist. Der Zusammenhang zwischen n_0 und n_1 ist durch die SAHA-gleichung gegeben:

$$\frac{n_1 \cdot n_e}{n_0} = \Phi(T) \tag{2}$$

n_e bezeichnet die Zahl pro cm^{-3} der freien Elektronen und $\Phi(T)$ (in cm^{-3}) die Funktion

$$\log \Phi(T) = -\chi_1 \frac{5040}{T} + \frac{3}{2} \log T + \log \frac{2u_1}{u_0} + 15{,}38$$

χ_1 ist die Ionisierungsenergie in eV, u_1 die Zustandssumme des einfach ionisierten Atoms.

Zwischen der Gesamtzahl N aller Teilchen und der Teilchenzahl des betrachteten Analysenelementes im Bogenplasma soll nun beim Gesamtdruck P ein bestimmtes Verhältnis bestehen, das am einfachsten durch den Molenbruch

$$\frac{n_0 + n_1}{N} = c \qquad (N = P/kT) \tag{3}$$

zu charakterisieren ist. c (z. B. in %) ist also ein Maß für die Konzentration der interessierenden Teilchensorte in der Strahlungsquelle.

Durch Einsetzen von (2) und (3) in (1) ergibt sich:

$$\varepsilon = \frac{1}{4\pi} A\, h\nu \frac{g_{0,a}}{u_0} c \frac{N}{1 + \Phi(T)/n_e} e^{-\chi_{0,a}/kT} \tag{4}$$

Der Emissionskoeffizient einer Spektrallinie hängt demnach nicht allein von der Konzentration c des betreffenden Elementes im Plasma ab, sondern außerdem von der Temperatur T und der Elektronendichte n_e [5, 6].

Für eine gegebene Zusammensetzung des Plasmas ist n_e natürlich eine Funktion der Temperatur. Ändert man aber die Plasmazusammensetzung, dann ergibt sich bei bestimmter Temperatur für n_e ein anderer Wert. Die Elektronendichte hängt also nicht nur von der Temperatur ab, sondern parametrisch auch von der Gesamtzusammensetzung des Plasmas.

Eine erste mögliche Ursache des Matrixeffektes besteht also darin, daß selbst bei gleicher Temperatur die Linienintensität des Analysenelementes über die Elektronendichte von allen anderen Plasmakomponenten beeinflußt wird. Dabei spielen Elemente mit geringer Ionisierungsenergie, die bereits bei kleinen Konzentrationen die Elektronendichte stark verändern, die Hauptrolle.

Prinzipiell ist man nun in der Lage, diesen Teil des Matrixeffektes theoretisch zu übersehen. Zu dem Zweck ist es erforderlich, die Teilchendichten n_0 und n_1 für verschiedene Zusammensetzung des Plasmas in Abhängigkeit von der Temperatur zu berechnen. Aus der Teilchenkonzentration des Analysenelementes ergibt sich dann leicht der Emissionskoeffizient und daraus die Intensität einer bestimmten Analysenlinie. Das Gleichungssystem, das man bei dieser Aufgabe zu bearbeiten hat, sieht z. B. für Luft mit den Komponenten N_2, O_2, NO, N, O, N^+, O^+ folgendermaßen aus:

1 DALTONsches Gesetz
1 Quasineutralitätsbedingung
3 Massenwirkungsgesetze
2 SAHAgleichungen
1 Massenverhältnis (N : O)

8 Gleichungen für die 8 unbekannten Teilchendichten $n(N)_2, \ldots, n(O^+)$ und n_e.

Mischt man der Luft noch Analysen- und Störelemente zu, dann erweitert sich der Umfang der Gleichungen für jedes hinzukommende Element um 2. Da die Gleichungen nichtlinear sind, ist der Aufwand bei der Lösung erheblich.

II

Eine Komplizierung des Matrixproblems hängt mit den Eigenschaften des Bogens zusammen. Die Schwierigkeit besteht insbesondere darin, daß die Bogentemperatur mit der Elektronendichte gekoppelt ist. Alle Änderungen der Elektronendichte führen damit notwendig zu Änderungen der Bogentemperatur. Einigermaßen übersichtlich sind die Verhältnisse noch bei einem Gleichstrombogen, der wie üblich mit konstanter Stromstärke betrieben werden soll. Bekanntlich sinkt bei einem solchen Bogen die Temperatur, wenn man die

Elektronendichte durch Zusatz leicht ionisierbarer Elemente erhöht. Trotz der nunmehr niedrigeren Bogentemperatur bleibt die Elektronendichte über dem anfänglichen Wert [5, 6, 7].

Eine zweite mögliche Ursache für den Matrixeffekt im Bogen besteht also darin, daß sich Temperatur und Elektronendichte des Bogens ändern, wenn sich die Plasmazusammensetzung ändert.

Der Mechanismus des Matrixeffektes läßt sich bis hierher wie folgt veranschaulichen. Bei gleichbleibender Konzentration des Analysenelementes im Plasma bewirkt eine Veränderung der übrigen Komponenten Verschiebungen von Elektronendichte und Temperatur. Beide Einflüsse verursachen nach Gleichung (4) Intensitätsänderungen der Analysenlinie, obwohl die Konzentration c des Analysenelementes konstant geblieben ist.

Auf der Grundlage des sog. Kanalmodells der Lichtbogensäule kann man die möglichen Intensitätsänderungen infolge des Matrixeffektes wenigstens näherungsweise quantitativ übersehen [7]. Eine genauere Betrachtung muß die radiale Temperaturverteilung im Bogen berücksichtigen (Lösung der ELENBAAS—HELLERschen Gleichung). Untersuchungen in dieser Richtung, die allerdings nur die Änderung der Temperaturverteilung bei Variation der Plasmazusammensetzung zum Inhalt haben, führte KRINBERG [8] durch.

III

Die bis jetzt angestellten Betrachtungen basierten auf der Voraussetzung, daß die im Lichtbogen auftretenden Feldstärken und Temperaturgradienten vernachlässigt werden können. Bei einem realen Bogen ist das nun keineswegs der Fall, und man muß deshalb die Frage stellen, wie sich Feldstärken und Temperaturgradienten auf die für die Spektralanalyse interessierenden Erscheinungen im Bogen auswirken. Diese Fragestellung führt zu dem komplizierten und noch wenig untersuchten Komplex der Diffusions- bzw. Entmischungsvorgänge. Es ist eigentlich seit langem bekannt, daß sich die Teilchen im Bogen weder in axialer noch in radialer Richtung gleichmäßig verteilen. Damit wird das Mischungsverhältnis der einzelnen Teilchensorten ortsabhängig.

Die Entmischungseffekte im Bogen sind vor allem beim Nachweis kleiner Gehalte wichtig. Sie können zur Verbesserung oder Verschlechterung der Nachweisempfindlichkeit führen.

Betrachtet man zunächst die Achsenrichtung, dann kann man den Einfluß eines Temperaturgradienten vernachlässigen. Das äußere elektrische Feld bewirkt nun, daß sich die Ionen vor der Kathode und die Neutralteilchen vor der Anode anreichern. Der spektroskopische Nachweis dieses Effektes stammt von MANNKOPFF und PETERS [9]. In der Spektralanalyse wird er als »Glimmschichtverfahren« zur Bestimmung kleiner Gehalte leicht ionisierbarer Elemente ausgenutzt.

In radialer Richtung besteht ein starker Temperaturgradient und ein inneres elektrisches Feld. Im Gleichgewicht resultiert eine Entmischung, die sich folgendermaßen charakterisieren läßt [10]. Die leicht ionisierbaren Elemente reichern sich in den äußeren Bogenbezirken an, wobei die Anreicherung mit zunehmender Konzentration kleiner wird. Zur Bogenachse hin folgen Linien mit wachsender Anregungsenergie. Der experimentelle Befund ist im wesentlichen bereits seit den Untersuchungen LENARDs im Jahre 1903 bekannt [11].

Die Berechnung solcher Entmischungsvorgänge im Bogen ist prinzipiell möglich, wenn auch nicht ganz einfach. Dazu sind hauptsächlich zwei Wege beschritten worden, die zum selben Ergebnis führen [12]. MAECKER und FRIE [13] gingen von der Thermodynamik irreversibler Prozesse aus und SCHLÜTER [14] vom hydrodynamischen Modell des Plasmas. Der Unterschied zur obigen Betrachtungsweise besteht vor allem darin, daß die konstanten Massenverhältnisse durch entsprechende Kontinuitäts- und Bewegungsgleichungen für jede diffundierende Teilchensorte ersetzt werden müssen. Neben den rein thermodynamischen Größen wie Partialdruck und Temperatur kommen also auch die Diffusionsgeschwindigkeiten der Teilchen als dynamische Größen ins Spiel. Eine weitere Schwierigkeit besteht darin, daß dieses Modell mit dem Temperaturfeld des Bogens verknüpft werden muß, das ja seinerseits in starkem wechselseitigem Zusammenhang mit der Teilchenverteilung steht. Diese Aufgabe, die über die Energie-Bilanzgleichung des Bogens, etwa in der ELENBAAS—HELLERschen Form, zu bewältigen wäre, ist offenbar noch nicht in Angriff genommen worden.

Die Kopplung zwischen Teilchenverteilung und Temperaturverteilung über dem Bogenquerschnitt ist nun eine dritte mögliche Ursache des Matrixeffektes. Sie besteht darin, daß Veränderungen der Teilchenverteilung der einen Sorte, die etwa durch wechselnde Zusammensetzung der Proben hervorgerufen sein mögen, zu Änderungen der Temperaturverteilung und der Verteilung aller anderen Teilchensorten und damit der Intensitäten führen.

IV

Schließlich ist noch die Zufuhr des Probedampfes in den Bogen und die Wechselwirkung mit dem Bogenplasma von Einfluß auf die Verteilung von Teilchendichte und Temperatur und damit auf die Linienintensitäten. Den oben beschriebenen Transporterscheinungen im Bogen überlagern sich nämlich Massenströme, die durch die Verdampfung der Probe bzw. der Elektrodensubstanz entstehen und die zu einer Modifizierung der Teilchen- und Temperaturverteilungen führen. Dabei findet wiederum eine gegenseitige Beeinflussung der einzelnen Teilchensorten statt, die eine vierte mögliche Ursache für den Matrixeffekt im Bogen darstellt.

Bei den in der Spektralanalyse zumeist verwendeten Anordnungen von gebohrten und gestopften Kohleelektroden erfolgt die Verdampfung in das Plasma asymmetrisch, weil die Entladung auf dem ringförmigen Rand der Elektrode ansetzt. Die Zuführung des Dampfes ist deshalb nicht rein axial, sondern es treten auch radiale und azimutale Geschwindigkeitskomponenten auf. Dadurch wird eine theoretische Behandlung sehr erschwert. Für axiale Masseneinströmung gibt es Ansätze von SCHMITZ und PATT [15], für radiale Masseneinströmung von DRUXES [16], die allerdings in beiden Fällen unter etwas anderer Zielsetzung aufgestellt wurden.

Eine mehr pauschale Beschreibung der stationären Teilchenverteilung im Bogen beruht auf der Betrachtung der Diffusionsvorgänge, die sich beim »Durchströmen« des Probedampfes durch die Entladungszone abspielen [17, 18, 19]. Dabei muß strenggenommen für jede Teilchensorte eine Diffusionsgleichung erfüllt sein, denen noch die spezifischen Gleichungen des Bogens hinzugefügt werden müßten. Die gegenseitige Wechselwirkung der einzelnen Teilchensorten wäre dann z. T. in den Diffusionskoeffizienten enthalten. Über den Einfluß der Plasmazusammensetzung auf die Diffusionskoeffizienten der einzelnen Teilchensorten im Bogen liegen allerdings nur wenige Untersuchungen vor [20, 21]. Zu bedenken ist endlich, daß der Diffusionstrom gewöhnlich nur eine Komponente im Gesamtkomplex der Ströme im Bogen ausmacht.

Die genannten vier Ursachen für den Matrixeffekt treten natürlich stets gekoppelt auf. Die vorliegende Darstellungsweise ist deshalb nicht ganz frei von Willkür. Es erschien trotzdem nützlich die Ursachen in dieser Form herauszustellen, weil sich daran zeigen läßt, wie kompliziert das Problem des Matrixeffektes wird, wenn man die Betrachtung verfeinert.

LITERATUR

1. RAUTSCHKE, R.: XIV. Coll. Spectr. Internat., Debrecen 1967, und Spectroch. Acta **23B** 55 (1967).
2. NICKEL, H.: XIV. Coll. Spectr. Internat., Debrecen 1967, und Spectroch. Acta **21**, 363 (1965).
3. SCHROLL, E.: XIV. Coll. Spectr. Internat. Debrecen 1967.
4. NICKEL, H., PFLUGMACHER, A.: Fres. Z. anal. Chem. **184**, 161 (1961).
5. BOUMANS, P. W. J. M.: in Reinststoffprobleme, Bd. 2 Reinststoffanalytik. Akademie-Verlag, Berlin, 1966 (Vorträge Dresden 1965).
6. VUKANOVIĆ, V.: XIV. Coll. Spectr. Internat., Debrecen 1967.
7. ROST, L.: XIV. Coll. Spectr. Internat., Debrecen 1967.
8. KRINBERG, I. A.: in: Spektralanalyse in Geologie und Geochemie (russ.). Materialien der II. sib. Konf. über Spektroskopie. Moskau, 1967.
9. MANNKOPFF, R., PETERS, A.: Z. Phys. **70**, 444 (1931).
10. EBERHAGEN, A.: Z. Phys. **143**, 312 (1955).
11. LENARD, P.: Ann. Phys. **11**, 636 (1903).
12. FRIE, W.: Z. Phys. **162**, 61 (1961).
13. MAECKER, H., FRIE, W.: Z. Phys. **162**, 69 (1961).
14. SCHLÜTER, A.: Naturforschung **5A**, 72 (1950) und **6A**, 73 (1951).

15. PATT, H. J., SCHMITZ, G.: Z. Phys. **185,** 1 (1965) und **188,** 1 (1965).
16. DRUXES, H.: Diss. Aachen 1966.
17. BOUMANS, P. W. J. M., DE GALAN, L.: Anal. Chem. **38,** 674 (1966).
18. BOUMANS, P. W. J. M.: XIV. Coll. Spectr. Internat., Debrecen 1967.
19. MALYCH, V. D., SERD, M. A.: in: Spektralanalyse in Geologie und Geochemie (russ.). Materialien der II. sib. Konf. über Spektroskopie. Moskau, 1967.
20. POLATBEKOV, P. P., ŽUKOV, I. A.: Vestnik AN Kaz. SSR No. **5,** 75 (1967).
21. VUKANOVIĆ, V.: in: Emissionsspektralanalyse (Vorträge Görlitz 1962). Akademie-Verlag Berlin, 1964.

Lothar ROST; Sektion Geowissenschaften der Bergakademie, DDR 92 Freiberg

Acta Chimica Academiae Scientiarum Hungaricae, Tomus 61 (3), pp. 279—287 (1969)

CALCULATION OF THE INFLUENCE OF THE OHMIC RESISTANCE OF THE CELL ON THE THIRD HARMONIC A.C. POLAROGRAPHIC CURRENT IN CASE OF A REVERSIBLE ELECTRODE REACTION

J. DÉVAY, L. MÉSZÁROS and T. GARAI

(Department of Physical Chemistry, University for Chemical Engineering, Veszprém and Research Group for Electrochemistry of the Hungarian Academy of Sciences, Veszprém)

Received August 8, 1968

The theoretical relationships derived for the third harmonic a.c. flowing through the cell under the effect of small amplitude sinusoidal voltage superimposed on the d.c. polarizing potential in case of reversible polarographic reaction were amended by correction terms taking into account the ohmic resistance of the cell. Calculation according to the correction terms show that the decrease of the third harmonic a.c. amplitudes under the effect of the ohmic resistance of the cell is greater when the angular frequency of the a.c. voltage and the concentration of the depolarizer are increased and when the number of the electrones involved in the electrode reaction is higher.

In a previous communication [1] we gave a theoretical treatment of the first and second as well as the third harmonic [2] component of the alternating current flowing through the cell when a sinusoidal voltage of small amplitude is superimposed onto the polarizing d.c. potential. The dependence of the amplitude of the harmonics on the overpotential, the angular frequency and the amplitude of the a.c. voltage as well as on the transfer coefficient and the exchange current was studied in the case of diffusion and charge transfer polarizations. The results were discussed in detail for the case of reversible polarographic reactions.

In a.c. polarography and especially in the study of electrode kinetics the ohmic potential drop on the measuring cell must be taken into consideration. The importance of this correction has been pointed out by many workers [3, 4], however, the contribution of the higher harmonics of the a.c. current to the ohmic potential drop was assumed to be negligible.

In a recent paper [5] we derived correction terms for the ohmic drop relating to the first and second harmonic component of the a.c. current precisely taking into account the cell impedance in the case of reversible polarographic reaction. In the present work these calculations are extended to the third harmonic component of the a.c. current.

The amplitude of the third harmonic a.c. current in the case of reversible polarographic reaction is given by the following formula [2]:

$$i_3 = \frac{\sqrt{3}}{192} \frac{(zF)^4}{(RT)^3} \eta_{\sim}^3 \sqrt{\omega}\,(C_{10}\sqrt{D_1} + C_{20}\sqrt{D_2}) \frac{\left| 3 - 2ch^2 \frac{zF}{2RT}(\eta_{=} - \eta_{½}) \right|}{ch^4 \frac{zF}{2RT}(\eta_{=} - \eta_{½})} \qquad (1)$$

where D_1 and D_2, C_{10} and C_{20} are the diffusion coefficients and the concentrations in the bulk of the solution of the reduced and oxidized form, respectively, of the component taking part in the electrode reaction, ω is the angular frequency of the a.c. voltage, $\eta_\sim$ is the amplitude of the a.c. voltage, $\eta_=$ is the time average value of the overpotential, $\eta_{1/2}$ is the half-wave potential, T is the temperature on the Kelvin scale, R is the universal gas constant and F is the Faraday constant.

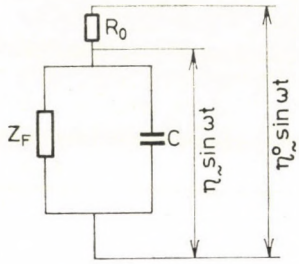

Fig. 1. Equivalent circuit of the electrode in the case of cell resistance R_0

The equivalent circuit of the cell is represented in Fig. 1 where R_0 is the ohmic resistance of the cell, C is the double layer capacity and Z_F is the faradaic impedance. The latter is the resultant of the parallelly connected R_p polarization resistance and C_p "pseudocapacity":

$$\frac{1}{Z_F} = \frac{1}{R_p} + j\omega C \tag{2}$$

where $j = \sqrt{-1}$

The polarization resistance and the pseudocapacity can be expressed by the following formula (*cf.* Ref. [5], Eq. [6])

$$\frac{1}{R_p} = \omega C_p = \frac{(zF)^2}{\sqrt{2RT}} \sqrt{\omega}\,(C_{10}\sqrt{D_1} + C_{20}\sqrt{D_2})\,\frac{e^{\frac{zF}{RT}(\eta_= - \eta_{1/2})}}{(1 + e^{\frac{zF}{RT}\eta_= - \eta_{1/2}})^2} \tag{3}$$

The a.c. voltage, $\eta_\sim^0 \sin \omega t$ imposed on the cell is not applied to the electrode impedance since a considerable ohmic drop arises on the ohmic resistance of the cell. The a.c. voltage amplitude on the electrode impedance is given by the following formula (*cf.* Ref [5], Eq. [3a]):

$$\eta_\sim = \frac{\eta_\sim^0}{\sqrt{\left(1 + \frac{R_0}{R_p}\right)^2 + \left(\frac{R_0}{R_p} + \omega R_0 C\right)^2}} \tag{4}$$

where $\eta_\sim^0$ is the amplitude of the a.c. voltage imposed on the cell.

In order to derive the exact correction term for the third harmonic component of the a.c. current, the ohmic drop expressed by Eq. (4), further the

shunting effect of the resistance R_0 are to be taken into account. Thus the equivalent circuit of the cell is to be transformed as in the case of the calculation of the correction term for the second harmonic a.c. current [5] (Fig. 2).

A sine-wave voltage of ω angular frequency that does not contain higher harmonic components is imposed to the points A and B of the cell *i.e.* to the resultant of R_0 and Z_e connected in series. Thus A and B are at equal potentials as far as the third harmonic a.c. component is concerned and they can be

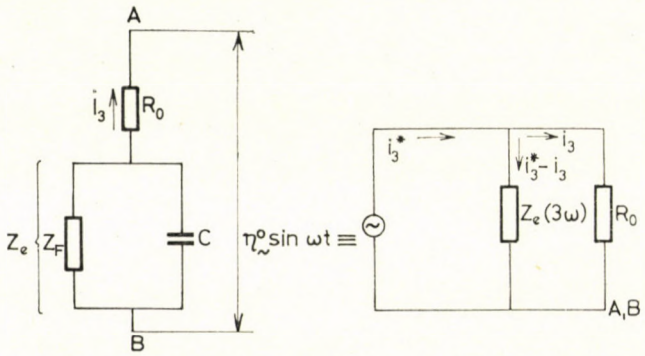

Fig. 2. Equivalent circuit of the electrode relating to the third harmonic component of the a.c. current

considered as short circuited in the equivalent circuit. Accordingly in this case the resistance R_0 and the electrode impedance Z_e can be represented in parallel connection. The electrode impedance, $Z_{e(3\omega)}$ is given by the following formula

$$\frac{1}{Z_{e(3\omega)}} = \frac{1}{Z_{F(3\omega)}} + j\,3\omega C \tag{5}$$

i.e. it is defined as in Eq. (2) but at the frequency 3ω of the third harmonic. The appearance of the third harmonic component in the a.c. current flowing through the cell is a consequence of the non-linearity of the electrode impedance, thus the latter can be represented as a current generator producing a current i_3^* and having an internal resistance equal to $Z_{e\,(3\omega)}$. According to the equivalent circuit of Fig. 2, taking into consideration Kirchhoff's law, we have

$$i_3 R_0 = (i_3^* - i_3)\, Z_{e(3\omega)},$$

$$i_3 = \frac{i_3^*}{1 + \dfrac{R_0}{Z_{e(3\omega)}}} = \frac{i_3^*}{\left[1 + \dfrac{R_0}{R_{p(3\omega)}} + j\left(\dfrac{R_0}{R_{p(3\omega)}} + 3\omega R_0 C\right)\right]}$$

where i_3 is the third harmonic current flowing through the electrode. Hence the absolute value of the third harmonic current density is

$$|i_3| = \frac{|i_3^*|}{\sqrt{\left(1 + \dfrac{R_0}{R_{p(3\omega)}}\right)^2 + \left(\dfrac{R_0}{R_{p(3\omega)}} + 3\omega R_0 C\right)^2}} \tag{6}$$

Finally uniting the correction terms we obtain:

$$i_3 = \frac{\sqrt{3}\,(zF)^4}{192\,(RT)^3}\sqrt{\omega}\,(C_{10}\sqrt{D_1} + C_{20}\sqrt{D_2})\,\frac{\left|3 - 2ch^2\,\frac{zF}{2RT}\,(\eta_= - \eta_{1/2})\right|}{ch^4\,\frac{zF}{2RT}\,(\eta_= - \eta_{1/2})}\cdot \tag{7}$$

$$\cdot\,\frac{\eta_{\sim}^{03}}{\left[\left(1 + \frac{R_0}{R_{p(\omega)}}\right)^2 + \left(\frac{R_0}{R_{p(\omega)}} + \omega R_0 C\right)^2\right]^{3/2}\sqrt{\left(1 + \frac{R_0}{R_{p(3\omega)}}\right)^2 + \left(\frac{R_0}{R_{p(3\omega)}} + 3\omega R_0 C\right)^2}}$$

Formula (7) represents the amplitude of the third harmonic a.c. current flowing through the cell under the effect of the sine wave a.c. voltage of amplitude $\eta_{\sim}^{0}$ superimposed on the direct potential $\eta_=$ as a function of z, C_{10}, C_{20}, $\sqrt{\omega}$, $\eta_=$, η^0 and R_0.

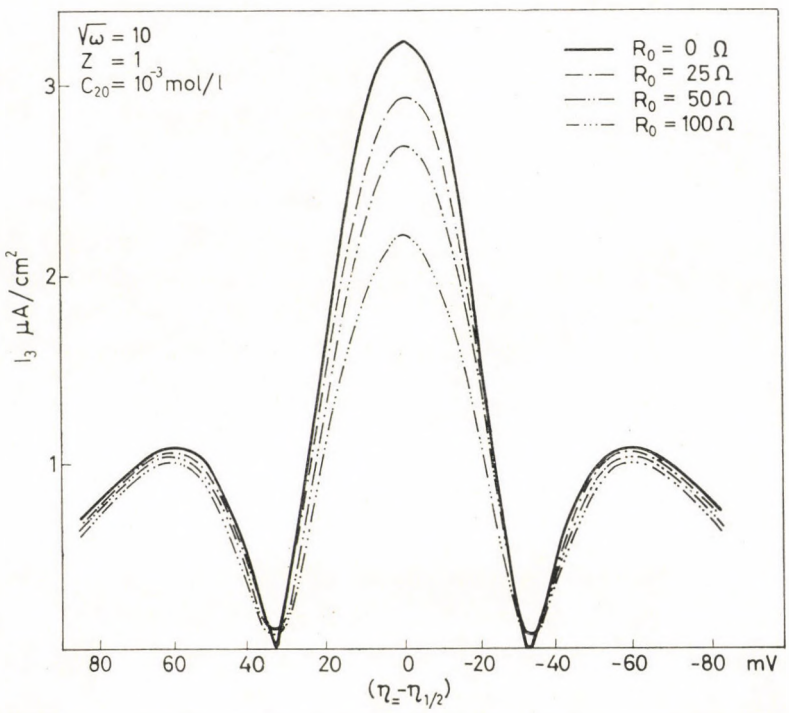

Fig. 3a

Fig. 3. The current density of the first harmonic a.c. component (i_3) *vs.* the d.c. potential ($\Delta\eta = \eta_= - \eta_{1/2}$) for $R_0 = 0$, 25, 50 and 100 Ohm resp. ($C_{10} = 0$, $C_{20} = 1 \cdot 10^{-3}$ mole/1 and $z = 1$); a) $\sqrt{\omega} = 10$; b) $\sqrt{\omega} = 20$; c) $\sqrt{\omega} = 50$

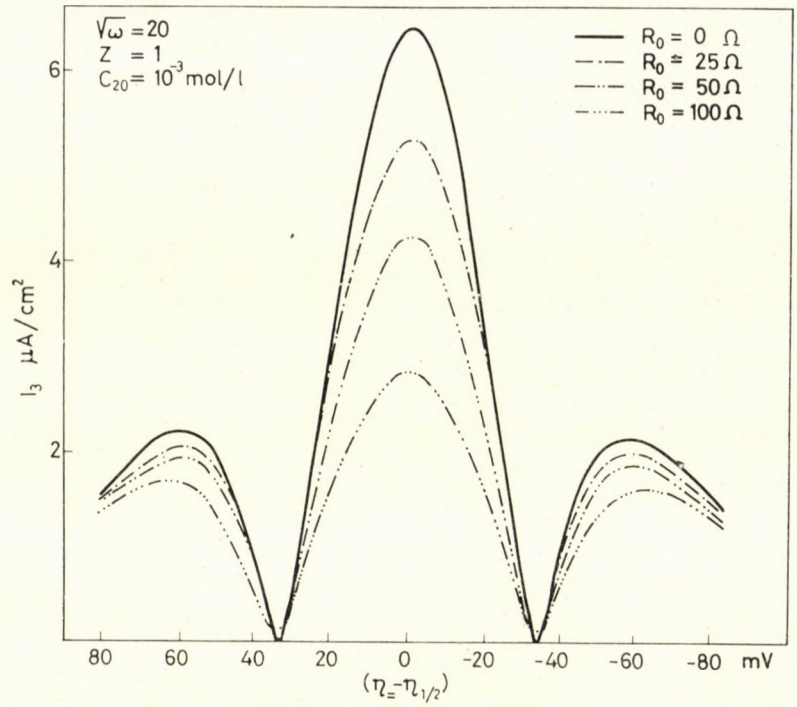
√ω = 20
Z = 1
C20 = 10⁻³ mol/l
R0 = 0 Ω
R0 = 25 Ω
R0 = 50 Ω
R0 = 100 Ω
I3 μA/cm²
6
4
2
80 60 40 20 0 -20 -40 -60 -80 mV
(η= - η1/2)

Fig. 3b

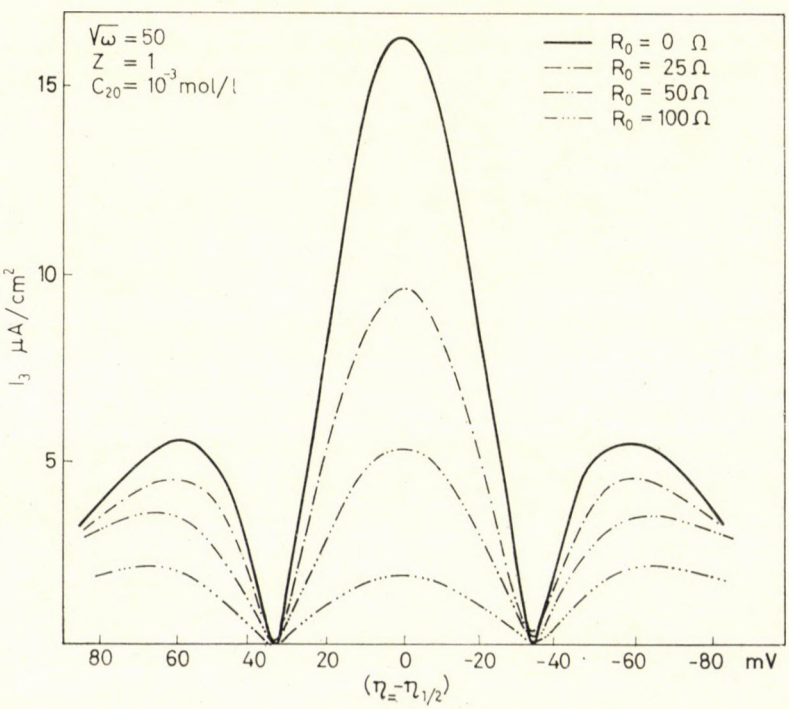
√ω = 50
Z = 1
C20 = 10⁻³ mol/l
R0 = 0 Ω
R0 = 25 Ω
R0 = 50 Ω
R0 = 100 Ω
I3 μA/cm²
15
10
5
80 60 40 20 0 -20 -40 -60 -80 mV
(η= - η1/2)

Fig. 3c

Calculations were made in order to evaluate Eq. (7) since the formula containing many variables is rather complicated. The results of these calculations are represented in Figs 3 to 7 plotted as a function of each variable. (For sake of convenience the values $D = 1 \cdot 10^{-5}$ cm^2 sec^{-1} and $\eta^0_{\sim} = 1 \cdot 10^{-2}$ V were assumed.)

Fig. 3 shows the amplitude of the third harmonic a.c. component as a function of $\eta_{=}$ in case of $z = 1$, for $R_0 = 0$, 25, 50 and 100 resp., while $C_{10} = 0$, $C_{20} = 1$, 10^{-3} mole/l, and $\sqrt{\omega} = 10$, 20 and 50, respectively. It is apparent from Fig. 3 that the amplitude of the third harmonic a.c. current density decreases by increasing R_0 and z.

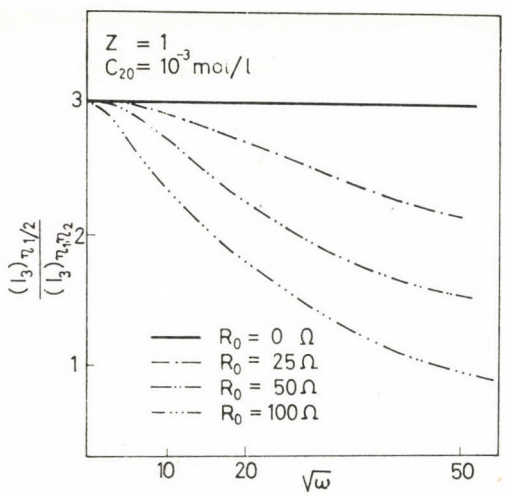

Fig. 4. The ratio of the maximum amplitudes of the third harmonic a.c. current density appearing at the half-wave potential and at more negative and positive potentials than the latter plotted as a function of the square root of the angular frequency of the a.c. voltage for $R_0 =$ $=0$, 25, 50 and 100 Ohm resp.

This effect is greater on the maximum amplitude of i_3 appearing at the half-wave potential than on the maximum amplitudes at more negative and more positive potentials referred to the half-wave potential. (In case of polarographically reversible electrode reaction the latter two amplitudes are equal.)

It is noteworthy that in the case of the third harmonic a.c. component the correction for the ohmic drop affects considerably the amplitude of the a.c. current while the difference of the more negative and more positive peak potentials, respectively, than the half-wave potential is changing much less than in the case of the second harmonic a.c. component [5]. It is interesting to note that the decrease of the ratio of the maximum amplitudes of the third harmonic a.c. component at the half-wave potential and at more negative (or positive) potential than the latter as a function of the angular frequency of the a.c.

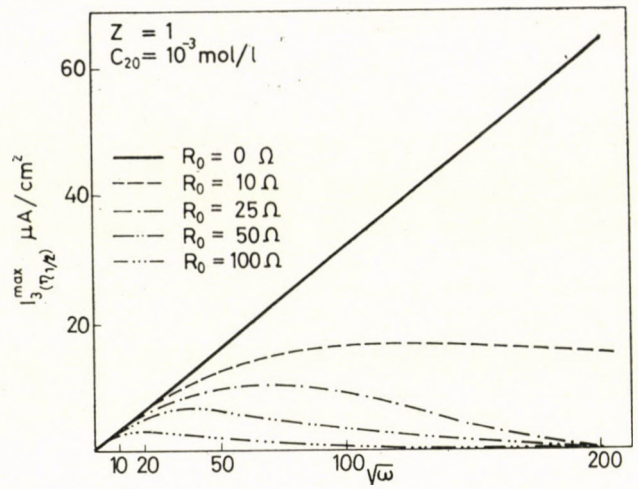

Fig. 5. The maximum of the current density of the third harmonic a.c. component $\left(i^{max}_{3(\eta_{1/2})}\right)$ plotted *vs.* the square root of the angular frequency of the a.c. voltage for $R_0 = 0$, 25, 50 and 100 Ohm resp. in the case of $C_{10} = 0$, $C_{20} = 1 \cdot 10^{-3}$ mole/l, $z = 1$

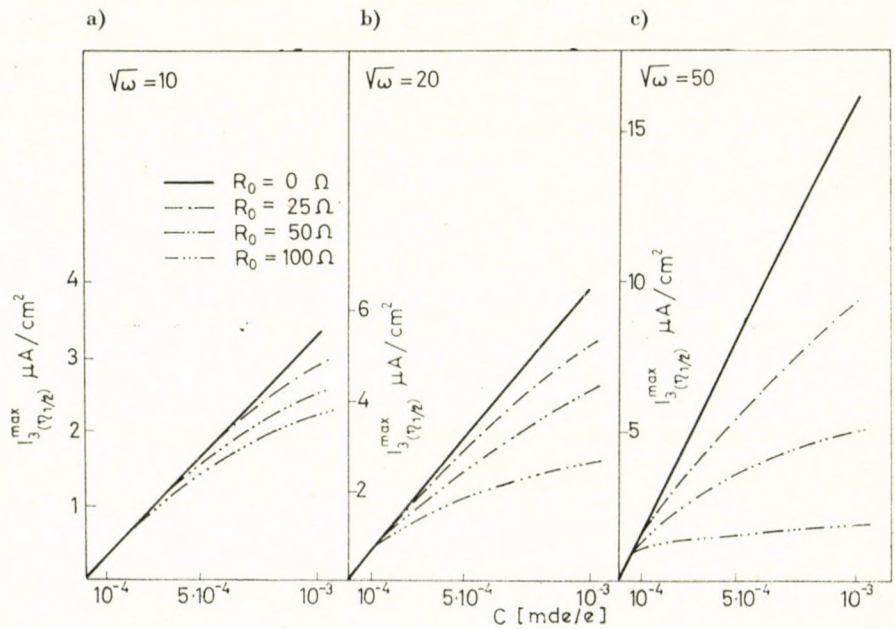

Fig. 6. The maximum amplitude of the third harmonic a.c. current density $\left(i^{max}_{3(\eta_{1/2})}\right)$ plotted *vs.* the concentration $C_{20}(C_{10} = 0)$ for $z = 1$ and $R_0 = 0$, 25, 50 and 100 Ohm resp. a) $\sqrt{\omega} = 10$; b) $\sqrt{\omega} = 20$; c) $\sqrt{\omega} = 50$

voltage and of the concentration, respectively, are similar in form to the curves representing the deviation from the theoretical value of the potential corresponding to the maximum amplitudes of the second harmonic a.c. current as functions of both the angular frequency of a.c. voltage and the concentration respectively.

Fig. 4 shows this phenomenon using the data of Fig. 3. The ratio of the maximum amplitudes appearing at the half-wave potential and at more nega-

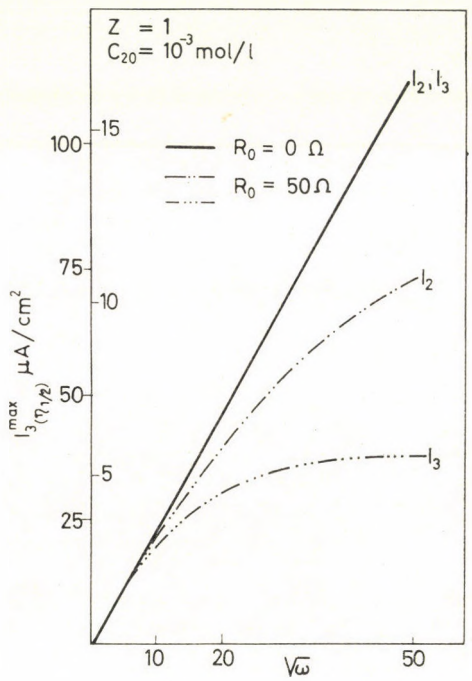

Fig. 7. The maximum amplitude of the second and third harmonic a.c. current density resp. plotted as a function of $\sqrt{\omega}$ in the case of $C_{10} = 0$, $C_{20} = 1 \cdot 10^{-3}$ mole/l, $z = 1$ and $R_0 = 0$ and 50 Ohm resp.

tive or positive potential than the latter are plotted as a function of the square root of the angular frequency in case of $R_0 = 0$, 25, 50 and 100 Ohm.

Fig. 5 represents the maximum amplitude of the third harmonic a.c. current at the half-wave potential plotted as a function of the square root of the angular frequency assuming various R_0 values, in case of $z = 1$, $C_{10} = 0$ and $C_{20} = 1 \cdot 10^{-3}$ mole/l.

Fig. 6 shows the maximum amplitude values as a function of the concentration in case of $\sqrt{\omega} = 10$, 20 and 50 and $z = 1$ as well as $R_0 = 0$, 25, 50 and 100 Ohm.

The ohmic correction is increasing by increasing values of the number of electrones involved in the electrode reaction as the Faraday admittance appearing in the correction term is increasing linearly with the square of the charge number.

It is evident from a comparison of the correction terms related to the second and third harmonic a.c. current intensity resp. [*cf.* Eq. (7)] that the effect of the ohmic drop is increasing in the case of higher harmonic components of a.c. current. This phenomenon is shown in Fig. 7, where the values of $i_2^{\max}$ and $i_{3(\eta_{1/2})}^{\max}$ respectively, are plotted as a function of $\sqrt{\omega}$. In both cases the following parameter values were assumed:

$$C_{20} = 1 \cdot 10^{-3} \text{ mole/l}, \; C_{10} = 0, z = 1 \text{ and } R_0 = 50 \text{ Ohm}.$$

Our calculations lead to the conclusion that the ohmic drop appearing on the resistance R_0 of the cell is considerably affecting the measurement of the higher a.c. harmonic components even in case of relatively low cell resistance.

REFERENCES

1. DÉVAY, J., MÉSZÁROS, L., GARAI, T.: Acta Chim. Acad. Sci. Hung. **58,** 141 (1968)
2. DÉVAY, J., MÉSZÁROS, L., GARAI, T.: Acta Chim. Acad. Sci. Hung. **60,** 67 (1969)
3. DELAHAY, P.: New Instrumental Methods in Electrochemistry. New York 1954
4. SMITH, D. E. Electroanalytical Chemistry, Vol. I. Ed. J. Bard, New York 1966
5. DÉVAY, J., MÉSZÁROS, L., GARAI, T.: Acta Chim. Acad. Sci. Hung. (in press)

József DÉVAY
Lajos MÉSZÁROS
Tibor GARAI
Veszprém, Schönherz Z. u. 12, Hungary

Acta Chimica Academiae Scientiarum Hungaricae, Tomus 61 (3), pp. 289—299 (1969)

BESTIMMUNG DER OBERFLÄCHE PULVERFÖRMIGER PLATINADSORBENTIEN DURCH MESSUNG DER JODADSORPTION MIT DER RADIOAKTIVEN INDIKATOR-METHODE

G. TÓTH und L. ZSINKA

(Institut für Isotope der Ungarischen Akademie der Wissenschaften, Budapest)

Eingegangen am 10. August 1968

Es wurde gezeigt, daß sich Jodidionen sowohl an vorher mit Wasserstoff bedeckten, als auch an mit chemisorbierter Oxydschicht bedeckten Platinoberflächen in Form von elementarem Jod abscheiden. Die Abscheidung erfolgt in beiden Fällen zufolge eines Austausches der Jodidionen mit den vorher adsorbierten Wasserstoff- bzw. Sauerstoffatomen. Während dieser Austausch an mit Wasserstoff bedeckten Adsorbentien durch die Bruttogleichung

$$Pt(H) + H^+ + J^- \rightarrow Pt(J) + H_2 \qquad (1)$$

beschrieben werden kann, erfolgt an mit Oxydschicht bedeckten Adsorbentien als erster Schritt die Auflösung der Platin-Oberflächenschicht laut Gl. (2)

$$Pt_2 - Pt_1 - O + 2H^+ + 2J^- \rightarrow (PtJX_n)^{4-(n+1)} + H_2O + J + Pt_2 \qquad (2)$$

sodann die Chemisorption des gebildeten elementaren Jods laut Gl. (2a)

$$Pt_2 + J \rightarrow Pt_2J, \qquad (2a)$$

wobei Pt_1 und Pt_2 die äußerste bzw. die darunter liegende Platinschicht und $(PtJX_n)^{4-(n+1)}$ den aus der ursprünglich mit chemisorbierter Oxydschicht bedeckten äußersten Platin-Oberflächenschicht gebildeten Platin–Jod-Komplex bedeutet.

Ein Vergleich der mit der BET-Methode gemessenen Oberfläche mit der adsorbierten maximalen Jodmenge zeigt, daß bei der Sättigung der Oberfläche eines mit Oxydschicht bedeckten Adsorbens eine monoatomare chemisorbierte Jodschicht gebildet wird, wobei jedem Oberflächen-Platinatom ein Jodatom zukommt. Hingegen erwies sich an mit Wasserstoff bedeckten Adsorbentien die adsorbierte maximale Jodmenge um 10—25% weniger als die einer monoatomaren, gesättigten Schicht entsprechende Menge. Die gute Übereinstimmung zwischen der mit der BET-Methode und der mittels Jodadsorption gemessenen Oberfläche ermöglicht die Bestimmung der Oberfläche von Platinkatalysatoren mit Hilfe der adsorbierten maximalen Jodmenge. Da die letztere Bestimmung bei Zimmertemperatur, ohne vorangehende und höhere Temperaturen erfordernde Entgasung vorgenommen werden kann, muß eine mögliche Alterung der Oberfläche des Adsorbens nicht in Betracht gezogen werden.

An pulverförmigen, durch die Reduktion von Wasserstoffchloroplatinat hergestellten Platinadsorbentien wurde die Adsorption von Jodidionen in Abhängigkeit von der Konzentration, vom pH-Wert sowie vom reduzierten bzw. oxydierten Zustand des Adsorbens untersucht. Die spezifische Oberfläche der Adsorbentien wurde mit der BET-Methode bestimmt, und diese Werte wurden mit den aus der adsorbierten Jodmenge berechneten verglichen. Die gute Übereinstimmung weist darauf hin, daß die Oberfläche pulverförmiger Platinadsor-

bentien bzw. -katalysatoren durch die Messung des Sättigungswertes der Jodadsorption bestimmt werden kann. Der Mechanismus der Jodadsorption an mit adsorbiertem Wasserstoff bzw. chemisorbierter Oxydschicht bedeckten Platinoberflächen wurde geklärt.

1. Einleitung

In den letzten Jahren befaßten sich zahlreiche Arbeiten mit der Abscheidung von Jodidionen an blanke und platinierte Platinoberflächen [1—10]. Obwohl in mancher Hinsicht zwischen den einzelnen Angaben sowie auch zwischen den aus diesen gezogenen Schlüssen wesentliche Wiedersprüche bestehen, sind sich die meisten Autoren darüber einig, daß die je Flächeneinheit adsorbierte maximale Jodmenge die der ionischen Monoschicht entsprechende Menge übertrifft [1—4], so daß die Abscheidung der Jodidionen nicht auf eine ionische Adsorption, sondern auf Chemisorption zurückzuführen ist.

Diese Feststellungen sowie unsere früheren experimentellen Ergebnisse [4, 5], die ebenfalls auf eine die ionische Monoschicht überschreitende Adsorption hinweisen, lassen folgern, daß es sich bei der Abscheidung von Jodidionen auf Platinoberflächen um Chemisorption handelt, doch können diese Befunde an sich nicht als klare Beweise betrachtet werden. Die Frage, ob tatsächlich eine Chemisorption erfolgt, könnte zwar durch den Nachweis der an der Adsorbens-Oberfläche zustande kommenden monoatomaren Jodschicht entschieden werden, doch können tatsächlich im Falle von Platten-Adsorbentien, für welche der Rauhigkeitsfaktor der Oberfläche nur annähernd bekannt is, nur indirekte und annähernde Schlüsse über das Verhältnis zwischen adsorbierter maximaler Jodmenge und monoatomarer Schicht gezogen werden, so daß im Falle von Platten-Adsorbentien der eindeutige Nachweis der Bildung einer monoatomaren Schicht durch Chemisorption sozusagen als unmöglich zu betrachten ist.

Außer der Bestimmung der Bedeckung der Oberfläche bereitet auch die Klärung des Adsorptionsmechanismus Schwierigkeiten, da sich bekanntlich an der Platinoberfläche bereits bei Zimmertemperatur und in Luft durch Chemisorption eine Oxydschicht — etwa mit der Zusammensetzung PtO — bildet. Derart wäre die Abscheidung von Jodidionen an mit chemisorbierter Oxydschicht bedeckten Platinadsorbentien nur durch einen Austausch mit den Sauerstoffatomen vorstellbar.

Hingegen erfolgt die Adsorption der Jodidionen an mit adsorbiertem Wasserstoff bedeckten Platinoberflächen durch den Austausch der Jodidionen und des vorher adsorbierten atomaren Wasserstoffes sowie der in der Lösung anwesenden Wasserstoffionen, wobei der Vorgang mit der folgenden Bruttogleichung beschrieben werden kann:

$$J^- + H^+ + H(Pt) \rightarrow J(Pt) + H_2 \qquad (1)$$

Obzwar die Gültigkeit der Gl. (1) für Platten-Adsorbentien durch die pH-Abhängigkeit der Adsorption sowie durch jene Beobachtung unterstützt wird, wonach vorher adsorbiertes Jod durch die Einleitung von Wasserstoff in die mit dem Adsorbens in Berührung stehende Lösung desorbiert wird [4, 5], kann der Adsorptionsmechanismus laut Gl. (1) für Platten-Adsorbentien quantitativ nicht bestätigt werden, denn die mit der Adsorption gleichzeitig stattfindende pH-Änderung kann wegen der kleinen Oberfläche meßtechnisch nicht erfaßt werden.

Die spezifische Oberfläche des durch Reduktion von Platinsalzen hergestellten Platinadsorbens beträgt im allgemeinen einige Quadratmeter je Gramm, so daß die spezifische Oberfläche mit volumetrischer Gasadsorption mit Hilfe der BET-Gleichung bestimmt und so auch die je effektive Oberflächeneinheit adsorbierte Jodmenge berechnet werden kann. Die beträchtliche spezifische Oberfläche der pulverförmigen Platinadsorbentien ermöglicht außerdem eine Messung der mit der Jodadsorption gleichzeitig erfolgenden pH-Änderung.

Die nachstehend beschriebenen Versuche bezweckten einerseits die Klärung des Mechanismus der Jodadsorption mit vorher mit Wasserstoff bzw. chemiesorbierter Oxydschicht bedeckten Platinadsorbentien und anderseits die Bestimmung des Verhältnisses zwischen der adsorbierten maximalen Jodmenge und der einer monoatomaren Schicht entsprechenden Jodmenge.

2. Versuchsanordnung

Das pulverförmige Platinadsorbens wurde durch die Reduktion von Wasserstoffchloroplatinat mit Formaldehyd in alkalischer Lösung hergestellt. In Abhängigkeit davon, ob ein Adsorbens mit kleinerer oder größerer spezifischer Oberfläche hergestellt werden sollte, wurde die Reduktion bei Zimmertemperatur bzw. bei 4—5°C vorgenommen. Nach der Reduktion wurde das Adsorbens mit destilliertem Wasser gewaschen und bei Zimmertemperatur getrocknet.

Die adsorbierte bzw. die in Lösung verbleibende Jodmenge wurde mit radioaktiver Indikatormethode bestimmt, indem die Gamma-Aktivität der markierten ^{131}I Ionen sowohl am Adsorbens als auch in der Lösung mit einem NaJ(Tl) Szintillations-Bohrlochkristall gemessen wurde. Bei Versuchen, die die Bestimmung der Abhängigkeit der adsorbierten Jodidmenge von der Jodidionenkonzentration bezweckten, wurden Adsorbens-Mengen von 10 mg zusammen mit der Versuchslösung in einem Glasrohr, dessen Durchmesser (20 mm) mit dem des Bohrlochs des Szintillationskristalls übereinstimmte, eingeführt. Die Lösung wurde mit einem Elektromotor gerührt, und in bestimmten Zeitabständen wurden die beiden Phasen zwecks Aktivitätsbestimmung getrennt. Nach Erreichen des Sättigungswertes der adsorbierten Jodmenge wurde die am Adsorbens haftende Flüssigkeitsschicht durch Einbringen des Adsorbens

in eine solche Lösung entfernt, die von gleicher Zusammensetzung war, wie die Versuchlösung, jedoch keine Jodidionen enthielt. Die Lösung wurde dann so lange gerührt, bis die Gamma-Aktivität des Adsorbens einen konstanten Wert erreichte.

In Versuchen zur Bestimmung der durch die Jodadsorption in der Versuchslösung hervorgerufenen pH-Änderung wurde ähnlich vorgegangen, mit dem Unterschied, daß zur Erhöhung der pH-Änderung zu jedem Versuch 100 mg Adsorbens verwendet wurden. Die pH-Änderung der Versuchslösung wurde mit einer Glaselektrode und einem Röhrenvoltmeter-Typ Radiometer gemessen.

Bei einem Teil der Versuche wurde das Adsorbens mit Wasserstoff gesättigt, während die übrigen Versuche ohne diese Vorbehandlung des Adsorbens durchgeführt wurden. In der Folge werden die mit elektrolytisch entwickeltem Wasserstoff gesättigten Adsorbentien als mit Wasserstoff bedeckt, die ohne reduzierende Vorbehandlung verwendeten Adsorbentien als mit Sauerstoff bedeckt bezeichnet.

Die spezifische Oberfläche der untersuchten Platinadsorbentien wurde bei der Temperatur des flüssigen Stickstoffs mit der BET-Methode bestimmt, wobei wir jedoch im Gegensatz zur allgemeinen Praxis Krypton verwendeten [10]. Die Oberfläche wurde bei 180 °C entgast. Die gemessenen Werte der spezifischen Oberfläche sind in Tabelle I angeführt. Die Jodidionenkonzentration der Versuchslösungen wurde mit Kaliumjodid, die Wasserstoffionenkonzentration mit Schwefelsäure eingestellt.

Tabelle I

Adsorbent Nummer	Spezifische Oberfläche (m^2/g)
1.	2,0
2.	11,9
3.	13,0
4.	24,3

3. Versuchsergebnisse

a) Die Konzentrationsabhängigkeit der Adsorption an mit Wasserstoff bedeckten Adsorbentien.

Ähnlich wie an Platten-Adsorbentien [4, 5], war die Ausscheidung der Jodidionen auch an pulverförmigen Platinadsorbentien ein schneller Vorgang. Der Sättigungswert der Adsorption stellte sich nach 20—40 Minuten ein. Die Darstellung der Adsorptions-Sättigungswerte als Funktion der Konzentration (Abb. 1) läßt darauf folgern, daß die adsorbierte Menge über eine gegebene

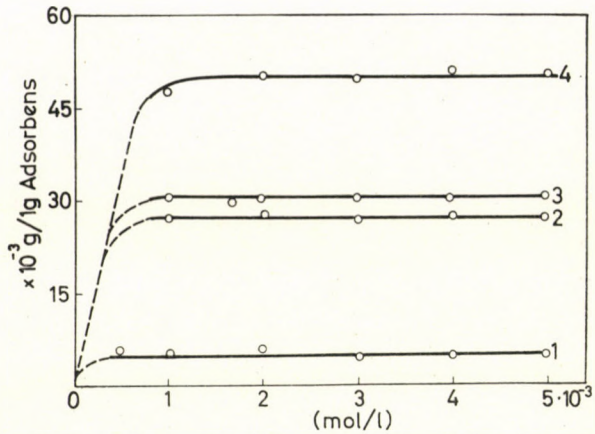

Abb. 1. Die adsorbierte Jodmenge in Abhängigkeit der Anfangskonzentration im Falle von wasserstoffbedeckten Adsorbentien in 1 *n* Schwefelsäure. (Die Kurven beziehen sich auf Adsorbentien der gleichen Nummer)

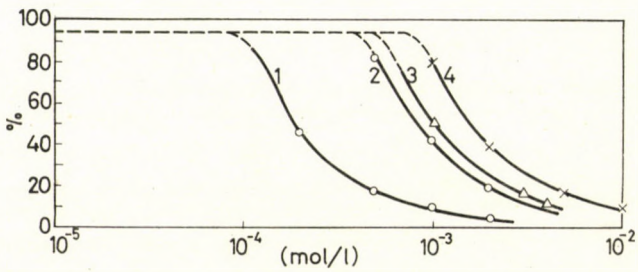

Abb. 2. Ausmaß der Adsorption an wasserstoffbedeckten Adsorbentien in Abhäng igkeit de Anfangskonzentration in 1 *n* Schwefelsäure. (Die Kurven beziehen sich auf Adsorbe ntien de gleichen Nummer)

Ausgangs-Jodidionenkonzetration bei Erhöhung der Konzentration nicht mehr weiter ansteigt, und die adsorbierte Jodmenge von der Jodidionenkonzentration unabhängig wird. Wenn man das Maß der Adsorption als Funktion der Jodidionenkonzentration darstellt, wird ersichtlich, daß bis zur Sättigung der Oberfläche die ganze ursprünglich in der Lösung anwesende Jodmenge adsorbiert wird (Abb. 2). Die an 1 g Adsorbens bzw. 1 cm² der Adsorbensoberfläche adsorbierten Jodmengen sind in Tabelle II zusammengefaßt.

Tabelle II

Adsorbent Nummer	Spezifische Oberfläche, m²/g	Maximalwert der adsorbierten Jodmenge	
		je 1 g Adsorbent, g	je 1 cm² Oberfläche, µg
1.	2,0	$5{,}0 \cdot 10^{-3}$	0,25
2.	11,9	$27 \cdot 10^{-3}$	0,23
3.	13,0	$31 \cdot 10^{-3}$	0,24
4.	24,3	$50 \cdot 10^{-3}$	0,21

Die in der letzten Rubrik der Tabelle II angeführten Daten zeigen, daß die je Oberflächeneinheit adsorbierte maximale Jodmenge in guter Annäherung als konstant zu betrachten ist. Auf die Frage des Verhältnisses der je Oberflächeneinheit adsorbierten Menge zur Monoschicht soll weiter unten eingegangen werden.

b) Die Konzentrationsabhängigkeit der Adsorption an mit Sauerstoff bedeckten Adsorbentien.

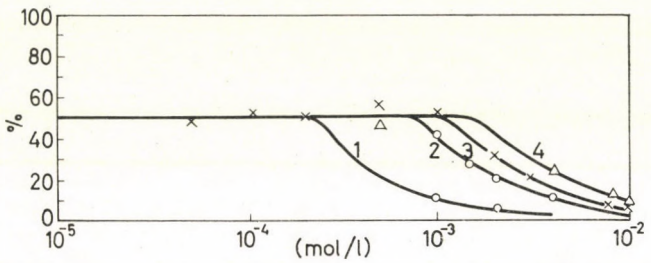

Abb. 3. Ausmaß der Adsorption an sauerstoffbedeckten Adsorbentien in Abhängigkeit der Anfangskonzentration in 1 *n* Schwefelsäure. (Die Kurven beziehen sich auf Adsorbentien der gleichen Nummer)

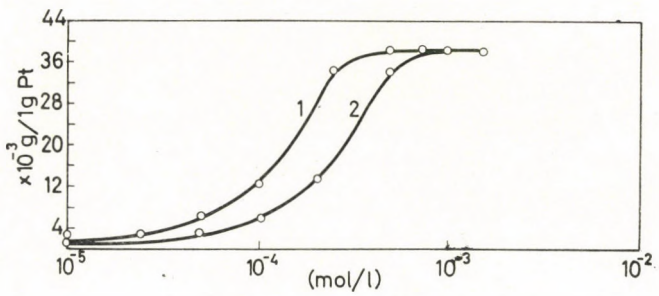

Abb. 4. Adsorbierte Jodmenge in Abhängigkeit der Anfangskonzentration (Kurve 2) und der Gleichgewichtskonzentration (Kurve 1) am sauerstoffbedeckten Adsorbens Nr. 3 in 1 *n* Schwefelsäure

Zum Unterschied zu den mit Wasserstoff bedeckten Adsorbentien, lag das Maß der Adsorption an mit chemisorbierter Oxydschicht bedeckten Adsorbentien selbst bei so niedrigen Ausgangs-Jodidionenkonzentrationen, bei denen eine Sättigung der Oberfläche noch gar nicht stattfinden konnte, stark unter 100%. Stellt man das Maß der Adsorption als Funktion der Ausgangskonzentration dar (Abb. 3), so wird ersichtlich, daß in einem ziemlich breiten Konzentrationsbereich nur etwa 50% der in der Lösung ursprünglich anwesenden Jodmenge adsorbiert wird. Werden die adsorbierten Mengen als Funktion der Konzentration dargestellt (Abb. 4), so erhält man Kurven, die einen ähn-

lichen Ablauf aufweisen, wie die für die Jodadsorption an mit Wasserstoff bedeckter Oberfläche erhaltenen Kurven, indem sie bei einer gegebenen Konzentration einen Sättigungswert erreichen. Nach Überschreiten dieses Wertes steigt die adsorbierte Menge bei weiterer Konzentrationserhöhung nicht mehr.

Der Befund, wonach das Maß der Adsorption an mit chemiesorbierter Oxydschicht bedeckten Platinadsorbentien in einem recht breiten Konzentrationsbereich einen Wert von nur etwa 50% erreicht, obzwar dabei keine Oberflächensättigung stattfindet, kann damit erklärt werden, daß gleichzeitig mit der Jodadsorption die äußerste Oberflächenschicht des Adsorbens in Form eines Platin—Jod-Komplexes aufgelöst wird. Weiter unten wird auf den Beweis der Richtigkeit dieser Annahme noch näher eingegangen, hier soll nur darauf hingewiesen werden, daß nach den Daten der Tabelle III die je cm^2 der Oberfläche adsorbierte maximale Jodmenge auch in diesem Fall in guter Näherung als konstant zu betrachten ist.

Tabelle III

Adsorbent Nummer	Spezifische Oberfläche, m^2/g	Maximal adsorbierte Jodmenge	
		je 1 g Adsorbent, g	je 1 cm^2 Oberfläche, $\mu g/cm^2$
1.	2,0	$6 \cdot 10^{-3}$	0,30
2.	11,9	$37 \cdot 10^{-3}$	0,31
3.	13,0	$38 \cdot 10^{-3}$	0,29
4.	24,3	$66 \cdot 10^{-3}$	0,27

Die in Abb. 3 dargestellten Kurven beweisen, daß man im Falle der mit Oxydschicht bedeckten Platinadsorbentien aus der bloßen Tatsache, daß nur ein Bruchteil der in der Versuchslösung anwesenden Jodmenge adsorbiert wird, nicht darauf folgern darf, daß eine Oberflächensättigung erfolgt ist.

Es soll bemerkt werden daß Gemische von vorher reduzierten, also mit Wasserstoff bedeckten bzw. mit chemisorbierter Oxydschicht bedeckten Platinadsorbentien, je nach dem Verhältnis der beiden Komponenten, eine Jodadsorption von 50 bis 100% aufweisen können. Wenn die adsorbierte Jodmenge für diese Fälle als Funktion der Anfangs- oder auch der Gleichgewichts-Jodidionenkonzentration dargestellt wird, erhält man ähnliche Kurven wie die in Abb. 4 dargestellten, deren Verlauf mit den von BALASCHOWA und KASARINOW beschriebenen sog. logarithmischen Isothermen [8, 9] übereinstimmt.

c) Vergleich des Oberflächenbedarfes der adsorbierten maximalen Jodmenge mit der mittels der BET-Methode bestimmten Oberfläche.

Die Kurven in Abb. 1 und 3 zeigen, daß im Falle sämtlicher, von uns untersuchter Platinadsorbentien eine Sättigung der Oberfläche zu beobachten ist, so daß eine weitere Erhöhung der Jodidionenkonzetration in der Versuchslösung keine weitere Änderung der adsorbierten Jodmenge mit sich bringt. Ein

Vergleich der Adsorptions-Sättigungswerte und der mit der BET-Methode bestimmten Oberfläche zeigt, daß sich die je Flächeneinheit adsorbierte maximale Jodmenge linear mit der BET-Oberfläche ändert (Tabellen I, II und III).

Zum Vergleich der adsorbierten maximalen Jodmenge und der der Monoschicht entsprechenden Menge wurde der Oberflächenbedarf des adsorbierten Jods unter der Annahme berechnet, daß im Falle einer Oberflächensättigung an jedes Platinatom der Oberfläche ein Jodatom gebunden wird. Unter Berücksichtigung des Kristallsystems und der Gitterkonstante (3,91 Å) des Platins ergibt sich für den Oberflächenbedarf eines Jodatoms 7,6 Å^2, bzw. es entfallen $0.28 \cdot 10^{-6}$ g Jod auf 1 cm^2 der Jod-Monoschicht.

Die so berechneten sowie die mit der BET-Methode bestimmten Oberflächenwerte, ferner das Verhältnis der berechneten und gemessenen Oberflächenwerte zueinander sind in Tabelle IV und V angeführt. Die Daten der Tabelle V beziehen sich auf mit Oxydschicht bedeckte, die der Tabelle IV auf vorher mit Wasserstoff gesättigte Adsorbentien.

Tabelle IV

Adsorbent Nummer	Spez. Oberfläche bestimmt nach der BET Methode, m^2/g	Spez. Oberfläche berechnet aus dem Platzbedarf	Verhältnis der bestimmten und berechneten Oberflächen
1.	2,0	1,8	1,1
2.	11,9	9,6	1,2
3.	13,0	11,1	1,2
4.	24,3	17,8	1,4

Tabelle V

Adsorbent Nummer	Spez. Oberfläche bestimmt nach der BET Methode, m^2/g	Spez. Oberfläche berechnet aus dem Platzbedarf	Verhältnis der bestimmten und berechneten Oberflächen
1.	2,0	2,1	0,9
2.	11,9	13,2	0,9
3.	13,0	13,6	1,0
4.	24,3	23,5	1,0

Die Daten der Tabellen IV und V zeigen, daß im Falle der vorher reduzierten Adsorbentien die berechneten spezifischen Oberflächenwerte um etwa 10—25% niedriger sind als die mit der BET-Methode bestimmten Werte. Hingegen wurde im Falle der ohne reduzierende Vorbehandlung verwendeten Adsorbentien eine sehr gute Übereinstimmung zwischen den berechneten und den mit der BET-Methode bestimmten Oberflächenwerten gefunden.

4. Adsorptionsmechanismus an mit Wasserstoff bzw. mit Sauerstoff bedeckten Platinadsorbentien

Das unterschiedliche Verhalten der vorher reduzierten bzw. der mit Oxydschicht bedeckten Platinadsorbentien in bezug auf die Konzentrationsabhängigkeit der Adsorption sowie der Ausscheidungsmechanismus des Jods können auf Grund unserer Versuchsergebnisse unter Berücksichtigung der Eigenschaften der chemisorbierten Wasserstoff- bzw. Sauerstoffschicht gedeutet werden.

Aus den diesbezüglichen Angaben der Literatur geht hervor, daß eine Platinoberfläche in Kontakt mit atmosphärischem Sauerstoff praktisch als mit chemisorbierter Oxydschicht bedeckt betrachtet werden kann. Versuchsergebnisse von TRAPNELL und LANYON [11] weisen auf die Bildung einer nahezu monoatomaren Oxydschicht hin; ANSON und LINGANE konnten das Vorhandensein einer Oxydschicht an der Oberfläche sogar mit der üblichen analytischen Methode nachweisen, und fanden einen Wert von 6 für das Verhältnis jeder Platinatome der Oberfläche, an denen ein bzw. zwei Sauerstoffatome gebunden sind [12].

Die Gegenwart einer chemisorbierten Oxydschicht an der Oberfläche kann auch mit verschiedenen elektrochemischen Verfahren nachgewiesen werden, doch sind zwischen den Versuchsergebnissen verschiedener Autoren in bezug auf das Verhältnis der Sauerstoff- und Platinatome an der Oberfläche gewisse Widersprüche zu finden. FELDBERG und Mitarbeiter sowie OHASHI und HOARE halten auch die Bildung einer mehr Sauerstoffatome enthaltenden Oberflächen-Oxydschicht für möglich [13, 14, 15], während BÖLD und BREITER auf Grund der Analyse von mit potentiostatischer Dreieckmethode aufgenommenen Strom-Spannungskurven bloß die Bildung von PtO fanden [16].

Wegen der beträchtlichen Energie der Chemisorption von Sauerstoff an Platinoberflächen findet die thermische Zersetzung der Oxyd-Oberflächenschicht selbst in der Nähe des Schmelzpunktes von Platin nicht statt. Zwar kann die chemisorbierte Oxydschicht mit Wasserstoffgas reduziert werden, doch erfolgt in diesem Fall eine gleichzeitige Wasserstoff-Adsorption; die so gebildete adsorbierte Wasserstoffschicht kann bei 1 atm Wasserstoff-Druck mit einem Bedeckungsgrad von 0,84 charakterisiert werden [17, 18].

Unter Berücksichtigung der Tatsache, daß die mit atmosphärischem Sauerstoff in Berührung stehende Platinoberfläche mit chemisorbiertem Sauerstoff, während die Oberfläche eines mit Wasserstoff reduzierten Adsorbens mit atomarem Wasserstoff bedeckt ist, erscheint die Annahme berechtigt, daß die Ausscheidung von Jodidionen weder an oxydierten noch an reduzierten Platinadsorbentien als eine einfache Adsorption zu betrachten ist, sondern vielmehr als ein Austausch zwischen den Jodidionen und den vorher adsorbierten Wasserstoff- bzw. Sauerstoffatomen.

An mit Wasserstoff bedeckten Platinadsorbentien kann dieser Austausch mit Gl. (1) beschrieben werden, hingegen erfolgt an mit Sauerstoff bedeckten Adsorbentien auch eine Lösung der Oberflächenschicht des Adsorbens:

$$Pt-O + 2H^+ + 2J^- \rightarrow (PtIX_n)^{4-(n+1)} + H_2O + J \qquad (2)$$

und das gebildete elementare Jod wird an der zweiten Oberflächenschicht adsorbiert:

$$Pt + J \rightarrow Pt\,(J) \qquad (2a)$$

In Gl. (2) bedeutet $(PtJX_n)^{4-(n+1)}$ den von der Oberfläche gebildeten Platin–Jod-Komplex, wobei 4 die Koordinationszahl und X irgendein im System anwesender einwertiger Ligand ist. Ohne auf die Frage der Zusammensetzung bzw. der Struktur dieses Komplexes eingehen zu wollen, soll erwähnt werden, daß die durch Gl. (1) bzw. (2) beschriebenen Mechanismen auch durch die Resultate bestätigt werden, die wir über die pH^+-Änderung während der Adsorption erhielten. Die diesbezüglichen Ergebnisse sind in Tabelle VI angeführt.

Tabelle VI

Zustand des Adsorbents	Adsorbierte Jodmenge, g.Äquiv.	pH+-Änderung g.Äquiv.	Verhältnis der pH+-Änderung und der adsorbierten Jodmenge
Sauerstoffbedeckt	$4{,}5 \cdot 10^{-5}$	$8{,}78 \cdot 10^{-5}$	1,95
Wasserstoffbedeckt	$8{,}2 \cdot 10^{-6}$	$7{,}64 \cdot 10^{-6}$	0,93

Die Messung der pH-Änderung in den Versuchslösungen während der Adsorption wurde zum Unterschied von Versuchen, die die Bestimmung der adsorbierten maximalen Jodmenge bezweckten, mit Lösungen in 0.01 *n* Schwefelsäure durchgeführt, um eine gut meßbare Änderung zu erhalten.

Die Daten in Tabelle VI zeigen, daß das Verhältnis der durch die Jodadsorption verursachten Wasserstoff-Konzentrationsabnahme zu der Jodidionen-Konzentrationsabnahme im Falle von mit Wasserstoff bedeckten Adsorbentien etwa 1, hingegen im Falle von mit Oxydschicht bedeckten Adsorbentien etwa das Doppelte beträgt, was die Gültigkeit der Gleichungen (1) bzw. (2) bestätigt.

Die Lösung äußerster Oberflächenschicht von Platinadsorbentien, die in salzsaurem Medium auch von ANSON und LINGANE beobachtet wurde [12], kann darauf zurückgeführt werden, daß infolge der beträchtlichen Chemisorptionsenergie des Sauerstoffs (nach HAYWARD and TRAPNELL 70 kcal/Mol [19]), die Oberflächenatome zum Teil aus dem Kristallgitter herausgerissen werden [20].

Ebenfalls auf diese Ursache ist zurückzuführen, daß selbst bei einer überschüssigen Jodidionenkonzentration nur die Lösung der Oberflächenschicht, also der mit chemisorbiertem Sauerstoff bedeckten Platinschicht stattfindet.

Jene Beobachtung, wonach vor der Erreichung der Oberflächensättigung nur etwa die Hälfte der anwesenden Jodmenge an mit Sauerstoff bedeckten Adsorbentien adsorbiert wird, kann mit Hilfe der Gleichung (2) gedeutet werden, die übrigens darauf hinweist, daß in diesem Fall der zwischen der adsorbierten Menge und der Konzentration gemessene Zusammenhang — eben weil ein Teil der Jodionen einen Platin–Jod-Komplex bildet — als eine Adsorptionsisotherme von anderem Typ zu betrachten ist.

Es soll bemerkt werden, daß bei der Entgasung der Adsorbentien vor der Oberflächenbestimmung mit der BET-Methode eine gewisse Oberflächenabnahme (Alterung) zu beobachten war, falls diese bei der üblichen Temperatur (160—200°C) vorgenommen wurde. Die Frage der Oberflächenalterung sowie die Bestimmung der Oberfläche anderer Edelmetall-Katalysatoren mittels Jodadsorption werden den Gegenstand eineru nserer nächsten Arbeiten bilden.

LITERATUR

1. Balaschowa, N. A.: Zh. Fiz. Khim. XXXII. No. **10**, 2266 (1968)
2. Chien Chang Lin, Chaun-ting Chang, Si Yung Yeh: J. Atomic Energy Soc. of Japan **5**, 187 (1963)
3. Schwabe, K., Wagner, K., Weissmantel, Ch.: Z. Phys. Chem. **206**, 309 (1956)
4. Tóth, G.: Radiokhimija V. **4**, 411 (1963)
5. Tóth, G.: Magyar Kémiai Folyóirat **70**, 361 (1964)
6. Schwabe, K.: Electrochimica Acta **6**, 223 (1962)
7. Scwabe, K., Weissmantel, Ch.: Z. Phys. Chem. **215**, 48 (1960)
8. Balaschowa, N. A., Kazarinov, V. E.: Radiokhimija VII. 739 (1965)
9. Kazarinov, N. E., Balaschowa, N. A.: Dokl. Ak. Nauk CCCP **134**, 864 (1960)
10. Király, J.: Magyar Kémiai Folyóirat **68**, 77 (1962)
11. Lanyon, M. A. H., Trapnell, B. M. W.: Proc. Roy. Soc. (London) A**227** 387 (1955)
12. Anson, C., Lingane, J. J.: J. Am. Chem. Soc. **79**, 4901 (1957).
13. Feldberg, S. W., Enke, C. G., Bricker, C. E.: J. Electrochem. Soc. **110**, 826 (1963)
14. Ohaski, K., Sasaki, K., Nagaura, Sh.: Bull. Chem. Soc. Japan **39**, 2066 (1966)
15. Hoare, J. P.: J. Electrochem. Soc. **111**, 988 (1964)
16. Böld, W., Breiter, M.: Electrochimica Acta **5**, 145 (1961).
17. Deborin, G., Erschler, B.: Acta physicochimica USSSR **13**, 347 (1940)
18. Breiter, M., Knorr, C. A., Völkl, W.: Z. Elektrochemie **59**, 681 (1955)
19. Hayward, D. O., Trapnell, B. M. W.: Chemisorption, London 1964
20. Ponec, V.: J. Catalysis **6**, 362 (1966)
21. Llopis, J., Gamboa, J. M., Alfayate, J. M.: Electrochimica Acta **12**, 57 (1967)

Géza Tóth
László Zsinka } Budapest XII., Konkoly Thege M. út

Acta Chimica Academiae Scientiarum Hungaricae, Tomus 61 (3), pp. 301—308 (1969)

METHANOLYSIS OF LUTEIN DITRICHLOROACETATE

PREPARATION OF 3-HYDROXY-3′-METHOXY-α-CAROTENE AND 3-HYDROXY-5′-METHOXY-4′,5′-DIHYDRO-3′,4′-DEHYDRO-α-CAROTENE

J. SZABOLCS and Á. RÓNAI

(Chemical Institute of the Medical University, Pécs)

Received July 4, 1968

Selective methanolysis of the 3′-trichloroacetoxy group of lutein ditrichloroacetate has been observed yielding two isomeric lutein monomethyl trichloroacetates, the structures of which have been proved. The methanolysis provides a new test for the detection of some OH groups in carotenoids which are in a position similar to that of the 3′-hydroxyl group of lutein.

The difference in behaviour between the 3- and 3′-hydroxyl groups of lutein I manifests itself in several reactions and, as it is to be expected, the 3′-OH group, *i.e.* the allylic one, is more reactive.

ZECHMEISTER [1, 2, 3] and SEASE observed 25 years ago that lutein gave desoxyluteins by water elimination during which the 3′-hydroxyl group was lost. Later, by the treatment of lutein with methanol and hydrochloric acid, CURL [4] succeeded in preparing 3-hydroxy-3′-methoxy-α-carotene. GROB and PFLUGSHAUPT [5] made similar observations on the ether formation of the 3′-hydroxyl group of lutein. More recently, JENSEN and HERTZBERG [6] have pointed out that the allylic hydroxyl group of lutein can be oxidized selectively with nickel peroxide into 3-hydroxy-3′-keto-α-carotene.

In our laboratory it was observed that selective methanolysis of the 3′-trichloroacetoxy group of lutein ditrichloroacetate occurs when the compound is allowed to stand in methanolic solution at room temperature. As this solvolysis was not only interesting, but also seemed to promise a new test for the detection of some OH groups in carotenoids, methanolysis was investigated more thoroughly.

Lutein I gives lutein ditrichloroacetate in a good yield with trichloroacetyl chloride in a mixture of anhydrous pyridine and benzene, and the product can be crystallized from acetone–petroleum ether, m.p. 130° C (lutein ditrichloroacetate furnishes lutein either by base-catalyzed hydrolysis, or on treatment with lithium aluminium hydride). Lutein ditrichloroacetate, however, yields two isomeric monomethoxylutein-3-trichloroacetates when it is dissolved in methanol and allowed to stand at room temperature. As chromatography alone failed to separate the two methoxy derivatives, they were submitted to hydrolysis before chromatography. One of the two main products proved to be identical with 3-hydroxy-3′-methoxy-α-carotene, V, whose struc-

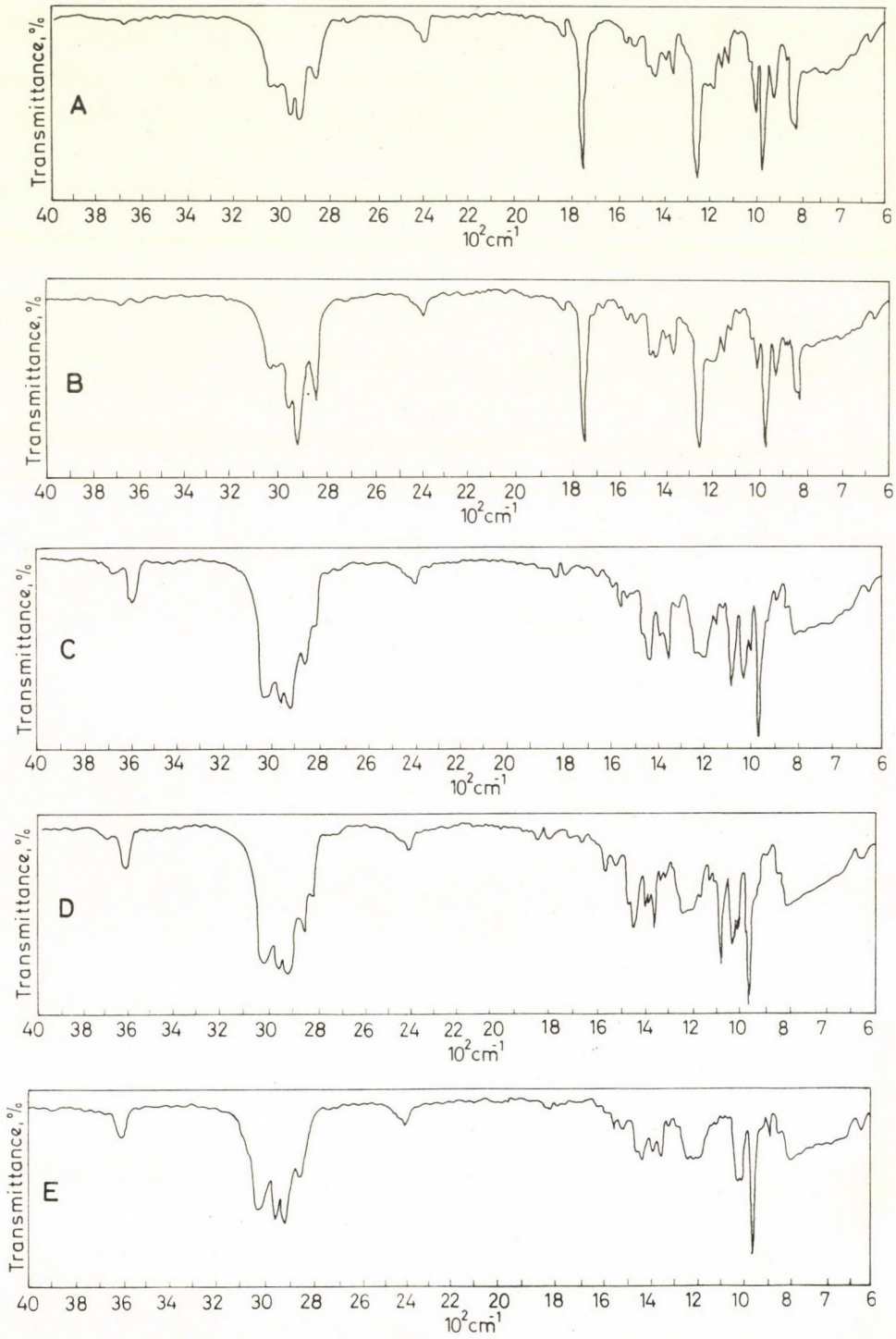

Fig. 1. IR spectra of trichloroacetates and of the products of methanolysis in $CHCl_3$. *A:* zeaxanthin ditrichloroacetate; *B:* lutein ditrichloroacetate; *C:* 3-hydroxy-3′-methoxy-α-carotene; *D:* 3-hydroxy-5′-methoxy-4′,5′-dihydro-3′,4′-dehydro-α-carotene; *E:* 3-hydroxy-2′,3′-dehydro-α-carotene

ture was demonstrated recently by JENSEN [6]. The light absorption properties of the other product (*cf.* Figs 1, 2, 3), which is adsorbed at a higher level in the calcium carbonate column, are identical with those of 3-hydroxy-3′--methoxy-α-carotene, and both products have the same molecular formula ($C_{41}H_{58}O_2$).

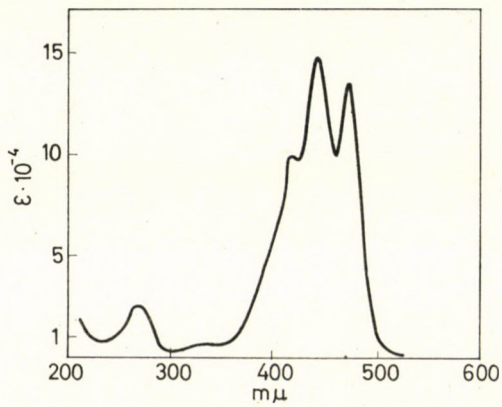

Fig. 2. Molecular extinction curve of 3-hydroxy-3′-methoxy-α-carotene in benzene

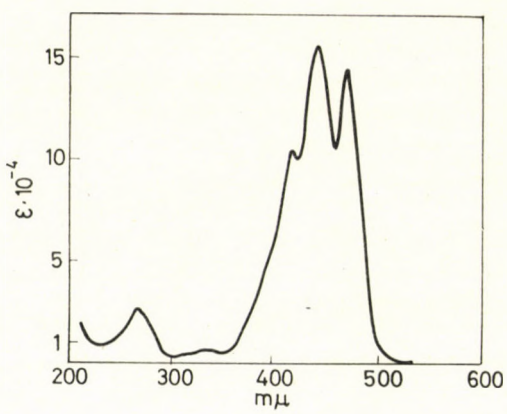

Fig. 3. Molecular extinction curve of 3-hydroxy-5′-methoxy-4′, 5′-dihydro-3′, 4′-dehydro--α-carotene in benzene

3-hydroxy-3′-methoxy-α-carotene and the isomeric derivative cannot be isomerized into each other either by refluxing or with iodine. In their UV spectra there is no *cis* peak, they give different isomer sets, and thus the possibility of *cis-trans* isomerism is to be ruled out. As zeaxanthin ditrichloroacetate (see Fig. 1*A*) fails to solvolyze under the conditions in which lutein ditrichloroacetate does, the 3-methoxy-3′-hydroxy-α-carotene structure cannot be taken into consideration.

It is assumed that the isomeric lutein monomethyl ether is 3-hydroxy--5′-methoxy-4′,5′-dihydro-3′,4′-dehydro-α-carotene, **VI**. The formation of the latter may be explained by allylic rearrangement — as shown in Table I — as proposed by ZECHMEISTER [2], who gave this "probable mechanism" as an explanation for the formation of desoxyluteins from lutein by water elimination.

The appearance of an allyl cation, and so the possibility of allylic rearrangement, is supported by the fact that an anhydrous derivative, **VII**, as a by-product, always appears in the trichloroacetylation of lutein. This derivative is obviously formed *via* a resonance hybrid cation (**III**, **IV**) by loss of proton. Considering that according to ZECHMEISTER [2], carbonium ion **III** can furnish only one derivative by losing a proton (3-hydroxy-2′,3′-dehydro-α--carotene; the so-called [2] desoxylutein „III"), but carbonium ion **IV** may give rise to two (desoxylutein "I" and desoxylutein "II"), it seems likely that the anhydrous derivative formed alone in the trichloroacetylation of lutein is identical with desoxylutein "III". The identity of the two compounds was also demonstrated experimentally.

Considering that trichloroacetylation and solvolysis take place in a good yield, this method is suitable for the detection of hydroxyl groups in a position similar to that of the 3′-hydroxyl group of lutein. A report on the structure of α-cryptoxanthin as revealed by this method will be published elsewhere.

It should be noted that reactivity of the allylic hydroxyl group of lutein can explain why in many cases, the melting point of lutein does not reach even after several re-chromatographies and recrystallizations the lit. value (193° C), and in fact, it may decrease on recrystallization.

Experimental

The visual absorption maxima (in mμ) were determined in a grid spectroscope Type Löwe-Schumm, and the melting points on a Kofler block. The visible and infrared absorption spectra were recorded on Beckman DU and Zeiss (Jena) UR 10 Spectrophotometer, respectively. The widths of zones are given in mm.

Lutein ditrichloroacetate

To a solution of 50 mg of lutein in 1 ml of absolute pyridine and 10 ml of absolute benzene there was added a solution of 0.2 ml trichloroacetyl chloride in 1 ml of absolute pyridine and 10 ml absolute benzene, and the mixture was shaken under dry nitrogen for 60 min. Then it was filtered, and the pigments transferred to 200 ml of petroleum ether in a separatory funnel, and washed thoroughly with water. The pyridine-free solution was then dried over anhydrous Na_2SO_4, the solvent removed in vacuum, and the residue crystallized from acetone–petroleum ether. Recrystallization gave 41 mg of yellow needles, m.p. 130° C. The pigment showed epiphasic behaviour between 95% methanol and petroleum ether, and had absorption maxima in hexane at 474, 444 and 420 mμ (10^{-3} E, 128.1, 138.7, and 93.2, respectively). The IR spectrum obtained in $CHCl_3$ is presented in Fig. 1.
$C_{44}H_{54}O_4Cl_6$. Calcd. C 61.47; H 6.45. Found C 62.23; H 7.00%

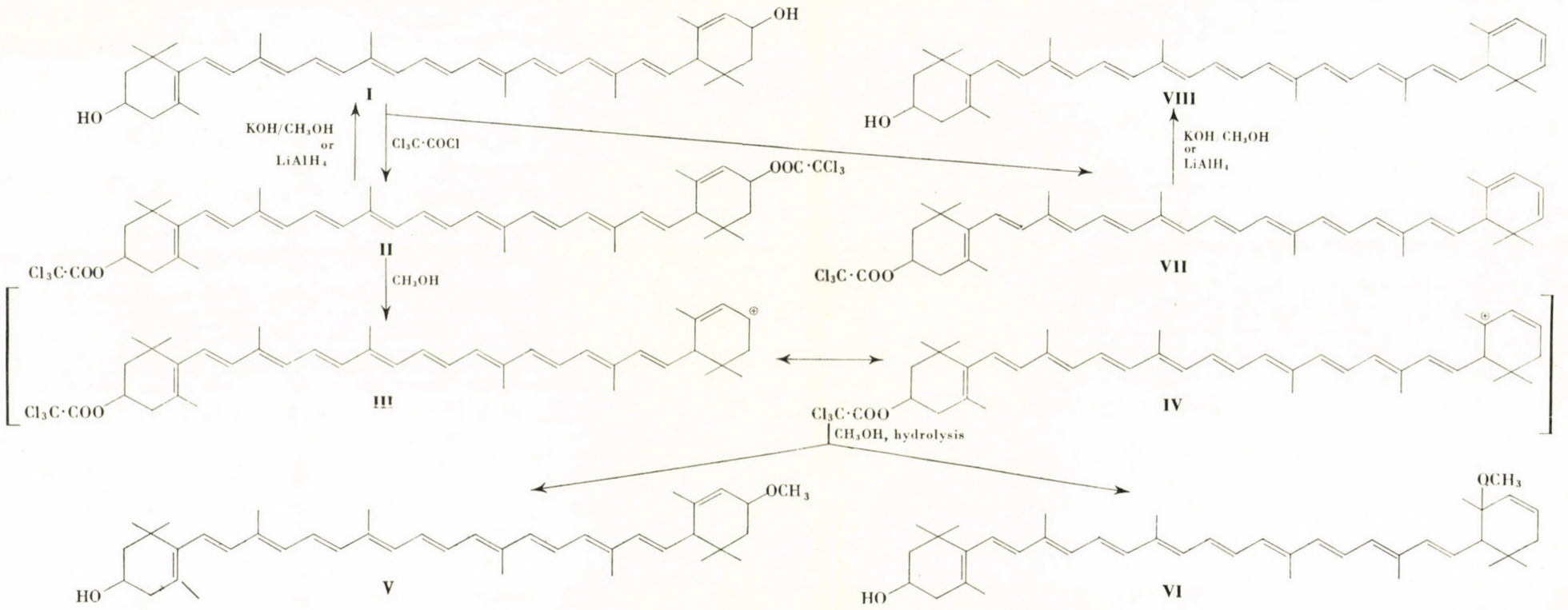
I
HO
OH
KOH/CH₃OH
or
LiAlH₄
Cl₃C·COCl
II
Cl₃C·COO
OOC·CCl₃
CH₃OH
III
Cl₃C·COO
IV
Cl₃C·COO
CH₃OH, hydrolysis
V
HO
OCH₃
VI
HO
OCH₃
VII
Cl₃C·COO
KOH/CH₃OH
or
LiAlH₄
VIII
HO

Base-catalyzed hydrolysis of lutein ditrichloroacetate

A solution of lutein ditrichloroacetate (10 mg) in ether (20 ml) was allowed to stand in the presence of 4 ml of a 30% KOH solution in methanol under nitrogen for 18 hrs. The hydrolyzed mixture was washed thoroughly with water, dried over anhydrous Na_2SO_4, and evaporated in vacuum. The residue was dissolved in a mixture of benzene and petroleum ether and submitted to chromatography on calcium carbonate.

Bands	Products	Abs. max. in petroleum ether	
1 brownish-yellow	unidentified	—	—
(1) 30 yellow	lutein	477	447
(2) 5 orange	desoxylutein "III"	477	447

Pigment 1 was hypophasic on partition between 90% methanol and petroleum ether, and did not separate from an authentic lutein sample in mixed chromatogram test.

Pigment 2 was mainly epiphasic between 95% methanol and petroleum ether, and was not separated in the mixed chromatogram from an authentic sample of desoxylutein "III".

Treatment of lutein ditrichloroacetate with $LiAlH_4$

Lutein ditrichloroacetate (10 mg) was dissolved in 30 ml anhydrous ether and added to a magnetically stirred slurry of lithium aluminium hydride (about 20 mg) in 10 ml of anhydrous ether. After 15 min the reaction was completed and the excess of hydride destroyed by the careful addition of moist ether and 10% potassium hydroxide solution. After the usual procedure, the product was chromatographed on calcium carbonate from benzene–petroleum ether (1 : 1).

Bands	Products	Abs. max. in petroleum ether	
(1) 1 yellow	unidentified	473	443
(2) 35 yellow	lutein	476	447
(3) 6 yellow	desoxylutein "III"	476	446

Pigment 2 was hypophasic between 90% methanol and petroleum ether. It did not separate from an authentic sample of lutein in a mixed chromatogram.

Pigment 3 was divided between 95% methanol and petroleum ether and did not show separation in the mixed chromatogram test from an authentic sample of desoxylutein "III".

Solvolysis of lutein ditrichloroacetate during crystallization from benzene–methanol at room temperature

600 mg of lutein was trichloroacetylated by the method described above, and then crystallized from 8 ml of benzene by the careful addition of 50 ml of methanol (the solution being kept at room temperature for 4 hrs, at 0° C for 12 hrs and finally, at —15° C for 5 hrs). As the precipitate did not give a sharp m.p. even after recrystallization, it was submitted to chromatography. In the adsorption column, however, probably owing to decomposition that took place in the column, it gave indistinct zones.

Therefore it was dissolved in 300 ml of ether and allowed to stand in the presence of a 30% KOH solution in methanol under nitrogen at room temperature for 16 hrs. After washing with water, drying, and evaporation in vacuum, the residue was chromatographed on calcium carbonate from benzene–petroleum ether.

Bands	Products	Abs. max. in petroleum ether	
5 brown	unidentified	—	—
(1) 30 yellow	3-hydroxy-5′-methoxy-4′,5′-dihydro-3′,4′-dehydro-α-carotene	476	445
1 light yellow	—	—	—
(2) 70 yellow	3-hydroxy-3′-methoxy-α-carotene	476	445
(3) 4 yellow	desoxylutein "III"	476	446
1 light yellow	—	—	—

The bands were eluted with a mixture of benzene and methanol, transferred to benzene in separatory funnels, washed with water, dried over anhydrous Na_2SO_4, evaporated in vacuum, and the residues crystallized.

Pigment 1 (3-hydroxy-5′-methoxy-4′,5′-dihydro-3′,4′-dehydro-α-carotene) was dissolved in 3 ml of benzene, then 20 ml of methanol was carefully added, and the mixture was allowed to stand at —15° C for 12 hrs. Recrystallization gave 45 mg of glittering plates, m.p. 130° C. On partition between 95% methanol and petroleum ether it was found in the upper phase. The visible and UV spectra are presented in Fig. 3, the IR spectrum obtained in chloroform is shown in Fig. 1*D*.

$C_{41}H_{58}O_2$. Calcd. C 84.48; H 10.03. Found C 83.78; H 10.09%.

Pigment 2 (3-hydroxy-3′-methoxy-α-carotene) was dissolved in 3 ml of benzene and crystallized by the addition of 35 ml of methanol at —15 °C. 160 mg of orange-coloured plates were obtained, m.p. 168 °C. The visible and UV spectra are shown in Fig. 2; the IR spectrum taken in chloroform, is presented in Fig. 1*C*. On partition between 95% methanol and petroleum ether both phases were coloured, the greater part of the pigment, however, was found in the epiphase.

$C_{41}H_{58}O_2$. Calcd. C 84.48; H 10.03. Found C 84.65; H 10.21%.

Pigment 3 (desoxylutein "III") was dissolved in a small amount of benzene, mixed with 4 ml of methanol and allowed to stand at —15° C. The pigment crystallized in glittering plates and did not separate from an authentic sample of desoxylutein "III" in a mixed chromatogram. The pigment was epiphasic between 95% methanol and petroleum ether. The IR spectrum obtained in chloroform is presented in Fig. 1*E*.
$C_{40}H_{54}O$. Calcd. C 87.21; H 9.88. Found C 87.44; H 10.27%.

Zeaxanthin ditrichloroacetate

50 mg of zeaxanthin was treated with trichloroacetyl chloride as described for the preparation of lutein ditrichloroacetate. Recrystallization from benzene–methanol yielded 35 mg of zeaxanthin ditrichloroacetate as long needles, m.p. 170° C.

The pigment exhibited entirely epiphasic properties. The IR spectrum recorded in $CHCl_3$ is presented in Fig. 1 *A*.
$C_{44}H_{54}O_4Cl_6$. Calcd. C 61.47; H 6.45. Found C 61.74; H 6.62%.

Solvolysis of lutein ditrichloroacetate in benzene–methanol

3 mg of lutein ditrichloroacetate in a mixture of benzene (3 ml) and methanol (12 ml) were allowed to stand under nitrogen at room temperature for 18 hrs. After completion of the solvolysis, the solution was washed with water, dried over anhydrous Na_2SO_4, evaporated in vacuum, and the residue dissolved in 20 ml of ether and hydrolyzed at room temperature in the presence of 4 ml 30% KOH solution in methanol for 18 hrs. Finally, it was transferred to ether, thoroughly washed with water, and chromatographed on calcium carbonate from a mixture of benzene and petroleum ether (1 : 5).

Bands	Products	Abs. max. in petroleum ether	
(1) 1 yellow	unidentified	479	448
(2) 5 yellow	lutein	477	447
(3) 15 yellow	3-hydroxy-5′-methoxy-4′,5′-dihydro-3′, 4′-dehydro-α-carotene	476	446
(4) 25 yellow	3-hydroxy-3′-methoxy-α-carotene	476	446
(5) 2 yellow	desoxylutein "III"	477	447

Pigment 1 was not identified because of lack of material.

Pigment 2 did not separate from an authentic sample of lutein in a mixed chromatogram, and it was found in the lower phase between 90% methanol and petroleum ether.

Pigments 3, 4 and 5 were identified, using the products obtained in the course of the previous experiments, by mixed chromatograms, partition tests, etc.

It should be mentioned that lutein ditrichloroacetate gave an entirely identical chromatogram when solvolyzed under similar conditions but decomposed by $LiAlH_4$.

Isomerization of 3-hydroxy-3′-methoxy-α-carotene

(a) Isomerization by refluxing in benzene solution. 3 mg of pigment **V** in 15 ml of benzene was refluxed under nitrogen in semidarkness for 2 hrs. Chromatography was carried out on calcium carbonate from benzene–petroleum ether (1 : 3).

Bands	Products	Abs. max. in petroleum ether	
1 brown	unidentified	—	—
(1) 30 yellow	3-hydroxy-3′-methoxy-α-carotene	476	446
(2) 10 yellow	*cis* isomer	473	442

In a mixed chromatogram pigment 1 proved to be identical with the starting material. Pigment 2 could be isomerized into pigment 1 by refluxing.

(b) Isomerization by iodine. 4 mg of pigment **V** in 40 ml of benzene and in the presence of 0.04 mg of iodine was allowed to stand at room temperature for 30 min. The solution was washed with aqueous sodium thiosulphate solution and water, and dried over anhydrous Na_2SO_4. It was then chromatographed on calcium carbonate from benzene–petroleum ether (1 : 5).

Bands	Products	Abs. max. in petroleum ether	
(1) 30 yellow	3-hydroxy-3-methoxy-α-carotene	476	446
(2) 5 light	*cis* isomer	467	437
(3) 20 yellow	*cis* isomer	471	441

Pigment 1 did not separate from the starting material in the mixed chromatogram. Pigments 2 and 3 could be isomerized into the starting material by refluxing.

Isomerization of 3-hydroxy-5′-methoxy-4′,5′-dihydro-3′,4′-dehydro-α-carotene

(a) Isomerization by refluxing in benzene solution. 3 mg of pigment **VI** was dissolved in 15 ml of benzene and refluxed under nitrogen for 2 hrs. The solution was chromatographed on calcium carbonate from benzene–petroleum ether (1 : 5).

Bands	Products	Abs. max. in petroleum ether	
(1) 12 yellow	*cis* isomer	471	441
(2) 30 yellow	3-hydroxy-5′-methoxy-4′,5′-dihydro-3′,4′-dehydro-α-carotene	476	446

Pigment 1 is a *cis* isomer and can be converted into pigment 2, which is the unchanged starting material; the conversion product did not separate from the starting material in a mixed chromatogram.

(b) Isomerization by iodine. 4 mg of pigment **VI** was dissolved in 40 ml of benzene and allowed to stand in the presence of 0.04 mg of iodine at room temperature for 30 min. The solution was washed with aqueous sodium thiosulphate solution and water, dried over anhydrous Na_2SO_4, and chromatographed on calcium carbonate from benzene–petroleum ether (1 : 5).

Bands	Products	Abs. max. in petroleum ether	
(1) 14 yellow	*cis* isomer	470	441
(2) 40 yellow	3-hydroxy-5′-methoxy-4′,5′-dihydro-3′, 4′-dehydro-α-carotene	476	446

Pigment 1 is a *cis* isomer, and can be isomerized into pigment 2, which is the unchanged starting material; the conversion product did not separate from the starting material in a mixed chromatogram.

*

We would like to express our thanks to Mr. L. TIMÁR for the elementary analyses, and to Miss M. HÁM for assistance in the chromatographic work.

REFERENCES

1. ZECHMEISTER, L., SEASE, J. W.: J. Am. Chem. Soc. **65**, 1951 (1943)
2. ZEICHMEISTER, L.: Fortschritte d. Chem. Org. Naturst. **XV**, 62 (1958)
3. ZECHMEISTER, L., PETRACEK, F. J.: Arch. Biochem. Biophys. **61**, 243 (1956)
4. CURL, L.: Food Res. **21**, 589 (1956)
5. GROB, E. C., PFLUGSHAUPT, R. P.: Helv. Chim. Acta **45**, 1592 (1962)
6. JENSEN, S. L., HERTZBERG, S.: Acta Chem. Scand. **20**, 1703 (1966)

József SZABOLCS
Ádám RÓNAI
Pécs, Rákóczi út 80, Hungary

Acta Chimica Academiae Scientiarum Hungaricae, Tomus 61 (3), pp. 309—313 (1969)

THE STRUCTURE OF α-CRYPTOXANTHIN AND THE IDENTITY OF ZEINOXANTHIN WITH α-CRYPTOXANTHIN

J. SZABOLCS and Á. RÓNAI

(Chemical Institute of the Medical University, Pécs)

Received July 4, 1968

On the basis of chemical evidence it has been shown that the structure of α-cryptoxanthin is 3-hydroxy-α-carotene, *i.e.* α-cryptoxanthin is identical with zeinoxanthin.

α-Cryptoxanthin was isolated from *Capsicum annuum* var. *Lycopersiciforme flavum* by CHOLNOKY *et al.* [1] in 1958. On the basis of its microanalysis, spectral properties, vitamin A potency, and pronounced similarity in many respects to β-cryptoxanthin, it was assumed that α-cryptoxanthin was 3'-hydroxy-α-carotene. BODEA [2, 3] also reported the isolation of 3'-hydroxy-α-carotene (with the name physoxanthin) from *Physalis Alkekengi* but, as revealed by other investigations [4, 5], "physoxanthin" was identical with neo-β-cryptoxanthin A. In 1960 PETZOLD and QUACKENBUSHE [6] reported the occurrence in maize of a new carotenol which was identified, first of all on the basis of its physical properties and lack of vitamin A potency, as 3-hydroxy-α-carotene and called zeinoxanthin. Thus it seemed that on the analogy of other phytoxanthins, both monohydroxy derivatives of α-carotene occurred in nature.

In view of the lack of chemical evidence for the structure of either α-cryptoxanthin or zeinoxanthin, it seemed worth-while to reinvestigate their structures. The necessity of such investigation was confirmed by a report in which FARKAS [7] identified α-cryptoxanthin with zeinoxanthin in a mixed chromatogram.

The molecular formula ($C_{40}H_{56}O$) shows that there is an isomeric relationship between α-cryptoxanthin and β-cryptoxanthin. The decaene chromophore [λ_{max} (C_6H_6) 488, 457 and 433 mμ; 10^{-3} E, 116.9, 130.0 and 86.5, respectively] and the presence of a hydroxyl group [ν_{max}($CHCl_3$) 3615 cm^{-1}] follow from the light absorption properties (see Fig. 1).

The 3'-hydroxy-α-carotene structure of α-cryptoxanthin, as proposed by CHOLNOKY *et al.* [1], could have been confirmed by a simple methanolysis test [8] of α-cryptoxanthin trichloroacetate. Namely, the 3'-hydroxyl group of α-cryptoxanthin occupies the same position as the 3'-OH group of lutein, of which it is known that, after trichloroacetylation, it undergoes methanolysis resulting in monomethoxy derivatives. The present experiments have, however,

revealed that α-cryptoxanthin trichloroacetate [ν_{max} (KBr) 1764 cm^{-1}; zeaxanthin ditrichloroacetate had ν_{max} (KBr) 1761 cm^{-1} !] fails to solvolyse under the conditions in which lutein ditrichloroacetate does (β-cryptoxanthin trichloroacetate, as is to be expected, does not undergo methanolysis). Therefore the 3'-hydroxy-α-carotene structure of α-cryptoxanthin must be ruled out.

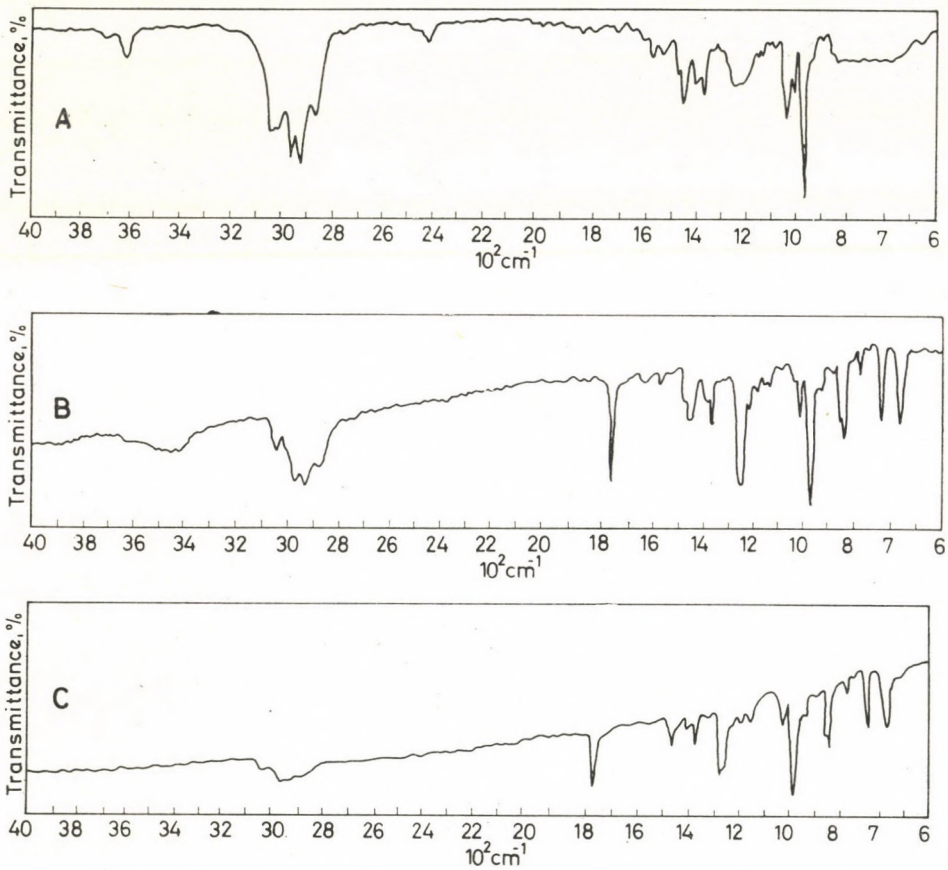

Fig. 1. IR spectra. A: Spectrum of α-cryptoxanthin in $CHCl_3$; B: Spectrum of α-cryptoxanthin trichloroacetate (KBr); C: Spectrum of β-cryptoxanthin trichloroacetate (KBr)

In agreement with the above result the isolation of α-apo-2-carotenal, II, in the potassium permanganate oxidation [9] of α-cryptoxanthin acetate provides evidence for the presence of an unsubstituted α-ionone ring in α-cryptoxanthin.

α-Cryptoxanthin trichloroacetate had τ ($CDCl_3$) 9.18, 9.12, 8.89—8.87, 8.26, 8.44, 8.10 and 8.04, of which 9.18, 9.12, 8.44 and 8.10 are in good agreement with those of ε-carotene, while 8.89—8.87 and 8.26 are also present in the spectrum of zeaxanthin [11]. The band at 8.04 is due to the in-chain methyls.

A doublet at 7.74 indicates a methylene group at C—4, similar to the end groups in zeaxanthin split by spin-spin coupling with the single proton at C—3 (see Fig. 2). On the other hand, the presence of the methylene group at C—4

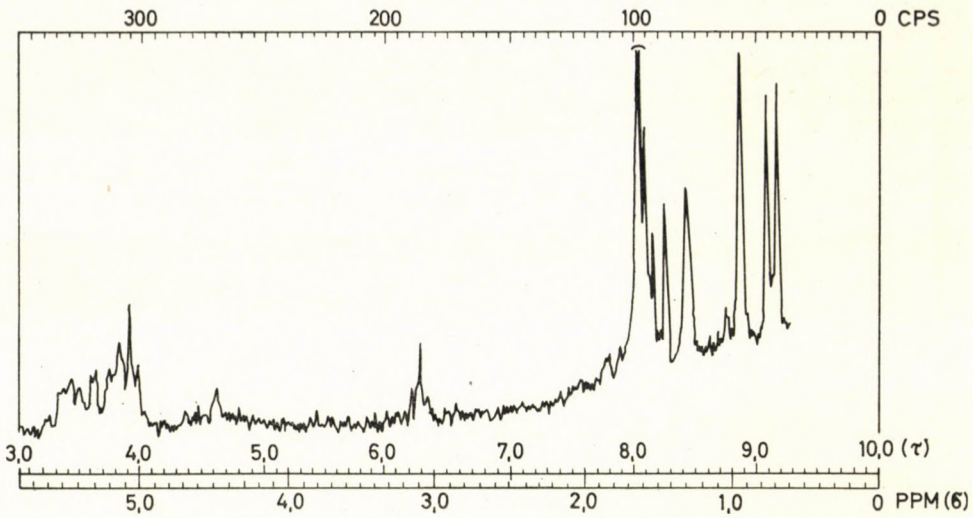

Fig. 2. NMR spectrum of α-cryptoxanthin trichloroacetate in $CDCl_3$ at 100 Mc/sec

was also confirmed by treatment of α-cryptoxanthin with hydrogen chloride in chloroform. If there were an OH group in allylic position at C—4, this dehydratation test [10] would result in anhydro-α-cryptoxanthin, which was never found.

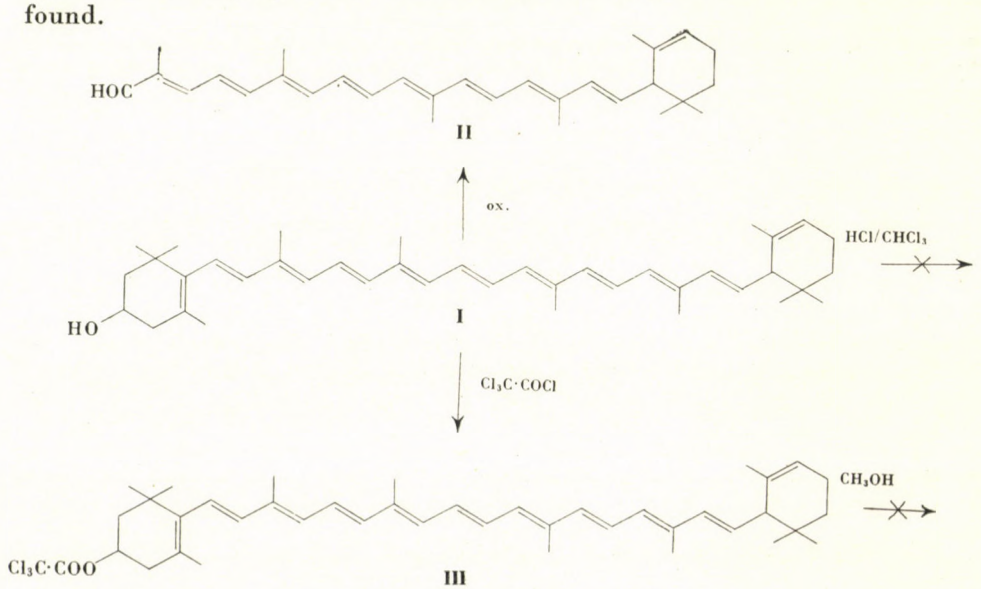

Chart 1

All these experiments are consistent with formula I (see Chart 1), in which one end group is similar to that of ε-carotene and the other to that of zeaxanthin, *i.e.* α-cryptoxanthin is 3-hydroxy-α-carotene.

The revised structure of α-cryptoxanthin is in good agreement with the fact already mentioned that α-cryptoxanthin did not separate from zeinoxanthin in a mixed chromatogram [7]. The vitamin A potency of α-cryptoxanthin had originally been demonstrated in a sample precipitated from mother liquors, thus it must have been due to the presence of impurities.

In future publications we shall refer to α-cryptoxanthin as 3-hydroxy-α-carotene.

*

The authors wish to express their thanks to Professor B.C.L. WEEDON for his valuable comment on the NMR spectrum of α-cryptoxanthin trichloroacetate.

Experimental

The routine procedures and measurements used in this work have been summarized in a previous publication [8]. α-Cryptoxanthin was isolated from *Capsicum annuum* var. *Lycopersiciforme flavum.*

α-Cryptoxanthin trichloroacetate

A solution of 25 mg of α-cryptoxanthin in 0.5 ml of anhydrous pyridine and 5 ml of absolute benzene was mixed with 4 drops of trichloroacetyl chloride in 0.5 ml of anhydrous pyridine and 3 ml of absolute benzene. The mixture was shaken at room temperature for 60 min. The rate of acylation was followed by TCL (Kieselgel G; developing solvent: benzene). After completing the reaction, the solution was diluted with petroleum ether, filtered into a separatory funnel, washed thoroughly with water, dried over anhydrous Na_2SO_4, and evaporated in vacuum. The residue was crystallized from a mixture of benzene and methanol to obtain 17 mg, m.p. 158°C; The IR spectrum (KBr disc) is presented in Fig. 1B. On partition between 95% methanol and petroleum ether the product was found entirely in the upper phase.

When α-cryptoxanthin trichloroacetate was allowed to stand in methanolic solution under conditions similar to those used for lutein ditrichloroacetate, it was recovered unchanged and no methanolysis occurred.

β-Cryptoxanthin trichloroacetate

β-Cryptoxanthin trichloroacetate was prepared in the usual manner from β-cryptoxanthin originating from *Capsicum annuum* var. *Lycopersiciforme rubrum.* It crystallized from benzene and methanol in yellow to orange plates, m. p. 148°C. The IR spectrum, recorded in chloroform, is presented in Fig. 1C.

$KMnO_4$ oxidation of α-cryptoxanthin acetate

7 mg of α-cryptoxanthin acetate in 20 ml of benzene was shaken with 20 ml of potassium permanganate solution (0.31 g of $KMnO_4$ and 0.5 g of anhydrous Na_2CO_3 in 100 ml of water) at room temperature for 4 hrs. The decomposition of α-cryptoxanthin acetate was followed by TLC. Manganese dioxide was then filtered off, the oxidation products were eluted with benzene containing some methanol, transferred into a separatory funnel, washed with water, dried over anhydrous Na_2SO_4, and the solvent evaporated in vacuum. The residue was dissolved in a small amount of petroleum ether and subjected to chromatography on calcium carbonate, and developed with petroleum ether.

Bands	Pigments	λ_{max} (mμ) in petroleum ether		
2 orange	α-apo-2-carotenal	(495)	457	427
2 yellow				439
30 orange		481	451	
		518*	484*	452*
5 yellow		477	(450)	(439)

* in CS_2

After the usual procedure described above, pigment 1 was identified as follows:

(i) By the spectral properties (λ_{max} in petroleum ether and carbon disulfide were at 481, 453 and 519, 486, 454 mμ, respectively).

(ii) On partition between 95% methanol and petroleum ether it was found in the upper phase (before the partition test pigment 1 had been kept under the conditions of hydrolysis).

(iii) In a mixed chromatogram, pigment 1 did not separate from an authentic sample of α-apo-2-carotenal ($R_F = 0.55$ on Kieselgel G; developing solvent: benzene), but it separated from α-citraurin and α-citraurin acetate ($R_F = 0.21$).

(iv) Pigment 1 gave a set of isomers similar to that from an authentic sample of α-apo-2-carotenal and differing from the set of β-apo-2-carotenal.

Isomerization with iodine in petroleum ether on a calcium carbonate column produced the following chromatogram:

Bands	Pigments	λ_{max} (mμ) in petroleum ether	
20 orange	α-apo-2-carotenal	481	452
2 pink		475	445
10 pale pink		474	445

We would like to express our thanks to Miss M. HÁM for assistance in the chromatographic work, and to Mr. L. TIMÁR for the IR spectra.

REFERENCES

1. CHOLNOKY, L., SZABOLCS, J., NAGY, E.: Ann. **616**, 207 (1958)
2. BODEA, C., NICOARA, E.: Ann. **609**, 181 (1957)
3. BODEA, C., NICOARA, E.: Ann. **635**, 137 (1960)
4. CHOLNOKY, L., SZABOLCS, J.: Ann. **626**, 206 (1959)
5. CHOLNOKY, L., SZABOLCS, J., TIMÁR, M.: Ann. **663**, 202 (1963)
6. PETZOLD, E. N., QUACKENBUSH, F. W.: Arch. Biochem. Biophys. **86**, 163 (1960)
7. FARKAS, M.: A Veszprémi Vegyipari Egyetem Közleményei **8**, 291 (1964)
8. SZABOLCS, J., RÓNAI, A.: Acta Chim. Acad. Sci. Hung. (In the press)
9. V. EULER, H., KARRER, P., SOLMSSEN, U.: Helv. Chim. Acta **21**, 211 (1938)
10. KARRER, P., LEUMANN, E.: Helv. Chim. Acta **34**, 445 (1951)
11. WEEDON, B. C. L.: Chemistry of the Carotenoids, Chapter 3, 92 (Chemistry and Biochemistry of Plant Pigments, edited by T. W. Goodwin). Academic Press, London and New York 1965.

József SZABOLCS
Ádám RÓNAI
Pécs, Rákóczi út 80, Hungary

Acta Chimica Academiae Scientiarum Hungaricae, Tomus 61 (3), pp. 315—324 (1969)

CHEMISTRY OF 1,3-BIFUNCTIONAL SYSTEMS, VI*

EXAMINATION OF THE TRANSFORMATIONS OF 4-METHYL-1,3-DIOXANE ON VARIOUS CATALYSTS BY MEANS OF THE MICRO REACTOR TECHNIQUE

M. Bartók, J. Apjok, R. A. Karakhanov** and K. Kovács

(Institute of Organic Chemistry, A. József University, Szeged)

Received June 24, 1968

The transformations of 4-methyl-1,3-dioxane have been studied in the presence of hydrogen, on thermolite-supported platinum, palladium and rhodium, further, on nickel-aluminium and copper-aluminium catalysts, using the micro reactor technique. The degree of decomposition of 4-methyl-1,3-dioxane and the relative ratio of the various reaction paths were examined as a function of the experimental parameters, such as the nature and amount of catalyst, and temperature. Under the conditions applied, the transformation of this compound proved to be a complex process, composed of several primary and secondary reactions. The main reaction paths are: total fragmentation giving rise to olefins and saturated hydrocarbons; partial fragmentations yielding butyraldehyde, butanol, methyl ethyl ketone, and *sec.*-butanol, and finally isomerization to *n*- and *sec.*-butyl formate. The observation of the isomerization of 1,3-dioxanes to esters means not only the recognition of a new reaction, but at the same time it represents a new type of 1,3-rearrangements proceeding through a four-membered transition state.

In the course of an examination of the chemical transformations of 1,3-bifunctional carbon compounds, experiments were carried out concerning the reactions of 1,3-dioxanes on different contact catalysts. In this work attention was focused mainly on the effect of metal contact catalysts upon the degree of decomposition, and the course of the conversions of 1,3-dioxanes of various structures. No publications had been found in the literature dealing with the reactions of 1,3-dioxanes on metal contact catalysts. Our results on the decomposition of 2-alkyl- and 2,2-dialkyl-1,3-dioxanes in the presence of platinum contact catalyst were reported in previous papers [1, 2].

The present communication deals with the decomposition of 4-methyl-1,3-dioxane on thermolite-supported platinum, palladium and rhodium catalysts (Pt/T, Pd/T, Rh/T), moreover on Raney-type nickel (Ni—Al) and copper (Cu—Al) catalysts. The impulse micro reactor technique [3] was chosen as the experimental method. The all-glass micro reactor was directly attached to a Willy Giede GCHF 18/2 gas chromatograph. The experiments were carried out in the temperature range between 180 and 400°C, in hydrogen carrier gas stream.

* Part IV: Acta Phys. et Chem. Szeged **14**, 99 (1968).

** Institute of Organic Chemistry named after Zelinsky, Academy of Sciences, USSR, Moscow.

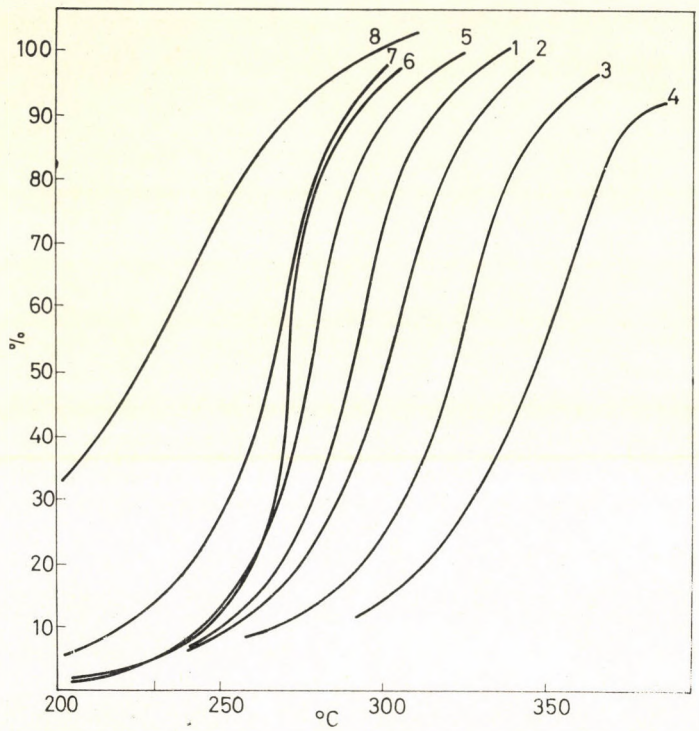

Fig. 1. Dependence of the decomposition of 4-methyl-1,3-dioxane on various catalysts as function of the temperature. *1* 1 ml Pt/T; *2* 0.5 ml Pt/T; *3* 0.25 ml Pt/T; *4* 0.125 ml Pt/T; *5* 1 ml Pd/T; *6* 1 ml Rh/T; *7* 0.2 ml Cu-Al; *8* 0.2 ml Ni-Al

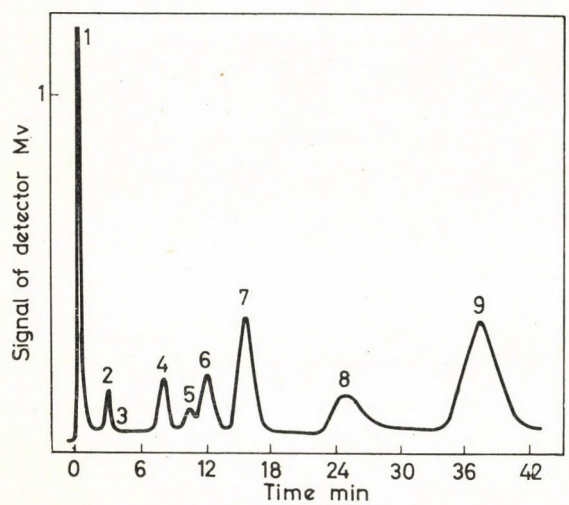

Fig. 2. Characteristic chromatogram of the decomposition products of 4-methyl-1,3-dioxane in the presence of 1 ml Pt/T catalyst at 305°. *1* gaseous decomposition products; *2* acetaldehyde; *3* methanol + ethanol; *4* butyraldehyde; *5* *sec.*-butyl formate; *6* *sec.*-butanol + methyl ethyl ketone; *7* *n*-butyl formate; *8* butanol; *9* 4-methyl-1,3-dioxane

According to the graphically represented data in Fig. 1, the catalysts can be arranged, on the basis of their effect upon the extent of decomposition, in the following order:

$$Ni-Al > Cu-Al > Rh/T > Pd/T > Pt/T$$

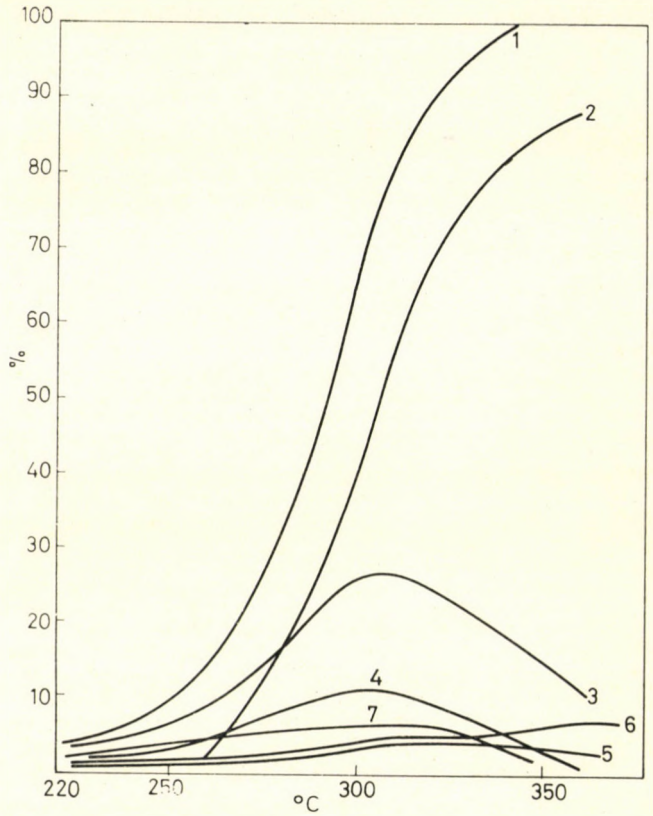

Fig. 3. Dependence of the conversion of 4-methyl-1,3-dioxane and its decomposition products in the presence of 1 ml Pt/T catalyst as a function of the temperature. *1* quantity of 4-methyl-1,3-dioxane transformed; *2* conversion of 4-methyl-1,3-dioxane to gaseous products; *3* conversion of 4-methyl-1,3-dioxane to liquid products; *4* *n*-butyl formate; *5* butyraldehyde; *6* *sec.*-butanol + methyl ethyl ketone; *7* butanol

The directions of the reactions can be determined by evaluating the chromatograms of the decomposition products. A characteristic chromatogram is shown in Fig. 2. The experimental data obtained by qualitative and quantitative evaluations of the chromatograms are tabulated (Table I), and the data obtained in the case of 1 ml Pt/T catalyst are also graphically shown in Fig. 3.

These experimental results reveal that the decomposition of 4-methyl-1,3-dioxane in the presence of various metal contact catalysts is a complex process, which can be summarized as follows:

Primary processes

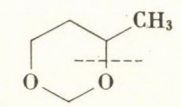

$$\longrightarrow \quad H-C(=O)-O-CH_2-CH_2-CH_2-CH_3 \qquad (1)$$

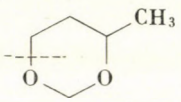

$$\longrightarrow \quad H-C(=O)-O-CH(CH_3)-CH_2-CH_3 \qquad (2)$$

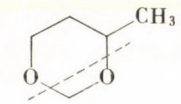

$$\longrightarrow \quad H_3C-CH_2-CH_2-C(=O)H + [CH_2O] \qquad (3)$$

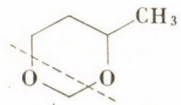

$$\longrightarrow \quad H_3C-C(=O)-CH_2-CH_3 + [CH_2O] \qquad (4)$$

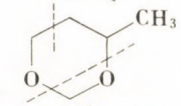

$$\longrightarrow \quad H_3C-CH=CH_2 + [2\,CH_2O] \qquad (5)$$

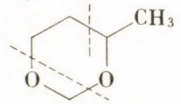

$$\longrightarrow \quad H_2C=CH_2 + [CH_2O] + H_3C-C(=O)H \qquad (6)$$

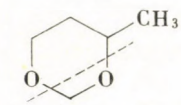

$$\xrightarrow{H_2} \quad H_3C-CH_2-CH_2-CH_2OH + CH_3OH \qquad (7)$$

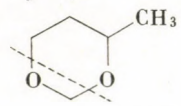

$$\xrightarrow{H_2} \quad H_3C-CH(OH)-CH_2-CH_3 + CH_3OH \qquad (8)$$

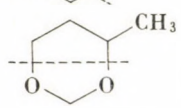

$$\xrightarrow{H_2} \quad H_3C-CH_2-CH_2-CH_3 + CH_2O + H_2O \qquad (9)$$

Secondary processes

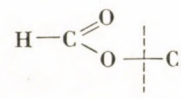

$$\xrightarrow{H_2} \quad C_4H_{10} + \left[H-C(=O)-OH\right] \qquad (10)$$

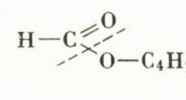

$$\xrightarrow{H_2} \quad C_4H_9-OH + [CH_2O] \qquad (11)$$

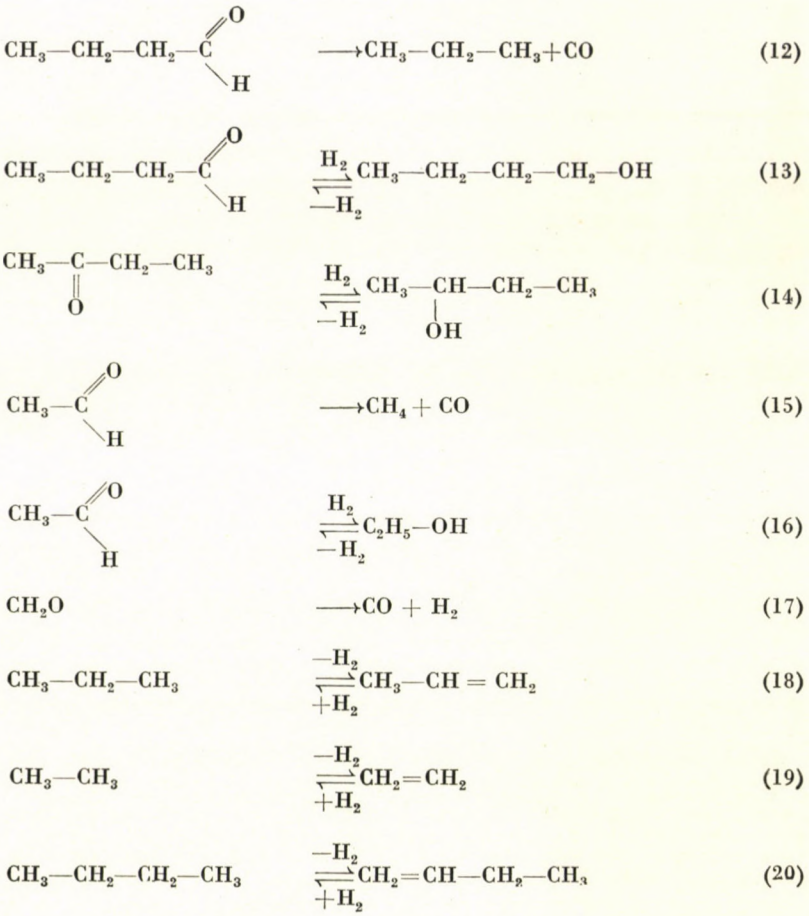

(12)

(13)

(14)

(15)

(16)

(17)

(18)

(19)

(20)

Two of the nine primary reactions (1, 2) are isomerization, three are hydrogenolysis (7, 8, 9), while the other four are fragmentational processes.

The experimental data in Table I clearly demonstrate that both the quality and quantity of the catalyst, as well as the temperature have decisive influence on the direction of the decomposition.

The observation of the isomerization of 4-methyl-1,3-dioxane to butyl formates means not only the recognition of a new reaction, but also demonstrates a new example of 1,3-rearrangements.

If the relative percentage distribution of the individual primary processes is considered, it can be stated that fragmentational transformations to hydrocarbons and hydrogenolysis are favoured in the presence of each catalyst.

The yield of oxo compounds and esters taken together reached its maximum value (25%) in the case of the Pt/T catalyst. The maximum yield of isomerization to *n*-butyl formate was 15%, and it was obtained with Pt/T catalyst

again. The other isomerization product of 4-methyl-1,3-dioxane occurred in quite a negligible amount in the catalysate. In the presence of Rh/T, Ni—Al and Cu—Al catalysts both isomerization processes are of secondary importance.

In order to throw more light upon the chemical changes under investigation, and as a complementary examination, the catalytic decomposition of the two isomerization products, *i.e.* primary and secondary butyl formates, was

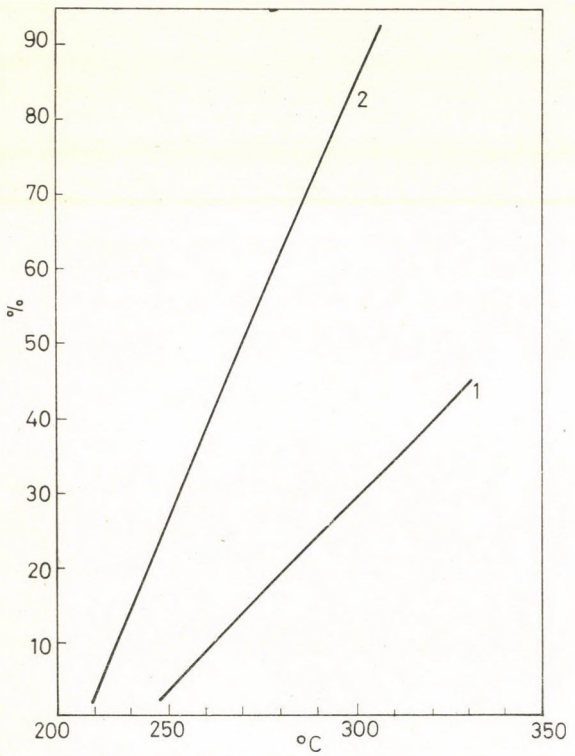

Fig. 4. Dependence of the decomposition of *n*-butyl formate (1) and *sec.*-butyl formate (2) on Pt/T catalyst as a function of temperature

studied under conditions identical with those used in the case of 4-methyl-1,3-dioxane. Fig. 4 shows the degree of decomposition of the two compounds as a function of the temperature. At the same time, the vapour-phase decomposition products of 4-methyl-1,3-dioxane and the two formates, obtained on 1 ml Pt/T catalyst at 300°C, were subjected to comparative examinations. A comparison of these experimental data afforded valuable information about the degree of the isomerization reactions. Namely, in determining the degree of isomerization, one has to take into consideration, in addition to the amount of formates detected in the catalysate, the amount of formates decomposed at that

Table I

Experimental data of the contact catalytic decomposition of 4-methyl-1,3-dioxane

Catalyst, ml	Temperature, °C	Conversion, %	Distribution* of the de composition products %						
			Gaseous products	Liquid products	Butyraldehyde	*sec.*-Butyl formate	*sec.*-Butanol + methyl ethyl ketone	Butyl formate	Butanol
Pt/T 1	225	5	min.	5	1	0	1	1	2
Pt/T 1	260	10	1	9	1	1	2	3	3
Pt/T 1	285	43	25	18	2	1	2	8	5
Pt/T 1	305	66	39	27	4	1	4	11	6
Pt/T 1	320	93	73	20	3	0	4	8	4
Pt/T 1	340	98	82	16	3	0	6	4	2
Pt/T 1	360	100	89	11	3	0	7	0	0
Pt/T 1	380	100	90	10	3	0	7	0	0
Pt/T 0.5	200	2	min.	2	min.	0	1	min.	1
Pt/T 0.5	230	5	1	4	min.	min.	1	1	2
Pt/T 0.5	270	18	7	11	1	1	3	3	3
Pt/T 0.5	295	50	25	25	2	2	4	9	7
Pt/T 0.5	320	61	35	26	3	1	4	7	8
Pt/T 0.5	333	84	60	23	3	min.	3	8	7
Pt/T 0.5	345	98	82	16	2	0	5	2	4
Pt/T 0.25	255	5	0	5	min.	min.	1	1	1
Pt/T 0.25	298	20	9	11	1	1	2	3	3
Pt/T 0.25	325	54	33	21	2	1	3	7	6
Pt/T 0.25	350	90	67	22	3	0	5	7	6
Pt/T 0.25	370	96	80	16	3	0	6	3	4
Pt/T 0.125	300	15	4	10	1	1	2	2	3
Pt/T 0.125	340	39	22	17	1	2	2	5	5
Pt/T 0.125	355	60	39	21	1	1	3	7	6
Pt/T 0.125	370	87	68	18	1	min.	4	8	5
Pt/T 0.125	392	92	76	16	1	0	4	5	5
Pd/T 1	200	2	min.	2	min.	0	min.	1	0
Pd/T 1	240	8	2	6	min.	1	1	3	min.
Pd/T 1	260	21	10	11	1	2	1	5	1
Pd/T 1	280	56	41	15	1	3	2	7	2
Pd/T 1	305	92	77	15	1	min.	4	6	3
Pd/T 1	330	100	91	9	2	0	4	1	2
Rh/T 1	200	2	min.	1	min.	min.	min.	0	0

Table I continued

Catalyst, ml	Temperature, °C	Conversion, %	Distribution* of the decomposition products %						
			Gaseous products	Liquid products	Butyraldehyde	*sec.*-Butyl formate	*sec.*-Butanol + methyl ethyl ketone	Butyl formate	Butanol
Rh/T 1	255	13	9	4	min.	1	1	1	0
Rh/T 1	275	70	65	5	1	1	2	1	0
Rh/T 1	300	95	88	7	1	0	4	1	0
Ni–Al 0.2	180	19	16	3	1	min.	min.	min.	2
Ni–Al 0.2	200	33	26	6	1	min.	1	min.	4
Ni–Al 0.2	240	62	48	14	3	0	4	min.	7
Ni–Al 0.2	255	73	57	16	3	min.	4	min.	9
Ni–Al 0.2	275	93	76	17	3	min.	4	min.	10
Ni–Al 0.2	300	100	86	14	2	0	1	0	11
Cu–Al 0.2	200	5	1	4	1	0	1	min.	2
Cu–Al 0.2	225	23	14	8	2	0	3	1	3
Cu–Al 0.2	245	25	11	14	3	min.	7	1	3
Cu–Al 0.2	270	58	43	16	3	min.	10	2	1
Cu–Al 0.2	295	93	77	16	3	min.	9	4	1
Retention time (min)		37.6			8.2	10.6	12.3	16.2	25.4

* The formation of traces of acetaldehyde, methanol and ethanol was always observed in the decomposition.

temperature. On this basis, the following data were obtained concerning the degree of isomerization of 4-methyl-1,3-dioxane to esters:

Temperature, °C	*n*-butyl formate, %	*sec.*-butyl formate, %
260	4	2
285	11	6
305	17	12

The decomposition of *sec.*-butyl formate gives, besides a negligible amount of *sec.*-butanol, C_4 hydrocarbons, while that of *n*-butyl formate yields, besides butyraldehyde and butanol, C_3 and C_4 hydrocarbons ($C_3/C_4 = 1/1$). In the decomposition of 4-methyl-1,3-dioxane, the C_3/C_4 ratio was found to be 1/4, indicating the significance of ring hydrogenolysis (reaction path 9).

Comparison of the amounts of butyraldehyde and butanol, taken together, with that of methyl ethyl ketone and *sec.*-butanol shows that not only the absolute, but also the relative quantities are highly dependent upon the catalyst applied:

Catalyst	Butyraldehyde + butanol, %	Methyl ethyl ketone + *sec.*-butanol, %
Ni–Al	12	4
Pt/T	8	4
Pd/T	4	4
Cu–Al	4	10
Rh/T	1	4

In our opinion, the reason why the formation of butyraldehyde, butanol, methyl ethyl ketone, *sec.*-butanol, *sec.*-butyl formate and *n*-butyl formate depend upon the nature of the catalyst lies not so much in the difference in the stability of these products, but is rather explained by the adsorption conditions of the starting material and the products, dependent on the catalyst.

The formation of the individual products, mainly those arising as a result of various secondary processes, can be explained in terms of different mechanisms. Investigation under identical experimental conditions of the secondary processes may result in the elucidation of the exact reaction mechanism.

Experimental

Preparation of the catalysts

The thermolite carrier of 0.2—0.4 mm particle size was boiled with hydrochloric acid and washed with distilled water several times until free of iron, and then dried. The metal components (10%) were applied on the carrier from $H_2PtCl_6 \cdot 6H_2O$, $RhCl_3 \cdot 4H_2O$ and $PdCl_2$, as described earlier [3]. 1.5 ml aqueous solution was applied to 1 g of the carrier. After adsorption, the catalyst was dried and reduced at 200—300°C in a stream of hydrogen. Th_e Raney-type catalysts were prepared as described earlier [4]. Apart from the Cu–Al contact, th_e activity of the catalysts did not change considerably in the course of application.

Experimental conditions

The impulse-micro reactor technique [3] was chosen for the experiments. The particle size of the catalyst was 0.2—0.4 mm. The chromatographic column was 1 m high and 5 mm in diameter, containing 20% β,β-oxydipropionitrile on thermolite. The thermostat was adjusted to 72°C, carrier gas: hydrogen; rate of flow of the carrier gas: 60 ml/min; detector current: 160 mA; max. displacement of the compensograph: 2 mV; diameter of the micro reactor: 8 mm; sample amount injected: 0.0033 ml. A Willy Giede type GCHF 18/2 gas chromatograph was used. The analysis of the gaseous products was accomplished at 80°C in a 1 m long Al_2O_3 column. The peaks were identified by means of suitable standard materials, and quantitatively $_e$valuated with the aid of calibration curves.

REFERENCES

1. APJOK, J., BARTÓK, M., KARAKHANOV, R. A., SHUIKIN, N. I.: Izv. Akad. Nauk SSSR, Ser. Chim. **1968,** 2357
2. APJOK, J., BARTÓK, M., KARAKHANOV, R. A., KOVÁCS, K.: Acta Phys. et Chem. Szeged, **14,** 99 (1968)
3. BARTÓK, M., FÉNYI, SZ.: Acta Phys. et Chem. Szeged, **12,** 157 (1966)
4. BARTÓK, M., KOZMA, B.: Acta Phys. et Chem. Szeged, **9,** 116 (1963)

Mihály BARTÓK, József APJOK } Szeged, Dóm tér 8, Hungary
R. A. KARAKHANOV; Institute of Organic Chemistry named after Zelinsky, Academy of Sciences USSR, Moscow
Kálmán KOVÁCS; Szeged, Dóm tér 8, Hungary

Acta Chimica Academiae Scientiarum Hungaricae, Tomus 61 (3), pp. 325—328 (1969)

XeF_2 AS AN ANALYTICAL REAGENT

(PRELIMINARY COMMUNICATION)

A. SCHNEER-ERDEY and K. KOZMUTZA

(Research Group for Inorganic Chemistry, Hungarian Academy of Sciences, and Institute of General and Inorganic Chemistry, L. Eötvös University, Budapest)

Received March 17, 1969

Due to its strong oxidizing power, good storage stability and portionability, solid XeF_2 is a convenient reagent both in qualitative and quantitative analyses. The determination of iodide ions as periodate and the detection of chromium as chromate are described.

The first paper on the preparation of compounds of noble gases appeared in 1962 [1]. One of the fluorine-containing compounds of Xe described in the above paper has been found to be XeF_2 [2]. It is a solid, translucent, crystalline compound at room temperature with a characteristic smell and a considerable vapour pressure (3 torr). The reactions of XeF_2 have been investigated by several workers [3]. It has been shown that the reaction of XeF_2 with water is of first order, and hydrolysis takes place according to the following equation:

$$XeF_2 + H_2O \rightarrow Xe \uparrow + 2\,HF + 1/2\,O_2$$

with a half-life of 7 hours.

The iodometric determination of XeF_2 is based on the titration of iodine formed in the reaction

$$XeF_2 + 2\,KI \rightarrow Xe \uparrow + 2\,KF + I_2$$

with $Na_2S_2O_3$ [3, 5].

The oxidizing effect of XeO_3 formed in the aqueous solution of XeF_6 has already been utilized for analytical purposes. After oxidizing organic acids to carbon dioxide and water, the excess XeO_3 was measured iodometrically [4].

Dissolving XeF_2 in water (the concentration of the saturated solution is 0.15 *M* at room temperature) the smell of ozone can be felt and also the presence of H_2O_2 detected [5]. The oxidizing properties of XeF_2 have long been known [7]. The redox potential of the system Xe/XeF_2 was found to be 2.2 V in an acidic medium [8]. This is comparable with the standard potentials of ozone ($E_0 = 2.07$ V) and elementary fluorine ($E_0 = 2.85$ V). A comparison

of these three oxidizing agents shows that XeF_2 has favourable properties such as its solid state, easy handling and good storage stability.

At room temperature XeF_2 can be stored in teflon bottles, while any kind of plastic vessel, *e.g.* polyethylene, is suitable in dry ice (—80° C).

The purpose of the present paper is to show that the strong oxidizing power of XeF_2 can be utilized in analytical chemistry. XeF_2 is not only a strong oxidant but can also serve as an effective fluorinating agent of organic compounds. It is planned to use this reagent in reactions which are very difficult to carry out under ordinary conditions. In the following, the application of XeF_2 for the oxidation of iodide to periodate and Cr(III)— ions to chromate in acidic medium will be outlined briefly.

Oxidation of iodide ions

After demonstrating that the amount of iodine released by XeF_2 from excess KI is about 95% of the amount equivalent to XeF_2 originally present, the extent of oxidation of iodine by excess XeF_2 was studied. For this purpose, to 5 ml aliquots of water of KI 5 ml of sulfuric acid and an excess XeF_2 were added in plastic beaker. Iodine appeared instantaneously. A few minutes later the brownish-yellow solutions faded. In order to make the reaction complete and to decompose the excess XeF_2, the colourless solutions containing gas bubbles were heated on a water bath. The solutions were cooled, and after adding 2 *N* HCl and excess KI iodine was titrated with a standard $Na_2S_2O_3$ solution in the presence of starch indicator.

The data in Table I indicate that the oxidation of iodide results in the formation of periodate.

Table I

KI taken (mg)	XeF_2 added (mg)	XeF_2 (mg) calculated for 8-equivalent oxidation	Volume of 0.01 *N* $Na_2S_2O_3$ (ml)	KI found (mg)	Deviation %
1.67	18.07	6.81	8.15	1.69	+1.3
1.52	22.98	6.20	7.60	1.58	+3.7
1.00	11.02	4.08	4.76	0.99	—1.0
0.90	15.66	3.67	4.23	0.88	—2.3
0.45	13.07	1.84	2.13	0.442	—1.8

In each case XeF_2 was added in large excess above the maximum amount required. The material of the plastic beakers did not influence the reaction. However, care must be taken to achieve complete decomposition of the excess reagent.

The results show that in acidic medium KI is quantitatively oxidized to KIO_4 by excess XeF_2. Since the volume of standard $Na_2S_2O_3$ solution is eight times that equivalent to the KI originally present, the method is suitable for the determination of small amounts of iodide with sufficient accuracy. When the analysis is performed by titration, 1 ml of 0.01 *N* $Na_2S_2O_3$ corresponds to 0.20751 mg of KI.

Oxidation of Cr(III) ions

Only a few reagents are capable of oxidizing chromium(III) to Cr(VI) in acidic media [6].

The oxidation of Cr(III) ions by XeF_2 has been found to occur almost quantitatively in half an hour at about pH = 2.

The solution containing Cr(III) ions was prepared from 1 *N* $K_2Cr_2O_7$ by reduction with H_2O_2 in dilute sulfuric acid. The solution was diluted to the required volume with doubly distilled water. The pH of the solution was 1.7. 1 ml of the solution oxidized to chromate corresponded to 1.005 ml of 0.1 *N* $Na_2S_2O_3$. When the solution was diluted tenfold, the pH increased to 2.3. After oxidation, 1 ml of the solution corresponded to 0.9993 ml 0.01 *N* $Na_2S_2O_3$.

When XeF_2 was added to 1 ml of Cr(III) solution in a glass or plastic beaker, the green solution began to turn yellow in a few minutes. After adding 2—40 ml of water, the solution was heated for 1/2 hour on a water bath, or it was poured in a glass beaker covered with a funnel and boiled for 20—30 minutes on a sand bath. After cooling 2 *N* HCl and an excess of KI were added. The iodine formed was titrated with 0.01 *N* $Na_2S_2O_3$ in the presence of starch as indicator. Smaller amounts of chromium can be determined photometrically. When glass beakers are used care must be taken to prevent concentration of the solution since this may lead to losses in chromium due to the evaporation of CrO_2F_2.

The results of two measurements are given in Table II.

Table II

Cr(III) taken expressed as 0.01 *N* $Na_2S_2O_3$ (ml)	XeF_2 (mg) for oxidation		Volume of 0.01 *N* $Na_2S_2O_3$ (ml) consumed	Deviation %
	necessary	used		
10.07	8.5	14.20	9.80	−2.7
9.99	8.5	73.0	10.20	+2.1

The data show that further work is necessary to make the procedure more accurate and reproducible. This work is in progress.

The drawbacks of the otherwise excellent reagent are its high price and the fact that it is difficult to obtain, which put certain limits on its application.

*

The authors are indebted to Mr. P. GRÓZ (Chemistry Department, Central Research Institute for Physics, Hungarian Academy of Sciences) for supplying the valuable XeF_2 sample.

REFERENCES

1. CLAASSEN, H. H., SELIG, H., MALM, J. G.: J. Amer. Chem. Soc. **84**, 3593 (1962); Science **138**, 136 (1962)
2. SMITH, D. F.: J. Chem. Phys. **38**, 270 (1963)
3. APPELMAN, E. H., MALM, J. G.: J. Amer. Chem. Soc. **85**, 110, 816, 825 (1963); **86**, 2141, 2297 (1964)
   BECK, M., DÓZSA, L.: Magyar Kém. Folyóirat **73** 522 (1967)
   FEHÉR, I., LŐRINCZ, M.: Magyar Kém. Folyóirat **74**, 232 (1968)
4. JASELSKIS, B., KRUEGER, R. H.: Talanta **13**, 945 (1966)
5. APPELMAN, E. H.: Inorg. Chem. **6**, 1268, 1305 (1967)
6. PASCAL, P.: Nouveau Traité de Chimie Minéral, Tome XIV pp. 102, 179. Masson et Cie Paris, 1960
7. HOPPE, R., MATTAUCH, H., RÖDDER, K. M., DÄHNE, W.: Z. anorg. allg. Chem. **324**, 214 (1963)
8. APPELMAN, H. H., MALM, J. G.: J. Amer. Chem. Soc. **86**, 2297 (1964)

Anna SCHNEER-ERDEY
Kornélia KOZMUTZA
Budapest VIII., Múzeum krt. 6—8

INDEX

INORGANIC AND ANALYTICAL CHEMISTRY — ANORGANISCHE UND ANALYTISCHE CHEMIE — НЕОРГАНИЧЕСКАЯ И АНАЛИТИЧЕСКАЯ ХИМИЯ

KISS, B. A.: Continuous Detection by Simultaneous TG and IR Measurements of NH_3 and H_2O Released in Thermal Decompositions 207

BOKSAY, Z. and GURMAI, M.: Conductivity of Mixed Alkali Glasses Containing Aluminium Oxide 223

SZÉKELY, T., RÖSNER, P. and GÖMÖRY, P.: Contribution to the Heterofunctional Condensation of Silanes. I. Investigation of the Preparation of Siloxanes with Regular Structures 233

PUNGOR, E. und WESER, A.: Die Untersuchung von Boriden, Carbiden und Nitriden auf ihre Eignung als Indikatorelektrode für potentiometrische Messungen (The Investigation of Borides, Carbides and Nitrides for their Suitability as Indicator Electrodes in Potentiometric Measurements)..... 241

BERÉNYI, M.: Platinum and Palladium Catalyzed Oxidation of Ammonia under the Experimental Conditions of Differential Thermoanalysis (DTA)..... 257

INCZÉDY, J., KLATSMÁNYI-GÁBOR, P. and ERDEY, L.: The Use of Complex-forming Agents in Ion Exchange Chromatography. I. Separation of Cobalt(II) and Nickel(II) Ions on Cation Exchange Column Using Oxalate Ions Containing Eluent..... 261

PHYSICAL CHEMISTRY — PHYSIKALISCHE CHEMIE — ФИЗИЧЕСКАЯ ХИМИЯ

ROST, L.: Physikalische Ursachen des Matrixeffektes bei der Spektralanalyse im Gleichstrombogen. (Physical Causes of the Matrix Effect in Spectral Analysis in a Direct-current Arc 271

DÉVAY, J., MÉSZÁROS, L. and GARAI, T.: Calculation of the Influence of the Ohmic Resistance of the Cell on the Third Harmonic a.c. Polarographic Current in Case of a Reversible Electrode Reaction 279

TÓTH, G. und ZSINKA, L.: Bestimmung der Oberfläche pulverförmiger Platinadsorbentien durch Messung der Jodadsorption mit der radioaktiven Indikator-Methode. (The Determination of the Surface of Powdered Platinum Adsorbents by the Measurement of Iodine Adsorption by Radioactive Tracer Method)..... 289

ORGANIC CHEMISTRY — ORGANISCHE CHEMIE — ОРГАНИЧЕСКАЯ ХИМИЯ

SZABOLCS, J. and RÓNAI, Á.: Methanolysis of Lutein Ditrichloroacetate. Preparation of 3-hydroxy-3'-methoxy-α-carotene and 3-hydroxy-5'-methoxy-4',5'-dihydro-3',4'-dehydro-α-carotene 301

SZABOLCS, J. and RÓNAI, Á.: The Structure of α-Cryptoxanthin and the Identity of Zeinoxanthin with α-Cryptoxanthin 309

BARTÓK, M., APJOK, J., KARAKHANOV, R. A. and KOVÁCS, K.: Chemistry of 1,3-bifunctional Systems, VI. Examination of the Transformations of 4-Methyl-1,3-Dioxane on Various Catalysts by Means of the Micro Reactor Technique..... 315

SCHNEER-ERDEY, A. and KOZMUTZA, K.: XeF_2 as an Analytical Reagent (Preliminary communication) 325

Printed in Hungary

A kiadásért felel az Akadémiai Kiadó igazgatója — Műszaki szerkesztő: Farkas Sándor

A kézirat nyomdába érkezett: 1969. IV. 28. — Terjedelem: 10,75 (A/5) ív, 56 ábra, 1 melléklet

69.67753 Akadémiai Nyomda, Budapest — Felelős vezető: Bernát György

ACTA CHIMICA

ТОМ 61—ВЫП 3

РЕЗЮМЕ

Термогравиметрическое и одновременно с этим ИК-спектрофотометрическое измерения количества паров NH_3 и H_2O, образующихся при термическом разложении

А. Б. КИШ

Был разработан ИК-спектрофотометрический метод для измерения количеств NH_3 и H_2O, образующихся в течение термического разложения. Изучались зависимости между навесками, скоростью потока газа-носителя, скоростью нагрева печи, а также измеренной площадью кривых с максимумом. Определялись те условия эксперимента, при которых площадь ИК-кривых с максимумом пропорциональна количеству выделяющегося газа.

Для измерения H_2O использовалась реакция с CaC_2, в связи с чем был измерен выход реакции превращения экспериментальным путем. Полученные для измерения H_2O кривые с максимумом калибровались с помощью $CuSO_4 \cdot 5H_2O$. На основе совместной оценки кривых ТГ и ИК-кривых с максимумом были получены такие экспериментальные данные, которые могут быть распространены и на до сих пор неисследованные, более уточненные детали реакции разложения парамолибдата аммония и паравольфрамата аммония.

Об электропроводности смешанных стекол, содержащих алюминий

З. БОКШАИ и М. ГУРМАИ

Определялись электрическое сопротивление стекол и число переноса катионов стекол в системе $Na_2O—K_2O—Al_2O_3—SiO_2$. В то время как сопротивление натрий-алюмосиликатных стекол изменяется при 400 °С лишь в пределах одного порядка в зависимости от отношения алюминия к щелочному металлу, сопротивление же калийных стекол в узком интервале изменения состава увеличивается почти на три порядка. Такое необычное высокое сопротивление $K_2O—Al_2O_3—SiO_2$-стекол с высоким содержанием алюминия объясняется тем, что дырки относительно больших размеров, необходимые для миграции ионов калия, образуются в жесткой скелетной структуре лишь за счет высоких энергий активации. Вследствие этого, поведение смешанных стекол, относящихся к данной системе также изменяется.

Некоторые данные к гетерофункциональной конденсации, I Изучение получения силоксанов регулярного строения

Т. СЕКЕИ, П. РЁЗНЕР и П. ГЁМЁРИ

Изучалась гетерофункциональная конденсация, протекающая между алкоксисиланами и хлор-силанами, с целью установления возможности её использования для получения силоксановых полимеров и олигомеров с заданным регулярным строением. Было установлено, что проведением реакции в растворе можно избежать равновесную реакцию, представляющую собой мешающую побочную реакцию. Однако, обмен заместителей ограничивает возможности построения молекул заданного регулярного строения в области низких молекулярных весов.

На основе изменения алкильной части алкоксигруппы можно судить о механизме реакции, а также о роли катализатора.

Изучение боридов, карбидов и нитридов с точки зрения применения их в качестве потенциометрических индикаторных электродов

Э. ПУНГОР и Ш. ВЕСЕР

Проводились исследования карбидов, боридов и нитридов переходных металлов для установления их применимости в качестве индикаторных электродов в растворах кислого ферроцианида и феррицианида. Авторами была установлена зависимость между кристаллическим строением вещества индикаторного электрода и окислительно-восстановительными индикаторными свойствами.

Каталитическое окисление аммиака с помощью платины и палладия в условиях дифференциального-термического анализа ДТА

М. БЕРЕНЬИ

В условиях дифференциального-термического анализа на держателе образца в виде платиновой пластинки, окисление аммиака начинается со значительной скоростью уже при 230°. С помощью катализаторов с большой удельной поверхностью, содержащих платину или палладий, был изготовлен такой детектор, который позволяет следить за процессами, сопровождаемыми выделением аммиака выше 100°. Детектор чувствителен к количеству аммиака, меньшего чем 1 мг.

Применение комплексообразователей в ионообменной хроматографии, I

Разделение ионов кобальта(II) и никеля(II) на катионообменной колонке с помощью элюэнта, содержащего ионы оксалата

Й. ИНЦЕДИ, П. ГАБОР-КЛАТШАНИ и Л. ЭРДЕИ

С помощью данных по ионобменным равновесиям, стабильностям комплексов и константам диссоциации были рассчитаны доли разделения ионов никеля(II) и кобальта(II) на катионообменной смоле из растворов, содержащих 0,1 моля щавеловой кислоты — оксалата натрия при различных величинах pH. Используя раствор элюэнта с рассчитанным оптимальным значением pH, удалось осуществить хроматографическое разделение ионов металлов. Рассчитанные и полученные из эксперимента значения объемов элюэнта совпадают удовлетворительно.

Физические причины матричного эффекта при спектральном анализе в дуге постоянного тока

Л. РОСТ

Матричные эффекты в количественном спектральном анализе обусловливаются двумя совокупностями причин, а именно, химическими процессами, происходящими при испарении образца (матричные эффекты по химическим причинам), и физическими процессами, происходящими в плазме источника излучения (матричные эффекты по физическим причинам). Настоящая работа занимается исключительно последними на примере свободно горящей дуги постоянного тока. По существу можно различать четыре причины, которые могут также находится в сложной зависимости друг от друга, а именно: влияние концентрации всех частиц, находящихся в плазме, влияние концентрации частиц и температуры, транспортные процессы, протекающие в дуге, и взаимодействие газового образца, текущего в зону разряда, с плазмой.

Расчет влияния сопротивления ячейки на третью гармоническую составляющую в полярографии с переменным током в случае обратимого электродного процесса

Й. ДЕВАИ, Л. МЕСАРОШ и Т. ГАРАИ

Учитывая омическое сопротивление ячейки были дополнены коррекционным фактором теоретические зависимости, касающиеся третьей гармонической составляющей переменного тока, возникающего в обратимых полярографических процессах под влиянием переменного напряжения синусной формы с небольшой амплитудой, налагающегося на постоянное напряжение. На основе расчетов, проведенных с помощью этой зависимости, было установлено, что под влиянием омического сопротивления раствора амплитуды третьей гармонической составляющей, по сравнению со случаем, когда $R_0 = 0$, уменьшаются тем значительнее, чем больше контурная частота переменного напряжения, концентрация компонентов, принимающих участие в электродной реакции, и изменение элементарного заряда.

Определение поверхности порошковобразных платиновых адсорбентов измерением адсорбции иода с помощью метода радиоактивной индикации

Г. ТОТ и Л. ЖИНКА

Было показано, что ионы иодида выделяются на поверхности платины предварительно покрытой как водородом, так и хемосорбированным слоем кислорода в виде элементарного иода. Выделение, в обоих случаях, является результатом обмена, протекающего между ионами иодида и предварительно адсорбированными атомами водорода или кислорода. В случае водородного покрытия обмен может быть описан следующим суммарным уравнением:

$$Pt{-}H + H^+ + I^- \rightarrow Pt{-}I + H_2 \qquad (1)$$

В случае же окисьного покрытия первая стадия — это растворение поверхностногопокрытия платины согласно уравнению (2):

$$Pt_2{-}Pt_1{-}O + 2H^+ + 2I^- \rightarrow (Pt\,IX_n)^{4-(n+I)} + H_2O + I + Pt_2 \qquad (2)$$

а следующая стадия — хемосорбция элементарного иода, образующегося по уравнению (2):

$$Pt_2 + I \rightarrow Pt_2I, \qquad (2a)$$

где через Pt_1 и Pt_2 обозначаются внешний и лежащий непосредственно под ним слой платины, соответственно; а $(PtIX_n)^{4-(n+I)}$ означает комплекс платины с иодом, образующийся из внешнего поверхностного слоя платины, покрытого первоначально хемосорбированным слоем кислорода.

Сравнение поверхности, измеренной методом БЕТ, с максимальным количеством адсорбированного иода указывает на то, что на поверхности адсорбента, покрытого слоем окиси, во время насыщения образуется монослой хемосорбированного иода, в котором на каждый атом платины на поверхности приходится один атом иода. В случае же адсорбентов с водородным покрытием максимальное количество адсорбированного иода оказалось на 10—25% меньше количества, соответствующего насыщенному монослою. Хорошее согласие между величинами поверхностей, определенными методом БЕТ и с помощью адсорбции иода, позволяют производить определение поверхности платиновых катализаторов путем измерения максимального количества адсорбированного иода. Т. к. последнее осуществляется и при комнатной температуре, то тем самым устраняется возможность старения поверхности адсорбента, вызванная применением высоких температур для обезгаживания.

Структура α-криптоксантина и идентичность зеиноксантина с α-криптоксантином

Й. САБОЛЬЧ и А. РОНАИ

Химическим путем было установлено, что структура α-криптоксантина соответствует 3-гидрокси-α-каротину и что α-криптоксантин идентичен с зеиноксантином.

Химия 1,3-бифункциональных систем, IV. Изучение превращений 3—метилдиоксана—1,3 с помощью микрореакторной техники на различных катализаторах

М. БАРТОК, Й. АПЙОК, Р. А. КАРАХАНОВ и К. КОВАЧ

С помощью микрореакторной техники проводились исследования превращения 4-метилдиоксана-1,3 в присутствии водорода на платиновых, палладиевых и родиевых катализаторах с термолитным носителем, а также на никель-алюминиевых и медь-алюминевых катализаторах. В зависимости от изменения экспериментальных условий — качество и количество катализатора, температура — были изучены степень и различные направления превращений 4-метилдиоксана-1,3. Превращения вышеупомянутого вещества — сложные; они складываются из нескольких первичных и вторичных процессов. Основными направлениями превращений являются: полная фрагментация с образованием олефинов и насыщенных углеводородов; частичная фрагментация с образованием бутиральдегида, бутанола и метилэтилкетона, а также *втор.*-бутанола; изомеризация с образованием *Н.*- и *втор.*-бутилформиата. На примере изомеризации 1,3-диоксанов в сложные эфиры были показаны не только новая реакция, но и новый тип 1,3-перегруппировки, протекающий через четырехчленное промежуточное состояние.

Метанолиз дитрихлорацетата лутеина

Получение 3-гидрокси-3′-метокси-α-каротинаи 3-гидрокси-5′--метокси-4′,5′-дигидро-3′,4′-дегидро-α-каротина

Й. САБОЛЬЧ и А. РОМАН

При селективном метанолизе 3′-трихлорацетоксигрупп дитрихлорацетата лутеина образуются два изомерных монометильных трихлорацетата лутеина, структура которых была доказана. Метанолиз представляет собой новый метод для обнаружения некоторых гидроксилных групп в каротиноидах, находяшихся в положении, подобном положению 3′-гидроксильной группы лутеина.

The Acta Chimica publish papers on chemistry, in English, German, French and Russian.

The Acta Chimica appear in volumes consisting of four parts of varying size, 4 volumes being published a year.

Manuscripts should be addressed to

Acta Chimica
Budapest 112/91 Műegyetem

Correspondence with the editors should be sent to the same address.

The rate of subscription is 165 forints a volume. Orders may be placed with "*Kultúra*" Foreign Trade Company for Books and Newspapers (Budapest I., Fő utca 32. Account No. 43-790-057-181) or with representatives abroad.

Les Acta Chimica paraissent en français, allemand, anglais et russe et publient des mémoires du domaine des sciences chimiques.

Les Acta Chimica sont publiés sous forme de fascicules. Quatre fascicules seront réunis en un volume (4 volumes par an).

On est prié d'envoyer les manuscrits destinés à la rédaction à l'adresse suivante:

Acta Chimica
Budapest 112/91 Műegyetem

Toute correspondance doit être envoyée à cette même adresse.

Le prix de l'abonnement est de 165 forints par volume.

On peut s'abonner à l'Entreprise pour le Commerce Extérieur de Livres et Journaux «*Kultúra*» (Budapest I., Fő utca 32. Compte-courant No. 43-790-057-181) ou à l'étranger chez tous les représentants ou dépositaires.

«*Acta Chimica*» издают трактаты из области химической науки на русском, французском, английском и немецком языках.

«*Acta Chimica*» выходят отдельными выпусками разного объема. 4 выпуска составляют один том. 4 тома публикуются в год.

Предназначенные для публикации рукописи следует направлять по адресу:

Acta Chimica
Budapest 112/91 Műegyetem

По этому же адресу направлять всякую корреспонденцию для редакции.

Подписная цена «*Acta Chimica*» — 165 форинтов за том. Заказы принимает предприятие по внешней торговле книг и газет «*Kultúra*» (Budapest I., Fő utca 32. Текущий счет № 43-790-057-181) или его заграничные представительства и уполномоченные.

Reviews of the Hungarian Academy of Sciences are obtainable at the following addresses:

ALBANIA
Ndermarja Shtetnore e Botimeve
Tirana

AUSTRALIA
A. Keesing
Box 4886, GPO
Sydney

AUSTRIA
Globus Buchvertrieb
Salzgries 16
Wien I

BELGIUM
Office International de Librairie
30, Avenue Marnix
Bruxelles 5
Du Monde Entier
5, Place St. Jean
Bruxelles

BULGARIA
Raznoiznos
1, Tzar Assen
Sofia

CANADA
Pannonia Books
2, Spadina Road
Toronto 4, Ont.

CHINA
Waiwen Shudian
Peking
P. O. B. 88

CZECHOSLOVAKIA
Artia
Ve Smečkách 30
Praha 2
Poštová novinová služba
Dovoz tisku
Vinohradská 46
Praha 2
Mad'arská Kultura
Václavské nám. 2
Praha I
Poštová novinová služba
Dovoz tlače
Leningradská 14
Bratislava

DENMARK
Ejnar Munksgaard
Nörregade 6
Copenhagen

FINLAND
Akateeminen Kirjakauppa
Keskuskatu 2
Helsinki

FRANCE
Office International de Documentation et Librairie
48, rue Gay Lussac
Paris 5

GERMAN DEMOCRATIC REPUBLIC
Deutscher Buch-Export und Import
Leninstraße 16
Leipzig 701
Zeitungsvertriebsamt
Fruchtstrasse 3—4
1004 Berlin

GERMAN FEDERAL REPUBLIC
Kunst und Wissen
Erich Bieber
Postfach 46
7 Stuttgart S.

GREAT BRITAIN
Collet's Holdings Ltd.
Dennington Estate
London Rd.
Wellingborough. Northants.
Robert Maxwell and Co. Ltd.
Waynflete Bldg. The Plain
Oxford

HOLLAND
Swetz & Zeitlinger
Keizersgracht 471—487
Amsterdam C.
Martinus Nijhof
Lange Voorhout 9
The Hague

INDIA
Current Technical Literature Co. Private Ltd.
India House OPP
GPO Post Box 1374
Bombay I

ITALY
Santo Vanasia
Via M. Macchi 71
Milano
Libreria Commissionaria Sansoni
Via La Marmora 45
Firenze

JAPAN
Nauka Ltd.
92, Ikebukur O-Higashi 1-chome
Toshima-ku
Tokyo
Maruzen and Co. Ltd.
P. O. Box 605
Tokyo-Centrai
Far Eastern Booksellers
Kanda P. O. Box 72
Tokyo

KOREA
Chulpanmul
Phenjan

NORWAY
Johan Grundt Tanum
Karl Johansgatan 43
Oslo

POLAND
RUCH
ul. Wronia 23
Warszawa

ROUMANIA
Cartimex
Str. Aristide Briand 14—18
Bucureşti

SOVIET UNION
Mezhdunarodnaya Kniga
Moscow G—200

SWEDEN
Almquist & Wiksell
Gamla Brogatan 26
Stockholm

USA
Stechert Hafner Inc.
31, East 10th Street
New York, N. Y. 10003
Walter J. Johnson
111, Fifth Avenue
New York, N. Y. 10003

VIETNAM
Xunhasaba
19, Tran Quoc Toan
Hanoi

YUGOSLAVIA
Forum
Vojvode Mišića broj 1
Novi Sad
Jugoslovenska Knjiga
Terazije 27
Beograd

ACTA CHIMICA

ACADEMIAE SCIENTIARUM HUNGARICAE

TOMUS 61 FASCICULUS 4

AKADÉMIAI KIADÓ, BUDAPEST

1969

ACTA CHIM. ACAD. SCI. HUNG.

ACTA CHIMICA

A MAGYAR TUDOMÁNYOS AKADÉMIA KÉMIAI TUDOMÁNYOK OSZTÁLYÁNAK IDEGEN NYELVŰ KÖZLEMÉNYEI

SZERKESZTI

LENGYEL BÉLA

TECHNIKAI SZERKESZTŐK

DEÁK GYULA és HARASZTHY-PAPP MELINDA

Az Acta Chimica német, angol, francia és orosz nyelven közöl értekezéseket a kémiai tudományok köréből.

Az Acta Chimica változó terjedelmű füzetekben jelenik meg, egy-egy kötet négy füzetből áll. Évente átlag négy kötet jelenik meg.

A közlésre szánt kéziratok a szerkesztőség címére (Budapest 112/91 Műegyetem) küldendők.

Ugyanerre a címre küldendő minden szerkesztőségi levelezés. A szerkesztőség kéziratokat nem ad vissza.

Az Acta Chimica előfizetési ára kötetenként belföldre 120 Ft, külföldre 165 Ft. Megrendelhető a belföld számára az „Akadémiai Kiadó"-nál (Budapest V., Alkotmány utca 21. Bankszámla 05-915-111-46), a külföld számára pedig a „Kultúra" Könyv- és Hírlap Külkereskedelmi Vállalatnál (Budapest I., Fő utca 32. Bankszámla: 43-790-057-181) vagy annak külföldi képviseleteinél és bizományosainál.

Die Acta Chimica veröffentlichen Abhandlungen aus dem Bereiche der chemischen Wissenschaften in deutscher, englischer, französischer und russischer Sprache.

Die Acta Chimica erscheinen in Heften wechselnden Umfanges. Vier Hefte bilden einen Band. Jährlich erscheinen 4 Bände.

Die zur Veröffentlichung bestimmten Manuskripte sind an folgende Adresse zu senden:

Acta Chimica
Budapest 112/91 Műegyetem

An die gleiche Anschrift ist auch jede für die Redaktion bestimmte Korrespondenz zu richten.

Abonnementspreis pro Band: 165 Forint. Bestellbar bei dem Buch- und Zeitungs-Außenhandels-Unternehmen »*Kultúra*« (Budapest I., Fő utca 32. Bankkonto Nr. 43-790-057-181) oder bei seinen Auslandsvertretungen und Kommissionären.

Acta Chimica Academiae Scientiarum Hungaricae, Tomus 61 (4), pp. 329—340 (1969)

DISTRIBUTION OF ARC TEMPERATURE USING CATHODE EXCITATION

Z. G. HANNA*, T. KÁNTOR and L. ERDEY

*(Institute of General and Analytical Chemistry, Technical University, Budapest, and *National Research Centre, Cairo, U. A. R.)*

Received June 26, 1968

Determination of the axial and radial distribution of temperature in d.c. carbon arc in air is described using cathode excitation. Particular attention is given to the effect of the low ionization potential element aluminium when evaporated into the plasma. It is concluded that aluminium affects the residence time of the thermometric element zinc.

1. Introduction

In a work published by us [1], we gave a detailed study on the most convenient and reproducible way to introduce the matrix material and the thermometric volatile element zinc into the arc gap using the CTE-device (device for controlled total evaporation) in order to maintain a steady and reproducible arc. In this paper we will use the experimental conditions established by us to determine the axial and radial distribution of temperature of carbon arc in air when the sample electrode is arced as cathode. Several workers have dealt with temperature determination of arcs anode excitation [2—17], but not with cathode excitation. Moreover, this study would be of interest for analysts who are dealing with cathode excitation in order to develop new spectrochemical methods. We will give an approximate estimation for the distribution of zinc concentration in the plasma. From this study it became apparent that the residence time of zinc was increased respectively when aluminium was evaporated into the plasma.

Scope of theory

The theory of temperature measurement of an arc as a thermal source is elaborated in the basic works of this field [2—17]. The following equation deduced from the BOLTZMANN statistics has been applied first by ORNSTEIN and BRINKMAN [2]

$$T = \frac{5040(V_a - V_b)}{\log \frac{(gA)_a}{(gA)_b} - \log \frac{I_a^o}{I_b^o}}, \qquad (1)$$

where $T(°K)$ represents temperature, $V(eV)$ the excitation potential, labels a and b are for the two monochromatic radiations respectively, emitted by one and the same species, g the statistical weight, A the transition probability and $I°$ (photons. sec^{-1}. $cm^{-2}sr^{-1}$) the emitted *absolute* intensity (radiance).

In practical spectrography by simple calibration methods of the emulsion it is only possible to measure the intensity in an arbitrary scale. This measured line intensity (irradiance) will be called by us *relative* intensity (I), which is proportional to the absolute intensity as a given optical and detecting system:

$$I = fI°, \tag{2}$$

where f is the instrumental factor (depending on the wavelength) which is unknown in these cases. It is conventional to use Y and ΔY symbols according to the following definitions:

$$Y = \log I = \log fI° \tag{3}$$

$$\Delta Y_{a,b} = \log \frac{I_a}{I_b} = \log \frac{f_a}{f_b} + \log \frac{I_a°}{I_b°} \tag{4}$$

Using the normal way of photographic photometry the respective contrast factors (γ_a and γ_b) are available and we can conclude to the variation of speed value of the emulsion by them: if the contrast factor ratio is about one, the ratio of speed values is about one too [18]. Assuming that the instrumental factor varies mostly with the speed value of the emulsion within a limited wavelength range in case of $\gamma_a/\gamma_b \simeq 1$ the respective instrumental factor ratio can be eliminated from Eq. (4).

Usually, two line pairs of zinc appear to be ideal in this respect given in Eqs (5) and (6) knowing that the relative (gA) values determined by SCHUTTEVAER [5] and SCHUTTEVAER and SMIT [6] which have the Somers correction and provided by BOUMANS [14] were used together with the practical formulas given below:

$$T = \frac{20510}{2.580 + \Delta Y \dfrac{\text{ZnI } 3076}{\text{ZnI } 3072}} \tag{5}$$

$$T = \frac{18850}{3.258 + \Delta Y \dfrac{\text{ZnI } 3076}{\text{ZnI } 3282}} \tag{6}$$

2. Experimental

The line pair ZnI 3076/ZnI 3072 is more advantageous than the other one from the emulsion calibration point of view. But on the other hand the use of this line pair is associated with other kind of evaluation problems. Namely, there is a quite large difference between the intensity of the two lines,

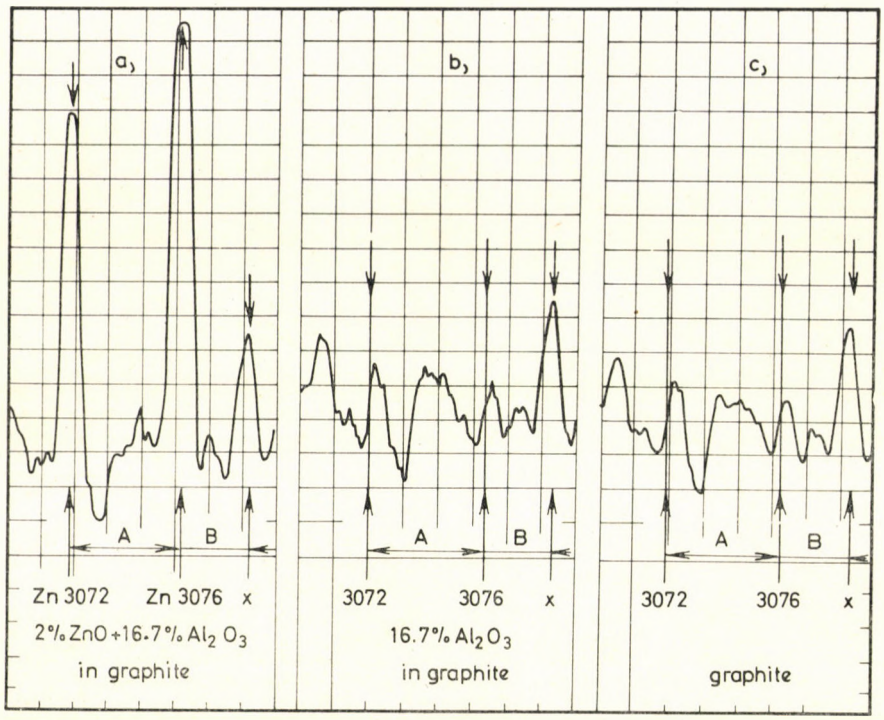

Fig. 1. Traces of spectra represent band interferences of zinc lines: *a* — admixture arc; *b* —admixture arc without zinc oxide, *c* — pure graphite arc

in addition they are disturbed by "carbon-air" bands which affect both unfavourable conditions for their evaluation. Although these problems have been investigated in case of anode excitation [15] yet we found that it is important to report them again in detail from the point of view of cathode excitation.

The band interferences for the two lines can be seen on traces of spectra represented by Fig. 1 (a, b, c). Total exposures were made at the middle region of the gap with powdered graphite (c), admixture having 16.7% Al_2O_3 (b) and admixture having the same amount of alumina and 2% ZnO. In addition what is seen from Fig. 1, the intensity of the zinc lines varied much along the gap especially the ZnI 3072, which was more disturbed by the band and had a lower intensity itself. This means that a band correction for this line is more important than for ZnI 3076. We had constructed a band correction formula using a third band peak (remarked by "x" on the traces) for the line ZnI 3072 and a conventional background correction was performed for ZnI 3076. Temperature data obtained by this way are given in Table I. Later we discovered that the intensity ratio of the band was about 3072 Å and the reference one (x) varied along the gap, as a result the constructed formula was invalid for the various regions of the arc gap.

However, it seems that the elimination of the above discussed problem can be achieved by using different concentrations of zinc oxide at the various regions of the arc gap, provided that these concentrations must be as high as possible to obtain considerable line intensities and at the same time without the interfering of self-absorption. In this case a normal background correction can provide good results.

The use of the other line pair ZnI 3282/ZnI 3076 was more favourable, as was also found by DE GALAN [15]. There was no large difference in the intensity of the two lines and a normal background correction was satisfactory. Moreover, it was possible to use one concentration of zinc oxide selected by the method published in a previous paper [1]. In case of the used type of emulsion the contrast factor for these two lines showed a slight deviation (*e. g.* $\gamma_{3282} = 1.37$ and $\gamma_{33076} = 1.31$).

Table I

Axial temperature data using ZnI 3076/ZnI 3072 line pair

Distance from cathode (mm)	Temperature (K)		$\frac{\Delta T}{T_1 - T_2}$
	Graphite arc (T_1)	Admixture arc (T_2)	
Anode			
5.7—6.7	5480	5480	0
5.0—6.0	5600	5570	30
4.0—5.0	5890	5760	130
3.0—4.0	6210	6050	160
2.0—3.0	6470	6260	210
1.0—2.0	6510	6330	180
0.3—1.3	6610	6380	230
Cathode			

Table II

Axial temperature data using ZnI 3076/ZnI 3282 line pair

Distance from cathode (mm)	Temperature (°K)		$\frac{\Delta T}{T_1 - T_2}$
	Graphite arc (T_1)	Admixture arc (T_2)	
Anode			
5.7—6.7	5830	5830	0
5.0—6.0	6000	5930	70
4.0—5.0	6180	6040	140
3.0—4.0	6360	6180	180
2.0—3.0	6460	6270	190
1.0—2.0	6530	6340	190
0.3—1.3	6600	6390	210
Cathode			

Tables I and II give results obtained for temperature measurement using both line pairs and their respective Eqs (5) and (6), with powdered graphite and admixture having 0.33% ZnO in both materials. It can be seen that both line pairs gave the same results within the cathode zone while there is a significant deviation within the anode one. This was because ZnI 3072 became weaker on moving towards the anode and the band interference affected this line more which appeared in the deviated results.

On the basis of the above described study Eq. (6) was selected for further work given in this paper; for characterising the precision of the temperature measurement fifteen replicate exposures were made at the middle region of the gap with the admixture using the working conditions summarised below. *Standard deviation* $\pm 43°K$ was obtained for the temperature, inserting the log intensity ratios of replicate measurements in Eq. (6).

Summary of the experimental conditions

Source: 220 V, d. c. generator, cathode excitation, 10 amps (in stable state of the arcings), 7 mm gap, operating with CTE-device [1] and using 90 sec pre-arcing with 240 sec exposure time.

Spectrograph: Zeiss Jena, Q-24 (medium, quartz), 0.015 mm slit, internal focusing. Diaphragm especially constructed for this purpose fixed on the "F—150" lens has an opening of 3×3 mm (1×1 mm of the actual gap).

Photography: Gevaert 23 D 50 emulsion, Kodak D-19 developer.

Photometry: Zeiss Jena "Schnell photometer" with recording system, evaluation on the basis of experimental density (H and D) curves using two-step filter method.

Materials: two standards were prepared, powdered graphite and admixture of graphite and 16.7% Al_2O_3 both containing 0.33% ZnO for the axial while the same materials were used with 0.83% ZnO in case of the radial investigation.

Sample electrode: (down) was cut from a graphite rod 3 mm diam. and 35 mm long. The crater was 2 mm diam. and 16 mm deep. The exposed length of the electrode was 6 mm. The filling of the electrode was performed as follows: 8 mg of a powdered graphite containing 0.33% or 0.83% ZnO was placed at the bottom of the crater for "axial" and "radial" investigations respectively followed by 25 mg standard mixture (with or without alumina) as a second layer. The empty portion of the crater was filled with powdered graphiteto the rim and well tapped.

Counter electrode: 6 mm diam. and 35 mm long graphite rod was used having a neck 3 mm in diam. and 5 mm long at the middle of the electrode.

3. Results

The "scope of theory" given above for the measurement of the temperature of plasma involves a remarkable simplification of the problem. Eq. (1) and Eqs (5) and (6) derived from the former, enable the temperature of the plasma, imagined as pressed into a "surface", to be calculated. To the calculation of the space distribution of temperature the spatial absolute intensity in Eq. (1) has to be interpreted and calculated, one possible solution being the Abel-transformation [14].

However, the application of zinc as the thermometric element offers oppurtunity to estimate, in which plasma zone exists the temperature calculat-

ed by Eqs (5) and (6). Since the ionization potential of zinc is high, its atom lines are most intensively emitted in the higher-temperature zone being near to the axis of the plasma within any chosen plasma section. Considering that the zinc atom concentration is highest also in the vicinity of the plasma axis the intensity of zinc atom lines comes mostly from the core of the plasma. Temperatures calculated on the basis of measuring these lines are therefore to be related to this part of the plasma. These "effective temperature" [14] data are given in this paper and they are related to the internal zone of the plasma in case of the measurement of the axial temperature distribution. In the estimation of the radial temperature distribution leaving out the Abel-transformation leads to greater inaccuracy in the spatial assignation of tem. peratures. This inaccuracy shows itself by the fact that a more uniform temperature fall is measured on going from the axis outward than the real one.

Axial distribution

Replicate exposures were taken for each of the seven selected axial regions of the arc gap moving from the cathode upwards to the anode. The axial variation of the *effective* temperature and the line intensities of the elemenst are given in Fig. 2. We can see from Fig. 2(b) the effect of the aluminium va-

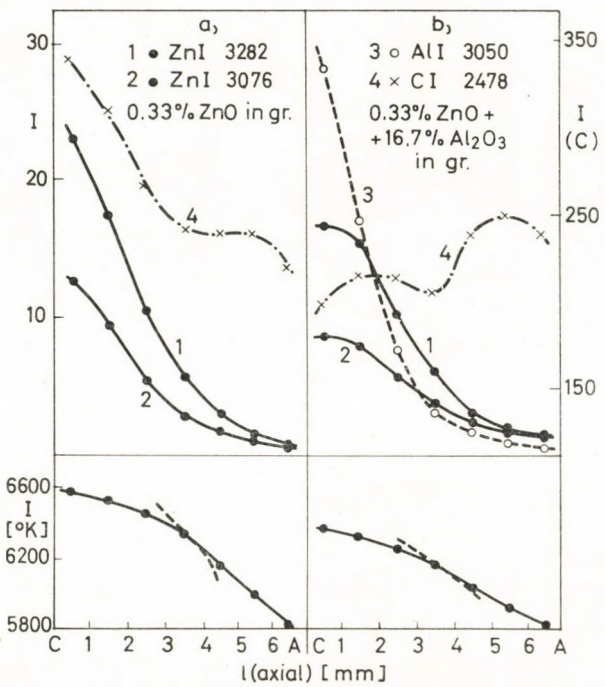

Fig. 2. Axial variation of temperature and line intensities: *a* — graphite arc, *b* — admixture arc

pours upon the behaviour of the temperature and the corresponding line intensities. An inflection separating two zones of the arc gap can be recognized in the middle of both temperature curves. These are a cathode zone with slight temperature variation values which extends from thecathode until the middle of the gap; and an anode zone characterised by a higher dropping of temperature which covers the upper half of the gap until the anode. Results of this study for the temperature values of the two arcs are given in Table II and the temperature difference (ΔT) between the two arcs for the same region of the gap.

We should like to mention here, that measuring the temperature of the whole gap using a diaphragm with an opening of 1×21 mm (0.3×7 mm actual dimensions in the gap) gave temperature values corresponding to 6590°K and 6390°K for powdered graphite and admixture respectively. These values are equivalent to that obtained near the cathode electrode for the respective arcs (see Table II). This was because the majority of the emitted light of zinc originated from the region near the cathode (see Fig. 2).

As a complement for our discussion we determined the electron pressure (P_e) adjacent regions to the cathode and anode for both arcs as given in Table III. For this measurement the MgII 2795/MgI 2852 line pair was used and for further details we refered to [14].

Table III

Axial electron pressure (P_e) data

Distance from cathode (mm)	log P_e(atm)	
	Graphite arc	Admixture arc
(near anode) 5.7—6.7	—3.5	—3.3
(near cathode) 0.3—1.3	—2.8	—2.5

Radial distribution

On considering that the visible arc column under the selected working conditions has a diameter of about 9 mm, the temperature was determined at five regions from the centre of the gap outwards. Replicate exposures were taken for each region following the conditions previously described. The radial decline of the effective temperature and the line intensities of the elements in both arcs are illustrated in Fig 3. Here again we can notice the effect of the aluminium vapours on the arc temperature and the line intensities of zinc and carbon. Results obtained are given in Table IV to show the temperature values for both arcs at variable distances from the centre and the temperature difference (ΔT) between the two arcs for the same region.

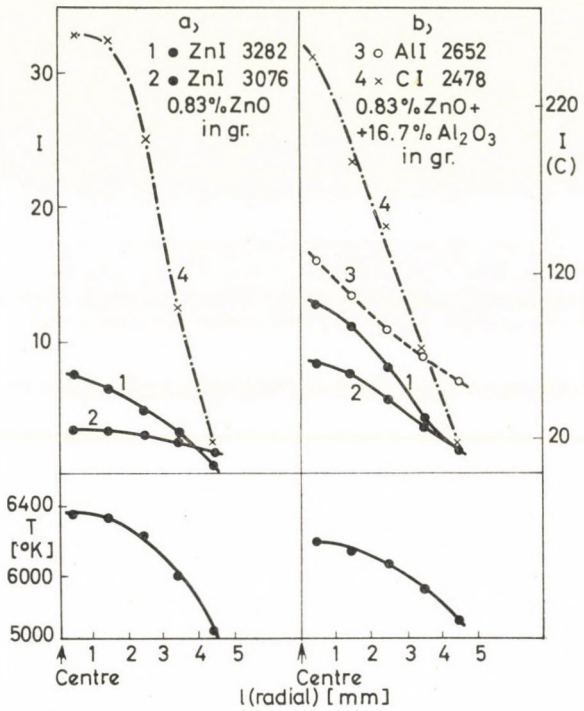

Fig. 3. Radial decline of temperature and line intensities in the middle of the arc gap: *a* —graphite arc, *b* — admixture arc

From Table IV it is more clear that in case of the admixture the outest point of the mantle indicates a higher temperature than in case of graphite. We assumed that this phenomenon was due to the heating effect resulting from the oxidation of aluminium vapours coming from the arc core.

Table IV

Radial temperature data

Distance from centre (mm) (middle of regions)	Temperature (°K)		ΔT $T_1 - T_2$
	Graphite arc (T_1)	Admixture arc (T_2)	
Centre			
0	6380	6180	200
1	6340	6150	190
2	6240	6060	180
3	5980	5900	80
4	5650	5720	—70
Mantle			

4. Discussion

Some contribution to the interpretation of axial transport process

Many interesting studies dealt with mean time spent by atoms in the plasma as *e. g.* [11, 14, 19, 20] and we want to investigate this question using our experimental data. It is known that the intensity of an emitted monochromatic radiation is determined by the atomic properties and the concentration of the free atoms in the arc plasma and by its temperature and electron pressure. Knowing the fundamental arc parameters and the atomic properties of the relevant element it is possible to calculate the concentration of this element in the plasma [14]. In this respect the zinc was handled as a relevant element by us. However, we had no absolute intensity data of the zinc lines and therefore we had only the possibility to calculate the relative distribution of the zinc atoms in the plasma. Using the selected ZnI 3282 line the following approximate equation was applied:

$$\log n_{Zn} = Y_{ZnI\ 3282} - \log K - 5040 \cdot 7.78/T, \qquad (7$$

where n_{Zn} is the number of the free and non-ionized atoms, K contains the instrumental factor, the emission properties and the partition function, the value, 7.78 is the excitation potential [V]. In Eq. (7) we considered that the partition function is independent of the temperature which is allowed here as an approximation [14]. The total number of the species (atoms, ions and molecules) (n°_{Zn}) can be expressed as:

$$n^{\circ}_{Zn} = \frac{1 - \alpha(1 - \beta)}{(1 - \alpha)\beta} n_{Zn} \qquad (8)$$

where α is the degree of ionization of zinc and β the degree of dissociation of zinc oxide.

According to the literature [14] and our temperature values in the core (Table II) the dissociation of zinc oxide can be considered as $\beta \simeq 1$ because its dissociation energy is 6.1 eV [21] which is relatively low. Moreover, α for zinc is negligible as a first approximation (particularly in the anode zone) because zinc has a relatively high ionization energy (9.29 eV). These mean that the data of n_{Zn} give a good information about the total zinc species.

Using Eq. (7) for the first region adjacent to the anode in the graphite arc the $n(\mathrm{rel})_{Zn} = 1$ was taken as an arbitrary step and the value of $\log K$ was calculated. Using this $\log K$ value the other $n(\mathrm{rel})_{Zn}$ data were determined for all regions of both arcs and plotted in Fig. 4.

Generally, we can see that the relative concentration of zinc is higher in the presence of aluminium vapours (curve 2) than in case of graphite arc

(curve 1), although the rate of entry of zinc in the case of both arcs was the same with good approximation. This was established by an earlier method [1] and we got that it was 0.0056 microgram atom Zn/sec.

In order to give a more explanatory reason for the increase of the concentration of the zinc in the presence of aluminium vapours, we draw the

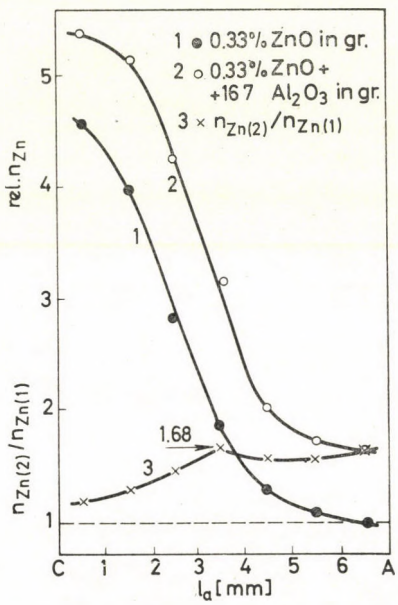

Fig. 4. Axial distribution of zinc in graphite arc (curve 1), and admixture arc (curve 2). Curve 3 represents the concentration ratios between the two arcs

relative concentration ratios between the two arcs represented by curve 3 in Fig. 4. Curve 3 may account for the general trend obtained experimentally as will be explained. Here we used label (1) and label (2) which mean in graphite and in admixture arc respectively.

Our aim is to explain the effect of the low ionization potential element aluminium, upon the axial transport velocity of zinc. With another form, the obtained experimental results can be written:

$$\frac{n_{Zn(2)}}{n_{Zn(1)}} = \frac{\tau_{Zn(2)}}{\tau_{Zn(1)}} = \frac{v_{Zn(1)}}{v_{Zn(2)}} > 1 \text{ or, } v_{Zn(1)} - v_{Zn(2)} > 0\,,$$

where τ is the residence time and v is the axial transport velocity of the relevant element in the arc.

BOUMANS proposed the equation below for describing the axial transport process when the lower sample electrode is switched on as cathode [14]:

$$v = v_c - E\alpha\mu_i, \tag{9}$$

where v_c is the convection velocity of the whole arc gases, E is the axial field strength, α the degree of ionization and μ_i the ion mobility of the relevant element. Applying this equation for our case we get:

$$v_{Zn(1)} - v_{Zn(2)} = \underbrace{v_{c(1)} - v_{c(2)}}_{A} + \underbrace{E_2 \alpha_{Zn(2)} \mu_{Zn^+(2)}}_{B} - \underbrace{E_1 \alpha_{Zn(1)} \mu_{Zn^+(1)}}_{C} \qquad (10)$$

At the first region near to the anode $T_1 = T_2$ and with respect to their low temperature values (Table II), the α values can be taken as equal nearly zero. In this case it means that only part "A" of Eq. (10) has significance in this respect. The convection velocity of the arc gases is larger when the temperature difference is bigger between the arc gas and the surrounding gas system (air) (see Table II), consequently:

$$v_{Zn(1)} - v_{Zn(2)} \simeq v_{c(1)} - v_{c(2)} > 0.$$

Moving towards the cathode the α value is becoming more and more important and therefore the "B" and "C" parts of Eq. (10) too. Here we can account that $E_2 < E_1$, $\alpha_{Zn(2)} < \alpha_{Zn(1)}$ and $\mu_{Zn^+(2)} < \mu_{Zn^+(1)}$, moreover moving towards the cathode the differences between the respective parameters are increasing. As a result the $v_{Zn(1)} - v_{Zn(2)}$ has to decrease monotonously if $v_{c(1)} - v_{c(2)} =$ constant.

According to our investigations $E_2 - E_1$ difference is negative but has not a big value as in case of anode excitation [1]. The negative enhancement of the difference $\alpha_{Zn(2)} - \alpha_{Zn(1)}$ in direction to the cathode is clear from considerations of Table II and on the basis of Table III. The mobility of the relevant ions according to the literature drops in the presence of foreign ions [22] or in general with the increasing of concentration of ions and excited atoms [23]. This was the case in the admixture arc and as a result the $\mu_{Zn^+(2)}$ became smaller and smaller towards the cathode because the concentration of the aluminium vapours became higher and higher. This picture is interfered with a certain limit because the increase of temperature enhances the ion mobility [23].

As a last point for our qualitative discussion of curve 3 in Fig. 4, is the explanation of the maximum point at the centre of the arc gap. According to the above mentioned reasons it seems that there is no possibility to understand this distinguished point on the basis of the variation of α and μ_i values. But we may account this to the variation of the convection velocity along the gap or perhaps there is another kind of process here which had not been taken into consideration.

5. Conclusion

From the described calculation it might be considered that the residence time of zinc was increased in the presence of aluminium as a matrix element. It seems that the proposed explanation of this phenomenon is a good basis for further investigations. However, it was not available to maintain a detailed study for both directions of the arc column due to the use of two different zinc concentrations. But this study is in progress in addition to the measuring of the electron concentration in the various regions.

REFERENCES

1. KÁNTOR, T., HANNA, Z. G., ERDEY, L.: Spectrochim. Acta **243,** 37 (1969).
2. ORNSTEIN, L. S., BRINKMAN, H.: Naturwissenschaften **19,** 462 (1931).
3. MANNKOPFF, R.: Z. Physik 86, (1933).
4. MANDELSHTAM, S. L.: Dokl. Akad. Nauk. SSSR **18,** 559 (1938).
5. SCHUTTEVAER, J. W.: Relative Probabilities of Transitions in Cadmium, Zinc and Strontium Atom, Ph. D. Thesis, University Utrecht (1942).
6. SCHUTTEVAER, J. W., SMIT, J. A.: Physica **10,** 502 (1943).
7. SEMENOVA, O. P.: Izvest. Akad. Nauk. SSSR, Ser. Fiz. **9,** 715 (1945).
8. HULDT, L.: Spectrochim. Acta **7,** 264 (1955).
9. EULER, J.: Ann. Physik **18,** 345 (1956).
10. DIKHOFF, J. A. M.: Spectrochim. Acta **11,** 162 (1957).
11. VUKANOVIČ, V. M.: Proc. of the VIII. Coll. Spectr. Int., Luzern, p. 62—66 (1959).
12. BOUMANS, P. W. J. M.: Some Fundamental Aspects of D. C. Arc Spectrochimical Analysis. Ph. D. Thesis, University of Amsterdam (1961).
13. SCHRIBNER, B. F., MARGOSHES, M.: Anal. Chem. **38,** 297 R (1966).
14. BOUMANS, P. W. J. M.: Theory of Spectrochemical Excitation. Hilger and Watts, London (1966).
15. DE GALAN, L.: Particle Distribution in the D. C. Carbon Arc. Ph. Thesis, University of Amsterdam (1965).
16. MARGOSHES, M.: Appl. Spectroscopy **21,** 92 (1967).
17. BOUMANS, P. W. J. M.: Proc. of the XIV. Coll. Spectr. Int. Debrecen, Hungary, 23 (1967).
18. KÁNTOR, T.: Mathematical Analysis of the Fundamental Relation of Photographic Photometry. Thesis, Technical University of Budapest (1965).
19. ZAIDEL, A. N., KALITEEVSKII, N. I., KUND, G. G., FRATKIN, S. G.: Opt. i Spektroskopiya **2,** 28 (1957).
20. SEMENOVA, O. P., LEVCHENKO, M. A.: *ibid* **13,** 609 (1962).
21. SUN, K. H.: J. Am. Ceramic Soc. **30,** 277 (1947).
22. MEEK, J. M., CRAGGS, J. D.: Electrical Breakdown of Gases, p. 33. Clarendon Press, Oxford, 1953.
23. VON ENGEL, A.: Ionized Gases, *ibid*, p. 112—122 (1965).

Zakaria G. HANNA, Cairo, National Research Centre
Tibor KÁNTOR, László ERDEY } Budapest XI., Gellért tér 4.

Acta Chimica Academiae Scientiarum Hungaricae, Tomus 61 (4), pp. 341—347 (1969)

ANALYSIS OF STEROIDS, IX*

SPECTROPHOTOMETRIC INVESTIGATION OF OESTRA-5(10)-EN-3,17-DIONE AND ITS 3,3-DIMETHYL KETAL

S. GÖRÖG

(Physico-chemical Research Laboratory, Chemical Works of Gedeon Richter Ltd., Budapest)

Received July 1, 1968

A spectrophotometric method has been developed for following of conversion of oestra-5(10)-en-3,17-dione (OeD) into its 3,3-dimethyl ketal (OeDK). The method is based on the fact that OeD reduced with sodium borohydride and treated with hydrochloric acid cannot be measured spectrophotometrically, while the same treatment of OeDK results in an intensely absorbing Δ^4-3-keto compound.

Determination of OeD and OeDK in the presence of each other was carried out by alkaline rearrangement of the OeD contaminant into the Δ^4-isomer; the quantity of the latter was measured by differential spectrophotometry. After treatment with hydrochloric acid, the total quantity of the two compounds was measured by means of the absorption band characteristic to Δ^4-3-keto compounds.

Recently $\Delta^{5(10)}$-3-ketosteroids have achieved increasing importance among 19-nor-steroids. As this bond structure is very sensitive, the 3-keto group is usually protected during the reactions. The most simple method is to prepare the dimethyl ketal.

The analytical method used for the investigation of the rate and conversion of the ketal-forming reaction and for the qualification of the obtained keto compounds should be suitable for the determination of the starting material and the reaction product in the presence of each other.

The possibility to solve the problem by spectrophotometric determination was studied on the pair of compounds shown below:

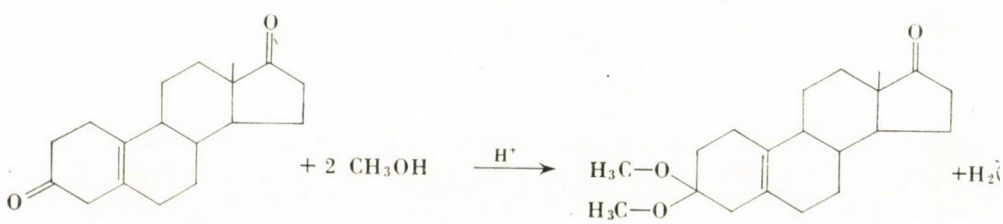

oestra-5(10)-en-3,17-dione
OeD

oestra-5-(10)-en-3,17-dione 3,3-dimethyl ketal
OeDK

* Part VIII: J. Pharm. Sci. **57,** 1737 (1968).

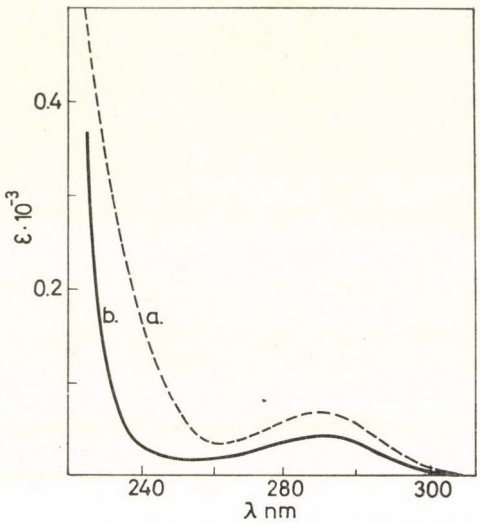

Fig. 1. Ultraviolet absorption spectra of oestra-5(10)-en-3,17-dione and its 3,3-dimethyl ketal in ethanol. Curve *a:* spectrum of oestra-5(10)-en-3,17-dione; Curve *b:* spectrum of oestra-5(10)-en-3,17-dione 3,3-dimethyl ketal

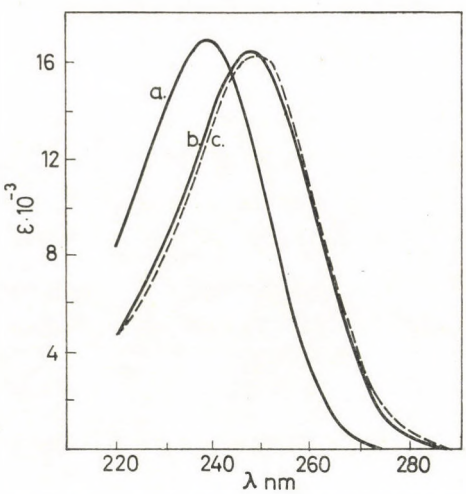

Fig. 2. Ultraviolet absorption spectra of oestra-4-en-3,17-dione and oestra-4-en-17β-ol-3-one. Curve *a:* spectrum of oestra-4-en-3,17-dione in ethanol; Curve *b:* spectrum of oestra-4-en-3,17-dione in water; Curve *c:* spectrum of oestra-4-en-17β-ol-3-one in water

Neither of the two compounds shows light absorption usable for analytical measurements (Fig. 1); treatment with strong acids gives the Δ^4-3-keto compound in both cases (Curve *a* in Fig. 2), so measurements based on the light absorption of this product allow only the determination of the total quantity of the two compounds together.

For a selective determination, reactions suitable to distinguish between the two compounds were required.

Following of the ketal-forming reaction

First our method for following the ketal-forming reaction is described. Our aim was to measure the quantity of the reaction product selectively. This was possible by reduction with sodium borohydride of the $\Delta^{5(10)}$-3-keto system which gives the $\Delta^{5(10)}$-3-hydroxy bond system, while, under the same conditions, the protected carbonyl group in the dimethyl ketal is not affected.

Treatment with sodium borohydride was followed by heating with hydrochloric acid. This has no effect on the $\Delta^{5(10)}$-3-hydroxy system obtained in the reduction of OeD, so no bond system with light absorption is formed; however, heating of the unchanged $\Delta^{5(10)}$-3-ketone dimethyl ketal system with hydrochloric acid converts it into the Δ^{4}-3-keto compound, oestra-4-en-17β-ol--3-one (19-nortestosterone), which has intense light absorption (Curve *c* in Fig. 2). This can be measured selectively, so the progress of the reaction may be followed on the basis of the increasing intensity of the absorption band due to the Δ^{4}-3-keto group.

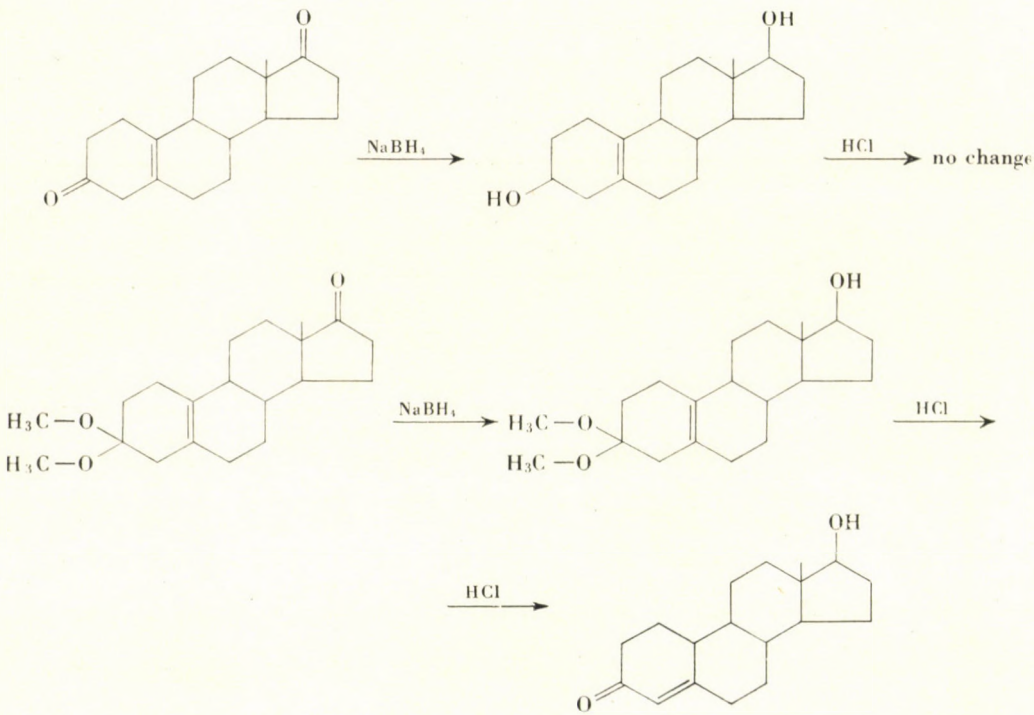

The reaction with sodium borohydride was carried out according to our method developed previously for the determination of unsaturated ketosteroids [1]. Unreacted sodium borohydride was decomposed by acetic acid before the hydrolysis, since direct treatment with hydrochloric acid also starts the simul-

taneous rapid hydrolysis of the dimethyl ketal. This results in the simultaneous presence of the 3-keto compound and sodium borohydride at least for a short time, and this may give rise to an interaction. The produced error would depend on the quantity of unchanged sodium borohydride present and the rate of addition of hydrochloric acid. Acetic acid decomposes sodium borohydride without hydrolysing the dimethyl ketal group, thus such an error can be avoided. Then, boiling the solution with hydrochloric acid effected the desired hydrolysis in a rapid and unambiguous reaction.

Thus the reaction was followed by treating the periodically taken samples with sodium borohydride, then with acetic acid, finally with hydrochloric acid, and the extinctions were measured in water solutions at 250 nm against a reference prepared in the same way but containing no steroid. Complete (100%) reaction is represented by the extinction obtained by the same procedure but without treatment with sodium borohydride, when both compounds are converted into the Δ^4-3-keto derivative.

Our measurements were carried out at 250 nm (which is on the descending side of the spectrum of Δ^4-3-ketosteroids, the maximum being at about 247 nm), because this band suffers a slight bathochromic shift due to reduction of the C-17 ketone group by sodium borohydride [2]. Thus comparison of the extinction with that of a solution hydrolyzed without reduction is possible only at the isoabsorption point of the spectra of oestra-4-en-17β-ol-3-one and oestra-4-en-3,17-dione; it was found to be at 250 nm in aqueous solution (Curves *c* and *b* in Fig. 2).

Determination of oestra-5(10)-en-3,17-dione impurity in its 3,3-dimethyl ketal

The dimethyl ketal obtained from oestra-5(10)-en-3,17-dione always contains more or less starting material. The knowledge of the quantity of this impurity is important in further conversions.

This determination was based on the fact that in mild alkaline medium the $\Delta^{5(10)}$-3-keto bond-system may be converted into a Δ^4-3-keto system, which is measurable spectrophotometrically, while under these conditions the dimethyl ketal remains unchanged.

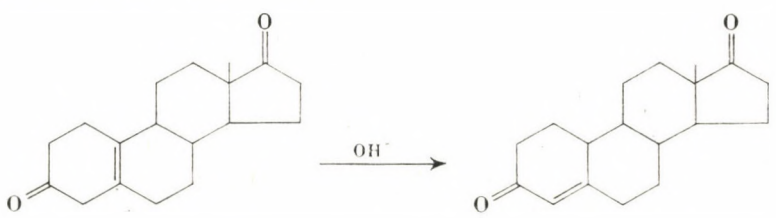

When the extinction of an alcoholic solution treated with an alkali is determined against a similar but untreated solution at 239 nm, the "background" due to light absorption of OeDK is cancelled and the read value will be characteristic to the OeD contamination. The low absorption of OeD makes measurements possible at relatively high concentrations, so high sensitivity can be attained.

As spectrophotometric measurements at 239 nm are rather problematic in alkaline medium, the solution was slightly acidified with acetic acid after the alkaline rearrangement. (Mineral acids cannot be used, because they convert OeDK into the Δ^4-3-keto compound even in cold solution.) The reference solution also contained the same quantities of sodium hydroxide and acetic acid, but they were added in reversed order to exclude the possibility of alkaline rearrangement.

Determination of oestra-5(10)-en-3,17-dione 3,3-dimethyl ketal

The conversion of OeD and OeDK into oestra-4-en-3,17-dione by boiling with hydrochloric acid has been used, as this can be measured spectrophotometrically and is equal to the total quantity of the two compounds. The result should be corrected with the OeD content determined by the above procedure taking into account the ratio of the molecular weights.

Experimental

Reagents of analytical grade were used. The spectrophotometric determinations were carried out on a Spectromom 201 spectrophotometer.

Following of the reaction OeD→OeDK

1.00 ml of the reaction mixture of the ketal formation (OeD content: about 0.03 g) is added to 10 ml of methanol and 1.0 ml of 0.1 *N* methanolic NaOH in a 100.0 ml measuring flask. (Sodium hydroxide is needed to neutralize the weak acid present as a catalyst.) 0.2 g (±5%) of sodium borohydride is added, and after dissolution, the solution is allowed to stand for 15 min. at room temperature. Then 0.5 ml of glacial acetic acid and, after standing for 2 min., 10 ml of 5 *N* HCl are added dropwise. The solution is boiled up and, after cooling, its volume adjusted to 100.0 ml with methanol. 3.00 ml of the obtained solution is pipetted into another 100.0 ml measuring flask, and filled with water up to the mark. The extinction of this diluted solution is determined at 250 nm against a solution prepared in the same way but containing no steroid.

After starting the reaction, a sample of 1.00 ml is withdrawn from the reaction mixture and treated according to the above described procedure except for the addition of sodium borohydride. The extinction of this solution is determined at 250 nm against the reference containing no steroid. The observed value represents the extinction in that case, when the conversion is completed to 100%. The extinctions measured after the reduction with sodium borohydride, given in per cents of this value, directly show the percentage progress of the reaction.

Determination of OeD contamination in OeDK

About 0.15 g of the substance is dissolved in ethanol and the volume adjusted to 50.0 ml. 10.00 ml of the solution is pipetted into a 100.0 ml measuring flask. 1.0 ml of 0.1 *N* aqueous NaOH solution is added, and the mixture allowed to stand for 15 min. at room temperature. 2.0 ml of 0.1 *N* acetic acid solution is then added, and the volume adjusted to 100.0 ml with ethanol.

2.0 ml of 0.1 *N* acetic acid and 1.0 ml of 0.1 *N* NaOH are added to another 10.00 ml portion of the stock solution, which is then filled up to 100.0 ml with ethanol. The extinction of the solution treated with NaOH is determined against this other solution at 239 nm.

The quantity of OeD contamination is calculated as follows:

$$\%_{\text{OeD}} = \frac{500 \cdot E}{E^{1\%}_{1\text{cm}} \cdot B}$$

where $E^{1\%}_{1\text{cm}} = 611$, the specific extinction of Δ^4-OeD at 239 nm in ethanolic medium, and B is the weighed quantity of the substance, in grams.

Determination of OeDK

2.00 ml of ethanolic stock solution prepared as described above, is boiled with 100 ml of water and 10 ml of 5 *N* HCl and, after cooling, its volume is adjusted to 250.0 ml with water, in a measuring flask. The extinction of the solution at 247 nm is compared with that of a similarly prepared solution containing no steroid.

The obtained results are to be corrected with the previously determined OeD content.

$$\%_{\text{OeDK}} = \frac{12500 \cdot E}{E^{1\%}_{1\text{cm}} \cdot B} - \frac{M_{\text{OeDK}}}{M_{\text{OeD}}} \%_{\text{OeD}}$$

where $E^{1\%}_{1\text{cm}} = 512$ is the specific extinction of OeDK after hydrolysis, M_{OeDK} and M_{OeD} are the molecular weights of OeDK and OeD respectively (318 and 272).

Results

Fig. 3 shows curves of the conversion OeD → OeDK at different temperatures.

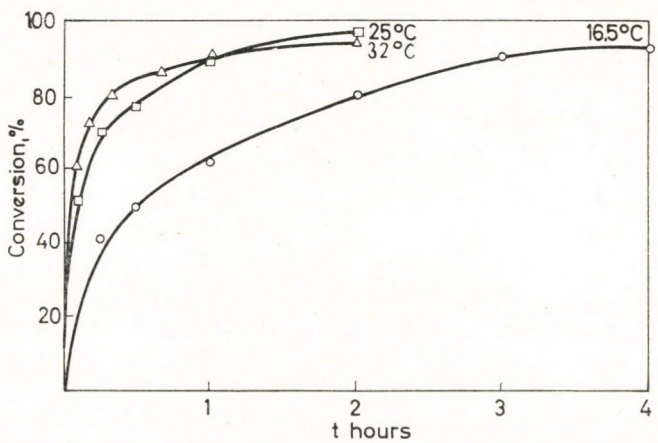

Fig. 3. Following of the conversion of oestra-5(10)-en-3,17-dione into its 3,3-dimethyl ketal. Solvent: methanol. Catalyst: malonic acid. Concentration of oestra-5(10)-en-3,17-dione: 3.0 g/100 ml

The curves cannot be evaluated kinetically, as after an apparently very fast starting period, they flatten considerably. This is caused by starting the reaction, according to the manufacturing technology, by dissolving OeD and malonic acid, the catalyst, simultaneously in methanol of appropriate temperature. Dissolution takes a few minutes, while the reaction is already in progress; however, the moment of perfect dissolution was considered as $t = 0$. On the basis of these curves, the time required for completion of the reaction and the degree of conversion (about 95%) can be stated.

To evaluate the above described methods, mixtures of the two substances were prepared whose OeD content varied between 0 and 5%. The results obtained are shown in Table I. The difference between the weighed amounts and found quantities of OeD did not exceed ± 0.15 absolute per cent, so this method gives results of satisfactory accuracy, even in the presence of 0.5% OeD contamination.

Table I

	OeD, %		OeDK, %	
	Weighed	Found	Weighed	Found
1.	4.76	4.81	95.2	95.6
2.	3.10	3.17	96.9	97.4
3.	1.92	1.80	98.1	98.9
4.	0.90	0.99	99.1	99.2
5.	0.51	0.46	99.5	99.0
6.	0.30	0.24	99.7	99.4

The corrected values regarding the quantity of OeDK present in excess, agree within $\pm 1\%$ with the calculated ones.

*

The author's thanks are due to Mrs. Gy. BERHIDAI for her useful assistance in the experiments.

REFERENCES

1. GÖRÖG, S.: Steroids **11**, 93 (1968)
2. ENGEL, L. L.: Physical Properties of the Steroid Hormones, p. 90. Pergamon Press, Oxford — London — New York — Paris, 1963

Sándor GÖRÖG; Budapest X., Gyömrői út 21.

Acta Chimica Academiae Scientiarum Hungaricae, Tomus 61 (4), pp. 349—366 (1969)

EXPERIMENTAL STUDY OF POSITIVE ION EMISSION FROM TUNGSTEN, I

O. KAPOSI and M. RIEDEL

(Physical, Chemical and Radiological Department of the L. Eötvös University Budapest)

Received July 15, 1968

A method was elaborated for the measurement of positive ion emission of metals by means of a time-of-flight mass spectrometer. The method permits the determination of the nature of the ions emitted and also the study of the very fast processes involved.

The mechanism of positive ion emission from helical tungsten filaments was studied in details by measuring temperature and time dependence of the emission in the cases of both not preheated and annealed spirals. Measurements on molybdenum resulted curves corresponding to those obtained for tungsten. Continuous and impulse-like (the latter caused by ion bursts) ion currents could be detected. The absolute value of both currents could be measured as well. Thus, height and shape of the ion burst pulses and the number of ions creating the pulses could be evaluated for various temperatures. Measurements on monocrystals and linear wires were performed too. Comparing their results with those on helical filaments for the role of additive materials and their position in tungsten could be explained.

As early as 1913, RICHARDSON [1] observed the emission of positive ions from hot metal surfaces. During the subsequent years this phenomenon has been investigated on various metals by a great number of authors [2, 3, 4]. With the recent developments in vacuum technique the interest has been focused more and more on the ionic emission from tungsten. It seems that many, practically important phenomena are closely related to the positive ion emission from tungsten. Such are the anomalous flicker effect observed in diodes [5, 6, 7, 8], the presence of a number of unusual background peaks in high-sensitivity solid sample mass spectroscopy with the use of multifilament surface ionization source [9], arcing occurring in electric bulbs [10—16], disturbances in certain types of mass spectrometry and in the application of the ionization gauge [17, 18], to mention only the most important problems.

The intensive positive ion emission in the cases mentioned above can be related to the technology used for the production of tungsten [19, 20]. It was discovered some decades ago that heated tungsten coils kept their shape remarkably well, if about 1% of other materials (KCl, SiO_2, Al_2O_3) are added to tungsten at an appropriate stage in the manufacturing process. During the shrinking process the major part of the additives evaporates but an extremely small fraction remains in the "fibre structured" drawn tungsten wire. During the recrystallization of the wire the presence of this small fraction

of additives leads to the formation of large crystals with longer boundaries between them. When the metal is heated the additives are gradually emitted and owing to the high degree of ionization of the alkali metal atoms on tungsten [21], ion emission of relatively high intensity can be observed.

In connection with this positive ion emission from tungsten, it is of practical importance to investigate the mechanism of the emission process. In the earlier experiments there has been a great fluctuation in the experimental data and it was difficult to obtain reproducible results. The experimental method to be described in the next section permits to obtain reproducible experimental data. It is possible to infere from the measurements not only the mechanism of the ion emission process but to obtain information on the location and motion of the impurities present in the metal if one compares the measured data with other experimental results on the structure of tungsten.

Experimental

The emission measurements were performed with the use of a linear ion path time-of-flight mass spectrometer developed and built in the Nuclear Chemistry Department of the Central Research Institute for Physics [22]. In principle of construction this equipment conforms to the Bendix apparatus [23]. The length of the flying tube is 1 m, the acceleration voltage is 1000 V and the operational frequency is 10 kc. With the time delayed ion focusing, similar to that developed by WILEY and MCLAREN [23] its resolving power is 100. This relatively low resolving power is not disadvantageous if one considers the small masses of ions which are emitted from tungsten. Its great speed and the continuous recording of spectra changing in time are a definite advantage for the study of rapidly varying processes, like ion emission.

During our measurements the tungsten filament to be investigated acted as a surface ionization ion source, and so only the spectrum of positive ions emitted as a result of heating the tungsten appeared on the detection oscilloscope. The sample was spot-welded on a sample holder (A) and placed directly into the ion source between the plate used for source backing (B) and the ion collector grid (C), as shown in Fig. 1.

In Fig. 1 the accelerator grids are lettered by D and E, the insulating rods prepared from teflon by F, the joints by G, and the flight tube by H.

For the investigation of the time behaviour of the emission processes, the temperature of the filament had to be increased at different rates in a reproducible manner. The heating voltage was therefore continuously and almost linearly variable by means of an electronic control circuit permitting to adjust the end temperature of the filament to any desired value.

The varying temperature of the filament was measured with an Uher-type electronic pyrometer which was calibrated with an Evershed high precision optical pyrometer. Since the time constant of the electronic pyrometer is 5 ms, the temperature of the filament could be measured continuously. The output voltage of the pyrometer which is proportional to the temperature and the emission spectrum was recorded on the same oscilloscope which could be filmed at different speeds, as desired. A microscope equipped with a micrometer was used to read the temperature mark and the peak height from the oscilloscope. The variance in the measured values of peak height was 1—2% and the accuracy of the temperature measurement was about ± 30 °C.

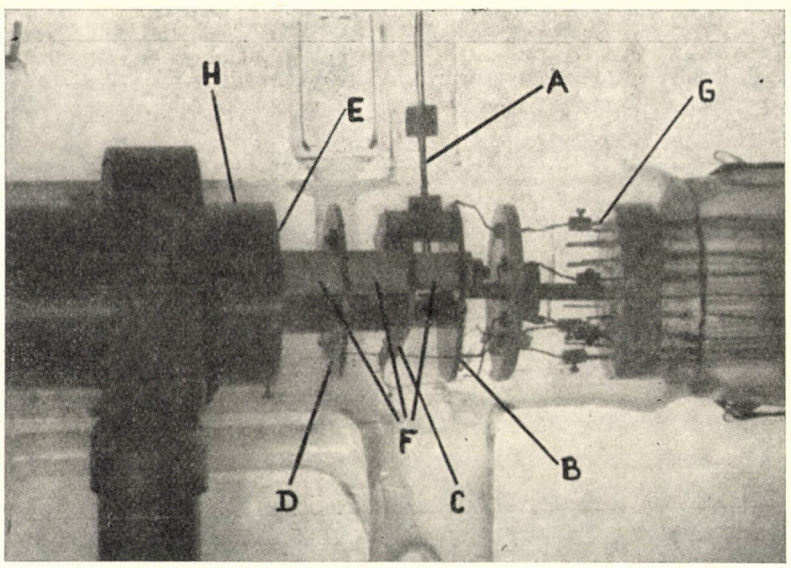

Fig. 1. The ion source of the time-of-flight mass spectrometer

In some cases the spectrum was measured with the KFKI-type multi-channel analyser or with selective automatic energy counter, type Gamma NK-108. Controlling the coincidence circuit of the multi-channel analyser by appropriate gating pulses, it was possible to analyze separately the peaks produced in the spectrum by different mass numbers.

The very low ion current output signal was amplified by EMI type multiplier and Gamma A-11-R2 high frequency amplifier before the oscilloscopic display and thus only relative ion intensity measurement could be performed. The measurement of the effective intensity of the ion current and the calibration of the mass spectrometer was performed with a 401/1 type Radelkis vacuum tube meter with $10^{11}\ \Omega$ internal resistance. With this the value of the voltage drop across 3.3 $M\Omega$ due to the ion current was measured.

Results

As a first step in the present measurements, the composition of the ion current emitted from 100 W electric bulb filament, (product of the United Incandescent Lamp and Electricity Co. Budapest) was evaluated. It was found, in agreement with other authors [3, 9, 14, 24, 25] that the emitted ion current is composed mostly of potassium and in less extent of sodium ions, and that the initial temperature for ion emission is at about 1100 °K. In some cases also Cs^+ and Rb^+ ions were detectable, but in spite of the very high ionization efficiency of these metals on tungsten, the detected quantities were very low.

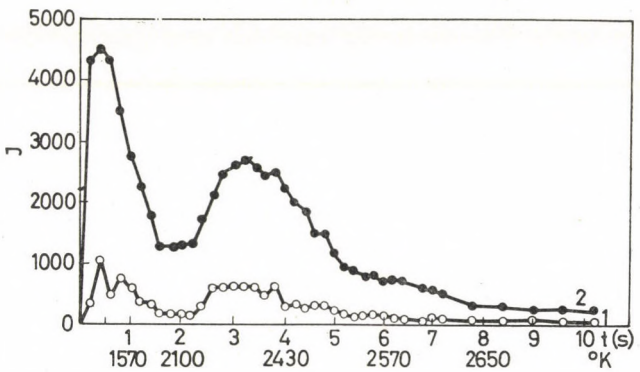

Fig. 2. Ion emission I (arbitrary units) of tungsten filament vs. time (seconds) and temperature (°K) with relatively slow heating up. Curve 1, for Na^+, curve 2, for K^+

Infrequently, rapidly decaying Li^+ and probably Al^+ ions could be identified. W^+ and WO^+ ions originating from the filament yielded very poor intensity and only above 2700 °K.

In each case only Na^+ and K^+ ions were emitted in measurable quantities. In case of strongly ignited filament (the heating temperature was about 2500 °K), the number of Na^+ ions substantially diminished, but the emission of K^+ ions could be measured even after several hours of heating. The time and temperature curves plotted for Na^+ and K^+ emission are shown in Fig. 2.

An unpreheated 100 W electric bulb spiral was investigated. The measurement from the initial temperature for ion emission up to 2650 °K takes 8 seconds and the filming of the spectrum yields 5 pictures/s. The two maxima visible on the curves (curve 1 for Na^+, curve 2 for K^+) appear sharply in each case of the numerous emission curves which were recorded and are seen to lie in about the same temperature interval. In the heating-up period the ion current is greater by a few orders of magnitude than after some minutes of annealing when the ion emission attains a steady value which in the case of potassium is nearly constant in time.

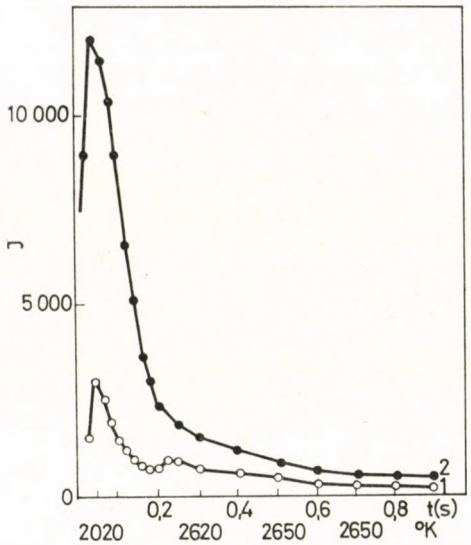

Fig. 3. Ion emission vs. time and temperature with high speed heating up

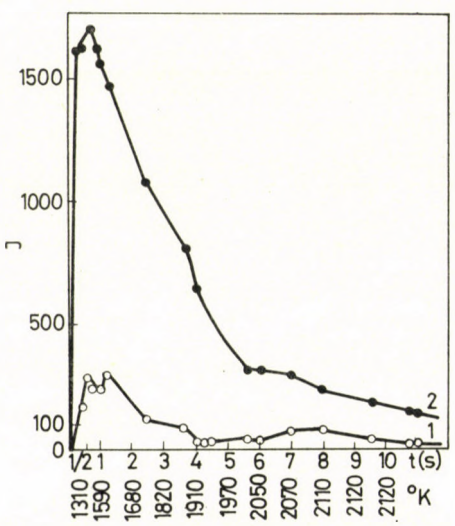

Fig. 4. The time and temperature curves for Na^+ and K^+ emission plotted on the heating up of Mo. The diameter of the Mo wire was 80 μ

On fast heating-up only one, well defined but higher maximum can be observed as apparent from Fig. 3 where the non-annealed filament was heated to 2650 °K in 0.3 s.

In order to see whether the shape of the ion emission curve and the nature of the emission is specific for tungsten, or similar to those obtained for other

metals, the ion emission from Mo prepared by the same powder metallurgical method, but without additives, was measured. Mo was chosen because it has the same crystal structure as tungsten, though its melting point is much lower. On the heating up of Mo relatively intensive but not so high Na^+ and K^+ ion emission and at times the presence of Rb^+ peaks, again much lower than in the case of tungsten, could be observed. The time and temperature curves for Na^+ and K^+ emission plotted on the heating up of Mo are shown in Fig. 4.

In contrast to the curves for tungsten, two separate maxima cannot be observed in the molybdenum curves. Owing to the lower melting point o

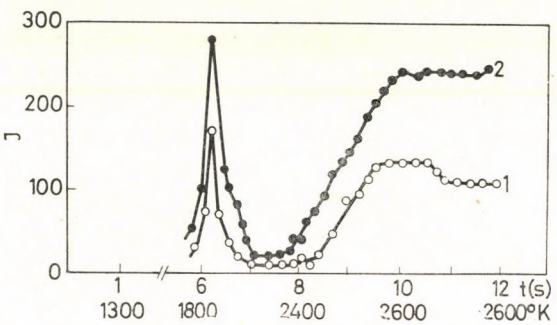

Fig. 5. The time and temperature behaviour of the ion emission in case of moderately annealed tungsten filament

Mo, the temperature interval for ion emission is much narrower and the filament could not be heated above 2100 °K without blowing out. In spite of the different heating-up temperatures, many similar characteristics are observable in the emission spectra of the two metals. The emission is markedly more intensive in the first period of heating [26]. A rapid decrease in the intensity is observable as the temperature continues to rise until finally the emission attains a steady value for both metals, which, as we shall see, is governed by a closely similar mechanism.

The time and temperature behaviour of the ion emission was studied also on tungsten filament which had been already moderately annealed (at 2500 °K). The results are shown in Fig. 5.

The zero point on the time scale in Fig. 5 coincides with that at which the heating was started and not with that of ion emission as in the non-annealed case. The curves in Fig. 5 considerably differ from those shown in Fig. 2. In Fig. 5 a brief transient peak is observable on the curve at about 1800 °K which appears on both increasing and decreasing the sample temperature and even in the case of strongly annealed filament when only the potassium current was detectable.

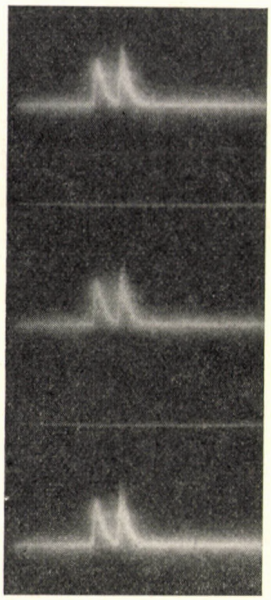

Fig. 6. Photograph of the Na^+ and K^+ spectra. The Na^+ peak is seen on the left hand side, the other is the K^+ peak

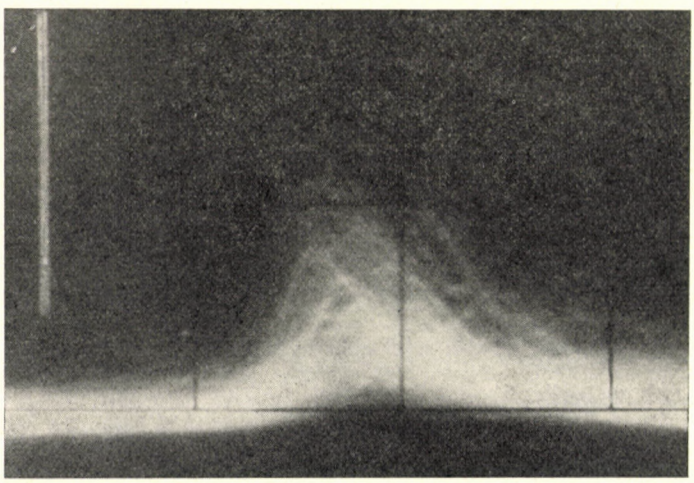

Fig. 7. The photograph of potassium ion peak. The sweeping time of the oscilloscope is 1 μs/cm. The vertical line is the temperature proportional sign

On repeated heating of the filament not only the shape of the time dependence but also the character of the ion emission was observed to undergo a change. It was found, in agreement with earlier authors [6, 7, 27] that not single ions but, in a far greater number, ion bursts of various sizes are emitted.

This observation was confirmed by the photographs taken of the Na^+ and K^+ spectra shown in Fig. 6.

The burstlike-character of the ion emission is indicated in Fig. 6 by the fact that the different mass peaks, specially in the case of potassium, have no definite ending because of the irregular burst amplitudes. The phenomenon is even more discernible in Fig. 7 where the potassium peak is pulled apart on the oscilloscope with a sweeping time of 1 μs/cm.

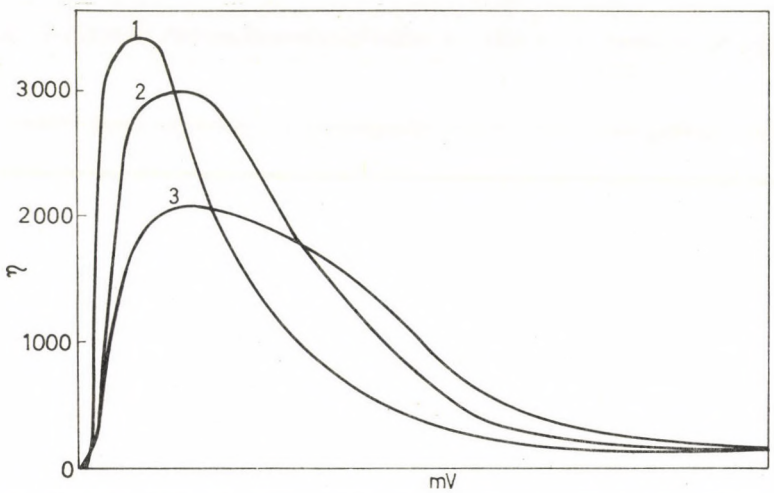

Fig. 8. The amplitude distribution of potassium ion bursts recorded in 20 s. The filament was heated up within 12 s from room temperature to 2800 °K. Curve 1 shows results of measurements from 0—20 s, curve from 40—60 s, and curve 3 after 5 min of heating

Using a multichannel pulse height analyzer we were able to follow the process of the emission becoming gradually burstlike with rising temperatures in the case of non-annealed filament. The amplitude distributions of Na^+ and K^+ bursts could be measured separately by the multichannel analyzer. The curves for K^+ bursts are shown in Fig. 8.

The filament was heated up from room temperature to 2800 °K in 12 seconds. The number of bursts (n) as a function of amplitude (mV) was recorded for 20 seconds of heating. Curve 1 was plotted for the period from 0 to 20, Curve 2 for that from 40 to 60 s and Curve 3 after annealing for 5 minutes. It can be seen that with the progress of heating time the ion burst distribution becomes increasingly heterogeneous and shifts towards greater amplitudes, that is, the burst-type emission starts to predominate. The same observation could be made in the Na^+ distribution.

To establish the size, duration, shape and number of ion bursts as a function of temperature, a filament already annealed at 2500 °K for 1 hour was

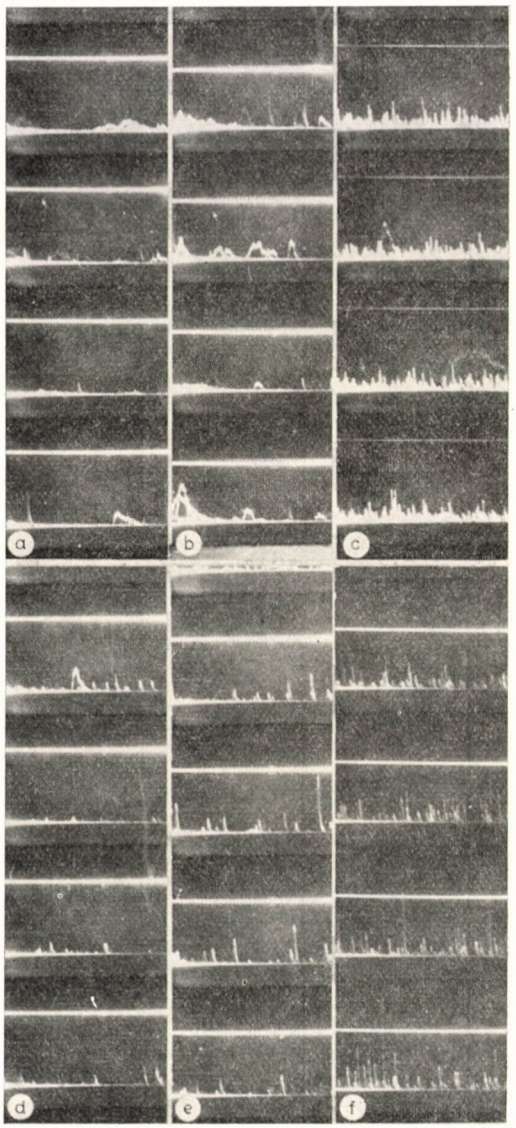

Fig. 9. The size, duration, shape and number of ion bursts as a function of temperature. The oscilloscope sweeping time was 10 μs/cm. The distances of the lines above the spectrums are proportional to the temperatures. Picture a) was taken at 1420 °K, b) at 1620 °K, c) at 1810 °K, d) at 2070 °K, e) at 2330 °K and f) at 2570 °K

heated to different temperatures while the oscilloscope screen was filmed (Fig. 9).

In this experiment the spectrometer was not operated in the usual manner, that is, the emitted ions were not accelerated per pulse but continuously. In this case the ion current was not focused and the ions reached thus the

collector successively as they were emitted. Owing to the strong annealing before the experiment, the ion bursts from the filament consisted predominantly of potassium. The pictures which were taken at different temperatures but otherwise under the same conditions, show the following. At temperatures above 2300 °K the number of ion bursts suddenly increases, their distribution becomes increasingly heterogeneous and the rise time decreases. As the oscilloscope sweeping time was 10 μs/cm the length of the ion bursts could be evaluated; it varied from 1 μs to 5 μs. At about 1650 °K, however, 10—20 μs values were found predominantly. A maximum in the number of bursts is

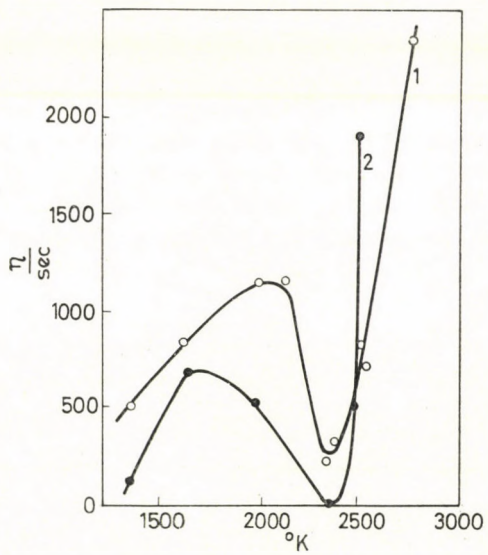

Fig. 10. The number of emitted ion bursts per seconds as a function of temperature. Curve 1 refers to the Na^+ ion and curve 2 to the K^+ ion

observed between 1700—1900 °K which diminishes at 2100 °K and increases again suddenly above 2300 °K.

To get a more accurate picture of this behaviour, the number of ion bursts emitted per second was evaluated as a function of temperature with the use of the multichannel analyzer. Since in this experiment an only slightly annealed filament was used, the number of Na^+ bursts was also considerable, as seen in Fig. 10 where Curve 1 stands for the Na^+ and Curve 2 for the K^+ bursts.

Fig. 10 shows the same results as the foregoing pictures. The temperature interval (1600—2000 °K) for transient ion emission is the same in the case of continuous and of periodical heating up, when the filament is kept for some minutes at the same temperature. The burstlike ion emission increases in both cases at the same values of temperature.

By determining the effective ion current some additional important informations could be obtained for the mechanism of the emission. The results indicated the ion current to be greater with three orders of magnitude, when a not annealed filament was heated up (in this case the ion emission predominantly continuous) than the stationary (mostly impulse-like ion current) of the annealed filaments. In the first case about 10^{-9} A ion current was recorded, while at the stationary emission this value decreased to 10^{-12} A. Owing to the rapid decrease during the first heating up period (see Fig. 2) the obtained results were inaccurate. The stationary emission current, however, showed only minor fluctuations. In order to evaluate the ratio of individual ions to those which emit in bursts in the stationary ion current, the total integrated current was measured with a vacuum tube meter, and the amplitude distribution of the ion bursts was analyzed using an automatic selective counter type Gamma NK 108. Performing the measurements at different temperatures, the length of the ion bursts and the number of ions composing them, could be calculated. The results obtained using tungsten wires and single-crystals, prepared from the same wire, are compiled in Table I.

Table I

The value of integrated and burstlike ion current as a function of temperature in case of tungsten wire and monocrystal

Temp. K°	Wire diam. 30 μ		Single-crystal diam. 30 μ	
	Impulselike curr. C/s	Integrated curr. C/s	Impulselike curr. C/s	Integrated curr. C/s
1260	$1.03 \cdot 10^{-15}$	$0.45 \cdot 10^{-15}$	$0.92 \cdot 10^{-15}$	$0.45 \cdot 10^{-15}$
1360	$8.18 \cdot 10^{-15}$	$5.86 \cdot 10^{-15}$	$1.54 \cdot 10^{-15}$	$0.48 \cdot 10^{-15}$
1650	$28.70 \cdot 10^{-15}$	$22.50 \cdot 10^{-15}$	$2.85 \cdot 10^{-15}$	$6.30 \cdot 10^{-15}$
1870	$18.80 \cdot 10^{-15}$	$13.50 \cdot 10^{-15}$	$1.44 \cdot 10^{-15}$	$2.70 \cdot 10^{-15}$
2150	$80.30 \cdot 10^{-15}$	$74.30 \cdot 10^{-15}$	$12.20 \cdot 10^{-15}$	$8.50 \cdot 10^{-15}$
2360	$807.00 \cdot 10^{-15}$	$568.00 \cdot 10^{-15}$	$128.00 \cdot 10^{-15}$	$79.00 \cdot 10^{-15}$

The results show that the currents measured in the two different ways are in the same order of magnitude. This means that the stationary emission is nearly completely impulse like. It can be seen from Table I that lower ion current was measured in case of single-crystal.

The number of ions which created a single ion eruption was calculated from ion current measurements and from analyses of the ion bursts. Some results are given in Table II.

The results show that the number of ions creating one burst varies from a few to several thousands.

Table II

The number of ions which create a single ion eruption at 1 μs; 5 μs and 20 μs burst lengths

The amplitude of ion current 3.10^{-13} A	The number of ions in case of diff. burst lengths		
	1 μs	5 μs	20 μs
1	2	10	37
10	19	94	375
100	188	940	3750

Some preliminary experiments indicated that the stationary ion emission of molybdenum had also a burstlike character. It was found that the amplitude and the length of the ion bursts were considerably less and the amplitude distribution was more homogeneous in the whole temperature interval when molybdenum was heated.

Discussion

Prior to the discussion of the experimental results, a brief summary of the experimental data on the structure of and particularly on the location and behaviour of trace impurities in tungsten is presented [28, 29].

Several authors [30, 31, 32] were able to show that drawn tungsten wires consist of bunches of fibres, 1—3 μ in diameter. This fibre structure disappears, if the wires are heated over 2000 °K and transforms to a microcrystalline type (primary recrystallization). After prolonged annealing at 2200°—2500 °K a secondary recrystallization takes place. The latter process is rapid [33]. In the presence of additives like K, Si, Al the length of the secondary crystallites (so-called GK wire) will be 10 to 100 times that of the wire diameter. The new crystallites are oriented parallel to the axis of the wire and result in a structure with longo verlapping boundaries [34, 35, 36] of excellent tensile properties.

MEIJERING and RIECK [30] assume the above crystallite structure to be due to the tube-like coverage of the surface of the fibrous crystallites by the additives, though this coverage cannot be regarded as homogeneous since the strands are blocked at several points. Assuming the distribution of barriers and leaks to be statistical, the growth of the secondary crystallites is far less impeded in the direction of the axis as compared with any growth in the lateral direction.

On the other hand MANNERKOSKI [35, 37] and MILLNER [19] claim, that the active impurities, like potassium, are present in the tungsten lattice before the recrystallization in the form of solutes and the tube-like coverage forms only during the formation of the secondary crystallites from the columnar structure which develops from the primary crystallites. In the columnar struc-

ture the overlapping boundaries of the texture elements along the axis the so-called tilt boundaries contain predominantly edge dislocations which can move only in the vertical direction. In contrast, the horizontal boundaries between the crystallites are so-called twist boundaries [38] containing overwhelmingly screw dislocations which can move mainly in the horizontal direction. On heating, the number of dislocations in the wire diminishes until the onset of thermodynamic equilibrium. During this process the dislocations move towards the surface of the lattice displacing also the impurity atoms.

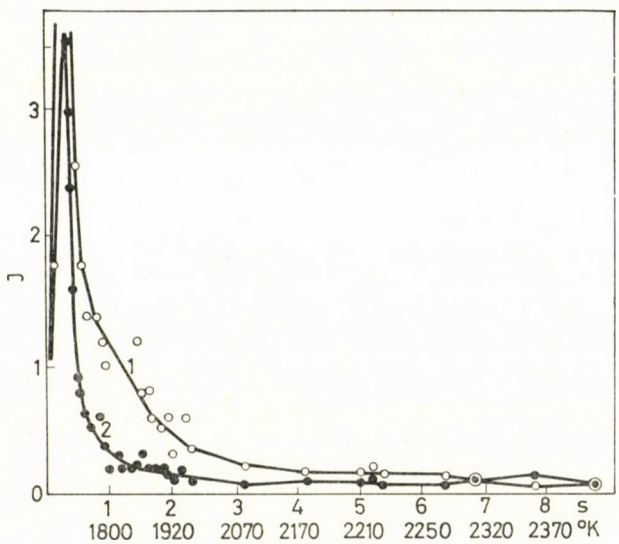

Fig. 11. Ion emission of a single-crystal tungsten wire vs. temperature with relatively slow heating up

As known [39, 40], the contaminant atoms are displaced primarily with the edge dislocations and as a result accumulate to constitute walls along the axis of the wire.

In the light of above theories our experimental data can be interpreted as follows. In Fig. 2 the first maximum, observed on the first heating up of non-preheated wires can be attributed mainly to the desorption of alkali impurities from the surface, the second to recrystallization effects in tungsten. As already shown in the autoradiography experiments performed by MILLNER *et al.* [41, 42, 43] on other metals, impurity atoms move along with the new crystallite boundaries under formation at a speed exceeding that of boundary diffusion [40] and are crowded therefore into inclusions formed along the reduced number of crystallite boundaries.

From these inclusions the impurity atoms travel to the surface mainly through dislocations by pipe diffusion [40]. For this there must exist a large

number of dislocations due to the internal stresses resulting from the machining (drawing, twisting) of the metal [30]. The dislocations act as centers for the gathering of the impurity atoms into so-called COTTRELL clouds [44], causing a stability for dislocations. On the slow heating-up of metals, the dislocations together with their COTTRELL atmosphere move slowly towards the crystal boundaries where they disappear. In case of fast heating-up the rapid temperature increase induces a great thermal activation for dislocation movement and the thermal motion of the dislocations becomes fast enough to leave

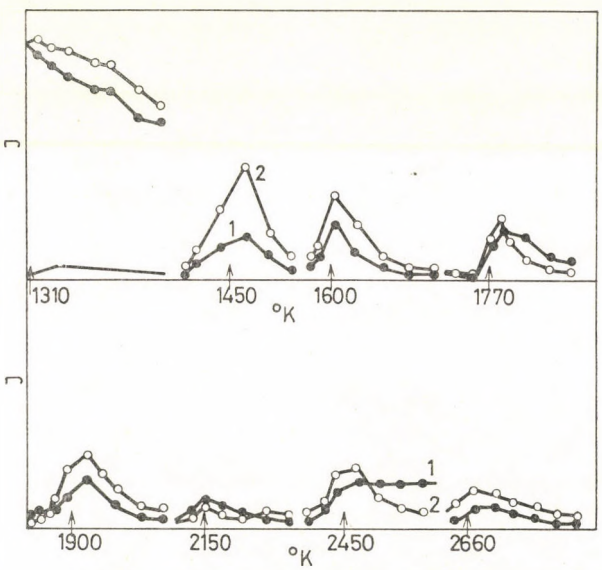

Fig. 12. Ion emission of non-annealed tungsten filament in case of stepped heating. The lowest curve at 1340 °K denotes the Cs^+ ion

behind the COTTRELL atmosphere moving by lattice diffusion. This explains why the second maximum could not be observed on fast heating up (Figs 2 and 3).

The assumption that the second maximum, observed when the sample was first and slowly heated up, is due to recrystallization, was confirmed by the measurement on single-crystal, when only one emission peak was observed under the same experimental conditions (Fig. 11).

The large number of dislocations required by this mechanism was revealed by the experiments of MINTURN, DATZ and TAYLOR [7] and the data reported by HEGEDÜS *et al.* [45]. The ion emission from tungsten was found to increase markedly, if the sample was under either mechanical or thermal stress which is known to produce dislocations. We have also observed this phenomenon on the stepped heating of non-annealed filaments (Fig. 12).

It is apparent from Fig. 12 that the ion emission exhibits a transient maximum before attaining a steady value whenever the non-annealed wire is rapidly heated up from any temperature. The highest peak is observed on the first heating-up and it becomes gradually lower with each repeated heating. It is of interest to note that the maximum obtained on heating up to 2150 °K is lower than that observed on the heating to either lower or higher temperatures. This observation is a further evidence of the minimum occurring in this temperature region obtained also in the case of continuous heating-up.

On continued heating after the second maximum, the ion emission shows an exponential decrease. This is due to the removal of the impurity centers close to the tungsten surface, *i.e.* to the decrease in the concentration gradient in the surface region.

At temperatures above that of secondary recrystallization (2500 °K) the activated random walk of the impurities in tungsten is accelerated to an extent at which the attraction of lattice defects cannot assert itself anymore and pipe diffusion through dislocations and grain boundaries is overwhelmingly replaced by lattice diffusion [40, 46]. This model can be used for the interpretation of the ion burst data in Fig. 9. The long (10—20 μs) bursts obtained at lower temperatures are the results of pipe diffusion by which the impurity atoms are brought to the surface in the form of the Cottrell clouds moving along with the dislocations. The front dislocation arriving to the surface acts as a piping aperture for the impurities which emerge from the surface by thermionic emission as determined by the Saha—Langmuir equation [21]. Since the duration of bursts probably depends on the pipe length and the emission rate, bursts of various lengths and amplitudes may appear along with that of predominant length. Thus, it is possible to estimate the number of dislocations from that of the different bursts. At 1800 °K this number was estimated as $10^6/cm^2$.

In the bursts characteristic of higher temperatures, the ions are brought to the surface by another mechanism, mainly by lattice diffusion. To explain the bursts above secondary recrystallization temperature, we have to consider the behaviour of the impurities arriving to the surface of tungsten. The impurities are first adsorbed on the metal surface and, depending on the temperature, they remain adsorbed *e.g.* in the range from 1000 to 2500 °K for 10^{-3}—10^{-5} s, on the average [21]. The activation energy for the adsorbed ions migrating on the surface corresponds to about 50% of the heat of desorption. Their migration rate is determined by the surface diffusion coefficient. Calculating with the data of POPP [48], at *e.g.* 2000 °K their average displacement while adsorbed on the tungsten surface, is $\sim 10^{-3}$ cm.

According to RASOR and VARNER [49] it can be estimated that surface systems for which E is greater than kT (where E is the mean energy difference between the atomic and ionic state and kT is the thermal energy) should cause

the adsorbed particles to uniformly cover crystal faces like a two dimensional gas. Systems in which E is small or negative should concentrate by condensation effects. In this case adsorbed particles should avoid uniform high work function crystal faces and concentrate at their boundaries or on low work function faces. In the case of potassium and sodium these two effects seem to complete at the temperature of incandescence, and depending on the temperature and surface inhomogeneities, the ions either condense or spread out over a large area.

The impurities are desorbed from the tungsten surface with a heat of desorption which depends on the surface coverage. Part of the impurities, with sufficient energy owing to the thermal energy distribution, leaves the surface, while the rest condense, as determined by the structural heterogeneities [21]. At these spots the presence of adsorbed gases and the covering of the surface by the alkali particles lead to a decrease in the energy required for the desorption [50, 51] and a large number of ions, with a lower thermal energy, can leave the surface at once, in the form of ion bursts. Thus, at lower temperatures the ion bursts are brought about by pipe diffusion, at higher temperatures mainly by surface migration.

At increasing temperatures the value of kT increases relative to E (in case of Na and K), that is the ion condensation rate increases simultaneously with the range of surface migration. As a result more ions leave the surface at the same time, that means the formation of more bursts with higher energies. This is apparent from the amplitude distribution of the burst analyzed in Fig. 8.

The number of particles creating one burst (characterized by the burst amplitude) depends thus on the measure of ion condensation and their thermal energy distribution. The energy distribution is Maxwellian, as apparent from curve 1 in Fig. 8, which can be described by the equation:

$$y = 13\,920 \sqrt{x} \exp\left(-\frac{x}{0.21}\right)$$

Considering the data reported on the physicochemical investigations of other authors it is possible to explain part of the present results. Any of the available models fails to account for the transient ion emission observed on annealed filaments. It has been suggested [25, 27] that an increased formation rate of tungsten oxide in this temperature interval leads to an increased tungsten evaporation owing to the volatility of oxides. This assumption is, however, contradicted by the observation that on fast repeated heating or cooling to the temperature of transient ion emission a maximum is observed even at very low partial oxygen pressure (10^{-7} mmHg). It has to be established whether this shape of the emission curve observed for annealed filaments is due to a

change in the surface emission of the alkali impurities or to the combination of several processes. This is the main object of our continued investigations.

*

Authors are indebted to Mr. GY. BAKTAI and Mr. S. SALY and to Dr. J. NEUGEBAUER (Tungsram Ltd.) for their courtesy of supplying the samples and the preparation of the single-crystals for the experiments and for many useful discussions.

REFERENCES

1. RICHARDSON, O. W.: Proc. Roy. Soc., (London) **89,** 507 (1913).
2. WAHLIN, H. B.: Phys. Rev. **34,** 164 (1929).
3. SMITH, L. P.: Phys. Rev. **35,** 381 (1930).
4. LICHTMANN, D.: The J. of Vac. Sci. and Tech. Vol. 2, No 2, 1965.
5. JOHNSON, J. B.: Phys. Rev. **26,** 71 (1925).
6. LINDEMANN, W. W., VAN der ZIEL, A.: J. Appl. Phys. **28,** 448 (1957).
7. MINTURN, R. E., DATZ, S., TAYLOR, E. H.: J. Appl. Phys. **31,** 876 (1960).
8. MINTURN, R. E., DATZ, S., TAYLOR, E. H.: J. Appl. Phys. **31,** 880 (1960).
9. FRAZER, J. W., BURNS, R. P., BARTON, G. W.: Rev. Sci. Instr. **30,** 370 (1959).
10. CLAPP, R. H.: Illum. Engng. **6,** 357 (1950).
11. SZELÉNYI, T.: Acta Techn. Acad. Sci. Hung. **34,** 453 (1961).
12. SZELÉNYI, T.: Acta Techn. Acad. Sci. Hung. **34,** 457 (1961).
13. BUCHANAR, A. G.: Trans. Illum. Eng. Soc. (London) **29,** 15 (1964).
14. ROBOZ, P., KOVÁCH, A.: Acta Techn. Acad. Sci. Hung. **51,** 277 (1965).
15. KAPOSI, O., MATUS, L., SÜLI, M.: Magy. Kém. Foly. **73,** 245 (1967).
16. KAPOSI, O., RIEDEL, M., BAKTAI, Gy.: XIV. Coll. Spectr. Internat. 7—12 August 1967, 1541—1551.
17. TAYLOR, J. B.: Z. Physik **57,** 242 (1929).
18. DATZ, S., TAYLOR, E. H.: J. Chem. Phys. **25,** 389 (1956).
19. MILLNER, T.: Acta Techn. Acad. Sci. Hung. **17,** 67 (1957).
20. SMITHELLS, C. J.: Tungsten. (III. Edition) Chapman and Hall Ltd. London, 1952.
21. KAMINSKY, M.: Atomic and Ionic Impact Phenomena on Metal Surfaces. Springer-Verlag, New York, 1965.
22. MATUS, L.: MTA Közp. Fiz. Kut. Int. Közl. **13,** 4 (1965).
23. WILEY, W. C., MCLAREN, I. H.: Rev. Sci. Instr. **26,** 1150 (1955).
24. SASAKI, N., INOUE, H.: J. Chem. Soc. Japan **76,** 473 (1955).
25. HORVÁTH, A., HEGEDÜS, A. J., KEREK, L.: Microchimica Acta 1967/3. 431—451.
26. LICHTMAN, D., KRIST, T. R.: J. Appl. Phys. **36,** 2323—24 (1965).
27. WINTERS, H. F., DENISON, D. R., BILLS, D. G., DONALDSON, E. E.: J. Appl. Phys. **34,** 1810 (1963).
28. JOHNSON, R. P.: Phys. Rev. **56,** 814 (1939).
29. MEIJERING, J. L.: Z. Plansee-Seminar 1955, Rentte, Warmfeste und korrosion-beständige Sinterwerkstoffe (1956) 305.
30. MEIJERING, J. L., RIECK, G. D.: Philips Technische Rundschau **19,** (1957/58) 129.
31. LAX, E., PIRÁNI, M.: Wolfram. J. Ambr osius Barth, Leipzig 1929.
32. MILLNER, T., PROHÁSZKA, J., NEUGEB AUER, J.: Festkörperphysik (Festkörperphysik Tagung in Balatonfüred, 1959) Akade mie Verlag, Berlin 1961, 219.
33. PROHÁSZKA, J., HORVÁTH, A., MILLNER, T.: Festkörperphysik (Festkörperphysik Tagung in Balatonfüred, 1959) Akademie Verlag, Berlin 1961, 60.
34. ROSI, F. D.: Sylvania Techn. **5,** 82 (1952).
35. MANNERKOSKI, M.: Institute of Metals **88,** 397 (1959—1960).
36. SWALIN, R. A., GEISLER, A. H.: J. Inst. Met. **86,** 129 (1957/58).
37. MANNERKOSKI, M.: Acta Metallurgica **10,** 982 (1962).
38. KITTEL, C.: Introduction to Solid State Physics. Second Ed. John Wiley and Sons, Inc. New York, 1961.
39. KOVÁCS, I., ZSOLDOS, L.: Diszlokációk és képlékeny alakváltozás. Műszaki Könyvkiadó, Budapest, 1965.
40. SHEWMAN, P. G.: Diffusion in Solids. Mc Graw-Hill Book Company, Inc. New York, 1963.

41. BARTHA, L., PROHÁSZKA, J., MILLNER, T.: (Festkörperphysik Tagung in Balatonfüred 1959) Akademie-Verlag, Berlin 1961, 143.
42. MILLNER, T., BARTHA, L., PROHÁSZKA, J.: Z. Metallkunde **51**, 639 (1960).
43. MILLNER, T., BARTHA, L., PROHÁSZKA, J.: Z. Metallkunde **54**, 17 (1963).
44. COTTRELL, A. H.: Dislocations and Plastic Flow in Crystals. Clarendon Press, Oxford, 1953.
45. HEGEDÜS, A., HORVÁTH, A., KEREK, L., KÜRTHY, M.: Magyar Kémiai Folyóirat **74**, 218 (1968).
46. KREIDER, K. G., BRUGGEMANN, G.: Trans. Met. Soc. of Aime, **239**, 1222—26 (1967).
47. SZABÓ, Z.: Kontakt katalízis. Akadémiai Kiadó, Budapest, 1967.
48. POPP, G.: Annalen der Physik **13**, 115 (1964).
49. RASOR, N., VARNER, Ch.: J. Appl. Phys. **35**, 2589 (1964).
50. TAYLOR, J., LANGMUIR, I.: Phys. Rev. **44**, 423 (1933).
51. LANGMUIR, I.: J. Amer. Chem. Soc. **54**, 2798 (1932).

Olivér KAPOSI
Miklós RIEDEL
Budapest VIII., Puskin u. 11—13.

Acta Chimica Academiae Scientiarum Hungaricae, Tomus 61 (4), pp. 367—380 (1969)

KINETIC STUDY OF HYDROCARBON ADSORPTION ON NICKEL CATALYST

P. TÉTÉNYI, L. BABERNICS and K. SCHÄCHTER

(Institute of Isotopes of the Hungarian Academy of Sciences, Budapest)

Received September 14, 1968

The adsorption of ethane, benzene, and cyclohexane on a nickel catalyst was studied by a kinetic method. The experimentally determined adsorption coefficients indicate chemical interaction between the surface and the substrate. The heats of adsorption are relatively small, the adsorption of ethane being endothermic.

The adsorption characteristics permit to draw conclusions on the nature of the adsorbed layer. The values for Q_{HNi}, Q_{CNi}, and Q_{ONi} can be calculated from the corresponding heats of adsorption.

Adsorption coefficients determined by the kinetic method, as well as the thermodynamic values calculated from them, can provide valuable information about the nature of adsorption on the catalytically active surface during the catalytic reaction, and about the catalyst–substrate interaction.

In earlier papers [1, 2] we reported the determination of adsorption coefficients for hydrogen on nickel and platinum catalysts. The investigation of the adsorption of different hydrocarbons is also important from the viewpoint of the mechanism of dehydrogenation. Therefore, the adsorption coefficients for benzene, which is another product in the dehydrogenation of cyclohexane, have been determined. It was not possible to determine the adsorption coefficients for the reacting cyclohexane by a direct method, therefore, an indirect method has been used. We determined the adsorption coefficients of cyclohexane relative to that of isopropyl alcohol. The adsorption coefficients for ethane were determined for the purpose of comparison with cyclohexane.

Experimental

a) *Method*

The experiments were performed with the earlier described [3] flow-reactor. The preparation and properties of the nickel catalyst have been reported [4]. The physical constants for cyclohexane, benzene, and isopropyl alcohol were in agreement with those in the literature. The purity of ethane was checked by gas chromatography. "F"-labelled argon was used in all the experiments. The cyclohexane–benzene and isopropyl alcohol–cyclohexane mixtures were prepared by weighing. Liquid cyclohexane was added at a

constant rate to the stream of argon or ethane before the reactor. The argon/ethane stream was adjusted using gas cylinders fitted with reducing valves. The fine control of the flow-rate was achieved with a capillary flow-meter. The amount of cyclohexane, reacted in unit time was determined from the refractive index of the condensate. The amount of dehydrogenated isopropyl alcohol was calculated from the volume of hydrogen evolved in unit time. The constant activity of the catalyst in both reactions was demonstrated by the constant rate of gas evolution.

b) *The adsorption coefficients for ethane and benzene*

The equilibrium constants for the adsorption of ethane and benzene were determined by a method which is, in its principle, identical with that used for hydrogen [1, 2]. As it has been shown earlier [1, 3], the dehydrogenation of cyclohexane in the presence of a non-reacting additive on the nickel catalyst used in our experiments can be described by the following equation

$$\frac{s}{x_i} = \alpha + \gamma_i \frac{v_i}{v_{CH}} \tag{1}$$

where

$$\alpha = \frac{A + Bb_{CH}}{kb_{CH}} \quad \text{and} \quad \gamma_i = \frac{A}{kb_{CH}}(1 + b_i)$$

$$A = 1 + \frac{k}{k'_{CH}}; \quad B = 1 + \frac{k}{k'_B} + \frac{k}{k'_H}$$

x_i — the amount of cyclohexane reacting in unit time in the binary mixture with the i-th additive;

v^{CH} and v_i — the flow-rates of cyclohexane and the additive, respectively;

k, k'_{CH}, k'_B and k'_H — the rate constants for the surface reaction, and the desorption of cyclohexane, benzene and hydrogen, respectively;

b_{CH} and b_i — the adsorption coefficients for cyclohexane and the additive, respectively;

s — the surface area of the catalyst.

The validity of an Eq. (1)-type expression has been established for both cyclohexane-ethane and cyclohexane-benzene mixtures, as demonstrated (for cyclohexane-ethane mixtures) by Fig. 1. The values for γ_E and γ_B at different temperatures, as well as the γ_{Ar} values obtained as the slopes of the straight lines corresponding to Eq. (1), are shown in Tables I and II. The equi-

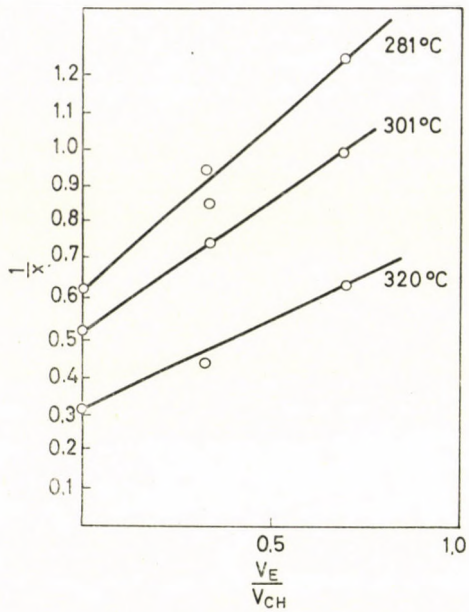

Fig. 1. Straight lines demonstrating the validity of expression (1) for ethane-cyclohexane mixtures

Table I

The adsorption coefficients of ethane

t C°	γ_E	γ_{Ar}	b_E atm^{-1}
272	1.27	0.290	2.25±0.3
281	1.03	0.288	2.57±0.1
301	0.63	0.145	3.35±0.1
320	0.50	0.085	4.88±0.2

Table II

The adsorption coefficients for benzene

t C°	γ_B	γ_{Ar}	b_B atm^{-1}
275	2.90	0.18	15.2±0.9
285	1.61	0.12	12.4±1.1
304	1.12	0.11	9.1±0.4
314	1.02	0.12	7.5±0.8

librium constants* for the adsorption of ethane and benzene (b_E and b_B) are easily calculated from the slopes:

$$b_i = \frac{\gamma_i}{\gamma_{Ar}} - 1 \tag{2}$$

The resulting values are given in Tables I and II.

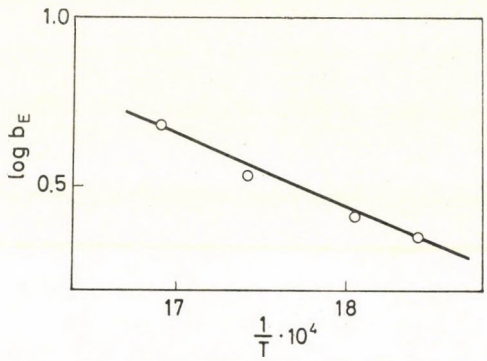

Fig. 2. The temperature dependence of the adsorption coefficients for ethane

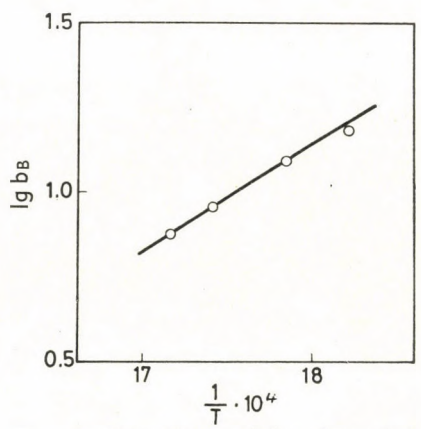

Fig. 3. The temperature dependence of the adsorption coefficients for benzene

The data in the tables show that the adsorption coefficients of ethane increase, while those of benzene decrease with increasing temperature. In both cases, the temperature dependence corresponds to that predicted by the FRENKEL-relationship [5],

$$b = b_0 \, e^{\frac{\lambda}{RT}} \tag{3}$$

as demonstrated by Figs 2 and 3.

The heats of adsorption are 12 and —10 kcal/mole for benzene and ethane, respectively.

* b_{Ar} was assumed to be zero at the temperature of the experiment (250—300 °C).

c) *The relative adsorption coefficients for cyclohexane*

The adsorption coefficient for cyclohexane as a reagent cannot be determined by the above described method. The extent of cyclohexane adsorption was, therefore, deduced from the dehydrogenation of isopropyl alcohol–cyclohexane mixtures. The reaction was run at a temperature (160—200 °C), where only isopropyl alcohol undergoes dehydrogenation and cyclohexane can be regarded as a non-reacting additive.

However, the dehydrogenation of isopropyl alcohol cannot be described by the kinetic equation (1).

In a previous paper [6], we have shown that, on the nickel catalyst used in our studies, the dehydrogenation of isopropyl alcohol in a binary mixture with a non-reacting additive takes place according to the kinetic equation

$$ks = A\left(\frac{b_{ac}}{b_a} + \frac{b_{\mathrm{H}}}{b_a} + \frac{v_i}{v_a}\,\frac{b_i}{b_a}\right) v_a \ln \frac{v_a}{v_a - x} - \left[A\left(\frac{b_{ac}}{b_a} + \frac{b_{\mathrm{H}}}{b_a}\right) - B\right] x\,, \tag{4}$$

where

$$A = 1 + \frac{k}{k'_a}\,;\quad B = 1 + \frac{k}{k'_{ac}} + \frac{k}{k'_{\mathrm{H}}}\,;$$

k — the rate constant for dehydrogenation;

k_a, k'_{ac} and k'_{H} — the rate constants for the desorption of isopropyl alcohol, acetone, and hydrogen, respectively;

b_a, b_{ac}, b_{H} and b_i — the adsorption coefficients for isopropyl alcohol, acetone, hydrogen, and the additive, respectively;

v_a and v_i — the amounts of isopropyl alcohol and the additive, respectively, fed in unit time (ml N.T.P./min);

x — the amount of isopropyl alcohol reacting in unit time (ml N.T.P./min).

The general form of Eq. (4) has been derived by one of the authors [7], on the basis of the BALANDIN—KIPERMAN equation [8]. In the derivation, none of the steps involved has been assumed to be rate-determining. The fact that one of the steps is rate-determining is expressed by the physical meaning of constants A and B. The form of Eq. (4), however, remains unchanged.

Upon introducing z_{ac}, z_H and z_i defined by

$$z_i = \frac{A}{B}\,\frac{b_i}{b_a} \tag{5}$$

Eq. (4) rearranges to

$$\frac{kS}{B} = \left(z_{ac} + z_H + \frac{v_i}{v_a} z_i\right) v_a \ln \frac{v_a}{v_a - x} - (z_{ac} + - z_H - 1)\, x \qquad (6)$$

Constants z_i are called apparent relative adsorption coefficients. In case when the chemical reaction on the surface is the rate-determining step, both A and B are equal to 1, the z_i-s being actual adsorption coefficients.

The apparent relative adsorption coefficients for cyclohexane were determined by comparing the rate of isopropyl alcohol dehydrogenation with those of isopropyl alcohol-cyclohexane binary mixtures. The z_{CH}-values were calculated from approximation formula (7)* derived from Eq. (6):

$$z_{CH} = \frac{\frac{x}{x_i} - 1}{\frac{1}{p} - 1}, \qquad (7)$$

where

x and x_i — the amount of isopropyl alcohol that has reacted in the case of pure alcohol and alcohol-cyclohexane binary mixture, respectively;

p — the mole fraction of isopropyl alcohol in the mixture.

The experimental results and the z_{CH}-values calculated from Eq. (7) for 161 °C are shown in Table III. The z_{CH} values calculated from the rate of

Table III

Rates of dehydrogenation of isopropyl alcohol–cyclohexane mixtures and apparent relative adsorption coefficients for cyclohexane

t C°	γ	x	z_{CH}	$\bar{z}_{CH}$
161	1.1	4.1	—	
161	0.16	2.2	0.17	
161	0.56	3.6	0.20	
161	1.0	4.1	—	0.18 ± 0.02
161	0.22	2.8	0.15	
161	0.44	3.0	0.22	
161	1.0	3.9	—	
161	0.22	2.5	0.16	

* According to its derivation, approximation formula (7) can only be used at conversions below 10%. With one or two exceptions, this was true for all the measurements. Incidentally, the comparison of the z_{ac} and z_H values calculated by different methods indicated [10] that, even at a conversion of 30%, the results of precise and approximate calculations only differed by less than 10%.

dehydrogenation of isopropyl alcohol–cyclohexane mixtures with various compositions are nearly identical at a given temperature. Similar results are obtained at other temperatures, as illustrated by the small deviation of the z_{CH} values (Table IV). These facts confirm that Eq. (6) correctly describes the

Table IV

Apparent relative adsorption coefficients of cyclohexane and hydrogen (z_{CH} and z_H) and their ratio (b_{CH}/b_H)

t °C	$\bar{z}_{CH}$	z_H	b_{CH}/b_H
161	0.18±0.02	0.59	0.31
170	0.24±0.01	0.39	0.62
178	0.26±0.01	0.31	0.84
188	0.32±0.03	0.22	1.45
207	0.44±0.03	0.11	4.00

rate of dehydrogenation for both pure alcohol, and alcohol–cyclohexane binary mixtures.

Dividing the z_{CH} values by the previously determined [4] values for z_H, the ratio of the adsorption coefficients for cyclohexane and hydrogen is obtained according to Eq. (5):

$$z_{CH}/z_H = b_{CH}/b_H \tag{8}$$

The b_{CH}/b_H values shown in Table IV have a logarithmic temperature dependence. The difference in heats of adsorption calculated from the temperature dependence is

$$\lambda_{CH} - \lambda_H = -22 \text{ kcal/mole} \tag{9}$$

The heat of adsorption for hydrogen was previously determined on the nickel catalyst used ($\lambda_H = 24$ kcal/mole). Using this value, 2 kcal/mole is obtained from Eq. (9) for the heat of adsorption of cyclohexane.

In the calculation of the λ_{CH} values, the dehydrogenation of both cyclohexane and isopropyl alcohol was assumed to take place on identical sites of the catalyst surface. Thus, the λ_H value obtained from cyclohexane dehydrogenation can be added to the $\lambda_{CH} - \lambda_H$ value measured for the dehydrogenation of isopropyl alcohol. This assumption is supported by the fact that the rates of these two reactions run parallel on nickel catalysts prepared by different methods. A parallel change of the two reaction rates is also observed over different catalyst metals [13].

It was an implicit assumption that the heat of adsorption for hydrogen does not change in the interval between 150—300 °C. This assumption is supported by the experimental results obtained in this laboratory by L. GUCZI, according to which the isosteric heat of adsorption for hydrogen on this nickel catalyst remains practically constant between 0 and 300 °C.

Discussion

The problem whether or not the adsorption coefficients determined by the kinetic method, and the heat of adsorption derived from their temperature dependence have any physical reality, could only be judged by comparing them with the results obtained by means of other techniques.

Only a limited amount of data is available about the adsorption of ethane, cyclohexane, and benzene which would be suitable for direct comparison. This is particularly true for the heats of adsorption.

The heat of adsorption for benzene on a chromium(III)oxide — aluminium oxide — potassium oxide catalyst was found by RUBINSTEIN *et al.* [14] to vary between 10 and 13 kcal/mole, depending on the fraction of the surface covered. Due to the fact that strongly different adsorbents were used, the agreement of this value with the one obtained by us does not constitute convincing evidence. Obtained in this laboratory results concerning the adsorption of benzene on a cobalt catalyst show that the heat of adsorption changes between 6 and 10 kcal/mole, depending on the fraction of the surface covered. The heat of adsorption of ethylene was shown to depend on the per cent *d*-character of the metallic bond of the catalyst [15]. Since these parameters for nickel and cobalt are almost identical, one can assume that the heats of adsorption on identically prepared samples of these two catalysts will not differ significantly.

At any rate, the heat of adsorption of benzene in the above two cases is close to the value determined by the kinetic method. This fact demonstrates the probable reality of the kinetic adsorption coefficients, similarly to the observations on the adsorption of hydrogen [1].

The very small heat of adsorption for cyclohexane, and a negative one for ethane, indicates the possibility of endothermic adsorption.

The existence of endothermic adsorption and its possible role in catalysis has been pointed out by DE BOER [16].The negative heat of adsorption for ethane seems to support the existence of endothermic adsorption. Although the heat of adsorption for cyclohexane is positive, it is smaller than the heat of condensation (7.9 kcal/mole). This indicates endothermic chemisorption in the case of cyclohexane, too, since the molecular interaction between substrate and adsorbent is, by all means, accompanied by a positive heat-effect.

It is worth mentioning that the heats of adsorption of saturated hydrocarbons on oxides have been found to be larger than on metals. Thus, the heat of adsorption of ethane on chabazite is 8.5 kcal/mole [17], while those of cyclohexane on silica gel [18] and on chabazite [14] equal 8.3 and 10 kcal/mole, respectively.

The endothermic chemisorption of saturated hydrocarbons is understandable since on metals this process involves C—H bond dissociation. This has been established for the adsorption of both ethane and cyclohexane on

nickel [19—21]. The energy of activation for the adsorption of cyclohexane during its dehydrogenation was found to be 23 kcal/mole on our catalyst [22] which is another indication for dissociative adsorption.

The heat effect associated with the breaking of the C—H bond on nickel can be expressed with the bond energies in the following way:

$$Q_{CH,Ni} = -Q_{CH} + Q_{CNi} + Q_{HNi} \tag{10}$$

The value for Q_{HNi} can be calculated from the heat of adsorption of hydrogen, using the expression

$$\lambda_H = -Q_{HH} + 2Q_{HNi} \tag{11}$$

Since $\lambda_H = 24$ and $Q_{HH} = 104$ kcal/mole [23], one obtains 64 kcal/mole for Q_{HNi}. In order that $Q_{CH,Ni}$ be positive, Q_{CNi} should be larger than 35 kcal/mole because the value of Q_{CH} for ethane is 99 kcal/mole [23]. However, the experimental results [24] give $Q_{CNi} = 18$ kcal/mole. The value for Q_{CNi} determined by the kinetic method is 21 kcal/mole [25]. It is extremely unlikely therefore that the C—Ni bond energy would be high enough to make $Q_{CH,Ni}$ positive. Consequently, the adsorption of ethane on the catalyst used in our experiments is endothermic. No data are available for the C—H bond energy in cyclohexane. A structural analogy suggests that the energy of the first bond is best approximated by the energy of fission of the $(CH_3)_2CH—H$ bond which is equal to 89 kcal/mole [26]. The difference of 10 kcal/mole between the C—H bond energies in ethane and cyclohexane may be the explanation for the observed difference of 12 kcal/mole in the adsorption heats.

Therefore, the heat of the C—H bond fission in saturated hydrocarbons is probably negative or close to zero. This is compensated for only to a small extent by the heat of molecular interaction between the substrate and the adsorbent.

These approximative calculations explain alltogether the low or even negative values for the heats of adsorption of saturated hydrocarbons. The higher positive values for the heats of adsorption of ethane and cyclohexane on oxides are probably due to the incompleteness, or absence, of C—H bond fission during adsorption. The fact that the heat of adsorption of cyclohexane on oxide catalysts exceeds the heat of condensation only by 1—2 kcal/mole, the two being almost identical on silicagel, lends support to this immagination.

The heat of adsorption of benzene is only slightly higher than that of its condensation. In spite of this, the adsorption cannot be considered weak, as demonstrated by the numerical values of the adsorption coefficients. The latter is 10 atm^{-1} at 300 °C, as opposed to a value of 0.2 atm^{-1} for hydrogen. The adsorption coefficients can be expressed with the mean time of lingering

in the following way:

$$b_i = \frac{\mu}{\sqrt{M_i}} \tau_i, \tag{12}$$

where

τ — the mean time of lingering,
M_i — the molecular weight of the substrate,
μ — the number of collisions of a substance having a molecular weight of *1*, with an active site in 1 second.

The relative time of lingering for two substrates [27] is obtained from (12)

$$\frac{\tau_i}{\tau_k} = \sqrt{\frac{M_i}{M_k}} \frac{b_i}{b_k} \tag{13}$$

The mean time of lingering for benzene on the surface of a nickel catalyst at 300 °C is 3.1×10^2 times longer than that of hydrogen, as calculated from Eq. (13). The time of lingering for ethane is 58 times that of hydrogen, *i.e.* somewhat less than 1/5th of the value for benzene. The magnitude of the heat of adsorption of hydrogen unambiguously proves that it is chemically bonded to the surface. Therefore, the much longer times of lingering for benzene and ethane is evidence for strong interaction between the surface and these substrates.

The following three pictures are the most likely ones for the adsorption of benzene:

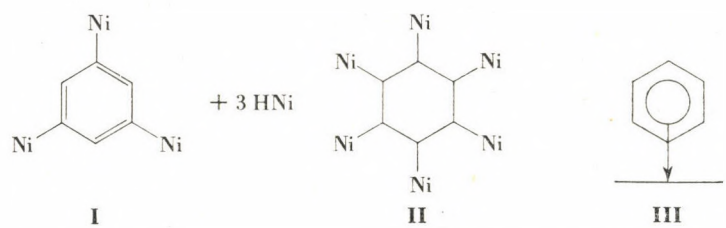

I **II** **III**

dissociative associative π-complex type adsorption

The existence of structure **I** proposed by PITKETHLY [28] has been established [29]. Its presence is probably confined to irreversible benzene adsorption. The occurrence of such type of adsorption seems unlikely on catalytically active sites which are most important during the reaction. In the opposite case, similarly to ethane, endothermic adsorption should have been found for benzene.

It is more difficult to make a decision in favour of one of the remaining structures **II** and **III**. Both structures would lead to a relatively low heat of

adsorption. In case of structure **II**, the energy change associated with the formation of the six C—Ni bonds is strongly decreased by the collapse of the aromatic structure. With structure **II** the heat of adsorption can only be equal to 12 kcal/mole if each C—Ni bond energy equals 40 kcal/mole. As it has been mentioned, this is very unlikely.

Thus the principle of exclusion leaves structure **III**, the existence of which is assumed in an increasing number of instances [30]. The small heat of adsorption is explained by relatively weak interaction. The free enthalpy and entropy of adsorption were calculated from the following expressions:

$$\Delta G_a^o = -RT \ln b_B ;$$
$$\Delta S_a^o = -\frac{\Delta G_a^o + \lambda}{T}. \tag{14}$$

The calculations gave 2—6 kcal/mole, and —16.5 e.u. for the free enthalpy and entropy of adsorption, respectively. The translational and rotational entropies for benzene at 300 °C are 42.2 and 22.6 e.u., respectively, as calculated from known formulae [31]. These values are in good agreement with those calculated by KEMBALL and RIDEAL [32].

If either structure **I** or **III** is operative, benzene should lose both its translational and rotational degrees of freedom. The resulting loss of entropy is only partly compensated for by the vibrational entropy due to the newly formed bonds. Earlier studies [29] on the chemisorption of benzene showed that the latter covers 3—4% of the surface at 300 °C. This value indicated that the configurational entropy under no circumstances can exceed 10—15 e.u. Therefore, this cannot explain the low entropy of adsorption, either.

The fact that the absolute value of the entropy of adsorption is by nearly 50 e.u. less than the sum of the translational and rotational entropies, indicates that the adsorbed molecules retain some translational and rotational freedom. The retention of one rotational and two translational degrees of freedom seems most likely, the former referring to rotation in the plane of the ring. Even in this case the entropy is expected to decrease by about 35 e.u. The difference of almost 20 e.u. between the expected and experimental entropies of adsorption can already be explained by the experimental error, the approximate character of the calculations, the vibrational entropy due to the bond between the surface and the ring, and by the vibration of the adsorbed molecule as a whole.

The results obtained for the entropy of adsorption, too, permit the conclusion that the interaction between the benzene ring and the metal surface is relatively weak. This is more likely with structure **III** than with either **I** or **II**. It would be premature however to draw definite conclusions about the mechanism of adsorption on the catalytic surface from the data which are available at present.

Summarizing the results, one may conclude that the hydrocarbons studied by us are adsorbed on nickel due to chemical interaction. However, the heats of adsorption are much smaller (negative for ethane) than the values expected for chemisorption. The latter result seems to support the DE BOER concept according to which endothermic adsorption plays an important role in heterogeneous catalysis [16].

The catalyst–substrate bond energies

The fact that hydrogen and various hydrocarbons are chemisorbed on catalytically active nickel surfaces permit the calculation of catalyst–substrate bond energies from the heats of adsorption. It has been mentioned that the heat of adsorption of hydrogen yields 64 kcal/mole for the H—Ni bond energy.

The C—Ni bond strength can be calculated from known values for the heats of adsorption of ethane and cyclohexane. The experimental results on the kinetics and mechanism of cyclohexane dehydrogenation [11, 22, 33], as well as those on the H—D exchange [34] show that the first step of dehydrogenation is the formation of a surface complex C_6H_{11}.Ni. Thus, the adsorption is associated with the rupture of a C—H bond. The formation of the C_2H_5.Ni radical during ethane adsorption has been demonstrated both by the results on the H—D exchange with ethane [35] and those on the kinetics of its cracking [36]. Therefore, as a first approximation, the heat of adsorption of both cyclohexane and ethane can be regarded equal to the energy change due to the C—H bond rupture. Thus the C—Ni bond energy can be calculated from formula (10). The result is 27 and 25 kcal/mole from the heat of adsorption of cyclohexane and ethane, respectively.

The following average value can be accepted:

$$Q_{\mathrm{CNi}} = 26 \text{ kcal/mole}$$

The O—Ni bond energy can be calculated from the heat of adsorption obtained from the apparent relative adsorption coefficients of acetone, which have been determined [4] in connection with the dehydrogenation of isopropyl alcohol. The difference between the heats of adsorption of acetone and hydrogen is

$$\lambda_{ac} - \lambda_{\mathrm{H}} = -11 \text{ kcal/mole}$$

Consequently, the heat of adsorption of acetone is 13 kcal/mole. The adsorption of acetone is presumably associated with the rupture of one of the C=O bonds. Therefore, the following expression is obtained for the heat of adsorption:

$$\lambda_{ac} = -Q_{\mathrm{C=O}} + Q_{\mathrm{CNi}} Q_{\mathrm{ONi}} \qquad (15)$$

Using the value of $Q_{C=O} = 165.2$ kcal/mole [23], the energy of the first bond to be ruptured is found to equal 83 kcal/mole. Thus, from Eq. (15)

$$Q_{ONi} = 70 \text{ kcal/mole}$$

The calculated bond energy values are summarized in Table V. The bond

Table V

Bond energies calculated from energies of activation and heats of adsorption (kcal/mole)

Base value for the calculations	ε	λ
Q_{HNi}	59	64
Q_{CNi}	21	26
Q_{ONi}	58	70

energies calculated from the activation energies determined by the kinetic method for our nickel catalyst [25] are also included in the Table. The values obtained by the two different methods differ by about 10—25%. The bond energies calculated from the heats of adsorption are in all cases larger than those obtained by the kinetic method.

This can be explained by two factors. It is conceivable that complete bond rupture does not take place in the process of adsorption. In the calculations this assumption involves smaller Q_{XNi} values. As an extension of this, one may also assume incomplete fission of the individual bonds of the molecule reacting in the adsorbed state. The introduction of this assumption into the calculations would result in the decrease of bond energies determined by the kinetic method. This is so because the original calculations based on the kinetic method have been carried out assuming complete bond rupture in the reacting substrate.

A more likely explanation for the existing differences would be the fact that in the kinetic method the energy barrier for bond fission was regarded as equal to the heat effect. This means that the processes which take place on metal surfaces do not require an energy of activation. Thus, the experimental energies of activation were regarded as the heat effects associated with the individual steps. Obviously, this resulted in lower bond energy values with the kinetic method. The fact that the bond energies calculated from the heats of adsorption are larger than those obtained by neglecting the activation energies of the individual steps indicates that processes on solid surfaces may require

an energy of activation. In other words, in catalytic reactions the components probably undergo activated adsorption.

The available experimental data, however, do not constitute a sound basis for the calculation of the energies of activation.

REFERENCES

1. TÉTÉNYI, P., KIRÁLY, J., BABERNICS, L.: Acta Chim. Acad. Sci. Hung. **29,** 35 (1961).
2. TÉTÉNYI, P., BABERNICS, L.: Acta Chim. Acad. Sci. Hung. **35,** 419 (1963).
3. TÉTÉNYI, P., BABERNICS, L., PETHŐ, Á.: Acta Chim. Acad. Sci. Hung. **28,** 375 (1961).
4. BALANDIN, A., TÉTÉNYI, P.: Dokl. Acad. Nauk USSR **115,** 727 (1957).
5. FRENKEL, J.: Z. Physik, **26,** 117 (1924).
6. TÉTÉNYI, P., SCHÄCHTER, K., BABERNICS, L.: Acta Chim. Acad. Sci. Hung. **42,** 325 (1964).
7. TÉTÉNYI, P.: Acta Chim. Acad. Sci. Hung. **22,** 247 (1960).
8. BALANDIN, A., KIPERMAN, S.: Zh. Fis. Khim. **31,** 140 (1957).
9. BALANDIN, A., BOGDANOVA, O., SCHEGLOVA, A.: Izv. Akad. Nauk. USSR OKHN 497 (1946).
10. TÉTÉNYI, P.: Ph. D. Thesis Moscow 1957.
11. TÉTÉNYI, P.: D. Sc. Thesis, Budapest 1965.
12. TÉTÉNYI, P., BABERNICS, L., GUCZI, L., SCHÄCHTER, K.: Acta Chim. Acad. Sci. Hung. **40,** 387 (1964).
13. TÉTÉNYI, P., SCHÄCHTER, K.: Acta Chim. Acad. Sci. Hung. **56,** 15 (1968).
14. RUBINSTEIN, A., SLOVETSKAYA, K., BRUEVA, T.: Dokl. Akad. Nauk USSR **151,** 580 (1963).
15. BEECK, O.: Disc. Farad. Soc. **8,** 118 (1950).
16. DE BOER, J. H.: Adv. Catalysis **8,** 17 (1956).
17. CHANG, T. S.: Proc. Roy. Soc. L. A, **169,** 512 (1939).
18. KISELEV, A., FROLOV, B.: Kinetika i Kataliz **3,** 767 (1962).
19. GALWEY, A., KEMBALL, C.: **55,** 1959 (1959).
20. SELWOOD, P. W.: „Adsorption and Collective Paramagnetism" Academic Press N. Y.—L. 1962.
21. FICHENS, R., PLISKIN, W.: Adv. Catalysis **10,** 1 (1958).
22. SCHAY, G., TÉTÉNYI, P.: Acta Chim. Acad. Sci. Hung. **51,** 39 (1967).
23. KONDRATIEF, V.: "Structura Atomov i Molekul" Fizmatgiz Moscow 1959.
24. MORTIMER, C.: "Reaction Heats and Bond Strengths. Pergamon Press, Oxford—London 1962.
25. TÉTÉNYI, P.: Acta Chim. Acad. Sci. Hung. **54,** 267 (1957).
26. SZWARC, M.: Chem. Rev. **47,** 75 (1950).
27. BALANDIN, A.: Zh. Obschei Khim. **12,** 160 (1942).
28. PITKETHLY, R., GOBLE, A.: Actes Congr. Intern. Catalyse 2e, Paris, 1960 **2,** 1851 (Technip., Paris (1961).
29. TÉTÉNYI, P., BABERNICS, L.: J. Catalysis **8,** 215 (1967).
30. BOND, G., WELLS, P.: Adv. Catalysis **15,** 91 (1964).
31. KEMBALL, C.: Adv. Catalysis **2,** 233 (1950).
32. KEMBALL, C., RIDEAL, E.: Proc. Roy. Soc. L. A, **187,** 53 (1946).
33. TÉTÉNYI, P., BABERNICS, L., THOMSON, S.: Acta Chim. Acad. Sci. Hung. **34,** 335 (1963).
34. ANDERSON, J., KEMBALL, C.: Proc. Roy. Soc. L. A, **226,** 472 (1954).
35. ANDERSON, J., KEMBALL, C.: Proc. Roy. Soc. L. A, **223,** 361 (1954).
36. KEMBALL, C., TAYLOR, H.: J. A. C. S. **70,** 345 (1948).

Pál TÉTÉNYI
Lajos BABERNICS
Klára SCHÄCHTER
Budapest XII., Konkoly Thege M. út.

Acta Chimica Academiae Scientiarum Hungaricae, Tomus 61 (4), pp. 381—390 (1969)

APPLICATION OF THE SEMIEMPIRICAL DIFFERENT ORBITALS FOR DIFFERENT SPINS SCF LCAO MO METHOD FOR THE CALCULATION OF SPIN DENSITIES OF SOME PHENYL NITROXIDE RADICALS

J. LADIK, G. BICZÓ, I. KENDE and L. SÜMEGI

(Central Research Institute for Chemistry of the Hungarian Academy of Sciences, Budapest)

Received September 23, 1968

The spin density distributions of the phenyl nitroxide radical and its *ortho*, *para* and *meta* halogenated (F, Cl, Br) derivatives were calculated with the aid of the semiempirical different orbitals for different spins (DODS) SCF LCAO MO method. According to the obtained results the agreement between the theoretical and experimental spin densities is for the ring carbon atoms comparatively the best if we use for the Coulomb integrals $\gamma_{i,j}$ 1.5 times the values approximated by the expression of MATAGA and NISHIMOTO. On the other hand, the agreement for the nitrogen and oxygen atoms is bad. This indicates that the introduction of spin projection is important also in the case of this semiempirical version of the DODS method. Work in these lines is in progress.

Introduction

In the last few years much attention has been focused on "neutral" radicals such as different types of the nitroxide radicals [1—10]. Therefore in the course of the ESR investigation of stabile free radicals we have calculated the spin densities of different radicals contaning the N—O· group with the aid of the semiempirical different orbitals for different spins *SCF LCAO MO* method of DEWAR [11]. The chemical formulas of the investigated radicals, phenyl-cyanopropyl nitroxide and its substituted derivatives, are given in Fig. 1.

At the same time we have studied also experimentally the coupling constants in the *ESR* spectra of these radicals [12].

Method

Within the framework of the π electron approximation the spin density due to the π electrons at atom i is defined by

$$\varrho_i = P^{\alpha}_{i,i} - P^{\beta}_{i,i}\,, \tag{1}$$

where $P^{\alpha}_{i,i}$ and $P^{\beta}_{i,i}$ are the π electron charge densities of electrons with spin α and β, respectively, $(n_\alpha \geq n_\beta)$ at atom i.

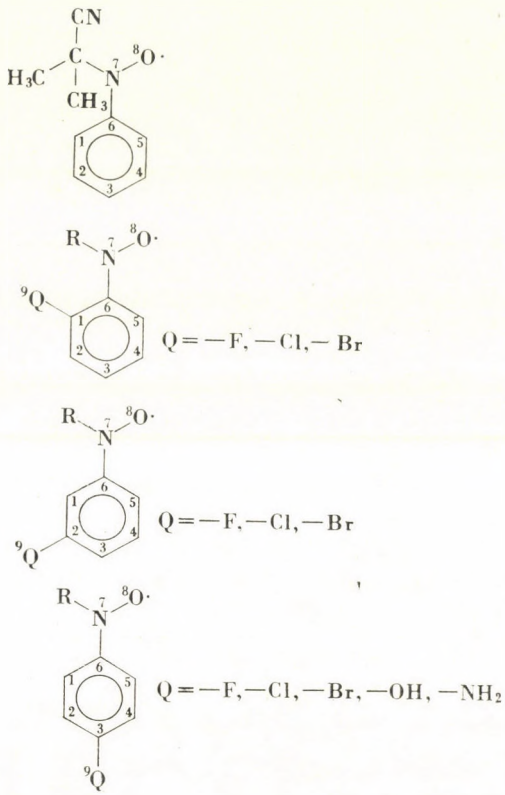

Fig. 1. The chemical formulas of the investigated radicals

To calculate the quantities $P^{\alpha}_{i,i}$ and $P^{\beta}_{i,i}$ in a tolerably good approximation the different orbitals for different spins method [13, 14] can be used in its *SCF LCAO MO* form [15, 16]. To simplify the very cumbersome integrations, necessary in the original non-empirical version of this method, DEWAR [11] has proposed a semiempirical form of the method which corresponds to the Pariser–Parr–Pople method for a closed shell system.

According to the method of DEWAR (extending it also to heterocycles) we have to determine simultaneously the *SCF* eigenvectors of the matrices $\mathbf{F}_{\alpha}$ and $\mathbf{F}_{\beta}$ which have the elements

$$F^{\alpha}_{i,i} = -I_i + P^{\beta}_{i,i}(I_i - E_i) + \sum_{j \neq i} (P^{\alpha}_{j,j} + P^{\beta}_{j,j} - Z_j)\,\gamma_{i,j}\,,$$
$$F^{\alpha}_{i,j} = \beta_{i,j} - P^{\alpha}_{i,j}\gamma_{ij} \tag{2}$$

and

$$F^{\beta}_{i,j} = -I_i + P^{\alpha}_{i,i}(I_i - E_i) + \sum_{j \neq i} (P^{\beta}_{j,j} + P^{\alpha}_{j,j} - Z_j)\,\gamma_{i,j}\,, \tag{3}$$
$$F^{\beta}_{i,j} = \beta_{i,j} - P^{\beta}_{i,j}\gamma_{i,j},$$

respectively. Here I_i, E_i and Z_i is the ionization potential, electron affinity and the number of π electrons, respectively, given by the atom i in its appropriate valence state, the $\gamma_{i,j}$-s are the Coulomb integrals between electrons belonging to atoms i and j, respectively, and the resonance integrals $\beta_{i,j} = (\varkappa_i \mid \mathrm{H}^{\mathrm{core}} \mid \varkappa_i)$, which should be taken into account only between nearest neighbours, are treated as empirical parameters. The elements of the matrices $\mathbf{P}^{\alpha}$ and $\mathbf{P}^{\beta}$ are defined by the expressions

$$P^{\alpha}_{i,j} = \sum_{k=1}^{n_f} c^{*\alpha}_{k,i}\, c^{\alpha}_{k,j},\quad P^{\beta}_{i,j} = \sum_{k=1}^{n_f-1} c^{*\beta}_{k,i}\, c^{\beta}_{k.j}\,, \tag{4}$$

where n_f denotes the highest MO filled by an electron with spin α.

To begin the calculation one has to start with initial charge and bond order matrices $\mathbf{P}^{(o)\alpha}$ and $\mathbf{P}^{(o)\beta}$ estimated for instance from the results of a previous Hückel calculation. Solving the matrix eigenvalue problems

$$\begin{aligned} \mathbf{F}^{(o)\alpha}\,\mathbf{c}_i^{(1)\alpha} &= \varepsilon_i^{(1)\alpha}\,\mathbf{c}_i^{(1)\alpha}\,, \\ \mathbf{F}^{(o)\beta}\,\mathbf{c}_i^{(1)\beta} &= \varepsilon_i^{(1)\beta}\,\mathbf{c}_i^{(1)\beta} \end{aligned} \tag{5}$$

simultaneously, from the obtained eigenvectors $\mathbf{c}_i^{(1)\alpha}$ and $\mathbf{c}_i^{(1)\beta}$ we can form the new matrices $\mathbf{P}^{(1)\alpha}$ and $\mathbf{P}^{(1)\beta}$. Substituting their elements into equations (2) and (3) we perform the matrices $\mathbf{F}^{(1)\alpha}$ and $\mathbf{F}^{(1)\beta}$. Repeating this procedure until self consistency we obtain the set of the *SCF* eigenvectors $\mathbf{c}_i^{(SCF)\alpha}$ and $\mathbf{c}_i^{(SCF)\beta}$. Substituting them into equations (4) we obtain the matrices $\mathbf{P}^{(SCF)\alpha}$ and $\mathbf{P}^{(SCF)\beta}$. The differences of the diagonal elements of these matrices,

$$(\mathbf{P}^{(SCF)\alpha})_{i,i} - (\mathbf{P}^{(SCF)\beta})_{i,i} = P^{(SCF)\alpha}_{i,i} - P^{(SCF)\beta}_{i,i} = \varrho_i^{(SCF)}\,, \tag{6}$$

give directly the desired spin densities.

In the actual calculations we have approximated the Coulomb integrals $\gamma_{i,j}$ with the aid of the expressions

$$\gamma_{i,j} = \frac{e^2}{R_{i,j} + a_{i,j}}\,;\quad \frac{e^2}{a_{i,j}} = \frac{1}{2}(I_i - E_i + I_j - E_j) \tag{7}$$

proposed by MATAGA and NISHIMOTO [17]. Here $R_{i,j}$ denotes the distance between centres i and j, and I_i and E_i is again the ionization potential and electron affinity, respectively.

For the above outlined method a program was written for the GIER computer. The program uses as input data the I_i, E_i and Z_i values, the geometrical matrix R and the Hückel matrix $\mathbf{H}(H_{i,i} = \alpha_i = (\varkappa_i \mid H^{core} \mid \varkappa_i);\ H_{i,j} = \beta_{i,j}\quad i \neq j)$. As an alternative the program is able to use only the off diagonal elements

of **H**, but in this case we have to give some initial matrices $\mathbf{P}^{(o)\alpha}$ and $\mathbf{P}^{(o)\beta}$, respectively. (According to our experiences with closed shell *SCF LCAO MO* calculations on series of similar molecules the $\mathbf{P}^{(SCF)}$ matrix of a molecule with rational changes can be very well used as $\mathbf{P}^{(o)}$ of a similar other molecule [18]. Since in this way it was possible to accelerate the convergence of the procedure in a great amount, we wanted to use the same trick in the present open shell case.) The criterion of self consistency was

$$| P_{i,j}^{(n)\alpha} - P_{i,j}^{(n-1)\alpha} |_{\max} < 0.001 \tag{8a}$$

and at the same time

$$| P_{i,j}^{(n)\beta} - P_{i,j}^{(n-1)\beta} |_{\max} < 0.001, \tag{8b}$$

where the index max refers to the maximal difference of the corresponding elements of the two matrices. As output data the program prints the *SCF* eigenvalues $\varepsilon_i^{(SCF)\alpha}$, $\varepsilon_i^{(SCF)\beta}$, the *SCF* eigenvectors $\mathbf{c}_i^{(SCF)\alpha}$, $\mathbf{c}_i^{(SCF)\beta}$ and finally the *SCF* charge and bond order matrices $\mathbf{P}^{(SCF)\alpha}$ and $\mathbf{P}^{(SCF)\beta}$, respectively. It is possible to print out also the same results for every iteration step.

In the experimental investigations the *ESR* spectra were obtained for phenyl nitroxide radicals derived from nitrosobenzene by addition of a cyanoisopropyl radical:

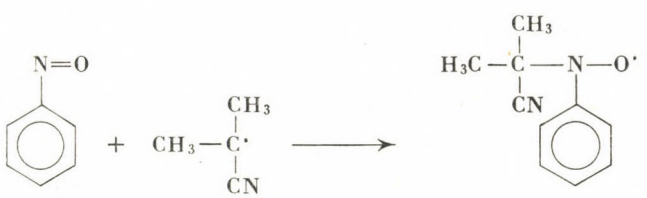

(We have used the thermal decomposition of azo-bisisobutyronitrile as a source of cyanoisopropyl radical.) All the *ESR* measurements were performed in benzene solution, in absence of oxygen at room temperature [12].

Results and discussion

In Table I we give the calculated spin densities for the phenyl nitroxide radical with different values of the Coulomb integrals $\gamma_{i,j}$. The calculations have been performed also for different values of the angle of rotation around the C—N bond. (In this case the relation $\beta_{C,N}^{\alpha^\circ} = \beta_{C,N}^{0^\circ} \cos \alpha$ has been used, where α is the angle of rotation, for the $\beta_{C,N}$ parameters and in calculating the integrals $\gamma_{i,j}$ the changed geometry has been taken into account.) In this way we have investigated the effect of rotation on the spin density distribution. As we can see from the Table, the agreement between the theoretical and experi-

Table I

Calculated spin densities of the phenyl nitroxide radical with different values of the Coulomb integrals and by different angles of rotation

	$\gamma^{M.N.}$			$1.2\gamma^{M.N.}$			$1.5\gamma^{M.N.}$			Experimental spin densities*
	0°	30°	60°	0°	30°	60°	0°	30°	60°	
1	0.249	0.266	0.258	0.095	0.080	0.046	0.052	0.040	0.019	0.101
2	−0.238	−0.258	−0.255	−0.080	−0.068	−0.042	−0.032	−0.025	−0.013	−0.039
3	0,244	0.263	0.257	0.089	0.075	0.044	0.045	0.035	0.017	0.101
4	−0.239	−0.259	−0.256	−0.080	−0.069	−0.042	−0.032	−0.025	−0.013	−0,039
5	0,249	0.267	0.259	0.095	0.080	0.046	0.053	0.041	0.019	0.101
6	−0.237	−0.256	−0.255	−0.091	−0.078	−0.046	−0.050	−0.040	−0.019	
7	0.171	0.175	0.184	0.218	0.223	0.231	0.306	0.312	0.323	a_N = 11.25 gauss
8	0.800	0.803	0.809	0.755	0.758	0.763	0.658	0.661	0.668	

* Using the McConnel relation $|a_H| = Q_{CH}|\varrho_C|$ with the value $Q_{CH} = 22.5$ gauss [10] for the calculation of the carbon spin densities from the experimentally found [12] hyperfine splitting constants.

mental π electron spin densities at the carbon atoms is comparatively the best if we use the values $\gamma_{i,j} = 1.5\,\gamma_{i.j}^{M.N.}$ for the Coulomb integrals ($\gamma_{i,j}^{M.N.}$ stands for the Coulomb integral calculated with the aid of the Mataga—Nishimoto approximation) and all the 8 atomic nuclei of the phenyl nitroxide radical which contribute a π orbital lie in the same plane (the angle of rotation is 0°). In this case the agreement for the *meta* positions (atoms 2 and 4) is quite good, while the values obtained for the *ortho* and *para* positions (atoms 1, 3 and 5) are too small.

The experimentally determined splitting constant of the nitrogen atom ($a_N = 11.25$ gauss) can be compared by the corresponding theoretical value, if we use for the latter the approximate expression

$$a_N| = ||\varrho_N|\,Q_N + |\varrho_O|\,Q_O| \tag{9}$$

suggested by Karplus and Fraenkel [19] with the values $Q_N = 30.5$ gauss and $Q_O = -13.6$ gauss found by Kikuchi and Someno [10] for phenyl nitroxide. If we substitute the theoretical spin densities obtained with $\gamma_{i,j} = 1.5\,\gamma_{i,j}^{M.N.}$ in the case of 0° rotation angle ($\varrho_N = 0.306$ and $\varrho_O = 0.658$) into (9) we obtain for a_N the extremely small value of 0.38 gauss which is in sharp contradiction with the experimental one. The reason of this discrepancy is that our method has resulted in a far too large spin density at the oxygen atom and a far too small one at the nitrogen atom. This explanation is in agreement with the fact that both our previous Hückel calculation [20] and the calculation of Kikuchi and Someno [10] performed in the Hückel and also in the McLachlan [21] approximation has given $\varrho_N > \varrho_O$.

As we can see from the comparison of the theoretical and experimental values in Table I the semiempirical different orbitals for different spins *SCF LCAO MO* method of DEWAR can account only partially for the spin density distribution of a radical containing also heteroatoms. The obvious way of the improvement of the method is to project out from the many electron π electron wave function the components which do not correspond to the doublet spin state. As it is well known, in the case of a doublet the next state which has the largest component in the unprojected many electron wave function is the quartet state. Therefore a rather complicated program is under construction which annihilates at least this undesired quartet component.

The fact that Coulomb integral values 1.5 $\gamma_{i,j}^{M.N.}$ (which are nearly equal with the theoretical $(\varkappa_i\varkappa_j \mid \frac{1}{r} \mid \varkappa_i\varkappa_j) \equiv \gamma_{i,j}^{theor.}$ Coulomb integral values), and not the much smaller $\gamma_{i,j.}^{M.N.}$ values have given for the spin densities at the carbon atoms the comparatively best agreement with experiment indicates also that the annihilation of the quartet component is necessary [22]. Further it seems probable that this annihilation by increasing the spin density of the N atom and decreasing it by the oxygen atom will give also a much more correct theoretical a_N value. This statement can be supported by the fact that according to another calculation performed for the spin densities of the triplet states of the nucleotide bases [23] the annihilation of the quintet component of the unprojected wave function has a rather large effect on the spin densities of certain atoms.

In Table II we give the calculated spin densities for ortho F-, Cl-, and Br-phenyl nitroxide radicals determined again for 0°, 30° and 60° angles of rotation around the C—N bond. The used $\gamma_{i,j}$ values were $\gamma_{i,j} = 1.5\ \gamma_{i,j}^{M.N.}$.

Table II

Calculated spin densities of ortho F-, Cl- and Br-phenyl nitroxide radicals with $\gamma_{i,j} = 1.5\ \gamma_{i,j}^{M.N.}$ *and by different angles of rotation*

	o—F			o—Cl			o—Br		
	0°	30°	60°	0°	30°	60°	0°	30°	60°
1	0.044	0.033	0.011	0.046	0.035	0.014	0.045	0.033	0.012
2	−0.025	−0.018	−0.006	−0.026	−0.019	−0.009	−0.025	−0.018	−0.006
3	0.037	0.027	0.010	0.039	0.029	0.013	0.038	0.028	0.010
4	−0.024	−0.017	−0.007	−0.026	−0.020	−0.009	−0.025	−0.017	−0.007
5	0.044	0.032	0.011	0.046	0.034	0.014	0.045	0.033	0.012
6	−0.043	−0.032	−0.011	−0.045	−0.034	−0.014	−0.043	−0.032	−0.012
7	0.317	0.320	0.328	0.312	0.317	0.326	0.309	0.315	0.325
8	0.648	0.654	0.663	0.652	0.657	0.665	0.665	0.659	0.667
9	0.003	0.002	0.001	0.002	0.002	0.001	0.001	0.001	0.000
Exp.	$a_N = 13{,}37$ gauss			$a_N = 13.44$ gauss			$a_N = 13.69$ gauss		

Table III

The calculated experimental spin densities of para F-, Cl-, Br-, -OH- and NH_2-phenyl nitroxide radicals ($\gamma_{i,j} = 1.5\,\gamma_{i,j}^{M.N.}$, $\alpha = 0°$)

	p—F		p—Cl		p—Br		p—OH		p—NH_2	
	Theor.	Exp.	Theor.	Exp.	Theor.	Exp.	Theor.	Exp.	Theor.	Exp.
1	0.046	0.101	0.046	0.104	0.049	0.099	0.046	0.100	0.046	
2	−0.026	−0.038	−0.026	−0.042	−0.029		−0.026	−0.035	−0.026	
3	0.039	—	0.039	—	0.042	—	0.038	—	0.040	—
4	−0.027	−0.038	−0.026	−0.042	−0.028		−0.027	−0.035	−0.028	
5	0.046	0.101	0.046	0.104	0.048	0.099	0.046	0.100	0.046	
6	−0.045	—	−0.045	—	−0.047	—	−0.045	—	−0.045	—
7	0.311	$a_N = 11{,}53$ gauss	0.312	$a_N = 10.94$ gauss	0.307	$a_N = 10.84$ gauss	0.311	$a_N = 11.87$ gauss	0.311	$a_N = 11{,}69$ gauss
8	0.654		0.653		0.657		0.654		0.653	
9	0.002	—	0.002	—	0.001	—	0.033	—	0.004	—

Comparing these results with those obtained for the unsubstituted radical (see in Table I the column $1.5\ \gamma^{M.N.}$) we can see that the substitution of the halogene atoms in the ortho position decreases somewhat the absolute values of the spin densities within the ring but it does not change their sign distribution. Since experimentally it was possible to measure only the a_N hyperfine splitting constant, the spin densities within the ring must be extremely small. Therefore the calculated values obtained for the rotation angle 60° are the most realistic ones. As in the case of the unsubstituted compound, the experimentally found a_N values cannot be interpreted on the basis of these results. Finally it should be noticed that the spin density on the halogen substituents is extremely small.

In Table III we give the calculated and experimental spin densities for para F-, Cl-, Br-, HO- and NH_2-phenyl nitroxide radicals. The calculated values were obtained with Coulomb integral values $\gamma_{i,j} = 1.5\ \gamma_{i,j}^{M.N.}$ and for $\alpha = 0°$. The experimental ones we have obtained again from the experimentally found hyperfine splitting constants using McConnel's relation with $Q_{C,H} = 22.5$ gauss.

Looking at the Table we can see again that the spin distribution of the radical is not much changed by the substitution (the spin density at the substituents is in all the five cases very small, the distribution of signs is unchanged, the absolute values of the spin densities within the ring is somewhat smaller and the spin densities in the N=O group change only very slightly). This fact is in agreement with the experimental values, which also change only in a very small amount in consequence of the different substituents. Therefore for the comparison of the theoretical and experimental values we can say the same,

Table IV

The calculated and experimental spin densities of meta F-, Cl- and Br-phenyl nitroxide radicals ($\gamma_{i,j} = 1{,}5\ \gamma_{i,j}^{M.N.}$ $\alpha = 0°$)

	m—F		m—Cl		m—Br	
	Theor.	Exp.	Theor.	Exp.	Theor.	Exp.
1	0.045	0.103	0.046	0.103	0.048	0.101
2	−0.025	—	−0.026	—	−0.028	—
3	0.040	0.103	0.040	0.103	0.041	0.101
4	−0.026	−0.036	−0.027	−0.036	−0.028	−0.036
5	0.046	0.103	0.047	0.103	0.048	0.101
6	−0.044	—	−0.045	—	−0.046	—
7	0.306	$a_N = 10.83$ gauss	0.307	$a_N = 10.94$ gauss	0.306	$a_N = 10.87$ gauss
8	0.658		0.657		0.658	
9	−0.001	—	−0.001	—	−0.003	—

as we did in the case of the unsubstituted radical. In this respect it should be mentioned that in the case of the HO-substituted radical we have performed the calculation also for Coulomb integral values $\gamma_{i,j} = \gamma_{i,j}^{M.N.}$ and $1.2\gamma_{i,j}^{M.N.}$, respectively. Again, as in the case of the unsubstituted radical, the comparatively best agreement could be achieved with $\gamma_{i,j} = 1.5\ \gamma_{i.j}^{M.N.}$.

Finally in Table IV we give the theoretical and experimental spin densities for the meta F-, Cl-, and Br-phenyl nitroxide radicals. The calculated values refer to $\gamma_{i,j} = 1.5\ \gamma_{i,j}^{M.N.}$ and $\alpha = 0°$. The experimental values were obtained in the same way as the previous ones. From the data included in the Table we can conclude once more that the substitution of the halogen atom influences neither the theoretical nor the experimental spin distribution in a greater amount.

We can draw the conclusion from our investigations with the aid of the semiempirical different orbitals for different spins *SCF LCAO MO* method that though this method describes correctly some features of the experimental spin distribution both in the case of parent radical and in the cases of its substituted derivatives, it is necessary to introduce spin projection to improve the agreement between the experimental and theoretical values. Work in these lines, as we have already mentioned previously, is in progress.

*

We should like to express our gratitude to Dr. F. TÜDŐS, for calling our attention to the problem and for fruitful discussions.

REFERENCES

1. LAMAIRE, H., MARECHAL, Y., RAMASSEUL, R., RASSAT, A.: Bull. Soc. Chim. **1965,** 322.
2. BRIÉRE, R., RASSAT, A.: Bull. Soc. Chim. **1965,** 378.
3. CHAPELET-LETOURNEUX, G., LAMAIRE, H., RASSAT, A.: Bull. Soc. Chim. **1965,** 444
4. CHAPELET-LETOURNEUX, G., LAMAIRE, H., RASSAT, A., RAVET, J. P.: Bull. Soc. Chim. **1965,** 1975.
5. DEGUCHI, Y.: Bull. Chem. Soc. Japan **35,** 260 (1962).
6. UMEMOTO, K., DEGUCHI, Y., TAKAKI, H.: Bull. Chem. Soc. Japan **36,** 560 (1963).
7. PANNELL, J.: Mol. Phys. **5,** 291 (1966).
8. BLACHLEY, W. D., REINHARD, R. R.: J. Am. Chem. Soc. **87,** 802 (1965).
9. KAWAMURA, T., MATSUNAMI, S., YONEZAWA, T.: Bull. Chem. Soc. Japan **40,** 1111 (1967).
10. KIKUCHI, O., SOMENO, K.: Bull. Chem. Soc. Japan **40,** 2549 (1967).
11. DEWAR, M. J. S.: Rev. Mod. Phys. **35,** 586 (1963).
12. KENDE, I., TÜDŐS, F., SÜMEGI, L.: Acta Chim. Acad. Sci. Hung. **54,** 315 (1967).
13. SLATER, J. C.: Phys. Rev. **82,** 538 (1951).
14. LÖWDIN, P.-O.: Phys. Rev. **97,** 1474 (1955).
15. BERTHIER, G.: J. Chim. Phys. **51,** 137 (1954): *ibid* **51,** 363 (1954).
16. BERTHIER, G. in: Molecular Orbitals in Chemistry, Physics and Biology, p. 57. ed. P.-O. Löwdin and B. Pullman. Academic Press, New York—London, 1964, p. 57.
17. MATAGA, N., NISHIMOTO, K.: Z. Physik. Chemie **13,** 140 (1957).
18. LADIK, J., BICZÓ, G. and RÉDLY, J.: (unpublished results).
19. KARPLUS, M., FRAENKEL, G.: J. Chem. Phys. **35,** 1312 (1961).

20. LADIK, J., BICZÓ, G., MOHOS, B., TÜDŐS, F., RÉDLY, J.: Proc. Conf. on Some Aspects of Physical Chemistry. Budapest, **427**, (1966).
21. MCLACHLAN, A. D.: Mol. Phys. **3**, 233 (1960).
22. SNYDER, L. (personal communication).
23. PACKER, J., AVERY, J., LADIK, J., BICZÓ, G.: Int. Quant. Chem. (submitted for publication).

János LADIK
Géza BICZÓ
Imre KENDE
László SÜMEGI

Budapest II., Pusztaszeri út 57—69.

Acta Chimica Academiae Scientiarum Hungaricae, Tomus 61 (4), pp. 391—406 (1969)

CALCULATION OF INFRARED BAND CONTOURS OF PLANAR ASYMMETRIC TOP MOLECULES, I

CONSTRUCTION OF GENERAL RELATIONSHIPS

É. PAÁL and GY. VARSÁNYI

(Institute of Physical Chemistry, Technical University, Budapest)

Received October 1, 1968

Using a method reported previously [6, 7, 8] the band contours of planar asymmetric top molecules of different asymmetry parameter and different rotational constants were calculated. The fraction-value widths of pure A-bands and B-bands as well as those of some AB hybrid bands having transition moments of different directions were determined. On the basis of the fraction-value widths $\varkappa - \Delta\tilde{\nu}_{1/n}, B - \Delta\tilde{\nu}_1/_n$ and $\varphi - \Delta\tilde{\nu}_{1/n}$ diagrams were constructed. The domains of $\varkappa$ and B in which the $\varphi - \Delta\tilde{\nu}_1/_n$ diagrams can be used for determining the direction of the transition moment were defined.

Introduction

The contours of vapour spectra of polyatomic molecules are determined by the rotational structure. The band contours depend on the direction of the transition moments. The transition moments of non-perpendicular vibrations of planar asymmetric top molecules having a C_s symmetry lie in the plane determined by axes A and B. If theoretical band contours of vibrations directed towards A and B are known, there is a possibility to determine the direction of the transition moment on the basis of experimental data of contours.

No explicit expression can be given for the values of energy levels of an asymmetric top. In order to calculate these values, the molecule can be regarded as an intermediate species between an oblate and a prolate symmetric top. There is a simple approximation, namely the graphical determination on the basis of the terms of symmetric tops [1, 2]. KING, HAINER and CROSS reported a relationship on the basis of quantum mechanical calculations [3].

The values of E_τ (*i.e.* the so-called reduced energy) were calculated up to $J = 40$ applying the method of KING, HAINER and CROSS [4].

The first calculation of band contours was carried out by BADGER and ZUMWALT [5]. They constructed a diagram on the basis of band contours obtained at different values of asymmetry parameter ($\varkappa$). This diagram has been recommended for quick estimation of $\varkappa$ and ϱ:

$$\varkappa = \frac{2B - A - C}{A - C} \tag{1}$$

$$\varrho = \frac{A}{B} \tag{2}$$

where A, B, C are the rotational constants.

Band contours of dihalogenobenzenes as well as vinyl haloids have been calculated by VARSÁNYI [6, 7, 8]. A graphical approximation was then used for the determination of energy values. This approximation proved to be satisfactory for every band of dihalogenobenzenes, in case of the C-bands of vinyl chloride and vinyl bromide, however, it was not able to reproduce the fine structure observed in the spectrum, thus the application of a second approximation was necessary [7]. The branch formulae for calculation of line positions related to the vibrational wave number were given in case of each subbranch with the aid of the term formulae.

As for the line intensities of an asymmetric top, calculation methods were reported first by KRAMERS and ITTMANN [9], then by CROSS, HAINER and KING [10]. The line intensities were calculated using the latter authors' method by SCHWENDEMANN and LAURIE [11] in case of $J \leq 12$, and by WACKER and PRATTO [12] in case of $J \leq 35$. Both calculations were carried out using different values of asymmetry parameter.

The calculation of line intensities reported in the paper [6] used the line intensities of a symmetric top as the base.

The values of F line intensities have been determined by DENNISON in case of symmetric tops [13]. VARSÁNYI has shown [6] that in case of $J > 10$, the ratio of the F values of asymmetric and symmetric tops (q) is an exclusive function of $S = K/J$. In this formula for S, K is the arithmetical mean value of K quantum numbers of the ground and excited states and J means the nutation quantum number belonging to the ground state. The $q - S$ curves for every subbranch have been determined and the relative intensities have been calculated for larger J values on this basis. The lines have been normalized to a 0.5 cm^{-1} line distance. (This normalizing is, in fact, an intensity transformation [8]). Some hybrid bands were then constructed by averaging the curves by weighting them by the cosine squares of the angles between the transition moment vector and the axis of the least inertia. Doing this, the triangular character of the finite slit of the spectrometer was taken into consideration. On the basis of the intensity = wave number diagrams, transmittance = wave number diagrams were constructed. The classification of the hybrid bands was carried out on the basis of the fraction-value widths (namely the half-, fifth- and tenth-value widths), since the band widths proved to be approximately independent of the resolution of the spectrum. The uncertainty originating from the inaccuracy of the measurement of the background transmittance was eliminated by calculating with more than one fraction-value width simultaneously.

Data of the calculated hypothetical molecules and the calculation of the terms

The present calculations were carried out using the described methods. It was not necessary to keep to real molecules for constructing general relationships but it was possible to choose arbitrary asymmetry parameters together with appropriate rotational constants. Since in case of planar molecules the largest moment of inertia is equal to the sum of the other two ones, it was sufficient to choose the asymmetry parameter and one rotational constant arbitrarily. The data of the hypothetical model molecules are listed in Table I.

The *C*-bands originate from perpendicular vibrations. In case of perpendicular excitation, the transition moment is perpendicular to the plane of the molecule, thus *C*-bands form no hybrides. Consequently, in the present work, only the calculation of *A*- and *B*-bands will be dealt with.

The bands were calculated subbranch by subbranch. The first graphical approximation was applied for calculating the terms, as this approximation is

Table I

$\varkappa$	A (cm^{-1})	B(cm^{-1})	C (cm^{-1})
−0.9	0.6710	0.1500	0.1226
	0.2237	0.0500	0.0409
	0.04477	0.0100	0.00817
−0.6	0.3354	0.1500	0.1036
	0.1120	0.0500	0.0345
	0.02236	0.0100	0.00691
0	0.2121	0.1500	0.0879
	0.0707	0.0500	0.0293
	0.01414	0.0100	0.00586

satisfactory in every case with the selected values of rotational constants, except for only one case, *i.e.* the case of Q_r *CI* subbranch (the symbol *CI* means the first subbranch in the *C*-band).

Calculation of line intensities

Relative intensities were calculated. The value of the statistical weight (g) was chosen in every case to be equal to $(2J + 1)$. The twofold statistical weight of the $K = 0$ line was taken into consideration when F line intensities were calculated. The F values of symmetric tops calculated according to DENNISON have been listed in paper [6].

Subbranch R_r can be found in both B-band and C-band. B-band contains two partial subbranches corresponding to $\Delta L = 1$ and $\Delta L = -1$. The subbranch in the C-band has a twofold weight thus the intensity of each component of the subbranch is equal to one quarter of the total intensity, except for the line pertaining to $K = 0$. In the latter case the twofold degeneration causes the intensities of each subbranch to be equal to one half of the total intensity. Subbranch R_p can be divided into four parts, too, according to the different values of ΔL; *i.e.*: R_pB I; R_p B II; R_p C I; R_p C II. The F values in each partial subbranch are equal to one quarter of the total value. The components of subbranch R_q are: R_q A I and R_q A II, thus the intensities are halved. On the basis of similar considerations, it is obvious that the F value of subbranch Q_r is also halved, whereas the intensity of subbranch Q_q remains unchanged.

The lower limit of the approximation with a prolate top is, according to KRAMERS and ITTMANN [9]:

$$S_K = \frac{2}{\pi} \operatorname{arctg} \sqrt{\frac{B-C}{A-B}} \tag{3}$$

The quotient $q(S)$ was obtained by relating the line intensities of the asymmetric top to the F values of symmetric tops: when $S < S_K$, to those of the oblate top, when $S > S_K$, to those of the prolate top, except for subbranch R_p B I and, in case of $\varkappa = -0.9$, for subbranches R_r B II, Q_r B and Q_q A. In the cases mentioned the basis of the comparison was the prolate top throughout the whole range of S values. In subbranch R_p B I, the values are as follows: $\Delta J = 1$, $\Delta K = -1$ and $\Delta L = 3$. In case of approximating with an oblate top, quantum numbers K and L are inverted. DENNISON's formulae of line intensity contain no expressions valid for $\Delta K = 3$. The comparison of subbranches R_r B II, Q_r B and Q_q A in case of $\varkappa = -0.9$ with an oblate top would have resulted greater deviation from unit than our procedure. The line intensities of the asymmetric top were obtained from the tables of SCHWENDEMANN and LAURIE [11] as well as those of WACKER and PRATTO [12]. Table II contains S_K values pertaining to the selected values of asymmetry parameter.

Table II

$\varkappa$	S_K
−0.9	0.1433
−0.6	0.2950
0	0.5018

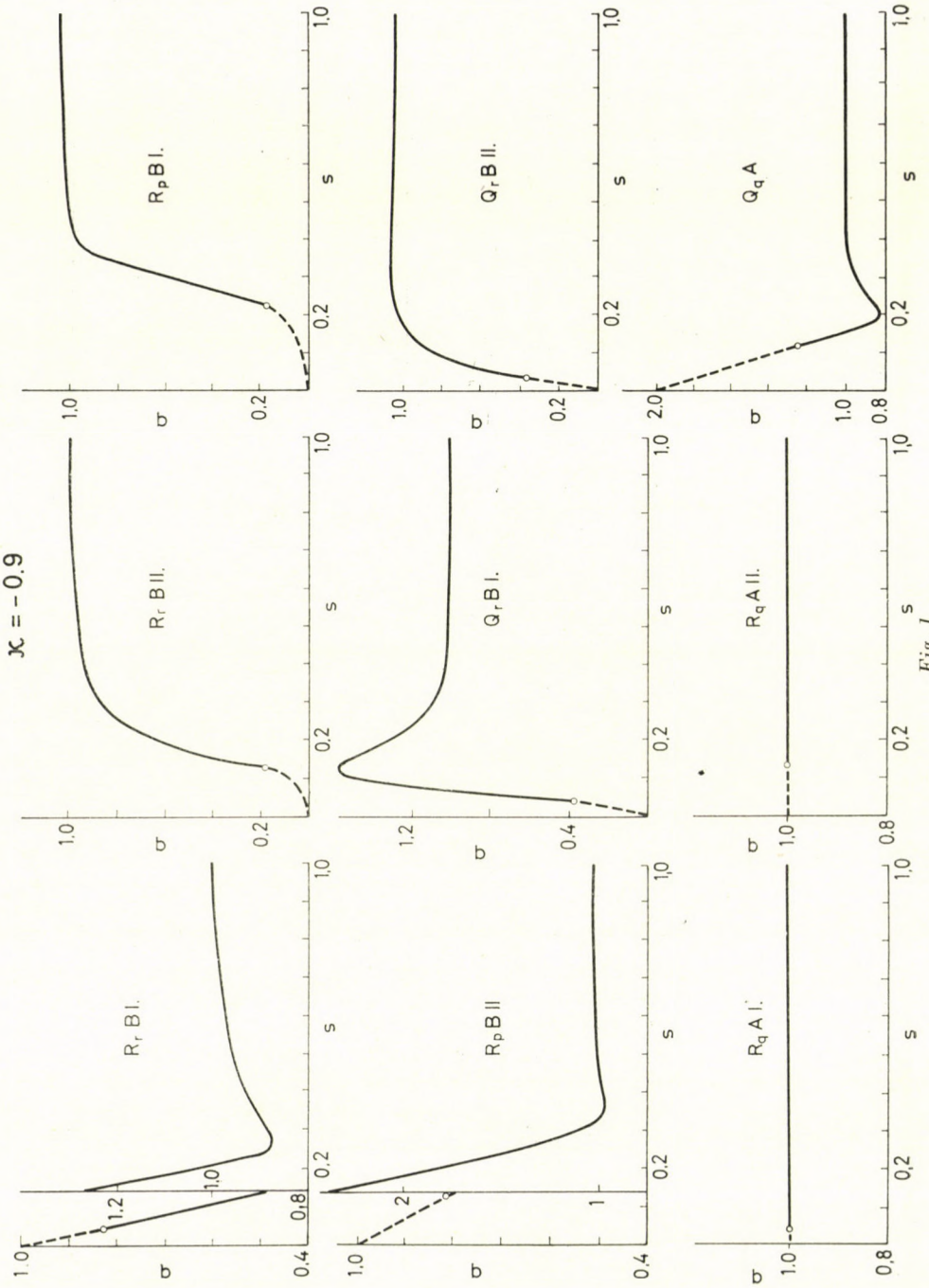
$\varkappa = -0.9$
R_r B I.
R_r B II.
R_p B I.
Q_r B I.
Q_r B II.
R_p B II
R_q A I.
R_q A II.
Q_q A
σ
s

Fig. 1

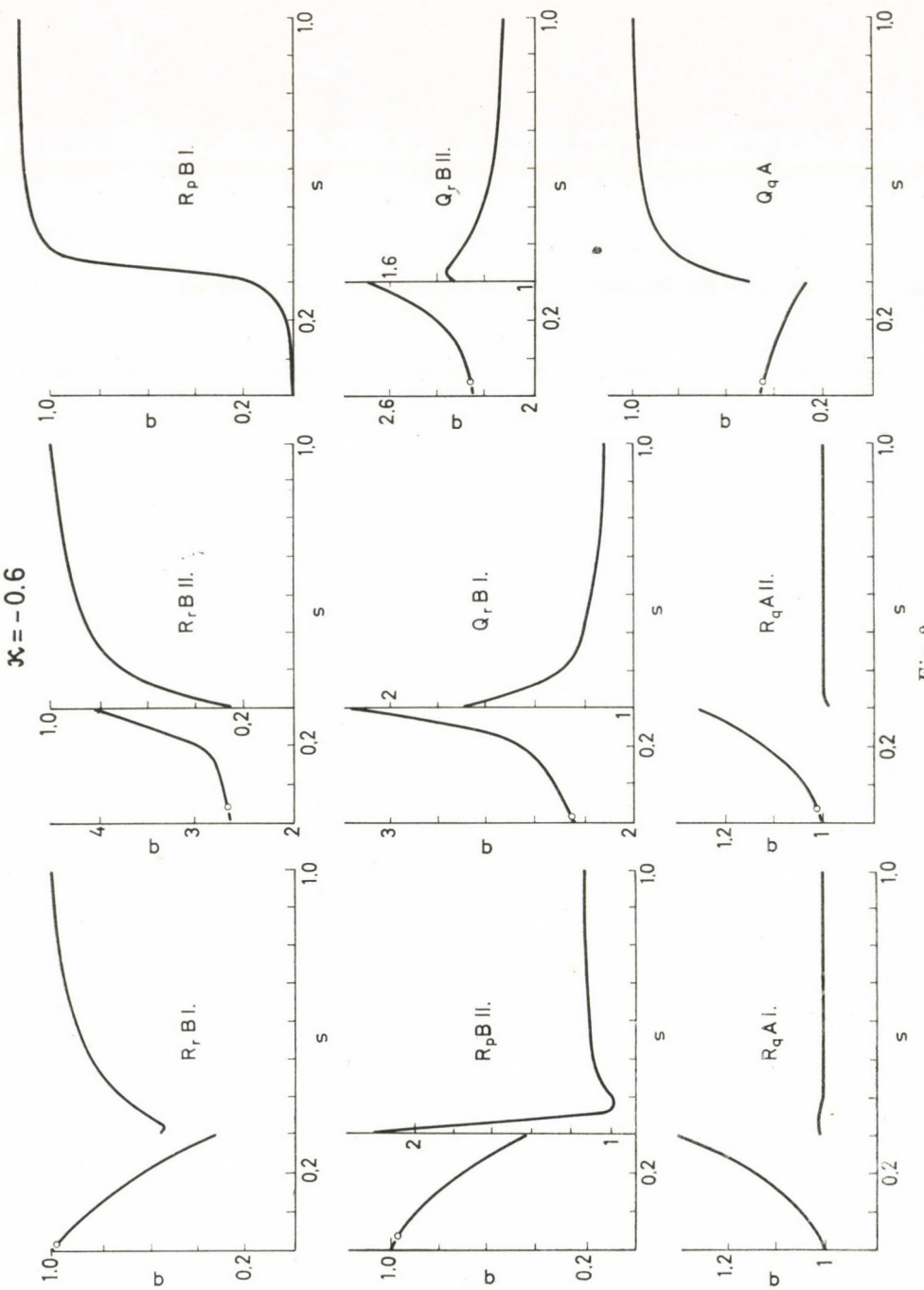

Fig. 2

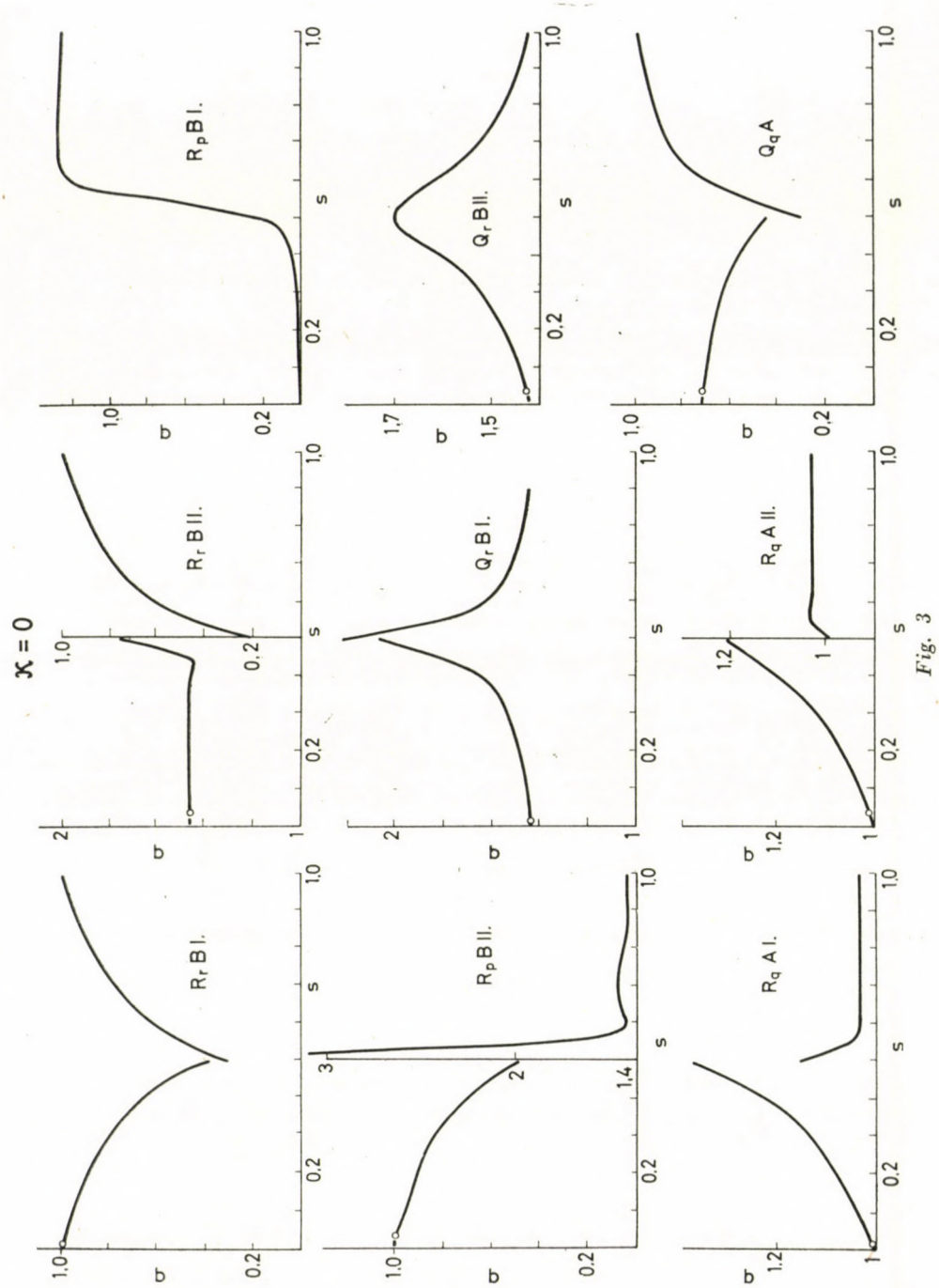
$\varkappa = 0$
$R_r B I.$
$R_r B II.$
$R_p B I.$
$R_p B II.$
$Q_r B I.$
$Q_r B II.$
$R_q A I.$
$R_q A II.$
$Q_q A$
σ
s

Fig. 3

The $q - S$ diagrams were constructed (Figs 1, 2, 3). The temperature in the cell was assumed to be 50 °C uniformly. The Boltzmann factor corresponding to this temperature was used in the expression of intensity. The calculations were continued until the line intensities corresponding to the values of J and K were less by three orders of magnitude than those of the most intensive line (Table III).

Table III

$\varkappa$	B(cm^{-1})	J_{max}	K_{max}
−0.9	0.1500	100	40
	0.0500	160	80
	0.0100	400	200
−0.6	0.1500	120	65
	0.0500	200	100
	0.0100	450	250
0	0.1500	140	70
	0.0500	220	120
	0.0100	500	300

The calculation of line positions

The line positions were determined using the branch formulas of [8]. The wave numbers of the line positions have been expressed as the multiples of the least rotational constant. The line bundles pertaining to the same K value are equidistant in each subbranch and the distance of the lines depends exclusively on $\varkappa$. A similar regularity can be observed if K quantum number will be gradually increased.

Construction of band contours

The envelopes of each subbranch were constructed so that the K quantum number be constant in case of the same curve. A summarized curve was constructed from the line bundle obtained. The summarized curve could be constructed in a more simple way in case of some of the subbranches. It was utilized that in the Q_q branch of every molecule the lines pertaining to the same L values have the same position, as well as the fact that if $\varkappa = 0$, the positions of lines in subbranches $R_r\,B$ II, $R_p\,B$ II and $Q_r\,B$ are independent of K. The summarized curves were normalized to a line distance equal to 0.5 cm^{-1} which

corresponded to the resolution of the Zeiss UR-10 spectrometer, and the triangular character of the finite slit of the spectrometer was also taken into consideration.

The intensity–wave number diagrams were then transformed into transmittance–wave number diagrams [8].

The background and maximum transmittances were taken arbitrarily as 90% and 20%, respectively. It may be done, for the fraction-value widths proved to be independent of the background as well as of the maximum transmittance.

Hybrid bands can be obtained from pure A- and B-bands if they are averaged by weighting them statistically by the cosine squares of the angles between the transition moment and the axis of the least moment of inertia (φ). Three hybrid bands were calculated, namely in cases of $\varphi = 30°$, $45°$ and $60°$, respectively. The fraction-value widths of both pure and hybrid bands were determined [8].

Results

The fraction-value widths ($\Delta\tilde{\nu}_{1/n}$) obtained in case of nine hypothetical molecules are tabulated in Table IV.

Diagrams were constructed on the basis of these fraction widths. Since in case of pure bands two parameters can be varied simultaneously (*i.e.* $\varkappa$ and B) it seemed to be useful to construct two types of diagrams being related to each other. One type of these is the $\varkappa - \Delta\tilde{\nu}_{1/n}$ diagram suitable for plotting series of curves belonging to different values of B. The other type is the $B - \Delta\tilde{\nu}_{1/n}$ diagram, in which the series of curves belong to different values of $\varkappa$. The fraction-value widths can then be determined unambiguously from these two types of diagrams in case of given values of B and $\varkappa$. The diagrams obtained are shown in Figs 4—9. In case of hybrid bands a third type of diagram must be added to the previous two ones: the $\Delta\tilde{\nu}_{1/n} - \varphi$ diagram (Figs 10—12). Using these three diagrams the direction of the transition moment can be determined from the experimental fraction-value widths.

It can be seen from Figs 10—12 that the determination of fraction-value widths does not give an unambiguous information in every case on the angle between the transition moment and the A axis. If the asymmetry parameter is $\varkappa = -0.9$, with the medium rotational constant (B) being in the 0.0500 cm^{-1} to 0.1500 cm^{-1} range, the half-, fifth- and tenth-value widths render it possible to determine the direction of the transition moment. If the value of B is equal to 0.0100 cm^{-1}, the difference between the half-value widths of the A-band and B-band is as small as 3 cm^{-1}, whereas the analogous differences between the fifth- and tenth-widths are 5.5 cm^{-1} and 7.8 cm^{-1}, respectively. Since the determination of the tenth-value widths of the bands is the least accurate,

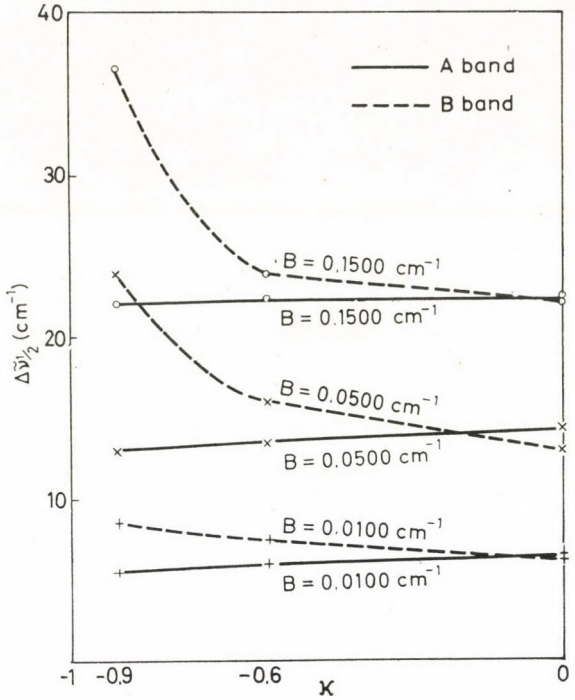
A band
B band
B = 0.1500 cm⁻¹
B = 0.1500 cm⁻¹
B = 0.0500 cm⁻¹
B = 0.0500 cm⁻¹
B = 0.0100 cm⁻¹
B = 0.0100 cm⁻¹
Δν̃½ (cm⁻¹)
40
30
20
10
-1
-0.9
-0.6
0
κ

Fig. 4

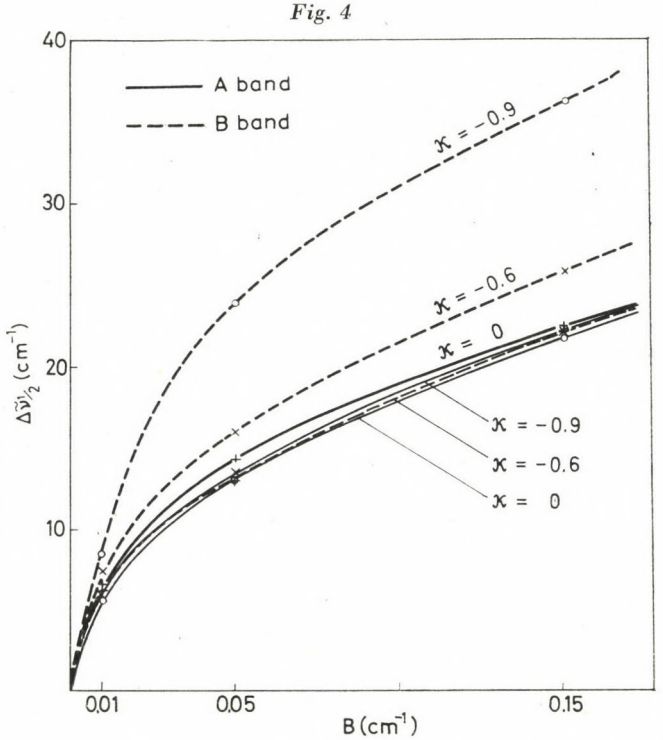
A band
B band
κ = −0.9
κ = −0.6
κ = 0
κ = −0.9
κ = −0.6
κ = 0
Δν̃½ (cm⁻¹)
40
30
20
10
0.01
0.05
0.15
B (cm⁻¹)

Fig. 5

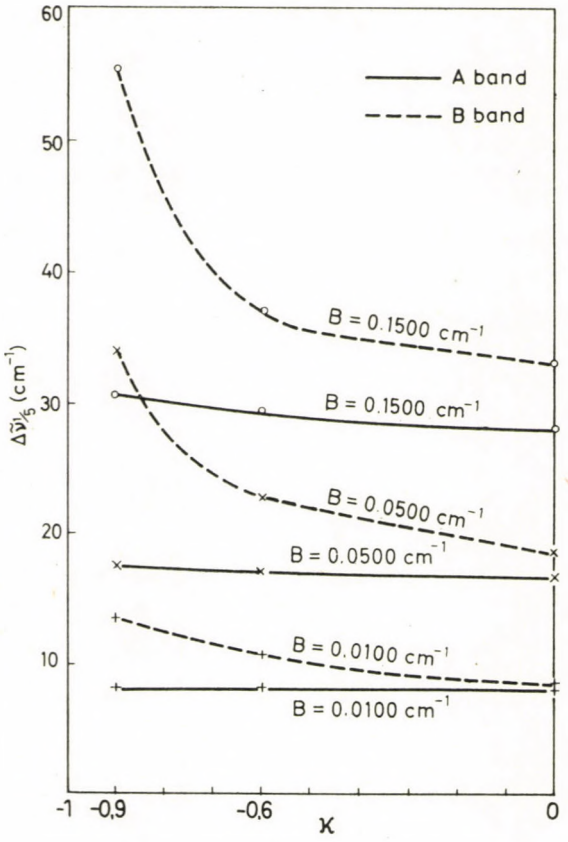
A band
B band
B = 0.1500 cm⁻¹
B = 0.1500 cm⁻¹
B = 0.0500 cm⁻¹
B = 0.0500 cm⁻¹
B = 0.0100 cm⁻¹
B = 0.0100 cm⁻¹
Δṽ½ (cm⁻¹)
60
50
40
30
20
10
-1
-0,9
-0,6
0
κ

Fig. 6

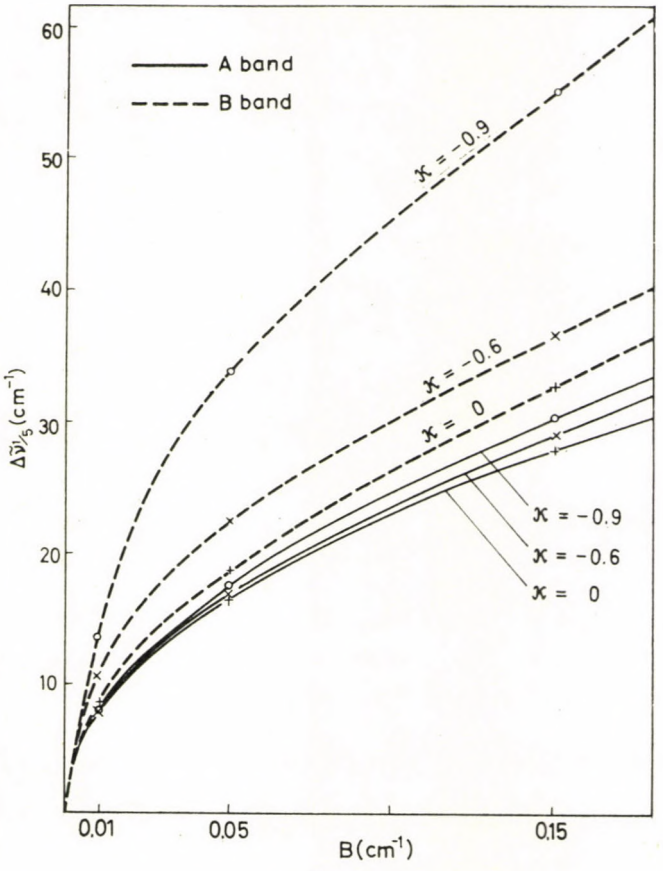
A band
B band
κ = −0.9
κ = −0.6
κ = 0
κ = −0.9
κ = −0.6
κ = 0
Δṽ½ (cm⁻¹)
60
50
40
30
20
10
0,01
0,05
0,15
B(cm⁻¹)

Fig. 7

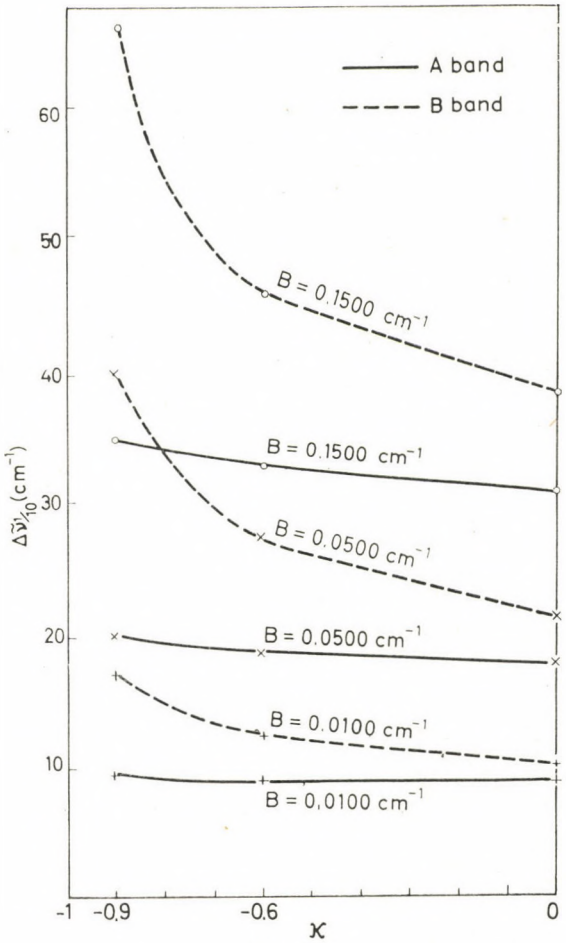
A band
B band
B = 0.1500 cm⁻¹
B = 0.1500 cm⁻¹
B = 0.0500 cm⁻¹
B = 0.0500 cm⁻¹
B = 0.0100 cm⁻¹
B = 0,0100 cm⁻¹
Δν̃1/2 (cm⁻¹)
60
50
40
30
20
10
-1
-0,9
-0,6
0
κ

Fig. 8

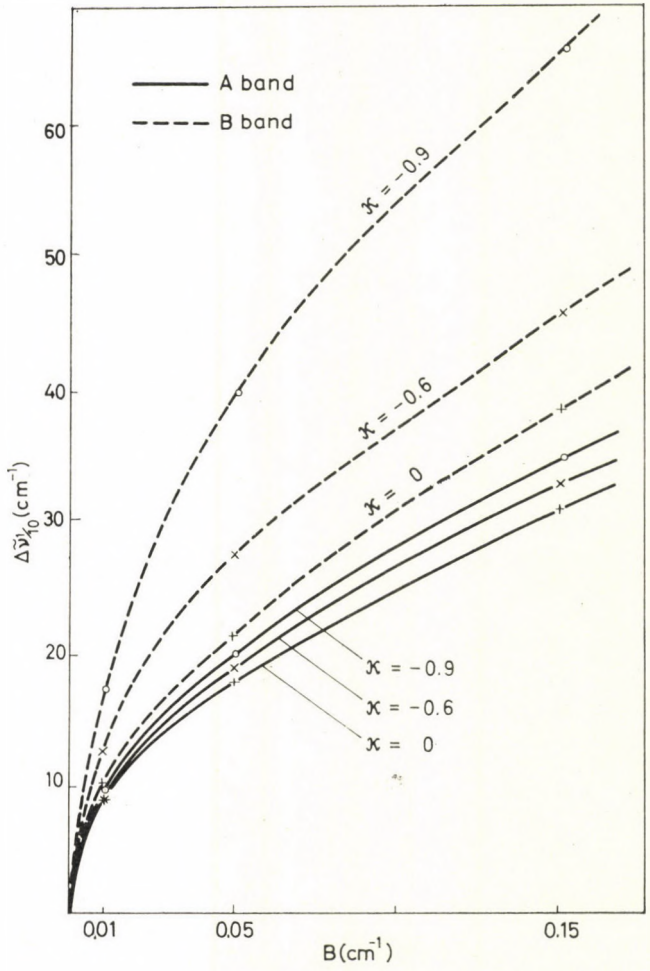
A band
B band
κ = -0.9
κ = -0.6
κ = 0
κ = -0.9
κ = -0.6
κ = 0
Δν̃1/2 (cm⁻¹)
60
50
40
30
20
10
0,01
0,05
0.15
B(cm⁻¹)

Fig. 9

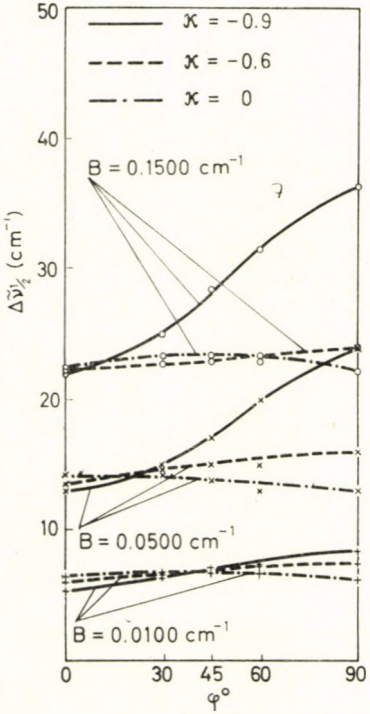

Fig. 10

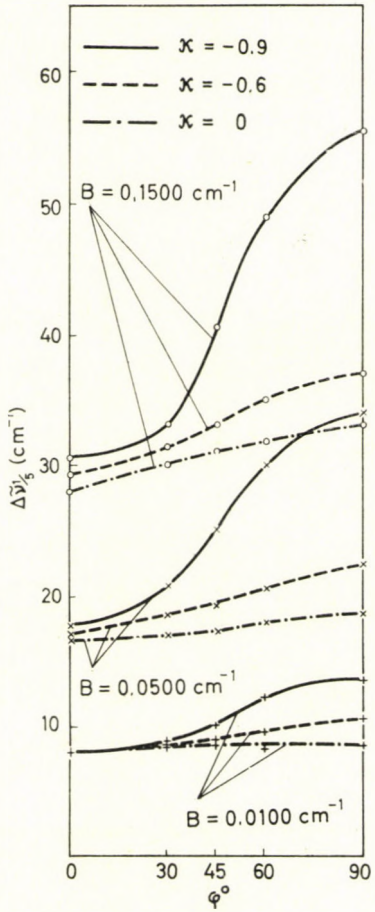

Fig. 11

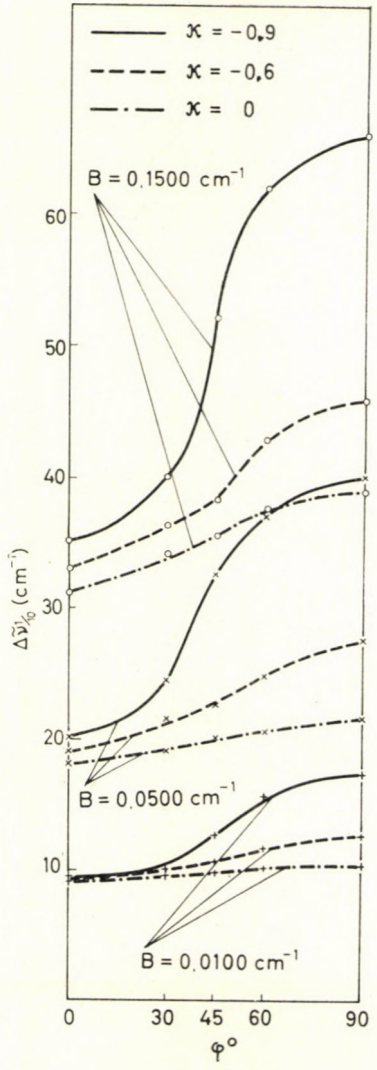

Fig. 12

Table IV

$\varkappa$	B (cm^{-1})	$\Delta\tilde{\nu}_{1/2}$ (cm^{-1})	$\Delta\tilde{\nu}_{1/5}$ (cm^{-1})	$\Delta\tilde{\nu}_{1/10}$ (cm^{-1})
		A-band ($\varphi = 0°$)		
−0.9	0.1500	22	30.5	35
	0.0500	13	17.5	20
	0.0100	5.5	8	9.5
−0.6	0.1500	22.3	29.3	33
	0.0500	13.5	17	19
	0.0100	6	8	9
0	0.1500	22.5	28	31
	0.0500	14.3	16.5	18
	0.0100	6.5	8	9
		AB hybrid band ($\varphi = 30°$)		
−0.9	0.1500	25	33	40
	0.0500	15	20.8	24.5
	0.0100	6.5	8.8	10
−0.6	0.1500	22.8	31.3	36.3
	0.0500	15	18.5	21.5
	0.0100	7	8.5	10
0	0.1500	23.5	30	34
	0.0500	14.3	17	19
	0.0100	6.8	8.5	9.5
		AB hybrid band ($\varphi = 45°$)		
−0.9	0.1500	28.5	40.5	52
	0.0500	17	25	32.5
	0.0100	7.3	10	12.5
−0.6	0.1500	23	33	38.3
	0.0500	15	19.3	22.5
	0.0100	7	9	10.5
0	0.1500	23.5	31	35.5
	0.0500	13.8	17.3	20
	0.0100	6.8	8.5	9.8
		AB hybrid band ($\varphi = 60°$)		
−0.9	0.1500	31.5	40	62
	0.0500	20	30	37
	0.0100	7.5	12.3	15.5
−0.6	0.1500	23.5	35	42.8
	0.0500	15	20.5	24.8
	0.0100	7	9.5	11.5
0	0.1500	23	31.8	37.5
	0.0500	13	18	20.5
	0.0100	6.5	8.3	10

Table IV (continued)

$\varkappa$	B (cm^{-1})	$\Delta\tilde{\nu}_{1/2}$ (cm^{-1})	$\Delta\nu_{1/5}$ (cm^{-1})	$\Delta\tilde{\nu}_{1/10}$ (cm^{-1})
		B-band ($\varphi = 90°$)		
−0.9	0.1500	36.5	55.5	66
	0.0500	24	34	40
	0.0100	8.5	13.5	17.3
−0.6	0.1500	24	37	46
	0.0500	16	22.5	27.5
	0.0100	7.5	10.5	12.5
0	0.1500	22.3	33	39
	0.0500	13	18.5	21.5
	0.0100	6.3	8.5	10.3

it is not possible to determine the direction of the transition moment with a sufficient accuracy on the basis of these data. If $\varkappa = -0.6$ and $B = 0.1500$ cm^{-1}, the differences between the half-, fifth- and tenth-value widhts of the A- and B-bands are 1.7 cm^{-1}, 7.7 cm^{-1} and 13 cm^{-1}, respectively. Though the half-value width provides no sufficient basis for determining the direction of the transition moment, the simultaneous determination of the fifth- and tenth-value widths may provide a useful information. The method cannot be applied if the parameters of the molecule are as follows: $\varkappa = -0.6$ and $B = 0.0500$ cm^{-1} or $\varkappa = -0.6$ and $B = 0.0100$ cm^{-1}. In case of the most asymmetric molecules ($\varkappa = 0$), the half-, fifth- and tenth-value widths of the hybrid bands give no information on the direction of the transition moment in the range from $B = 0.1500$ cm^{-1} to $B = 0.0100$ cm^{-1}.

In our next publication the accuracy of the diagrams concerning pure A-bands and B-bands will be dealt with.

REFERENCES

1. Gordy, W., Smith, W. V., Trambarulo, R. F.: Microwave Spectroscopy. J. Wiley and Sons, New York, 1953.
2. Herzberg, G.: Molecular Spectra and Molecular Structure II. Infrared and Raman Spectra of Polyatomic Molecules. D. Van Nostrand Co. New York, 1949.
3. King, G. W., Hainer, R. M., Cross, P. C.: J. Chem. Phys. **11,** 27 (1943).
4. Allen, H. C., Jr., Cross, P. C.: Molecular Vib-Rotors. J. Wiley, New York, 1963.
5. Badger, R. M., Zumwalt, L. R.: J. Chem. Phys. **6,** 711 (1938).
6. Varsányi, Gy.: Acta Chim. Acad. Sci. Hung. **25,** 255 (1960).
7. Varsányi, Gy., Szőke, S., Faragó, T.: Acta Chim. Acad. Sci. Hung. **34,** 411 (1962).
8. Varsányi, Gy.: Acta Chim. Acad. Sci. Hung. **43,** 315 (1965).
9. Kramers, H. A., Ittmann, G. P.: Z. Physik, **58,** 217 (1929).
10. Cross, P. C., Hainer, R. M., King, G. W.: J. Chem. Phys. **12,** 210 (1944).
11. Schwendemann, R. H., Laurie, V. W.: Tables of Line Strengths for Rotational Transitions of Asymmetric Rotor Molecules. Pergamon Press.
12. Wacker, P. F., Pratto, M. R.: Microwave Spectra Tables. Line Strengths of Asymmetric Rotors. National Bureau of Standards Monograph 70 — Vol. II, 1964.
13. Dennison, D. M.: Rev. Modern Phys. **3,** 280 (1931).

Éva Paál
György Varsányi
} Budapest XI., Budafoki út 8.

Acta Chimica Academiae Scientiarum Hungaricae, Tomus 61 (4), pp. 407—415 (1969)

PREPARATION OF ^{18}O-LABELLED METHYLSILOXANES

P. GÖMÖRY and L. SZEPES

(Department of General and Inorganic Chemistry, L. Eötvös University, Budapest, and Inorganic Research Group, Hungarian Academy of Sciences, Budapest)

Received September 19, 1968

A preparative method has been developed for the hydrolysis of mono- and bifunctional methylchlorosilanes with ^{18}O-enriched water. By means of hydrolysis, polymerization, pyrolysis, and equilibration, the following ^{18}O-enriched cyclic and linear siloxanes have been prepared in gas chromatographic purity:
$[(CH_3)_2SiO]_n$ with $n = 3, 4, 5, 6, 7$;
$(CH_3)_3Si—O—[Si(CH_3)_2—O]_k—Si(CH_3)_3$ with $k = 0, 1, 2, 3, 4, 5$. In the hydrolysis of dimethyldichlorosilane with a nearly stoichiometric amount of water, the amount of cyclic pentasiloxanes increased at the expense of that of the cyclic tetrasiloxane.

Mass-spectrometric studies [1] on the molecular structure of methylsiloxanes have indicated that labelling by ^{18}O may help to clarify the reaction routes leading to the observed fragmentation patterns.

As known, methylsiloxanes are usually prepared by the hydrolysis of the corresponding monomeric chlorosilanes in the presence of a large excess of water.

Methylsiloxanes containing oxygen in an isotope ratio other than that of the natural mixture, can be prepared by hydrolysis in ^{18}O-enriched water. However, owing to the high price of ^{18}O-enriched water, it cannot be used in a large excess. Therefore, we have modified the procedure so that chlorosilanes are hydrolysed with nearly the stoichiometric amount of water, and even the small excess of the latter is recovered with unchanged isotope composition. The ^{18}O-content can only be kept constant if special care is taken to avoid contamination by water having the natural isotope composition, and properly purified starting materials are used.

Using trimethylchlorosilane and dimethyldichlorosilane containing less than 0.1% impurities (as demonstrated by GC analysis), the following ^{18}O-labelled (4.5 and 30%) linear and cyclic methylsiloxanes have been prepared:

M_2	D_3
M_2D	D_4
M_2D_2	D_5
M_2D_3	D_6
M_2D_4	D_7
M_2D_5	

where $M = (CH_3)_3SiO_{0.5}$ and $D = (CH_3)_2SiO$.

The purity of the isolated products was checked by gas chromatography. The amount of impurities was found to be less than 0.2% in all cases*. The procedure is illustrated by the following scheme:

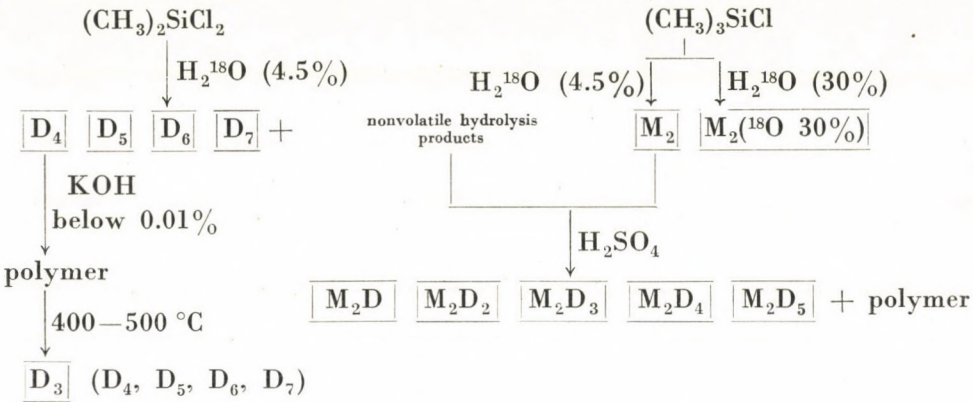

It should be noted that if the hydrolysis is carried out with ^{17}O-enriched water, the present technique allows the preparation of ^{17}O-labelled linear and cyclic siloxanes, which are especially suitable for NMR studies. The amount of ^{17}O in octamethylcyclotetrasiloxane prepared by hydrolysis with natural water is so small** that its NMR spectrum can only be obtained and evaluated if a very powerful instrument is used [2].

I. Hydrolysis of chlorosilanes

(1) *Hydrolysis of dimethyldichlorosilane in the presence of* 10% *and* 100% *excess of water above the stoichiometric amount*

The majority of papers dealing with the hydrolysis of dimethyldichlorosilane is concerned with the technological problem of finding the best conditions for the formation of cyclic siloxanes, first of all octamethylcyclotetrasiloxane, the starting material for manufacturing silicone rubber. The overall process is approximately described by the equation

$$n\,(CH_3)_2SiCl_2 + n\,H_2O \rightarrow [(CH_3)_2SiO]_n + 2n\,HCl,$$

the reaction being carried out in a large excess of water. Since the product of hydrolysis is a strongly hydrophobic mixture of siloxanes, the reaction is heterogeneous. The ratio of cyclic siloxanes in the crude hydrolysis product is known

* This purity will be described in the following as "GC purity".

** The natural abundance of the three oxygen isotopes is: approx. 99.759% ^{16}O, 0.204% ^{18}O, and 0.037% ^{17}O.

to increase in the presence of a solvent(*e.g.*, diethyl ether) which is miscible with water to a limited extent [3]. Furthermore, such solvents increase the rate of hydrolysis. The amount of cycles is further increased if the hydrolysis is carried out in strongly acidic medium (*e.g.*, in 6 *N* HCl) with intensive stirring and cooling [3].

There are two possibilities for performing the hydrolysis with ^{18}O-enriched water:

— absolute diethyl ether is saturated wth labelled water, and the hydrolysis is carried out in this solvent, using nearly stoichiometric quantities of the reagents, in *homogeneous* solution;

— the hydrolysis is carried out in a *heterogeneous* system in the presence of a suitable excess of water, which is subsequently recovered.

The amount of hydrolysis products obtainable in homogeneous solutions in the laboratory is limited by the solubility of water in the solvent. We have found that properly dehydrated diethyl ether, which does not consume Karl-Fischer reagent, dissolves about 0.8—0.9% of water (instead of 1.3%, given in the literature) after vigorous shaking for 24 hours. Therefore, not more than 5—6 g of cyclic tetrasiloxane per liter of solution can be expected. The advantage of this method is in its simplicity and the small (5—10 g) water consumption.

Larger amounts of cyclic methylsiloxanes were prepared by heterogeneous hydrolysis in the presence of a 100% excess of water. The amount of D_4 isolated from 1 liter of the solution is about 35—40 g. Interestingly enough, hydrochloric acid released in the hydrolysis gives a homogeneous phase with ether, water, and the produced methylsiloxanes, which dissolves about 1/4 of the total amount of siloxanes. Therefore, the upper solution containing ether, siloxane, and hydrochloric acid should be processed separately from the lower phase containing labelled water.

During the evaporation of the solvent from the ethereal phase, most of the hydrochloric acid is also removed. The evaporation residue was neutralized with dry gaseous ammonia before fractional distillation to avoid changes in the isotope ratio.

The volume of the lower phase which contained the excess of labelled water was, surprisingly, nearly equal to that of the upper phase. The ratio of the phase volumes was expected to be 1 : 10, since the excess water to ether ratio after hydrolysis was about 1 : 10. The strong change in solubility is due to the high concentration of hydrochloric acid. This is indicated by the composition of the lower phase: ether 61.2, hydrochloric acid 26.4, methylsiloxane 6.9, and labelled water 5.5%. From the lower phase hydrochloric acid — ether is evaporated first. Simultaneously, the homogeneous solution separates to concentrated aqueous hydrochloric acid and a siloxane phase. The valuable labelled water is thus recovered as concentrated aqueous hydrochloric acid.

In order to regenerate the labelled water, metallic sodium was reacted with water having an isotope composition identical with that of the water used in the reaction. The recovered hydrochloric acid solution was then neutralized with the $Na^{18}OH$ solution. Labelled water can be carefully distilled from the alkaline solution saturated with NaCl. By this technique, in addition to the amount of water used for the reaction with sodium, 64% of the excess water was recovered.

It is worth mentioning that the amount of cyclic siloxanes in the volatile siloxane fraction obtained by hydrolysis under the above conditions is different from that given in the literature. In particular, the amount of the D_5 fraction has strongly increased at the expense of the D_4 fraction in the higher density phase. The compositions of siloxane fractions separated from the upper ether — —hydrochloric acid—siloxane *(I)* phase and the lower, aqueous *(II)* phase, as well as those of the volatile fractions obtainable by distillation from *I* and *II* at 3 torr up to 100 °C, are shown in Table I.

The composition was determined by fractional distillation using a rotating column equivalent to 30 theoretical plates, followed by comparing the amounts of the individual fractions and their GC analyses. The volatile fractions were directly analyzed by gas chromatography. The agreement between the values obtained by the above two methods was very good.

Table I

Composition of the siloxane mixtures in the crude hydrolysis product and in the volatile fraction

	I		II	
	Composition of the fraction (%)	Composition of the volatile part (%)	Composition of the fraction (%)	Composition of the volatile part (%)
D_3	0.04	0.09	—	—
D_4	25.0	52.0	17.5	37.7
D_5	14.9	31.0	21.9	47.3
D_6	4.1	8.6	3.7	7.9
D_7	—	—	0.6	1.2
Et_2O	4.0	8.3	3.0	6.5
non-volatile	51.8	—	52.6	—

(2) *Hydrolysis of trimethylchlorosilane in the presence of a* 20% *excess of water above the stoichiometric amount*

M_2-free trimethylchlorosilane (of GC purity) was hydrolysed in absolute ether solution. The labelled water (20% excess above the stoichiometric quantity) was added to the ethereal solution of the silane. Since only unhydrolyzed

chlorosilane may contaminate the product if external humidity is excluded, it is necessary to achieve as complete a hydrolysis as possible. After prolonged stirring and refluxing, the ethereal phase was separated from the slight lower layer of aqueous hydrochloric acid, and subjected to fractional distillation. Labelled water was recovered from the aqueous hydrochloric acid as described in Section 1.

The labelled hexamethyldisiloxane could only be isolated in chromatographic purity if extreme care was taken to avoid the presence of toluene, because its last traces cannot be removed from hexamethyldisiloxane by fractional distillation. Therefore, in the preparation of absolute ether it is not advisable to use metallic sodium which has been in contact with toluene.

(1/a) Preparation of ^{18}O-octamethylcyclotetrasiloxane in homogeneous phase

Perfectly anhydrous diethyl ether, which did not consume any amount of the Karl-Fischer reagent, was saturated with water containing 4.5% of ^{18}O by means of vigorous shaking for 24 hrs. The wated content of the resulting solution was found to be 0.79 g/100 ml by the Karl-Fischer method. In a 2 l round-bottomed flask equipped with a stirrer, a reflux condenser, a thermometer, and a dropping funnel, 740 ml of the labelled aqueous ether was placed, and 37.5 g (0.29 mole) of $(CH_3)_2SiCl_2$ dissolved in 80 ml of absolute ether was added dropwise, under vigorous stirring and cooling. The system was isolated from its environment by a $Mg(ClO_4)_2$ tower and scrubbers with paraffin oil. The rate of dropwise addition was adjusted so that the temperature of the reaction mixture did not exceed 32 °C. After stirring for 4 hrs., the dissolved hydrochloric acid was neutralized with gaseous NH_3 dried over solid KOH, sodium wire, and sodium amalgam. After evaporating most of the ether, the hydrolysis product was distilled using a rotating column equivalent to 30 theoretical plates, to obtain 3.05 g (14.2%) of GC-pure $D_4(^{18}O)$.

The saturation of absolute ether with labelled water may be performed in the vessel used for the hydrolysis. To 740 ml of absolute ether there was added 5.6 g of $H_2{}^{18}O$ (4.5%) by drops, under stirring and refluxing. After stirring and refluxing for 1 hr., the above method gave 6.16 g (28.6%) of $D_4(^{18}O)$ which contained 2.5% impurities, as shown by GC analysis. (The yield can be increased if high purity is not required.)

(1/b)Preparation of ^{18}O-octamethylcyclotetrasiloxane in heterogeneous phase

In a flask with a stirrer, an efficient reflux condenser, and two dropping funnels, a mixture of 1000 ml of absolute ether and 72 g (4 moles) of $H_2{}^{18}O$ (4.5%) was placed, and 516 g (4 moles) of GC-purity $(CH_3)_2SiCl_2$ as a 1 : 1 ether solution, and 72 ml (4 moles) of $H_2{}^{18}O$ (4.5%) were added simultaneously by drops, under intensive stirring and cooling, during 1.5 hrs. The temperature did not exceed 20 °C. After further stirring for 4 hrs., the two phases were separated in a separatory funnel. The weight of the upper layer was 859 g, that of the lower one 853 g.

The *upper phase* was processed as described under (1/a). Up to 100°/3 torr, 48.2% (92.8 g) of the siloxane mixture (original total weight 192.2 g) distilled over. The amounts of isolated substances are shown in Table II.

After distilling of 662 g of the mixture ether-hydrochloric acid from the lower phase ($d^{22} = 0.861$), it separated into two layers (59.7 g of siloxane and 73.1 g of aqueous HCl). The amounts of the isolated substances as well as the yields, calculated for dimethyldichlorosilane, are shown in Table II.

The labelled water was recovered as follows: 17 g of metallic sodium was allowed to react with a mixture of 50 g of $H_2{}^{18}O$ (4.5%) and 200 ml of absolute methanol. The resulting $Na^{18}OH$ solution was used to make alkaline the HCl solution containing the labelled water which had been separated from the lower layer. Methanol and labelled water were finally separated on a fractionating column.

Table II

^{18}O-labelled cyclosiloxanes obtained by heterogeneous hydrolysis

	Upper phase (g)	Lower phase (g)	Yield (%)
$D_3(^{18}O)$	0.08	—	0.03
$D_4(^{18}O)$	48.19	11.10	20.1
$D_5(^{18}O)$	28.62	13.82	14.3
$D_6(^{18}O)$	7.95	2.32	3.5
$D_7(^{18}O)$	—	0.35	0.12

(2) Preparation of ^{18}O-hexamethyldisiloxane

In a 1 l flask equipped with a stirrer, an efficient reflux condenser, and a dropping funnel, a solution of 217 g (2 moles) of GC-pure $(CH_3)_3SiCl$ in 300 ml absolute ether was placed, and 21.6 g (1.2 mole) of $H_2{}^{18}O$ (30%) was added by drops during 3 hrs., under constant stirring and refluxing. After stirring and refluxing for 8 hrs., the ether phase was subjected to fractional distillation to obtain 95.2 g (58%) of labelled hexamethyldisiloxane (GC-purity).

Hexamethyldisiloxane was similarly prepared with $H_2{}^{18}O$ (4.5%), and used in the equilibration reactions.

II. Pyrolysis of alkaline $D_4(^{18}O)$ polymer

The pyrolysis of linear dimethylpolysiloxanes of high molecular weight in the absence of oxygen is known to result in the formation of D_3 [3]. The simplest way of preparing the high polymer is the alkaline polymerization of the highly purified cyclic tetramer. Less than 0.01% of solid KOH was used to polymerize D_4, thus the decrease of the ^{18}O isotope fraction was negligible. The amount of catalyst had an important effect on the molecular weight of the polymer [4]. In order to obtain the desired molecular weight (several hundred thousand), dissolved CO_2 had to be removed from D_4 by bubbling N_2 through this compound, in order to avoid carbonate formation which would have hindered the reaching of the molecular weight required.

The yield of $D_3(^{18}O)$ in direct pyrolysis of a polymer containing Si—OK terminal groups is rather low. If the latter, which act as equilibration catalysts, are removed, the pyrolysis product will contain more of the $D_3(^{18}O)$, $D_6(^{18}O)$ and $D_7(^{18}O)$ fractions. The results shown in Table III were obtained by GC analysis of the pyrolysis products.

Table III

Pyrolysis products of ^{18}O-dimethylpolysiloxane

	Si-OK-containing polymer (%)	Si-OK-free polymer (%)
D_3	10.4	19.9
D_4	56.7	36.6
D_5	25.2	19.3
D_6	6.4	15.3
D_7	1.5	7.1
D_8	—	1.7

In order to remove the Si—OK terminal groups, dry CO_2 was bubbled through a 10% solution of the polymer in benzene for 24 hours. After filtration and removal of the solvent, the pyrolysis was performed. A copper vessel was used for pyrolysing small amounts. A slow stream of dry N_2 was passed through the system to exclude air.

During the distillation of $D_3(^{18}O)$, the condenser had to be maintained at 70 °C to avoid solidification of the product (m.p. 65 °C).

Preparation of hexamethylcyclotrisiloxane by pyrolysis

In a 50 ml flask equipped with a stirrer, inlet and outlet tubes for N_2, and immersed into an oil bath (150°), 14.2 g of GC-pure $D_4(^{18}O$ 4.5%) was placed, dry nitrogen was bubbled through the system for 1 hr., then 0.0112 g (0.0079%) of solid KOH was added. Vigorous stirring was applied until complete dissolution of KOH. In about 20—25 min. a strong increase of viscosity was observed indicating that polymerization had begun. The molecular weight after 2 hrs. at 150° increased to several hundred thousand.

The polymer was heated at 400—500 °C in the pyrolysing vessel under dry N_2 for 15 min., when degradation was complete. Yield: 13.04 g (92%). 1.36 g (9.6%) of labelled hexamethylcyclotrisiloxane was isolated in GC purity.

III. Equilibration of dimethylsiloxanes with sulphuric acid

In dimethylsiloxane systems containing mono- and bifunctional units, rearrangements leading to equilibria take place under the influence of so-called equilibration catalysts (*e. g.*, conc. H_2SO_4) [5]. LENGYEL, PRÉKOPA and TÖRÖK [6] described a method for calculating the equilibrium distribution of molecular weights. In the equilibrium mixture the number of the molecules terminating in monofunctional units, built from k bifunctional units is:

$$N'_k = R \frac{R}{R+N} \left(\frac{N}{R+N} \right)^k, \qquad (1)$$

where

k — the number of D-units in the molecules M_2D_k,
R — the total number of molecules in the equilibrium mixture, *i. e.* the number of molecules M_2 in the *initial* mixture,
N — the number of D-units in the *initial* mixture.

The above formula derived by introducing some simplifying assumptions can be used as a good approximation if the M/D ratio is not too small, *i. e.* the formation of cycles is negligible.

For a possible preparative use of the equilibration procedure, it is necessary to know the initial composition required to obtain maximum amount of molecules with the composition M_2D_k. The question can be answered by means of Eq. (1). Introducing

$$p = \frac{N}{R + N} \tag{2}$$

Eq. (1) can be written as

$$N'_k = R(1 - p)p^k. \tag{3}$$

Obviously, N'_k has maximum value if

$$\frac{dN'_k}{dp} = 0\,. \tag{4}$$

From Eqs (4) and (3) we get:

$$\frac{d(Rp^k - Rp^{k+1})}{dp} = kRp^{k-1} - (k + 1)Rp^k = 0\,; \tag{5}$$

if $R \neq 0$

$$p = \frac{k}{k + 1}, \tag{6}$$

Substitution of this expression into Eq. (2) gives

$$N = kR.$$

Thus, molecules with M_2D_k composition should form in maximum yield in the *equilibrium* mixture, if the number of bifunctional units in the initial mixture equals k-time the number of the molecules M_2.

In order to have all members of the series M_2D_k ($k = 1, 2, 3, 4, 5$) present in isolable amounts in the equilibrium mixture, we chose an initial composition that would lead to an optimum amount of M_2D_2.

Equilibration was carried out using the residue (free of volatile components) obtained in the hydrolysis of dimethyldichlorosilane with $H_2{}^{18}O$ (4.5%). This is mainly a mixture of α, ω-dimethylpolysiloxanediols, but the presence

of Si—Cl terminal groups is also probable. The rate of reaching the equilibrium in such heterogeneous systems was found to be much lower than, *e.g.*, during the equilibration of a $M_2 + D_4$ mixture. The results of 5- and 10-hour equilibrations catalyzed by 5 and 10% conc. H_2SO_4, respectively, are shown in Table IV together with the corresponding data calculated from Eq. (1). The composition was determined by GC analysis. The results show that increasing amount of the catalyst and longer equilibration times shift the system closer to the equilibrium.

Table IV

Calculated and found amounts of siloxane oligomers in the equilibrated mixtures

	Calculated		5% conc. H_2SO_4, 5 hrs.		5% conc. H_2SO_4, 10 hrs.		10% conc. H_2SO_4, 10 hrs.	
	moles	g	moles	g	moles	g	moles	g
M_2	0.067	10.87	—	—	0.078	12.65	0.051	8.25
M_2D	0.045	10.60	0.019	4.45	0.038	8.88	0.032	7.56
M_2D_2	0.030	9.25	0.011	3.39	0.014	4.51	0.020	6.18
M_2D_3	0.020	7.62	0.006	2.49	0.007	2.72	0.011	4.45
M_2D_4	0.013	6.06	0.003	1.61	0.005	2.36	0.006	2.96
M_2D_5	0.0088	4.69	0.0026	1.38	0.0034	1.82	0.0037	1.97
M_2D_6	0.0059	3.57	0.0016	0.94	—	—	0.0027	1.64
M_2D_7	0.0039	2.66	0.0008	0.59	—	—	0.0022	1.52
M_2D_8	0.0026	1.97	0.0006	0.44	—	—	0.0010	0.75

Preparation of the $M_2D_k(^{18}O)$ series (k = 1, 2, 3, 4, 5)

A mixture of 30.00 g (0.405 mole) of volatile-free polysiloxane, obtained by heterogeneous hydrolysis as described in Section *I* (^{18}O 4.5%) and 32.72 g (0.202 mole) of ^{18}O-hexamethyldisiloxane (^{18}O 4.5%) was mixed with 3.13 g (5%) or 6.27 g (10%) of conc. H_2SO_4. The vessels containing the two-phase systems were vigorously shaken for 5 and 10 hrs., respectively. The content of the vessels was then transferred to a separatory funnel half-filled with water, and washed acid-free with water, aqueous Na_2CO_3, and water again, followed by drying over Na_2SO_4. The mixture was separated on a preparative gas chromatograph (*cf.* Table IV). Species with $k = 6$, 7 and 8 were not isolated in pure form.

REFERENCES

1. Tamás, J., Újszászy, K., Székely, T., Bujtás, Gy.: Acta Chim. Acad. Sci. Hung. (In the press).
2. Weawer, H. E., Tolbert, B. M., LaForce, R. C.: J. Chem. Phys. **23**, 1956 (1955).
3. Gmelins Handbuch der anorganische Chemie, Silicium Teil C, 8. Auflage, p. 260. Verlag Chemie, Weinheim, 1958.
4. Török, F., Gömöry, P.: Magyar Kém. Foly. **66**, 70 (1960).
5. Patnode, W. I., Wilcock, D. F.: J. Am. Chem. Soc. **68**, 358 (1946).
6. Lengyel, B., Prékopa, A., Török, F.: Z. Physik. Chem. (Leipzig) **206**, 161 (1965).

Pál Gömöry
László Szepes
Budapest VIII., Múzeum krt. 6—8.

Acta Chimica Academiae Scientiarum Hungaricae, Tomus 61 (4), pp. 417—421 (1969)

A NEW METHOD FOR THE PREPARATION OF AMINO ALCOHOLS FROM AMINO ACIDS

J. SZAMMER

(Central Research Institute for Chemistry of the Hungarian Academy of Sciences, Budapest)

Received September 21, 1968

The N-trityl derivatives of amino acid methyl esters are reduced to the corresponding N-tritylamino alcohols by $LiAlH_4$ in excellent yields. By this method, the N-trityl derivatives of glycine, DL-alanine and DL-serine were converted to the corresponding N-trityl amino alcohols in yields of 94, 92 and 95%, respectively. This procedure appears to be a new general method for the preparation of amino alcohols from amino acids.

The $LiAlH_4$ reduction of amino acids and their derivatives to amino alcohols has been the subject of many investigations [1—3]. However, starting with certain amino acids, the reduction gives amino alcohols in very low yield. According to the literature, the $LiAlH_4$ reduction of serine methyl ester gives serinol only in about 30% yield, and the preparation of ethanolamine affords similarly poor results [1a].

In this communication, some results obtained in the $LiAlH_4$ reduction of N-trityl amino acid methyl esters are reported. This appears to be a new general method for the preparation of amino alcohols from amino acids.

The procedure is shown in Fig. 1.

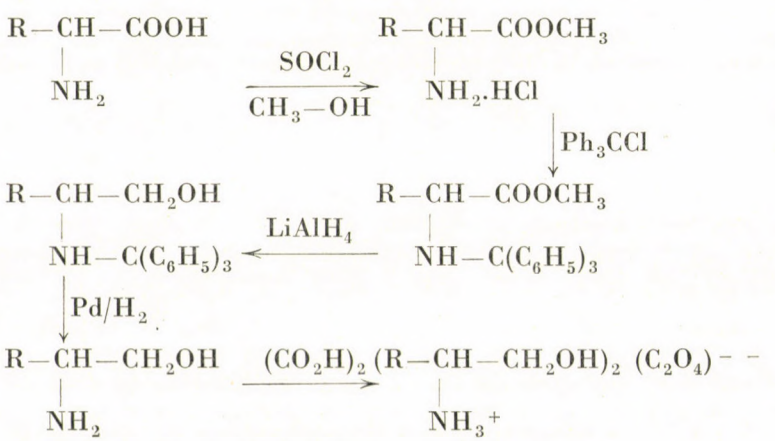

Fig. 1

The reaction steps shown in Fig. 1 can be carried out readily and in good yields (Table I). The overall yields of ethanolamine, alaninol, and serinol obtained from the corresponding amino acids are 73, 70 and 76, respectively. Presumably, similarly good results can also be obtained with other amino acids.

The method described above is especially preferable for the preparation of amino alcohols labelled with isotopes [4], all the more so, since a number of excellent procedures are known for the preparation of amino acids labelled isotopically in some position.

Table I

Yields and melting points of reaction products

Compound	m. p., C°	Yield,* %
Glycine methyl ester. HCl	176	92
N-tritylglycine methyl ester	106—7	88
N-tritylethanolamine	85—6	94
Ethanolamine oxalate	203	96
DL-alanine methyl ester · HCl	157	95
N-trityl-DL-alanine methyl ester	96	84
N-trityl-DL-alaninol	96—8	92
DL-alaninol oxalate	166	95
DL-serine methyl ester · HCl	168	98
N-trityl-DL-serine methyl ester	146	88
N-tritylserinol	132—3	95
Serinol oxalate	202—3	94

* The values refer to the steps indicated in Fig. 1

Experimental

N-trityl amino acid methyl ester

The amino acids were esterified with methanol in the presence of thionyl chloride [5], and treated with trityl chloride to obtain the N-trityl-esters [6].

N-trityl amino alcohol

The N-trityl amino acid methyl ester (0.028 mole) was added in small portions, with stirring, to a solution of 2.7 g of $LiAlH_4$ in 200 ml of ether at 0 °C. After stirring for 1 hr. at this temperature, the mixture was refluxed for 2 hrs. After adding 10 ml of methanol and 10 ml of water, the precipitate was filtered off, washed with ether and the ether solution dried over Na_2SO_4. The ether was evaporated and the residue washed with petroleum ether, and recrystallized from cyclohexane.

Amino alcohol oxalate

Hydrogenolysis of a solution of the N-trityl amino alcohol (0.05 mole) in abs. ethanol (200 ml) was effected in the presence of Pd-charcoal (10%; 0.8 g). After absorption of the theoretical amount of hydrogen, the catalyst was filtered off, the ethanol evaporated and an alcoholic ether solution of oxalic acid was added to the mixture. The crude oxalate is usually quite pure, but may be further purified by recrystallization from ethanol or ethanol-water.

REFERENCES

1. (*a*) KARRER, P., PORTMANN, P., SUTER, M.: Helv. Chim. Acta **31,** 1617 (1948).
   (*b*) KARRER, P., PORTMANN, P.: Helv. Chim. Acta **31,** 2088 (1948).
2. (*a*) VOGL, O., PÖHM, M.: Monatsh. **83,** 541 (1952).
   (*b*) VOGL, O., PÖHM, M.: Monatsh. **84,** 1097 (1953).
3. DORNOW, A., MESSWARB, G., and FREY, H. H.: Chem. Ber. **83,** 445 (1950).
4. ÖTVÖS, L., SZAMMER, J., NOSZKÓ, L.: Belgique Atom. Bulletin, 317 (1968).
5. GUTTMANN, ST., BOISSONAS, R. A.: Helv. Chim. Acta **41,** 1852 (1958).
6. CHILLEMI, F.: Gaz. Chim. Ital. **93,** 1079 (1963).

János SZAMMER Budapest II., Pusztaszeri út 57/69.

Acta Chimica Academiae Scientiarum Hungaricae, Tomus 61 (4), pp. 421—427 (1969)

QUARTERNÄRE BORORGANISCHE VERBINDUNGEN

P. NENNING und H. HOLZAPFEL

(Sektion Chemie der Karl-Marx-Universität Leipzig und Forschungsabteilung des VEB Laborchemie Apolda — DDR)

Eingegangen am 1. Oktober 1968

Es wurden quarternäre und bisquarternäre bororganische Verbindungen synthetisiert und ihre Alkalimetallsalzbildung sowie ihr Verhalten in wäßriger Lösung untersucht. Wir stellten fest, daß die Alkalimetallsalze zum Teil in Wasser sehr schwer löslich sind. Allerdings lassen sich einzelne Alkalimetallkationen nicht spezifisch ausfällen, so daß die hergestellten Verbindungen als analytische Reagenzien wahrscheinlich keine Zukunft haben.

Die hergestellten bororganischen Komplexe sind gegen hydrolytische Zersetzung beständig, wenn die Elektronegativitätsdifferenz zwischen Zentralatom und Liganden gering ist und im Liganden Mesomerie nicht möglich ist.

Die Synthese quarternärer bororganischer Verbindungen mit aromatischen Liganden gelang erstmalig G. WITTIG und Mitarbeitern [15, 17]. Seither sind eine große Anzahl Substanzen dieses Verbindungstyps dargestellt worden, die zum Teil wegen ihrer Fähigkeit zur Bildung schwerlöslicher Alkalimetallsalze das Interesse der Analytiker hervorriefen. Im Hinblick auf ihre Verwendbarkeit zur Alkalimetallbestimmung wurden das Natriumtetraphenylboranat [14], Natriumtriphenylcyanoboranat [3], Lithiumtetra-*p*-tolylboranat [10] und Kaliumtetra-2-phenylboranat [11] ausführlicher untersucht. Über die Haltbarkeit wäßriger Reagenzlösungen wird Unterschiedliches berichtet. Während Natriumtetraphenylboranatlösungen wochenlang ohne Veränderungen aufbewahrt werden können, trüben sich Lithiumtetra-*p*-tolylboranatlösungen bei Luftzutritt schon nach wenigen Stunden. Über die Ursachen dieses unterschiedlichen Verhaltens ist wenig bekannt.

Wir untersuchten bei quarternären bororganischen Verbindungen den Einfluß verschiedener Liganden auf die Löslichkeit der Alkalimetallsalze und die Resistenz der erhaltenen wäßrigen Lösungen gegen Hydrolyse.

Im Tetraphenylboranatanion sind die vier Bindungen zwischen dem Boratom und den Phenylgruppen gleichartig, da man annehmen kann, daß das Bor in seinen quarternären Komplexverbindungen sp^3-hybridisiert ist. Nach der PAULINGschen Elektronegativitätsskala [7] hat Bor die Elektronegativität 2,0. Eine Phenylgruppe hat die Gruppenelektronegativität 2,5 [12], so daß man nach der PAULINGschen Näherungsformel

$$\text{Ionencharakter} = 1 - e^{-\frac{1}{4}(x_A - x_B)^2}$$

x_A = Elektronegativität des Zentralatoms
x_B = Elektronegativität des Liganden

den Ionencharakter der Bindung zwischen dem Zentralatom Bor und jeder Phenylgruppe zu annähernd 6% berechnet.

Die vorwiegend kovalente Bindung gibt einem polaren hydrolysierenden Agenz keinen bevorzugten Angriffspunkt, so daß eine wäßrige Lösung eines Tetraphenylboranates bei Raumtemperatur recht hydrolyseresistent ist.

Substituiert man einen Liganden im quarternären Komplex, wird die Symmetrie der Elektronenverteilung um das Zentralatom gestört. Die Störung ist um so ausgeprägter, je mehr sich nunmehr die Elektronegativität des Liganden von der des Boratoms unterscheidet und je stärker Mesomerie im Liganden auftreten kann. Bei den von uns hergestellten Verbindungen Natriumtriphenyl-*p*-bromphenylboranat (**I**), Natriumtriphenyl-*p*-diphenylboranat (**II**) und Natriumtriphenyl-*p*-bromdiphenylboranat (**III**) läßt sich dieser Einfluß durch Messung der Hydrolysegeschwindigkeit in wäßriger Lösung verfolgen. Während die Bindung zwischen dem Zentralatom Bor und den drei Phenylgruppen im wesentlichen unbeeinflußt bleibt, ist die Bindung zum vierten Liganden stärker polar, so daß die hydrolytische Zersetzung des Komplexes an dieser Stelle seinen Ausgang nimmt. Die im vierten Liganden mögliche Mesomerie kann bei den Substanzen **I** bis **III** als die Hauptursache für die Unbeständigkeit der Verbindungen in wäßriger Lösung angesehen werden.

Um eine stabile quarternäre bororganische Verbindung zu erhalten, muß der vierte Ligand nicht unbedingt ein aromatischer Rest sein. Bekannt ist das Natriumtriphenylcyanoboranat (**IV**) als Reagenz auf Cäsium [3]. Unsere Messungen über einen längeren Zeitraum haben gezeigt, daß eine $10^{-2}\,M$ Lösung von **IV** weniger hydrolyseresistent ist als eine Lösung von Natriumtetraphenylboranat (**V**) gleicher Konzentration. Allerdings sind die Unterschiede nur gering. Wir führen das auf die Tatsache zurück, daß die Phenylgruppe und die Cyanidgruppe die gleiche Gruppenelektronegativität haben [12] und deshalb in ihrem Bindungsverhalten gegenüber dem Zentralatom keine wesentlichen Unterschiede zeigen. Der früher von anderer Seite [17] vorgeschlagenen Formulierung mesomerer Grenzformen innerhalb der Cyanidgruppe stimmen wir deshalb nicht zu, weil die dort postulierte Verschiebung der bindenden Elektronenpaare zwischen Zentralatom und Liganden zu einer starken Polarisierung der Bindungen und damit zu einer hydrolyseanfälligen Verbindung führen müßte. Natriumtriphenylcyanoboranat aber ist in wäßriger Lösung relativ beständig.

Aus den oben angegebenen Gründen ist es auch nicht gelungen, eine farbige quarternäre bororganische Verbindung herzustellen. Als Chromophore könnten nur ein oder mehrere Liganden wirken, die ein Resonanzsystem ausbilden können. Das bindende Elektronenpaar würde aber in die Resonanz

einbezogen, wodurch die Bindung Bor-Ligand so polar wird, daß der Komplex stark hydrolyseanfällig wird und für den Analytiker nicht mehr wertvoll ist.

In wäßriger Lösung hydrolysieren Natriumsalze quarternärer bororganischer Verbindungen zu Diarylborsäure bzw. Arylborsäure und Natronlauge, was sich in einer pH-Verschiebung zum alkalischen Milieu hin äußert. Die Zeitabhängigkeit der pH-Verschiebung ist ein Maß für die Hydrolyseanfälligkeit des quarternären Borkomplexes. Stellt man eine 10^{-2} *M* Lösung der Substanz **I** her und bringt sie auf pH = 6, verschiebt sich innerhalb von 8 Tagen der pH-Wert auf 6,6, im Falle der Verbindung **II** verschiebt er sich innerhalb von 3 Tagen bis zum Wert 7,5 und im Falle der Verbindung **III** innerhalb von 8 Tagen auf 7,7, um sich dann kaum noch zu erhöhen. In einer entsprechenden Natriumtetraphenylboranatlösung bleibt der pH-Wert über 14 Tage unverändert, ebenso bei Lösungen der Verbindungen **XI** und **XII** (siehe unten). Eine 10^{-2} *M* Lösung von **IV** verändert innerhalb dieses Zeitraumes den pH-Wert um 0,2 Einheiten.

Um quarternäre bororganische Verbindungen zu analytischen Zwecken einsetzen zu können, ist es wünschenswert, die Löslichkeit der Alkalimetallsalze in Wasser zu verringern. Die Löslichkeit wird offenbar beeinflußt durch den hydrophoben Charakter der Liganden, der unter anderem von ihrer Größe abhängt. Salze von quarternären bororganischen Verbindungen, die *p*-Diphenylgruppen bzw. Naphthylgruppen als Liganden enthalten, sollten im allgemeinen schwerer löslich sein als Salze von Tetraphenyl- oder Tetraalkylphenylboranaten. Andererseits ist bekannt, daß größere Liganden am Boratom sterische Hinderungen hervorrufen können, die von einem starken Anstieg der Löslichkeit der Alkalimetallsalze begleitet sind. So ist es aus räumlichen Gründen nicht möglich, das Tetra-*o*-diphenylboranat [16] oder das Tetra-*a*-naphthylboranat darzustellen. Es gelingt aber, Tri-*o*-diphenyl-phenylboranat (**VI**) [16] und Tri-*a*-naphthyl-phenylboranat (**VII**) [8] sowie Tri-*a*-naphthylcyanoboranat (**VIII**) [4] darzustellen. Alkalimetallsalze von **VI** sind generell löslich, während die entsprechenden Salze von **VII** und **VIII** sich zwar weniger gut lösen, aber immer noch besser als die Salze von **V**, was aufgrund der Größe der Liganden unerwartet ist. Sterische Gründe dürften für dieses Verhalten ebenso maßgebend sein, wie bei den von G. WITTIG und Mitarbeitern untersuchten *o*-und *m* Tetratolylboranaten [16].

Um unerwünschte sterische Effekte zu vermeiden, stellten wir das Tetra-*p*-diphenylboranat (**IX**) [9] und das Tri-*p*-diphenylcyanoboranat (**X**) her. In der Tat sind die Alkalimetallsalze dieser Verbindungen in Wasser sehr schwer löslich, doch ist an eine analytische Verwendung der Verbindungen als Reagenzien auf Alkalimetallkationen nicht zu denken, weil sie jegliche Selektivität vermissen lassen. Schon die Lithiumsalze sind in Wasser sehr wenig löslich. Untersuchungen der Hydrolyseresistenz der Komplexe waren aus diesem Grunde unmöglich.

Als zweiten Weg zur Verminderung der Löslichkeit der Alkalimetallsalze wählten wir die Synthese bisquarternärer bororganischer Verbindungen. Die Umsetzung von Triarylbor mit *p*-Dilithiumphenyl oder -diphenyl führte zu den Verbindungen

p-Phenylenbis-(triphenylboranat)	**(XI)**	
p-Diphenylenbis-(triphenylboranat)	**(XII)**	
p-Phenylenbis-(tri-*a*-naphthylboranat)	**(XIII)**	[13]
p-Diphenylenbis-(tri-*a*-naphthylboranat)	**(XIV)**	[13]

Die Lithiumsalze (und auch die Natriumsalze) sind in Wasser gut löslich. K^+, Rb^+ und Cs^+ lassen sich mit einer verdünnten Lithiumsalzlösung ausfällen. Die Wasserlöslichkeit der Kalium-, Rubidium- und Cäsiumsalze sinkt in der Reihenfolge der Verbindungen **XI—XII—XIII—XIV.** Das Cäsiumsalz von **XI** ist aber nur unwesentlich schwerer löslich als das Cäsiumtetraphenylboranat ($4{,}5 \cdot 10^{-5}$ Mol/l gegenüber $4{,}8 \cdot 10^{-5}$ Mol/l), während sich die Kaliumsalze von **XIV** und **V** immerhin um eine Zehnerpotenz in der Löslichkeit unterscheiden ($4 \cdot 10^{-5}$ Mol/l gegenüber $3{,}4 \cdot 10^{-4}$ Mol/l). Am Beispiel der Verbindung **XI** wurde festgestellt, daß bei pH = 6 außer K^+, Rb^+, Cs^+ noch NH_4^+, Ag^+ und Cu^{++} (unter teilweiser Zersetzung des Komplexes) Niederschläge geben, während Mg^{++}, Ca^{++}, Sr^{++}, Ba^{++}, Co^{++}, Ni^{++}, Al^{+++}, Zn^{++}, Cd^{++}, Pb^{++}, Mn^{++}, Bi^{+++}, $(UO_2)^{++}$ keine schwerlöslichen Salze bilden. Starke Oxidationsmittel, konzentrierte Säuren und Laugen zersetzen den Komplex, Verbindung **XI** gibt z. B. mit conc. Ammoniak Bortriphenylammoniakat.

Die angegebenen Werte der Löslichkeit haben wir durch Leitfähigkeitsmessungen in gesättigten wäßrigen Lösungen bestimmt. Dabei erhielten wir für die Ionenbeweglichkeit des Anions von **XI** den Wert 15 $cm^2/Ohm \cdot val$.

Die Tatsache, daß die Kalium-, Rubidium- und Cäsiumsalze des *p*-Diphenylenbis-(triphenylboranat)-anions, das man sich formal aus zwei Tetraphenylboranatanionen aufgebaut denken kann, nicht wesentlich schwerer löslich sind als die entsprechenden Tetraphenylboranate, zeigt, daß auch die bisquarternären bororganischen Verbindungen als analytische Reagenzien gegenüber dem Natriumtetraphenylboranat keine Vorteile bieten. Wir stellten fest, daß bei der Fällung des Cäsiumsalzes von **XI** in saurer Lösung (pH = 3) keine Hydrogensalze entstehen, ebensowenig haben wir die Existenz gemischter Natrium-Cäsiumsalze nachweisen können. Das Verhältnis Alkalimetallkation : komplexem Anion ist stets 2 : 1, wobei die beiden Kationen identisch sind.

Wir müssen also feststellen, daß Vergrößerung der Liganden bei Tetraphenylboranatverbindungen zu einer unspezifischen, alle Alkalimetallkationen umfassenden Löslichkeitsverminderung führt. Bisquarternäre bororganische

Verbindungen sind in ihrem Löslichkeitsverhalten den Tetraarylboranaten ähnlich. Die Erfassungsgrenze für große Alkalimetallkationen liegt im Falle bisquarternärer bororganischer Verbindungen allerdings — durch die Zusammensetzung des Komplexes bedingt — ungünstiger.

Die Konstitution der erhaltenen Verbindungen wurde durch Elementaranalyse, flammenfotometrische Alkalimetallbestimmung, Sublimatabbau [1], Molekulargewichtsbestimmung und IR-Spektren sichergestellt.

Bei dem Vergleich der IR-Spektren von 25 quarternären bororganischen Verbindungen stellten wir fest, daß mit geringen Abweichungen stets die Banden bei 1260 cm^{-1} und 860 cm^{-1} auftreten, die von C. RICHTER [9] einer Bor–Kohlenstoff-Bindung zugeordnet werden. Die Banden treten nur auf, wenn mindestens 3 aromatische Liganden im Komplex vorhanden sind.

Experimenteller Teil

1. Darstellung der Verbindungen I bis III

Zu einer Lösung von *p*-Bromphenyl-, *p*-Diphenyl- bzw. *p*-Bromdiphenylmagnesiumbromid in Äther oder Tetrahydrofuran (THF) fügt man unter strengem Luftausschluß (Schutzgas Argon) die berechnete Menge Bortriphenyl [6] in Äther. Nach Abflauen der stürmischen Reaktion erwärmt man noch 2 Stunden am Rückfluß. Der GILMAN-Test [2] ist jetzt negativ. Die abgekühlte Reaktionsmischung gibt man in eiskalte Sodalösung, dabei scheidet sich $MgCO_3$ ab. Die organische Phase wird im Scheidetrichter abgetrennt, die wäßrige Phase dreimal mit Äther extrahiert. Die Extrakte werden mit Soda sicc. getrocknet, im Vakuum unter Ar eingeengt, Benzol wird zugefügt und der letzte Äther abdestilliert. Das ausfallende mikrokristalline Pulver wird über einen Filtertiegel G 4 abfiltriert, mit Benzol gewaschen und im Vakuum getrocknet. Zur weiteren Reinigung wird die Substanz in Äther gelöst, die Lösung wird filtriert und erneut mit Benzol eingedampft. Ausbeuten ca. 30% Th.

Darstellung der Verbindung X

Zu einer Lösung von *p*-Diphenylmagnesiumbromid, erhalten aus 4 g Mg und 38 g *p*-Bromdiphenyl, in THF fügt man tropfenweise 8 g BF_3-ätherat. Nach Abflauen der Reaktion kocht man 2 Stunden am Rückfluß, destilliert die größte Menge THF ab und extrahiert den Rückstand mit Benzol. Die Extrakte werden vereinigt, 100 ml Tetralin und 20 g NaCN zugefügt, auf dem Luftbad das Benzol größtenteils abdestilliert und 30 Minuten bei 110 °C gehalten. Man läßt abkühlen, filtriert vom Tetralin ab, löst den Niederschlag in einer Wasser—Aceton-Mischung, filtriert und fällt die bororganischen Komplexverbindungen mit K^+, Rb^+ oder Cs^+ aus. Der farblose Niederschlag wird abfiltriert und über P_2O_5 getrocknet.

Darstellung der Verbindungen XI und XII

Zu einer Suspension von Dilithiumphenyl (**XV**) bzw. Dilithiumdiphenyl (**XVI**) in Petroläther tropft man in der Kälte eine Lösung von Bortriphenyl in Äther. Die Reaktion geht unter schwacher Wärmetönung vor sich und ein kristalliner Niederschlag fällt aus. Das Lösungsmittel wird dekantiert, der Niederschlag wird mit Petroläther und dann mit Benzol gewaschen. Er wird in Aceton gelöst, die Lösung wird filtriert und nach Benzolzusatz im Vakuum eingeengt. Man erhält die reine Verbindung in ca. 25%iger Ausbeute.

Darstellung der Verbindungen XIII und XIV

Zu einer Suspension von **XV** bzw. **XVI** in Petroläther (30—50 °C) tropft man die in Petroläther gelöste berechnete Menge Tri-*a*-naphthylbor zu. Als Schutzgas findet wie stets Ar Verwendung. Man kocht 30 Stunden am Rückfluß, engt die Lösung ein, filtriert ab und löst den Niederschlag in Wasser. Man neutralisiert sofort mit Essigsäure und fällt die Kalium-, Rubidium-, Cäsium- und Ammoniumsalze aus.

Messung der Hydrolysegeschwindigkeit

In 10^{-2} *M* Lösungen der entsprechenden Natriumsalze werden bei 20 °C aller 24 Stunden mit einer Glaselektrode die pH-Werte gemessen. Als Anzeigegerät dient das pH-Meßgerät MV 11 S der Fa. Clamann und Grahnert, Dresden.

Messung der Ionenbeweglichkeit von XI

Eine besonders gereinigte Probe von **XI** wird eingewogen (60.63 mg) und mit Leitfähigkeitswasser auf 100 ml aufgefüllt. Wir stellten eine Verdünnungsreihe her und haben die Leitfähigkeit mit dem Leitfähigkeitsmeßgerät der Fa. Radelkis gemessen.

c	4/3 k(')	Λ_c
$1 \cdot 10^{-4}$	$2{,}4 \cdot 10^{-5}$	90
$2 \cdot 10^{-4}$	$4{,}1 \cdot 10^{-5}$	77
$3 \cdot 10^{-4}$	$6{,}0 \cdot 10^{-5}$	75
$4 \cdot 10^{-4}$	$6{,}9 \cdot 10^{-5}$	65
$5 \cdot 10^{-4}$	$8{,}1 \cdot 10^{-5}$	61

(') 4/3 ist die Gefäßkonstante.

Durch graphische Extrapolation ergibt sich eine Ionenbeweglichkeit von 15 $cm^2/Ohm \cdot val$.

Bestimmung der Schmelzpunkte

Die Schmelzpunkte haben wir auf einem Mikroheiztisch nach BOETIUS bestimmt.

Verbindung	Na-salz	K-salz	Rb-salz	Cs-salz
	°C	°C	°C	°C
I	440	490	410	440
II	400	440	410	420
III	315	300	360	340
VII	178*	—	340	360
VIII	265	280	—	—
X	—	220	240	270
XI	450	470	430	390
XII	—	450	490	470

* Lithiumsalz

Die Substanzen schmelzen nach Braunfärbung unter Zersetzung. Die Angabe de Schmelzpunkte ist deshalb notwendigerweise mit einem größeren Fehler als normal behaftet

Die Infrarotspektren

Die IR-Spektren wurden an einem UR 10 der Fa. Carl Zeiß aufgenommen (KBr-Tablette).

I: 3060 m, 3005 w, 2985 w,2880 w, 1610 w, 1580 w, 1480 m, 1430 m, 1260 w, 1185 w, 1155 w, 1070 w, 1050 w, 1035 w, 1010 w, 860 w, 815 w, 750 s, 720 ss, 622 w, 607 m.
II: 3065 s, 3010 s, 2995 m, 2975 m, 1610 m, 1590 m, 1490 ss, 1435 s, 1395 w, 1260 w, 1190 w, 1160 m, 1075 w, 1035 w, 1010 w, 870 w, 860 w, 825 s, 760 ss, 750 ss, 730 ss, 720 ss, 700 ss, 663 w, 627 m, 620 m, 610 s, 500 w, 490 m.
III: 3065 m, 3005 m, 1585 w, 1485 ss, 1435 m, 1380 w, 1270 w, 1190 w, 1165 m, 1080 w, 1035 w, 1010 m, 860 w, 815 ss, 765 ss, 745 ss, 725 ss, 715 ss, 610 m.
X: 3060 w, 3025 m, 2175 m, 1600 m, 1485 ss, 1450 w, 1390 w, 1255 w, 1160 w, 1115 w, 1080 w, 1010 m, 895 w, 830 s, 770 ss, 750 s, 705 s, 560 w, 510 w.
XI: 3065 s, 3000 s, 2975 s, 1620 m, 1590 m, 1570 w, 1485 ss, 1435 s, 1315 w, 1265 m, 1190 s, 1180 m, 1160 s, 1130 w, 1075 m, 1035 m, 1010 w, 1000 w, 875 m, 860 s, 815 m, 750 ss, 720 ss, 630 s, 620 s, 610 ss, 490 m, 470 m.
XII: 3065 ss, 3050 s, 3010 s, 2995 s, 1625 w, 1590 m, 1490 ss, 1440 s, 1390 w, 1275 m, 1190 m, 1165 s, 1075 m, 1040 m, 1015 m, 865 m, 855 m, 820 s, 770 s, 750 ss, 720 ss, 685 s, 620 s, 610 s, 500 m, 475 m, 465 m.

REFERENCES

1. Flaschka, H., Amin, A. M., Holasek, A.: Z. anal. Chem. **138**, 241 (1953).
2. Gilman, H.: J. Amer. Chem. Soc. **47**, 2002 (1925).
3. Havir, J.: Collect. czecholov. chem. Commun. **26**, 1775 (1961).
4. Holzapfel, H., Nenning, P., Döpel, P.: Z. Chem. **5**, 315 (1965).
5. Krause, E., Nitsche, P.: Ber. dtsch. chem. Ges. **54**, 2784 (1921).
6. Krause, E., Nitsche, P.: Ber. dtsch. chem. Ges. **55**, 1261 (1922).
7. Pauling, L.: Die Natur der chemischen Bindung. Verlag Chemie, Weinheim, 1964.
8. Rasuwajew, G. A., Brilkina, T. G.: Ber. Akad. Wiss. UdSSR **91**, 861 (1953).
9. Richter, C.: Dissertation. Leipzig, 1962.
10. Sasonowa, W. A., Leonow, W. W.: J. anal. Chemie (russ.) **14**, 483 (1959).
11. Sasonowa, W. A.: Ber. Akad. Wiss. UdSSR 1295 (1957).
12. Staab, H. A.: Einführung in die theoretische organische Chemie. Verlag Chemie, Weinheim, 1962.
13. Stirn, H.: Diplomarbeit. Leipzig, 1966.
14. Tollert, H.: Analytik des Kaliums. Enke Verlag, Stuttgart, 1962.
15. Wittig, G.: Naturwissenschaften **34**, 216 (1947).
16. Wittig, G., Herwig, W.: Chem. Ber. **88**, 962 (1955).
17. Wittig, G., Raff, P.: Liebigs Ann. Chemie **573**, 195 (1950).

Peter Nenning
Heinz Holzapfel
701 Leipzig, Liebigstr. 18. DDR.

K. KÜHNE: *Glas, seine Herstellung und Anwendung.* Theodor Steinkopff, Dresden 1968. 98 Seiten, 26 Abb. 62 Qu.

Die theoretischen und praktischen Kenntnisse der einzelnen Industriezweige sind in den mittlerweile erschienenen Handbüchern ausführlich zusammengefaßt. Über Entwicklungen während und seit ihrer Erscheinung berichten jedoch nur Fachzeitschriften, deren Studium viel Zeit und Mühe beansprucht. Die einzelnen Bände der Technischen Fortschrittsberichte wollen über diese Schwierigkeit hinweg helfen. Die im vorigen Jahr erschienene Monographie der Serie befaßt sich mit Glas.

Der erste Abschnitt des Buches schildert die geschichtliche Entwicklung des Glases, unter Betonung der beiden sprunghaften Wendepunkte, namentlich: die Entdeckung der Pfeife und die Tätigkeit von SCHOTT.

Der zweite Abschnitt befaßt sich mit der Chemie und Physik des Glases. Die Begründungen des Verfassers, warum die Glas- und keramische Industrie in der Entwicklung hinter der Metallurgie zurückblieb, sind beachtenswert. Die letztere diente nämlich zur Erzeugung von Waffen und Kriegsausrüstungen, worauf großes Gewicht gelegt wurde. Sodann werden die gegenwärtig bekannten Glassorten auf Grund ihrer Verwendung in Gruppen aufgeteilt, und die chemischen und physikalischen Eigenschaften des Glases beschrieben.

In dem den glasartigen Zustand behandelnden Abschnitt faßt der Verfasser die von ZACCHARIASEN, LEBEDEW, VOGEL und WEYL ausgearbeiteten Theorien zusammen, um dann auf deren Grundlage eine neue Definition aufzustellen. Anschließend werden die Zusammenhänge zwischen den in die Gläser eingebauten Ionen und den Glaseigenschaften besprochen.

Der nächste Abschnitt beschreibt besondere Glassysteme, die durch nachträgliche Behandlung zu neuen Produkten führten, wie z. B. die Vycor-, Chemcor-, Photoform- und Photoceram-Gläser und das Laser.

In dem Abschnitt über Glasschmelzen wird die Entwicklung der Schmelzöfen beschrieben, und jene Eigenschaften festgelegt, über die ein Schmelzofen verfügen muß, um wirtschaftlich eine homogene Schmelze zu liefern. Sodann wird die Bearbeitung der Schmelze mittels Blasen, Ziehen, Pressen und Walzen diskutiert, und abschließend die Erzeugungstechnologien von Quarzglas beschrieben.

Der wertvollste Abschnitt der Monographie behandelt die in der Zukunft zu erwartende Entwicklung der Glaserzeugung und -verwendung. Diese Entwicklung hängt natürlich mit jener der Glas verwendenden Industrien zusammen, wo die Forderungen stets größer werden. Das Glas wird bei mancher Verwendung durch die konkurrierenden Produkte, durch Kunststoffe ersetzt, doch wird das Glas in der Bau-, Verpackungs- und optischen Industrie seine Hegemonie bewahren. Gläser für Laboratoriums- und Industriegeräte, sowie vakuumtechnische Gläser stehen auch vor einer großen Entwicklung. Eine allgemeine Verbreitung der Nicht-Silikatgläser, so z. B. der glasartigen Metallkarbide und Metallnitride, die bereits jetzt für Spezialzwecke eingesetzt werden, ist in der Zukunft zu erwarten. Es ist ferner zu erwarten, daß Gläser und polymere Kunstharze kombiniert werden, um damit die Nachteile einerseits der organischen, andererseits der anorganischen glasartigen Produkte zu kompensieren. Auch die Hochdruck- und Vakuumschmelzen werden zu neuen Technologien und wertvolleren Gläser führen. Obzwar Voraussagungen stets Unsicherheiten in sich bergen, steht ohne Zweifel fest, daß die Resultate auf dem Gebiet der Glasforschung zu vielen neuen Produkten und Anwendungsmöglichkeiten führen werden.

Die Monographie behandelt das Thema logisch und konsequent. Das Buch bezweckt weder die theoretische noch die praktische Beschreibung des Glases, was ja in Handbüchern eingehend beschrieben wird. Es sollen vielmehr die mit dem Glaszustand zusammenhängenden theoretischen Fragen, Verfahrenstechnologien und Anwendungsmöglichkeiten besprochen

werden, indem eine zusammenfassende Übersicht jener Verwendungen gegeben wird, für welche sich das Glas eignet.

Dieser Zielsetzung wird in vollem Maße Genüge geleistet. Der Autor bereicherte die Fachliteratur des Glases mit einer Monographie, die sowohl den Fachleuten als auch den sich für Glas interessierenden, auf anderen Gebieten der Technik tätigen Lesern wertvolle und Lehrreiche Kenntnisse vermittelt.

O. KNAPP

W. A. BINGEL: *Theorie der Molekülspektren* (Theory of molecular spectra) Verlag-Chemie 1967. Chemische Taschenbücher 2. pp. 206, 67 figures, 21 tables.

W. A. BINGEL is professor of chemistry at the University of Göttingen. His name became known among those working in the field of quantum chemistry by his complex theory of atoms. His present handbook discusses over about 200 pages the fundamental problems of molecular spectroscopy, its recent developments and tendencies.

The book discusses diatomic and simple polyatomic molecules. The spectra of several of these types of molecules can be recorded also in the gaseous state, so that the study of all the fine details exhibited by the spectra, rotational structure included, as well as that of underlying phenomena becomes possible.

The book is concerned to an equal extent with the experimental and theoretical aspects of the subject, however, at a level, which is easily understood by research workers of up-to-date education, interested in physical chemistry and chemistry.

Thus, though the discussion of the results of wave mechanics begins with the fundamental principles, the reader is led by very simple means to group theoretical interpretation and classification. Emphasis is laid on the problems of electronic spectra and electronic states, but also rotational and vibrational spectra are considered. The problem of the intensities in the vibrational structure of electronic transitions, the assignation of electronic states on the basis of quantum numbers, fundamental principles in the calculation of potential energy and potential surfaces are dealt with extensively.

Particular mention should be made of the part devoted to the interpretation of the spectra of molecules with lower number of atoms, in which chemical reactions are dealt with including "short life" intermediates.

In the general part, the classification and the frequency range of the spectra, further the pure rotational and rotational-vibrational spectra are discussed. The problems of potential energy functions are elucidated precisely and with the briefness of definitions with the aid of electronic transitions, and those of relative intensities with the aid of the selection rules.

The last three chapters of the book discuss the relationships of molecular spectroscopy and theoretical quantum chemistry in connection with the systemization of the electronic transitions of di- and triatomic molecules.

In summary, the book of Professor BINGEL gives a very good survey of the theoretical problems and relationships of structural investigation and molecular spectroscopy.

S. SZŐKE

L. A. PAQUETTE: *Principles of Modern Heterocyclic Chemistry*. W. A. Benjamin, Inc., New York—Amsterdam, 1968. 401 + X pp.

This is the most recent Volume of the well known Organic Chemistry Monograph Series edited by Professor Ronald BRESLOW. The goal of the Series is to furnish teachers and, of course, students of organic chemistry with relatively short monographs of intermediate level, to be used as supplements of the current texts.

If there is any topic which generally becomes somewhat short in courses of organic chemistry and which, therefore, absolutely needs to be supplemented by a monograph of the kind outlined above, this is the topic of Heterocyclic Chemistry. The task of writing such a

highly needed intermediate level textbook of heterocyclic chemistry was undertaken, in the United States, by Professor PAQUETTE of Ohio State University, whose name and contributions to this field of organic chemistry are well known.

In the opinion of the reviewer, the task has been brilliantly performed by the author. The book is equally modern in the selection of the topics, the way of their treatment, and in the arrangement of the subject-matter. For instance, ring systems of the same size and containing the same number of hetero atoms have, in contrast to the usual practice of earlier texts, not been treated as separate groups according to the kind of the hetero atom (or atoms), but as related sub-groups of the same group. This procedure, of course, yields deeper insight into, and better understanding of, heterocyclic chemistry. Accordingly, for instance, Chapter 1 deals with the chemistry of three-membered rings with one hetero atom irrespective whether this is oxygen, sulfur or nitrogen; three-membered rings with two hetero atoms are similarly treated in Chapter 2; furan, thiophene and pyrrole are jointly discussed in Chapter 4, etc. The subject matter of the individual chapters has been arranged throughout the book mostly into three sections: synthesis, reactions, and problems. In discussing the first two topics, effort has been made to call special attention to analogies between ring systems differing only in the kind of the hetero atom, and to general synthetic approaches and reactions. Some of the problems are quite difficult to solve and often require more than the knowledge of the text material, namely that of the pertinent literature. In order to facilitate checking of the correctness of the solutions worked out by the reader, or to help in obtaining the solutions of the more difficult problems, references to the literature are added to each problem. This seems to the reviewer an excellent and original idea. It is a further advantage that the presented exercise problems are based on the most recent literature.

On the other hand, great emphasis is laid, in harmony with modern practice, throughout the whole book upon presenting mechanistic, stereochemical and, if necessary, stereoelectronic details of the reactions treated.

The titles of the individual chapters (not yet mentioned) are as follows: Four-membered heterocycles; Condensed five-membered heterocycles; The azoles; The pyridine group; Quinoline and isoquinoline; The diazines and *s*-triazine; Further principles of heterocyclic synthesis; Some heterocycles of biological interest; and, finally, a short Appendix on the nomenclature of heterocyclic compounds.

As it may be seen from the above enumeration, the choice of the material presented is somewhat arbitrary; for instance, pyrane and its many naturally occurring important derivatives are not included and, among the azines, only the chemistry of the diazines and *s*-triazine is briefly reviewed. The greatest part of medium ring systems has also been omitted (although the author himself has made many important contributions to this branch of heterocyclic chemistry) and the same applies to partially or completely saturated, *i.e.* non-aromatic, derivatives of five- and six-membered heterocyclic compounds. It is, however, clear that the whole topic of heterocyclic chemistry cannot be presented in a volume of the present size, therefore, omissions even of important topics are unavoidable; in this respect, free choice has to be granted to the author.

The reader may find compensation for the omissions mentioned by two truly excellent chapters: the first, dealing with three-membered rings with one hetero atom (62 pages — this is 15%, and a total of as high as 25% of the space available has been devoted to the chemistry of small ring heterocycles, reflecting the growing importance of these compounds), and the tenth, presenting "Further principles of heterocyclic synthesis", which is — to the knowledge of the reviewer — almost quite unprecedented with regard to its point of view and style. Sections of the latter chapter are: Cycloaddition reactions; Valence-bond isomerizations; Enamine condensations — all dealing with modern topics currently under active investigation —; and, again, Problems with references.

The printing of the book is very good; the formulas are clear, misprints and errors were not found.

Summing up, it is the opinion of the reviewer that "Principles of modern heterocyclic chemistry" is a very well written short textbook of intermediate level, which may be recommended not only to students of chemistry but also for more advanced chemists.

K. LEMPERT

Advances in Macromolecular Chemistry, Vol. I. Edited by W. M. Pasika, Academic Press, London and New York 1968. XXVII sheets, 432, pp., 89 figures, 37 tables

The Academic Press Publishers and Mr. W. M. PASIKA can be only congratulated for their decision to start a new macromolecular chemical series, the aim of which — as indicated by its foreword — is to be a medium for delineating the frontiers of macromolecular research and to provide informative reviews on the more established aspects of the macromolecular science.

The first volume of the series, published recently, deals with the following subjects:
ferrocene polymers,
popcorn, polymerization,
electron acceptors as initiators of charge-transfer polymerization,
non-newtonian viscosity and the macromolecule,
solid-state polymerization,
polysulphones: organic and physical chemistry.

Owing to its content the first volume will undoubtedly win high acclaim among the macromolecular chemists, because each chapter is closely related to specific subjects originating or rapidly developing during the past few years. For readers in Hungary, it is of particular interest that the work of Prof. G. HARDY and co-workers is extensively referred to in the part of solid-state polymerization.

The contributors of the first volume of this series are researchers of international repute who have made considerable contributions to the literature in the field they are reviewing.

The work is of great interest for both specialists and non-specialists in this field enabling them to apply concepts and advancement in related branches of polymer science to their own fields without spending precious time and energy on compiling data from literature.

I. GÉCZY

H. DALLMANN, K. H. ELSTER: *Einführung in die höhere Mathematik für Naturwissenschaftler und Ingenieure*, Band I. VEB Gustav Fischer Verlag. 718 Seiten

Das Studium von Naturwissenschaften an Universitäten und Hochschulen beansprucht heutzutage beträchtliche mathematische Kenntnisse. Um den Ansprüchen von Physikern und Studenten von technischen Hochschulen nachzukommen, sind schon bisher in der ganzen Welt zahlreiche Lehrbücher der höheren Mathematik erschienen. Diese Bücher behandeln in verschiedenem Umfang und mit verschiedenen Methoden die zum Studium von Naturwissenschaften und des Ingenieurswesens benötigten mathematischen Kenntnisse, mit Beispielen und unter verschiedenartiger Anordnung des behandelten Materials. Doch werden oft die strengeren mathematischen Beweisführungen und solche Teile, die genauere und exaktere Gedankengänge enthalten — so daß sie auch die Aufmerksamkeit und die Abstrahierfähigkeit des Lesers beanspruchen —, von Lesern, die angewandte Mathematik beanspruchen, einfach überblättert. Viele Lehrbücher lassen deshalb diese Teile einfach weg und verweisen auf die die besonderen mathematischen Kenntnisse liefernde Literatur, oder man druckt solche Teile in Minuskelschrift, mit der Bemerkung, daß sie für anspruchvollere Leser gedacht sind. Die jähe Entwicklung der Naturwissenschaften und der Technik in den vergangenen Jahren erhöhte auch die mathematischen Anforderungen, und zwar nicht nur in bezug auf Umfang, sondern auch hinsichtlich Präzisität und Exaktheit. Eben deshalb ist die Herausgabe eines Lehrbuches der höheren Mathematik, welches vor allem die Bedürfnisse von zukünftigen Naturwissenschaftlern und Ingenieuren sowie der wissenschaftlichen Forscher in der Industrie vor Augen hält, und dabei den Anforderungen der strengen Mathematik genügt, wünschenswert. Daher wird das Erscheinen des I. Bandes dieses Lehrbuchs der höheren Mathematik mit größter Freude begrüßt, und wir hoffen, daß auch der zweite Band erscheinen wird.

Im wesentlichen behandelt das Buch die Differential- und Integralrechnung von reellen Funktionen mit einer Veränderlichen, mit einer entsprechenden Einleitung und Anwendungsbeispielen. Wer nun dieses Buch in die Hand nimmt, wird sofort sehen, daß es auch den Ansprüchen von Studenten mit rein mathematischem Interesse von »theoretischer mathematischer Einstellung« auf einer Anfangsstufe Genüge leistet. Die Behandlungsweise des Buches ist nämlich vollkommen exakt, und es umfaßt als Grundlage das System der reellen und komplexen Zahlen, die elementaren Kennwerte von Zahlen- und Punktmengen sowie die eingehende

Beschreibung der Zahlenfolgen. Das gute Verständnis des Buches wird durch die klaren Abbildungen und durch die aus den Naturwissenschaften genommenen sehr gut gewählten Beispiele erleichtert. In der Diskussion der konvergenten Zahlenfolgen ist z. B. das Linienspektrumsystem des Wasserstoffatoms angeführt, wodurch ein anschauliches Bild über den Begriff des Häufungswertes vermittelt wird. In Verbindung mit den Zahlenreihen wird auch der Begriff des oberen und unteren Limes erörtert, und bei der Diskussion der reellen Zahlen wird z. B. bewiesen, daß die Menge der reellen Zahlen unabzählbar ist. In Verbindung mit der Diskussion der Häufungswerte wird z. B. der berühmte Überdeckungssatz von BOREL, welcher bei Beweisführungen der reellen Funktionslehre oft verwendet wird, erörtert. Die Behandlung des Funktionsbegriffes ist auch sehr eingehend und gründlich, und wird außer einer modernen und exakten Begriffserklärung durch zahlreiche Beispiele aus den Naturwissenschaften sowie durch Abbildungen demonstriert. Die Veranschaulichung ist eine Stärke des Buches; dies erleichtert jedenfalls das Verständnis und die Aneignung der Begriffe der höheren Mathematik. Es liegt an der Natur des Buches, daß bei der Erörterung der einzelnen Begriffe auch auf deren praktische Anwendung großes Gewicht gelegt wird. So kann man z. B. bei der Behandlung der kontinuierlichen Funktionen das zur annähernden Lösung der Gleichungen dienende »regula falsi« Verfahren, und im Abschnitt über rationelle Funktionen die Interpolationsformeln von Lagrange und Newton finden, und der Darlegung der Formel zur Lösung der Gleichungen dritten Grades folgt eine eingehende Diskussion der zur annähernden Lösung der algebraischen Gleichungen dienenden Verfahren. Nach der anschaulichen und erschöpfenden Behandlung der exponentiellen und logarithmischen Funktionen findet man die trigonometrischen und arcus Funktionen, die mit zahlreichen, aus der Schwingungslehre genommenen praktischen Beispiele illustriert werden. Diese Beispiele erleichtern wesentlich die Aneignung dieses Wissensgebietes, und fördern außerdem die Erkenntnis der praktischen Verwendbarkeit. Die Differentialrechnung umfaßt das für Bücher dieser Art übliche Gebiet; ein Fortschritt gegenüber den bisheringen Lehrbüchern ist die Illustration der numerischen Anwendungen an Hand von zahlreichen Beispielen, die eingehende Diskussion der graphischen Methoden sowie zahlreiche Abbildungen zur Veranschaulichung. Bei der Anführung der einzelnen Teile wurden die entsprechendsten physikalischen und chemischen Probleme, die das Verständnis des gegebenen mathematischen Materials erleichtern, mit glücklicher Hand gewählt.

Die Integralrechnung beginnt in der üblichen We se, mit dem Begriff des bestimmten Integrals und dessen Analyse, wobei aus jedem Gebiet deriMechanik und Physik viele Beispiele gegeben werden, so daß der Leser ein klares Bild über die Bedeutung des bestimmten Integrals in den verschiedensten Gebieten der Naturwissenschafte n erhält. Das unbestimmte Integral wird auch sehr eingehend behandelt, und die Technik de r Integralrechung wird an Hand von zahlreichen Beispielen gezeigt. Dieser Teil schließt mit einigen geometrischen Anwendungen, graphischer und numerischer Integrierung und mit der Beschreibung einfacher, zur Integrierung verwendeter Geräte.

Der Differential- und Integralrechnung folgt der Abschnitt über die unendlichen Reihen. Nach den exakten Begriffseinleitungen werden die bekannten Konvergenzkriterien der positiven Reihen sowie Berechungen von Reihen mit beliebiger Gliederzahl behandelt. Bei der Diskussion der Funktionsreihen wird der Begriff der gleichmäßigen Konvergenz mit großer Sorgfalt erörtert, und ihr Verständnis durch Heranziehung von Abbildungen erleichtert. Auch die eingehende Erörterung der Anwendung der Potenzreihen ist mustergültig.

Das Buch gibt eine ziemlich genaue Diskussion der bei der Beschreibung der periodischen Vorgänge eine wichtige Rolle spielenden trigonometrischen Fourier-Reihen, wobei dieser Abschnitt durch eine kurze Übersicht der orthogonalen Funktionssysteme ergänzt wird.

Zum Unterschied von der üblichen Anordnungsweise, werden Vektoralgebra und Determinanten zum Schluß behandelt. Dieser interessante Abschnitt endet mit zahlreichen praktischen Beispielen und der Beschreibung von Kurven und Oberflächen zweiten Grades.

Zusammenfassend kann festgestellt werden, daß das neue Lehrbuch der Professoren DALLMANN und ELSTER ein wertvoller Gewinn der mathematischen Lehrbuchliteratur von einführendem Charakter ist. Nicht nur das große Gebiet des behandelten Themenkreises, sondern auch die relative Anordnung der einzelnen Teile sowie die Art ihrer Diskussion bringen viel Interessantes und Neues für den Leser, wobei die Behandlung der Themen durch viele treffende praktische Beispiele und Anwendungen illustriert und verständlich gemacht wird. Eben deshalb wird das Buch für jeden sich mit Naturwissenschaften beschäftigenden Universitätsstudenten, aber auch für Hochschullehrer von großem Nutzen sein. Die an dem Unterricht Beteiligten werden in dem Buch viele geschickte pädagogische Gesichtspunkte und Ideen finden, die ihnen zur Verbesserung ihrer bisherigen Vorlesungen verhelfen werden. Das oben Gesagte macht es verständlich, daß wir dem Erscheinen des zweiten Bandes mit großer Erwartung entgegensehen.

D. KRÁLIK

INDEX

INORGANIC AND ANALYTICAL CHEMISTRY — ANORGANISCHE UND ANALYTISCHE CHEMIE — НЕОРГАНИЧЕСКАЯ И АНАЛИТИЧЕСКАЯ ХИМИЯ

HANNA, Z. G., KÁNTOR, T. and ERDEY, L.: Distribution of Arc Temperature Using Cathode Excitation 329

GÖRÖG, S.: Analysis of Steroids, IX. Spectrophotometric Investigation of Oestra-5(10)-en--3,17-dione and its 3,3-dimethyl Ketal 341

PHYSICAL CHEMISTRY — PHYSIKALISCHE CHEMIE — ФИЗИЧЕСКАЯ ХИМИЯ

KAPOSI, O. and RIEDEL, M.: Experimental Study of Positive Ion Emission From Tungsten, I 349

TÉTÉNYI, P., BABERNICS, L. and SCHÄCHTER, K.: Kinetic Study of Hydrocarbon Adsorption on Nickel Catalyst 367

LADIK, J., BICZÓ, G., KENDE, L. and SÜMEGI, L.: Application of the Semiempirical Different Orbitals for Different Spins SCF LCAO MO Method for the Calculation of Spin Densities of Some Phenyl Nitroxide Radicals 381

PAÁL, É. and VARSÁNYI, GY.: Calculation of Infrared Band Contours of Planar Asymmetric Top Molecules, I. Construction of General Relationships 391

ORGANIC CHEMISTRY — ORGANISCHE CHEMIE — ОРГАНИЧЕСКАЯ ХИМИЯ

GÖMÖRY, P. and SZEPES, L.: Preparation of ^{18}O-Labelled Methylsiloxanes 407

SZAMMER, J.: A New Method for the Preparation of Amino Alcohols from Amino Acids 419

NENNING, P. und HOLZAPFEL, H.: Quarternäre bororganische Verbindungen. (Quaternary Boron-organic Compounds) 421

Book Reviews—Buchbesprechungen—Рецензии книг 429

Printed in Hungary

A kiadásért felel az Akadémiai Kiadó igazgatója Műszaki szerkesztő: Farkas Sándor
A kézirat nyomdába érkezett: 1969. V. 13. — Terjedelem: 9,75 (A/5) ív, 40 ábra

69.67649 Akadémiai Nyomda, Budapest — Felelős vezető: Bernát György

ACTA CHIMICA

ТОМ 61 — ВЫП. 4.

РЕЗЮМЕ

Распределение температуры дуги прикатодном возбуждении

З. Г. ХАННА, Т. КАНТОР и Л. ЭРДЕИ

Описывается определение продольного и радиального распределения температуры в угольной дуге постоянного тока в воздухе при катодном возбуждении. Особое внимание уделяется эффекту, наблюдаемому при испарении в плазму алюминия, обладающего низким потенциалом ионизации. Было заключено, что алюминий оказывает влияние на время пребывания цинка, применяемого в качестве термометрического элемента.

Аналитическая химия стероидов, IX

Спектрофотометрическое изучение (эстра-5) 10-ен-3,17-диона и его 3,3-диметил-кеталя

Ш. ГЁРЁГ

Был разработан спектрофотометрический метод для изучения превращений эстра-5(10)-ен-3,17-диона (ЭД) в его 3,3-диметил-кеталь (ЭДК). Основой метода служит то, что ЭД при восстановлении борогидридом натрия с последующей солянокислой обработкой не может быть измерен спектрофотометрически, в то время как ЭДК под влиянием той же самой обработки дает Δ^4-3-кето-соединение, обладающее интенсивным поглащением света.

Определение ЭД наряду с ЭДК, присутствующих вместе, проводилось таким образом, что вначале ЭД, присутствующее в виде загрязнения, подвергалось щелочной обработке и превращалось в Δ^4-изомер; количество последнего измерялось дифференциальной спектрофотометрией. Общее количество двух соединений можно было измерять после солянокислой обработки на основе полосы поглащения, характерной для Δ^4-3-кето-соединений.

Исследование эмиссии положительных ионов вольфрама, I

О. КАПОШИ и М. РИДЕЛЬ

Был разработан способ для изучения эмиссии положительных ионов металлов с помощью масс-спектрометра типа время полета. Метод позволяет определить не только качество испускаемых ионов, но является пригодным и для исследования очень быстрых процессов, протекающих во время эмиссии.

Подробно изучалась зависимость механизма эмиссии положительных ионов вольфрамовых спиралей, и сырых и предварительно подвергнутых термической обработке, от температуры и времени накаливания. Проводились сравнительные исследования с молибденовой проволокой. При измерениях удалось различить непрерывные и пульсирующие, вызванные «ионными вспышками» ионные токи. Кроме отношения этих ионных токов были определены и их абсолютные величины. Из размеров, формы и числа ионных вспышек рассчитывались при различных температурах количества ионов, образующих вспышки. На основе сравнения этих измерений с измерениями, полученными для монокристаллического вольфрама и неспиральной вольфрамовой проволоки, были сделаны заключения о положении и роли добавок в вольфраме.

Изучение адсорбции углеводородов на никелевом катализаторе кинетическим методом

П. ТЕТЕНИ, Л. БАБЕРНИЧ и К. ШЕХТЕР

Авторами изучалась адсорбция этана, бензола и циклогексана кинетическим методом на никелевом катализаторе. Величины измеренных адсорбционных коэффициентов доказывают наличие химического взаимодействия между поверхностью и субстратом. Величины теплоты адсорбции относительно малы; адсорбция этана эндотермична.

На основе величин, характеризующих адсорбцию, могут быть сделаны выводы относительно природы адсорбированного слоя. Из величин теплоты адсорбции могут быть рассчитаны значения. Энергии связи водорода, углерода и кислорода с катализатором: Q_{CNi}, Q_{HNi} и Q_{ONi}.

Применение полуэмпирического метода ССП МО ЛКАО с использованием различных орбиталей для различных спинов к расчету спиновой плотности радикалов некоторых производных N-окиси фенилазота

Я. ЛАДИК, Г. БИЦО, И. КЕНДЕ и Л. ШЮМЕГИ

Распределение спиновых плотностей в радикалах N-окиси фенилазота, а также ее орто, пара и мета-галогенизированных (F, Cl, Br) производных рассчитывалось с помощью полуэмпирического метода ССП МО ЛКАО с использованием различных орбиталей для различных спинов (POPC). На основе полученных результатов, согласие между теоретическими и экспериментальными значениями спиновой плотности для углеродных атомов кольца является относительно наилучшим тогда, когда для значения кулоновского интеграла $\gamma_{i,j}$ было взято 1,5-ов значение от рассчитанного по уравнению Матага—Нишимото. В этом случае, однако, согласие для атомов азота и кислорода является плохим. Это указывает на то, что важным является также применение проектирования спина в полуэмпирической модификации метода POPC. Продолжается работа в этом направлении.

Расчет контуров ИК-полос для плоских и молекул типа асимметрического ротатора, I

Построение общих зависимостей

Э. ПААЛ и ДЬ. ВАРШАНИ

Рассчитывались контуры полос для плоских молекул типа асимметрического ротатора с различными параметрами асимметрии и коэффициентами инерции различных величин, с помощью уже ранее описанного метода [6, 7, 8]. Определялись ширины чистых полос A и B, а также нескольких гибридных полос AB различного направления при некоторой доле высоты. Из полученных значений ширины полосы при некоторой доле ее высоты строились диаграммы $\varkappa - \Delta\nu_{1/n}$, $B - \Delta\tilde{\nu}_{1/n}$ и $\varphi - \Delta\tilde{\nu}_{1/n}$. Определялись область значений н и B, в которой диаграммы $\varphi - \Delta\tilde{\nu}_{1/n}$ могут быть использованы для определения направления переходного момента.

Получение метилсилоксанов, меченных и зотопом O^{18}

П. ГЁМЁРИ и Л. СЕПЕШ

Был разработан препаративный метод для гидролиза ди- и моно-функциональных метил-хлор-силанов с использованием воды, обогащенной изотопом O^{18}. При помощи гидролиза, полимеризации и пиролиза, а также эквилибрации были синтезированы циклические силоксаны $[(CH_3)_2SiO]_n$ (где $n = 3,4,5,6,7$) газовохроматографической чистоты, обогащенные изотопом O^{18}, и линейные силоксаны $(CH_3)_3\ Si - O - [Si(CH_3)_2 - O]_k - Si(CH_3)_3$, где $\kappa = 0,1,2,3,4,5$. При гидролизе диметил-дихлорсилана почти стехиометрическим количеством воды наблюдалось увеличение количества циклического пентасилоксана в ущерб тетрасилоксана.

Новый метод получения аминоспиртов из аминокислот

Я. САММЕР

N-Тритил-производные метиловых эфиров аминокислот при восстановлении их с помощью $LiATH_4$ превращаются с хорошим выходом в соответствующие N-тритил-аминоспирты. N-Тритил-производные метиловых эфиров глицина, DL-аланина и DL-серина восстанавливаются в соответствующие N-тритил-аминоспирты с выходами 94, 92 и 95%, соответственно. Этот способ кажется общеприменяемым для получения аминоспиртов из аминокислот.

Четвертичные бороорганические соединения

П. НЕННИНГ и Х. ХОЛЦАПФЕЛ

Были синтезированы четвертичные и бис-четвертичные бороорганические соединения и изучалось как образование их солей со щелочными металлами, так и их поведение в водных растворах. Было найдено, что их соли со щелочными металлами являются почти нерастворимыми в воде. Несмотря на это считается, что катионы щелочных металлов не могут быть высаждены специфическим путем, и поэтому эти соединения, возможно не являются перспективными в качестве аналитических реагентов.

Полученные бороорганические комплексы являются устойчивыми к гидролизу, если различие электроотрицательностей центрального атома и лиганда невелико и изомерия невозможна.

The Acta Chimica publish papers on chemistry in English, German, French and Russian.

The Acta Chimica appear in volumes consisting of four parts of varying size, 4 volumes being published a year.

Manuscripts should be addressed to

Acta Chimica
Budapest 112/91 Műegyetem

Correspondence with the editors should be sent to the same address.

The rate of subscription is 165 forints a volume. Orders may be placed with "*Kultúra*" Foreign Trade Company for Books and Newspapers (Budapest I., Fő utca 32. Account No. 43-790-057-181) or with representatives abroad.

Les Acta Chimica paraissent en français, allemand, anglais et russe et publient des mémoires du domaine des sciences chimiques.

Les Acta Chimica sont publiés sous forme de fascicules. Quatre fascicules seront réunis en un volume (4 volumes par an).

On est prié d'envoyer les manuscrits destinés à la rédaction à l'adresse suivante:

Acta Chimica
Budapest 112/91 Műegyetem

Toute correspondance doit être envoyée à cette même adresse.

Le prix de l'abonnement est de 165 forints par volume.

On peut s'abonner à l'Entreprise pour le Commerce Extérieur de Livres et Journaux «*Kultúra*» (Budapest I., Fő utca 32. Compte-courant No. 43-790-057-181) ou à l'étranger chez tous les représentants ou dépositaires.

«*Acta Chimica*» издают трактаты из области химической науки на русском, французском, английском и немецком языках.

«*Acta Chimica*» выходят отдельными выпусками разного объема. 4 выпуска составляют один том. 4 тома публикуются в год.

Предназначенные для публикации рукописи следует направлять по адресу:

Acta Chimica
Budapest 112/91 Műegyetem

По этому же адресу направлять всякую корреспонденцию для редакции.

Подписная цена «*Acta Chimica*» — 165 форинтов за том. Заказы принимает предприятие по внешней торговле книг и газет «*Kultúra*» (Budapest I., Fő utca 32. Текущий счет № 43-790-057-181) или его заграничные представительства и уполномоченные.

Reviews of the Hungarian Academy of Sciences are obtainable at the following addresses:

ALBANIA
Ndermarja Shtetnore e Botimeve
Tirana

AUSTRALIA
A. Keesing
Box 4886, GPO
Sydney

AUSTRIA
Globus Buchvertrieb
Salzgries 16
Wien I

BELGIUM
Office International de Librairie
30, Avenue Marnix
Bruxelles 5
Du Monde Entier
5, Place St. Jean
Bruxelles

BULGARIA
Raznoiznos
1, Tzar Assen
Sofia

CANADA
Pannonia Books
2, Spadina Road
Toronto 4, Ont.

CHINA
Waiwen Shudian
Peking
P. O. B. 88

CZECHOSLOVAKIA
Artia
Ve Směčkách 30
Praha 2
Poštovná Novinová Služba
Dovoz tisku
Vinohradská 46
Praha 2
Mad'arská Kultura
Václavské nám. 2
Praha I
Poštová Novinová Služba
Dovoz tlače
Leningradská 14
Bratislava

DENMARK
Ejnar Munksgaard
Nörregade 6
Copenhagen

FINLAND
Akateeminen Kirjakauppa
Keskuskatu 2
Helsinki

FRANCE
Office International de Documentation et Librairie
48, rue Gay Lussac
Paris 5

GERMAN DEMOCRATIC REPUBLIC
Deutscher Buch-Export und Import
Leninstraße 16
Leipzig 701
Zeitungsvertriebsamt
Fruchtstrasse 3—4
1004 Berlin

GERMAN FEDERAL REPUBLIC
Kunst und Wissen
Erich Bieber
Postfach 46
7 Stuttgart S.

GREAT BRITAIN
Collet's Holdings Ltd.
Dennington Estate
London Rd.
Wellingborough, Northants.
Robert Maxwell and Co. Ltd.
Waynflete Bldg. The Plain
Oxford

HOLLAND
Swetz and Zeitlinger
Keizersgracht 471—487
Amsterdam C.
Martinus Nijhof
Lange Voorhout 9
The Hague

INDIA
Current Technical Literature
Co. Private Ltd.
India House OPP
GPO Post Box 1374
Bombay I

ITALY
Santo Vanasia
Via M. Macchi 71
Milano
Libreria Commissionaria Sansoni
Via La Marmora 45
Firenze

JAPAN
Nauka Ltd.
92, Ikebukur O-Higashi 1-chome
Toshima-ku
Tokyo
Maruzen and Co. Ltd.
P. O. Box 605
Tokyo-Central
Far Eastern Booksellers
Kanda P. O. Box 72
Tokyo

KOREA
Chulpanmul
Phenjan

NORWAY
Johan Grundt Tanum
Karl Johansgatan 43
Oslo

POLAND
RUCH
ul. Wronia 23
Warszawa

ROUMANIA
Cartimex
Str. Aristide Briand 14—18
Bucureşti

SOVIET UNION
Mezhdunarodnaya Kniga
Moscow G—200

SWEDEN
Almquist and Wiksell
Gamla Brogatan 26
Stockholm

USA
Stechert Hafner Inc.
31. East 10th Street
New York, N. Y. 10003
Walter J. Johnson
111, Fifth Avenue
New York, N. Y. 10003

VIETNAM
Xunhasaba
19, Tran Quoc Toan
Hanoi

YUGOSLAVIA
Forum
Vojvode Mišića broj 1
Novi Sad
Jugoslovenska Knjiga
Terazije 27
Beograd

30. IX. 1969 Index: 26.007